ADVANCES AND NOVEL TECHNOLOGIES IN SURGICAL INSTRUMENTS FOR THE TREATMENT OF CANCER

EDITED BY: Patrick J. Schuler and Lueder Alexander Kahrs
PUBLISHED IN: Frontiers in Oncology and Frontiers in Surgery

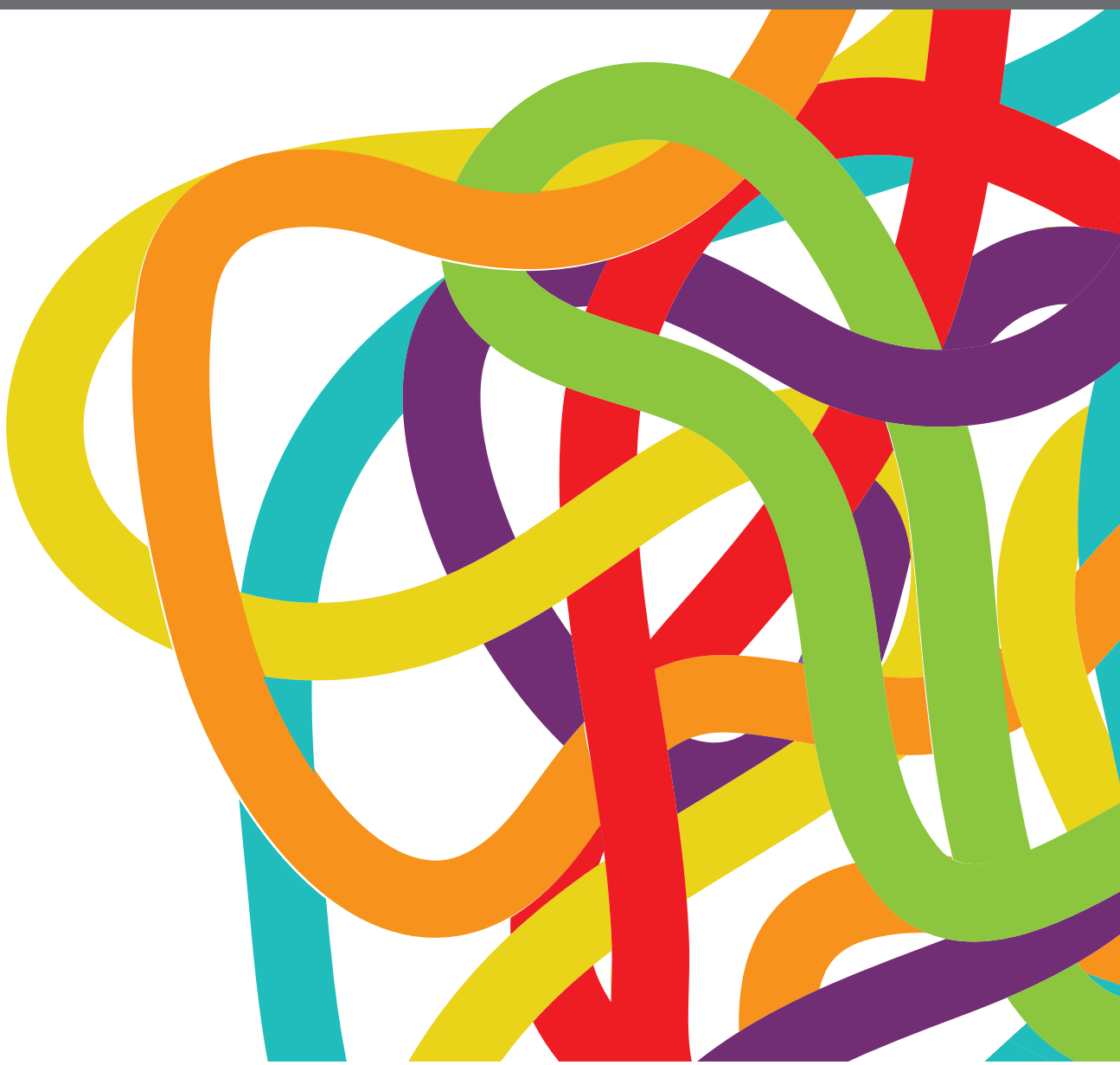

frontiers Research Topics

ISSN 1664-8714
ISBN 978-2-88976-737-3
DOI 10.3389/978-2-88976-737-3

About Frontiers

Frontiers is more than just an open-access publisher of scholarly articles: it is a pioneering approach to the world of academia, radically improving the way scholarly research is managed. The grand vision of Frontiers is a world where all people have an equal opportunity to seek, share and generate knowledge. Frontiers provides immediate and permanent online open access to all its publications, but this alone is not enough to realize our grand goals.

Frontiers Journal Series

The Frontiers Journal Series is a multi-tier and interdisciplinary set of open-access, online journals, promising a paradigm shift from the current review, selection and dissemination processes in academic publishing. All Frontiers journals are driven by researchers for researchers; therefore, they constitute a service to the scholarly community. At the same time, the Frontiers Journal Series operates on a revolutionary invention, the tiered publishing system, initially addressing specific communities of scholars, and gradually climbing up to broader public understanding, thus serving the interests of the lay society, too.

Dedication to Quality

Each Frontiers article is a landmark of the highest quality, thanks to genuinely collaborative interactions between authors and review editors, who include some of the world's best academicians. Research must be certified by peers before entering a stream of knowledge that may eventually reach the public - and shape society; therefore, Frontiers only applies the most rigorous and unbiased reviews.
Frontiers revolutionizes research publishing by freely delivering the most outstanding research, evaluated with no bias from both the academic and social point of view. By applying the most advanced information technologies, Frontiers is catapulting scholarly publishing into a new generation.

What are Frontiers Research Topics?

Frontiers Research Topics are very popular trademarks of the Frontiers Journals Series: they are collections of at least ten articles, all centered on a particular subject. With their unique mix of varied contributions from Original Research to Review Articles, Frontiers Research Topics unify the most influential researchers, the latest key findings and historical advances in a hot research area! Find out more on how to host your own Frontiers Research Topic or contribute to one as an author by contacting the Frontiers Editorial Office: frontiersin.org/about/contact

ADVANCES AND NOVEL TECHNOLOGIES IN SURGICAL INSTRUMENTS FOR THE TREATMENT OF CANCER

Topic Editors:
Patrick J. Schuler, Ulm University Medical Center, Germany
Lueder Alexander Kahrs, University of Toronto Mississauga, Canada

Citation: Schuler, P. J., Kahrs, L. A., eds. (2022). Advances and Novel Technologies in Surgical Instruments for the Treatment of Cancer. Lausanne: Frontiers Media SA. doi: 10.3389/978-2-88976-737-3

Table of Contents

frontiers | Frontiers in Oncology

TYPE Editorial
PUBLISHED 04 October 2022
DOI 10.3389/fonc.2022.1012750

OPEN ACCESS

EDITED BY
Pasquale Cianci,
Azienda Sanitaria Localedella Provincia di Barletta Andri Trani (ASL BT), Italy

REVIEWED BY
Vincenzo Neri,
University of Foggia, Italy
Dimitri Krizzuk,
Aurelia Hospital, Italy

*CORRESPONDENCE
P.J. Schuler
patrick.schuler@uniklinik-ulm.de

SPECIALTY SECTION
This article was submitted to Surgical Oncology, a section of the journal Frontiers in Oncology

RECEIVED 05 August 2022
ACCEPTED 22 September 2022
PUBLISHED 04 October 2022

CITATION
Schuler PJ, Hoffmann TK and Kahrs LA (2022) Editorial: Advances and novel technologies in surgical instruments for the treatment of cancer. *Front. Oncol.* 12:1012750. doi: 10.3389/fonc.2022.1012750

Editorial: Advances and novel technologies in surgical instruments for the treatment of cancer

P.J. Schuler[1,2]*, T.K. Hoffmann[1,2] and L.A. Kahrs[3,4]

[1]Department of Otorhinolaryngology, Head and Neck Surgery, Ulm University Medical Centre, Ulm, Germany, [2]Surgical Oncology Ulm, i2SOUL Consortium, Ulm, Germany, [3]Department of Mathematical and Computational Sciences, University of TorontoMississauga, Toronto, ON, Canada, [4]Institute of Biomedical Engineering, University of Toronto, Toronto, ON, Canada

KEYWORDS

cancer, technology, instruments, surgery, imaging

Editorial on the Research Topic
Advances and novel technologies in surgical instruments for the treatment of cancer

Traditional surgery for patients with malignant diseases is increasingly supported by robotic systems, artificial intelligence, augmented reality and smart instruments. These new techniques help the surgeons to plan and perform the surgical task in a better or faster way. Although in the last years the technical development has produced a long list of excellent opportunities in this field, the majority fails to find their way in into the clinical routine. The reasons often include the questionable benefit for the patients, difficulties in handling the device in a feasible manner or overwhelming costs, which are not covered by the medical insurance. In addition, devices, which are regularly used for the treatment of patients in the clinic, often lack the verification of their benefit by randomized clinical trials.

The goal of the special issue is to bring together technical developers and clinical physicians already in an early stage of development in order to discuss the technical potential and the clinical needs in the treatment of cancer patients. We believe that within every technical development, the patients' needs and the potential benefit for the treatment of their tumor burden should be in the center of interest. To this end, this special issue offers an open platform for both, technical and clinical contributions, which aim to improve the treatment of oncologic patients by the means of novel technical ideas.

A series of the accepted manuscripts focus on endoscopic techniques in the field of surgery describing procedures in a variety of organs including liver, esophagus, vagina, parotid gland, rectum and prostate. This demonstrates that almost all surgical specialties have adapted to this form of visualization in some form.

A publication reports on the consensus meeting on operating specifications for laparoscopic radical resection of hilar cholangiocarcinoma (HCCA). It lists 16 recommendations for preoperative management of HCCA in a laparoscopic setting. At the same time the experts agree that the laparoscopic approach for HCCA is still in the early phase of development.

A population-based analysis on the surgical therapy for early esophagogastric junction adenocarcinoma has received its data from the worldwide Surveillance, Epidemiology, and End Results (SEER) database including 3,708 patients. The analysis aimed to define the risk for lymph node metastasis comparing the endoscopic versus the open surgical setting. In conclusion, the endoscopic approach is non-inferior to open surgery in terms of risk for lymph node metastasis.

A very similar approach on elderly patients with endometrial cancer also investigated the outcome of laparoscopic surgery. The total study population of 537 patients was retrospectively recruited from seven institutions and divided into groups with laparoscopic or robotic surgery. The study concluded that there was no difference in survival. However robotic surgery was associated with lower blood loss and longer operating times.

The collection of manuscripts is continued by five meta-analysis publications, which compare endoscopic, robotic and other surgical approaches in large patient cohorts. The first analysis included 572 patients with parotid tumors and compared endoscopic/robotic parotidectomy with conventional open parotidectomy (CP) in terms of safety and efficacy. Based on their findings, the authors conclude that endoscopic and robotic parotidectomy should be reserved to those patients with strong cosmetic needs after adequate preoperative evaluation.

The second meta-analysis compared the laparoscopic approach with the robotic approach in 510 patients with intersphincteric resection of low rectal cancer. In contrast to the parotid study, the potential benefits of robotic surgery are considered a safe and feasible alternative for the treatment of low rectal tumors.

Robotic surgery for prostate cancer is considered to be a well-established clinical routine in most developed countries around the world. Different robotic approaches a therefore compared in the following meta-analysis on 3,129 patients with prostate cancer. The authors conclude, that resection of the Retzius space during radical prostatectomy is associated with worse recovery of continence, longer operation time and higher incidence of herniation. Although there was no significant difference in overall survival, this approach should still be considered in lesions of the anterior prostate.

Two meta-analyses reported on the treatment of hepatocellular carcinoma in 803 and 1,158 patients, respectively. The transcatheter arterial chemoembolization in combination with high-intensity focused ultrasound was associated with longer overall survival and should be recommended for patients with advanced hepatocellular carcinoma. In addition, fusion imaging in radiofrequency ablation was reported to have some effects on improving safety and efficacy as compared to standard ultrasound. However, currently fusion imaging should only be recommended for large lesions or those, which are difficult to ablate.

The second group of manuscripts in this special issue deals with novel surgical approaches and their potential benefit for the patients. In these publications, surgeons directly report on their experiences in the treatment of their patients, which make these contributions especially valuable.

The first retrospective interventional cohort study included 366 patients with intraocular tumors and a mean follow-up of 87 months. The authors state, that in their hands partial transscleral sclerouvectomy in combination with microinvasive vitrectomy is safe procedure, which can preserve the usefull vision in these patients and should be discussed as an alternative to enucleation.

Two working groups reported on the surgical therapy of limb tumors. The first retrospective study recommended an extended curettage as a feasible treatment option for giant cell tumor (n=29) of the proximal femur as an alternative to segmental resection. In the second case-series the authors reported on the experience with limb salvage surgery in 56 patients with malignant forearm tumors and gave recommendations for risk evaluation.

Another retrospective study approached the problem of ischemia reperfusion injury in liver transplantation. The authors demonstrated in 226 patients with hepatocellular carcinoma that an ischemic-free surgical procedure can significantly reduce hepatocyte necrosis and apoptosis after liver transplantation.

A small, prospective randomized trial in 30 patients with lung cancer compared to different sequences for the procedural steps during video-assisted thoracoscopic surgery. Another retrospective case-series evaluated the feasibility of endotracheal stent placement in combination with intra-arterial chemoembolization in patient with lung cancer (n=42). The authors demonstrated, that this may be an appropriate approach in this palliative patient collective.

Finally, in a human ex vivo trial (n=12), the authors demonstrated who the quality of fresh urinary tract biopsies can be improved by applying a cryobiopsy technique.

The last three manuscripts focus on the development of instruments and software in order to facilitate surgery.

To this end, a modular MR-compatible robot was developed, which can independently place multiple needles into a tissue for e.g. brachytherapy of the prostate. The whole procedure is guided by MR-imaging.

In a second study, the comparison of cutting qualities between CO_2 laser and diode-pumped Er-YAG laser was performed on an *ex vivo* animal model. According to the

authors, the CO_2 laser was inferior in terms of cutting efficacy and thermal damage width.

Finally, based on a data set of 195 patients with gallbladder polypoid lesions, the authors have developed a preoperative nomogram of clinical and radiomic features. This nomogram was validated for predicting benign and malignant lesions.

In conclusion, the publications in this special issue present a variety of new surgical approaches and technical developments, which help to better treat our patients with oncologic diseases.

Author contributions

PJS wrote the manuscript, TKH and LAK reviewed the manuscript. All authors contributed to the article and approved the submitted version.

Conflict of interest

The authors declare that the research was conducted in the absence of any commercial or financial relationships that could be construed as a potential conflict of interest.

Publisher's note

frontiers in Oncology

ORIGINAL RESEARCH
published: 22 September 2021
doi: 10.3389/fonc.2021.724886

Comparison Between Laparoscopic and Robotic Surgery in Elderly Patients With Endometrial Cancer: A Retrospective Multicentric Study

Giacomo Corrado[1], Enrico Vizza[2], Anna Myriam Perrone[3], Liliana Mereu[4], Vito Cela[5], Francesco Legge[6], Georgios Hilaris[7,8], Tina Pasciuto[9], Marco D'Indinosante[1], Eleonora La Fera[1], Camilla Certelli[2], Valentina Bruno[2], Stylianos Kogeorgos[7], Francesco Fanfani[9], Pierandrea De Iaco[3], Giovanni Scambia[1,10] and Valerio Gallotta[1]*

[1] Dipartimento Scienze della Salute della Donna, del Bambino, e di Sanità Pubblica, Ginecologia Oncologica, Fondazione Policlinico Universitario A. Gemelli IRCCS, Rome, Italy, [2] Department of Experimental Clinical Oncology, Gynecologic Oncology Unit, IRCCS "Regina Elena" National Cancer Institute, Rome, Italy, [3] Division of Oncologic Gynaecology, IRCCS Azienda Ospedaliero-Universitaria di Bologna, University of Bologna, Bologna, Italy, [4] Obstetrics and Gynecological Department, Santa Chiara Hospital, Trento, Italy, [5] Department of Obstetrics and Gynecology, University of Pisa, Pisa, Italy, [6] Department of Obstetrics and Gynecology, Division of Gynecology, "F. Miulli" General Hospital, Bari, Italy, [7] 2nd Department of Gynecologic Oncology, Hygeia Hospital, Marousi, Athens, Greece, [8] Department of Obstetrics and Gynecology, Division of Gynecologic Oncology, Stanford University Hospital, Stanford, CA, United States, [9] Research Core Facilty Data Collection G-STeP, Fondazione Policlinico Universitario Agostino Gemelli IRCCS, Rome, Italy, [10] Dipartimento Scienze della Salute della Donna, del Bambino, e di Sanità Pubblica, Ginecologia Oncologica, Fondazione Policlinico Universitario A. Gemelli—IRCCS, Università Cattolica del Sacro Cuore, Rome, Italy*

Introduction: Elderly endometrial cancer (EEC) patients represent a challenging clinical situation because of the increasing number of clinical morbidities. In this setting of patients, minimally invasive surgery (MIS) has been shown to improve surgical and clinical outcomes. The aim of this study was to evaluate the peri-operative and oncological outcomes of EEC patients who had undergone laparoscopic (LS) or robotic surgery (RS).

Materials and Methods: This is a retrospective multi-institutional study in which endometrial cancer patients of 70 years or older who had undergone MIS for EC from April 2002 to October 2018 were considered. Owing to the non-randomized nature of the study design and the possible allocation biases arising from the retrospective comparison between LS and RS groups, we also performed a propensity score-matched analysis (PSMA).

Results: A total of 537 patients with EC were included in the study: 346 who underwent LS and 191 who underwent RS. No significant statistical differences were found between the two groups in terms of surgical and survival outcomes. 188 were analyzed after PSMA (94 patients in the LS group were matched with 94 patients in the RS group). The median estimated blood loss was higher in the LS group (p=0.001) and the median operative time was higher in the RS group (p=0.0003). No differences emerged between LS and RS in terms of disease free survival (DFS) (p=0.890) and overall survival (OS) (p=0.683).

OPEN ACCESS

Edited by:
Stefano Restaino, Ospedale Santa Maria della Misericordia di Udine, Italy

Reviewed by:
Giuseppe Vizzielli, Azienda Sanitaria Universitaria Integrata di Udine, Italy
Giulia Pomati, Sapienza University of Rome, Italy

***Correspondence:**
Giacomo Corrado
giac.cor73@gmail.com

Specialty section:
This article was submitted to Gynecological Oncology, a section of the journal Frontiers in Oncology

Received: *14 June 2021*
Accepted: *06 September 2021*
Published: *22 September 2021*

Citation:
Corrado G, Vizza E, Perrone AM, Mereu L, Cela V, Legge F, Hilaris G, Pasciuto T, D'Indinosante M, La Fera E, Certelli C, Bruno V, Kogeorgos S, Fanfani F, De Iaco P, Scambia G and Gallotta V (2021) Comparison Between Laparoscopic and Robotic Surgery in Elderly Patients With Endometrial Cancer: A Retrospective Multicentric Study. Front. Oncol. 11:724886. doi: 10.3389/fonc.2021.724886

Conclusions: Our study showed that when compared LS and RS, RS showed lower blood losses and higher operative times. However, none of the two approaches demonstrated to be superior in terms of survival outcomes. For this reason, each patient should be evaluated individually to determine the best surgical approach.

Keywords: endometrial cancer, elderly patients, laparoscopic surgery (LS), robotic surgery, minimally invasive surgery (MIS)

INTRODUCTION

Endometrial cancer (EC) is the most common gynecological cancer in developed countries. A relevant percentage (15-25%) of women are older than 70 years at the diagnosis and the risk of EC increases according to the age (1, 2). Elderly patients present a higher rate of negative prognostic factors and the age itself represents a risk factor to consider in the choice of the adjuvant therapy (3). In fact, in this kind of patients more aggressive and advanced cancers are often diagnosed (4). The standard treatment is surgery in the majority of the cases. However, the main problem in the management of elderly patients is the comorbidities that increase the risk of surgical complications. For this reason, it is important on the one hand to obtain the best oncological outcome through radical surgery, and on the other hand, to reduce peri- and post-operative complications and to improve recovery times after surgery.

Several studies have investigated the feasibility of minimally invasive surgery (MIS) compared with laparotomic surgery and relevant advantages in terms of surgical outcomes have been demonstrated (5–10). However, studies in which different types of MIS in elderly patients are compared are missing.

In this study we evaluated the surgical and oncological outcomes of patients of 70 years or older who had undergone laparoscopic or robotic surgery for EC.

MATERIAL AND METHODS

This is a retrospective multi-institutional study that involved patients from seven Institutes: Fondazione Policlinico Universitario A. Gemelli of Rome, Regina Elena National Cancer Institute of Rome, Santa Chiara Hospital of Trento, Azienda Ospedaliero-Universitaria di Bologna, University of Pisa, "Miulli hospital" of Acquaviva delle Fonti in Bari, Hygeia Hospital, Marousi, Athens Greece. Approval to conduct the study was obtained independently from an internal review board at each participating institution. Informed consent to laparoscopic or robotic surgery was obtained from all the patients in accordance with local and international legislation (Declaration of Helsinki) (11).

Study Design

The data refer to a period from April 2002 to October 2018. All the EC patients of 70 years or older who had undergone MIS were considered. In the majority of the centers surgeons performed both laparoscopic and robotic surgery and the surgical approach was chosen according to clinical conditions or surgeons' preference. The robotic platforms used were Da Vinci Si or Xi (Intuitive Surgical Sunnyvale, CA). The cut-off of 70 years was based on previous studies, in which the incidence of comorbidities relevant for surgery had been considered (5, 12). All the patients were evaluated before surgery by means of a medical history, physical examination, vaginal-pelvic examination, chest X-ray, ultrasound scans, pelvic magnetic resonance imaging (MRI) or computed tomography (CT) scans. The number of relevant comorbidities was collected for each patients. Because of the retrospective nature of the study, no comorbidity scoring systems were available. Details relative to the surgical procedure and lymph node assessment [i.e. systematic lymphadenectomy or lymph node sampling or sentinel lymph node technique (SLN)] were collected in both groups. Intra-operative and post-operative complications were defined according to Common Terminology Criteria for Adverse Events (CTCAE) version 5 (13).

Adjuvant therapy was tailored to the pathologic findings at the primary surgery after multidisciplinary tumor board (gynecologic oncology, pathology, radiation oncology, medical oncology) discussion. Treatment was based on the National Comprehensive Cancer Network (NCCN) guidelines (www.nccn.org > professionals > physician_gls) as well as ESGO, and ESTRO guidelines (14). Follow-up data were recorded through phone calls, if not available from medical records. Study data were stored using REDCap electronic data capture tools hosted at Fondazione Policlinico Universitario A. Gemellli, IRCCS (https://redcap-irccs.policlinicogemelli.it/) (15, 16).

Statistical Analysis

Patient's characteristics were described as absolute frequency and percentage for nominal variables and as median (min-max) and mean (standard deviation) for continuous variables. For the analysis, patients were divided into two groups according to the surgical procedure adopted. We distinguished women who underwent LPS (LPS group) and those who underwent RS (RS group). Moreover, in order to assess the impact of age on LPS and RS, patients were stratified according to four age classes: 70-74 years old, 75-79 years old, 80-85 years old, more than 85 years old. Comparisons between groups were made with Mann-Whitney test or Kruskal–Wallis test for continuous variables and $\chi 2$ or Fisher exact test for nominal variables, as appropriate. The normality of continuous variables was assessed with Shapiro–Francia test. In order to assess the rule of age, BMI, comorbidity, previous abdominal surgery, FIGO stage (17), histotype, grading, presence of metastasis, surgical approach (LPS *vs* RS), operative time (OT) and adjuvant therapy on surgical complications, univariable logistic regression analyses

were run to identify possible factors significantly associated with intra-operative, early post-operative (≤30 days) and late post-operative (> 30 days) complications. The parameters were selected according to their clinical relevance and results were presented as Odds ratios (95% Confidence Intervals).

Owing to the non-randomized nature of the study design and the possible allocation biases arising from the retrospective comparison between LPS and RS groups, we also performed a propensity score-matched analysis (PSMA) (18). The PSMA was used to minimize potential selection bias and compare the treatment effects by taking into account all covariates that may influence the selection of the surgical approach (19, 20) namely laparoscopy or robotic surgery. Propensity score was developed through multivariable logistic regression model adjusting for: age, body mass index, comorbidity (present/absent), previous abdominal surgery, lymphadenectomy, histotype and FIGO stage. A 1:1 "nearest neighbor" match without replacement was applied (21) meaning that each patient treated by robotic surgery was matched with one patient treated by laparoscopy who had the closest estimated propensity score.

Survival analysis was performed both for the whole study and PSMA population in terms of DFS and OS. DFS was defined as the time elapsed from first diagnosis to recurrence or last follow-up while OS was defined as the time from first diagnosis to death or last follow-up. Median follow-up was calculated according to the inverted Kaplan-Meier technique (22) OS and DFS curves were estimated by Kaplan-Meier product limit method (23) and compared by log-rank test (24). For PSMA population, Cox proportional hazards models (25) were applied to evaluate the impact on DFS and OS of age, BMI, comorbidity, previous abdominal surgery, FIGO stage, histotype, grading, presence of metastasis, surgical approach (LPS *vs* RS) and adjuvant therapy. The parameters were selected according to their clinical relevance. All estimates were presented with two-sided 95% Confidence Intervals (CIs). All statistical calculations were performed using the STATA software version 13.0 (Stata Corp, College Station, TX). Two-sided tests were used and the significance level was set at $p< 0.05$. No imputation was carried out for missing data.

RESULTS

A total of 537 patients with EC were included in the study: 346 who underwent laparoscopic surgery (LS) and 191 who underwent robotic surgery (RS). Each center contributed with patients: Fondazione Policlinico Universitario A. Gemelli with 130 patients (54 LS and 76 RS), Regina Elena National Cancer Institute with 168 patients (143 LS and 25 RS), Santa Chiara Hospital with 75 patients (36 LS and 39 RS), Azienda Ospedaliero-Universitaria of Bologna with 83 patients (71 LS and 12 RS), University of Pisa with 18 patients (18 RS), "Miulli hospital" with 40 patients (24 LS and 16 RS), Hygeia Hospital with 23 patients (18 LS and 5 RS).

Patient Characteristics

Clinical and pathological characteristics are shown in **Table 1**. The median age was 76 (range 70-94) and 75 (range 70-88) years, respectively, in the LS and the RS group. The distribution of patients according to age and BMI was not normally distributed and is shown, respectively, in **Supplementary Figures S1** and **S2**. Analyses within both LS and RS groups didn't show any significant statistical differences in terms of histology, grading, prior abdominal surgery and medical comorbidities. These results were also confirmed in a stratified analysis according to class age (**Supplementary Table S1**). The majority of the patients in both groups had FIGO stage I (81.5% and 82.2%, respectively, in the LS and the RS group). The 18% of the patients had a FIGO stage higher than II (**Table 1**).

Surgical Outcomes

Surgical, adjuvant and follow up characteristics are shown in **Table 2**. No significant statistical differences were found between the two groups in terms of type of surgery, intra-operative and post-operative complication and laparotomic conversion. In particular, the rate of intraoperative complications was 1.9%. Six intraoperative complications were documented in the LS group: 2 bowel injuries, 2 bladder injuries, 2 vaginal lacerations. Four intraoperative complications were documented in the RS group: 1 bladder injury, 1 iliac artery injury, 1 vaginal laceration, 1 bowel injury. All the intraoperative complications occurred in the two groups were classified as grade < 3 according the CTCAE. There were 4 grade 3 early postoperative complications: 1 bowel perforation in RS group and 1 bladder-vaginal fistula and 2 urinary site infections in LS group. Among late postoperative complications only 3 were classified as grade 3 according to the CTCAE: 2 laparocele or incisional hernia (1 in LS and 1 in RS group) and 1 bowel perforation in RS group. Furthermore, the total number of laparotomic conversions was 10: 5 in the LS group due to obesity reasons and an excessive visceral adipose tissue, 5 in the RS due to vessel lesion (2 cases), sigma infiltration (1case) and vessel involvement by the tumor (2 cases). One patient was converted from robotic to laparoscopic surgery to due obesity reasons. Lymphadenectomy was performed in 70.2% of RS compared to 38.9% of the LS ($p<0.0001$). Even if the number of the lymph nodes retrieved was the same in the two groups the rate of lymph nodes metastases was higher in the robotic group ($p<0.002$).

The mean hospital stay was 4 days in LS group and 3 days in RS. This difference was statistically significant ($p=0.0001$). Days of hospitalization was statistically significant lower in robotic groups ranging from 75 to 85 years compared to laparoscopic groups (**Supplementary Table S2**). The absence of statistical significant differences between the two groups in terms of intra and post operative complications was also confirmed at univariable analysis (**Supplementary Table S1**).

Analysis According to the Age Class

Clinical and pathological characteristics according to the age class are shown in **Supplementary Table S2**. As regards the surgical outcomes, no differences emerged in terms of EBL, OT, laparotomic conversions and intra-operative and post-operative complications when the age increased, although the median OT was higher in the RS group of each age class (**Supplementary Table S3**).

TABLE 1 | Clinical and pathological characteristics of 537 patients with endometrial cancer according to the type of surgery.

Characteristic	All cases	LPS	RS	p value
All cases	537	346	191	
Age, years				**0.001**
Mean (standard deviation)	76.3 (4.8)	76.8 (5.0)	75.3 (4.2)	
Median (min-max)	75 (70-94)	76 (70-94)	75 (70-88)	
BMI kg/m^{2†}				0.059
Mean (standard deviation)	29.4 (6.0)	29.0 (5.6)	30.2 (6.5)	
Median (min-max)	28.9 (12.5-62)	28.4 (12.5-62)	29.1 (17.6-53)	
Comorbidities				0.066
0	60/528 (11.4)	40/343 (11.7)	20/185 (10.8)	
1	203/528 (38.4)	142/343 (41.4)	61/185 (33.0)	
2	144/528 (27.3)	94/343 (27.4)	50/185 (27.0)	
>2	121/528 (22.9)	67/343 (19.5)	54/185 (29.2)	
Previous abdominal surgery	188 (35.0)	130 (37.6)	58 (30.4)	0.094
FIGO stage				**0.003**
IA	258 (48.0)	165 (47.7)	93 (48.7)	
IB	181 (33.7)	117 (33.8)	64 (33.5)	
II	44 (8.2)	35 (10.1)	9 (4.7)	
IIIA	10 (1.9)	4 (1.2)	6 (3.1)	
IIIB	7 (1.3)	6 (1.7)	1 (0.5)	
IIIC	26 (4.8)	9 (2.6)	17 (8.9)	
IVA	3 (0.6)	3 (0.9)	0 (0)	
IVB	8 (1.5)	7 (2.0)	1 (0.5)	
Histotype				
Endometrioid	468 (87.2)	302 (87.3)	166 (86.9)	0.902
NEEC	69 (12.8)	44 (12.7)	25 (13.1)	
Grading				0.384
1	103/532 (19.4)	63/341 (18.5)	40/191 (20.9)	
2	272/532 (51.1)	182/341 (53.4)	90/191 (47.1)	
3	157/532 (29.5)	96/341 (28.2)	61/191 (31.9)	
Number of lymph nodes retrieved‡				0.476
Mean (standard deviation)	14.8 (9.7)	15.3 (9.9)	14.3 (9.4)	
Median (min-max)	13 (1-56)	14 (1-56)	13 (1-42)	
Lymph node metastasis				**0.002**
No	506 (94.2)	334 (96.5)	172 (90.1)	
Yes	31 (5.8)	12 (3.5)	19 (9.9)	

Results are presented as n (%) except where indicated. p value was calculated with two sided Pearson's Chi Square test or Mann-Whitney U test for categorical and continuous not normally distributed characteristics respectively. Bold font highlights statistically significant difference. LPS, Laparoscopic Surgery; RS, Robotic Surgery; BMI, Body Mass Index; NEEC, Not endometrioid endometrial cancer. †Information available for 522/537 patients. ‡Information available for 241 patients.

Study Population After PSMA

One hundred eighty-eight were analyzed after PSMA (94 patients in the LS group were matched with 94 patients in the RS group). After matching, no differences emerged between the clinical and pathological characteristics of the two groups, (**Table 3**). Furthermore, there were no differences in terms of surgical procedures and adjuvant therapies (respectively, p=0.605 and p=0.461), as shown in **Table 4**. Although the median estimated blood loss (EBL) was higher in the LS group (p=0.001) and the median OT was higher in the RS group (p=0.0003), no differences were observed between the two groups in terms of intra-operative and post-operative complications rate (**Table 4**). Moreover, our results did not show differences in the laparotomic conversion rate (p=0.248).

Survival Outcomes

No significant differences were found between the two groups regarding the rate of patients who underwent adjuvant therapy (p=0.707 and p=0.461 for the whole study and PSMA population respectively). Similarly, no significant differences were detected in terms of modality of adjuvant therapy (p=0.171 and p=0.493 for the whole study and PSMA population respectively). Median follow up was 46.0 months (95% CI: 41.5-51.1) and 46.0 months (95% CI: 40.7-53.4) for the whole study and PSMA population respectively. In this period, in the whole study population, we observed 77 recurrences: 15.0% and 13.1% had recurrence in LS and RS groups respectively (p=0.539); while in the PSMA population, we observed 31 recurrences: 17.0% and 16.6% had recurrence in LH and RH groups respectively (p=0.844) (**Tables 2** and **4**).

No differences emerged between LS and RS in terms of disease free survival (DFS) (p=0.614 and p=0.890 for the whole study and PSMA population respectively) and overall survival (OS) (p=0.171 and p=0.683 for the whole study and PSMA population respectively), as shown in **Figure 1**. At the univariable analysis, there were no differences in the DFS and the OS according to the age of the PSMA patients (**Table 5**). The only variables that affected survival were, respectively, the FIGO stage for DFS and the histotype for OS.

TABLE 2 | Surgical, adjuvant and follow up characteristics of 537 patients with endometrial cancer according to the type of surgery.

Characteristic	All cases	LPS	RS	p value
All cases	537	346	191	
Surgical procedures				
TRH	7 (1.3)	6 (1.7)	1 (0.5)	0.484
TRH + BSO/MSO	509 (94.8)	327 (94.5)	182 (95.3)	
TRH ± BSO/MSO + Omentectomy	21 (3.9)	13 (3.8)	8 (4.2)	
Lymphadenectomy				**<0.0001**
Not performed	272 (50.7)	215 (62.1)	57 (29.8)	
Sentinel lymph node	21 (3.9)	0 (0)	21 (11.0)	
Pelvic	225 (41.9)	121 (35.0)	104 (54.5)	
Pelvic and aortic	19 (3.5)	10 (2.9)	9 (4.7)	
Estimated blood loss, mL[ǂ]				0.244
Mean (standard deviation)	77 (79.6)	73.8 (56.0)	83.2 (112.1)	
Median (min-max)	50 (0-800)	50 (0-400)	50 (0-800)	
Operative time, min[ŧ]				**<0.0001**
Mean (standard deviation)	142.4 (71.4)	122.0 (60.2)	177.1 (75.6)	
Median (min-max)	130 (25-530)	110 (35-389)	170 (25-530)	
Hospital stay, days[ǂ]				**<0.0001**
Mean (standard deviation)	3.9 (2.7)	4.2 (2.7)	3.3 (2.8)	
Median (min-max)	3 (1-32)	4 (1-32)	3 (1-31)	
Laparotomic conversion*	11 (2.0)	5 (1.4)	6 (3.1)	0.184
Patients with intra-operative complication	10 (1.9)	6 (1.7)	4 (2.1)	0.768
Patients with post-operative complication within 30 days from surgery	31 (5.8)	22 (6.4)	9 (4.7)	0.434
Patients with post-operative complication beyond 30 days from surgery	17/533 (3.2)	11/344 (3.2)	6/189 (3.2)	0.988
Adjuvant therapy				0.707
No	287 (53.4)	187 (54)	100 (52.4)	
Yes	250 (46.6)	159 (46)	91 (47.6)	
Type of adjuvant therapy[†]				0.182
CHT	45/249 (18.1)	29/158 (18.4)	16/91 (17.6)	
EBRT	91/249 (36.5)	64/158 (40.5)	27/91 (29.7)	
BRT	47/249 (18.9)	30/158 (19)	17/91 (18.7)	
CHT+EBRT	33/249 (13.3)	16/158 (10.1)	17/91 (18.7)	
CHT+BRT	2/249 (0.8)	0/158 (0)	2/91 (2.2)	
EBRT+BRT	27/249 (10.8)	17/158 (10.8)	10/91 (11.0)	
CHT+EBRT+BRT	4/249 (1.6)	2/158 (1.3)	2/91 (2.2)	
Recurrences	77 (14.3)	52 (15.0)	25 (13.1)	0.539
Deaths	100 (18.6)	77 (22.3)	23 (12.0)	**0.004**
Median FU (95% CI), months[§]	46.0 (41.5-51.1)	58.6 (50.6-61.9)	36.0 (33.1-40.6)	nc

*Results are presented as n (%) except where indicated. p value was calculated with two sided Pearson's Chi Square test or Mann-Whitney U test for categorical and continuous not normally distributed characteristics respectively, except where indicated. Bold font highlights statistically significant difference. LPS, Laparoscopic Surgery; RS, Robotic Surgery; TRH, Total Radical Hysterectomy; BSO, Bilateral Salpingo-Oophorectomy; MSO, Monolateral Salpingo-Oophorectomy; CHT, Chemotherapy; EBRT, External brachytherapy; BRT, Brachytherapy; AWD, Alive with disease; NED, No evidence of disease; FU, follow-up; CI, Confidence interval; nc, not calculated. [ǂ]Information available for 442/537 patients. [ŧ]Information available for 517/537 patients. [ǂ]Information available for 486/537 patients. *One patient of 82 years old was converted from Robotic to laparoscopic surgery for obesity reason. [†]In one case the type of adjuvant therapy was not available. [§]Calculated with the inverse Kaplan-Meier technique.*

DISCUSSION

This study confirms the benefit of the MIS approach in elderly endometrial cancer patients (4–10). After 4 years of follow-up, the present data suggest that MIS in EEC patients is safe from an oncological standpoint in terms of comparable DFS and OS rates.

Based on our multicentric experience, we can assert that robotic and laparoscopic approach for elderly endometrial cancer patients can be well tolerated with no increase in complications. Although, the RS required longer operative time, on the other hand it showed advantages in terms of reduced blood loss and hospital stay compared to LS.

Overall, our data confirm the available lines of evidence supporting the safety of MIS. The incidence of overall post-operative complications in our cohort was 5.8%, a frequency in agreement with some previous results (4–10), without significant difference between the two groups, despite about 40% of obese patients in each group.

Since elderly patients usually present a higher comorbidity rate and a higher surgical risk, in recent years the efforts have focused on the choice of the best surgical approach for this kind of patients. The main issues related to MIS were anesthesiological: the maintenance of Trendelemburg position and the pneumoperitoneum increase abdominal pressure reducing cardiac output and respiratory movements (5, 6, 26). For this reason, the management of these patients require a close collaboration within a multidisciplinary team consisting of anesthesia, geriatric and gynecologic specialists in order to obtain a greater synergy for determining surgical indications and tailored approaches in these fragile patients (27, 28). However, the increasing expertise of the surgeons with lower operative times may reduce the relevance of these issues. Furthermore, MIS has shown good results in terms of lower

TABLE 3 | Clinical and pathological characteristics of 188 matched patients with endometrial cancer according to the type of surgery.

Characteristic	All cases	LPS	RS	p value
All cases	188	94	94	
Age, years				0.161
Mean (standard deviation)	74.4 (3.5)	74.9 (3.9)	73.9 (3.0)	
Median (min-max)	74 (70-87)	74 (70-87)	73.5 (70-85)	
BMI kg/m^2				0.626
Mean (standard deviation)	29.5 (6)	29.0 (5.2)	30 (6.7)	
Median (min-max)	29 (17.6-52)	28.3 (18.8-48)	29 (17.6-52)	
Comorbidities				0.742
0	24/186 (12.9)	11/93 (11.8)	13/93 (14.0)	
1	69/186 (37.1)	38/93 (40.9)	31/93 (33.3)	
2	47/186 (25.3)	23/93 (24.7)	24/93 (25.8)	
>2	46/186 (24.7)	21/93 (22.6)	25/93 (26.9)	
Previous abdominal surgery	49 (26.1)	26 (27.7)	23 (24.5)	0.618
FIGO stage				0.106
IA	83 (44.1)	44 (46.8)	39 (41.5)	
IB	69 (36.7)	35 (37.2)	34 (36.2)	
II	10 (5.3)	8 (8.5)	2 (2.1)	
IIIA	5 (2.7)	1 (1.1)	4 (4.3)	
IIIB	2 (1.1)	1 (1.1)	1 (1.1)	
IIIC	17 (9.0)	4 (4.3)	13 (13.8)	
IVA	0 (0)	0 (0)	0 (0)	
IVB	2 (1.1)	1 (1.1)	1 (1.1)	
Histotype				0.835
Endometrioid	161 (85.6)	80 (85.1)	81 (86.2)	
NEEC	27 (14.4)	14 (14.9)	13 (13.8)	
Grading				0.679
1	32/188 (17)	14/94 (14.9)	18/94 (19.1)	
2	97/188 (51.6)	51/94 (54.3)	46/94 (48.9)	
3	59/188 (31.4)	29/94 (30.9)	30/94 (31.9)	
Number of lymph nodes retrieved[‡]				0.729
Mean (standard deviation)	15.4 (9.1)	15.7 (9.3)	15.1 (8.9)	
Median (min-max)	15 (1-42)	15 (2-39)	14 (1-42)	
Lymph node metastasis				0.058
No	168 (89.4)	88 (93.6)	80 (85.1)	
Yes	20 (10.6)	6 (6.4)	14 (14.9)	

Results are presented as n (%) except where indicated. p value was calculated with two sided Pearson's Chi Square test or Mann-Whitney U test for categorical and continuous not normally distributed characteristics respectively. Bold font highlights statistically significant difference. LPS, Laparoscopic Surgery; RS, Robotic Surgery; BMI, Body Mass Index; NEEC, Not endometrioid endometrial cancer. [‡]Information available for 168 patients.

complication rates and faster recovery times. Our series confirmed that MIS is associated with good post-operative results, with clinical benefits in terms of post-operative complications (29). When compared with laparotomic surgery in EC patients aged 70 years or older, RS showed a reduction of EBL, OT, complications and days of hospitalization (5, 9). Even when elderly and not elderly patients were compared, RS maintained its advantages (7) with no differences between robotic and laparotomic approaches in terms of survival (5). In the same way, LS showed better surgical outcomes when compared with a laparotomic approach. Laparotomy, in fact, was associated with a higher risk of thromboembolism, due to a longer recovery time, and higher surgical site infections rate (6). Furthermore, prolonged hospitalization times may delay the start of adjuvant therapies, compromising their efficacy. Although some recent studies compared the three different approaches (LS, RS and laparotomic surgery) according to the age of the patients, confirming an advantage of minimally invasive surgery (30, 31), studies in which the best minimally invasive approach was evaluated are missing. In our study we compared LS and RS in elderly patients (70 years and older) with EC and no differences emerged between the two surgical approaches in terms of complication rates, both intra-operative and post-operative. The LS group showed a higher median EBL, probably because of a better surgical field control with robotic arms, whereas the OT were longer in the RS group, due to docking times. In a recent study, de' Angelis et al, who evaluated the LS and the RS in elderly patients with colorectal cancer, showed similar results with no differences in terms of surgical outcomes between the two approaches, except for a longer OT in the RS group (32). On the one hand, the increased OT in RS may be a disadvantage for elderly patients, since it may be related to a prolonged Trendelemburg position which is not reversible without the un-docking of the robot (5). On the other hand, in RS the insufflation system is different and the pressure of the pneumoperitoneum may be reduced, taking advantage from the lifting of the trocars and the abdomen during docking time.

Our results did not show a worsening of the surgical outcomes when the age increased, in agreement with Uccella et al. who demonstrated the maintenance of an advantage of LS compared with laparotomy even in patients aged 80 years or older (6) and Lowe et al. who showed a 96% successful robotic

TABLE 4 | Surgical, adjuvant and follow up characteristics of 188 matched patients with endometrial cancer according to the type of surgery.

Characteristic	All cases	LPS	RS	p value
All cases	188	94	94	
Surgical procedures				0.605
TRH	1 (0.5)	0 (0)	1 (1.1)	
TRH + BSO/MSO	175 (93.1)	88 (93.6)	87 (92.6)	
TRH ± BSO/MSO + Omentectomy	12 (6.4)	6 (6.4)	6 (6.4)	
Lymphadenectomy				0.484
Not performed	18 (9.6)	8 (8.5)	10 (10.6)	
Sentinel lymph node	2 (1.1)	0 (0)	2 (2.1)	
Pelvic	153 (81.4)	79 (84.0)	74 (78.7)	
Pelvic and aortic	15 (8)	7 (7.4)	8 (8.5)	
Estimated blood loss, mL[ǂ]				**0.001**
Mean (standard deviation)	82.1 (96.4)	87.8 (63.5)	75.5 (124.2)	
Median (min-max)	50 (0-800)	99 (9-400)	50 (0-800)	
Operative time, min[ŧ]				**0.0003**
Mean (standard deviation)	178.6 (75.7)	158.6 (64.1)	197.5 (81.1)	
Median (min-max)	178 (25-530)	150 (60-389)	187.5 (25-530)	
Hospital stay, days[ǂ]				**0.0002**
Mean (standard deviation)	4.1 (3.4)	4.9 (4.3)	3.3 (2.0)	
Median (min-max)	3 (1-32)	4 (1-32)	3 (1-12)	
Laparotomic conversion	7 (3.7)	2 (2.1)	5 (5.3)	0.248
Patients with intra-operative complication	6 (3.2)	3 (3.2)	3 (3.2)	1
Patients with post-operative complication within 30 days from surgery	15 (8.0)	10 (10.6)	5 (5.3)	0.178
Patients with post-operative complication beyond 30 days from surgery	10/186 (5.4)	6/94 (6.4)	4/92 (4.3)	0.538
Adjuvant therapy				0.461
No	81 (43.1)	43 (45.7)	38 (40.4)	
Yes	107 (56.9)	51 (54.3)	56 (59.6)	
Type of adjuvant therapy				0.493
CHT	22/107 (20.6)	11/51 (21.6)	11/56 (19.6)	
EBRT	27/107 (25.2)	13/51 (25.5)	14/56 (25.0)	
BRT	30/107 (28.0)	18/51 (35.3)	12/56 (21.4)	
CHT+EBRT	14/107 (13.1)	4/51 (7.8)	10/56 (17.9)	
CHT+BRT	1/107 (0.9)	0/51 (0)	1/56 (1.8)	
EBRT+BRT	11/107 (10.3)	4/51 (7.8)	7/56 (12.5)	
CHT+EBRT+BRT	2/107 (1.9)	1/51 (2.0)	1/56 (1.8)	
Recurrences	31 (16.5)	16 (17.0)	15 (16.0)	0.844
Deaths	35 (18.6)	22 (23.4)	13 (13.8)	0.092
Median FU (95% CI), months[§]	46.0 (40.7-53.4)	57.9 (48.5-70.8)	40.4 (34.8-45.8)	nc

Results are presented as n (%) except where indicated. p value was calculated with two sided Pearson's Chi Square test or Mann-Whitney U test for categorical and continuous not normally distributed characteristics respectively, except where indicated. Bold font highlights statistically significant difference. LPS, Laparoscopic Surgery; RS, Robotic Surgery; TRH, Total Radical Hysterectomy; BSO, Bilateral Salpingo-Oophorectomy; MSO, Monolateral Salpingo-Oophorectomy; CHT, Chemotherapy; EBRT, External brachytherapy; BRT, Brachytherapy; AWD, Alive with disease; NED, No evidence of disease; FU, follow-up; CI, Confidence interval; nc, not calculated. [ǂ]Information available for 155/188 patients. [ŧ]Information available for 183/188 patients. [ǂ]Information available for 174/188 patients. [§]Calculated with the inverse Kaplan-Meier technique.

procedures in octogenarians and nonagenarians (33). Furthermore, although Walker et al. showed an increased conversion rate (from LS to Laparotomy) for each decade of age (34), our analysis did not reveal any differences in the conversion rate according to the age class. Another important aspect of surgery in elderly patients that emerged in some studies is the reduction of the lymphadenectomy rate (31), probably in order to reduce the invasiveness of the surgical procedure in this kind of patients. In our study, although the number of patients who underwent lymphadenectomy was lower when the age increased, the difference did not reach a statistical relevance. As regards survival outcomes, none of the two approaches demonstrated to be superior.

The major strengths of this study are represented by the number of patients included in the study, the PSMA and its specific focus on the role of MIS in EEC patients. Limitations include the retrospective nature of the study, which can result in underreporting adequate pre-operative frailty evaluation (28, 35) of the patients.

CONCLUSIONS

In conclusion, thanks to the successful cooperative efforts of multiple referral Gynecologic Oncology Units, we confirmed in a large series that MIS for EEC is feasible and safe, and provides survival outcomes comparable to those obtained with open surgical approach. In particular, when compared LS and RS, RS showed lower blood losses and higher operative times. However, none of the two approaches demonstrated to be superior in terms of survival outcomes.

Several efforts should be made and prospective collaborative study are needed to provide adequate preoperative work up and availability of a dedicated multidisciplinary approach, which

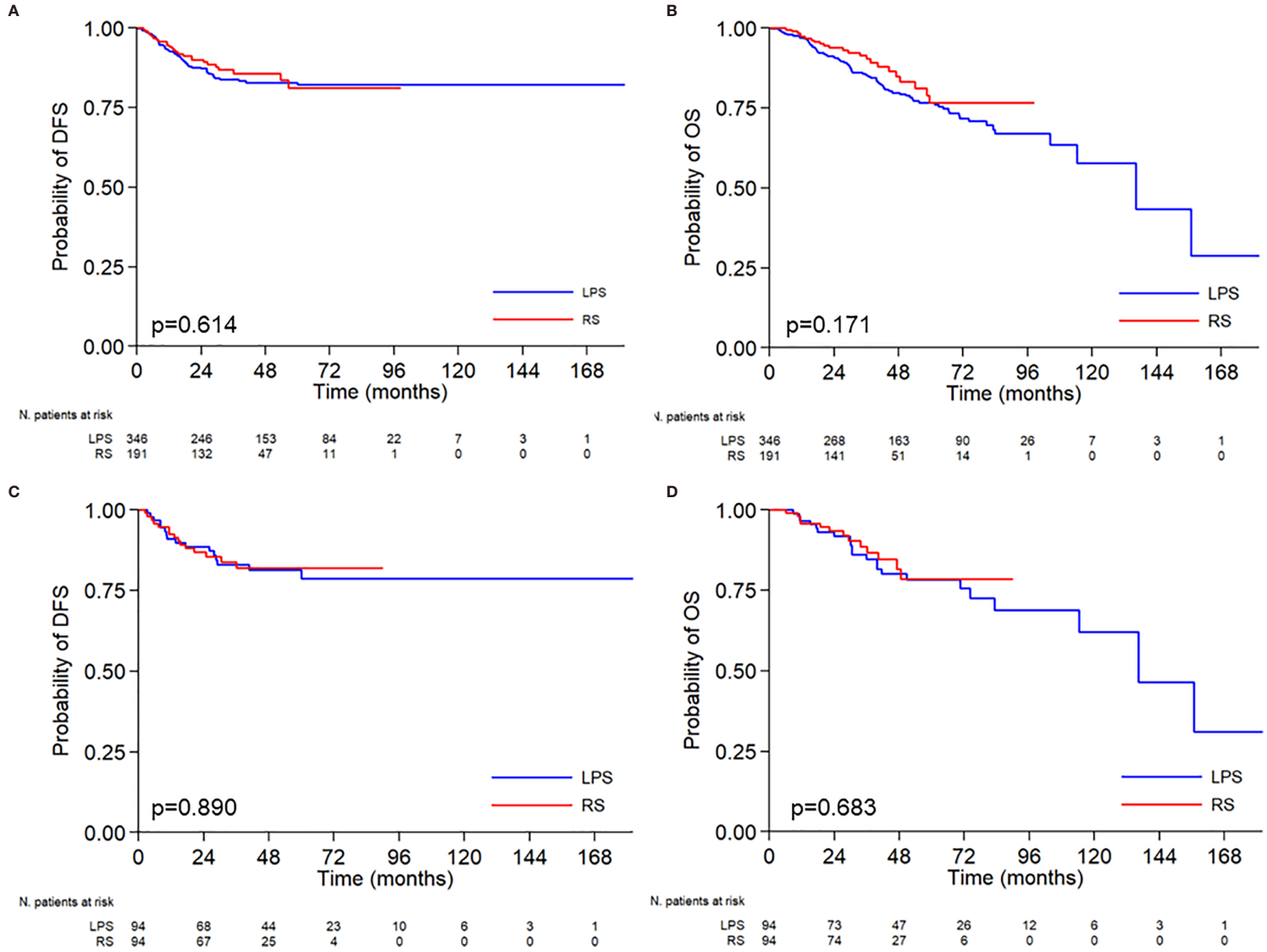

FIGURE 1 | Kaplan-Meier curves relative to disease free survival-DFS **(A–C)**, and overall survival-OS **(B–D)** according to the surgical approach. Median DFS: not reached *vs* not reached. Probability of DFS at 5 years 78.8% *vs* 81.9%. Median OS: 136.2 months *vs* not reached. Probability of OS at 5 years 78.2% *vs* 78.6%.

TABLE 5 | Univariable analysis of clinical, pathological and treatment characteristics of 188 matched patients with endometrial cancer according to DFS and OS.

Characteristic	Patient at risk	Disease free survival			Overall survival		
		N° events	HR (95% CI)	p value	N° events	HR (95% CI)	p value
Age	188	31	0.93 (0.83-1.04)	0.204	35	0.96 (0.87-1.05)	0.391
Age class							
70-74 years	105	20	1.00		20	1.00	
75-79 years	66	8	0.64 (0.28-1.46)	0.289	14	0.99 (0.49-2.02)	0.986
80-84 years	14	1	0.31 (0.04-2.29)	0.249	0	1.00 (empty class)	–
85+ years	3	2	3.3 (0.77-14.15)	0.107	1	1.12 (0.15-8.55)	0.909
BMI	188	31	1.02 (0.96-1.08)	0.498	35	1 (0.95-1.06)	0.942
Comorbidities							
0	24		1.00		5	1.00	
1	69		0.59 (0.21-1.61)	0.302	14	0.91 (0.32-2.55)	0.850
2	47		0.63 (0.21-1.88)	0.406	6	0.72 (0.22-2.38)	0.593
>2	46		0.70 (0.24-2.01)	0.505	10	1.13 (0.38-3.33)	0.823
Previous abdominal surgery							
No	139	23	1.00		28	1.00	
Yes	49	8	0.94 (0.42-2.09)	0.871	7	0.7 (0.3-1.62)	0.408
FIGO stage							
IA	83	7	1.00		10	1.00	
IB	69	11	2.02 (0.78-5.21)	0.147	14	1.81 (0.79-4.11)	0.158
II	10	4	5.28 (1.54-18.06)	**0.008**	3	2.21 (0.61-8.07)	0.229
IIIA	5	3	13.37 (3.45-51.85)	**<0.0001**	1	2.3 (0.29-18.11)	0.431
IIIB	2	2	29.06 (5.68-148.82)	**<0.0001**	1	7.67 (0.97-60.65)	0.053
IIIC	17	3	2.22 (0.57-8.59)	0.248	5	2.52 (0.86-7.4)	0.092
IVB	2	1	11.5 (1.38-95.54)	**0.024**	1	13.53 (1.63-112.51)	**0.016**
Histotype							
Endometrioid	161	25	1.00		22	1.00	
NEEC	27	6	1.54 (0.63-3.75)	0.343	13	3.56 (1.78-7.11)	**<0.0001**
Grading							
1	32	6	1.00		3	1.00	
2	97	10	0.48 (0.17-1.32)	0.156	12	1.12 (0.32-3.99)	0.859
3	59	15	1.34 (0.52-3.45)	0.547	20	3.08 (0.91-10.48)	0.071
Lymph node metastasis							
No	168	27	1.00		31	1.00	
Yes	20	4	1.28 (0.45-3.67)	0.643	4	1.18 (0.42-3.37)	0.754
Surgical approach							
LPS	94	16	1.00		22	1.00	
RS	94	15	0.95 (0.47-1.93)	0.890	13	0.86 (0.42-1.77)	0.683
Adjuvant therapy							
No	81	9	1.00		11	1.00	
Yes	107	22	2 (0.92-4.35)	0.080	24	1.79 (0.87-3.65)	0.111

Bold font highlights statistically significant difference. HR, Hazard Ratio; CI, Confidence Interval; BMI, Body Mass Index; NEEC, Not endometrioid endometrial cancer; LPS, Laparoscopic Surgery; RS, Robotic Surgery.

plays a major role in the selection of patients for the optimal management strategy in elderly endometrial cancer patients.

DATA AVAILABILITY STATEMENT

The raw data supporting the conclusions of this article will be made available by the authors, without undue reservation.

ETHICS STATEMENT

Ethical review and approval was not required for the study on human participants in accordance with the local legislation and institutional requirements. The patients/participants provided their written informed consent to participate in this study.

AUTHOR CONTRIBUTIONS

Conceived and designed the study: GC and VG. Collected the data: AP, LM, VC, FL, GH, MD'I, EF, CC, and VB. Data analysis: TP. Manuscript writing: CC and GC. Manuscript revision: VG. Supervision and validation: PI, EV, FF, SK, and GS. All authors contributed to the article and approved the submitted version.

SUPPLEMENTARY MATERIAL

The Supplementary Material for this article can be found online at: https://www.frontiersin.org/articles/10.3389/fonc.2021.724886/full#supplementary-material

Supplementary Figure 1 | Histograms of the distribution of the patients according to the age.

Supplementary Figure 2 | Histograms of the distribution of the patients according to body mass index (BMI).

REFERENCES

1. Siegel RL, Miller KD, Jemal A. Cancer Statistics, 2019. *CA Cancer J Clin* (2019) 69(1):7–34. doi: 10.3322/caac.21551
2. Bishop EA, Java JJ, Moore KN, Walker JL. Pathologic and Treatment Outcomes Among a Geriatric Population of Endometrial Cancer Patients: An NRG Oncology/ Gynecologic Oncology Group Ancillary Data Analysis of LAP2. *Int J Gynecol Cancer* (2017) 27(4):730–7. doi: 10.1097/IGC.0000000000000947
3. National Comprehensive Cancer Network guidelines. Available at: https://www.nccn.org/store/login/login.aspx?ReturnURL=https://www.nccn.org/professionals/physician_gls/pdf/uterine.pdf.
4. Koual M, Ngo C, Girault A, Lécuru F, Bats AS. Endometrial Cancer in the Elderly: Does Age Influence Surgical Treatments, Outcomes, and Prognosis? *Menopause* (2018) 25(9):968–76. doi: 10.1097/GME.0000000000001119
5. Lavoue V, Zeng X, Lau S, Press JZ, Abitbol J, Gotlieb R, et al. Impact of Robotics on the Outcome of Elderly Patients With Endometrial Cancer. *Gynecol Oncol* (2014) 133(3):556–62. doi: 10.1016/j.ygyno.2014.03.572
6. Uccella S, Bonzini M, Palomba S, Fanfani F, Malzoni M, Ceccaroni M, et al. Laparoscopic *vs.* Open Treatment of Endometrial Cancer in the Elderly and Very Elderly: An Age-Stratified Multicenter Study on 1606 Women. *Gynecol Oncol* (2016) 141(2):211–7. doi: 10.1016/j.ygyno.2016.02.029
7. Guy MS, Sheeder J, Behbakht K, Wright JD, Guntupalli SR. Comparative Outcomes in Older and Younger Women Undergoing Laparotomy or Robotic Surgical Staging for Endometrial Cancer. *Am J Obstet Gynecol* (2016) 214(3):350.e1–e10. doi: 10.1016/j.ajog.2015.09.085
8. Gallotta V, Conte C, D'Indinosante M, Federico A, Biscione A, Vizzielli G, et al. Robotic Surgery in Elderly and Very Elderly Gynecologic Cancer Patients. *J Minim Invasive Gynecol* (2018) 25(5):872–7. doi: 10.1016/j.jmig.2018.01.007
9. Lindfors A, Åkesson Å, Staf C, Sjöli P, Sundfeldt K, Dahm-Kähler P. Robotic *vs* Open Surgery for Endometrial Cancer in Elderly Patients: Surgical Outcome, Survival, and Cost Analysis. *Int J Gynecol Cancer* (2018) 28 (4):692–6994. doi: 10.1097/IGC.0000000000001240
10. Perrone AM, Di Marcoberardino B, Rossi M, Pozzati F, Pellegrini A, Procaccini M, et al. Laparoscopic *Versus* Laparotomic Approach to Endometrial Cancer. *Eur J Gynaecol Oncol* (2012) 33(4):376–81.
11. World Medical Association Inc. Declaration of Helsinki. Ethical Principles for Medical Research Involving Human Subjects. *J Indian Med Assoc* (2009) 107:403–5.
12. Vaknin Z, Perri T, Lau S, Deland C, Drummond N, Rosberger Z, et al. Outcome and Quality of Life in a Prospective Cohort of the First 100 Robotic Surgeries for Endometrial Cancer, With Focus on Elderly Patients. *Int J Gynecol Cancer* (2010) 20(8):1367–73.
13. National Cancer Institute, National Institutes of Health and US Department of Health and Human Services. *Common Terminology Criteria for Adverse Events (CTCAE). Version 5.0. Published November 27, 2017*. Available at: https://ctep.cancer.gov/protocoldevelopment/electronic_applications/docs/CTCAE_v5_Quick_Reference_8.5x11.pdf.
14. European Society of Gynaecological Oncology Guidelines. Available at: https://guidelines.esgo.org/uterine-cancer/guidelines/early-stage-algorithms/.
15. Harris PA, Taylor R, Thielke R, Payne J, Gonzalez N, Conde JG. Research Electronic Data Capture (REDCap) – A Metadata-Driven Methodology and Workflow Process for Providing Translational Research Informatics Support. *J BioMed Inform* (2009) 42(2):377–81. doi: 10.1016/j.jbi.2008.08.010
16. Harris PA, Taylor R, Minor BL, Elliot V, Fernandez M, O'Neal L, et al. REDCap Consortium, The REDCap Consortium: Building an International Community of Software Partners. *J BioMed Inform* (2019). doi: 10.1016/j.jbi.2019.103208
17. Pecorelli S. Revised FIGO Staging for Carcinoma of the Vulva, Cervix, and Endometrium. *Int J Gynaecol Obstet* (2009) 105(2):103–4. doi: 10.1016/j.ijgo.2009.02.012
18. Stuart EA. Matching Methods for Causal Inference: A Review and a Look Forward. *Stat Sci* (2010) 25:1–21. doi: 10.1214/09-STS313
19. Heinze G, Juni P. An Overview of the Objectives of and the Approaches to Propensity Score Analyses. *Eur Heart J* (2011) 32:1704–8. doi: 10.1093/eurheartj/ehr031
20. Austin PC. An Introduction to Propensity Score Methods for Reducing the Effects of Confounding in Observational Studies. *Multivariate Behav Res* (2011) 46:399–424. doi: 10.1080/00273171.2011.568786
21. Austin PC. Balance Diagnostics for Comparing the Distribution of Baseline Covariates Between Treatment Groups in Propensity-Score Matched Samples. *Stat Med* (2009) 28:3083–107. doi: 10.1002/sim.3697
22. Schemper M, Smith TL. A Note on Quantifying Follow-Up in Studies of Failure Time. *Control Clin Trials* (1996) 17:343–6. doi: 10.1016/0197-2456(96)00075-X
23. Kaplan EL, Meier P. Nonparametric Estimation From Incomplete Observation. *J Am Stat Assoc* (1958) 53:457–81. doi: 10.1080/01621459.1958.10501452
24. Mantel N. Evaluation of Survival Data and Two New Rank Order Statistics Arising in its Consideration. *Cancer Chem Rep* (1966) 50:163–70.
25. Cox DR. Regression Models and Life Tables. *J R Stat Soc B* (1972) 34:187–220. doi: 10.1111/j.2517-6161.1972.tb00899.x
26. Grieco DL, Anzellotti GM, Russo A, Bongiovanni F, Costantini B, D'Indinosante M, et al. Airway Closure During Surgical Pneumoperitoneum in Obese Patients. *Anesthesiology*. (2019) 131(1):58–73. doi: 10.1097/ALN.0000000000002662
27. Colloca G, Corsonello A, Marzetti E, Balducci L, Landi F, Extermann M, et al. Treating Cancer in Older and Oldest Old Patients. *Curr Pharm Des* (2015) 21 (13):1699–705. doi: 10.2174/1381612821666150130122536
28. Aloisi A, Tseng J, Kuhn T, Feinberg J, Chi DS, Brown CL, Mueller JJ, et al. Robotic Surgery in the Frail Elderly: Analysis of Perioperative Outcomes. *Ann Surg Oncol* (2020) 27(10):3772–80. doi: 10.1245/s10434-020-08475-w
29. Madden N, Frey MK, Joo L, Lee J, Musselman K, CHern JY, et al. Safety of Robotic-Assisted Gynecologic Surgery and Early Hospital Discharge in Elderly Patients. *Am J Obstet Gynecol* (2019) 220(3):253.e1–7. doi: 10.1016/j.ajog.2018.12.014
30. Bishop EA, Java JJ, Moore KN, Spirtos NM, Pearl ML, Zivanovic O, et al. Surgical Outcomes Among Elderly Women With Endometrial Cancer Treated by Laparoscopic Hysterectomy: A NRG/Gynecologic Oncology Group Study. *Am J Obstet Gynecol* (2018) 218(1):109.e1–e11. doi: 10.1016/j.ajog.2017.09.026
31. Bourgin C, Lambaudie E, Houvenaeghel G, Foucher F, Leveque J, Lavoue V. Impact of Age on Surgical Staging and Approaches (Laparotomy, Laparoscopy and Robotic Surgery) in Endometrial Cancer Management. *Eur J Surg Oncol* (2017) 43:703e709. doi: 10.1016/j.ejso.2016.10.022
32. de'Angelis N, Abdalla S, Bianchi G, Memeo R, Charpy C, Petrucciani N, et al. Robotic *Versus* Laparoscopic Colorectal Cancer Surgery in Elderly Patients: A Propensity Score Match Analysis. *J Laparoendosc Adv Surg Tech A* (2018) 28 (11):1334–45. doi: 10.1089/lap.2018.0115
33. Lowe MP, Kumar S, Johnson PR, Kamelle SA, Chamberlain DH, Tillmanns TD. Robotic Surgical Management of Endometrial Cancer in Octogenarians and Nonagenarians: Analysis of Perioperative Outcomes and Review of the Literature. *J Robotic Surg* (2010) 4:109–15. doi: 10.1007/s11701-010-0195-x
34. Walker JL, Piedmonte MR, Spirtos NM, Eisenkop SM, Schlaerth JB, Mannel RS, et al. Laparoscopy Compared With Laparotomy for Comprehensive Surgical Staging of Uterine Cancer: Gynecologic Oncology Group Study Lap2. *J Clin Oncol* (2009) 27:5331–6. doi: 10.1200/JCO.2009.22.3248
35. Charlson ME, Pompei P, Ales KL, MacKenzie CR. A New Method of Classifying Prognostic Comorbidity in Longitudinal Studies: Development and Validation. *J Chronic Dis* (1987) 40:373–83. doi: 10.1016/0021-9681(87)90171-8

Conflict of Interest: The authors declare that the research was conducted in the absence of any commercial or financial relationships that could be construed as a potential conflict of interest.

frontiers in Surgery

SYSTEMATIC REVIEW
published: 30 September 2021
doi: 10.3389/fsurg.2021.738421

Comparison of Retzius-Sparing Robot-Assisted Radical Prostatectomy vs. Conventional Robot-Assisted Radical Prostatectomy: An Up-to-Date Meta-Analysis

Jiang-Nan Xu[1†], *Zhen-Yu Xu*[2†] *and Hu-Ming Yin*[1*]

[1] *Department of Urology, The First Affiliated Hospital of Soochow University, Suzhou, China,* [2] *Department of Urology, Kunshan Chinese Medicine Hospital Affiliated to Nanjing University of Chinese Medicine, Suzhou, China*

OPEN ACCESS

Edited by:
Patrick J. Schuler, Ulm University Medical Center, Germany

Reviewed by:
Clemens Mathias Rosenbaum, Asklepios Klinik Barmbek, Germany
Xuefeng Qiu, Nanjing Drum Tower Hospital, China

****Correspondence:***
Hu-Ming Yin
1163051167@qq.com

†These authors have contributed equally to this work and share first authorship

Specialty section:
This article was submitted to Surgical Oncology, a section of the journal Frontiers in Surgery

Received: *08 July 2021*
Accepted: *26 August 2021*
Published: *30 September 2021*

Citation:
Xu J-N, Xu Z-Y and Yin H-M (2021) Comparison of Retzius-Sparing Robot-Assisted Radical Prostatectomy vs. Conventional Robot-Assisted Radical Prostatectomy: An Up-to-Date Meta-Analysis. Front. Surg. 8:738421. doi: 10.3389/fsurg.2021.738421

Background: The Retzius space-sparing robot-assisted radical prostatectomy (RS-RARP) has shown better results in urinary continence, but its efficacy and safety compared to conventional robot-assisted radical prostatectomy (c-RARP) remain controversial.

Material and Methods: A research was conducted in Medline *via* PubMed, Cochrane Library, EMBASE, and Web of Science up to January 4, 2021, to identify studies comparing RS-RARP to c-RARP. We used RevMan 5.3 and STATA 14.0 for meta-analysis.

Results: A total of 14 studies involving 3,129 participants were included. Meta-analysis showed no significant difference in positive surgical margins (PSMs), but the RS-RARP group had significantly higher PSM rates in the anterior site [odds ratio (OR) = 2.25, 95% CI: 1.22–4.16, $P = 0.01$]. Postoperative continence in RS-RARP group at 1 month (OR = 5.72, 95% CI: 3.56–9.19, $P < 0.01$), 3 months (OR = 6.44, 95% CI: 4.50–9.22, $P < 0.01$), 6 months (OR = 8.68, 95% CI: 4.01–18.82, $P < 0.01$), and 12 months (OR = 2.37, 95% CI: 1.20–4.70, $P = 0.01$) was significantly better than that in the c-RARP group. In addition, the RS-RARP group had a shorter console time (mean difference = −16.28, 95% CI: −27.04 to −5.53, $P = 0.003$) and a lower incidence of hernia (OR = 0.35, 95% CI: 0.19–0.67, $P = 0.001$). However, there were no significant differences in estimated blood loss, pelvic lymph node dissection rate, postoperative complications, 1-year-biochemical recurrence rate, and postoperative sexual function.

Conclusions: Compared with c-RARP, RS-RARP showed better recovery of continence, shorter console time, and lower incidence of hernia. Although there was no significant difference in overall PSM, we suggest that the surgeon should be more careful if the lesion is in the anterior prostate.

Keywords: prostate cancer, Retzius sparing, robot-assisted radical prostatectomy, urinary continence, systematic review and meta-analysis

INTRODUCTION

Prostate cancer is the most common malignant tumor in men. The American Cancer Society estimates that there will be 1,919,930 new cases of prostate cancer and 33,330 cancer-related deaths in 2020 (1). In patients with clinically localized prostate cancer, treatment is determined based on risk stratification and life expectancy, including active surveillance, radical prostatectomy, whole gland ablation, and external beam radiation therapy (2). Radical prostatectomy plays an important role in reducing mortality and increasing longevity in patients with clinically localized prostate cancer (3).

In recent years, robot-assisted radical prostatectomy (RARP) has been widely used because of its fine operation in the limited retropubic space. Conventional RARP (c-RARP) was first introduced by Abbou (4) and modified by Menon (5), which is characterized by dissecting the Retzius space to incise and mobilize the bladder and prostate. Despite the good operational advantages of c-RARP, there are some possible adverse consequences, such as urinary incontinence and erectile dysfunction. Among them, urinary incontinence is one of the most serious complications after c-RARP. More than 50% of patients suffer from urinary incontinence at 1 month following radical prostatectomy, which seriously affects the postoperative quality of life (6). With a growing understanding of the anatomy of the prostate and its surrounding structures, many surgical modifications have been proposed in an attempt to improve postoperative functional outcomes while ensuring satisfactory oncological outcomes (7).

Galfano et al. (8) first reported in 2010 that Retzius space-sparing (RS) during RARP was effective in achieving good urinary continence rates. In their subsequent prospective, uncontrolled case series, more than 90% of the 200 patients treated with Retzius space-sparing robot-assisted radical prostatectomy (RS-RARP) achieved immediate continence (9). This surgical approach is characterized by passing through the rectovesical pouch instead of the Retzius space, thus preserving the arcus tendinous, endopelvic fascia, neurovascular bundle, puboprostatic ligament, and deep dorsal vein plexus, which are key structures for maintaining normal urinary continence (10). The efficacy of RS-RARP in urinary continence was also verified in several subsequent studies (11–17).

Despite the better outcomes in urinary continence, several studies have shown that RS-RARP has a higher positive rate of a surgical margin than c-RARP (11–13, 15, 17). However, a recent meta-analysis found the opposite (18). Due to the small sample size of the previous studies and the few references included in the previous meta-analyses, the safety and efficacy of RS-RARP compared with c-RARP are not clear at present. Several new studies have been published in 2020, which may yield new results and new outcome indicators (19–24). Our study aims to systematically compare the clinical, oncological, and functional outcomes of RS-RARP and c-RARP through meta-analysis, to obtain reliable results and provide a basis for future studies and clinical guidance.

METHODS

Search Strategy

Two researchers independently conducted systematic retrieval of PubMed, EMBASE, Cochrane, and Web of Science, and the retrieval time was up to January 4, 2021. The search terms used include ("Retzius" OR "Bocciardi") and ("robot" OR "robotic") and "prostate." We also browsed references of key articles and manually searched the gray literature to make sure no relevant articles were omitted. Our research was conducted according to the preferred reporting items for systematic reviews and meta-analyses (PRISMA) (25).

Inclusion and Exclusion Criteria

Inclusion criteria were the following: (a) the subjects were patients with clinically localized prostate cancer; (b) the types of studies were randomized controlled trials (RCTs) or observational controlled studies; (c) studies that involved the comparison of RS-RARP and c-RARP; (d) include at least one of the following outcomes: console time, estimated blood loss, pelvic lymph node dissection (PLND), positive surgical margins, location of positive margins, postoperative continence, complications, hernia, and 1-year-biochemical recurrence rate.

Exclusion criteria were the following: (a) the study was designed as a single-arm trial without a control group; (b) there were no relevant outcome indicators; (c) conference abstracts, case reports, comments, and republished literature; (d) insufficient data or unable to obtain the required data.

Selection Process and Data Abstraction

The two authors first scanned the titles and abstracts for preliminary screening of all relevant literature. Works of literature that initially meet the inclusion and exclusion criteria or that are controversial will be directly included in the full-text assessment to make sure that all relevant studies are not missed. At the full-text evaluation stage, disputes are negotiated by two authors, and if an agreement cannot be reached, a third author is consulted.

The authors used a predesigned data extraction table to independently extract baseline data and data required for meta-analysis. Baseline data included the following: first author and year of publication, country, study type, mean age, the number of cases, follow-up, outcomes, and quality scores. Outcome indicators included in our study are as follows: console time, estimated blood loss, PLND, positive surgical margins, location of positive margins, postoperative continence, complications, hernia, 1-year-biochemical recurrence rate, and sexual function.

Literature Quality and Risk of Bias Assessment

To assess literature quality and risk of bias, we evaluated RCTs using the Jadad score (26) and evaluated observational controlled studies using the Newcastle–Ottawa Scale (NOS) (27). In this study, RCTs with a Jadad score of $\geq$4 were considered to be of high quality, and observational studies with a NOS score of $\geq$7 were also considered of high quality (26, 27).

Statistical Analysis

All statistical analyses in our study were performed using RevMan 5.3 (China Cochrane Centre, China; 2014) and Stata (StataCorp, College Station, TX, USA) software, and the significance level was $P < 0.05$. We estimated the effect size of continuous variables by the mean difference (MD) and its 95% CI and estimated the effect size of binary variables by the odds ratio (OR) of the calculated results and its 95% CI. We used inconsistencies (I^2) statistics to assess heterogeneity. If $I^2 > 50\%$, the heterogeneity is very significant and the random-effects model should be adopted. If $I^2 < 50\%$, it indicates that the heterogeneity is acceptable, and a fixed-effect model should be adopted. Subgroup analysis was conducted according to study type and population.

Sensitivity Analysis and Publication Bias

Sensitivity analysis was conducted by eliminating each literature article one by one, we calculated the change of I^2 through RevMan 5.3 (China Cochrane Centre, China; 2014) and obtained the forest plot of sensitivity analysis through Stata 14. After discovering the source of heterogeneity, we will make a detailed

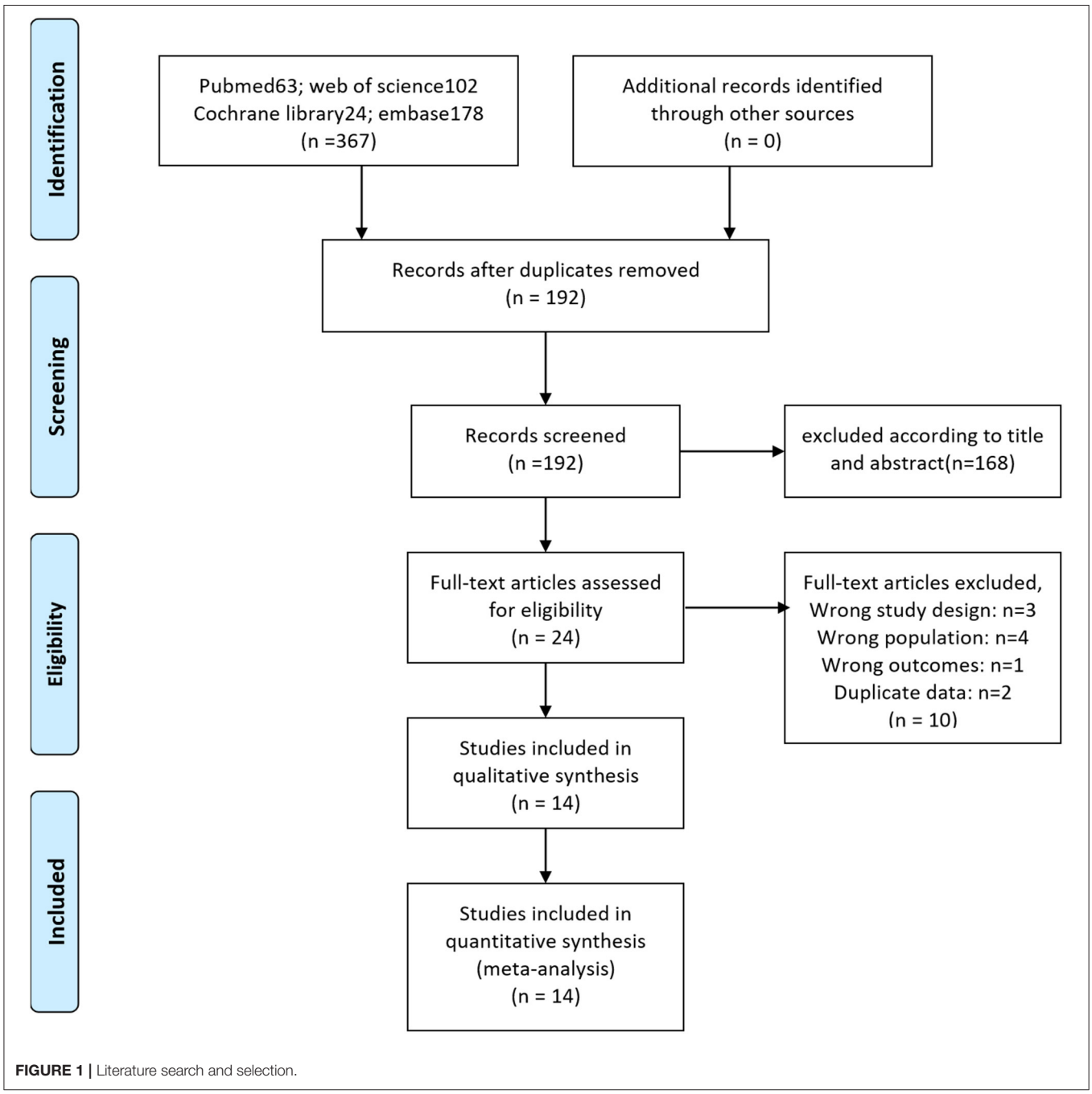

FIGURE 1 | Literature search and selection.

TABLE 1 | Literature basic information and literature quality evaluation results.

Study	Country	Study type	Mean age		Sample size		Follow-up	Outcomes	Quality scores	
			RS	Non-RS	RS	Non-RS		(mon)	Jadad	NOS
Lim (17)	Korea	PPSM	65.7	66.2	50	50	6	ABCDEF	NA	9
Chang (28)	Korea	CS	65.0	65.0	298	541	24	G	NA	8
Dalela (16) Menon (12)	USA	RCT	61.0	61.5	60	60	12	ACDEFH	4	NA
Sayyid (15)	USA	PS	61.0	62.0	100	100	12	ACDEF	NA	8
Chang (14)	China	PPSM	64.4	67.5	30	30	12	BDEH	NA	9
Eden (13)	UK	PS	63.0	65.0	40	40	3	BDEFI	NA	7
Asimakopoulos (11)	Italy	RCT	66.0	65.0	39	40	6	CDEF	4	NA
Egan (24) Kowalczyk (23)	USA	PS	62.1	61.9	70	70	12	ABDEFGH	NA	9
Lee (22)	Korea	PPSM	65.0	66.0	609	609	6	BDEFI	NA	8
Liao (21)	China	RC	64.8	65.6	41	92	12	BDEH	NA	7
Ota (20)	Japan	RC	67.0	69	25	25	12	ABDEFG	NA	8
Qiu (19)	China	RCT	68.0	67.0	55	55	12	ABCDEF	4	NA

A: console time; B: estimated blood loss; C: pelvic lymph node dissection; D: positive surgical margins; E: postoperative continence; F: complications; G: hernia; H: 1-year-biochemical recurrence rate; I: Sexual function RS: Retzius-sparing; PPSM: Prospective propensity score matching; CS: case-control; RCT: Randomized controlled trial; PS: Prospective study; RC: Retrospective cohort.

analysis of the target literature to find out the intrinsic reasons for it to be the source of heterogeneity.

Publication bias was assessed quantitatively by Egger's test. When the *p*-value *is* > 0.05, it means there is no significant publication bias. If $P < 0.05$, it indicated the existence of publication bias. In this case, the rim and fill method will be used to assess the impact of publication bias on our results. If publication bias is found to have a significant effect on results, we will discuss it in our discussion.

RESULTS

Literature Retrieval Results and Basic Characteristics

We searched the literature, carefully scanned and screened them, and the specific process is shown in **Figure 1**. According to the established retrieval formula, we searched a total of 367 related studies, deleted duplicates, and made preliminary screening according to titles and abstracts, and the remaining 24 pieces of literature entered the full-text reading stage. After reading through the full text of 24 articles, a total of 14 studies including 3,129 participants were finally included in our meta-analysis (11–17, 19–24, 28). Of the 14 studies, four were RCTs (11, 12, 16, 20) and the rest were observational controlled studies (13–15, 17, 19, 21–24, 28). Among them, Dalela (16) and Menon (12) were from the same randomized controlled study, and Egan (24) and Kowalczyk (23) were from the same prospective cohort study. The baseline data of the studies included in our meta-analysis are shown in **Table 1**.

Methodological Quality Assessment

We evaluated RCTs using the Jadad score (26) and evaluated observational controlled studies using the NOS (27). After detailed evaluation according to the scoring protocol, we found that all RCTs had a Jadad score greater than or equal to 4, and all observational studies had a NOS score greater than or equal to 7, indicating that all included studies had good methodological quality (**Table 1**).

Meta-Analysis Results

Console Time

Five studies (12, 15, 17, 19, 24) reported the difference in console time between RS-RARP and c-RARP. Due to the high heterogeneity ($I^2 = 93\%$), the meta-analysis results using the random-effects model showed that the console time of RS-RARP was significantly shorter than that of c-RARP (MD $= -16.28$, 95% CI: -27.04 to -5.53, $P = 0.003$) (**Figure 2**).

Estimated Blood Loss

Eight studies (13, 14, 17, 19–22, 24) reported the difference in estimated blood loss between RS-RARP and c-RARP. Due to the high heterogeneity ($I^2 = 85\%$), the meta-analysis results using the random-effects model showed that there was no significant difference in estimated blood loss between RS-RARP and c-RARP (MD $= -14.27$, 95% CI: -72.89 to 44.36, $P = 0.63$) (**Figure 3**).

Pelvic Lymph Node Dissection

Five studies (11, 12, 15, 17, 19), including 609 participants, reported PLND rate. Meta-analysis using a fixed-effects model showed that there was no significant difference in PLND rate between the RS-RARP group and the c-RARP group (OR $= 0.7$, 95% CI: 0.47–1.04, $P = 0.08$). $I^2 = 34\%$, the heterogeneity was in the acceptable range (**Figure 4**).

Positive Surgical Margins

PSM data were reported in 11 studies (11–15, 17, 19–22, 24) involving a total of 2,290 participants. Our meta-analysis showed

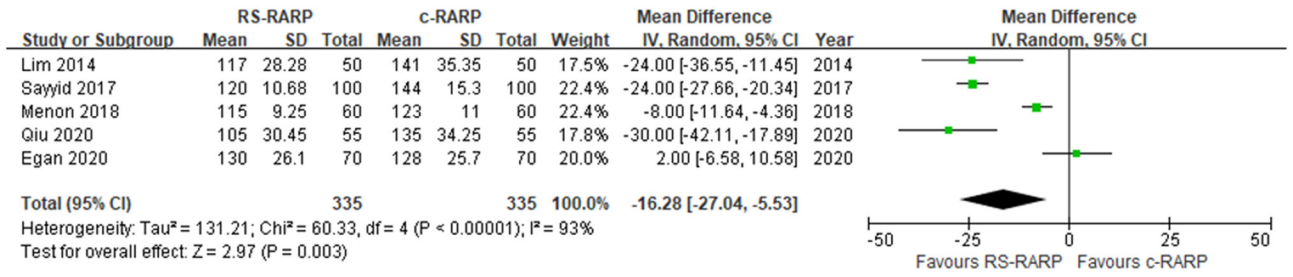

FIGURE 2 | Forest plot of console time.

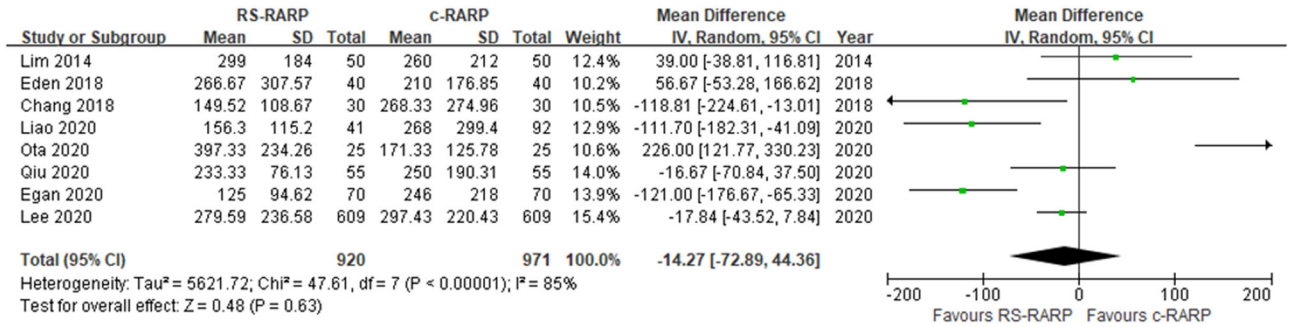

FIGURE 3 | Forest plot of estimated blood loss.

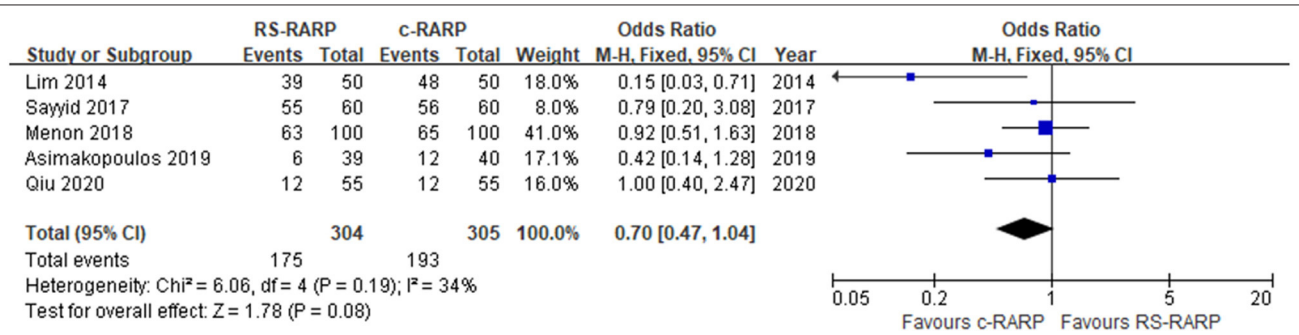

FIGURE 4 | Forest plot of pelvic lymph node dissection (PLND).

that there was no significant difference in PSM rates between RS-RARP and c-RARP (OR = 1.16, 95% CI: 0.95–1.42, $P = 0.16$). $I^2 = 0$, no obvious heterogeneity was observed. In the subgroup based on pathological stage, we found that no matter if pathological stage ≤ pT2 (OR = 1.08, 95% CI: 0.78–1.51, $P = 0.63$) or > pT2 (OR = 1.22, 95% CI: 0.90–1.67, $P = 0.20$), there was no significant difference in PSM rates between the two surgical methods (**Figure 5**).

We also conducted in-depth analysis according to the location of positive margins. Six studies (12, 13, 15, 17, 19, 24) reported data on the location of positive surgical margins, and we found that compared with c-RARP, RS-RARP had significantly higher PSM rates in the anterior site (OR = 2.25, 95% CI: 1.22–4.16, $P = 0.01$). In the other three sites, including apex (OR = 1.30, 95% CI: 0.76–2.22, $P = 0.34$), base (OR = 1.39, 95% CI: 0.55–3.54, $P = 0.48$), and posterior (OR = 1.37, 95% CI: 0.79–2.40, $P = 0.26$), there was no significant difference in PSM rates between the two surgical methods (**Figure 6**).

Postoperative Continence

Ten studies (11, 13–17, 19–22) reported data on early urine continence (≤1 month), and the random-effects model results showed that RS-RARP was significantly better than c-RARP in early urine continence (OR = 5.72, 95% CI: 3.56–9.19, $P < 0.001$, $I^2 = 68\%$) (**Figure 7**).

Seven studies (11, 14–16, 20–22) reported data on 3-month continence, and the results of the fixed-effect model showed that RS-RARP was significantly better than c-RARP in 3-month

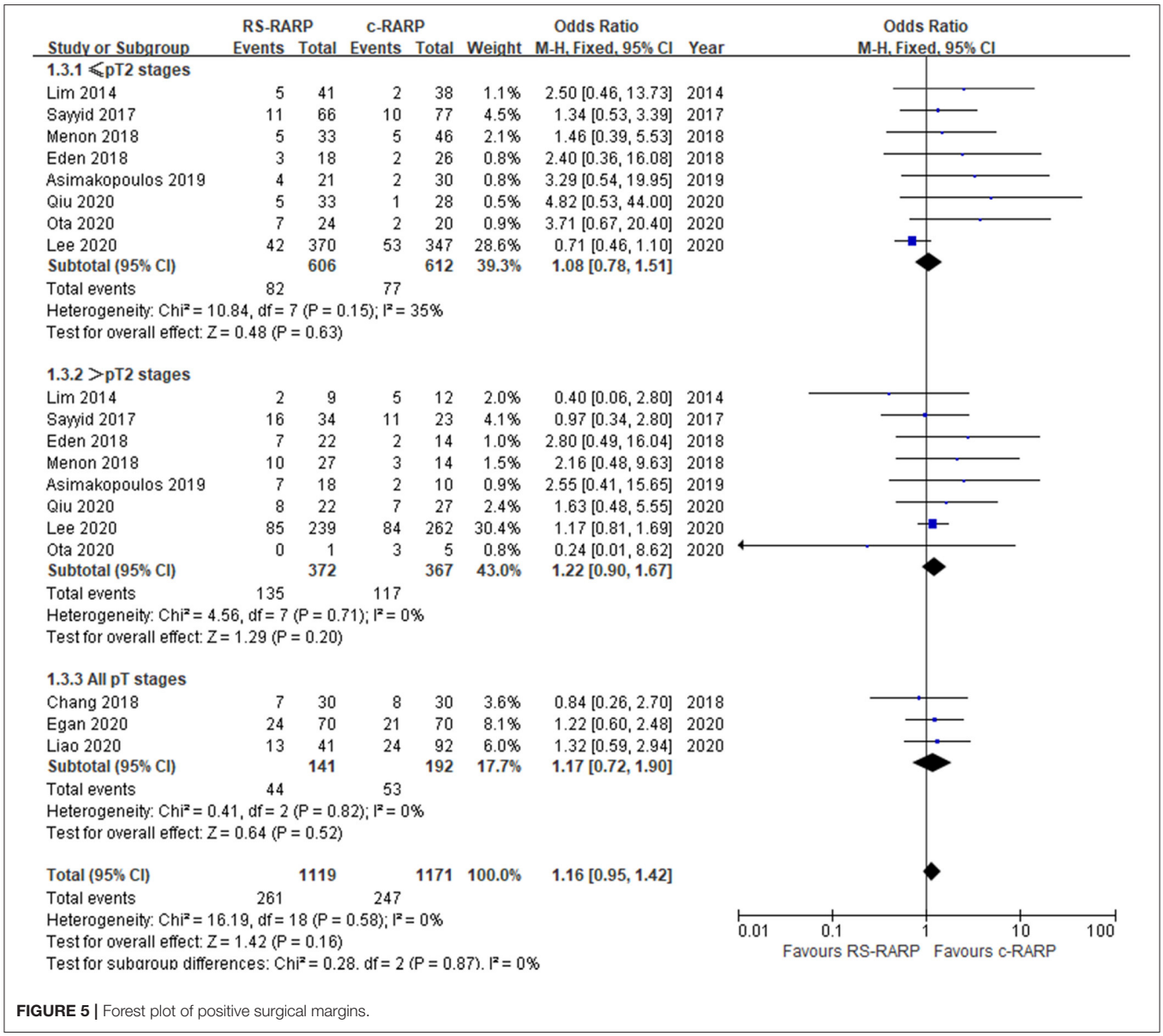

FIGURE 5 | Forest plot of positive surgical margins.

continence (OR = 6.44, 95% CI: 4.50–9.22, $P < 0.001$, $I^2 = 18\%$) (**Figure 7**).

Seven studies (11, 12, 14, 15, 20–22) reported data on 6-month continence, and the random-effect model results showed that RS-RARP was significantly better than c-RARP in 6-month continence (OR = 8.68, 95% CI: 4.01–18.82, $P < 0.001$, $I^2 = 52\%$) (**Figure 7**).

Six studies (12, 14, 15, 20, 21, 24) reported data on 12-month continence, and the fixed-effects model results showed that RS-RARP was significantly better than c-RARP in 12-month continence (OR = 2.37, 95% CI: 1.20–4.07, $P = 0.01$, $I^2 = 0\%$) (**Figure 7**).

Complications and Hernia

A total of nine studies (11–13, 15, 17, 19, 20, 22, 24) reported postoperative complications, and three studies (20, 23, 28) reported postoperative hernia incidence. Results of the meta-analysis showed that although there was no significant difference in postoperative complications between the two surgical procedures (OR = 0.88, 95% CI: 0.59–1.32, $P = 0.54$, $I^2 = 16\%$) (**Figure 8**), the incidence of postoperative hernia in the RS-RARP group was significantly lower than that in the c-RARP group (OR = 0.35, 95% CI: 0.19–0.67, $P = 0.001$, $I^2 = 14\%$) (**Figure 9**).

1-Year-Biochemical Recurrence Rate

Biochemical recurrence data were reported in four studies (12, 21, 24, 28), and meta-analysis using a random-effects model showed no significant difference in the rate of 1-year-biochemical recurrence between the two surgical procedures (OR = 0.87, 95% CI: 0.35–2.18, $P = 0.77$, $I^2 = 69\%$) (**Figure 10**).

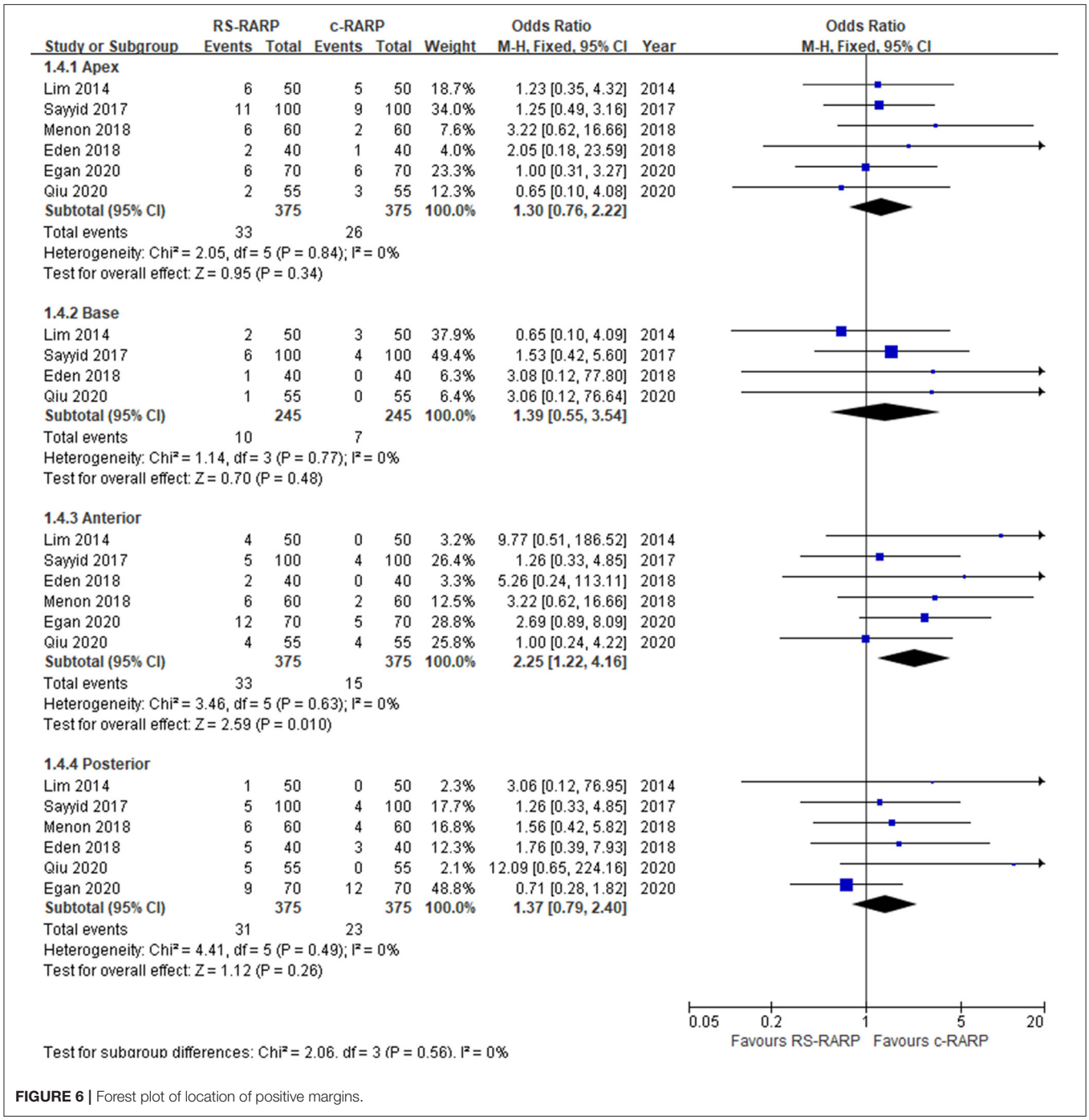

FIGURE 6 | Forest plot of location of positive margins.

Postoperative Sexual Function

The study of Egan et al. (24) [expanded prostate cancer index composite for clinical practice (EPIC-CP) sexual function scores: 4.6 ± 3.4 vs. 5.3 ± 2.6; $P = 0.417$] and Lee et al. (22) [international index of erectile function-5 scores (IIEF-5) score: 13 ± 7.2 vs. 13 ± 7.4; $P = 0.9$] showed no significant difference in postoperative sexual function between the two surgical methods.

Subgroup Analysis

We performed the subgroup analyses of functional and oncological outcomes by study type and population. As shown in **Table 2**, the results of the observational study subgroup were consistent with the overall results of our meta-analysis, while in the RCT subgroup, the RS-RARP group seemed to have a higher margin positive rate and biochemical recurrence rate than the c-RARP group. In population-based subgroup analysis, we found

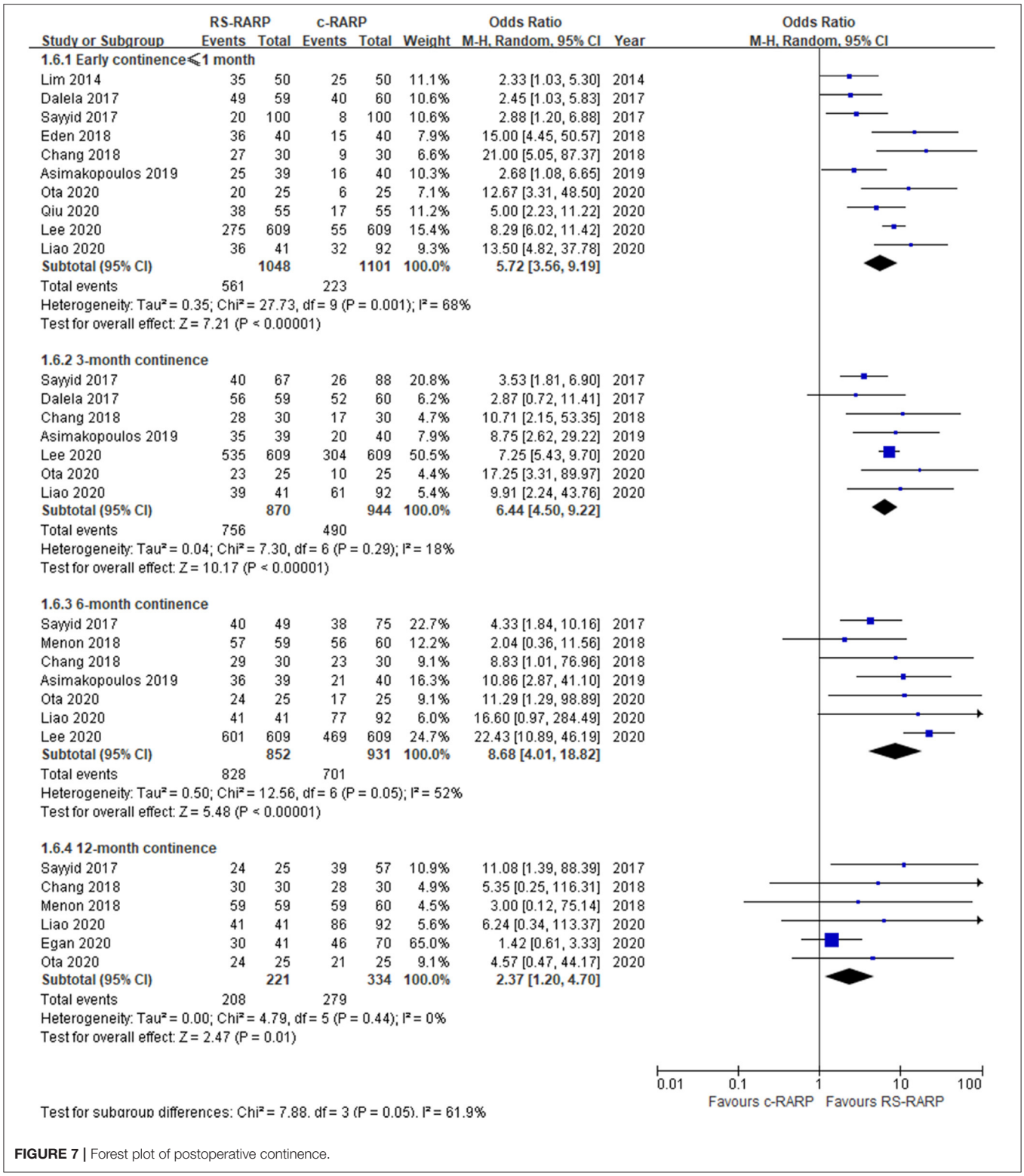

FIGURE 7 | Forest plot of postoperative continence.

that the advantage of RS-RARP in urine continence appeared to be more pronounced in the Asian population. In addition, in the western population subgroup, the positive rate of surgical margin in the RS-RARP group still seemed to be higher than that in the C-RARP group. Specific subgroup analysis results are shown in **Table 2**.

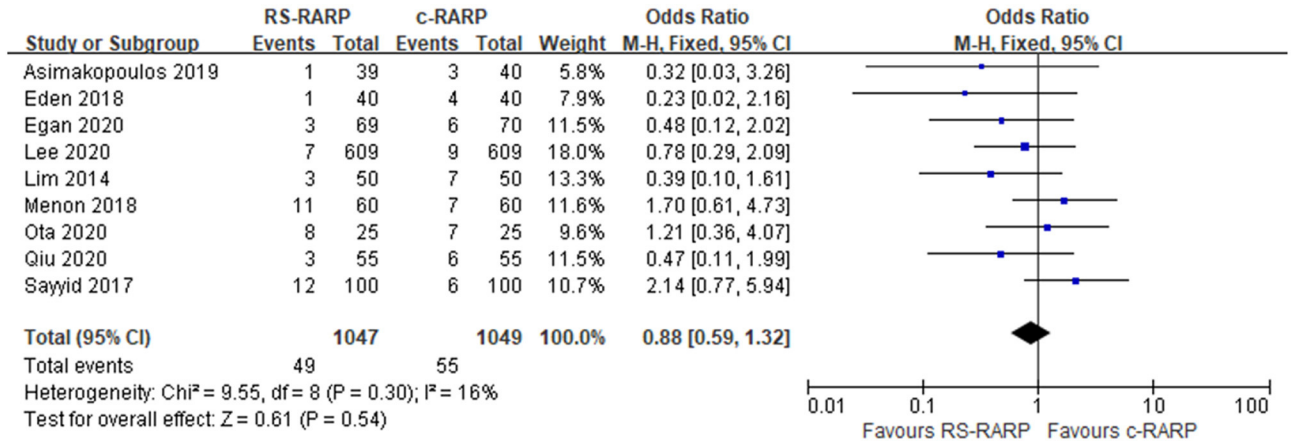

FIGURE 8 | Forest plot of complications.

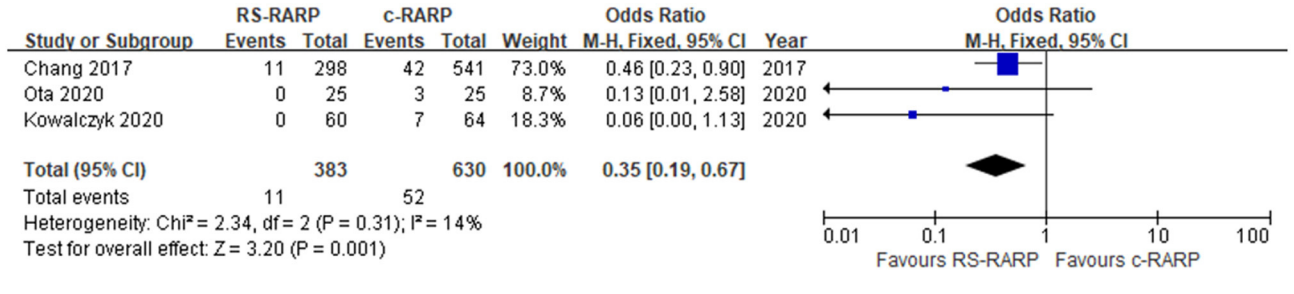

FIGURE 9 | Forest plot of hernia.

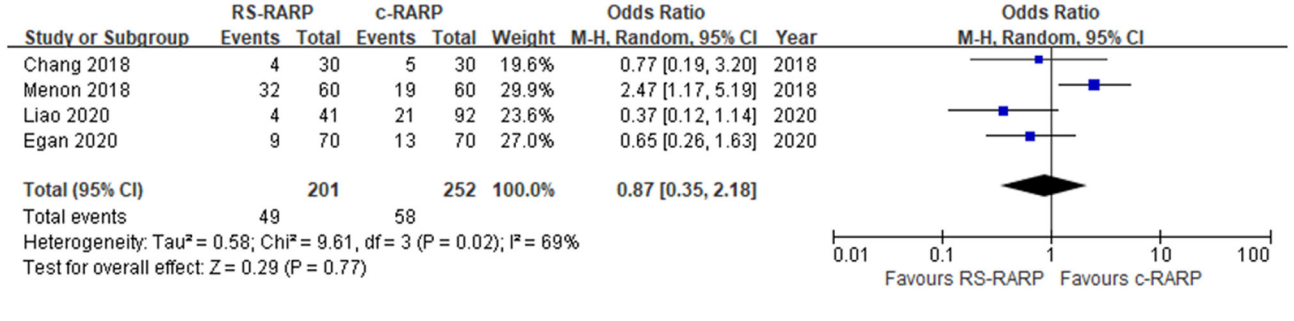

FIGURE 10 | Forest plot and of 1-year-biochemical recurrence rate.

Sensitivity Analysis

In the meta-analysis of console time, blood loss, early continence, 6-month continence, and 1-year-biochemical recurrence rate, we found significant heterogeneity (93, 85, 68, 52, and 69%, respectively). We performed a sensitivity analysis using the Stata software and produced forest plots after each study was sequentially removed. As shown in **Figure 11**, we found that in the outcome index group of console time, Sayyid (15) and Egan (24) may be sources of heterogeneity. In the remaining four outcome indicator groups, the combined effect value after each study was successively removed and was between the two reference lines. At the same time, when we changed the random-effects model to the fixed-effects model, the results of the meta-analysis did not significantly change. It can be seen that in the remaining four outcome indicator groups, although heterogeneity existed and sensitivity analysis did not find a clear source of heterogeneity, it did not bring significant bias to our results, and our results were still stable.

Publication Bias

We quantitatively evaluated publication bias by Egger's test, and the results showed that no obvious publication bias was found

TABLE 2 | Subgroup analysis.

Subgroup analysis	Positive surgical margins (≤pT2)	Positive surgical margins (>pT2)	Positive surgical margins (All)	Early-continence (≤1month)	12-month continence	1-year-biochemical recurrence rate
Study type						
RCT	2.42 [0.95, 6.16]	1.97 [0.86, 4.55]	2.16 [1.16, 4.02]	3.29 [2.00, 5.40]	3.00 [0.12, 75.14]	2.47 [1.17, 5.19]
Observational	0.96 [0.67, 1.37]	1.17 [0.83, 1.64]	1.17 [0.72, 1.90]	7.50 [4.21, 13.38]	2.91 [1.19, 7.11]	0.56 [0.29, 1.06]
Population						
Asian	0.98 [0.69, 1.41]	1.14 [0.81, 1.61]	1.05 [0.83, 1.34]	7.41 [4.26, 12.89]	5.19 [1.11, 24.36]	0.49 [0.20, 1.19]
western	2.06 [0.82, 5.18]	1.64 [0.82, 3.29]	1.50 [1.01, 2.23]	3.73 [1.83, 7.61]	2.82 [0.69, 11.49]	1.30 [0.35, 4.82]

RCT, Randomized controlled trial.

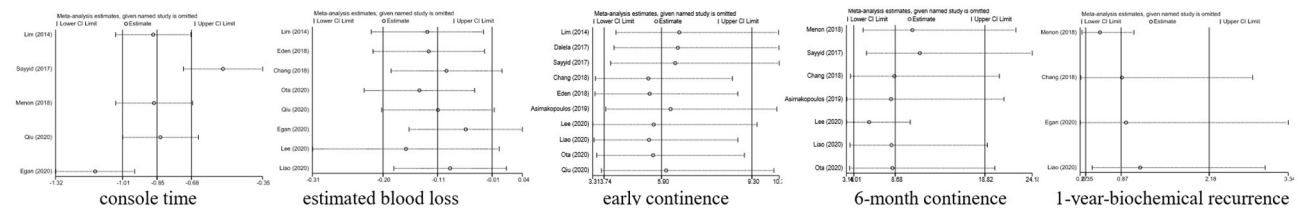

FIGURE 11 | Sensitivity analysis.

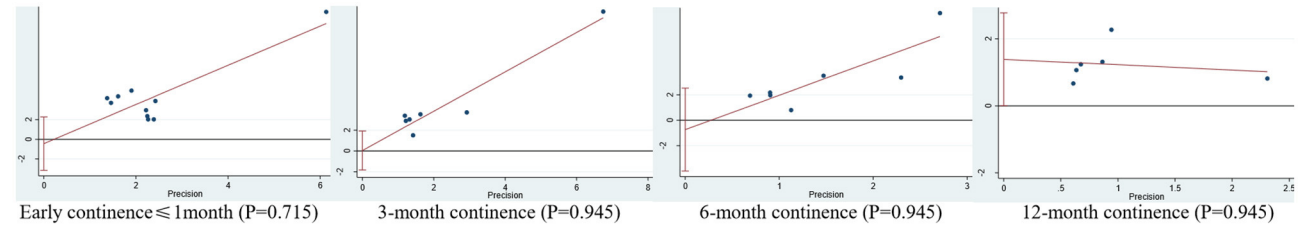

FIGURE 12 | Publication bias.

in all the outcome indicator groups. We showed the Egger graph and the *p*-value of some major outcome indicators in **Figure 12**.

DISCUSSION

To our knowledge, our meta-analysis is the most up-to-date and comprehensive. Due to the inclusion of several recent high-quality works of literature (19–24), we have obtained some more stable results in some outcome indicators that were different from the previous meta-analyses (18, 29, 30). In addition, we are the first study to include the PLND rate in the meta-analysis, and also the first study to conduct the subgroup analysis based on the population. Meta-analysis showed no significant difference in PSM, but the RS-RARP group had significantly higher PSM rates in the anterior site. The postoperative continence rate of the RS group at 1, 3, 6, and 12 months was significantly higher than that of the c-RARP group. In addition, the RS-RARP group had a shorter console time and a lower incidence of hernia. However, there were no significant differences in estimated blood loss, PLND rate, postoperative complications, and 1-year-biochemical recurrence rate. Our subgroup analysis found that RS-RARP seemed to have a higher margin positive rate in the RCT subgroup. In the subgroup analysis by population, we found that the advantage of RS-RARP in urine continence appeared to be more pronounced in the Asian population.

RS-RARP can be called "reverse perineal or RP" in a sense because it combines the advantages of perineal RP and retropubic RP (17). Perineal RP can accurately dissect the urethra and preserve the Retzius space and dorsal venous complex (DVC), but it damages the pelvic floor muscles and can lead to severe urinary incontinence (31). In contrast, the retropubic RP avoids damage to the pelvic floor muscles, but requires dissection of the Retzius space, resulting in the injury of critical structures involved in urine continence, such as arcus tendineus, endopelvic fascia, and neurovascular bundle (31). RS-RARP preserves both Retzius space and pelvic floor muscles, minimizes surgical trauma, and retains normal anatomical structure to the greatest extent. Although c-RARP also includes several remedial steps that have been shown to improve postoperative urine continence, such as the posterior reconstruction of the rhabdosphincter (32), bladder neck ultradissection (33), puboperineoplasty (34),

and nerve-sparing dissection (35), postinjury reparation is never as effective as outright injury avoidance. This explains why RS-RARP is significantly better than c-RARP in early urine continence.

In terms of clinical outcomes, we found that the RS-RARP group had shorter console time and a lower incidence of hernia, but no significant differences in estimated blood loss and complications. The difference in operative time may be due to the fact that RS-RARP maximizes the preservation of natural anatomy and does not require remedial reconstruction. As for the difference in hernia incidence, Shimbo et al. (36) noted that urethrovesical anastomosis during c-RARP surgery might lead to overstretching of the peritoneum and vas deferens, resulting in medial displacement and enlargement of the inner ring, leading to increased hernia incidence. Compared with c-RARP, RS-RARP can maximize the protection of the anterior compartment and myopectineal orifice to prevent the displacement of the internal ring, thus greatly reducing the incidence of hernia (17, 37). Although RS-RARP is theoretically less invasive than c-RARP, there is no significant difference in estimated blood loss. This might be due to the fact that during c-RARP, urine spills less from the bladder, but during RS-RARP, urine constantly spills from the bladder neck, which is open above the lens, due to gravity (22). This difference in urine content might bias the estimation of blood loss.

The results of some preliminary studies (11, 13) and meta-analysis (29) suggested that RS-RARP might have a higher PSM rate than c-RARP, while our meta-analysis showed no significant difference in PSM rate between the two surgical methods, which may be due to the learning curve of a new surgical procedure. Galfano et al. (9) reported an incidence of PSM of 32% in the first 100 patients who underwent RS-RARP and 19% in the next 100 patients. Recent studies have shown that the PSM rate of RS-RARP is very low when the operator is experienced (19, 22, 24). Lee et al. (22) based on a large sample found no significant difference in PSM between RS-RARP and c-RARP. The study of Egan et al. (24) also showed the same result. Although there was no significant difference in overall PSM, our subgroup analysis showed that the RS-RARP group had significantly higher PSM rates in the anterior site. In particular, in the study of Egan et al. (24), the PSM rates in the anterior site in the RS-RARP group were 2.69 times that of c-RARP. Despite the high literature quality of the study of Egan et al. (24), to avoid bias, we tried to remove the data of this study and found that although the difference became not statistically significant (OR = 2.07, 95% CI: 0.99–4.36, $P = 0.05$), the clinical trend was still obvious. Lim et al. (17) suggested that part of the reason for PSMs at the anterior margins may be related to anatomy. There is no clear plane between the prostatic stroma and the urethral sphincter muscle fibers at the apex and anterior (38). In addition, Kim et al. (39) believed that surgeons had a certain degree of vision limitation when performing the anterior aspect, which may also be one of the reasons. Our results are also somewhat supported by a recent study showing that patients with transitional zone tumors receiving RS-RARP had a higher rate of PSM, with most PSMs (39.8%) located in the anterior part of the prostatic gland (40). This study also indicates that the anterior part of the prostate capsule is often defective, resulting in a lack of a clear plane between the prostate capsule and the fibromuscular stroma. Therefore, patients with tumors located in the transitional zone, especially in the anterior part, are more likely to develop PSM during RS-RARP, which is characterized by anterior preservation (40). Perhaps, in theory, the RS-RARP approach is more suitable for posterior rather than anterior tumors. Therefore, when facing anterior tumors with higher pathological stages, surgeons can move slightly forward away from the prostate during the operation and remove more periprostatic fat to avoid PSM, or they can also consider choosing c-RARP (17). At present, there is no significant difference in the 1-year-biochemical recurrence rate between the two surgical methods, which is consistent with the results of PSM and reflects the oncologic safety of RS-RARP to a certain extent. Further follow-up is still needed.

Whether PLND is performed or not affects the clinical, functional, and oncological outcomes of patients (17). To avoid bias caused by differences in PLND rates between the groups, we included the PLND rate as one of the outcome indicators in our meta-analysis. Our results showed that there was no significant difference in PLND rate between the groups, which not only confirmed the operability of PLND in RS-RARP but also basically excluded the possibility that PLND rate could bring about bias to the results.

In our subgroup analysis, we found that the Asian population seemed to be more suitable for RS-RARP and had better function and oncological outcomes. This might be due to the fact that most of the studies (19–22) on the Asian populations were published recently, surgeons have gained more experience than earlier studies (12, 13, 15, 16) on the Western populations, and the RS-RARP technique itself also has been improved in many details. Whether this difference is really meaningful is unknown and may require further anatomical studies to confirm.

In our sensitivity analysis, the vast majority of the heterogeneity was not sourced, but despite the heterogeneity, our results were robust. Our heterogeneity mainly existed in the operation time and urine control outcome indicator group. The operation time may be related to the learning curve and recording method, and the definition of urine continence may also have some differences in various medical institutions, which may be the reason for the high heterogeneity.

LIMITATIONS

There are some limitations to our study. First, although we have explored postoperative sexual function, there are few solid results due to the limited data available. Second, there is a lack of long-term survival data. Third, we cannot yet fully explain the differences in outcomes between different populations.

CONCLUSION

Compared with c-RARP, RS-RARP showed better recovery of continence, shorter console time, and lower incidence of hernia. Although there was no significant difference in overall PSM, we suggest that the surgeon should be more careful if the lesion is in the anterior prostate.

DATA AVAILABILITY STATEMENT

The original contributions presented in the study are included in the article/supplementary material, further inquiries can be directed to the corresponding author.

ETHICS STATEMENT

The authors are accountable for all aspects of the work in ensuring that questions related to the accuracy or integrity of any part of the work are appropriately investigated and resolved.

AUTHOR CONTRIBUTIONS

H-MY conception, design, and administrative support. J-NX and Z-YX provision of study materials or patients, collection and assembly of data, data analysis, and interpretation. All authors write the manuscript and approval of manuscript.

REFERENCES

1. Siegel RL, Miller KD, Jemal A. Cancer statistics, 2020. *CA Cancer J Clin.* (2020) 70:7–30. doi: 10.3322/caac.21590
2. Mohler JL, Antonarakis ES, Armstrong AJ, D'Amico AV, Davis BJ, Dorff T, et al. Prostate cancer, version 2.2019, NCCN clinical practice guidelines in oncology. *J Natl Compr Canc Netw.* (2019) 17:479–505. doi: 10.6004/jnccn.2019.0023
3. Wilt TJ, Vo TN, Langsetmo L, Dahm P, Wheeler T, Aronson WJ, et al. Radical prostatectomy or observation for clinically localized prostate cancer: extended follow-up of the prostate cancer intervention versus observation trial (PIVOT). *Eur Urol.* (2020) 77:713–24. doi: 10.1016/j.eururo.2020.02.009
4. Abbou CC, Hoznek A, Salomon L, Olsson LE, Lobontiu A, Saint F, et al. Laparoscopic radical prostatectomy with a remote controlled robot. *J Urol.* (2001) 165:1964–6. doi: 10.1097/00005392-200106000-00027
5. Tewari A, Peabody J, Sarle R, Balakrishnan G, Hemal A, Shrivastava A, et al. Technique of da Vinci robot-assisted anatomic radical prostatectomy. *Urology.* (2002) 60:569–72. doi: 10.1016/S0090-4295(02)01852-6
6. Dev HS, Sooriakumaran P, Srivastava A, Tewari AK. Optimizing radical prostatectomy for the early recovery of urinary continence. *Nat Rev Urol.* (2012) 9:189–95. doi: 10.1038/nrurol.2012.2
7. Jacobs EF, Boris R, Masterson TA. Advances in robotic-assisted radical prostatectomy over time. *Prostate Cancer.* (2013) 2013:902686. doi: 10.1155/2013/902686
8. Galfano A, Ascione A, Grimaldi S, Petralia G, Strada E, Bocciardi AM, et al. New anatomic approach for robot-assisted laparoscopic prostatectomy: a feasibility study for completely intrafascial surgery. *Eur Urol.* (2010) 58:457–61. doi: 10.1016/j.eururo.2010.06.008
9. Galfano A, Di Trapani D, Sozzi F, Strada E, Petralia G, Bramerio M, et al. Beyond the learning curve of the Retzius-sparing approach for robot-assisted laparoscopic radical prostatectomy: oncologic and functional results of the first 200 patients with $\geq$ 1 year of follow-up. *Eur Urol.* (2013) 64:974–80. doi: 10.1016/j.eururo.2013.06.046
10. Wirth MP, Froehner M. Radical prostatectomy-only centers: the future in genitourinary surgery? *Eur Urol.* (2010) 57:953–4. doi: 10.1016/j.eururo.2010.02.032
11. Asimakopoulos AD, Topazio L, De Angelis M, Agrò EF, Pastore AL, Fuschi A, et al. Retzius-sparing versus standard robot-assisted radical prostatectomy: a prospective randomized comparison on immediate continence rates. *Surg Endosc.* (2019) 33:2187–96. doi: 10.1007/s00464-018-6499-z
12. Menon M, Dalela D, Jamil M, Diaz M, Tallman C, Abdollah F, et al. Functional recovery, oncologic outcomes and postoperative complications after robot-assisted radical prostatectomy: an evidence-based analysis comparing the retzius sparing and standard approaches. *J Urol.* (2018) 199:1210–7. doi: 10.1016/j.juro.2017.11.115
13. Eden CG, Moschonas D, Soares R. Urinary continence four weeks following Retzius-sparing robotic radical prostatectomy: the UK experience. *J Clin Urol.* (2018) 11:15–20. doi: 10.1177/2051415817706635
14. Chang LW, Hung SC, Hu JC, Chiu KY. Retzius-sparing robotic-assisted radical prostatectomy associated with less bladder neck descent and better early continence outcome. *Anticancer Res.* (2018) 38:345–51. doi: 10.21873/anticanres.12228
15. Sayyid RK, Simpson WG, Lu C, Terris MK, Klaassen Z, Madi R. Retzius-sparing robotic-assisted laparoscopic radical prostatectomy: a safe surgical technique with superior continence outcomes. *J Endourol.* (2017) 31:1244–50. doi: 10.1089/end.2017.0490
16. Dalela D, Jeong W, Prasad MA, Sood A, Abdollah F, Diaz M, et al. A pragmatic randomized controlled trial examining the impact of the retzius-sparing approach on early urinary continence recovery after robot-assisted radical prostatectomy. *Eur Urol.* (2017) 72:677–85. doi: 10.1016/j.eururo.2017.04.029
17. Lim SK, Kim KH, Shin TY, Han WK, Chung BH, Hong SJ, et al. Retzius-sparing robot-assisted laparoscopic radical prostatectomy: combining the best of retropubic and perineal approaches. *BJU Int.* (2014) 114:236–44. doi: 10.1111/bju.12705
18. Jiang YL, Zheng GF, Jiang ZP, Zhen L, Zhou XL, Zhou J, et al. Comparison of Retzius-sparing robot-assisted laparoscopic radical prostatectomy vs standard robot-assisted radical prostatectomy: a meta-analysis. *BMC Urol.* (2020) 20:114. doi: 10.1186/s12894-020-00685-4
19. Qiu X, Li Y, Chen M, Xu L, Guo S, Marra G, et al. Retzius-sparing robot-assisted radical prostatectomy improves early recovery of urinary continence: a randomized, controlled, single-blind trial with a 1-year follow-up. *BJU Int.* (2020) 126:633–40. doi: 10.1111/bju.15195
20. Ota Y, Hamamoto S, Matsuyama N, Hamakawa T, Iwatsuki S, Etani T, et al. Pelvic anatomical features after retzius-sparing robot-assisted radical prostatectomy intended for early recovery of urinary symptoms. *J Endourol.* (2020). doi: 10.1089/end.2020.0463
21. Liao PC, Hung SC, Hu JC, Chiu KY. Retzius-sparing robotic-assisted radical prostatectomy facilitates early continence regardless of neurovascular bundle sparing. *Anticancer Res.* (2020) 40:4075–80. doi: 10.21873/anticanres.14405
22. Lee J, Kim HY, Goh HJ, Heo JE, Almujalhem A, Alqahtani AA, et al. Retzius sparing robot-assisted radical prostatectomy conveys early regain of continence over conventional robot-assisted radical prostatectomy: a propensity score matched analysis of 1,863 patients. *J Urol.* (2020) 203:137–44. doi: 10.1097/JU.0000000000000461
23. Kowalczyk KJ, Davis M, O'Neill J, Lee H, Orzel J, Rubin RS, et al. Impact of retzius-sparing versus standard robotic-assisted radical prostatectomy on penile shortening, peyronie's disease, and inguinal hernia sequelae. *Eur Urol Open Sci.* (2020) 22:17–22. doi: 10.1016/j.euros.2020.09.004
24. Egan J, Marhamati S, Carvalho FLF, Davis M, O'Neill J, Lee H, et al. Retzius-sparing robot-assisted radical prostatectomy leads to durable improvement in urinary function and quality of life versus standard robot-assisted radical prostatectomy without compromise on oncologic efficacy: single-surgeon series and step-by-step guide. *Eur Urol.* (2020). doi: 10.1016/j.eururo.2020.05.010
25. Moher D, Liberati A, Tetzlaff J, Altman DG, Group P. Preferred reporting items for systematic reviews and meta-analyses: the PRISMA statement. *Int J Surg.* (2010) 8:336–41. doi: 10.1016/j.ijsu.2010.02.007

26. Berger VW. Is the Jadad score the proper evaluation of trials? J Rheumatol 2006 33:1710-1 author reply 1-2.
27. Cook DA, Reed DA. Appraising the quality of medical education research methods: the medical education research study quality instrument and the newcastle-ottawa scale-education. *Acad Med.* (2015) 90:1067–76. doi: 10.1097/ACM.0000000000000786
28. Chang KD, Abdel Raheem A, Santok GDR, Kim LHC, Lum TGH, Lee SH, et al. Anatomical Retzius-space preservation is associated with lower incidence of postoperative inguinal hernia development after robot-assisted radical prostatectomy. *Hernia.* (2017) 21:555–61. doi: 10.1007/s10029-017-1588-9
29. Tai TE, Wu CC, Kang YN, Wu JC. Effects of Retzius sparing on robot-assisted laparoscopic prostatectomy: a systematic review with meta-analysis. *Surg Endosc.* (2020) 34:4020–9. doi: 10.1007/s00464-019-07190-2
30. Phukan C, McLean A, Nambiar A, Mukherjee A, Somani B, Krishnamoorthy R, et al. Retzius sparing robotic assisted radical prostatectomy vs. conventional robotic assisted radical prostatectomy: a systematic review and meta-analysis. *World J Urol.* (2020) 38:1123–34. doi: 10.1007/s00345-019-02798-4
31. Imperatore V, Cantiello F, Fusco F, Iannuzzo M, Di Meo S, Imbimbo C, et al. Radical perineal prostatectomy versus radical retropubic prostatectomy after previous prostate surgery: surgical and functional outcomes. *Urol Int.* (2011) 86:140–5. doi: 10.1159/000317326
32. Gondo T, Yoshioka K, Hashimoto T, Nakagami Y, Hamada R, Kashima T, et al. The powerful impact of double-layered posterior rhabdosphincter reconstruction on early recovery of urinary continence after robot-assisted radical prostatectomy. *J Endourol.* (2012) 26:1159–64. doi: 10.1089/end.2012.0067
33. Cusumano S, Annino F, Selas ER, Hanna S, Piechaud T, Gaston R. Feasibility, technique, and principles of tension- and energy-free laparoscopic radical prostatectomy with lateral intrafascial dissection of the neurovascular bundles with the use of a high-definition optical device. *J Endourol.* (2008) 22:1981–7. doi: 10.1089/end.2008.9762
34. Eastham JA, Kattan MW, Rogers E, Goad JR, Ohori M, Boone TB, et al. Risk factors for urinary incontinence after radical prostatectomy. *J Urol.* (1996) 156:1707–13. doi: 10.1016/S0022-5347(01)65488-0
35. Curto F, Benijts J, Pansadoro A, Barmoshe S, Hoepffner JL, Mugnier C, et al. Nerve sparing laparoscopic radical prostatectomy: our technique. *Eur Urol.* (2006) 49:344–52. doi: 10.1016/j.eururo.2005.11.029
36. Shimbo M, Endo F, Matsushita K, Iwabuchi T, Fujisaki A, Kyono Y, et al. Incidence, risk factors and a novel prevention technique for inguinal hernia after robot-assisted radical prostatectomy. *Urol Int.* (2017) 98:54–60. doi: 10.1159/000448339
37. Hori S, Oyama N, Miyake M, Toyoshima Y, Takada S, Fujimoto K, et al. Prevention technique of postoperative inguinal hernia in patients undergoing radical prostatectomy for localized prostate cancer. *Indian J Surg Oncol.* (2017) 8:9–13. doi: 10.1007/s13193-016-0526-0
38. Walz J, Burnett AL, Costello AJ, Eastham JA, Graefen M, Guillonneau B, et al. A critical analysis of the current knowledge of surgical anatomy related to optimization of cancer control and preservation of continence and erection in candidates for radical prostatectomy. *Eur Urol.* (2010) 57:179–92. doi: 10.1016/j.eururo.2009.11.009
39. Kim LHC, Santok GD, Raheem AA, Alabdulaali I, Choi YD, Rha KH. Incidence and location of positive surgical margin following Retzius- Sparing Robot-Assisted Radical Prostatectomy and its significance on oncological outcome. *BJU Int.* (2016) 118:8.
40. Li Y, Fu Y, Li W, Xu L, Zhang Q, Gao J, et al. Tumour location determined by preoperative MRI is an independent predictor for positive surgical margin status after Retzius-sparing robot-assisted radical prostatectomy. *BJU Int.* (2020) 126:152–8. doi: 10.1111/bju.15060

Conflict of Interest: The authors declare that the research was conducted in the absence of any commercial or financial relationships that could be construed as a potential conflict of interest.

frontiers in Oncology

SYSTEMATIC REVIEW
published: 10 November 2021
doi: 10.3389/fonc.2021.748885

Endoscopic and Robotic Parotidectomy for the Treatment of Parotid Tumors: A Systematic Review and Meta-Analysis

Shanwen Chen[1†], Mei Zhao[2†], Dong Wang[1], Yi Zhao[1], Jianxin Qiu[1] and Yehai Liu[1]*

[1] Department of Otorhinolaryngology - Head and Neck Surgery, The First Affiliated Hospital of Anhui Medical University, Hefei, China, [2] Oncology Department of Integrated Traditional Chinese and Western Medicine, The First Affiliated Hospital of Anhui Medical University, Hefei, China

OPEN ACCESS

Edited by:
Patrick J. Schuler, Ulm University Medical Center, Germany

Reviewed by:
Boguslaw Mikaszewski, Medical University of Gdansk, Poland
AB Zulkiflee, University Malaya Medical Centre, Malaysia

****Correspondence:***
Yehai Liu
liuyehai@ahmu.edu.cn

[†]These authors share first authorship

Specialty section:
This article was submitted to Surgical Oncology, a section of the journal Frontiers in Oncology

Received: *28 July 2021*
Accepted: *18 October 2021*
Published: *10 November 2021*

Citation:
Chen S, Zhao M, Wang D, Zhao Y, Qiu J and Liu Y (2021) Endoscopic and Robotic Parotidectomy for the Treatment of Parotid Tumors: A Systematic Review and Meta-Analysis. Front. Oncol. 11:748885. doi: 10.3389/fonc.2021.748885

Background: The goal of this review was to introduce endoscopic/robotic parotidectomy (EP/RP) and compare EP/RP against conventional parotidectomy (CP) regarding the intraoperative and postoperative parameters in the treatment of parotid tumors.

Methods: A systematic literature search of medical databases (PubMed, Embase, and Cochrane Central Register of Controlled Trials) was performed from inception to November 2020 to generate relevant studies.

Results: A total of 13 eligible studies (572 patients) were included for systematic review, and 7 out of 13 comparable studies for the quantitative synthesis of outcomes. Patients who underwent EP were characterized by less intraoperative bleeding volume, shorter incision length, and higher satisfaction postoperatively (WMD, 95% CI, -42.80; - 58.23 to -27.37; $p < 0.01$; WMD, 95% CI, -5.64; -7.88 to -3.39; $p < 0.01$; SMD, 95% CI, 1.88; 1.46 to 2.31; $p < 0.01$, respectively). However, operative time and risk of facial palsy exhibited no significant differences (WMD, 95% CI, -11.17; -26.71 to 4.34; $p = 0.16$; OR, 95% CI,0.71; 0.39 to 1.32; $p = 0.28$, respectively).

Conclusions: Our findings suggest that the current evidence does not adequately support EP is equally safe and effective as CP. In certain selected cases, endoscopic technology has its unique advantages. For patients with strong cosmetic needs, endoscopic or robotic techniques may be an alternative through adequate preoperative evaluations.

Systematic Review Registration: International Prospective Register of Systematic Reviews, identifier CRD42020210299.

Keywords: endoscopic surgery, robotic surgery, parotid gland, oncology, complication

INTRODUCTION

Benign parotid tumors account for the majority of parotid tumors (1). The preferred treatment of choice tends to be surgical resection. Currently, the majority of clinical methods are traditional "S" incisions, which can fully expose the parotid tissue while preserving important structures such as the facial nerve. Unfortunately, this conventional method will ultimately leave a large facial scar from preauricular to submandibular nodes, causing a non-negligible psychological burden and reducing the quality of life of patients (2, 3).

Additionally, modified incisions to the parotid have been used in patients with benign parotid tumors to improve the postoperative appearance. These minimally invasive approaches, however, have not been extensively used due to the high risk of structure injury (4). In the past two decades, the use of endoscopy and robotics techniques, as an emerging alternative strategy, has been demonstrated in many studies, leading to the gradual popularization and adoption of the concept of minimally invasive surgery. These procedures possess the advantages of small trauma, well exposure, and satisfying cosmetic effects. In particular, endoscopic techniques have been applied in head and neck lesions, including thyroid lesions, thyroglossal duct cysts, parapharyngeal space tumors, and even neck dissection (5–8). More importantly, it can obtain an excellent cosmetic effect on the premise of safety. Benefitting from the advantages of magnifying endoscopy, it is accessible to identify nerves and small vessels during operation. Thus, small incision approaches, including preauricular, retroauricular, hairline, or transoral have been largely developed in parotidectomy with endoscopic assistance (9, 10).

Although minimally invasive surgical techniques, particularly endoscopic-assisted parotid surgery, have been introduced more than 10 years, the progressive development of technology is less than that of thyroid. One reason is certainly the difference of incidence, the ease of use and safety of the new technology warrant consideration as well. To date, there is no systematic review summarizing the findings on this technique. In this regard, the present study aimed to perform a systematic review and meta-analysis introducing the safety and efficacy of endoscopic or robotic-assisted parotid gland surgery.

METHODS

This review was conducted following the Preferred Reporting Items for Systematic Reviews and Meta-Analyses (PRISMA) guidelines (11). Two of the authors (S.C. and M.Z.) independently searched the electronic databases including PubMed, Embase, and the Cochrane Central Register of Controlled Trials (CENTRAL) for articles of interest published before November 2020.

This study was registered in the International Prospective Register of Systematic Reviews (CRD42020210299). The search of the databases was performed by combining the Mesh terms and keywords, including "endoscopy" OR "endoscopic" OR "robotic surgical procedures" OR "robot" OR "robotic" OR" minimally invasive" AND "parotid gland" OR "parotid" OR "parotidectomy" OR "parotid surgery". Articles that fulfilled the inclusion criteria were included in the review. The authors also reviewed the reference lists of the included studies to optimize screening and selection. All analyses were based on previous published studies; thus, no ethical approval and patient consent are required.

Study Selection

Inclusion criteria included: (1) both randomized clinical trials (RCTs) and observational studies, (2) studies that reported the outcomes of endoscopic or robotic-assisted parotidectomy, (3) articles reported in English language, and (4) if more than one study presented data from the same study participants, either the study of the higher quality or the most comprehensive was included. Exclusion criteria included: (1) any publication that did not meet the above inclusion criteria, (2) sialendoscopy, (3) salivary calculus, and (4) conference abstracts, editorials, and case report ≤ 5.

Data Extraction and Quality Assessment

The following data variables were extracted: first author, year of publication, country, study design, surgery approach, number of patients, gender and age, operative details, and outcomes. The main surgical outcomes included operative time, bleeding volume, incision length, cosmetic satisfaction, and facial never palsy. The secondary outcomes included drainage volume, length of hospital stay, and other complications. Finally, surgical completeness and tumor recurrence were also documented.

Further, the same authors independently assessed the quality of the included studies. The Methodological Index for Non-Randomized Studies (MINORS) scale was applied to evaluate the non-RCTs and Cochrane Collaboration tools for RCTs (12, 13).

Data Synthesis and Analysis

When the included studies were comparable, a meta-analysis was performed, otherwise, only a systematic review would have been conducted. Cosmetic satisfaction was assessed with a visual analog scale (VAS). When necessary, we subtracted the mean from the possible extremum while keeping the standard deviation unchanged to ensure that the directionality of the variables was consistent with higher values indicating high satisfaction. Medians were converted to means using a previously described methodology (14). Review Manager program version 5.4 was applied to perform statistical data analysis. For summarized continuous data, weighted mean difference (WMD) and/or standardized mean difference (SMD) were expressed, while dichotomous variables were examined using odds ratio (OR), reported with 95% CIs. Overall results were pooled using a random-effects model based on the variation between studies. The homogeneity test among studies was analyzed using I^2 tests, which was interpreted on the following scale: I^2 value of 25% indicates low heterogeneity, > 50% moderate heterogeneity, and > 75% high heterogeneity. A value of $p < .05$ was considered statistically significant. Sensitivity analyses were carried out when appropriate.

RESULTS

The initial literature search strategy yielded a total of 1043 studies. After comprehensive screening of abstracts, only 43 articles were included in the full-text review. Of these papers, we excluded 8 non-English articles, 5 conference abstracts, 1 animal study, 6 case studies ≤ 5, 8 irrelevant articles, and 2 studies with overlapping participants. The remaining 13 papers including 302 patients with EP and 270 patients with CP met the eligibility criteria for qualitative synthesis (9, 15–26). Then, 7 studies providing a control group for comparison were included in the final quantitative analysis of outcomes (9, 21–26). A flow diagram of the identification and selection of eligible studies is shown in **Figure 1**.

Characteristics of Included Studies

In total, 6 of 13 included studies were single-arm (15–20) while others provided a control group for comparison (9, 21–26). Four studies (22–24, 26) adopted prospective design whereas others were retrospective. The earliest included study was published in 2000 and the latest was published in 2020. The included studies were all performed in China and Korea. The latest study involved robotic-assisted parotid surgery (15), while the others were endoscopic assisted surgery. Among the 13 studies, no patients were converted to open surgery and only two patients were found to have tumor recurrence during the follow-up period. The first study used a modified "Blair" incision (20), the other used a transoral approach (22), and the rest used preauricular, retroauricular, hairline, or submandibular incisions. The region of most studies was limited to the superficial lobe of the parotid gland. However, 3 studies (9, 15, 21) were involved in deep lobe lesions while the other 2 studies were concentrated on accessory parotid (16, 22). Characteristics of included studies are shown in **Table 1**. Intraoperative and postoperative parameters of included studies are shown in **Table 2**.

Quality Assessment

Cochrane tool scores for 3 RCTs are shown in **eTable 1** and the MINORS scores are summarized in **eTable 2**. For both researchers

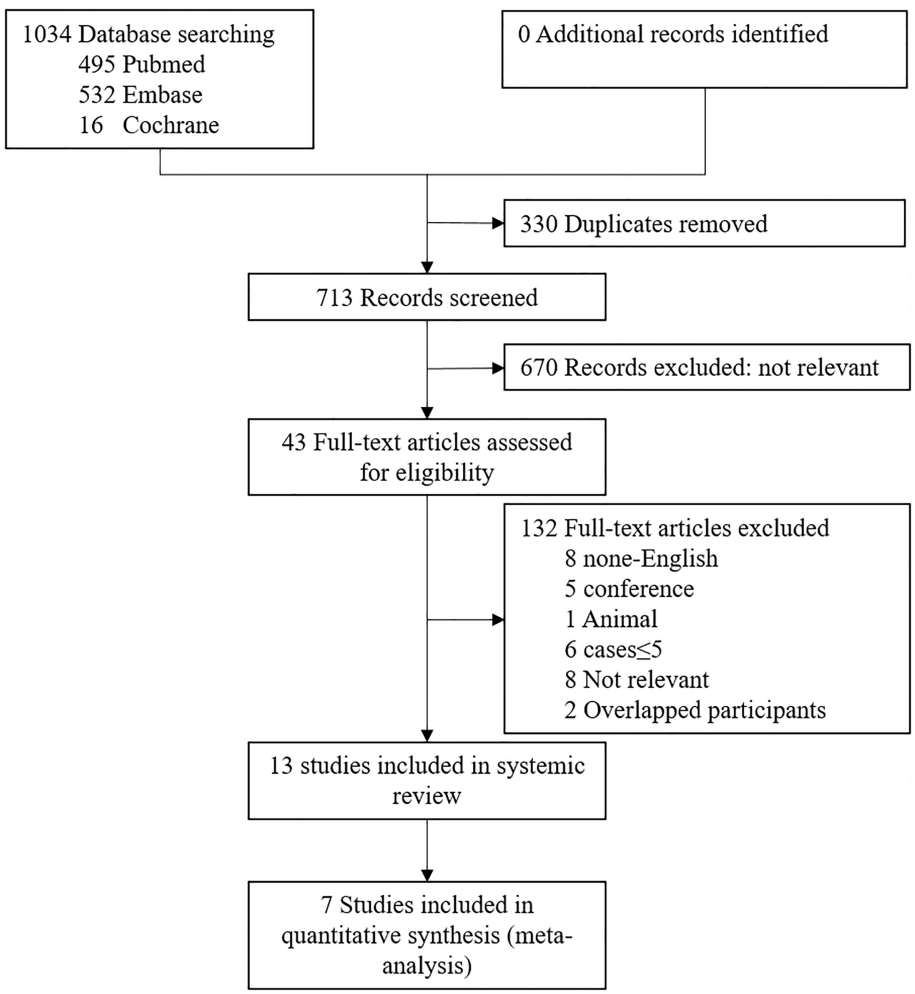

FIGURE 1 | Flow Diagram of the Literature Search.

TABLE 1 | Characteristics of the included studies.

Study	Year	Country	Study Type	No. (Male/Female)		Age, mean (SD), y		Tumor size, mean (SD), cm		Surgical region		Approach	Follow-up, median, months	
				EP	CP	EP	CP	EP	CP	EP	CP	EP	EP	CP
Park et al.	2020	Korea	R	25/28[a]	NA	39	NA	NR	NA	SL, DL	NA	RAHI	NR	NA
Zhang et al.	2015	China	R	5/8	NA	14.2 (6.3)	NA	2.0×2.6	NA	AP	NA	PA	3-14	NA
Woo et al.	2015	Korea	R	5/13	NA	27.3 (6.6)	NA	2.1×1.8	NA	SL	NA	HI	16	NA
Huang et al	2009	China	R	13/5	NA	17-62	NA	2.5 (0.4)	NA	SL	NA	RA	26-42	NA
Chen et al.	2007	China	R	12/2	NA	41.8	NA	3.9×2.4×1.7[b]	NA	NR	NA	RA	26[c]	NA
Lin et al.	2000	China	R	12/4	NA	40-75	NA	NR	NA	NR	NA	Modified 'Blair'	NR	NA
Li et al.	2019	China	R	8/7	39/18	53.0 (17.1)	52.5 (15.4)	2.3	3.0	SL, DL	SL, DL	RA	33	33
Kim et al.	2019	Korea	P	11/9	12/10	34.30 (8.61)	36.81 (8.77)	2.80 (0.89)	2.59 (0.81)	AP	AP	Transoral	13.4 (1.27)	14.45 (1.76)
Gao et al.	2019	China	R	17/20	55/32	47.00 (16.97)	51.37 (15.27)	2.35 (0.76)	2.38 (1.11)	SL, DL	SL, DL	RAHI, RM, THI	12	14
Fan rt al.	2017	China	P	14/7	15/10	38.7[b]	43.3	2.7 (1.6)	2.8 (1.9)	SL	SL	RA	25	27
Yan et al.	2015	China	P	9/20	10/19	45.1 (16.4)	45.7 (15.8)	2.8 (1.8)	2.9 (1.0)	SL	SL	RA	3-72	3-72
Chen et al.	2014	China	R	15/15	17/13	48 (11)	47 (12)	2.4 (0.5)	2.5 (0.4)	SL	SL	RA	9-36	9-36
Huang et al	2009	China	P	13/5	14/6	44.22 (16.18)	45.50 (14.17)	2.36 (0.53)	2.43 (0.47)	SL	SL	RA+RM	30	32

P, prospective; R, retrospective, EP, endoscopic-assisted parotidectomy; CP, conventional parotidectomy; SL, superficial lobe; DL, deep lobe; AP, accessory parotid; PA, preauricular; RA, retroauricular; HI, hairline; RAHI, retroauricular and hairline; THI, temporal hairline; RM, retromandibular; NR, not reported; NA, not available.

[a]*Robotic group. One patient underwent parotidectomy and thyroid lobectomy.*

[b]*Median.*

[c]*Mean.*

and patients in all included studies, the treatment methods were known. Due to insufficient follow-up time to monitor recurrence, all studies did not receive a high score in follow-up items.

Primary Outcomes

A total of 12 studies reported on the operative time of which 7 compared with CP (9, 21–26). Pooled data analysis revealed that operative time was insignificantly different for the EP group compared with the CP group (WMD, 95% CI, -11.17; -26.71 to 4.34; p = 0.16) with high heterogeneity (I^2 = 92%) (**Figure 2A**).

The intraoperative bleeding volume was reported in 12 studies, of which 7 compared with CP (9, 21–26). However, the authors of three studies provided no numerical data. The results of pooled data analysis were significant for the EP group compared with the CP group (WMD, 95% CI, -42.80; - 58.23 to -27.37; p < 0.01) with high heterogeneity (I^2 = 96%) (**Figure 2B**).

Incision length was observed in 10 studies in which 5 compared with CP (9, 22–25). Pooled results showed that the incision length was shorter in the EP group (WMD, 95% CI, -5.64; -7.88 to -3.39; p < 0.01) with high heterogeneity (I^2 = 98%) (**Figure 2C**).

The satisfaction was reported in all included studies, but 6 of which just presented with satisfaction. Compared with the CP group (21–25), pooled data of VAS score was significantly higher in the EP group (SMD, 95% CI, 1.88; 1.46 to 2.31; p < 0.01) with moderate heterogeneity (I^2 = 51%) (**Figure 2D**).

Facial palsy, as the main complication, was reported in all included studies with a total of 26 cases in the EP group and 45 in the CP group. However, all of those cases were transient and recovered in the follow-up period. Pooled data analysis was insignificantly different for the two method (OR, 95% CI,0.71; 0.39 to 1.32; p = 0.28) with low heterogeneity (I^2 = 2%) (**Figure 2E**).

Secondary Outcomes

Two articles respectively compared the length of hospital stay and drainage volume between the EP and CP groups (9, 21, 23). Notably, pooled data of both results supported endoscopic group (WMD, 95% CI, -2.33; -3.04 to -1.62; p < 0.01; 95% CI, -25.05; -31.15 to -18.94; p < 0.01; respectively) (**Figures 3A, B**). Additionally, the result indicates that other complications were fewer in the EP group than in the CP group (OR, 95% CI,0.23; 0.10 to 0.54; p < 0.01) (**Figure 3C**).

Sensitivity Analysis

Considering the difference of surgical approach and the potential error of data conversion, we performed a sensitivity analysis on the primary outcome by removing Kim et al. (22) and Li et al. (21) studies. Our results revealed that the influence of these two studies set on the pooled results was insignificant.

DISCUSSIONS

Traditional parotidectomy using Blair incision or its improved incision has been demonstrated to expose all parotid tissues well, but it leaves a 10 cm long incision on the cheek, severely affecting the postoperative aesthetics, especially in patients with scar

TABLE 2 | Summary of Intraoperative and postoperative parameters.

Study	Year	Operative time mean (SD), min		Incision length mean (SD), cm		Intraoperative bleeding mean (SD), ml		Satisfaction mean (SD)		Complications, No.				Drainage volume mean (SD), ml		Length of stay mean (SD), days		Recurrence No.	
										FN palsy		others							
		EP	CP	EP	CP	EP	CP	EP	CP	EP	CP	EP	CP	EP	CP	EP	CP	EP	CP
Park et al.[a]	2020	272	NA	NR	NA	24	NA	1.1	NA	3	NA	0	NA	152	NA	6.3	NA	NR	NA
Zhang et al.	2015	54	NA	2	NA	4-15	NA	satisfied	NA	0	NA	0	NA	NR	NA	NR	NA	0	NA
Woo et al.	2015	82.5	NA	5.5	NA	minimal	NA	9.77	NA	1	NA	0	NA	NR	NA	NR	NA	0	NA
Huang et al	2009	98.7	NA	3.3	NA	14.7	NA	satisfied	NA	2	NA	0	NA	NR	NA	NR	NA	0	NA
Chen et al.	2007	114	NA	3.1	NA	minimal	NA	satisfied	NA	2	NA	0	NA	NR	NA	NR	NA	1	NA
Lin et al.	2000	NR	NA	6.9	NA	NR	NA	satisfied	NA	0	NA	0	NA	NR	NA	NR	NA	NR	NA
Li et al.[b]	2019	98	115	NR	NR	30	50	0	3	3	8	1	22	35	59	5	6	0	0
Kim et al.	2019	47.5 (9.93)	82.72 (15.86)	3.55 (0.99)	6.40 (1.18)	minimal	minimal	9.66 (0.47)	6.72 (1.80)	1	3	0	6	NR	NR	NR	NR	0	0
Gao et al.	2019	97.84 (23.7)	120.34 (80.95)	4.66 (0.78)	12.98 (1.28)	26.76 (12.2)	65.29 (141.42)	satisfied	NR	8	18	39[c]	49[c]	NR	NR	9.12 (1.12)	11.33 (3.94)	0	1
Fan rt al.	2017	83.1 (21.3)	79.4 (17.5)	3.6 (0.5)	9.1 (1.9)	23.6 (8.9)	90.7 (34.4)	9.1 (1.4)	6.3 (2.6)	2	6	4	10	30.8 (8.7)	54.9 (12.7)	NR	NR	0	0
Yan et al.	2015	141.7 (51.2)	138.1 (34.2)	4.3 (0.5)	9.3 (1.2)	26.6 (10.4)	108.6 (40.2)	8.9 (0.7)	6.7 (1.8)	2	8	2	9	NR	NR	NR	NR	0	0
Chen et al.	2014	74.8 (15.7)	103.2 (10.3)	4.8 (0.4)	12.2 (1.4)	12.7 (3.9)	31.0 (8.9)	8.6 (1.2)	5.4 (1.3)	1	0	0	0	NR	NR	NR	NR	0	0
Huang et al	2009	108.61 (11.86)	105.25 (10.70)	NR	NR	13.89 (3.23)	30.25 (7.86)	satisfied	NR	1	2	1	1	NR	NR	NR	NR	0	0

EP, endoscopic-assisted parotidectomy; CP, conventional parotidectomy; NR, not reported; NA, not available; FN, facial nerve.

[a]*Exclude data of one patient with thyroidectomy.*

[b]*Continuous variables were expressed in median.*

[c]*Original data were not considered accurate.*

A Operative time

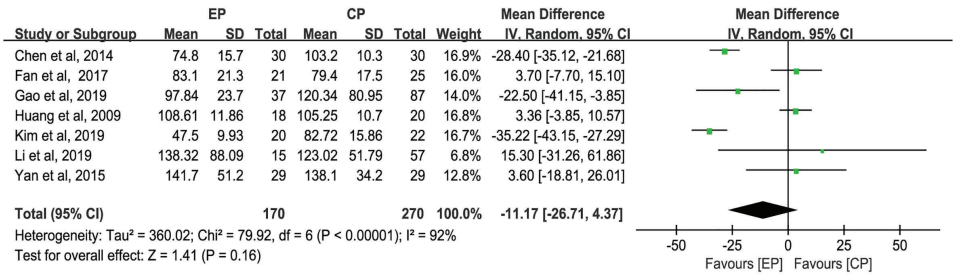

B Intraoperative bleeding

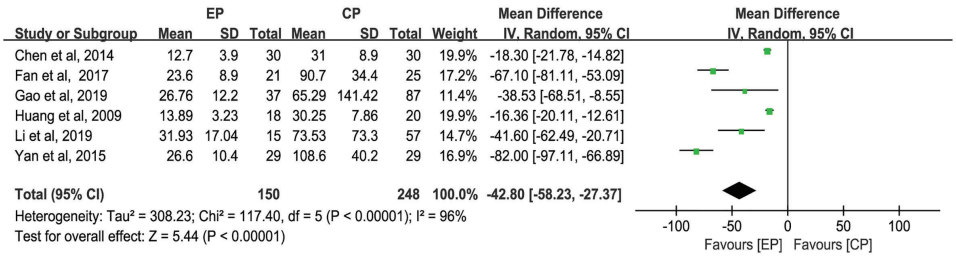

C Incision length

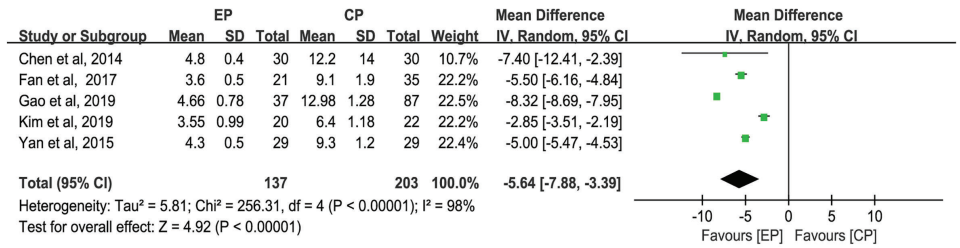

D Satisfication

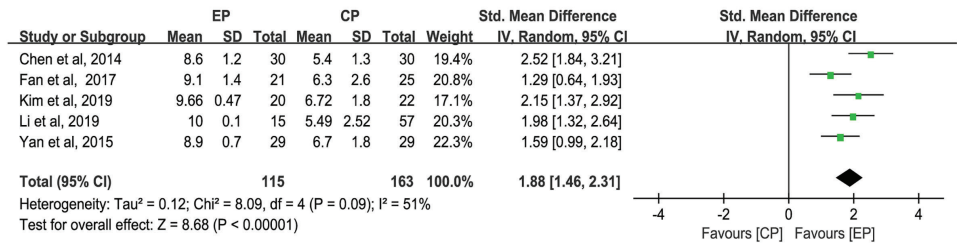

E Transctient FN palsy

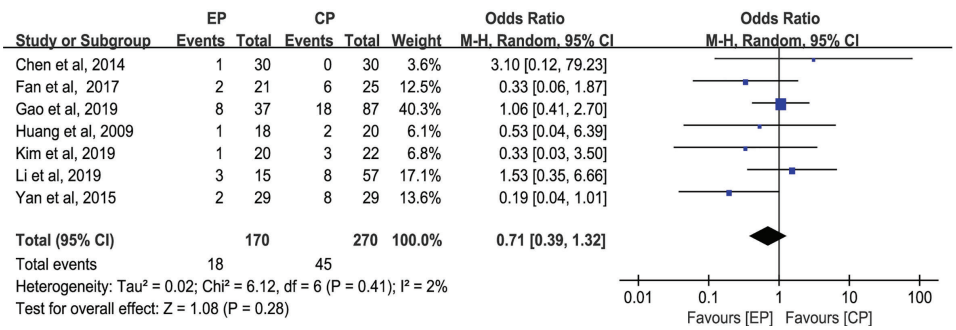

FIGURE 2 | Primary outcome.

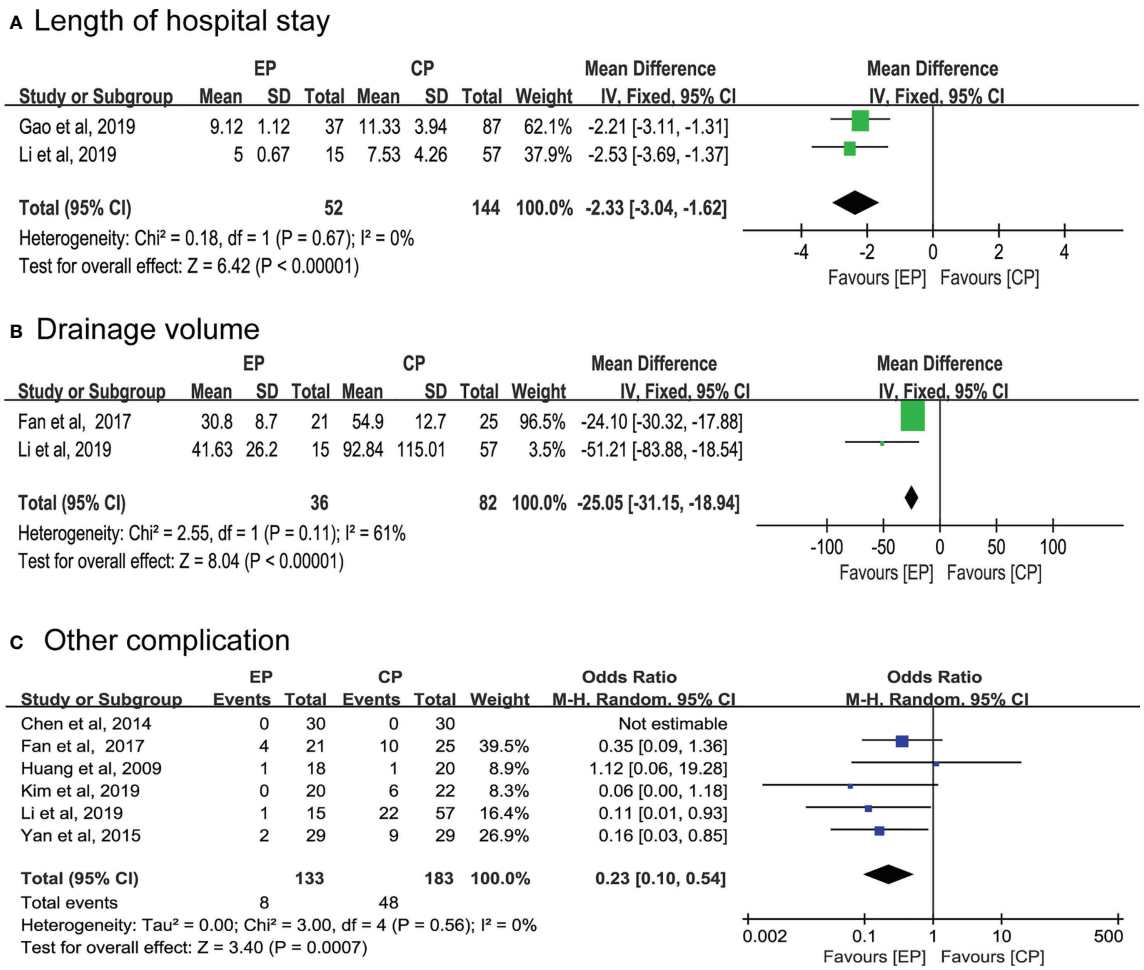

FIGURE 3 | Secondary outcome.

constitution (27). Recently, endoscopic assisted management has shown good prospects in a variety of head and neck surgeries, such as thyroid surgery, parapharyngeal space surgery, and selective neck dissection, among others. Similarly, the benefits of minimally invasive and magnifying endoscopy are also suitable for parotid surgery in theory. We therefore conducted this review and meta-analysis to systematically introduce the application of endoscopy in parotid gland surgery, as well as evaluate the advantages and disadvantages of this technique compared with traditional parotidectomy.

Our data indicate that the operative time was insignificant in the EP group than in the CP group with high heterogeneity. We observed in different study groups, the operation time of CP was comparable. Compared with the EP group, we noted that the master of CP was high, but the mastery of EP was different. The operation time of EP is expected to be shortened in the future, particularly with the increase in proficiency.

Traditional parotidectomy is usually performed using a Y-shaped or S-shaped incision, with an incision length close to 10 cm. Although new incision designs have been proposed, such as V-shaped periauricular incision, the incision length is often insignificantly shortened and cannot be covered well (4). One approach to overcome this problem is to apply the advantages of the endoscope to shorten the incision length as much as possible. The second is to use the natural masking effect of mastoid hair behind the parotid gland to place the incision in the hairline. Herein, we found the incision length of the EP group was less than 5 cm, while that of the CP group was more than 5 cm. These findings imply that the incision length of the EP group was significantly better than that of the CP group. We also uncovered that although different research groups used different incisions, including preauricular, postauricular, hairline, and oral mucosa, they all achieved good cosmetic effects based on successful completion of the operation and had higher cosmetic satisfaction compared with the CP group. Presently, there is a paucity of published literature that has examined how non-endoscope-assisted parotidectomy is performed through the facelift approach. However, this operation requires more traction and skin flap separation than endoscopically assisted parotidectomy (28).

Facial nerve injury is the most significant complication of parotidectomy. Large institutional series report transient facial nerve dysfunction occurring in up to 65% of parotidectomy patients and permanent facial nerve weakness in approximately 5% of cases (29, 30). In this review, six of the included studies (15, 17, 19, 21–23) used intraoperative nerve detectors, and the final pooled results suggest that there is no significant difference in the incidence of postoperative nerve palsy between EP and CP groups. We strongly believe that although it is difficult to fully expose all surgical fields at one time under endoscopy, with the improvement of endoscopic visualization technology, skilled surgeons can easily expose nerves to show their location and accurately determine their course. Additionally, the nerve detector can be applied for intraoperative nerve protection. Current studies have confirmed that in primary cases of parotidectomy, intraoperative facial nerve monitor decreases the risk of immediate postoperative facial nerve weakness (31). However, in other complications, except facial paralysis, the EP group was significantly better than the control group. Furthermore, the number of postoperative numbness in the EP group was lower than that of the CP group due to small incisions.

In addition to the advantages of EP discussed above, another point that cannot be ignored is the surgical indications. The classic Y-shaped or S-shaped incision can fully expose the parotid gland, which is suitable for the treatment of any parotid gland lesions, including benign and malignant lesions. To achieve the postoperative aesthetic effect, EP has obvious limitations on the surgical indications, mainly including the following points: (1) the size of lesions depends on the length of the incision design; (2) the lesions are limited to the superficial lobe of the parotid gland; (3) benign tumors; and (4) no history of radiotherapy and surgery. Radiotherapy or surgical history can make local tissue adhesion tight, even damage the original location mark, which will significantly increase the difficulty of surgery. Recent studies have shown that malignant tumors of the parotid gland and deep lobe lesions of the parotid gland can significantly increase the difficulty of the operation and the incidence of postoperative facial weakness (32). Therefore, in this study, most researchers excluded such patients before surgery. Li et al. (21) enrolled patients with low-grade T1 and T2 tumors without lymph node metastasis, and endoscopic assisted total parotidectomy was completed with the help of a nerve monitor. However, as the researchers noted, the surgeon must be skilled in the use of a nasal endoscope as well as enriched experience of parotid surgery. Robot-assisted neck lymph node dissection has been reported in many studies (33–35). Park et al. successfully completed parotid gland operation and neck lymph node dissection using robot-assisted technique through the posterior hairline incision, which greatly expanded the indications of parotid surgery and achieved good cosmetic results (15). Nevertheless, limited by the hardware conditions, the popularization of this technology still needs a long time.

Limitations

There still exist some limitations in this review. First, all included studies were conducted in China and Korea, potentially limiting the generalizability of our findings. Second, some between-study heterogeneity was checked in some comparisons, possibly due to differences in surgical approaches, inaccuracy of data conversion, and surgeon experience. Third, most of the studies included were nonrandomized trials, three studies with randomized design could not be completely blinded due to the nature of the surgery, which might over- or underestimate the measured effect. Fourth, the length of follow-up of the included studies is insufficient, which raises the question of undocumented recurrence.

CONCLUSION

Taking into account the above shortcomings and the small sample size, we suggest that the current evidence does not adequately support EP is equally safe and effective as CP. In certain selected cases, endoscopic technology has its unique advantages. For patients with strong cosmetic needs, endoscopic or robotic techniques may be an alternative through adequate preoperative evaluations.

DATA AVAILABILITY STATEMENT

The original contributions presented in the study are included in the article/**Supplementary Material**. Further inquiries can be directed to the corresponding author.

AUTHOR CONTRIBUTIONS

Concept and design: All authors. Acquisition, analysis, or interpretation of data: SC, MZ, and YL. Drafting of the manuscript: SC and MZ. Critical revision of the manuscript for important intellectual content: All authors. Statistical analysis: SC and MZ. Administrative, technical, or material support: All authors. Supervision: JQ and YL. All authors contributed to the article and approved the submitted version.

SUPPLEMENTARY MATERIAL

The Supplementary Material for this article can be found online at: https://www.frontiersin.org/articles/10.3389/fonc.2021.748885/full#supplementary-material

REFERENCES

1. Spiro RH. Salivary Neoplasms: Overview of a 35-Year Experience With 2,807 Patients. *Head Neck Surg* (1986) 8(3):177–84. doi: 10.1002/hed.2890080309
2. Nitzan D, Kronenberg J, Horowitz Z, Wolf M, Bedrin L, Chaushu G, et al. Quality of Life Following Parotidectomy for Malignant and Benign Disease. *Plast Reconstr Surg* (2004) 114(5):1060–7. doi: 10.1097/01.PRS.0000135326.50939.C1
3. Fiacchini G, Cerchiai N, Tricò D, Sellari-Franceschini S, Casani AP, Dallan I, et al. Frey Syndrome, First Bite Syndrome, Great Auricular Nerve Morbidity, and Quality of Life Following Parotidectomy. *Eur Arch Oto-Rhino-Laryngol Off J Eur Fed Oto-Rhino-Laryngol Soc EUFOS Affil Ger Soc Oto-Rhino-*

Laryngol - Head Neck Surg (2018) 275(7):1893–902. doi: 10.1007/s00405-018-5014-4
4. Wu PA, Lu ZQ, Guan YF, Zhu HL, Liang XN, Liang WY, et al. Application of Functional Parotidectomy *via* Retroauricular Hairline Incision in the Excising Superficial Parotid Tumor. *Zhonghua Er Bi Yan Hou Tou Jing Wai Ke Za Zhi* (2017) 52(12):905–8. doi: 10.3760/cma.j.issn.1673-0860.2017.12.006
5. Pawar P, Vaishampayan S, Shah DH, Pai A. Retro-Auricular Endo Assisted Selective Neck Dissection (How I do it). *Oral Oncol* (2020) 110:104942. doi: 10.1016/j.oraloncology.2020.104942
6. Iseri M, Ozturk M, Kara A, Ucar S, Aydin O, Keskin G. Endoscope-Assisted Transoral Approach to Parapharyngeal Space Tumors. *Head Neck* (2015) 37 (2):243–8. doi: 10.1002/hed.23592
7. Woo SH, Park JJ, Hong JC, Wang S-G, Park GC, Eun YG, et al. Endoscope-Assisted Transoral Removal of a Thyroglossal Duct Cyst Using a Frenotomy Incision: A Prospective Clinical Trial. *Laryngoscope* (2015) 125(12):2730–5. doi: 10.1002/lary.25508
8. Park J-O, Kim S-Y, Chun B-J, Joo Y-H, Cho K-J, Park YH, et al. Endoscope-Assisted Facelift Thyroid Surgery: An Initial Experience Using a New Endoscopic Technique. *Surg Endosc* (2015) 29(6):1469–75. doi: 10.1007/s00464-014-3826-x
9. Gao L, Liang Q-L, Ren W-H, Li S-M, Xue L-F, Zhi Y, et al. Comparison of Endoscope-Assisted Versus Conventional Resection of Parotid Tumors. *Br J Oral Maxillofac Surg* (2019) 57(10):1003–8. doi: 10.1016/j.bjoms.2019.08.010
10. Woo SH. Endoscope-Assisted Transoral Accessory Parotid Mass Excision. *Head Neck* (2016) 38(1):E7–12. doi: 10.1002/hed.24092
11. Moher D, Liberati A, Tetzlaff J, Altman DGPRISMA Group. Preferred Reporting Items for Systematic Reviews and Meta-Analyses: The PRISMA Statement. *PloS Med* (2009) 6(7):e1000097. doi: 10.1371/journal.pmed.1000097
12. Higgins JPT, Altman DG, Gøtzsche PC, Jüni P, Moher D, Oxman AD, et al. The Cochrane Collaboration's Tool for Assessing Risk of Bias in Randomised Trials. *BMJ* (2011) 343:d5928. doi: 10.1136/bmj.d5928
13. Slim K, Nini E, Forestier D, Kwiatkowski F, Panis Y, Chipponi J. Methodological Index for Non-Randomized Studies (Minors): Development and Validation of a New Instrument. *ANZ J Surg* (2003) 73(9):712–6. doi: 10.1046/j.1445-2197.2003.02748.x
14. McGrath S, Zhao X, Steele R, Thombs BD, Benedetti ADEPRESsion Screening Data (DEPRESSD) Collaboration. Estimating the Sample Mean and Standard Deviation From Commonly Reported Quantiles in Meta-Analysis. *Stat Methods Med Res* (2020) 29(9):2520–37. doi: 10.1177/0962280219889080
15. Park YM, Kim DH, Kang MS, Lim J-Y, Kim S-H, Choi EC, et al. Real Impact of Surgical Robotic System for Precision Surgery of Parotidectomy: Retroauricular Parotidectomy Using Da Vinci Surgical System. *Gland Surg* (2020) 9(2):183–91. doi: 10.21037/gs.2020.01.05
16. Zhang D, Wang Y, Liang Q, Song F, Chen W, Zhang B. Endoscopic-Assisted Resection of Benign Tumors of the Accessory Parotid Gland. *J Oral Maxillofac Surg Off J Am Assoc Oral Maxillofac Surg* (2015) 73(8):1499–504. doi: 10.1016/j.joms.2015.01.032
17. Woo SH, Kim JP, Baek C-H. Endoscope-Assisted Extracapsular Dissection of Benign Parotid Tumors Using Hairline Incision. *Head Neck* (2016) 38(3):375–9. doi: 10.1002/hed.23901
18. Huang X, Sun W, Liu X, Liu W, Guan Z, Xu Y, et al. Endoscope-Assisted Partial-Superficial Parotidectomy Through a Concealed Postauricular Skin Incision. *Surg Endosc* (2009) 23(7):1614–9. doi: 10.1007/s00464-009-0435-1
19. Chen M-K, Chang C-C. Minimally Invasive Endoscope-Assisted Parotidectomy: A New Approach. *Laryngoscope* (2007) 117(11):1934–7. doi: 10.1097/MLG.0b013e3181255ead
20. Lin SD, Tsai CC, Lai CS, Lee SS, Chang KP. Endoscope-Assisted Parotidectomy for Benign Parotid Tumors. *Ann Plast Surg* (2000) 45 (3):269–73. doi: 10.1097/00000637-200045030-00008
21. Li T, Liu Y, Wang Q, Qin Y, Gao W, Li Q, et al. Parotidectomy by an Endoscopic-Assisted Postauricular-Groove Approach. *Head Neck* (2019) 41 (9):2851–9. doi: 10.1002/hed.25720
22. Kim JP, Lee DK, Moon JH, Ryu JS, Woo SH. Endoscope-Assisted Transoral Accessory Parotid Mass Excision: Multicenter Prospective Observational Study. *Laryngoscope* (2020) 130(5):1218–26. doi: 10.1002/lary.28190
23. Fan S, Pan G-K, Chen W-L, Lin Z-Y, Liang F-Y, Li Q-X, et al. Endoscope-Assisted Extracapsular Dissection of Benign Parotid Tumors Through a Single Cephaloauricular Furrow Incision Versus a Conventional Approach. *Surg Endosc* (2017) 31(8):3203–9. doi: 10.1007/s00464-016-5345-4
24. Yan Y, Chen X. Endoscopic Resection for Benign Parotid Tumor Through a Cosmetic Retroauricular Incision With Water Sac Establishing Operative Space: A New Approach. *J Laparoendosc Adv Surg Tech A* (2015) 25(6):508–13. doi: 10.1089/lap.2015.0046
25. Chen J, Chen W, Zhang J, He F, Zhu Z, Tang S, et al. Modified Endoscope-Assisted Partial-Superficial Parotidectomy Through a Retroauricular Incision. *ORL J Oto-Rhino-Laryngol Its Relat Spec* (2014) 76(3):121–6. doi: 10.1159/000362605
26. Huang X, Zheng Y, Liu X, Sun W, Zeng L, Cai X, et al. A Comparison Between Endoscope-Assisted Partial Parotidectomy and Conventional Partial Parotidectomy. *Otolaryngol–Head Neck Surg Off J Am Acad Otolaryngol-Head Neck Surg* (2009) 140(1):70–5. doi: 10.1016/j.otohns.2008.09.015
27. Lee HJ, Jang YJ. Recent Understandings of Biology, Prophylaxis and Treatment Strategies for Hypertrophic Scars and Keloids. *Int J Mol Sci* (2018) 19:711. doi: 10.3390/ijms19030711
28. Grover N, D'Souza A. Facelift Approach for Parotidectomy: An Evolving Aesthetic Technique. *Otolaryngol–Head Neck Surg Off J Am Acad Otolaryngol-Head Neck Surg* (2013) 148(4):548–56. doi: 10.1177/0194599812475221
29. Terrell JE, Kileny PR, Yian C, Esclamado RM, Bradford CR, Pillsbury MS, et al. Clinical Outcome of Continuous Facial Nerve Monitoring During Primary Parotidectomy. *Arch Otolaryngol Head Neck Surg* (1997) 123 (10):1081–7. doi: 10.1001/archotol.1997.01900100055008
30. Jin H, Kim BY, Kim H, Lee E, Park W, Choi S, et al. Incidence of Postoperative Facial Weakness in Parotid Tumor Surgery: A Tumor Subsite Analysis of 794 Parotidectomies. *BMC Surg* (2019) 19:199. doi: 10.1186/s12893-019-0666-6
31. Sood AJ, Houlton JJ, Nguyen SA, Gillespie MB. Facial Nerve Monitoring During Parotidectomy: A Systematic Review and Meta-Analysis. *Otolaryngol–Head Neck Surg Off J Am Acad Otolaryngol-Head Neck Surg* (2015) 152 (4):631–7. doi: 10.1177/0194599814568779
32. Roh J-L, Kim HS, Park CI. Randomized Clinical Trial Comparing Partial Parotidectomy Versus Superficial or Total Parotidectomy. *Br J Surg* (2007) 94 (9):1081–7. doi: 10.1002/bjs.5947
33. Paek SH, Lee HA, Kwon H, Kang KH, Park SJ. Comparison of Robot-Assisted Modified Radical Neck Dissection Using a Bilateral Axillary Breast Approach With a Conventional Open Procedure After Propensity Score Matching. *Surg Endosc* (2020) 34(2):622–7. doi: 10.1007/s00464-019-06808-9
34. Shin YS, Choi EC, Kim C-H, Koh YW. Robot-Assisted Selective Neck Dissection Combined With Facelift Parotidectomy in Parotid Cancer. *Head Neck* (2014) 36(4):592–5. doi: 10.1002/hed.23441
35. Park YM, Holsinger FC, Kim WS, Park SC, Lee EJ, Choi EC, et al. Robot-Assisted Selective Neck Dissection of Levels II to V *via* a Modified Facelift or Retroauricular Approach. *Otolaryngol–Head Neck Surg Off J Am Acad Otolaryngol-Head Neck Surg* (2013) 148(5):778–85. doi: 10.1177/0194599813478934

Conflict of Interest: The authors declare that the research was conducted in the absence of any commercial or financial relationships that could be construed as a potential conflict of interest.

Publisher's Note: All claims expressed in this article are solely those of the authors and do not necessarily represent those of their affiliated organizations, or those of the publisher, the editors and the reviewers. Any product that may be evaluated in this article, or claim that may be made by its manufacturer, is not guaranteed or endorsed by the publisher.

frontiers in Surgery

SYSTEMATIC REVIEW
published: 23 November 2021
doi: 10.3389/fsurg.2021.731448

A Consensus Meeting on Expert Recommendations on Operating Specifications for Laparoscopic Radical Resection of Hilar Cholangiocarcinoma

Yongfu Xiong[1,2,3,4], *Li Jingdong*[1,2,3]*, *Tang Zhaohui*[5]* and *Joseph Lau*[6]*

[1] Department of Hepatobiliary Surgery, Affiliated Hospital of North Sichuan Medical College, Nanchong, China, [2] Institute of Hepato-Biliary-Pancreatic-Intestinal Disease, North Sichuan Medical College, Nanchong, China, [3] Research Office of Hepato-Biliary-Pancreatic-Intestinal Disease, Affiliated Hospital of North Sichuan Medical College, Nanchong, China, [4] Department of General Surgery, Wusheng County People's Hospital, Guang'an, China, [5] Department of General Surgery, Xinhua Hospital, School of Medicine, Shanghai Jiao Tong University, Shanghai, China, [6] Faculty of Medicine the Chinese University of Hong Kong, Prince of Wales Hospital, Shatin, Hong Kong SAR, China

OPEN ACCESS

Edited by:
Patrick J. Schuler,
Ulm University Medical Center, Germany

Reviewed by:
Mikel Prieto,
Cruces University Hospital, Spain
Somaiah Aroori,
Plymouth Hospitals NHS Trust, United Kingdom

***Correspondence:**
Joseph Lau
josephlau@cuhk.edu.hk
Tang Zhaohui
tangzhaohui@yahoo.com
Li Jingdong
li-jingdong@hotmail.com

Specialty section:
This article was submitted to Surgical Oncology, a section of the journal Frontiers in Surgery

Received: 27 June 2021
Accepted: 22 October 2021
Published: 23 November 2021

Citation:
Xiong Y, Jingdong L, Zhaohui T and Lau J (2021) A Consensus Meeting on Expert Recommendations on Operating Specifications for Laparoscopic Radical Resection of Hilar Cholangiocarcinoma. Front. Surg. 8:731448. doi: 10.3389/fsurg.2021.731448

Background: With advances in techniques and technologies, laparoscopic radical resection of hilar cholangiocarcinoma (HCCA) has gradually been carried out in major medical centers in China. Its feasibility and safety have been accepted by a group of Chinese surgical experts.

Methods: To standardize perioperative management of HCCA by using laparoscopic resectional approach, to ensure safety of the patient with standardized management, improve prognosis of the patient, and enable proper application and refinement of this surgical approach, the expert group on specifications for laparoscopic radical resection of HCCA in China organized a consensus meeting.

Results: Laparoscopic radical resection of HCCA is difficult and associated with high risks. Appropriate patients should be carefully selected and this surgical approach should be promoted gradually. The experts met and arrived at 16 recommendations on perioperative management of HCCA by using laparoscopic surgery. There were three recommendations on preoperative diagnosis and evaluation; one recommendation on surgical principles of treatment; one recommendation on indications and contraindications; one recommendation on credentialing, staffing, and equipment; nine recommendations on laparoscopic techniques in different stages of operation; and one recommendation on indications for conversion to open surgery.

Conclusion: Laparoscopic surgery for HCCA is still in the early phase of development. This consensus provides a clinical reference with the aim to promote and to facilitate its further development.

Keywords: expert recommendations, operating specifications, laparoscopic radical resection, hilar cholangiocarcinoma, consensus meeting

INTRODUCTION

Hilar cholangiocarcinoma (HCCA) is a common malignant biliary tract tumor. Improvements in medical imaging have led to better diagnosis and staging of this disease. Radical resection is still the only treatment that can offer a chance of cure. However, the special anatomical location of HCCA, with its proximity to hepatic artery, portal vein, and caudate lobe makes excisional surgery extremely difficult (1, 2). Recent advances in minimally invasive surgery have attracted pioneer surgeons to perform laparoscopic radical resection of HCCA in selected patients. With gradual establishment of this operation on its feasibility, safety, and short-term treatment outcomes, this approach has now been gradually adopted by expert biliary surgeons in China as an alternative approach to open surgery on highly selected patients. To standardize the perioperative management of HCCA and the technical steps in laparoscopic radical resection of HCC, to ensure safety of the patient and improve prognosis, the expert group on specifications for laparoscopic radical resection of HCCA organized a consensus meeting for all the biliary expert surgeons in this field in China to formulate expert recommendations for laparoscopic radical resection of HCCA and its perioperative management.

An expert consensus meeting was held on April 19, 2021, during the Second Congress of the Hilar Cholangiocarcinoma Study Group of Surgeons. Experts in HCCA surgery were invited to participate in the meeting and to present specific issues with respect to laparoscopic surgery for HCCA including oncologic concerns, selection criteria, surgical techniques, and future aspects of this procedure. Presentations were followed by panel discussions and open discussions with the audience. After meeting, a first draft including summaries of the presentations and discussions was circulated to the panels, discussed, and edited. This document, including expert consensus statements, was formulated by all the attending experts in this field.

The categories of evidence used in this current expert recommendation are shown in **Table 1** and the recommendation grades are given in **Table 2**.

TABLE 1 | Level of evidence.

Level (quality) of evidence	Requirements
Class 1	• High-quality evidence from more than 1 RCT • Meta-analyses of high-quality RCTs • One or more RCTs corroborated by high-quality registry studies
Class 2	• Moderate-quality evidence from 1 or more RCTs • Meta-analyses of moderate-quality RCTs
Class 3	• Moderate-quality evidence from 1 or more well-designed, well-executed non-randomized studies, observational studies, or registry studies • Meta-analyses of such studies
Class 4	• Randomized or non-randomized observational or registry studies with limitations of design or execution • Meta-analyses of such studies • Physiological or mechanistic studies in human subjects
Class 5	• Consensus of expert opinion based on clinical experience

RCTs, randomized clinical trials.

TABLE 2 | Recommendation grades for this current expert recommendation.

Recommendation grade	Criteria
Grade I	Strong recommendation
Grade II	Moderate recommendation
Grade III	Weak recommendation
Grade IV	No recommendation

PREOPERATIVE DIAGNOSIS, PREPARATION, AND EVALUATION OF LAPAROSCOPIC RADICAL RESECTION OF HCCA

Key Points in Preoperative Diagnosis and Preparation

A comprehensive, effective, and complete evaluation should be carried out based on clinical symptoms/signs, laboratory findings, and medical imaging results (**Table 3**). The key findings used in preoperative diagnosis of open radical resection of HCCA should be the same as in laparoscopic surgery (1, 2).

Expert Recommendation 1

Multidetector CT (MDCT) (class 1, grade I) and magnetic resonance cholangiopancreatography (MRCP) (class 1, grade I) are recommended as the most important investigations because they can clearly delineate tumor location, size, level of biliary obstruction, blood vessel invasion, and atrophy of different parts of liver. Before surgery, a proper drainage procedure, such as percutaneous transhepatic cholangiodrainage (PTCD) or endoscopic nasobiliary drainage (ENBD), should be performed to relieve jaundice and any obstruction (class 1, grade I). Portal vein embolization (PVE) can be used to increase the size of future liver remnant (FLR) and has been shown to be effective in inducing liver hypertrophy with minimal risks. Biliary drainage should be established before PVE in patients with biliary dilatation in FLR (class 2, grade I).

Importance of Classifications and Stagings for Laparoscopic Radical Resection of HCCA

Classifications and stagings were considered to be of extreme importance in determining resectability of the tumor (**Table 4**). The Bismuth–Corlette classification is recommended for HCCA (class 1, grade I). Based on the level and extent of invasion of the biliary tract, this classification was considered by the experts in providing a sound basis to determine local extent of resection and degree of combined liver resection before surgery (**Figure 1**).

The American Joint Committee on Cancer (AJCC) and the Union for International Cancer Control (UICC) tumor–node–metastasis (TNM) stagings are based on comprehensive analysis of postoperative pathological findings. They should be used

TABLE 3 | List of recommending preoperative examinations for hilar cholangiocarcinoma.

List of examinations	Features	Category of recommendation
B-ultrasound	Evaluates degree of tumor invasion. Doppler ultrasound is helpful to evaluate portal vein invasion.	II
CT (MDCT)	Thin-slice scan is helpful to show vascular invasion. It has advantages in defining tumor location, size, biliary obstruction level, liver atrophy, and three-dimensional imaging of blood vessels. It has a high accuracy in determining resectability.	I
MRI+MRCP	Provides high resolution of soft tissues, with adequate display of biliary system, and secondary changes to bile ducts. It has special values in evaluating the longitudinal extent of bile duct tumor.	I
ERCP/ENBD	Invasive investigations which can accurately show the whole bile duct. It can be used for preoperative drainage to reduce jaundice.	III
PTCD	First choice to reduce obstructive jaundice before surgery. It is not recommended as a diagnostic procedure.	II
Endoscopic ultrasound	Has certain value for tumors with associated bile duct stones or cystic dilatation of the bile duct.	III
PET-CT	Is not recommended for early or intermediate stages of tumors, but has value to determine distant metastases.	II
Laparoscopic exploration	Useful for clinical staging of tumors.	III

TABLE 4 | Preoperative classification and staging for hilar cholangiocarcinoma.

Classification or staging	Application characteristics	Category of recommendation
Bismuth-Corlette classification	The most widely used clinical classification. It considers the level and scope of biliary invasion but does not consider vascular invasion or lymphatic or distant metastasis.	I
AJCC/UICC	Can be used to assess local or distant metastasis with guiding significance on prognosis of surgical treatment of tumors.	I
MSKCC staging	Has value as it includes vascular invasion and liver atrophy and is recommended to assist clinical decision	II
The international cholangiocarcinoma working group staging	Combines multiple types of classification and staging for comprehensive assessment but lacks good clinical trials with large samples to support.	II

in predicting prognosis and postoperative survival of patients. The Memorial Sloan Kettering Cancer Center (MSKCC) staging (class 2, grade II) should be used to systematically evaluate blood vessel invasion, lymph node metastasis, liver atrophy, and distant metastasis.

Expert Recommendation 2

The Bismuth–Corlette classification (class 1, grade I) should be used to make a preliminary decision on the surgical method used. It is recommended to supplement the Bismuth–Corlette classification with the AJCC- and the UICC-related TNM stagings (class 1, grade I) and the International Cholangiocarcinoma Working Group Staging (class 2, grade II) to predict resectability of HCCA and long survival outcomes after treatment (3).

Preoperative Evaluation

Preoperative evaluation for laparoscopic radical resection of HCCA should be the same as in open surgery and should cover the following:

(1) Evaluation of degree of bile duct involvement: This is the primary target in preoperative evaluation. Magnetic resonance cholangiopancreatography combined with MDCT should be used to evaluate the degree of bile duct invasion, with visual display of the structural characteristics of the whole biliary system, length and extent of tumor involvement, and depth of invasion of bile duct wall (1, 2).
(2) Evaluation of adjacent vascular invasion: Preoperative imaging examinations combined with three-dimensional reconstruction should be used to determine whether adjacent blood vessels are invaded and the location and extent of invasion are important in determining resectability of the tumor.
(3) Three-dimensional CT reconstruction, visualization, and assessment: First, this technique can be used to display the anatomies of intrahepatic bile ducts and blood vessels from multiple angles and multiple levels, thus helping to assess any anatomical anomalies to avoid unnecessary injuries during operation and to better protect the structures and function of the remnant liver (4). Second, this assessment can help to quantitatively analyze tumor volume and volumes of each liver segment and its combination. It can also be used to carry out simulation surgery in planning operations and in selecting an optimal liver transection plane and to calculate residual liver volumes (3, 4).
(4) Evaluation of lymph node metastasis: PET-CT should be used to evaluate lymph node metastasis and extent of involvement.

Expert Recommendation 3

Preoperative MDCT (class 1, grade I) and MRCP (class 1, grade I) should be used routinely to assess the extent of bile duct and blood vessel invasion. Three-dimensional CT reconstruction, visualization, and assessment system (class 2, grade I) should be used routinely to evaluate anomalies of bile ducts and blood vessels and to calculate residual liver volumes. PET-CT is recommended to detect possible lymph node metastasis (class 2, grade II).

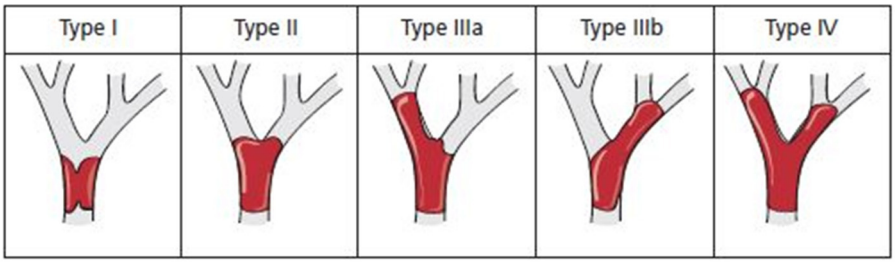

FIGURE 1 | Schematic diagram of the Bismuth–Corlette classification of hilar cholangiocarcinoma (HCCA).

INDICATIONS AND TREATMENT PRINCIPLES FOR LAPAROSCOPIC RADICAL RESECTION OF HCCA

Indications and Contraindications

The indications for laparoscopic radical resection of HCCA should be more stringent than in open surgery. Preoperative CT, MRCP, CT angiography, or magnetic resonance angiography should be used to clarify the relationship between the tumor and the hepatic artery and portal vein and to determine whether there is any invasion. The indications include the Bismuth–Corlette type I, type II, and some types III and IV tumors with no portal vein or hepatic artery invasion. In addition to all the contraindications to open radical resection of HCCA, the contraindications should also include intolerance to prolonged pneumoperitoneum, failure to establish pneumoperitoneum, extensive abdominal adhesions, difficulties in dissecting or exposing the lesion, extensive tumor invasion of portal vein or common hepatic artery, difficulties in obtaining adequate laparoscopic view, or presence of portal hypertension resulting in high surgical risks (4).

Expert Recommendation 4

The indications and contraindications should be strictly followed to select suitable patients for laparoscopic resection of HCCA. The Bismuth–Corlette type I and type II can be successfully resected and reconstructed by using laparoscopic surgery in expert hands. Laparoscopic surgery is also feasible for some Bismuth–Corlette types III and IV. For any Bismuth–Corlette type with tumor invasion of portal vein, common hepatic artery and their branches and vascular resection and reconstruction are recommended, if technically feasible. Otherwise, conversion to open surgery is recommended (class 1, grade I).

Principles of Treatment

The principles of laparoscopic radical resection of HCCA should be the same as in open radical resection of HCCA. The current standard of open surgery includes partial hepatectomy with en bloc resection of the tumor-invaded bile duct, regional lymph node and nerve dissection, and hepatic duct–jejunum Roux-en-Y anastomosis, with emphasis on complete tumor resection (R0 resection) with negative margins, including the invaded bile duct with the adjacent tissues and restoration of biliary-intestinal continuity of the functional residual liver remnant (4, 5). Anatomical liver resection is the standard procedure for HCCA. To achieve R0 resection, it is recommended to carry out intraoperative frozen sections to confirm negative proximal and distal bile duct resection margins (5–8).

Expert Recommendation 5

The principles of laparoscopic radical resection of HCCA should be the same as in open surgery. However, due to the limitations of laparoscopic operations in intraoperative assessment of liver resection margins, it is recommended to routinely perform anatomical major liver resections, e.g., hemihepatectomies or trisectionectomies combined with caudate lobe resection. Limited liver resections aiming to preserve functional liver parenchyma with local excision of adjacent liver parenchyma are not recommended (class 1, grade I).

REQUIREMENTS FOR HOSPITAL CREDENTIALING ON ADEQUATE STAFFING AND SURGICAL EQUIPMENT FOR LAPAROSCOPIC RADICAL RESECTION OF HCCA

In the early phase of promoting this surgery, laparoscopic radial resection of HCCA should only be confined to credentialed hospitals with good experience in major laparoscopic surgeries and with adequate staffing to form a fixed surgical team consisting of a chief surgeon, a first assistant, a scope operator, a scrub nurse, and an anesthesiologist. This surgical team should be proficient in carrying out complex laparoscopic operations, including laparoscopic liver resection and laparoscopic pancreaticoduodenectomy, and has crossed the required learning curves for these operations (recommended number of cases >50 for each of these types of surgery) (9). For surgical equipment, in addition to the conventional laparoscopic equipment and instruments, a good quality laparoscopic system, a LigaSure, ultrasonic knife, or Cavitron Ultrasonic Surgical Aspirator (CUSA) is recommended.

During the process of development and promotion of this surgery, patients should be highly selected during the learning curve to gradually step up from less complex to more complex

operations. The surgical team must have adequate experience in open radical resection of HCCA and the ability to complete the operation when conversion to open surgery is required and to deal with any complications, which may arise out of the laparoscopic operations.

Expert Recommendation 6

Laparoscopic radical resection of HCCA should only be carried out in large medical centers with adequate experience in laparoscopic hepatectomy and laparoscopic pancreaticoduodenectomy, after passing the learning curves, and with adequate experience in complex laparoscopic hepatectomy and bile duct reconstruction (class 1, grade I). There should be a fixed team in carrying out laparoscopic resection of HCCA (class 1, grade I). In the early phase of development, patients with less complex pathologies should be selected. There should be a gradual move to operate on more complex pathologies after accumulation of adequate operative experience (class 1, grade I).

SURGICAL PROCEDURES

Establishment of Operating Ports in Laparoscopic Radical Resection of HCCA

Generally, the five-port technique and split-leg position of patient are used. The port sites are recommended to center on the hepatic hilum in a V-shaped distribution. The specific port sites should be determined according to the planned operative procedure, taking into consideration of the requirements of liver resection and biliary reconstruction. Ancillary ports should be added when needed (**Figure 2**).

Expert Recommendation 7

When establishing the operating ports, the camera port is recommended to be placed under the umbilicus to facilitate reconstruction and anastomosis. The remaining ports should be centered on the hepatic hilum and should be distributed in a V shape. However, specific port layout should be individualized according to the planned operation. Operating ports should be added if necessary to facilitate surgery and to speed up the operative process (class 1, grade I).

Procedures for Intraoperative Laparoscopic Exploration

Routine exploration should be conducted to access whether there is any intraperitoneal metastasis. The hilar region should be dissected to determine the size, location, and extent of the hilar tumor. The depth of tumor involvement of bile duct, the relationship between the tumor with the portal vein and hepatic artery, the extent of vascular invasion, if any, and the involvement of caudate lobe should be assessed to reach to a preliminary decision on the possibility of radical resection and the extent of resection (1, 10–13) (**Figure 2**).

Expert Recommendation 8

Routine laparoscopic exploration should be carried out to exclude peritoneal metastases and small liver metastases. Laparoscopic ultrasonography should be used routinely to increase the accuracy of assessment (class 1, grade I).

Extent of Regional Lymphatic and Nerve Plexus Dissection in Laparoscopic Radical Resection of HCCA

The extent of routine lymphatic and nerve plexus dissection should include the hilar region, hepatoduodenal ligament, tissues around the common hepatic artery, and lymph nodes and nerve plexus behind the head of pancreas. Different surgical approaches can be used according to the usual practice of the surgeon, the extent and location of the tumor, and the approach used in the laparoscopic operation. A combined left- and right-sided approach is recommended.

Left-sided approach: The omental bursa (lesser sac) is opened, followed by dissection of lymph nodes around the common hepatic artery (8a, 8p) and lymph nodes around the celiac trunk. The common hepatic artery and the gastroduodenal artery (the latter can be transected if needed to better expose the portal vein) are slinged and the right gastric artery is transected. Skeletonized dissection of all the lymph nodes, fat, and nerve tissues in the hepatoduodenal ligament (12h, 12e, 12b, 12a, and 12p) then follows. The 13a lymph nodes in the posterior edge of the pancreas are then dissected, together with the lymph nodes adjacent to the abdominal aorta (no. 16).

Right-sided approach: The peritoneum on the side of duodenal peritoneum is opened to dissect the 13a lymph nodes on the posterior edge of pancreas, which should be immediately sent for intraoperative frozen section. If positive, no. 16 lymph nodes need to be removed and if no. 16 lymph nodes are positive, radical resection should be abandoned. If negative, all the tissues in the hepatoduodenal ligament, with the exception of the hepatic artery and portal vein are removed en bloc. The lymph nodes around the common hepatic artery (8a, 8p) and those around the celiac trunk, together with the surrounding fatty tissues, are then dissected (14–16) (**Figure 2**).

Expert Recommendation 9

Lymph node dissection should be standardized. Attention should be paid in protecting the surrounding blood vessel walls. There is no special rule for the sequence of dissection. Appropriate sequences of regional lymph node and nerve plexus dissection should be based on the intraoperative findings, the laparoscopic approaches used, and the usual practice of the operating surgeon (class 1, grade I).

Important Technical Points to Achieve Laparoscopic R0 Resection of HCCA

During laparoscopic surgery, the relatively small operating space of the hilum can be zoomed in to allow anatomical structures of the hilum to be displayed more clearly and three-dimensionally.

To dissect the hepatic hilum, the common bile duct is first isolated, ligated at the upper edge of the pancreas, and then transected. The lower resection margin of the bile duct should routinely be sent for frozen section examination. Bile duct dissection is then continued from a caudal to cranial direction.

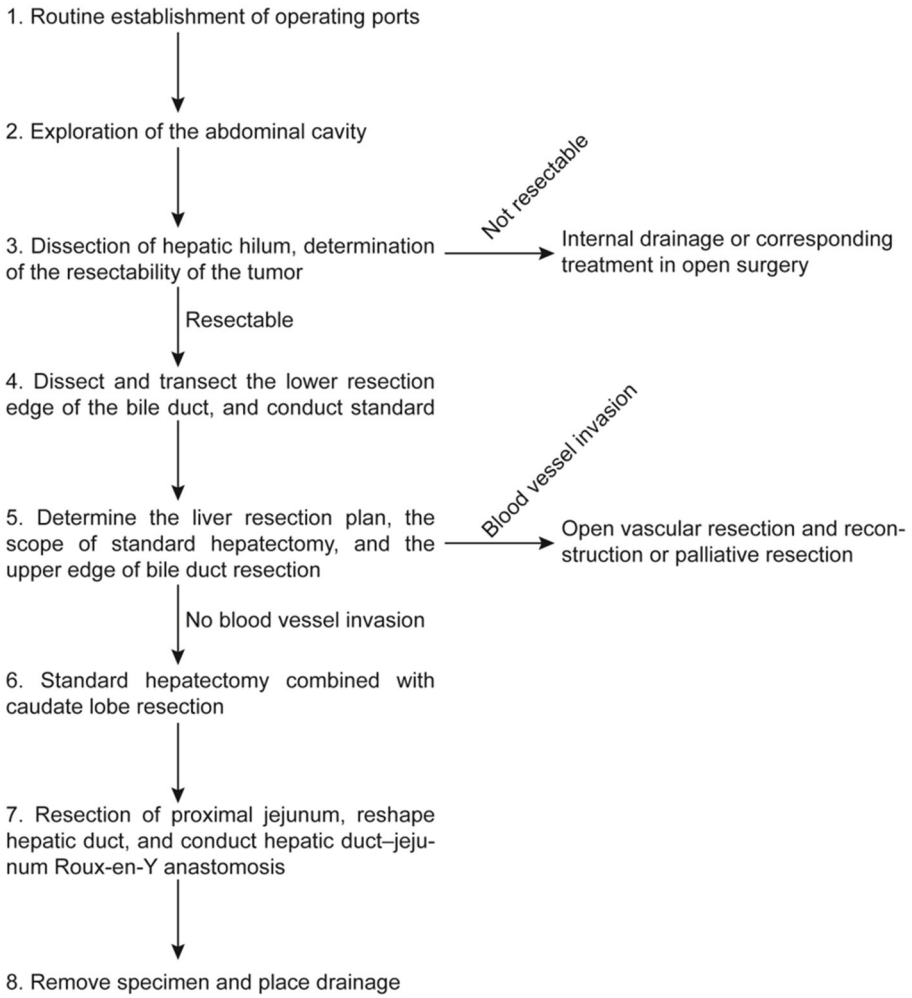

FIGURE 2 | Operation flowchart. This operation procedure was based on the recommendations of the experts who participated in the consensus meeting to provide a clinical reference for less experienced surgeons. Surgeons should carry out his/her operation procedures according to the specific situations during operation.

The skeletonized hepatic artery and portal vein are suspended to facilitate subsequent procedures. After assessing the extent of tumor invasion of the bile duct for resectability, the hepatic artery, portal vein, and their branches are dissected to determine whether the tumor has any vascular invasion. If the blood vessel supplying the hemiliver, which is planned to be preserved is found to be invaded, the surgery should be converted to open surgery. For any difficulties in determining the upper extent of biliary involvement by tumor, the liver parenchyma can be split to reveal the upper extent of the HCCA. When the upper extent of tumor has far exceeded the U point or P point, palliative surgery in reducing jaundice can be carried out. For resectable HCCA, the hepatic duct on the side of the liver to be preserved should be resected and the upper resection margin of the bile duct should be sent for frozen section examination. Repeated frozen sections and pathological examinations during the operation should be done to ensure negative resection margins with R0 resection (10, 15) (**Figure 2**).

Expert Recommendation 10

The hilar structures should be dissected to clarify whether the tumor has invaded blood vessels and to determine the extent of anatomical liver resection and the extent of bile duct resection based on preoperative and intraoperative findings. During the operation, frozen sections should be repeatedly conducted to assure negative margins of bile ducts, blood vessels, and liver to achieve R0 resection (class 1, grade I).

Important Technical Points in Handling the Caudate Lobe

In laparoscopic radical resection of HCCA, when combined with anatomical hemihepatectomy, extended hemihepatectomy, or trisectionectomy, the short hepatic veins can be clearly seen laparoscopically, thus facilitating en bloc resection of the caudate lobe.

Turning the liver and Spigelian lobe to the right allows good exposure for ligation and division of the short hepatic veins

on the left side of the inferior vena cava upto the suprahepatic portion. The short hepatic veins on the right of the inferior vena cava are dealt with using the right-sided approach with dissection from bottom to top. As for the short hepatic veins near the confluence of hepatic veins, it is safer to treat them after splitting the liver parenchyma down to the inferior vena cava (15–17). The thin backflow branches of the short hepatic veins can be transected with an ultrasonic knife or LigaSure and the larger branches can be transected after ligation. If necessary, they can be transected and sutured. After the portal vein branches to the caudate lobe are exposed and disconnected, the whole caudate lobe together with the resected portion of liver containing the resected bile ducts with the tumor can be resected en bloc (18, 19) (**Figure 2**).

Expert Recommendation 11

A combined approach to mobilize the caudate lobe from left to right and from right to left to deal with the short hepatic veins should be used. After complete mobilizing the caudate lobe, the portion of the liver to be resected together with the bile ducts containing the tumor can be resected en bloc (class 2, grade II).

Important Technical Points on Liver Resection in Laparoscopic Radical Resection of HCCA

The important technical points on liver resection in laparoscopic radical resection of HCCA are roughly the same as those in laparoscopic or open hepatectomy for other liver tumors or hepatolithiasis. The main difference lies in that in laparoscopic hepatectomy for HCCA, special efforts should be made to combine preoperative imaging (including three-dimensional reconstruction) and intraoperative findings to determine the plane and extent of liver resection (e.g., left or right hemihepatectomy, extended left or right hemihepatectomy) plus caudate lobe resection.

When right hepatectomy plus total caudate lobectomy is required for a patient with HCCA, the surgeon should choose instruments for liver parenchymal transection that he/she is most familiar with (such as an ultrasound knife or a laparoscopic CUSA). After ligating and dividing the right hepatic artery and the right portal vein, the liver parenchyma can be transected from a caudal to cranial direction along the ischemic line on the liver surface. Small blood vessels (<3 mm) on the transected liver raw area can be cauterized, while larger and thicker branches are transected after ligation. The right hepatic vein can be treated with an endoscopic cutting and vascular closure device (10, 20–22). The short hepatic veins are then transected along the inferior vena cava. After dividing the hepatocaval ligament and mobilizing the caudate lobe, the whole resected specimen can be removed en bloc (23, 24).

Left hepatectomy plus total caudate lobectomy is technically similar to the right-sided operation, although the operation is relatively easier. Patients with the Bismuth–Corlette type IV HCCA should be strictly and carefully selected. The surgical operation should be chosen based on the location of tumor, the extent of bile duct invasion, and any atrophy affecting the liver. Extended right hepatectomy, extended left hepatectomy, or resection of right or left hemiliver can be carried out in well-selected patients. A right-sided liver resection is safer than a left-sided liver resection because the right hepatic artery runs behind the common hepatic duct and is more susceptible to invasion by tumor and there is a longer length of the left hepatic duct than the right hepatic duct (25, 26) (**Figure 2**).

Expert Recommendation 12

Accurate preoperative and intraoperative decision on the extent of liver resection and the plane of liver transection are the key technical points for laparoscopic radical resection of HCCA. In the process of liver resection, tumor-free resection margins of bile ducts, blood vessels, and liver planes should be achieved. In the presence of severe liver cirrhosis or insufficient preoperative jaundice reduction, combined major hepatectomy aiming to achieve R0 resection should not be aggressively carried out. Palliative surgery should be used as an alternative treatment to ensure safety of the patient (class 2, grade II).

Important Technical Points on Hepatic Duct–Jejunum Anastomosis for Laparoscopic Radical Resection of HCCA

The technique of laparoscopic hepatic duct–jejunum anastomosis is more difficult and more demanding when compared with open surgery. When the open end of the hepatic duct is relatively large and its position is shallow, anastomosis is easier; otherwise, it can be technically very difficult. The number of hepatic duct openings on the liver remnant would depend on the plane and extent of resection.

For the hepatic duct–jejunum anastomosis, whether the anastomosis should be completed antecolic or retrocolic would depend on the body build of the patient and the findings of the operation. Tension should be avoided. Before the anastomosis, the hepatic duct should be properly shaped and anastomosed to a Roux-en Y jejunal loop. Continuous suturing is recommended for the posterior wall and for the anterior wall either continuous or intermittent suturing can be used, according to the size, position, and angle of the bile duct (10, 21, 27). For type IIIb HCCA, resection is relatively easier, but the right hepatic duct to jejunum anastomosis is more difficult. Right hemihepatectomy plus caudate lobectomy for type IIIa HCCA is technically more difficult, but the hepatic duct and jejunum reconstruction are relatively easier (28–31). The intestinal–intestinal anastomosis should be more than 45–60 cm away from the biliary–enteric anastomosis. If necessary, an external drainage decompression tube can be placed across the hepatic–enteric anastomosis (**Figure 2**).

Expert Recommendation 13

For HCCA, bile duct resection should be combined with major liver resection plus caudate lobe resection. When the number of bile ducts left in the liver remnant is large, temporary stay stitches can help to expose the bile duct openings to improve the quality of the cholangiojejunostomy. For those patients with difficult anastomoses, conversion to open surgery by using a median small incision to construct a difficult anastomosis helps. Placement of an external drainage decompression tube can help in better

healing of the anastomosis. For patients who cannot undergo major liver resection, palliative resection or bile duct–jejunum bypass should be considered (class 1, grade I).

Important Technical Points in Managing the Raw Transected Liver Surfaces, Placement of Drainage Tubes, and Removal of Specimens

After liver transection, the raw liver surface should be carefully inspected. Small biliary leakage and bleeding points should be closed by using suitable sutures (10, 22, 30, 31). The resected specimen should be placed into a specimen bag and removed through a small suprapubic transverse incision in the lower abdomen. A drainage tube should be routinely placed below the biliary–enteric anastomosis and on the raw liver area. The specimen should be routinely examined histopathologically to determine the tumor location and the extent of tumor involvement (**Figure 2**).

Expert Recommendation 14

The transected raw liver surface should be careful dealt with to stop all the bleeding and bile leakage points. Drainage tubes should be placed posterior to the biliary–enteric anastomosis and on the raw liver area. Care should be taken to ensure that the drainage tubes are not obstructed by kinking (class 1, grade I).

Laparoscopic Radical Resection for Patients With HCCA Requiring Vascular Resection and Reconstruction

Hilar cholangiocarcinoma resection, when combined with vascular resection and reconstruction, can lead to a higher chance of achieving R0 resection for patients with vascular invasion, thereby improving survival of these patients (32, 33). Invasion of blood vessels significantly increases the difficulty of laparoscopic radical resection of HCCA. Resection and reconstruction of hilar blood vessels under laparoscopic surgery are technically difficult. Once invasion of portal vein or hepatic artery supplying the planned-preserved hemiliver or the main trunks is found during operation, conversion to open surgery is recommended (**Figure 2**).

Expert Recommendation 15

If vascular resection and reconstruction are necessary due to invasion found on the hemiliver, which is planned to be preserved, prompt conversion to laparotomy is recommended (class 1, grade I).

INDICATIONS FOR CONVERSION TO LAPAROTOMY

Conversion to laparotomy should be carried out for the following conditions: uncontrollable bleeding; intolerance to pneumoperitoneum; difficulties in exposing or resecting the lesion; intraoperative detection of invasion of main vascular trunk or blood vessels of the side of the liver to be preserved; multiple open ends of the transected bile duct; difficulty in bile duct reshaping and biliary–intestinal anastomosis; unsatisfactory anastomosis; or difficulty/failure to continue the operation under laparoscopy. Timely conversion to laparotomy can reduce serious complications and is beneficial to patients.

Expert Recommendation 16

Timely conversion to laparotomy to ensure safety of the patient should be the primary consideration for laparoscopic surgeons (class 1, grade I).

SUMMARY

Laparoscopic radical resection of HCCA is technically difficult and it is still associated with high operative risks. Appropriate patients should be carefully selected. This surgical approach should be promoted carefully and gradually. It is recommended that only hepatobiliary and pancreatic laparoscopic surgery centers in large general hospitals with adequate experience in laparoscopic operations in other less complex hepaticopancreatobiliary operations should be acquired before attempting to develop this operation to come up with a safe and feasible operation for others to follow. It is also recommended to conduct clinical studies on this operation, focusing on safety of the patient and treatment effectiveness after standardizing the surgical procedures involved in this operation. The ultimate aim is to improve the quality and quantity of life for patients with HCCA.

DATA AVAILABILITY STATEMENT

The original contributions presented in the study are included in the article/supplementary material, further inquiries can be directed to the corresponding author/s.

AUTHOR CONTRIBUTIONS

All authors listed have made a substantial, direct, and intellectual contribution to the work and approved it for publication.

FUNDING

Doctoral research start-up fund of North Sichuan Medical College (201901 to YX) Project of multicentre clinical research of Shanghai Jiaotong University School of Medicine (DLY201807, to TZ). We declare that all sources of funding received for the research being submitted.

ACKNOWLEDGMENTS

Thanks to all the experts who participated in the formulation of the recommendations; they were Chen Yajin (Sun Yat-sen Memorial Hospital of Sun Yat-sen University), Qiu Yudong (Gulou Hospital Affiliated to Medical College of Nanjing University), Li Jing (Editorial Department of Chinese Journal of Surgery), Li Jiangtao (Affiliated Hospital of the Second

Hospital of Zhejiang University), LJ (Affiliated Hospital of North Sichuan Medical College), Xiong Yongfu (Affiliated Hospital of North Sichuan Medical College), Li Fuyu (West China Hospital of Sichuan University), He Yu (Southwest Hospital Affiliated to Army Military Medical University), Liu Houbao (Zhongshan Hospital Affiliated to Fudan University in Shanghai), Liu Jianhua (Second Affiliated Hospital of Hebei Medical University), Geng Zhimin (Xi'an Jiaotong University), Liang Xiao (Run Run Shaw Hospital Affiliated to Zhejiang University), Peng Bing (West China Hospital of Sichuan University), Wang Jian (Renji Hospital Affiliated to Tongji Medical College of Huazhong University of Science and Technology), Wang Jianming (Tongji Hospital Affiliated to Tongji Medical College of Huazhong University of Science and Technology), Zhang Yongjie (Oriental Hepatobiliary Surgery Hospital Affiliated to Naval Military Medical University), Zheng Shuguo (Southwest Hospital Affiliated to Army Military Medical University), Yin Xinmin (Hunan Provincial People's Hospital), Yang Yang (Third Affiliated Hospital of Sun Yat-sen University), Tang Chao Hui (Xinhua Hospital Affiliated to Shanghai Jiaotong University Medical College), and Lau Wan Yee (Prince of Wales Hospital, the Chinese University of Hong Kong).

REFERENCES

1. China A-cAO. Guideline for the diagnosis and therapy of hilar cholangiocarcinoma (2015). *Chin J Hepatobil Surg.* (2015). 21:505–11. doi: 10.3760/cma.j.issn.1007-8118.2015.08.001
2. Sharpe SM, Talamonti MS, Wang CE, Prinz RA, Roggin KK, Bentrem DJ, et al. Early national experience with laparoscopic pancreaticoduodenectomy for ductal adenocarcinoma: a comparison of laparoscopic pancreaticoduodenectomy and open pancreaticoduodenectomy from the national cancer data base. *J Am Coll Surg.* (2015) 221:175–84. doi: 10.1016/j.jamcollsurg.2015.04.021
3. Deoliveira ML, Schulick RD, Nimura Y, Rosen C, Gores G, Neuhaus P, et al. New staging system and a registry for perihilar cholangiocarcinoma. *Hepatology.* (2011) 53:1363–71. doi: 10.1002/hep.24227
4. Zhang J, Qiao QL, Guo XC, Zhao JX. Application of three-dimensional visualization technique in preoperative planning of progressive hilar cholangiocarcinoma. *Am J Transl Res.* (2018) 10:1730–5.
5. Cho A, Yamamoto H, Kainuma O, Muto Y, Yanagibashi H, Tonooka T, et al. Laparoscopy in the management of hilar cholangiocarcinoma. *World J Gastroenterol.* (2014) 20:15153–7. doi: 10.3748/wjg.v20.i41.15153
6. Zhang CW, Liu J, Hong DF, Wang ZF, Hu ZM, Huang DS, et al. Pure laparoscopic radical resection for type IIIa hilar cholangiocarcinoma. *Surg Endosc.* (2018) 32:1581–2. doi: 10.1007/s00464-017-5741-4
7. Zhi-qiang H. Management of hilar cholangiocarcinoma: review of a 25-year experience. *Chin J Digest Surg*. (2010). 9:161–4. doi: 10.3760/cma.j.issn.1673-9752.2010.03.001
8. Öter V, Özer I, Dalgiç T, Binarbaşi C, Ulaş M, Bostanci EB. Results of positive proximal margin after resection for hilar cholangiocarcinoma: an analysis of 42 cases. *Turk J Gastroenterol.* (2019) 30:88–94. doi: 10.5152/tjg.2018.17752
9. Tan CL, Zhang H, Peng B, Li KZ. Outcome and costs of laparoscopic pancreaticoduodenectomy during the initial learning curve vs laparotomy. *World J Gastroenterol.* (2015) 21:5311–9. doi: 10.3748/wjg.v21.i17.5311
10. Yin Xinming LY, Wei C, Yifei W, Yi L, Siwei Z, Chunhong L. Clinical application value of total laparoscopic radical resection of IV-type hilar choangiocarcinoma: video attached. *Chin J Hepat Surg.* (2018) 7:110—4. doi: 10.3877/cma.j.issn.2095-3232.2018.02.007
11. Puntambekar S, Sharma V, Kumar S, Mitkare S, Joshi G, Parikh H. Laparoscopic management of hilar cholangiocarcinoma: a case report. *Ind J Surg.* (2016) 78:57–9. doi: 10.1007/s12262-015-1345-1
12. Ito F, Agni R, Rettammel RJ, Been MJ, Cho CS, Mahvi, DM, et al. Resection of hilar cholangiocarcinoma: concomitant liver resection decreases hepatic recurrence. *Ann Surg.* (2008) 248:273–9. doi: 10.1097/SLA.0b013e31817f2bfd
13. Association for Medical and Healthcare; Pancreas Minimally Invasive Group in Pancreatic Diseases Committee of Chinese Research Hospital Association; Pancreas Minimally Invasive Group in Pancreatic Cancer Committee of Chinese Anti-Cancer Association Expert consensus of laparoscopic pancreaticoduodenectomy(postscript of operation process and main steps). *Zhonghua Wai Ke Za Zhi*. (2017). 55:335–9. doi: 10.3760/cma.j.issn.0529-5815.2017.05.004
14. Mayo SC, Austin DF, Sheppard BC, Mori M, Shipley DK, Billingsley KG. Evolving preoperative evaluation of patients with pancreatic cancer: does laparoscopy have a role in the current era? *J Am Coll Surg.* (2009) 208:87–95. doi: 10.1016/j.jamcollsurg.2008.10.014
15. Yi B, Zhang BH, Zhang YJ, Jiang XQ, Zhang BH, Yu WL, et al. Analysis of the relation between surgery and prognosis of hilar cholangiocarcinoma. *Zhonghua Wai Ke Za Zhi.* (2005) 43:842–5. doi: 10.3760/j:issn:0529-5815.2005.13.004
16. Molina V, Sampson J, Ferrer J, Sanchez-Cabus S, Calatayud D, Pavel MC, et al. Klatskin tumor: diagnosis, preoperative evaluation and surgical considerations. *Cir Esp.* (2015) 93:552–60. doi: 10.1016/j.cireng.2015.07.002
17. Han IW, Jang JY, Kang MJ, Kwon W, Park JW, Chang YR, et al. Role of resection for Bismuth type IV hilar cholangiocarcinoma and analysis of determining factors for curative resection. *Ann Surg Treat Res.* (2014) 87:87–93. doi: 10.4174/astr.2014.87.2.87
18. Gumbs AA, Jarufe N, Gayet B. Minimally invasive approaches to extrapancreatic cholangiocarcinoma. *Surg Endosc.* (2013) 27:406–14. doi: 10.1007/s00464-012-2489-8
19. Ercolani G, Zanello M, Grazi GL, Cescon M, Ravaioli M, Del Gaudio M, et al. Changes in the surgical approach to hilar cholangiocarcinoma during an 18-year period in a Western single center. *J Hepatobiliary Pancreat Sci.* (2010) 17:329–37. doi: 10.1007/s00534-009-0249-5
20. Bryant R, Laurent A, Tayar C, Cherqui D. Laparoscopic liver resection-understanding its role in current practice: the Henri Mondor Hospital experience. *Ann Surg.* (2009) 250:103–11. doi: 10.1097/SLA.0b013e3181ad6660
21. Hidalgo E, Asthana S, Nishio H, Wyatt J, Toogood GJ, Prasad KR, et al. Surgery for hilar cholangiocarcinoma: the Leeds experience. *Eur J Surg Oncol.* (2008) 34:787–94. doi: 10.1016/j.ejso.2007.10.005
22. Zheng S, Zhenping HE, Dong J, Wang S, Bie P, Cai J, et al. Twenty-year experience in surgical treatment of hilar cholangiocarcinoma. *Chin J Gen Surg.* (2001) 10:6–10. doi: 10.3969/j.issn.1005-6947.2001.01.003
23. Shu-you PJ-tL. Choice of surgical procedures for hilar cholangiocarcinoma. *J Clin Surg*. (2006). 14:70—2. doi: 10.3969/j.issn.1005-6483.2006.02.005
24. Jang JY, Kim SW, Park DJ, Ahn YJ, Yoon YS, Choi MG, et al. Actual long-term outcome of extrahepatic bile duct cancer after surgical resection. *Ann Surg.* (2005) 241:77–84. doi: 10.1097/01.sla.0000150166.94732.88
25. Palanivelu C, Jani K, Senthilnathan P, Parthasarathi R, Rajapandian S, Madhankumar MV. Laparoscopic pancreaticoduodenectomy: technique and outcomes. *J Am Coll Surg.* (2007) 205:222–30. doi: 10.1016/j.jamcollsurg.2007.04.004
26. Kendrick ML, Cusati D. Total laparoscopic pancreaticoduodenectomy: feasibility and outcome in an early experience. *Arch Surg.* (2010). 145:19–23. doi: 10.1001/archsurg.2009.243
27. Yu H, Wu SD, Chen DX, Zhu G. Laparoscopic resection of Bismuth type I and II hilar cholangiocarcinoma: an audit of 14 cases from two institutions. *Dig Surg.* (2011) 28:44–9. doi: 10.1159/000322398
28. Lu Z, Wang DD. Operation treatment method of Bismuth-Corlette III, IV hilar cholangiocarcinoma. *Zhonghua Wai Ke Za Zhi.* (2016) 54:488–91. doi: 10.3760/cma.j.issn.0529-5815.2016.07.003

29. Machado MAC, Makdissi FF, Surjan RC, Mochizuki M. Laparoscopic resection of hilar cholangiocarcinoma. *J Laparoendosc Adv Surg Tech A*. (2012) 22:954–6. doi: 10.1089/lap.2012.0339
30. Han HS, Cho JY, Yoon YS, Hwang DW, Kim YK, Shin HK, et al. Total laparoscopic living donor right hepatectomy. *Surg Endosc*. (2015) 29:184. doi: 10.1007/s00464-014-3649-9
31. Rassam F, Roos E, van Lienden KP, van Hooft JE, Klümpen HJ, van Tienhoven G, et al. Modern work-up and extended resection in perihilar cholangiocarcinoma: the AMC experience. *Langenbecks Arch Surg*. (2018) 403:289–307. doi: 10.1007/s00423-018-1649-2
32. Li JD, Zhao ZL. Current status of laparoscopic techniques in the surgical treatment of biliary carcinoma. *Zhonghua Wai Ke Za Zhi*. (2018) 56:338–41. doi: 10.3760/cma.j.issn.0529-5815.2018.05.004
33. Lee Y, Choi D, Han S, Han IW, Heo JS, Choi SH. Comparison analysis of left-side versus right-side resection in bismuth type III hilar cholangiocarcinoma. *Ann Hepatobiliary Pancreat Surg*. (2018) 22:350–8. doi: 10.14701/ahbps.2018.22.4.350

Conflict of Interest: The authors declare that the research was conducted in the absence of any commercial or financial relationships that could be construed as a potential conflict of interest.

frontiers in Surgery

SYSTEMATIC REVIEW
published: 02 December 2021
doi: 10.3389/fsurg.2021.752009

Comparison of Clinical Efficacy and Safety Between da Vinci Robotic and Laparoscopic Intersphincteric Resection for Low Rectal Cancer: A Meta-Analysis

Jie Zhang [1,2†], Xingshun Qi [3†], Fangfang Yi [2,3†], Rongrong Cao [3,4], Guangrong Gao [1] and Cheng Zhang [1]*

[1] Department of General Surgery, General Hospital of Northern Theater Command (Formerly Called General Hospital of Shenyang Military Area), Shenyang, China, [2] Postgraduate College, Dalian Medical University, Dalian, China, [3] Department of Gastroenterology, General Hospital of Northern Theater Command (Formerly Called General Hospital of Shenyang Military Area), Shenyang, China, [4] Postgraduate College, Jinzhou Medical University, Jinzhou, China

OPEN ACCESS

Edited by:
Patrick J. Schuler,
Ulm University Medical Center, Germany

Reviewed by:
Luca Morelli,
University of Pisa, Italy
Rocco Cappellesso,
University Hospital of Padua, Italy

***Correspondence:**
Cheng Zhang
cz1791@163.com

[†] These authors share first authorship

Specialty section:
This article was submitted to Surgical Oncology, a section of the journal Frontiers in Surgery

Received: 02 August 2021
Accepted: 02 November 2021
Published: 02 December 2021

Citation:
Zhang J, Qi X, Yi F, Cao R, Gao G and Zhang C (2021) Comparison of Clinical Efficacy and Safety Between da Vinci Robotic and Laparoscopic Intersphincteric Resection for Low Rectal Cancer: A Meta-Analysis. Front. Surg. 8:752009. doi: 10.3389/fsurg.2021.752009

Background and Aims: The intersphincteric resection (ISR) is beneficial for saving patients' anus to a large extent and restoring original bowel continuity. Laparoscopic ISR (L-ISR) has its drawbacks, such as two-dimensional images, low motion flexibility, and unstable lens. Recently, da Vinci robotic ISR (R-ISR) is increasingly used worldwide. The purpose of this article is to compare the feasibility, safety, oncological outcomes, and clinical efficacy of R-ISR vs. L-ISR for low rectal cancer.

Methods: PubMed, EMBASE, Cochrane Library, and Web of Science were searched to identify comparative studies of R-ISR vs. L-ISR. Demographic, clinical, and outcome data were extracted. Mean difference (MD) and risk ratio (RR) with their corresponding confidence intervals (CIs) were calculated.

Results: Five studies were included. In total, 510 patients were included, of whom 273 underwent R-ISR and 237 L-ISR. Compared with L-ISR, R-ISR has significantly lower estimated intraoperative blood loss (MD = −23.31, 95% CI [−41.98, −4.64], $P = 0.01$), longer operative time (MD = 51.77, 95% CI [25.68, 77.86], $P = 0.0001$), hospitalization days (MD = −1.52, 95% CI [−2.10, 0.94], $P < 0.00001$), and postoperative urinary complications (RR = 0.36, 95% CI [0.16, 0.82], $P = 0.02$).

Conclusions: The potential benefits of R-ISR are considered as a safe and feasible alternative choice for the treatment of low rectal tumors.

Keywords: da Vinci robot, intersphincteric resection, laparoscope, low rectal cancer, clinical efficacy

INTRODUCTION

According to recent cancer statistics, colorectal cancer is the third most common malignancy (1). However, 75% of rectal cancer is low rectal cancer, which is usually defined as the lower rectum within 5 cm from the anal verge (2). Surgery is considered the first choice for low rectal cancer. The treatment goal for surgeons is to preserve anal function under the premise of tumor resection in low rectal cancer. Abdominoperineal resection has been the standard surgery for advanced low rectal cancer for over a century, but its efficacy was less than satisfactory, resulting in a permanent colostomy, which greatly influences the patient's quality of life (3). In recent years, several new techniques have emerged aiming to preserve anal function under the premise of tumor resection in low rectal cancer. Intersphincteric resection (ISR) is one of the new operations, based on the dissection of the anatomical plane between the internal anal sphincter and the external anal sphincter, making it possible to increase the preservation of the sphincter and avoid a permanent colostomy (4, 5).

The laparoscope has the effect of magnifying the field of vision, which is more clear than open surgery. It can avoid the blindness of resection of the low pelvic tumor. In addition, it can also avoid tumor implantation caused by compression (6–8). Meanwhile, in many studies, laparoscope had lower blood loss, less analgesics, better recovery speed and quality, earlier restoration of intestinal function, and shorter hospital stay as compared with open surgery (6–8). However, laparoscope has its drawbacks, such as two-dimensional images, low motion flexibility, and unstable lens. For obese patients and male patients with pelvic stenosis, laparoscopic visual field exposure and operation space are particularly limited, which not only makes the anatomy difficult, but also easily damages the pelvic autonomic nerve during operation. In addition, the surgeons have to stand for a long time during the operation, which increases their fatigue. At the same time, laparoscopic surgery requires the coordination of the operator and the lens holder. These objective factors have limited the development of laparoscopic ISR (L-ISR). By comparison, da Vinci robotic ISR (R-ISR) has more advantages, such as three-dimensional vision, tremor filtering, flexible EndoWrist instruments, and better ergonomics to reduce fatigue (9–12).

The purpose of this article is to compare the feasibility, safety, clinical efficacy, and short-term oncological outcomes of L-ISR vs. R-ISR for the treatment of low rectal cancer.

METHODS

Registration

This meta-analysis was registered on the PROSPERO database and performed in accordance with the preferred reporting items for systematic review and meta-analysis (PRISMA) guidelines (13). The registration number of PROSPERO was CRD42021265545.

Search Strategy

The relevant publications were searched *via* PubMed, EMBASE, Cochrane library, and Web of Science databases. The search items were as follows: (rectal neoplasms OR rectal cancer OR rectal adenocarcinoma OR rectal tumor OR rectum cancer OR rectum adenocarcinoma OR rectum tumor) AND (da Vinci robot OR da Vinci OR robotics OR robot OR robotic OR robotically OR robot-assisted OR robotic-assisted) AND (laparoscopy OR laparoscope OR laparoscopic) AND (ISR OR internal sphincterectomy OR intersphincteric resection). The date of the last search was July 20, 2021.

Study Selection

The inclusion criteria were as follows: (1) Patients should be histologically diagnosed with low rectal cancer; (2) R-ISR should be the treatment choice in the experimental group, and L-ISR should be the treatment choice in the control group; (3) studies should provide the data regarding feasibility, safety, clinical efficacy, and/or short-term oncological outcomes; and (4) the publication language was not limited. The exclusion criteria were as follows:(1) duplicate articles; (2) review articles; (3) comments and correspondences; (4) meta-analyses; (5) irrelevant topics; (6) case reports; (7) unable to extract the data regarding patients with low rectal cancer; and (8) overlapping data.

Data Extraction

Data were extracted from the included studies by two reviewers independently. The following data were extracted, including first author, publication year, regions, number of patients, age, gender, BMI, American Society of Anesthesiologists (ASA) score, proportion of radiotherapy and chemotherapy, distance from the tumor to the anus, intraoperative blood loss, operative time, lymph node harvest, circumferential resection margin, distal resection margin, conversion rate, time to first flatus, time to postoperative diet, duration of hospital stay, postoperative complications, anastomotic leakage, postoperative ileus, postoperative urinary complications, and intra-abdominal abscess.

Study Quality Assessment

The Newcastle-Ottawa Scale (NOS) was used to evaluate the quality of non-randomized studies. The scale consists of three parts, namely, selection of research subjects (4 points), intergroup comparability (2 points), and outcome measurement (3 points). The highest score should be 9 points. A score of <6 points is considered to be of low quality, while a score of ≥ 6 points is considered to be of high quality.

Statistical Analysis

The difference was compared between L-ISR vs. R-ISR for the treatment of low rectal cancer. Only a random-effect model was employed. Continuous data were expressed as mean difference (MD) with a 95% CI as the effect size. For dichotomous variables, pooled risk ratios (RRs) with 95% CI were calculated to assess the treatment efficacy. $P < 0.05$ was considered as a statistically

Abbreviations: ISR, intersphincteric resection; R-ISR, robotic intersphincteric resection; L-ISR, laparoscopic intersphincteric resection; TME, total mesorectal excision; NOS, Newcastle-Ottawa Scale; RR, risk ratio; MD, mean difference; CI, confidence interval; BMI, body mass index; ASA, American Society of Anesthesiologists.

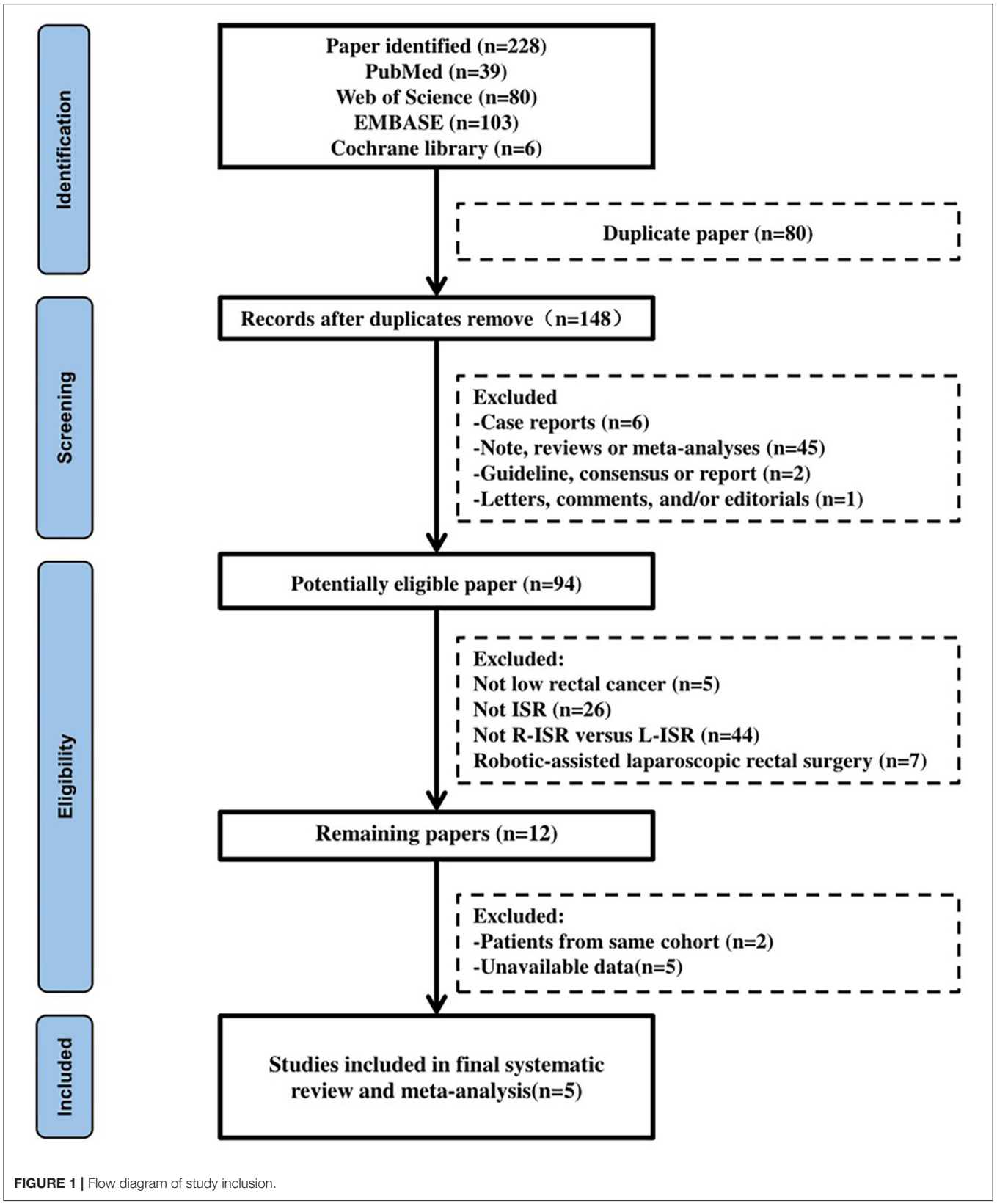

FIGURE 1 | Flow diagram of study inclusion.

TABLE 1 | Characteristics of included studies.

References	Setting		Study Design	Enrollment period		Patients, n	
	Country	Institution		Start	End	R-ISR	L-ISR
Baek et al. (14)	Korea	Single	Retrospective cohort study	2007.01	2010.12	47	**37**
Park et al. (16)	Korea	Single	Retrospective cohort study	2008.03	2011.03	40	40
Kuo et al. (18)	Korea	Single	Retrospective cohort study	2009.11	2013.07	36	28
Park et al. (17)	Korea	Multi	Retrospective cohort study	2008.01	2011.05	106	106
Yoo et al. (15)	Taiwan, China	Single	Retrospective cohort study	2006.09	2011.08	44	26

R-ISR, robotic intersphincteric resection; L-ISR, laparoscopic intersphincteric resection.

significant difference. The heterogeneity was evaluated by the I^2 statistics and chi-square test. $I^2 > 50\%$ and/or $P < 0.1$ were considered to have a statistically significant heterogeneity. Publication bias was not assessed by the funnel plot due to a small number of included studies. Data were analyzed using the Review Manager Version 5.4 (Cochrane collaboration, the Nordic Cochrane Centre, Copenhagen, Denmark).

RESULTS

Study Selection

A total of 228 articles were identified: 39 articles in the PubMed database, 103 articles in EMBASE database, 6 articles in the Cochrane Library database, and 80 papers in Web of Science. Five studies were finally included (**Figure 1**) (14–18). All five studies were of retrospective nature. Four studies were conducted in Korea, and one study in Taiwan. The characteristics of studies are shown in **Table 1**.

Characteristics of Study Participants

A total of 510 patients were analyzed: 273 patients underwent R-ISR and 237 patients L-ISR. The sample size varied from 26 to 106 among these studies, and 68.6% (350/510) of patients were men. With respect to the chemoradiotherapy, 63% (172/273) of patients undergoing R-ISR and 42.6% (101/207) of patients undergoing L-ISR were treated by chemoradiotherapy, respectively. The characteristics of patients are shown in **Table 2**.

Study Quality

The study quality assessment is shown in **Table 3**. All of the five studies were of high quality.

Meta-Analyses

Intraoperative Blood Loss

Intraoperative blood loss was significantly lower in patients undergoing R-ISR than in those undergoing L-ISR (MD = −23.31, 95% CI [−41.98, −4.64], $P = 0.01$) (**Figure 2A**). Among the studies, the heterogeneity was not significant ($I^2 = 24\%$, $P = 0.26$).

Operative Time

Operative time of R-ISR was significantly longer than that of L-ISR (MD = 51.77, 95% CI [25.68, 77.86], $P = 0.0001$) (**Figure 2B**). Among the studies, the heterogeneity was significant ($I^2 = 68\%$, $P = 0.03$).

Number of Retrieved Lymph Nodes

The number of lymph node harvested was not significantly different between patients undergoing R-ISR and L-ISR (MD = −1.83, 95% CI [−3.70, 0.04], $P = 0.06$) (**Figure 2C**). Among the studies, the heterogeneity was not significant ($I^2 = 30\%$, $P = 0.22$).

Circumferential Resection Margin

Circumferential resection margin was not significantly different between patients undergoing R-ISR and L-ISR (RR = 0.65, 95% CI [0.31, 1.36], $P = 0.25$) (**Figure 2D**). Among the studies, the heterogeneity was not significant ($I^2 = 0\%$, $P = 0.60$).

Distal Resection Margin

Distal resection margin was not significantly different between patients undergoing R-ISR and L-ISR (MD = 0.01, 95% CI [−0.16, 0.18], $P = 0.88$) (**Figure 2E**). Among the studies, the heterogeneity was not significant ($I^2 = 0\%$, $P = 0.50$).

Conversion Rate

Conversion rate was not significantly different between patients undergoing R-ISR and L-ISR (RR = 0.23, 95% CI [0.05, 1.12], $P = 0.07$) (**Figure 2F**). Among the studies, the heterogeneity was not significant ($I^2 = 0\%$, $P = 0.40$).

Time to First Flatus

Time to first flatus was not significantly different between patients undergoing R-ISR and L-ISR (MD = −0.21, 95% CI [−0.75, 0.33], $P = 0.44$) (**Figure 3A**). Among the studies, the heterogeneity was not significant ($I^2 = 0\%$, $P = 0.51$).

Time to Resume a Regular Diet

Time to resume regular diet was not significantly different between patients undergoing R-ISR and L-ISR (MD = −0.20, 95% CI [−0.67, 0.27], $P = 0.41$) (**Figure 3B**). Among the studies, the heterogeneity was not significant ($I^2 = 0\%$, $P = 0.53$).

Duration of Hospital Stay

Duration of hospital stay was significantly lower in patients undergoing R-ISR than in those undergoing L-ISR (MD = −1.52, 95% CI [−2.10, 0.94], $P < 0.00001$) (**Figure 3C**). Among the studies, the heterogeneity was not significant ($I^2 = 2\%$, $P = 0.40$).

TABLE 2 | Patient characteristics.

References	Age	Male	BMI	Chemoradiotherapy	Tumor stage, T0–T2, %		Tumor stage, T3–T4, %		ASA score		Distanced from the anal margin
	(R-ISR/L-ISR, years)	(R-ISR /L-ISR)	(R-ISR/L-ISR, kg/m2)	(R-ISR /L-ISR)	R-ISR	L-ISR	R-ISR	L-ISR	R-ISR (I/II/III)	L-ISR (I/II/III)	(R-ISR/L-ISR, cm)
Baek et al. (14)	58.0 ± 12.9	31/28	23.37 ± 3.27	20/12	76.6	70.2	23.4	29.7	22/24/1	25/12	4.39 ± 2.25
	/61.8 ± 12.8		/23.4 ± 2.73								/5.52 ± 3.74
Park et al. (16)	57.3 ± 12.1	28/25	23.9 ± 2.4	32/20	50.0	35.0	50.0	65.0	27/9/4	24/14/2	3.4 ± 1.1
	/63.6 ± 10.6		/24.3 ± 3.1								/3.6 ± 1.3
Kuo et al. (18)	55.9 (30–89)	21/17	23.78/23.32 (median)	28/28	16.7	10.7	83.3	89.3	0/33/3	4/22/2	3.83 (1.5–5.0)
	/54.9 (25–88)										/3.71 (2.0–6.0)
Park et al. (17)	59.6 ± 10.8	75/71	24.3 ± 2.8	68/60	55.7	54.7	44.3	45.3	48/52/6	42/50/14	3.2 ± 1.0
	/61.7 ± 9.6		/23.8 ± 3.3								/3.3 ± 1.1
Yoo et al. (15)	59.77 ± 12.33	35/19	24.13 ± 3.33	24/7	38.6	26.9	61.4	73.1	26/17/1	15/11	3.24 ± 0.78
	/60.5 ± 10.75		/21.42 ± 3.13								/3.71 ± 0.89

TABLE 3 | Newcastle-Ottawa Scale for bias risk assessment of non-randomized studies.

Study	Selection				Comparability	Outcomes		Total
	Representativeness of the exposed cohort	Selection of the non-exposed cohort	Ascertainment of exposure	Definition that outcome of interest was not present at the start of study		Ascertainment of outcome	Was follow-up long enough for outcomes to occur	Adequacy of follow-up of cohorts	
Park et al. (16)	1	1	1	1	2	1	0	0	7
Baek et al. (14)	1	1	1	1	1	1	0	0	6
Kuo et al. (18)	1	1	1	1	1	1	1	1	8
Yoo et al. (15)	1	1	1	1	1	1	0	1	7
Park et al. (17)	1	1	1	1	1	1	0	1	7

Postoperative Complications

The incidence of postoperative complications was not significantly different between patients undergoing R-ISR and L-ISR (RR = 0.81, 95% CI [0.59, 1.11], $P = 0.2$) (**Figure 3D**). Among the studies, the heterogeneity was not significant ($I^2 = 1\%$, $P = 0.40$).

Anastomotic Leakage

The incidence of anastomotic leakage was not significantly different between patients undergoing R-ISR and L-ISR (RR = 1.05, 95% CI [0.54, 2.03], $P = 0.89$) (**Figure 3E**). Among the studies, the heterogeneity was not significant ($I^2 = 0\%$, $P = 0.67$).

Postoperative Ileus

The incidence of postoperative ileus was not significantly different between patients undergoing R-ISR and L-ISR (RR = 0.90, 95% CI [0.41, 1.99], $P = 0.80$) (**Figure 3F**). Among the studies, the heterogeneity was not significant ($I^2 = 0\%$, $P = 0.69$).

Postoperative Urinary Complications

The incidence of postoperative urinary complications was significantly lower in patients undergoing R-ISR than in those undergoing L-ISR (RR = 0.36, 95% CI [0.16, 0.82], $P = 0.02$) (**Figure 3G**). Among the studies, the heterogeneity was not significant ($I^2 = 0\%$, $P = 0.61$).

Intra-Abdominal Abscess

The incidence of intra-abdominal abscess was not significantly different between patients undergoing R-ISR and L-ISR (RR = 0.63, 95% CI [0.18, 2.29], $P = 0.49$) (**Figure 3H**). Among the studies, the heterogeneity was not significant ($I^2 = 0\%$, $P = 0.78$).

DISCUSSION

This meta-analysis has several following findings: (1) R-ISR had significantly lower estimated intraoperative blood loss and risk of postoperative urinary complications, shorter duration of hospitalization, and longer operative time than L-ISR. (2) There was no significant difference in number of retrieved lymph nodes, circumferential resection margin, distal resection margin, conversion rate, time to first flatus, time to resume regular diet, postoperative complications, anastomotic leakage, postoperative ileus, or intra-abdominal abscess between the two groups.

Previous studies have suggested that the amount of blood loss is an independent risk factor for postoperative adverse events, cancer recurrence, and poorer overall survival (19, 20). In our meta-analysis, intraoperative blood loss was significantly lower in the R-ISR group than in the L-ISR group. This is because da Vinci robot has more advantages, such as three-dimensional vision, tremor filtering, and a 7-degree of EndoWrist instrument. Such benefits provide an access to the narrow pelvis with articulating instruments and identify blood vessels and clear lymph nodes in the surgical area more clearly as compared with laparoscope (21). Furthermore, by reducing blood loss, R-ISR is helpful for improving postoperative recovery and may allow greater preservation of immune function in cancer patients,

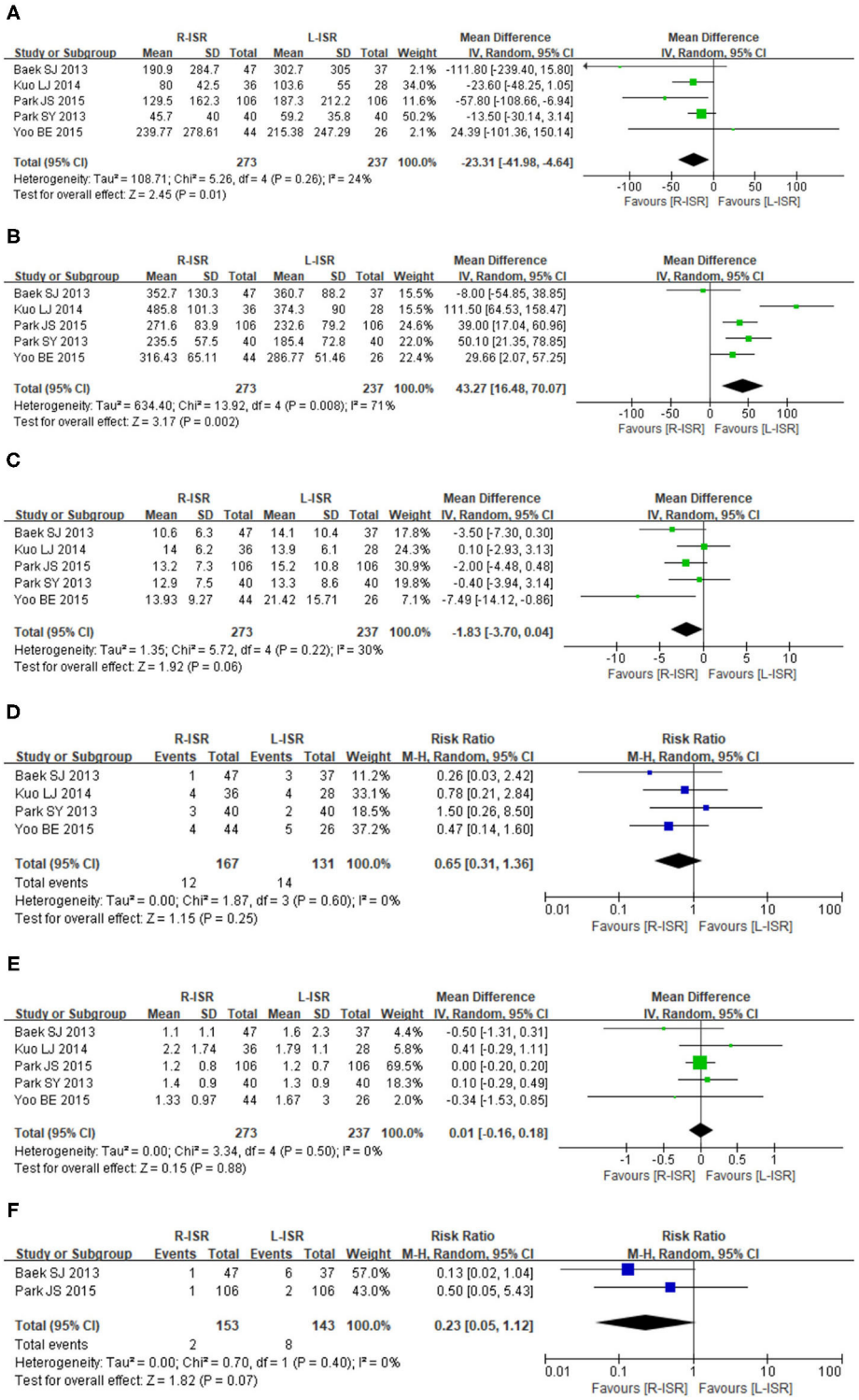

FIGURE 2 | Forest plots of perioperative outcomes comparing intraoperative blood loss **(A)**, operative time **(B)**, the number of retrieved lymph nodes **(C)**, circumferential resection margin **(D)**, distal resection margin **(E)**, and conversion rate **(F)**.

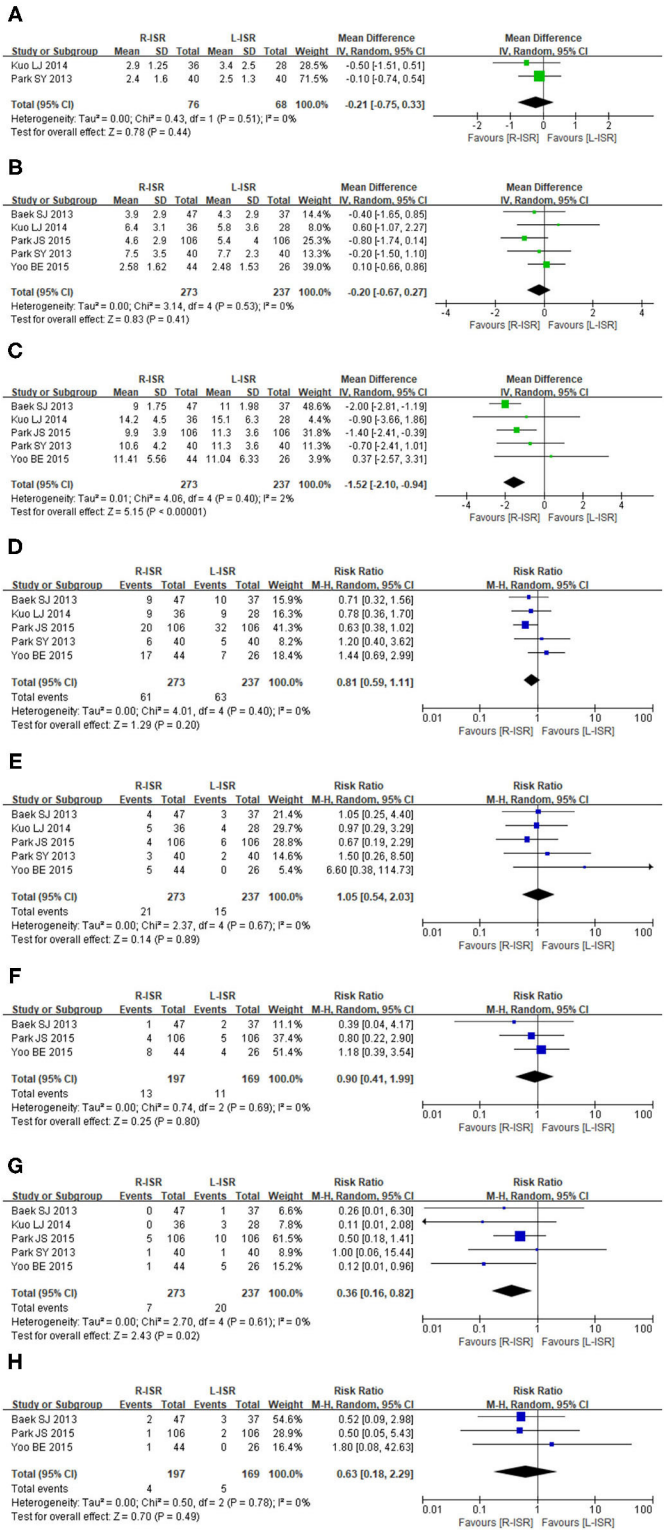

FIGURE 3 | Forest plots postoperative outcomes comparing time to first flatus **(A)**, time to resume regular diet **(B)**, duration of hospital stay **(C)**, postoperative complications **(D)**, anastomotic leakage **(E)**, postoperative ileus **(F)**, postoperative urinary complications **(G)**, intra-abdominal abscess **(H)**.

possibly thereby enhancing anti-neoplasm immune response and reducing the risk of tumor progression (22).

Our meta-analysis showed that the operative time was significantly longer in patients undergoing R-ISR than in those undergoing L-ISR. This is mainly because robotic surgery requires the docking robot and the replacement of the robotic EndoWrist (23). However, the recently invented Xi system's multi-quadrant capability can shorten the operation time by reducing redocking. In addition, the operative time is related to the skills of the surgeons. Kuo et al. showed that the mean time to complete robotic surgery was 519.5 min in the first 19 cases and only 448.2 min in the last 17 cases (24). Therefore, the operative time can be gradually decreased with increased surgeons' experiences, especially after rapidly overcoming the learning curve. Indeed, we observed that the operative time of R-ISR was heterogeneous among studies. Among the included studies, some surgeons may have less experiences of R-ISR as compared with L-ISR, which lead to a longer operative time in the R-ISR group. Another possible reason why the operative time was longer in the R-ISR group was that the robot can observe more lymph nodes in the low rectum with a more clear field of view as compared with laparoscope, thus increasing the time of lymph node dissection (21). Prolonged operative time can increase the risk of surgical site infection (SSI) (25) and may increase surgical team fatigue and room for more technical errors (26, 27). Regardless, it should be recognized that the duration of hospital stay was significantly lower in patients undergoing R-ISR than in those undergoing L-ISR, suggesting that the speed and quality of postoperative recovery should not be influenced by operative time in our meta-analysis.

Dissection of lymph nodes during radical surgery is related to the degree of radical resection and the survival and quality of life after surgery (28). Our meta-analysis showed that the mean number of lymph nodes harvested in patients undergoing R-ISR was a bit smaller than those undergoing L-ISR, but the difference was not significant between the two groups. There are some explanations for this unexpected phenomenon. First, the number of harvested lymph nodes is a parameter of the quality of the surgery and the minimum should be 12 lymph nodes for a correct pathological staging (29). It is pity that the number of lymph nodes harvested in the L-ISR of Baek's study was <12, which might cause the result inaccurate (14). Second, ISR surgery is more applicable for patients with T1 and T2 (30). Surgeons usually performed shorter resections with minimal lymph node dissection for this kind of tumors (31). Third, the scope of lymph node dissection may be smaller in the R-ISR group than in the L-ISR group. Moreover, there are a higher proportion of patients undergoing chemoradiotherapy before R-ISR, which might have affected the number of retrieved lymph nodes. In four of the included studies (14–17), more patients underwent chemoradiotherapy before R-ISR as compared with L-ISR.

The effect of the extent of anal sphincter resection on anal function is controversial among studies (32–35). Some studies suggested that anal function had no relationship with the extent of anal sphincter resection (32, 33), but others held the opposite view that the risk of fecal incontinence depended mainly on the height of the tumor and anastomotic site (34, 35). Notably, our included studies did not provide any relevant data regarding the extent of anal sphincter resection. Besides, J-type pouch coloanal anastomosis may be superior to direct anastomosis in protecting anal function (36). When anal function changes after surgery, anal lavage (37), biofeedback therapy (38), and sacral nerve stimulation therapy (39) can be used to promote the recovery of anal function.

The urinary function is mainly controlled by the sympathetic nerves from the superior hypogastric plexus and the parasympathetic nerves from the pelvic plexus and its branches (40). Surgical injury to the sympathetic nerve may lead to ejaculation dysfunction and injury to the parasympathetic nerve results in dysfunction of bladder detractor in male patients (41). Our meta-analysis showed that postoperative urinary complications occurred less frequently in the R-ISR group than in the L-ISR group. Because the mesorectum was anatomically in proximity to the pelvic nerves, it should be dissected as carefully as possible to reduce the damage of pelvic nerves (42). During the L-ISR surgery, it is often difficult to clearly identify subtle anatomical structures, probably increasing the risk of postoperative urinary dysfunction. By comparison, using a small and highly flexible robotic EndoWrist, the surgeons can more sufficiently expose the vascularless plane between the proper fascia of rectum and the anterior sacral fascia under the clear vision of the da Vinci robot. Considering a limited number of patients included in this study, more concrete evidence is needed to demonstrate the benefits of R-ISR on reproduction function over L-ISR.

This meta-analysis had several limitations. First, the data regarding the extent of anal sphincter resection, anastomosis methods, and neoadjuvant radiotherapy and chemotherapy were insufficiently reported, which prevented further subgroup analyses. Second, all included studies were non-randomized controlled studies with moderate quality. Third, the sample size is not adequate, and large-scale and multicenter randomized controlled studies are lacking to evaluate the long-term efficacy of R-ISR.

In conclusion, the potential benefits of R-ISR may be a safe and feasible choice for the treatment of low rectal tumors compared with L-ISR, including lower estimated intraoperative blood loss, postoperative urinary complications, and hospitalization days. However, high-quality large-scale randomized controlled trials are needed to compare R-ISR and L-ISR to guide the clinicians to choose the optimal approach for the treatment of low rectal tumors.

DATA AVAILABILITY STATEMENT

The original contributions presented in the study are included in the article/supplementary material, further inquiries can be directed to the corresponding author/s.

AUTHOR CONTRIBUTIONS

CZ involved in conceptualization. JZ, XQ, and CZ involved in methodology, data curation, and writing the original draft. XQ, FY, and CZ involved in validation.

JZ, GG, FY, and CZ involved in formal analysis. GG, RC, and CZ involved in the investigation. XQ, FY, GG, and RC involved in writing the review and editing. CZ involved in supervision and project administration. All authors contributed to the article and approved the submitted version.

REFERENCES

1. Siegel RL, Miller KD, Jemal A. Cancer statistics, 2019. *CA Cancer J Clin.* (2019) 69:7–34. doi: 10.3322/caac.21551
2. Rullier E, Denost Q, Vendrely V, Rullier A, Laurent C. Low rectal cancer: classification and standardization of surgery. *Dis Colon Rectum.* (2013) 56:560–7. doi: 10.1097/DCR.0b013e31827c4a8c
3. Perry WB, Connaughton JC. Abdominoperineal resection: how is it done and what are the results? *Clin Colon Rectal Surg.* (2007) 20:213–20. doi: 10.1055/s-2007-984865
4. Collard M, Lefevre JH. Ultimate functional preservation with intersphincteric resection for rectal cancer. *Front Oncol.* (2020) 10:297. doi: 10.3389/fonc.2020.00297
5. Peng B, Lu J, Wu Z, Li G, Wei F, Cao J, et al. Intersphincteric resection versus abdominoperineal resection for low rectal cancer: a meta-analysis. *Surg Innov.* (2020) 27:392–401. doi: 10.1177/1553350620918414
6. Saito N, Moriya Y, Shirouzu K, Maeda K, Mochizuki H, Koda K, et al. Intersphincteric resection in patients with very low rectal cancer: a review of the Japanese experience. *Dis Colon Rectum.* (2006) 49:S13–22. doi: 10.1007/s10350-006-0598-y
7. Serra-Aracil X, Gálvez A, Mora-López L, Rebasa P, Serra-Pla S, Pallisera-Lloveras A, et al. Endorectal ultrasound in the identification of rectal tumors for transanal endoscopic surgery: factors influencing its accuracy. *Surg Endosc.* (2018) 32:2831–8. doi: 10.1007/s00464-017-5988-9
8. Fan Z, Cong Y, Zhang Z, Li R, Wang S, Yan K. Shear wave elastography in rectal cancer staging, compared with endorectal ultrasonography and magnetic resonance imaging. *Ultrasound Med Biol.* (2019) 45:1586–93. doi: 10.1016/j.ultrasmedbio.2019.03.006
9. Hartley JE, Mehigan BJ, Qureshi AE, Duthie GS, Lee PW, Monson JR. Total mesorectal excision: assessment of the laparoscopic approach. *Dis Colon Rectum.* (2001) 44:315–21. doi: 10.1007/BF02234726
10. Scheidbach H, Schneider C, Konradt J, Bärlehner E, Köhler L, Wittekind C, et al. Laparoscopic abdominoperineal resection and anterior resection with curative intent for carcinoma of the rectum. *Surg Endosc.* (2002) 16:7–13. doi: 10.1007/s00464-001-8314-4
11. Weiser MR, Milsom JW. Laparoscopic total mesorectal excision with autonomic nerve preservation. *Semin Surg Oncol.* (2000) 19:396–403. doi: 10.1002/ssu.10
12. Watanabe M, Teramoto T, Hasegawa H, Kitajima M. Laparoscopic ultralow anterior resection combined with per anum intersphincteric rectal dissection for lower rectal cancer. *Dis Colon Rectum.* (2000) 43:S94–7. doi: 10.1007/BF02237232
13. Moher D, Liberati A, Tetzlaff J, Altman DG. Preferred reporting items for systematic reviews and meta-analyses: the PRISMA statement. *PLoS Med.* (2009) 6:e1000097. doi: 10.1371/journal.pmed.1000097
14. Baek SJ, Al-Asari S, Jeong DH, Hur H, Min BS, Baik SH, et al. Robotic versus laparoscopic coloanal anastomosis with or without intersphincteric resection for rectal cancer. *Surg Endosc.* (2013) 27:4157–63. doi: 10.1007/s00464-013-3014-4
15. Yoo BE, Cho JS, Shin JW, Lee DW, Kwak JM, Kim J, et al. Robotic versus laparoscopic intersphincteric resection for low rectal cancer: comparison of the operative, oncological, and functional outcomes. *Ann Surg Oncol.* (2015) 22:1219–25. doi: 10.1245/s10434-014-4177-5
16. Park SY, Choi GS, Park JS, Kim HJ, Ryuk JP. Short-term clinical outcome of robot-assisted intersphincteric resection for low rectal cancer: a retrospective comparison with conventional laparoscopy. *Surg Endosc.* (2013) 27:48–55. doi: 10.1007/s00464-012-2405-2
17. Park JS, Kim NK, Kim SH, Lee KY, Lee KY, Shin JY, et al. Multicentre study of robotic intersphincteric resection for low rectal cancer. *Br J Surg.* (2015) 102:1567–73. doi: 10.1002/bjs.9914
18. Kuo LJ, Lin YK, Chang CC, Tai CJ, Chiou JF, Chang YJ. Clinical outcomes of robot-assisted intersphincteric resection for low rectal cancer: comparison with conventional laparoscopy and multifactorial analysis of the learning curve for robotic surgery. *Int J Colorectal Dis.* (2014) 29:555–62. doi: 10.1007/s00384-014-1841-y
19. Egenvall M, Mörner M, Påhlman L, Gunnarsson U. Degree of blood loss during surgery for rectal cancer: a population-based epidemiologic study of surgical complications and survival. *Colorectal Dis.* (2014) 16:696–702. doi: 10.1111/codi.12630
20. Okamura R, Hida K, Hasegawa S, Sakai Y, Hamada M, Yasui M, et al. Impact of intraoperative blood loss on morbidity and survival after radical surgery for colorectal cancer patients aged 80 years or older. *Int J Colorectal Dis.* (2016) 31:327–34. doi: 10.1007/s00384-015-2405-5
21. Wells KO, Peters WR. Minimally invasive surgery for locally advanced rectal cancer. *Surg Oncol Clin N Am.* (2019) 28:297–308. doi: 10.1016/j.soc.2018.11.005
22. Breukink S, Pierie J, Wiggers T. Laparoscopic versus open total mesorectal excision for rectal cancer. *Cochrane Database Syst Rev.* (2006) Cd005200. doi: 10.1002/14651858.CD005200.pub2
23. Morelli L, Guadagni S, Di Franco G, Palmeri M, Caprili G, D'Isidoro C, et al. Use of the new da Vinci Xi® during robotic rectal resection for cancer: a pilot matched-case comparison with the da Vinci Si®. *Int J Med Robot.* (2017) 13:e1728. doi: 10.1002/rcs.1728
24. Ngu JC, Sim S, Yusof S, Ng CY, Wong AS. Insight into the da Vinci® Xi - technical notes for single-docking left-sided colorectal procedures. *Int J Med Robot.* (2017) 13:e1798. doi: 10.1002/rcs.1798
25. Cheng H, Chen BP, Soleas IM, Ferko NC, Cameron CG, Hinoul P. Prolonged operative duration increases risk of surgical site infections: a systematic review. *Surg Infect.* (2017) 18:722–35. doi: 10.1089/sur.2017.089
26. Bennett-Guerrero E, Welsby I, Dunn TJ, Young LR, Wahl TA, Diers TL, et al. The use of a postoperative morbidity survey to evaluate patients with prolonged hospitalization after routine, moderate-risk, elective surgery. *Anesth Analg.* (1999) 89:514–9. doi: 10.1213/00000539-199908000-00050
27. Hoekstra LT, van Trigt JD, Reiniers MJ, Busch OR, Gouma DJ, van Gulik TM. Vascular occlusion or not during liver resection: the continuing story. *Dig Surg.* (2012) 29:35–42. doi: 10.1159/000335724
28. Liang JT, Lai HS, Lee PH. Laparoscopic pelvic autonomic nerve-preserving surgery for patients with lower rectal cancer after chemoradiation therapy. *Ann Surg Oncol.* (2007) 14:1285–7. doi: 10.1245/s10434-006-9052-6
29. Compton CC, Fielding LP, Burgart LJ, Conley B, Cooper HS, Hamilton SR, et al. Prognostic factors in colorectal cancer. College of American Pathologists Consensus Statement 1999. *Arch Pathol Lab Med.* (2000) 124:979–94. doi: 10.5858/2000-124-0979-PFICC
30. Denost Q, Rullier E. Intersphincteric resection pushing the envelope for sphincter preservation. *Clin Colon Rectal Surg.* (2017) 30:368–76. doi: 10.1055/s-0037-1606114
31. Cappellesso R, Nicolè L, Zanco F, Lo Mele M, Fassina A, Ventura L, et al. Synchronous nodal metastatic risk in screening detected and endoscopically removed pT1 colorectal cancers. *Pathol Res Pract.* (2020) 216:152966. doi: 10.1016/j.prp.2020.152966
32. Ito M, Saito N, Sugito M, Kobayashi A, Nishizawa Y, Tsunoda Y. Analysis of clinical factors associated with anal function after intersphincteric resection for very low rectal cancer. *Dis Colon Rectum.* (2009) 52:64–70. doi: 10.1007/DCR.0b013e31819739a0
33. Saito N, Ito M, Kobayashi A, Nishizawa Y, Kojima M, Nishizawa Y, et al. Long-term outcomes after intersphincteric resection for low-lying rectal cancer. *Ann Surg Oncol.* (2014) 21:3608–15. doi: 10.1245/s10434-014-3762-y
34. Kim JC, Lee JL, Bong JW, Seo JH, Kim CW, Park SH, et al. Oncological and anorectal functional outcomes of robot-assisted intersphincteric resection in lower rectal cancer, particularly the extent of sphincter resection and sphincter saving. *Surg Endosc.* (2020) 34:2082–94. doi: 10.1007/s00464-019-06989-3

35. Denost Q, Laurent C, Capdepont M, Zerbib F, Rullier E. Risk factors for fecal incontinence after intersphincteric resection for rectal cancer. *Dis Colon Rectum.* (2011) 54:963–8. doi: 10.1097/DCR.0b013e31821d3677
36. Tilney HS, Tekkis PP. Extending the horizons of restorative rectal surgery: intersphincteric resection for low rectal cancer. *Colorectal Dis.* (2008) 10:736–7. doi: 10.1111/j.1463-1318.2008.01530.x
37. Martellucci J, Sturiale A, Bergamini C, Boni L, Cianchi F, Coratti A, et al. Role of transanal irrigation in the treatment of anterior resection syndrome. *Tech Coloproctol.* (2018) 22:519–27. doi: 10.1007/s10151-018-1829-7
38. Nishigori H, Ishii M, Kokado Y, Fujimoto K, Higashiyama H. Effectiveness of pelvic floor rehabilitation for bowel dysfunction after intersphincteric resection for lower rectal cancer. *World J Surg.* (2018) 42:3415–21. doi: 10.1007/s00268-018-4596-8
39. Noblett KL, Buono K. Sacral nerve stimulation as a therapy for patients with refractory voiding and bowel dysfunction. *Obstet Gynecol.* (2018) 132:1337–45. doi: 10.1097/AOG.0000000000002968
40. Masui H, Ike H, Yamaguchi S, Oki S, Shimada H. Male sexual function after autonomic nerve-preserving operation for rectal cancer. *Dis Colon Rectum.* (1996) 39:1140–5. doi: 10.1007/BF02081416
41. Ozeki S, Maeda K, Hanai T, Masumori K, Katsuno H, Takahashi H. Effects of robotic rectal surgery on sexual and urinary functions in male patients. *Surg Today.* (2016) 46:491–500. doi: 10.1007/s00595-015-1217-0
42. Hojo K, Vernava AM III, Sugihara K, Katumata K. Preservation of urine voiding and sexual function after rectal cancer surgery. *Dis Colon Rectum.* (1991) 34:532–9. doi: 10.1007/BF02049890

Conflict of Interest: The authors declare that the research was conducted in the absence of any commercial or financial relationships that could be construed as a potential conflict of interest.

Publisher's Note: All claims expressed in this article are solely those of the authors and do not necessarily represent those of their affiliated organizations, or those of the publisher, the editors and the reviewers. Any product that may be evaluated in this article, or claim that may be made by its manufacturer, is not guaranteed or endorsed by the publisher.

frontiers in Surgery

SYSTEMATIC REVIEW
published: 06 December 2021
doi: 10.3389/fsurg.2021.728098

Efficacy and Safety of Fusion Imaging in Radiofrequency Ablation of Hepatocellular Carcinoma Compared to Ultrasound: A Meta-Analysis

Tao Jie[1†], *Feng Guoying*[1†], *Tang Gang*[1], *Shi Zhengrong*[2*] *and Li Maoping*[3*]

[1] *Department of General Surgery, Chongqing Medical University, Chongqing, China,* [2] *Department of General Surgery, The First Affiliated Hospital of Chongqing Medical University, Chongqing, China,* [3] *Department of Ultrasound, The First Affiliated Hospital of Chongqing Medical University, Chongqing, China*

Background: Radiofrequency ablation (RFA), generally performed under real-time guidance of ultrasound which is safe and effective, is a common minimally invasive therapy for treating hepatocellular carcinoma. Fusion imaging (FI) is a newly developed imaging method, which integrates CT/MRI accurate imaging and matches the characteristics of real-time ultrasound imaging, thereby providing a new approach to guide tumor ablation therapy. However, the efficacy and safety of FI as opposed to ultrasound in tumor ablation remains unclear.

Objective: The present study sought to evaluate the difference in the efficacy and safety between FI and ultrasound in radiofrequency surgery for the treatment of hepatocellular carcinoma through a metaanalysis.

Materials and Methods: Searching for studies comparing the efficacy and safety of FI and ultrasound in radiofrequency of hepatocellular carcinoma in PubMed, Embase, and Cochrane Library databases for articles published until April 2021. Random or fixed effect models were used for statistical analysis. Metaanalysis and sensitivity analysis were used on the included studies.

Results: A total of six studies met predefined inclusion criteria, and were finally included in the analysis. Sensitivity and subgroup analyses, based on predetermined patient characteristics, allowed minimization of bias. In the RFA of hepatocellular carcinoma, FI decreased 1-year overall survival (OS) when compared with ultrasound. But FI was not significantly different from ultrasound in terms of technical efficiency, 1-, 2-, and 3-year local tumor progression (LTP), complications, as well as 2-year OS. Subgroup analysis, based on tumor mean diameter, showed that FI reduced the rate of 1- and 2-year LTP in patients with tumors of mean diameter $\geq$15 mm when compared with ultrasound. Moreover, operative complications could be reduced in patients with tumor mean diameter $<$15 mm using FI, compared with ultrasound.

Conclusion: Overall, these results showed that FI may have some effects on improving efficacy and safety of thermal ablation in HCC patients, relative to ultrasound. However, it may be a more effective method for managing large lesions, as well as those that are difficult to ablate. Further large-scale and well-designed randomized controlled trials are needed to validate these findings.

Keywords: curative effect, fusion imaging, meta-analysis, security, ultrasound

OPEN ACCESS

Edited by:
Patrick J. Schuler, Ulm University Medical Center, Germany

Reviewed by:
Xiao-Wan Bo, Tongji University, China
Thanongchai Siriapisith, Mahidol University, Thailand

***Correspondence:**
Li Maoping
limaoping@hospital.cqmu.edu.cn
Shi Zhengrong
shizr@hospital.cqmu.edu.cn

[†]These authors have contributed equally to this work and share first authorship

Specialty section:
This article was submitted to Surgical Oncology, a section of the journal Frontiers in Surgery

Received: *20 June 2021*
Accepted: *18 October 2021*
Published: *06 December 2021*

Citation:
Jie T, Guoying F, Gang T, Zhengrong S and Maoping L (2021) Efficacy and Safety of Fusion Imaging in Radiofrequency Ablation of Hepatocellular Carcinoma Compared to Ultrasound: A Meta-Analysis. Front. Surg. 8:728098. doi: 10.3389/fsurg.2021.728098

INTRODUCTION

Radiofrequency ablation (RFA) is a safe and effective method for treating patients with early hepatocellular carcinoma who cannot tolerate surgery or are reluctant to undergo surgery (1, 2), while imaging holds the key to the curative effect and prognosis of frequency ablation (3). On the other hand, ultrasound (US) remains the most commonly used imaging technique (4, 5) due to its economic convenience, nonionizing radiation, and real-time characteristics (6, 7). However, the imaging of ultrasound is relatively fuzzy in the face of lesions <2 cm (8), isoechoic, located in the center or top of the liver, as well as interference from adjacent structures and tissues (9). Therefore, contrast-enhanced ultrasound (CEUS) is required. However, the positioning ability for CEUS is also limited for tumors with poor blood supply and the situation where it is difficult to evaluate the ablation range, which may lead to tumor residue (10). In addition, tumors that are not visible in ultrasound, remain a major challenge during RFA (8). Therefore, RFA under ultrasound alone is constrained by numerous limitations.

Advancements in computer graphics, 3D image processing technology, and the emergence of fusion imaging (FI) have all improved RFA (11). FI, which overlaps images from different image sources and combines real-time images of ultrasound with the high resolution of CT/MRI (9), has been developed. Notably, this technique is more accurate than ultrasound alone in identifying target lesions, thereby allowing ablation of that are invisible or ablate tumors that are difficult to ablate (8). In addition, FI can also determine the ablation edge and evaluate treatment response in real time (12), has excellent efficacy and safety (13, 14), and may become an important imaging technique for RFA of hepatocellular carcinoma. In fact, the technique can also be used in needle biopsy for disease diagnosis (15), and is also a promising application in prostate (16), liver (17), heart (18), and brain diseases (19), among others.

However, published studies have yielded conflicting results with regards to efficacy and safety of FI relative to that of ultrasound. While some studies have shown that FI is more superior than ultrasound (20, 21), others have found no significant differences in the two technologies (22, 23). Therefore, the present metaanalysis was designed to systematically evaluate efficacy and safety of FI relative to ultrasound in radiofrequency surgery for the treatment of hepatocellular carcinoma. Specifically, patients with hepatocellular carcinoma undergoing RFA were selected as the research objects, and technical efficiency, local tumor progression (LTP), and complications [thoracic hemorrhage, biliary injury, so on (24)] were taken as the main evaluation indexes, whereas survival (OS) was considered the secondary evaluation.

MATERIALS AND METHODS

Literature Search

Articles from PubMed, Embase, and Cochrane library databases were searched and relevant articles were retrieved. Search strategy involved the following keywords: hepatocellular carcinoma, RFA, FI, and ultrasound. Due to the relatively new development of FI in hepatocellular carcinoma radiofrequency, studies published were screened until April 1, 2021, and studies published after that date were not included. References of selected literatures were also screened to prevent the omission of relevant studies. In the initial screening, we read the title and abstract to determine if it met our inclusion criteria. The available full-text articles were then reviewed as described (**Figure 1**). Specifically, two reviewers (Tao and Tang) conducted literature retrieval and data extraction, and any questions were resolved through discussion with other reviewers (Feng and Shi and Li).

Inclusion and Exclusion Criteria

Inclusion criteria were: (1) Studies to compare application of FI and ultrasound or FI and CEUS in RFA of patients with nonrecurrent hepatocellular carcinoma; (2) reported results included at least one of the technical efficiencies, LTP, complications, and OS. Exclusion criteria were: (1) non-English papers or repetitive articles; (2) Unpublished data or gray literature including conference abstracts, dissertation, brief reports, book chapters, editorials, and patents. Any discrepancies regarding selection of a qualified article were resolved through discussion or consultation with other reviewers (Feng and shi and li).

Data Extraction

To reduce chances of human error, data extraction for each study was performed independently by two reviewers (Tao and Tang) using a developed form. Data collected included, name of the first author, study design, country, and year of publication, sample diameter, participants' gender, and their mean age, liver function (Child-Pugh class), tumor diameter, type of intervention in the control group, and main outcomes. There were minimal disagreements between the two researchers with regards to data extraction or quality assessment, and these issues were resolved through discussion and consensus.

Quality Assessment

Since the included articles included both a cohort study and a randomized controlled studies, the two reviewers (Tao and Tang) evaluated the quality of each cohort study using the Newcastle–Ottawa quality assessment scale, whereas that of randomized controlled studies was performed using the risk of bias assessment scale in the Cochrane manual of systematic evaluation of interventions. If both reviewers had different views on the results, following the separate assessment, other researchers (Feng and Shi and Li) were called upon to help to reach a consensus. Quality of the cohort studies was assessed based on three factors, namely selection, comparability and outcome. On the other hand, risk of bias in randomized controlled studies was assessed based on seven criteria, namely randomization, distribution hiding, blindness of participants and operators, detection blindness, incomplete data, selective reporting, and other biases.

Statistical Analyses

The primary endpoints in the meta-analysis included technical efficiency, 1-, 2-, and 3-year LTP, and complications, whereas

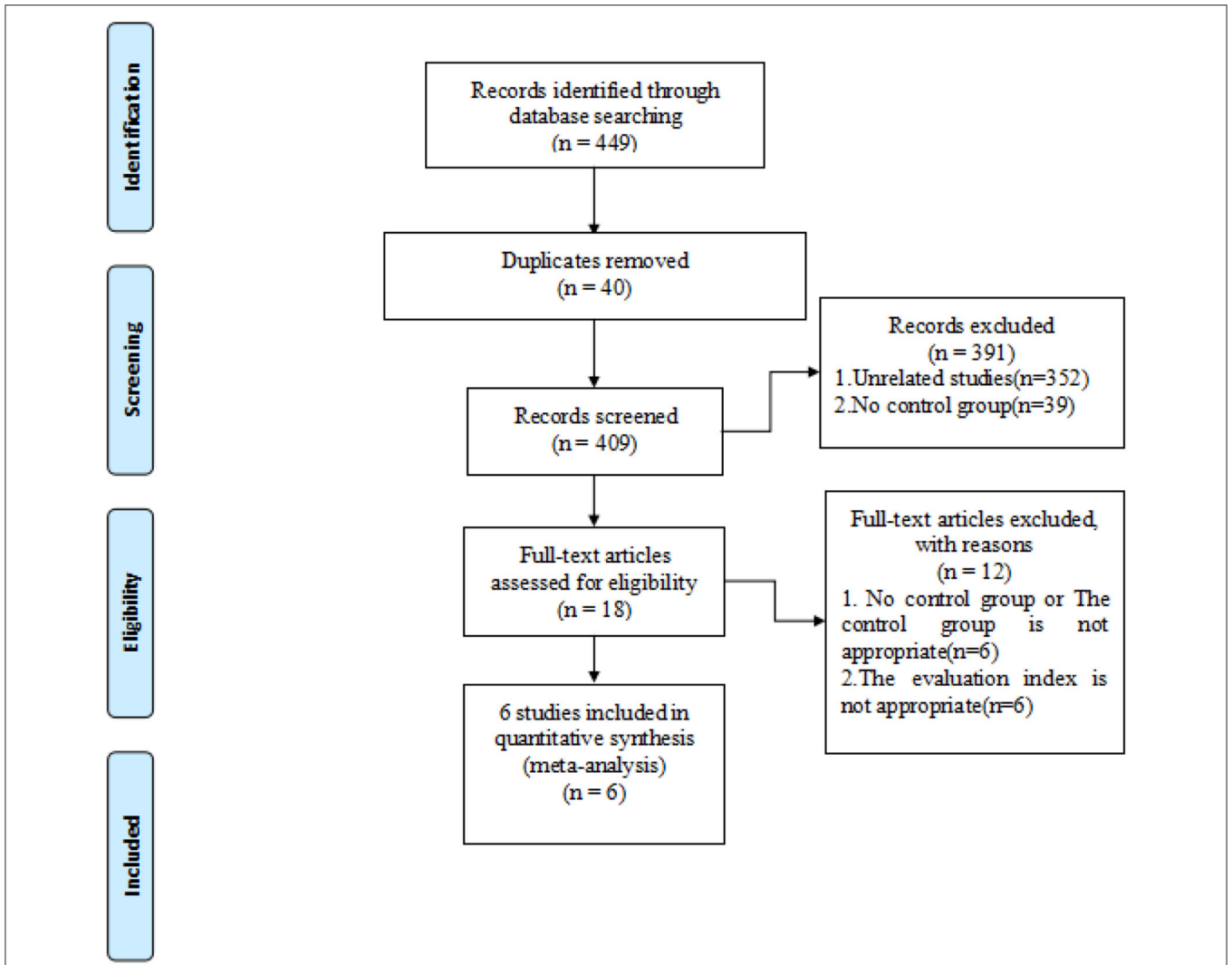

FIGURE 1 | PRISMA flow diagram of study selection process.

secondary endpoints were 1- and 2-year OS. Heterogeneity among studies was assessed using the *I*-square (I^2) and *Q* tests. When $I^2 < 50\%$ and $P > 0.1$ in the *Q*-value test, a fixed-effect model was applied. Otherwise, the random effects model was employed. Assessment of potential sources of interstudy heterogeneity was performed using subgroup analyses, based on baseline tumor mean diameter (tumor mean diameters ≥15 and <15 mm, the data was obtained by looking at all the literatures) and control type (US and CEUS). The proportion of each study to the overall outcome was assessed using sensitivity analysis, while publication bias was evaluated by grade correlation based on Begg and regression asymmetry test of Egger. Statistical analyses were performed using Stata 15.1 software (Statacorp, College Station, Texas, USA) and Review Manager5.3, by two investigators (Tao and Tang), and reviewed by the other researchers (Feng and Shi and Li).

RESULTS

Literature Search

The selection process of the present study is shown using the PRISMA flow diagram (**Figure 1**). Search strategy resulted in a total of 449 records, of which 40 were duplicates and were subsequently eliminated. The remaining 409 records were screened by title/abstract, and 18 selected for full-text assessment. An additional 12 records did not meet our inclusion criteria, leaving a final six full-text articles for metaanalysis (10, 21–23, 25, 26).

Characteristics of the Included Studies

Characteristics of the included studies, comprising six articles with 1,158 patients aged between 29 and 88 years from Asia, are summarized in **Table 1**. The studies were three arm tests (22, 26), treating them as four two-arm tests [Huang (22) (1): contrasting

TABLE 1 | Characteristics of included trials.

References	Country	Sample diameter (Number of cases, number of tumor)		Study type	Age	Gender (M/F)	Intervention		Child-Pugh class (A/B)	Tumor mean diameter (mm)	Outcomes
		case	Control				case	Control			
Ma et al. (21)	China	97, 110	83, 90	Cohort study	52.3	160/20	CT/MRI-US	US	162/18	18.9 (10–48)	Technical efficiency, LTP, RFS, OS, complications
You et al. (23)	China	14, unknown	13, unknown	Cohort study	54	25/2	MRI-US	US	26/1	20.1 (9–49)	LTP, complications
Toshikuni et al. (25)	Japan	25, unknown	20, unknown	Cohort study	73.4	22/23	CT/MRI-US	US	38/7	19 (<25)	complications
Minami et al. (26)	Japan	37, 57	192, 344	Cohort study	69	161/68	CT/MRI-CEUS	CEUS	Unknown	14.7 (5–60)	Technical efficiency, LTP, RFS, OS, complications
Minami et al. (26)	Japan	123, 155	192, 344	Cohort study	70.1	229/86	CT/MRI-US	CEUS	Unknown	14.7 (5–60)	Technical efficiency, LTP, RFS, OS, complications
Ju et al. (10)	China	98, 126	92, 120	Cohort study	53.7	181/9	CT/MRI-CEUS	CEUS	166/24	20.5 (10–60)	Technical efficiency, LTP, RFS, OS, complications
Huang et al. (22)	China	124, 153	125, 150	Randomized controlled trial	53.6	226/23	CT/MRI-CEUS	CEUS	238/11	18.9 (10–49)	Technical, efficiency, LTP, RFS, OS, complications
Huang et al. (22)	China	125, 153	125, 150	Randomized controlled trial	54.6	227/23	3DUS-CEUS	CEUS	239/11	18.7 (10–44)	Technical efficiency, LTP, RFS, OS, complications

LTP, local tumor progression rate; RFS, recurrence-free survival; OS, overall survival.

FI combined with CEUS and CEUS; Huang (22) (2): contrasting FI and CEUS; (26) (1): contrasting FI combined with CEUS and CEUS; (26) (2): contrasting FI and CEUS]. Six studies reported 1- and 2-year LTP, four reported on 3-year LTP, while eight analyzed complications of RFA. Moreover, six and two studies were cohort and randomized controlled studies, respectively. Five cohort studies were assessed using the Newcastle–Ottawa quality assessment scale (**Table 2**), whereas one randomized controlled study was assessed using the Cochrane risk bias assessment tool (**Table 3**).

Effect on Technical Efficiency

Pooled effect diameter analysis did not reveal any significant differences in the technical efficiency between ultrasonic image fusion and the control group, across the six included trials (RR, RE: 1.02; 95% CI: 0.98, 1.06, $p = 0.28$; **Figure 2**). However, there was significant heterogeneity between the effect diameter of included studies ($I^2 = 83\%$, $p < 0.0001$). Moreover, subgroup analysis, based on mean diameter (<15 mm) revealed no heterogeneity ($I^2 = 0.0\%$, $p = 0.77$). Results of sensitivity analysis, used to examine the effect of each study on pooled effect diameter, revealed that exclusion of Ma's study (21) from the analysis altered the overall effect diameter (RR, RE:1; 95% CI: 0.99, 1.02, $p = 0.84$).

Moreover, no evidence of significant publication bias was found across the included studies with regards to technical efficiency ($p = 0.81$, Begg's test and $p = 0.65$, Egger's test). Results of subgroup analyses on technical efficiency are presented in **Table 4**.

Effect on LTP

Six trials reported data on 1-year LTP, and their pooled effect diameter based on ultrasonic image fusion, relative to the control group was (OR, RE: 0.67; 95% CI: 0.36, 1.25, $p = 0.21$), with a heterogeneity ($I^2 = 55\%$, $p = 0.05$; **Figure 3A**). When the metaanalysis was subgrouped by mean diameter, heterogeneity was attenuated in studies with ≥15 mm ($I^2 = 42\%$, $p = 0.16$, test for overall effect: $z = 2.1$, $p = 0.04$) and in studies with <15 mm ($I^2 = 0\%$, $p = 0.67$). Notably, we found significant differences between subgroup heterogeneity ($I^2 = 77.8\%$, $p = 0.03$). Results from sensitivity analysis revealed that exclusion of Ma's study (21) altered the overall effect diameter (OR, RE: 0.86; 95% CI: 0.52, 1.41, $p = 0.55$).

The pooled mean difference for the six datasets, with regards to the effect of ultrasonic image fusion on 2-year LTP, was (OR, RE: 0.61; 95% CI: 0.35, 1.07, $p = 0.08$) relative to ultrasonoscopy (**Figure 3B**), with a heterogeneity of ($I^2 = 60.0\%$, $p = 0.03$). When the metaanalysis was subgrouped by mean diameter, heterogeneity was attenuated in studies with ≥15 mm ($I^2 = 40\%$, $p = 0.17$, test for overall effect: $z = 2.99$, $p = 0.003$), and in studies with <15 mm ($I^2 = 0\%$, $p = 0.67$). Then, there was a significant between-subgroup heterogeneity ($I^2 = 84.3\%$, $p = 0.01$). To examine the effect of each study on pooled effect diameter, we performed sensitivity analyses and found that (26) (2)'s study (26) altered the overall effect diameter (OR, RE: 0.50; 95% CI: 0.31, 0.82, $p = 0.007$).

TABLE 2 | Outcome of assessment of the quality of nonrandomised studies using the Newcastle-Ottawa scale study.

Study	Selection			Comparability			Outcome			Total score
	Representativeness of the exposed cohort	Selection of non-exposed cohort	Ascertainment of exposure	Outcome not presented at the start	Age and sex	Additional factors	Assessment of outcome	Follow-up long enough	Adequacy of follow up	
Minami et al. (26)	–	*	*	*	*	*	*	*	*	8/9
Toshikuni et al. (25)	*	*	*	*	*	*	–	*	*	8/9
Ju et al. (10)	*	*	*	*	*	*	*	*	*	9/9
Ma et al. (21)	*	*	*	*	*	–	*	*	*	8/9
You et al. (23)	*	*	*	*	*	–	*	*	*	8/9

A single asterisk (*) indicates 1 score, and dash (–) indicates 0 score.

TABLE 3 | Risk of bias table.

Bias	Authors' judgement	Support for judgement
Random sequence generation (selection bias)	Low risk	Random number
Allocation concealment (selection bias)	High risk	Doctors and data collectors know the results of the assignment
Blinding of participants and personnel (performance bias)	High risk	No blinded
Blinding of outcome assessment (detection bias)	Unclear risk	Insufficient information to judge
Incomplete outcome data (attrition bias)	Low risk	Data is balanced between groups
Selective reporting (reporting bias)	Low risk	Non-selective reporting
Other bias	Low risk	There was no obvious other bias

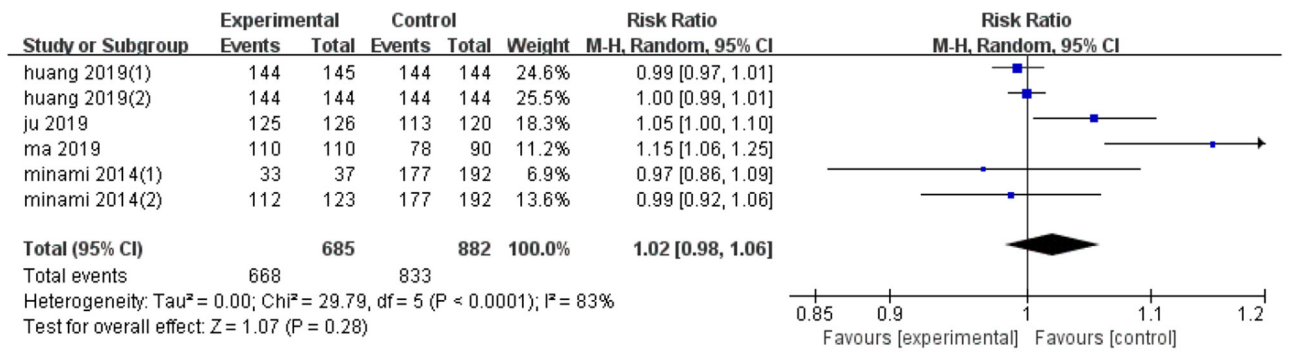

FIGURE 2 | Forest plot of the effects of ultrasonic image fusion on technical efficiency.

We also examined the effect of ultrasonic image fusion on 3-year LTP in four clinical trials. Overall, metaanalysis revealed no significant effects of the ultrasonic image fusion on 3-year LTP, relative to the control group (OR, RE: 0.71; 95% CI: 0.29, 1.79, $p = 0.47$), with heterogeneity across studies ($I^2 = 74\%$, $p = 0.008$; **Figure 3C**). Moreover, sensitivity analysis showed that excluding Ma's study (21) from the analysis changed the overall effect (OR, RE: 1.14; 95% CI: 0.67, 1.93, $p = 0.63$).

Begg's and Egger's tests did not reveal evidence of publication bias for LTP across 1-year ($p = 0.26$ and $p = 0.272$, respectively), 2-year ($p = 1.00$ and $p = 0.915$, respectively), and 3-year ($p = 0.73$ and $p = 0.901$, respectively) periods. The result of subgroup analysis on LTP are presented in **Table 4**.

Effect on Complications

Eight trials reported the effect of ultrasonic image fusion on complications. Metaanalysis showed that ultrasonic image fusion had no significant decrease on the complications (RD, RE: −0.02; 95% CI: −0.04, 0.01, $p = 0.3$; **Figure 4**), with a heterogeneity of ($I^2 = 67\%$, $p = 0.004$). When the metaanalysis was subgrouped by mean diameter, heterogeneity was attenuated in studies with ≥15 mm ($I^2 = 33\%$, $p = 0.19$) and studies with <15 mm ($I^2 = 0\%$, $p = 0.37$, test for overall effect: $z = 2.29$, $p = 0.02$). Then, there was a significant between-subgroup heterogeneity ($I^2 = 77.7\%$, $p = 0.03$). In addition, sensitivity analysis revealed that the study by You et al. (23) had a significant influence on the effect value (RD, RE: −0.01; 95% CI: −0.03, 0.01, $p = 0.45$).

TABLE 4 | Subgroup analysis to assess the effects of ultrasonic image fusion on radiofrequency ablation.

Indicators	Subgrouped by	The number of studies	Effect diameter	95%CI	I^2 (%)	*P* for between subgroup heterogeneity
Technical efficiency	Baseline mean diameter				39.3	0.2
	≥15 mm	4	1.04	0.98, 1.1	95	<0.0001
	<15 mm	2	0.98	0.93, 1.04	0	0.77
1-year LTP	Baseline mean diameter				77.8	0.03
	≥15 mm	4	0.48	0.24, 0.95	42	0.16
	<15 mm	2	1.34	0.69, 2.62	0	0.67
2-year LTP	Baseline mean diameter				84.3	0.01
	≥15 mm	4	0.45	0.27, 0.76	40	0.17
	<15 mm	2	1.34	0.69, 2.62	0	0.67
Complications	Baseline mean diameter				77.7	0.03
	≥15 mm	6	0	−0.02, 0.02	33	0.19
	<15 mm	2	−0.07	−0.12, −0.01	0	0.37
	Control group				0	0.74
	US	3	−0.04	−0.15, 0.07	76	0.01
	CEUS	5	−0.02	−0.05, 0.01	68	0.01

Notably, there was no publication bias, possibly due to the small sample diameter and short follow-up times reported in the studies. Results of subgroup analyses on complications are presented in **Table 4**.

Effect on Overall Survival

Quantitative analysis of overall survival, across four trials, revealed significantly lower 1-year overall survival in the ultrasonic image fusion, relative to the control group (OR, FE: 0.47; 95% CI: 0.23, 0.97, $p = 0.04$), with no evidence of heterogeneity across the studies ($I^2 = 0\%$, $p = 0.67$; **Figure 5A**). Moreover, ultrasonic image fusion had no effect on 2-year overall survival of patients across four studies that evaluated this technique, relative to controls (OR, FE: 0.95; 95% CI: 0.55, 1.63, $p = 0.85$; **Figure 5B**). Low heterogeneity across studies was seen ($I^2 = 43\%$, $p = 0.15$).

Begg's and Egger's tests for 2-year overall survival was ($p = 0.174$, $p = 0.041$, respectively). Due to the small sample diameter and short follow-up time of the studies, publication bias could not be confirmed. There was no evidence of publication bias for 1-year OS ($p = 0.734$, Begg's test and $p = 0.453$, Egger's test). The results of subgroup analysis on overall survival are presented in **Table 4**.

DISCUSSION

Hepatocellular carcinoma is now the sixth most common type of cancer, and the fourth most common cause of cancer-related deaths worldwide (27), while early hepatocellular carcinoma and OS with RFA are comparable to surgical resection (28). Moreover, FI, which can apply information obtained from different imaging methods to generate excellent efficacy and safety by combining the advantages of real-time ultrasound and high resolution CT/MRI, may be more useful than ultrasound in RFA (29). Therefore, the metaanalysis systematically analyzed six studies (10, 21–23, 25, 26), comprising 1,168 patients, and found that in the RFA of hepatocellular carcinoma, FI decreased 1-year OS, and thereis no significant changes in the efficiency of ablation technology, 1–3 year LTP, 2-year OS, and complications compared to ultrasound. Notably, there was clinical heterogeneity which might affect the result due to the difference in the type of control group included in the study. Therefore, the article further compared the differences about efficacy and safety of CEUS, FI (10, 22, 26), and the differences about efficacy and safety of ultrasound and FI in RFA (21, 23, 25). When studying the efficacy and safety of FI and CEUS, there was also no significant change in the results (technical efficiency, $P = 0.84$; 1-year LTP, $P = 0.55$; 2-year LTP, $P = 0.21$; 3-year LTP, $P = 0.63$; Complications, $P = 0.3$; 1-year OS, $P = 0.04$; 2-years OS, $P = 0.18$). Since there were few studies comparing FI and ultrasound, only analyzing the complications found no significant difference in the study results ($P = 0.52$).

The high echo of the gas generated by heating immediately after ablation will greatly blur the ultrasound image of the lesion and make the next puncture difficult, while there is no the interference of vaporization in FI. In addition, when the lesion is not obvious in ultrasound examination, FI can clearly show the lesion, which helps to reduce the difficulty of surgery (30, 31). Moreover, FI has been shown to increase visibility of liver lesions, which significantly increases the confidence of operators when performing RFA (32, 33), thereby improving surgical outcomes and reducing the associated risks and complications (34). Results of our subgroup analyses corroborated these findings, as evidenced by fewer complications in studies that used FI protocol for tumors with a mean diameter <15 mm. Notably, conventional intraoperative residual tumor detection in CEUS has mainly depended on characteristic enhancement of tumors (35), while FI can show the spatial relationship between the original tumor and the ablation area (36, 37), thereby improving accuracy of evaluating intraoperative ablation edge

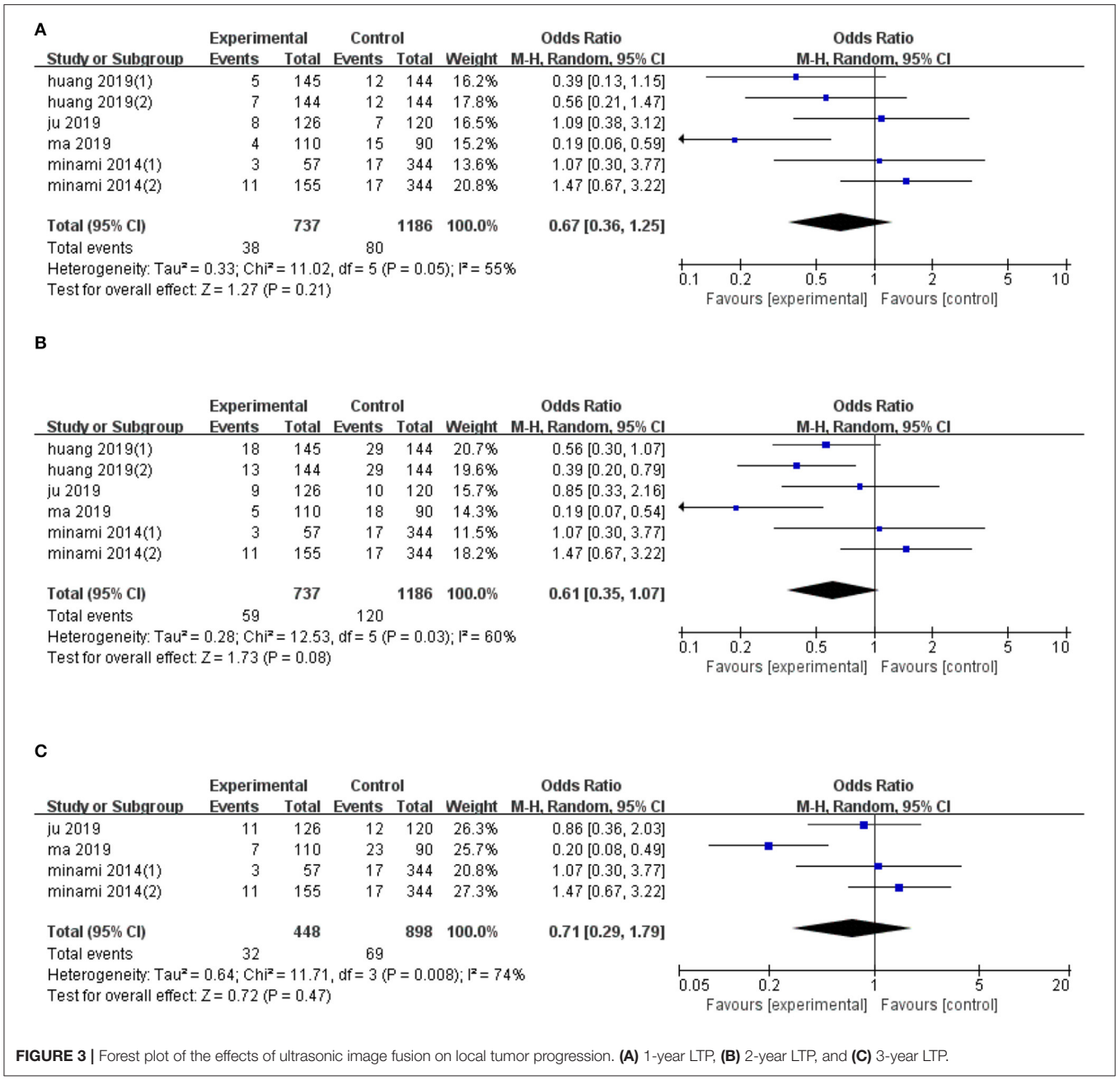

FIGURE 3 | Forest plot of the effects of ultrasonic image fusion on local tumor progression. **(A)** 1-year LTP, **(B)** 2-year LTP, and **(C)** 3-year LTP.

and reducing the residual tumor. Therefore, FI may improve efficacy of ablation surgery, and expand its indications (20, 21), which is consistent with the findings of our subgroup analyses. Specifically, this technique resulted in significantly lower 1- and 2-year LTP, relative to ultrasound in FI for tumors with a mean diameter >15 mm, and the subgroup analyses also confirmed that tumor diameter was the source of heterogeneity.

However, FI has its limitations. Firstly, inherent image distortion between US and CT/MR images is inevitable, especially when patients undergo changes in position, artificial ascites, pleural effusion, or other adjuvant surgery (38). Secondly, location of subcapsular tumors represents an important factor affecting misdiagnosis after fusion image-guided HCC ablation (10). Large anatomical markers, such as the portal vein branch, cannot be used for the localization of such tumors, while the rib shadow can obscure the line of sight of the tumor. These phenomenon increase the difficulty of ablation and may affect the accuracy of FI registration. It also suggests that FI may have limited effect on improving the efficacy and safety of thermal ablation of in HCC patients. So, FI was not significantly different from ultrasound in the efficiency of ablation technology, 1–3 year LTP, and 2-year OS. But the study (39) has found that the distance between the tumor and the surrounding anatomical markers (<3 cm) can significantly reduce the surgical efficacy using FI,

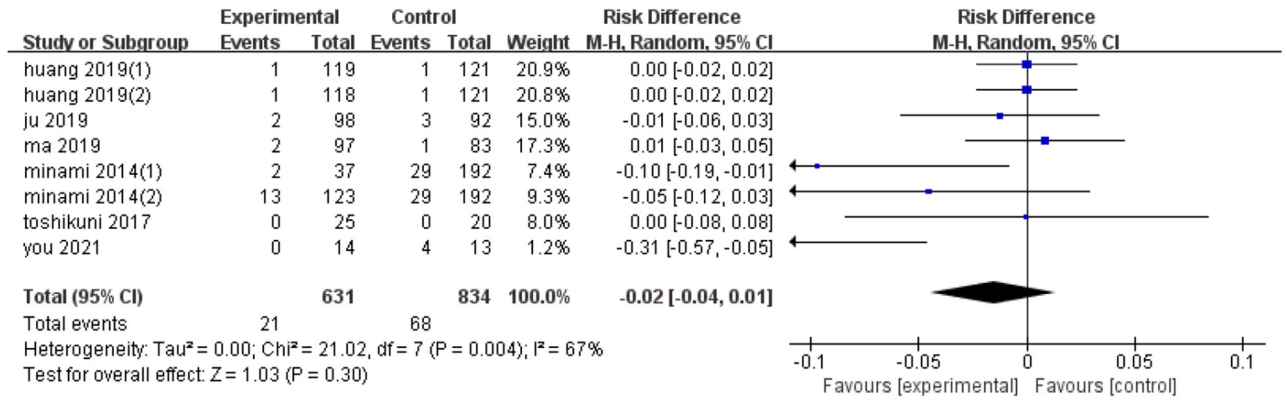

FIGURE 4 | Forest plot of the effects of ultrasonic image fusion on complications.

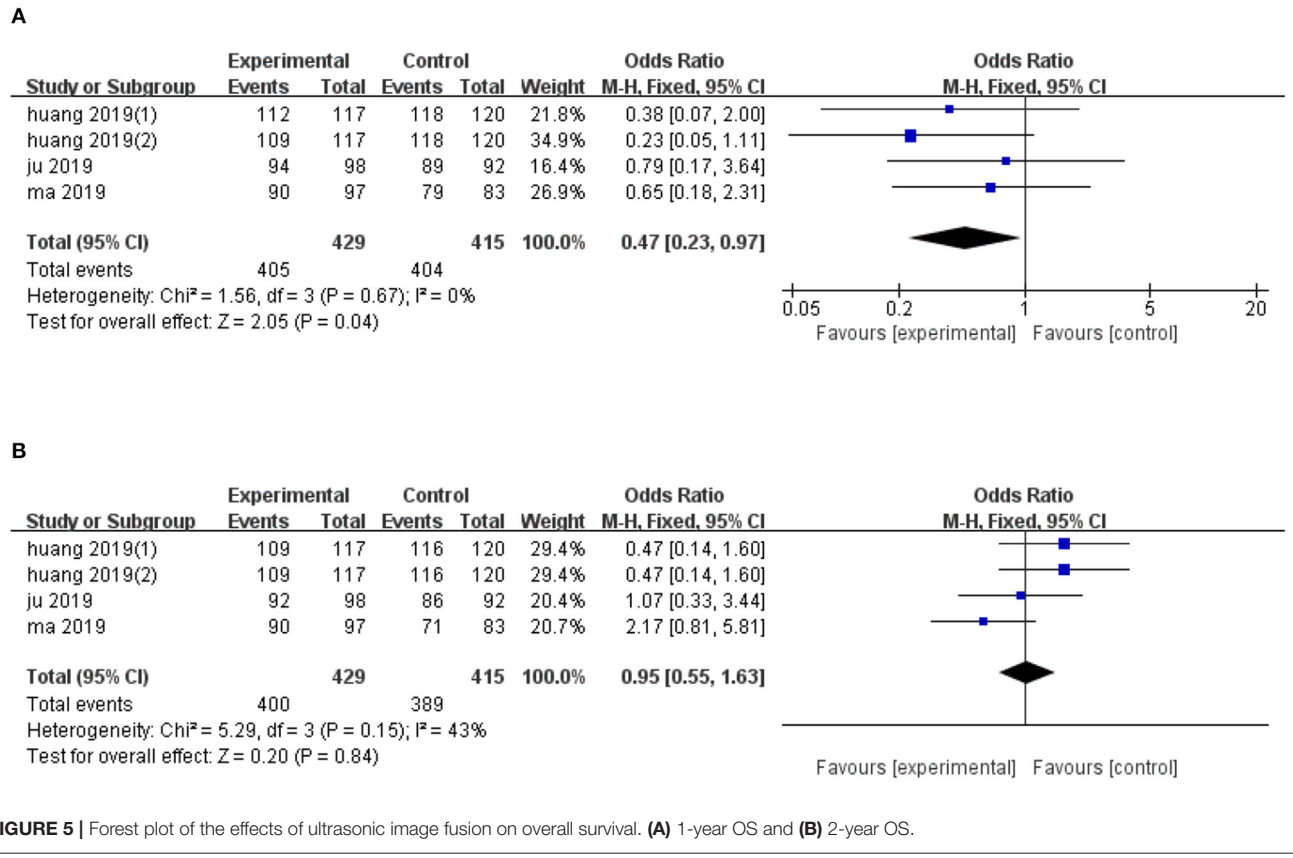

FIGURE 5 | Forest plot of the effects of ultrasonic image fusion on overall survival. **(A)** 1-year OS and **(B)** 2-year OS.

which has nothing to do with the location and diameter of the tumor or the patient's voluntary breathing, etc. Therefore, further research is needed to explore the limitations of FI.

The advantage of this study is that the difference in efficacy and safety between contrastive FI and ultrasound in RFA is controversial and there has not been a relevant metaanalysis. Secondly, this study evaluated the effectiveness of the ablation technique, 1–3 years of LTP, complications, and 1–2 years of OS, and performed subgroup analysis based on tumor diameter and type of control group. In addition, any bias in the review process can be minimized by conducting a comprehensive search of the literature and by following PRISMA guidelines for conducting and reporting reviews.

The study also had some limitations. Firstly, it was difficult to conduct randomization due to the nature of the intervention, so most of the included studies are cohort studies, with a few

high-quality studies. Secondly, differences in geographical regions, ages, and sexes of the patients might have introduced some bias (40). Thirdly, further studies are needed to investigate the indications of FI in RFA due to inconsistent definitions for evaluating liver function and difficult lesions. Fourthly, since there are many FI schemes and FI has certain efficacy for tumors of a certain diameter (3–5 cm) (41), it is necessary to find perfect relevant studies on the differences between FI schemes and their application value.

CONCLUSION

Currently, FI may play a role in improving the efficacy and safety of thermal ablation of HCC, compared to ultrasound, and may be more suitable for cases involving large lesions and difficult ablation. What is important is this study may provide a kind of research idea for the application value of FI. However, rigorous randomized controlled trials, with a larger sample diameter, are needed to validate these conclusions.

DATA AVAILABILITY STATEMENT

The original contributions presented in the study are included in the article/supplementary material, further inquiries can be directed to the corresponding author/s.

AUTHOR CONTRIBUTIONS

TJ, SZ, and LM contributed to the research concept and design. TJ, TG, and FG participated in literature retrieval, data collection, and data analysis. TJ, FG, SZ, and LM contributed to the drafting and review of the final manuscript. All authors read and approved the final manuscript.

FUNDING

This work was supported by the National Natural Science Foundation of China (Grant No. 81601513), Young and Middle-aged High-end Talents Program of Medical Research Program of Chongqing Health and Family Planning Commission (No. 2019GDRC002), and Chongqing Science and Technology Bureau (cstc2019jcyj-msxmX0837).

REFERENCES

1. Benson AB 3rd, D'Angelica MI, Abbott DE, Abrams TA, Alberts SR, Saenz DA, et al. NCCN guidelines insights: hepatobiliary cancers, Version 1, 2017. *J Natl Compr Canc Netw.* (2017) 15:563–73. doi: 10.6004/jnccn.2017.0059
2. Xu XL, Liu XD, Liang M, Luo BM. Radiofrequency ablation versus hepatic resection for small hepatocellular carcinoma: systematic review of randomized controlled trials with meta-analysis and trial sequential analysis. *Radiology.* (2018) 287:461–72. doi: 10.1148/radiol.2017162756
3. Auloge P, Cazzato RL, Koch G, Caudrelier J, De Marini P, Garnon J, et al. [Percutaneous tumor ablation]. *Presse Med.* (2019) 48:1146–55. doi: 10.1016/j.lpm.2019.10.011
4. Villanueva A. Hepatocellular carcinoma. *N Engl J Med.* (2019) 380:1450–62. doi: 10.1056/NEJMra1713263
5. Weinstein JL, Ahmed M. Percutaneous ablation for hepatocellular carcinoma. *AJR Am J Roentgenol.* (2018) 210:1368–75. doi: 10.2214/AJR.17.18695
6. Hui TC, Kwan J, Pua U. Advanced techniques in the percutaneous ablation of liver tumours. *Diagnostics (Basel).* (2021) 11:585. doi: 10.3390/diagnostics11040585
7. Izzo F, Granata V, Grassi R, Fusco R, Palaia R, Delrio P, et al. Radiofrequency ablation and microwave ablation in liver tumors: an update. *Oncologist.* (2019) 24:e990–e1005. doi: 10.1634/theoncologist.2018-0337
8. Xu E, Long Y, Li K, Zeng Q, Tan L, Luo L, et al. Comparison of CT/MRI-CEUS and US-CEUS fusion imaging techniques in the assessment of the thermal ablation of liver tumors. *Int J Hyperthermia.* (2019) 35:159–67. doi: 10.1080/02656736.2018.1487591
9. Calandri M, Mauri G, Yevich S, Gazzera C, Basile D, Gatti M, et al. Fusion imaging and virtual navigation to guide percutaneous thermal ablation of hepatocellular carcinoma: a review of the literature. *Cardiovasc Intervent Radiol.* (2019) 42:639–47. doi: 10.1007/s00270-019-02167-z
10. Ju JX, Zeng QJ, Xu EJ, He XQ, Tan L, Huang QN, et al. Intraprocedural contrast-enhanced ultrasound-CT/MR fusion imaging assessment in HCC thermal ablation to reduce local tumor progression: compared with routine contrast-enhanced ultrasound. *Int J Hyperthermia.* (2019) 36:785–93. doi: 10.1080/02656736.2019.1640899
11. Carriero S, Della Pepa G, Monfardini L, Vitale R, Rossi D, Masperi A, et al. Role of fusion imaging in image-guided thermal ablations. *Diagnostics (Basel).* (2021) 11:549. doi: 10.3390/diagnostics11030549
12. Lee DH, Lee JM. Recent advances in the image-guided tumor ablation of liver malignancies: radiofrequency ablation with multiple electrodes, real-time multimodality fusion imaging, and new energy sources. *Korean J Radiol.* (2018) 19:545–59. doi: 10.3348/kjr.2018.19.4.545
13. Xu E, Li K, Long Y, Luo L, Zeng Q, Tan L, et al. Intra-procedural CT/MR-ultrasound fusion imaging helps to improve outcomes of thermal ablation for hepatocellular carcinoma: results in 502 nodules. *Ultraschall Med.* (2021) 42:e9–e19. doi: 10.1055/a-1021-1616
14. Luo L, He X, Li K, Long Y, Zeng Q, Tan L, et al. Thermal ablation of medium-sized hepatocellular carcinomas using intraoperative ultrasound fusion imaging: a propensity score-matched analysis. *Clin Res Hepatol Gastroenterol.* (2021) 45:101581. doi: 10.1016/j.clinre.2020.11.011
15. Aj L, Kalra N, Bhatia A, Srinivasan R, Gulati A, Kapoor R, et al. Fusion image-guided and ultrasound-guided fine needle aspiration in patients with suspected hepatic metastases. *J Clin Exp Hepatol.* (2019) 9:547–53. doi: 10.1016/j.jceh.2019.01.003
16. Boesen L. Magnetic resonance imaging-transrectal ultrasound image fusion guidance of prostate biopsies: current status, challenges and future perspectives. *Scand J Urol.* (2019) 53:89–96. doi: 10.1080/21681805.2019.1600581
17. Kobe A, Kindler Y, Klotz E, Puippe G, Messmer F, Alkadhi H, et al. Fusion of preinterventional MR imaging with liver perfusion CT after RFA of hepatocellular carcinoma: early quantitative prediction of local recurrence. *Invest Radiol.* (2021) 56:188–96. doi: 10.1097/RLI.0000000000000726
18. Nobre C, Oliveira-Santos M, Paiva L, Costa M, Gonçalves L. Fusion imaging in interventional cardiology. *Rev Port Cardiol.* (2020) 39:463–73. doi: 10.1016/j.repc.2020.03.014
19. Wu DF, He W, Lin S, Zee CS, Han B. The real-time ultrasonography for fusion image in glioma neurosugery. *Clin Neurol Neurosurg.* (2018) 175:84–90. doi: 10.1016/j.clineuro.2018.10.009
20. Long Y, Xu E, Zeng Q, Ju J, Huang Q, Liang P, et al. Intra-procedural real-time ultrasound fusion imaging improves the therapeutic effect and safety of liver tumor ablation in difficult cases. *Am J Cancer Res.* (2020) 10:2174–84.
21. Ma QP, Xu EJ, Zeng QJ, Su ZZ, Tan L, Chen JX, et al. Intraprocedural computed tomography/magnetic resonance-contrast-enhanced ultrasound fusion imaging improved thermal ablation effect of hepatocellular carcinoma: comparison with conventional ultrasound. *Hepatol Res.* (2019) 49:799–809. doi: 10.1111/hepr.13336

22. Huang Q, Zeng Q, Long Y, Tan L, Zheng R, Xu E, et al. Fusion imaging techniques and contrast-enhanced ultrasound for thermal ablation of hepatocellular carcinoma - a prospective randomized controlled trial. *Int J Hyperthermia.* (2019) 36:1207–15. doi: 10.1080/02656736.2019.1687945
23. You Y, Long Y, Yan R, Luo L, Zhang M, Li L, et al. Improving ablation safety for hepatocellular carcinoma proximal to the hilar bile ducts by ultrasound-MR fusion imaging: a preliminary comparative study. *Front Oncol.* (2021) 11:570312. doi: 10.3389/fonc.2021.570312
24. Shiina S, Sato K, Tateishi R, Shimizu M, Ohama H, Hatanaka T, et al. Percutaneous ablation for hepatocellular carcinoma: comparison of various ablation techniques and surgery. *Can J Gastroenterol Hepatol.* (2018) 2018:4756147. doi: 10.1155/2018/4756147
25. Toshikuni N, Matsue Y, Ozaki K, Yamada K, Hayashi N, Tsuchishima M, et al. An image fusion system for estimating the therapeutic effects of radiofrequency ablation on hepatocellular carcinoma. *Radiol Oncol.* (2017) 51:263–9. doi: 10.1515/raon-2017-0028
26. Minami T, Minami Y, Chishina H, Arizumi T, Takita M, Kitai S, et al. Combination guidance of contrast-enhanced US and fusion imaging in radiofrequency ablation for hepatocellular carcinoma with poor conspicuity on contrast-enhanced US/fusion imaging. *Oncology.* (2014) 87(Suppl. 1) 55–62. doi: 10.1159/000368146
27. Bray F, Ferlay J, Soerjomataram I, Siegel RL, Torre LA, Jemal A. Global cancer statistics 2018: GLOBOCAN estimates of incidence and mortality worldwide for 36 cancers in 185 countries. *CA Cancer J Clin.* (2018) 68:394–424. doi: 10.3322/caac.21492
28. Zhu F, Rhim H. Thermal ablation for hepatocellular carcinoma: what's new in 2019. *Chin Clin Oncol.* (2019) 8:58. doi: 10.21037/cco.2019.11.03
29. Wang F, Numata K, Nihonmatsu H, Okada M, Maeda S. Application of new ultrasound techniques for focal liver lesions. *J Med Ultrason.* (2020) 47:215–37. doi: 10.1007/s10396-019-01001-w
30. Thamtorawat S, Hicks RM, Yu J, Siripongsakun S, Lin WC, Raman SS, et al. Preliminary outcome of microwave ablation of hepatocellular carcinoma: breaking the 3-cm barrier? *J Vasc Interv Radiol.* (2016) 27:623–30. doi: 10.1016/j.jvir.2016.01.011
31. Ahn SJ, Lee JM, Lee DH, Lee SM, Yoon JH, Kim YJ, et al. Real-time US-CT/MR fusion imaging for percutaneous radiofrequency ablation of hepatocellular carcinoma. *J Hepatol.* (2017) 66:347–54. doi: 10.1016/j.jhep.2016.09.003
32. Hakime A, Yevich S, Tselikas L, Deschamps F, Petrover D, De Baere T. Percutaneous thermal ablation with ultrasound guidance, fusion imaging guidance to improve conspicuity of liver metastasis. *Cardiovasc Intervent Radiol.* (2017) 40:721–7. doi: 10.1007/s00270-016-1561-5
33. Schwarze V, Rübenthaler J, Marschner C, Fabritius MP, Rueckel J, Fink N, et al. Advanced fusion imaging and contrast-enhanced imaging (CT/MRI-CEUS) in oncology. *Cancers (Basel).* (2020) 12:2821. doi: 10.3390/cancers12102821
34. Song KD, Lee MW, Rhim H, Kang TW, Cha DI, Sinn DH, et al. Percutaneous US/MRI fusion-guided radiofrequency ablation for recurrent subcentimeter hepatocellular carcinoma: technical feasibility and therapeutic outcomes. *Radiology.* (2018) 288:878–86. doi: 10.1148/radiol.2018172743
35. Xuan M, Zhou F, Ding Y, Zhu Q, Dong J, Zhou H, et al. Diagnostic accuracy of contrast-enhanced ultrasound in assessing the therapeutic response to radio frequency ablation for liver tumors: systematic review and meta-analysis. *Surg Endosc.* (2018) 32:2067–75. doi: 10.1007/s00464-017-5903-4
36. Ye J, Huang G, Zhang X, Xu M, Zhou X, Lin M, et al. Three-dimensional contrast-enhanced ultrasound fusion imaging predicts local tumor progression by evaluating ablative margin of radiofrequency ablation for hepatocellular carcinoma: a preliminary report. *Int J Hyperthermia.* (2019) 36:55–64. doi: 10.1080/02656736.2018.1530460
37. Li K, Su Z, Xu E, Huang Q, Zeng Q, Zheng E. Evaluation of the ablation margin of hepatocellular carcinoma using CEUS-CT/MR image fusion in a phantom model and in patients. *BMC Cancer.* (2017) 17:61. doi: 10.1186/s12885-017-3061-7
38. Minami Y, Kudo M. Image guidance in ablation for hepatocellular carcinoma: contrast-enhanced ultrasound and fusion imaging. *Front Oncol.* (2021) 11:593636. doi: 10.3389/fonc.2021.593636
39. Calandri M, Ruggeri V, Carucci P, Mirabella S, Veltri A, Fonio P, et al. Thermal ablation with fusion imaging guidance of hepatocellular carcinoma without conspicuity on conventional or contrast-enhanced US: surrounding anatomical landmarks matter. *Radiol Med.* (2019) 124:1043–8. doi: 10.1007/s11547-019-01057-1
40. Tang A, Hallouch O, Chernyak V, Kamaya A, Sirlin CB. Epidemiology of hepatocellular carcinoma: target population for surveillance and diagnosis. *Abdom Radiol (NY).* (2018) 43:13–25. doi: 10.1007/s00261-017-1209-1
41. Luo L, Yan R, Li K, Zeng Q, Tan L, Long Y, et al. The value of ultrasound fusion imaging technology in assisting thermal ablation of 3 5 cm liver cancer. *Chin J Ultrasound Imaging.* (2019) 28:1102–1103. doi: 10.3760/cma.j.issn.1004-4477.2019.04.008

Conflict of Interest: The authors declare that the research was conducted in the absence of any commercial or financial relationships that could be construed as a potential conflict of interest.

frontiers in Oncology

ORIGINAL RESEARCH
published: 13 December 2021
doi: 10.3389/fonc.2021.773535

Ischemic-Free Liver Transplantation Reduces the Recurrence of Hepatocellular Carcinoma After Liver Transplantation

Yunhua Tang[1,2,3†], *Tielong Wang*[1,2,3†], *Weiqiang Ju*[1,2,3†], *Fangcong Li*[1,2,3], *Qi Zhang*[1,2,3], *Zhitao Chen*[1,2,3], *Jinlong Gong*[1,2,3], *Qiang Zhao*[1,2,3], *Dongping Wang*[1,2,3], *Maogen Chen*[1,2,3*], *Zhiyong Guo*[1,2,3*] *and Xiaoshun He*[1,2,3*]

[1] Organ Transplant Center, The First Affiliated Hospital, Sun Yat-sen University, Guangzhou, China, [2] Guangdong Provincial Key Laboratory of Organ Donation and Transplant Immunology, Guangzhou, China, [3] Guangdong Provincial International Cooperation Base of Science and Technology (Organ Transplantation), Guangzhou, China

Ischemia reperfusion injury (IRI) is an adverse factor for hepatocellular carcinoma (HCC) recurrence after liver transplantation. Ischemic-free liver transplantation (IFLT) is a novel transplant procedure that can largely reduce or even prevent IRI, but the clinical relevance of IFLT and the recurrence of HCC after liver transplantation are still unknown. This retrospective study compared survival outcomes, HCC recurrence, perioperative data and IRI severity following liver transplantation (LT). 30 patients received IFLT and 196 patients received conventional liver transplantation (CLT) were chosen for the entire cohort between June 2017 and August 2020. A 1:3 propensity score matching was performed, 30 IFLT recipients and 85 matched CLT patients were enrolled in propensity-matched cohorts. An univariate and multivariate Cox regression analysis was performed, and showed surgical procedure (CLT *vs* IFLT) was an independent prognostic factor (HR 3.728, 95% CI 1.172-11.861, *P*=0.026) for recurrence free survival (RFS) in HCC patients following liver transplantation. In the Kaplan–Meier analysis, the RFS rates at 1 and 3 years after LT in recipients with HCC in the IFLT group were significantly higher than those in the CLT group both in the entire cohort and propensity-matched cohort (*P*=0.006 and *P*=0.048, respectively). In addition, patients in the IFLT group had a lower serum lactate level, lower serum ALT level and serum AST level on postoperative Day 1. LT recipients with HCC in the IFLT group had a lower incidence of early allograft dysfunction than LT recipients with HCC in the CLT group. Histological analysis showed no

OPEN ACCESS

Edited by:
Patrick J. Schuler, Ulm University Medical Center, Germany

Reviewed by:
Roberto Montalti, Federico II University Hospital, Italy
Tommaso Maria Manzia, University of Rome Tor Vergata, Italy

***Correspondence:**
Maogen Chen
maogen2000@163.com
Zhiyong Guo
rockyucsf1981@126.com
Xiaoshun He
gdtrc@163.com

[†]*These authors have contributed equally to this work and share first authorship*

Specialty section:
This article was submitted to Surgical Oncology, a section of the journal Frontiers in Oncology

Received: *10 September 2021*
Accepted: *22 November 2021*
Published: *13 December 2021*

Citation:
Tang Y, Wang T, Ju W, Li F, Zhang Q, Chen Z, Gong J, Zhao Q, Wang D, Chen M, Guo Z and He X (2021) Ischemic-Free Liver Transplantation Reduces the Recurrence of Hepatocellular Carcinoma After Liver Transplantation. Front. Oncol. 11:773535. doi: 10.3389/fonc.2021.773535

obvious hepatocyte necrosis or apoptosis in IFLT group. In conclusion, IFLT can significantly reduce IRI damage and has the potential to be a useful strategy to reduce HCC recurrence after liver transplantation.

Keywords: ischemia reperfusion injury, hepatocellular carcinoma, ischemic-free liver transplantation, prognosis, propensity-matched analysis

INTRODUCTION

Hepatocellular carcinoma (HCC) is the fifth most common cancer and the third cause of cancer-related mortality worldwide (1). Liver transplantation (LT) offers the most effective treatment for selected patients with HCC compared to liver resection or local ablation (2). However, the high incidence of postoperative recurrence has become a major concern and remains the main limitation of long-term outcomes of liver transplantation (3). Risk factors for HCC recurrence have been extensively investigated and are related to tumor size and number, microvascular invasion and poorly differentiated tumor grade (4, 5). In addition to tumor biology, increasing animal studies and clinical evidence suggest that ischemia reperfusion injury (IRI) promotes the recurrence of HCC after liver transplantation (6–8).

Liver grafts will inevitably be subject to varying degrees of IRI when organ procurement occurs after rapid cold flush, subsequent cold preservation and warm reperfusion after implantation into the recipient. Several studies have shown that liver IRI results in microvascular dysfunction, immune cell recruitment to liver grafts, and the release of pro-inflammatory and pro-proliferation mediators, facilitating the growth of circulating liver cancer cells in the injured liver (9, 10). For decades, great efforts have been made to reverse IRI and reduce the recurrence of HCC after liver transplantation, including ischemia preconditioning, immunological therapy and gene therapy (6, 11–13). However, few studies could be translated to the clinic. Obviously, none of the reported methods could effectively prevent IRI, which is an inevitable consequence due to cold preservation during liver transplantation. Ischemia-free liver transplantation (IFLT) is a novel transplant procedure that is able to procure, preserve and implant liver grafts without stopping the blood and oxygen supply for liver grafts. It has been well established that IRI was largely alleviated and even entirely prevented in IFLT in our previous studies (14, 15). However, to date, no reports have examined the clinical relevance of IFLT and the recurrence of HCC after liver transplantation.

Abbreviations: IRI, ischemia reperfusion injury; HCC, hepatocellular carcinoma; IFLT, ischemic-free liver transplantation; LT, liver transplantation; CLT, conventional liver transplantation; ALT, alanine aminotransferase; AST, aspartate aminotransferase; EAD, early allograft dysfunction; DBD, donation after brain death; DCD, donation after circulatory death; BMI, body mass index; MELD, Model for End-Stage Liver Disease; AFP, alpha-fetoprotein; RFA, radiofrequency ablation; TACE, transcatheter arterial chemoembolization; ICU, intensive care unit; SCS, static cold storage; HA, hepatic artery; NMP, normothermic machine perfusion; HE, hematoxylin and eosin; TUNEL, terminal deoxynucleotidyl transferase dUTP nick end labeling; SD, means ± standard deviation; RFS, recurrence-free survival; OS, overall survival; PNF, primary nonfunctioning; POD, post-operative day.

In this study, we aimed to compare the transplant outcomes and graft IRI severity in recipients with HCC between IFLT and conventional liver transplantation (CLT), further assessing the impact of IFLT on the risk of HCC recurrence after liver transplantation.

PATIENTS AND METHODS

Study Population

This was a retrospective cohort design study. We included adult (18 years of age and older) patients diagnosed with HCC preoperatively who underwent CLT or IFLT at The First Affiliated Hospital of Sun Yat-sen University, Guangzhou, China, between June 2017 and August 2020. Split LT, liver-kidney combined transplantation or multivisceral transplantation were excluded, and patients who died within 30 days of LT were also excluded. Because patients who underwent IFLT only received donors from donation after brain death (DBD), donation after circulatory death (DCD) or living donors were excluded from the current study. Thus, patients identified as having HCC were chosen for the study population (n=226); 30 of 226 patients received IFLT, and the remaining 196 patients received CLT. All 226 donors were enrolled in a voluntary organ donation program for deceased Chinese citizens, and informed consent was obtained from relatives of the donors. No organ donations were from executed prisoners. This study was approved by the Institutional Review Board of the First Affiliated Hospital of Sun Yat-sen University.

The donor variables were age, BMI, donor serum creatinine, donor total bilirubin, donor serum sodium, and cold ischemia time. The recipient variables were age at transplant, BMI, preoperative laboratory MELD score, and positive hepatitis B surface antigen. Tumor parameters were pretransplant AFP, most radiologic tumor diameter, number of lesions (1,2, 3+), Milan criteria, liver resection history, neoadjuvant therapy (RFA or TACE), tumor differentiation (well, moderate, poor), and microvascular invasion. Intraoperative and posttransplantation data included operation duration, anhepatic phase, total blood loss, blood transfusion, ICU stay, hospital stay, early allograft dysfunction (EAD), serum INR, lactate, ALT, AST and creatinine level on the first day posttransplantation, recurrence, date of recurrence, and site of recurrence.

To evaluate whether the outcomes of HCC recipients who underwent IFLT or CLT were different, propensity-matched analyses were performed. IFLT recipients were matched 1:3 with patients who had undergone CLT during the same time period utilizing a propensity match score, matching for the following variables: pretransplant tumor characteristics (serum

AFP, the most radiologic tumor diameter, multiple/single, portal vein tumor thrombosis, liver resection history, RFA/TACE neoadjuvant therapy) and explant tumor characteristics (differentiation and microvascular invasion). The caliper width was 0.2 standard deviations of the logit-transformed propensity score. The absolute standardized differences method was used to diagnose the balance after matching, and all were confirmed to be less than 0.25.

The primary endpoint of this study was tumor recurrence. Secondary endpoints included operation time, intensive care and hospital stay, EAD, serum ALT and AST levels on the first day posttransplantation, histological analysis of liver tissues before procurement, at the end of preservation and after revascularization, and overall survival. EAD was defined by the presence of one or more of the following after LT (16): bilirubin of ≥10 mg/dL on Day 7, international normalized ratio of ≥1.6 on Day 7, and alanine aminotransferase or aspartate aminotransferase >2000 IU/L within the first 7 days. To estimate overall survival, survival time was calculated from the date of LT to death or last known follow-up, and status was recorded at the last point of contact with the patient who died or lived. To estimate recurrence-free survival (RFS), patients with no evidence of recurrence were censored at the time, of last follow-up or death.

CLT and IFLT Procedure

The CLT procedure included organ procurement after rapid cold flush, subsequent static cold storage (SCS) and back-table preparation, and then implantation. The surgical procedures of IFLT were as described in our previous study (14, 15). Briefly, after the liver was fully mobilized, a 4 cm-long segment of the external iliac vein from the blood donor was harvested and end-to-side anastomosed to the portal vein of liver donors, serving as an access point for portal vein cannulation while still permitting native blood flow through the portal vein. A 12 Fr cannula was inserted into the splenic artery (or gastroduodenal artery) without interruption of arterial supply to the liver from the celiac artery. A 32 Fr cannula was placed in the infrahepatic inferior vena cava for outflow. A straight 24 Fr cannula connected to the portal vein perfusion line of Liver Assist (Organ Assist, Groningen, The Netherlands) was inserted into the portal vein *via* the interposition vein. The arterial cannula was then connected to the hepatic artery (HA) perfusion line of Liver Assist. After the *in situ* normothermic mechanical perfusion (NMP) circuit for the livers was established, the livers were harvested and moved to the organ reservoir under continuous NMP. So that the graft did not suffer ischemia during procurement. Hereafter, the liver underwent ex situ NMP. The perfusate contained approximately 1.3 L cross-matched leucocyte-depleted washed red cells, 1.4 L Succinylated gelatinor, 30 mL 5% sodium bicarbonate, 0.5 g metronidazole, 37500 U heparin, 1.5 g cefoperazone sodium and sulbactam sodium, 30 mL 10% calcium gluconate, 3 mL 25% magnesium sulfate and 250 mL compound amino acid injection. In IFLT, no back-table preparation is needed, and the liver is implanted under continuous NMP. Briefly, the splenic artery (or gastroduodenal artery) and interposition vein and all vascular anastomoses (donor suprahepatic vena cava to recipient suprahepatic vena cava, donor portal vein to recipient portal vein, and donor celiac artery/common hepatic artery to recipient common hepatic artery) were performed without interruption of the blood supply to the graft under continuous NMP. After the native blood supply from the recipient's portal vein and hepatic artery to the graft was re-established, the *in situ* NMP was stopped, and the cannulas were removed. The donor splenic artery (or gastroduodenal artery) was ligated closed, and the interposition vein was sutured closed. The donor infrahepatic vena cava and common bile duct were anastomosed to the recipient counterparts. Graphic rendering of the ischemia-free liver transplantation procedure is shown in **Figure 1**.

Sample Collection

In *ex vivo* perfusion, samples from the perfusate were collected for analysis of the blood gas parameters (pO2, pCO2, PH and lactate). Perfusate samples were also collected and centrifuged, and the supernatant was stored at -80°C for liver function tests, such as aspartate aminotransferase (AST), alanine aminotransferase (ALT), and total bilirubin (Tbil), using standard biochemical methods. Bile production was collected every 60 minutes from the biliary draining tube for bile production calculation and detection of PH and $HCO3^-$ of bile. Liver tissue biopsy was performed for histology studies before procurement, at the end of preservation and after revascularization, including hematoxylin and eosin (HE) staining for histological scoring and terminal deoxynucleotidyl transferase dUTP nick end labeling (TUNEL) assay for hepatocyte apoptosis.

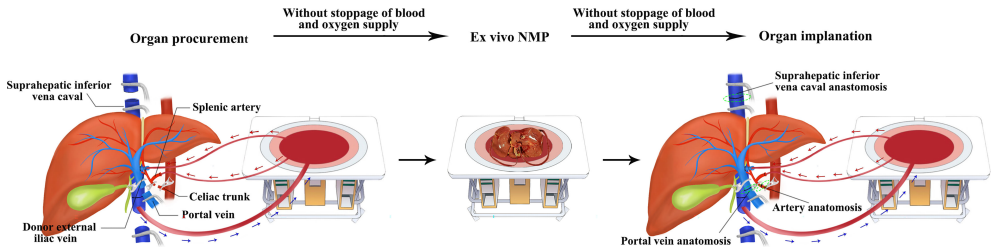

FIGURE 1 | Graphic rendering of the ischemia-free liver transplantation procedure.

Transplantation Procedures and Postoperative Management

After CLT or IFLT, all patients were admitted to the intensive care unit. The immunosuppressive regimen was 20 mg basiliximab induction therapy administered during the operation and on postoperative Day 4. Both a calcineurin inhibitor and mycophenolate mofetil were administered for immunosuppressive maintenance therapy beginning on postoperative Day 4.

Statistical Analysis

The donor and recipient characteristics were expressed as the means ± standard deviation (SD) for metric parameters and as percentages for nominal parameters. Continuous data were compared using t-tests, whereas categorical variables were compared using the chi-square test or Fisher's exact test. We used Kaplan-Meier statistics and the log-rank test to analyze the recurrence-free survival (RFS) and overall survival (OS) rates of the patients both in the entire cohort and propensity-matched cohorts. To identify independent predictors of RFS in entire cohort, an univariate and multivariate Cox proportional hazard regression was conducted for all candidate predictors of RFS. Pretransplant serum AFP levels were categorized into two groups according to interquartile range 3 (IQR3). Variables with a $P < 0.05$ in univariate analysis were subjected to multivariate Cox proportional hazards regression *via* the forward stepwise method; the results were presented as hazard ratios (HRs) with 95% confidence intervals (CIs). The data analysis was performed using STATA 14.0 software (Stata Corp). $P < 0.05$ was considered to be statistically significant.

RESULTS

Recipient and Donor Clinical Characteristics Between the IFLT group and CLT Group

Patients identified as having HCC were chosen for the study population (n=226) between June 2017 and August 2020 in the entire cohort; 30 of 226 patients received IFLT, and the remaining 196 patients received CLT. To correct selection biases and confounding factors, propensity score matching was performed at a 1:3 ratio. After matching, 30 IFLT recipients and 85 matched CLT patients from our center were enrolled in propensity-matched cohorts during the same period. In the entire cohort, the duration of follow-up was 22.9 ± 11.2 months in the IFLT group and 22.6 ± 11.4 months in the CLT group with no significant differences, securing a minimal follow-up of 6 months in the two groups.

There were no significant differences in donor and recipient characteristics between the IFLT group and the CLT group both in the entire cohort and in the propensity-matched cohort, including

TABLE 1 | Recipient and donor characteristics in IFLT and CLT groups before and after propensity score matching.

	Entire cohort			Propensity-matched cohort		
	IFLT group (n = 30)	CLT group (n = 196)	P	IFLT group (n = 30)	CLT group (n = 85)	P
Donor Characteristics						
Donor age (years)	41.4 ± 14.2	36.8 ± 14.9	0.117	41.4 ± 14.2	35.1 ± 14.3	0.053
Gender: male	66.7% (20/30)	74.0% (145/196)	0.401	66.7% (20/30	71.8% (61/85)	0.599
BMI, kg/m^2	22.3 ± 2.3	23.3 ± 9.8	0.771	22.3 ± 2.3	22.2 ± 3.1	0.896
Donor serum creatinine (ummol/L)	87.3 ± 67.2	139.2 ± 155.6	0.074	87.3 ± 67.2	125.6 ± 107.7	0.071
Donor total bilirubin (umol/L)	27.7 ± 21.5	23.4 ± 17.6	0.250	27.7 ± 21.5	22.9 ± 14.5	0.180
Donor serum sodium (mmol/L)	147.6 ± 12.6	149.7 ± 16.7	0.508	147.6 ± 12.6	148.3 ± 20.8	0.870
Cold ischemia time (hours)	NA	6.7 ± 2.1	NA	NA	6.8 ± 2.2	NA
Recipient Characteristics						
Age at transplant (years)	54.2 ± 9.9	50.2 ± 73	0.088	54.2 ± 9.9	50.74 ± 9.9	0.106
Gender: male	96.7% (29/30)	92.9% (182/196)	0.435	96.7% (29/30)	90.6% (77/85)	0.287
BMI, kg/m^2	23.4 ± 3.1	23.2 ± 3.2	0.793	23.4 ± 3.1	23.5 ± 3.5	0.822
Preoperative lab MELD score	15.4 ± 7.7	13.7 ± 8.1	0.279	15.4 ± 7.7	13 ± 7.8	0.174
Positive Hepatitis B surface antigen	90.0% (27/30)	86.7% (170/196)	0.618	90.0% (27/30)	85.9% (73/85)	0.565
Tumor parameter						
Pretransplant AFP (ug/l)	167.9 ± 428.5	12899.4 ± 729.2	**0.016**	167.9 ± 428.5	97.9 ± 342.8	0.371
Size biggest HCC lesion (mm)	43.47 ± 16.7	54.23 ± 41.74	0.129	43.47 ± 16.7	44.5 ± 33.8	0.751
Number of lesions						
single	46.7% (14/30)	39.3% (77/196)	0.443	46.7% (14/30)	42.4% (36/85)	0.682
Multiple	53.3% (16/30)	60.7% (119/196)		53.3% (16/30)	57.6% (49/85)	
Within Milan criteria	56.7% (17/30)	36.2% (71/196)	**0.032**	56.7% (17/30)	48.2% (41/85)	0.427
tumor differentiation						
Well	3.3% (1/30)	3.1% (6/196)	0.994	3.3% (1/30)	4.7% (4/85)	0.839
Moderate	73.3% (22/30)	73.0%%(143/196)		73.3% (22/30)	76.5% (65/85)	
Poor	23.3% (7/30)	24.0% (47/196)		23.3% (7/30)	18.8% (16/85)	
Microvascular invasion	16.7% (5/30)	33.7% (66/196)	**0.042**	16.7% (5/30)	18.8% (16/85)	0.793
Liver resection history	23.3% (7/30)	17.9% (35/196)	0.772	23.3% (7/30)	21.2% (18/85)	0.806
neoadjuvant therapy (RFA or TACE)	46.7% (14/30)	52.0% (102/196)	0.328	46.7% (14/30)	52.9% (45/85)	0.554
Duration of follow-up (days)	22.9 ± 11.2	22.6 ± 11.4	0.917	22.9 ± 11.2	24.8 ± 11.9	0.441

The bold emphasis of P value means that the value less than 0.05 has statistical significance.

donor characteristics (age, gender, donor BMI, donor serum creatinine, donor serum total bilirubin and donor serum sodium) and recipient characteristics (age, gender, BMI, laboratory MELD scores and positive hepatitis B surface antigen). The cold ischemia time in the CLT group was 6.7 ± 2.1 hours in the entire cohort and 6.8 ± 2.2 hours in the propensity-matched cohort. Donor and recipient characteristics were summarized in **Table 1**.

Comparison of Tumor Parameters Between the IFLT Group and CLT Group

In the entire cohort, the pretransplant AFP level was higher in the CLT group than in the IFLT group (P=0.016). The percentage of LT recipients within the Milan criteria and microvascular invasion was higher in the CLT group than in the IFLT group (P=0.032 and P = 0.042, respectively). There were no differences in the size largest HCC lesion, number of lesions, tumor differentiation, liver resection history and neoadjuvant therapy (RFA or TACE) history between the two groups. In the propensity-matched cohort, there were no differences in all tumor parameters between the two groups. Comparison of tumor parameters were summarized in **Table 1**.

IFLT Provides a Larger Benefit for the Reduction in Post-LT HCC Recurrence Than CLT

To analysis whether IFLT has potential as an independent prognostic factor in HCC patients following liver transplantation, Cox regression analysis was performed to examine RFS in the entire cohort. Univariate analysis indicated that pretransplant AFP (≥ 300 ug/l *vs.* < 300 ug/l)(HR 3.830, 95% CI 2.447-5.997, P <0.001), biggest HCC diameter (≥ 5cm *vs.* < 5cm) (HR 1.753, 95% CI 1.119-2.746, P =0.014), poor tumor differentiation (HR 2.738, 95% CI 1.226-6.112, P = 0.014), microvascular invasion (HR 3.453, 95% CI 2.213-5.388, P <0.001) and surgical procedure (CLT *vs* IFLT) (HR 4.371, 95% CI 1.371-13.864, P =0.012) were associated with RFS. Furthermore, multivariate analysis demonstrated that pretransplant AFP (≥ 300 ug/l *vs.* < 300 ug/l) (HR 2.262, 95% CI 1.597-4.318, P <0.001), microvascular invasion (HR 2.309, 95% CI 1.403-3.801, P <0.001) and surgical procedure (CLT *vs* IFLT) (HR 3.728, 95% CI 1.172-11.861, P =0.026) were independent prognostic factors for DFS in HCC patients following liver transplantation (**Table 2**).

In the entire cohort, Kaplan–Meier analysis showed the RFS rates at 1 and 3 years after LT in recipients with HCC in the IFLT group were 92.2% and 86.7%, respectively, which were significantly higher than those (73.0% and 46.3%) in the CLT group (P=0.006, **Figure 2A**). The overall survival rates at 1 and 3 years after LT in recipients with HCC in the IFLT group were 96.7% and 90.6%, respectively, which tended to be higher than those (90.2% and 68.1%) in the CLT group, but with no significant differences (P=0.089, **Figure 2B**). In the propensity-matched cohort, the RFS rates at 1 and 3 years after LT in recipients with HCC in the IFLT group were 92.2% and 86.7%, respectively, which were significantly higher than those (88.1% and 53.6%, respectively) in the CLT group (P=0.048, **Figure 2C**). The overall survival rates at 1 and 3 years after LT in recipients with HCC in the IFLT group were 96.7% and 90.6%, respectively, which tended to be higher than those (94.1% and 70.6%) in the CLT group, but with no significant differences (P=0.442, **Figure 2D**). These results indicate that IFLT provides greater benefits than CLT in terms of the reduction in post-LT HCC recurrence.

TABLE 2 | Univariate and multivariate analyses of risk factors for recurrence-free survival in the entire cohort.

	Univariate analysis			Multivariate analysis		
	HR	**95% CI**	**P**	**HR**	**95% CI**	**P**
Recipient Characteristics						
age at transplant (years)	0.980	0.959-1.001	0.062			
Gender: male *vs* female	1.030	0.448-2.371	0.944			
BMI, kg/m^2	1.006	0.940-1.077	0.860			
Preoperative lab MELD score	1.008	0.979-1.037	0.599			
Positive Hepatitis B surface antigen	1.382	0.418-4.569	0.596			
Pretransplant AFP: ≥ 300 *vs.* < 300 ug/l	3.830	2.447-5.997	**<0.001**	2.626	1.597-4.318	**<0.001**
biggest HCC diameter: ≥ 5cm *vs.* < 5cm	1.753	1.119-2.746	**0.014**			
Tumor Number (single *vs.* multiple)	1.009	0.643-1.582	0.969			
Tumor differentiation: Moderate *vs.* Well	1.702	0.801-3.614	0.167			
Tumor differentiation: Poor *vs.* Well	2.738	1.226-6.112	**0.014**			
Microvascular invasion	3.453	2.213-5.388	**<0.001**	2.309	1.403-3.801	**0.001**
Liver resection history	0.983	0.560-1.725	0.952			
Neoadjuvant therapy (RFA or TACE)	1.113	0.715-1.732	0.636			
Donor Characteristics						
Donor age (years)	1.002	0.987-1.017	0.824			
BMI, kg/m^2	0.946	0.878-1.019	0.144			
Donor serum creatinine (ummol/L)	1.001	0.999-1.003	0.393			
Donor total bilirubin (umol/L)	0.994	0.980-1.008	0.382			
Donor serum sodium (mmol/L)	1.001	0.988-1.014	0.899			
surgical procedure: CLT *vs.* IFLT	4.371	1.371-13.864	**0.012**	3.728	1.172-11.861	**0.026**

The bold emphasis of P value means that the value less than 0.05 has statistical significance.

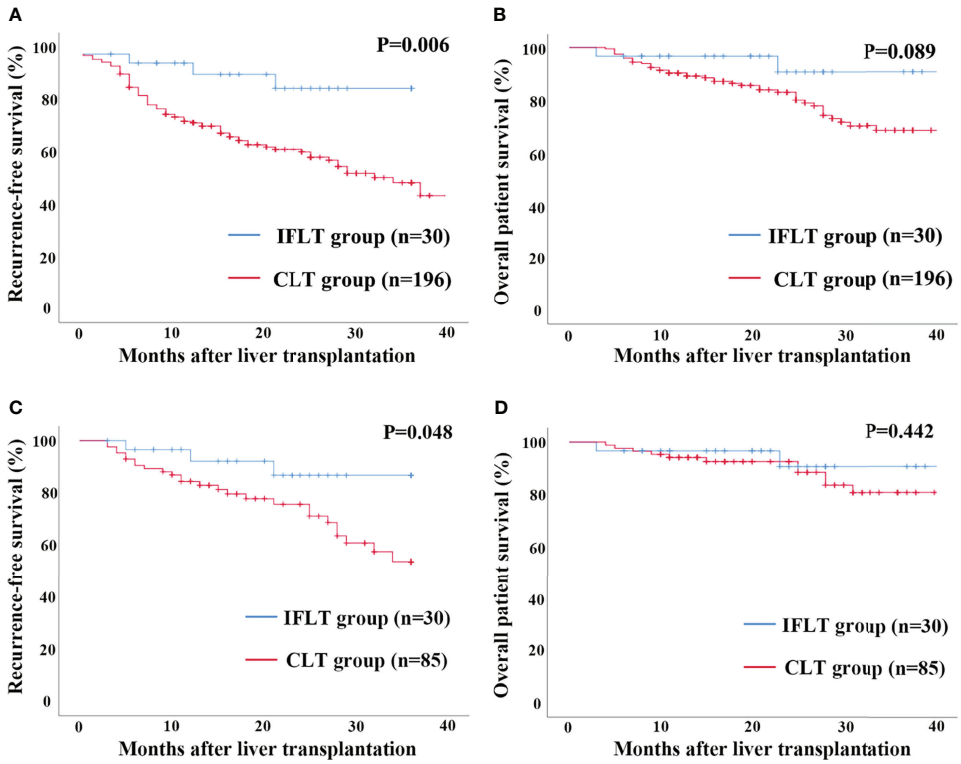

FIGURE 2 | Recurrence-free survival and overall survival by Kaplan-Meier survival analysis for patients transplanted for HCC between the IFLT and CLT group for 3 years' follow-up. **(A)** Recurrence-free survival in the entire cohort. **(B)** Overall survival in the entire cohort. **(C)** Recurrence-free survival in the propensity-matched cohort. **(D)** Overall survival in the propensity-matched cohort.

Comparison of Operative and Postoperative Outcomes Between the IFLT Group and CLT Group

In the entire cohort, LT recipients with HCC in the IFLT group had a shorter operation duration than LT recipients with HCC in the CLT group (6.3 ± 1.4 hours *vs.* 6.9 ± 1.5 hours, *P*=0.016). The anhepatic time was not different between the IFLT and CLT groups (52.2 ± 16.9 mins *vs.* 53.3 ± 14.8 mins, *P*=0.980). There were no differences in total blood loss or blood transfusion between the two groups. The ICU stay (52.4 ± 50.7 hours *vs.* 53.8 ± 50.2 hours, *P*=0.895) and hospital stay (23.8 ± 17.6 days *vs.* 25.8 ± 15.1 days, *P*=0.772) were similar between the two groups. LT recipients with HCC in the IFLT group had a lower incidence of EAD than LT recipients with HCC in the CLT group (3.3% *vs.* 29.6%, *P*=0.002). Patients in the IFLT group had a lower serum lactate level (1.9 ± 1.2 mmol/L *vs.* 2.7 ± 1.3 mmol/L, *P*=0.005), lower serum ALT level (198.8 ± 157.9 U/L *vs.* 633.8 ± 706.2 U/L, *P*=0.001) and serum AST level (437.1 ± 328.9 U/L *vs.* 1571.6 ± 1764.6 U/L, *P*=0.001) on postoperative Day 1. There were no differences in serum creatine levels or serum INR levels between the two groups on postoperative Day 1.

In the propensity-matched cohort, the indicators mentioned above had the same trend. Operative and postoperative outcomes are summarized in **Table 3**.

IFLT Is Feasible, Safe and Effective, and Can Largely Reduce IRI in LT Recipients With HCC

The NMP device provided adequate O2 and extraction of CO2 of the perfusion fluid with stable pressure and flow of both the portal vein and hepatic artery throughout the whole IFLT procedure (**Figures 3A, B**). The lactate levels in the perfusate dropped quickly from 4.73 ± 2.22 mmol/L to normal, and the pH value in the perfusate was within the normal physiological range, reflecting active metabolism by the liver grafts (**Figure 3C**). The liver grafts presented a vivid appearance during procurement, ex vivo NMP and implantation (**Figure 3D**). Continuous bile production with a high sodium bicarbonate and pH level indicated good quality of the bile (**Figures 3E, F**). Altogether, these results indicate the effectiveness of IFLT and suggest excellent organ viability.

Hematoxylin and eosin (HE) staining evaluation of IFLT allograft biopsies showed stable and low Suzuki scores, whereas increased Suzuki scores were observed in the CLT allograft biopsies at the end of preservation graft and after revascularization (**Figure 4A**). The TUNEL assay showed no significant increase in apoptotic hepatocytes throughout the whole IFLT procedure in the IFLT group, while a significant increase in apoptotic hepatocytes was observed at the end of the

TABLE 3 | Operative and postoperative outcomes in IFLT and CLT groups before and after propensity score matching.

	Entire cohort			Propensity-matched cohort		
	IFLT group (n = 30)	CLT group (n = 196)	P	IFLT group (n = 30)	CLT group (n = 85)	P
Operation duration (hours)	6.3 ± 1.4	6.9 ± 1.5	**0.016**	6.3 ± 1.4	7.0 ± 1.4	**0.017**
Anhepatic phase (mins)	52.2 ± 16.9	53.3 ± 14.8	0.980	52.2 ± 16.9	52.7 ± 13.2	0.086
Total blood loss (mL)	1726 ± 830	1626 ± 1649	0.775	1726 ± 830	1418 ± 1069	0.259
Blood transfusion (ml)	960 ± 860	940 ± 960	0.908	960 ± 860	820 ± 780	0.395
ICU stay (h)	52.4 ± 50.7	53.8 ± 50.2	0.895	52.4 ± 50.7	55.1 ± 47.2	0.798
Hospital stay (day)	23.8 ± 17.6	25.8 ± 15.1	0.772	23.8 ± 17.6	24.6 ± 14.1	0.816
EAD	3.3% (1/30)	29.6%(58/196)	**0.002**	3.3% (1/30)	29.4%(25/85)	**0.003**
INR day 1	1.5 ± 0.4	1.4 ± 0.3	0.179	1.5 ± 0.4	1.5 ± 0.3	0.575
Serum lactate day 1	1.9 ± 1.2	2.7 ± 1.3	**0.005**	1.9 ± 1.2	2.6 ± 1.3	**0.021**
ALT day 1, U/L	198.8 ± 157.9	633.8 ± 706.2	**0.001**	198.8 ± 157.9	617.6 ± 819.5	**0.007**
AST day 1, U/L	437.1 ± 328.9	1571.6 ± 1764.6	**0.001**	437.1 ± 328.9	1393 ± 1610	**0.002**
Creatinine day 1, mmol/L	95.7 ± 43.2	84.8 ± 35.3	0.129	95.7 ± 43.2	84.3 ± 37.3	0.186

The bold emphasis of P value means that the value less than 0.05 has statistical significance.

preservation graft and after revascularization (**Figure 4B**). These results suggest that IFLT can largely reduce IRI in LT recipients with HCC.

DISCUSSION

IRI is an unavoidable adverse factor in liver transplantation. IRI can impair the function of transplanted organs, leading to EAD or even primary nonfunctioning (PNF), increasing the incidence of complications and mortality in recipients after surgery (17). In addition, IRI is associated with tumor recurrence and metastasis after liver transplantation. Much effort has been devoted to reducing the degree of IRI, including ischemia preconditioning and the use of protective gases, stem cells or gene therapy. However, few methods have been translated into clinical practice (18). Recently, great achievements have been made in *ex vivo* machine perfusion of organs. In particular, NMP could offer oxygen and nutrients and allow functional testing of liver grafts, which have been demonstrated to be obviously superior to static cold storage in minimizing IRI (19). In the current NMP setting, the organs still suffer cold storage injury and ischemia due to cold flush before procurement, back-table preparation on ice and normal saline flush after NMP. Research has shown that a short period of cold ischemia time still results in significant sinusoidal endothelial cell dysfunction and Kupffer cell activation in the liver (20). Therefore, we established IFLT without stopping the blood and oxygen supply and any cold preservation for the

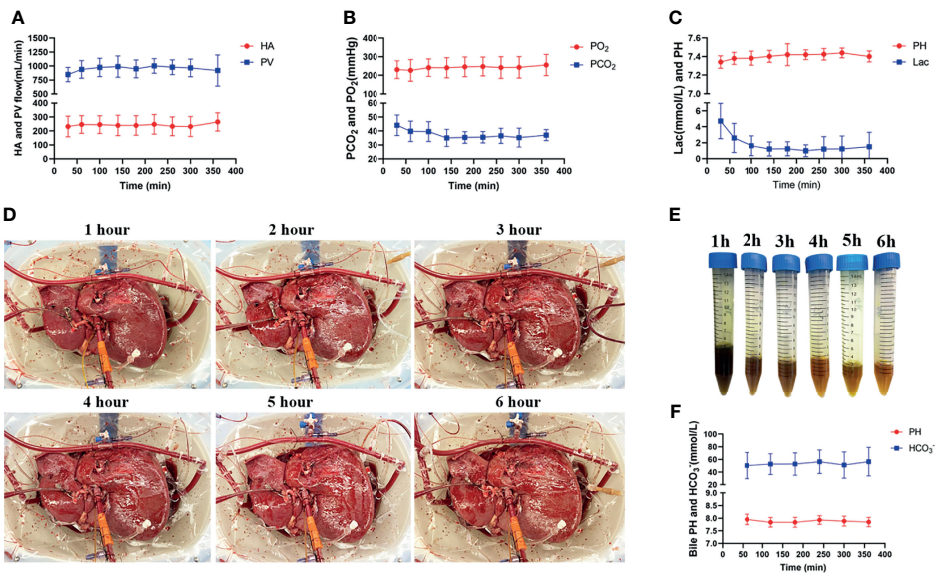

FIGURE 3 | Normothermic machine perfusion. **(A)** The arterial and portal venous flow rates; **(B)** The O2 and CO2 tension in the perfusate. **(C)** pH values and lactate levels in the perfusate. **(D)** The grafts presented a vivid appearance during ex vivo perfusion; **(E)** The produced bile during ex vivo perfusion; **(F)** PH value and bicarbonate levels of the produced bile.

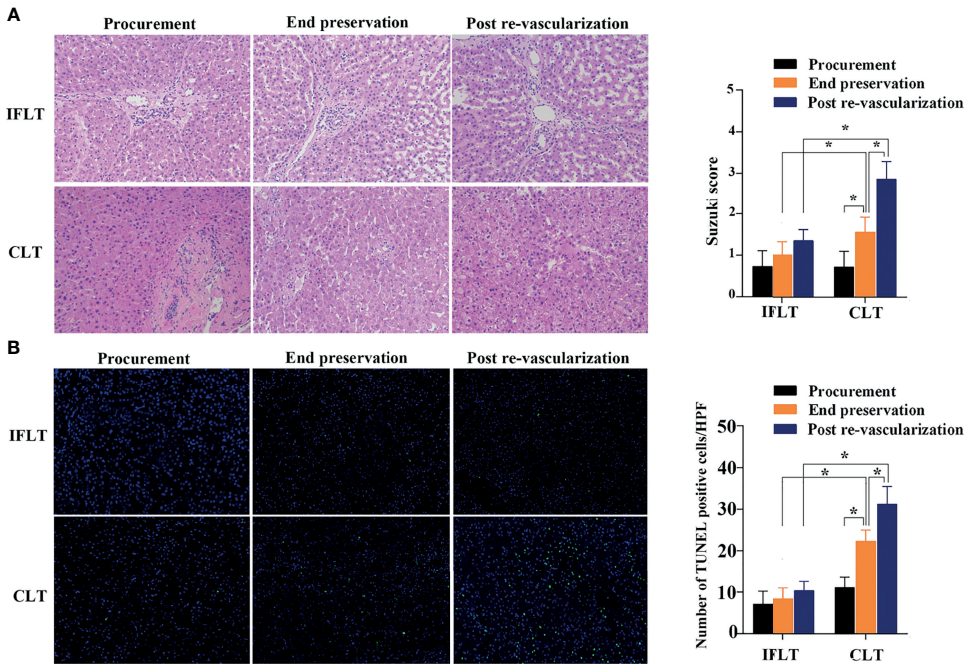

FIGURE 4 | Histological analysis of liver tissues. **(A)** Hematoxylin and eosin (HE) of donor liver tissue biopsies before procurement, at the end of preservation and post-reperfusion in the IFLT and CLT. **(B)** The TdT-mediated dUTP nick end labelling (TUNEL) assay revealed that the number of apoptotic hepatocytes per high power field (HPF) before procurement, at the end of preservation and post-reperfusion in the IFLT and CLT. *P<0.001.

liver grafts during the whole transplant procedure. The protective effect of IFLT in reducing IRI on the donor liver was obvious. Peak transaminase levels within 1 week after LT correlated with both cold ischemia time and warm ischemia time, which can reflect the severity of IRI (21) and is regarded as a well-defined surrogate marker for long-term graft function and survival (21). In the current study, the peak value of transaminase on posttransplant Day 1 in the IFLT group was significantly lower than that in the CLT group. In addition, EAD suggests the initial poor function of liver grafts and represents the clinical phenotype of severe IRI after liver transplantation. Our results showed that LT recipients with HCC in the IFLT group had a lower incidence of EAD than LT recipients with HCC in the CLT group (3.3% *vs.* 29.4%, *P*=0.003), which was also much lower than the incidence of EAD of 20.0–30.0% reported by other centers in Western countries (16, 22, 23). Furthermore, histological analysis showed no significant increase in the Suzuki score or apoptotic hepatocytes during the whole transplant procedure in the IFLT group. In the IFLT group, the amount of blood loss and blood transfusion did not increase, and the postoperative ICU hospital stay and total hospital stay did not increase. These results suggested that IFLT did not increase the difficulty and complexity of the operation, nor did it increase the complications and hospitalization costs. Together, these findings indicate that IRI can be largely prevented in IFLT.

Clinically, previous studies have shown that posttransplant cancer recurrence and metastasis are significantly correlated with many factors, including tumor size and number (24), microvascular invasion (25), elevated AFP level (26, 27) and poorly differentiated tumor grade (4). In addition to liver tumor biology itself, increasing evidence supports the adverse effect of liver ischemia on the risk of liver cancer recurrence after liver transplantation. Nagai et al. (28) showed that prolonged cold and warm ischemia times of the liver graft are independent predictors of HCC recurrence one year after liver transplantation. Orci et al. (29) confirmed that LT recipients of organs from DCD donors with long warm ischemia times had higher HCC recurrence after liver transplantation. Several transplantation centers have reported that the rate of HCC recurrence was significantly higher following living donor liver transplantation than following deceased donor liver transplantation because the liver graft from a living donor is usually small for the recipient and more vulnerable to IRI (30, 31). On the other hand, several attempts targeting graft IRI effectively decreased the risk of early HCC recurrence after liver transplantation. Kornberg et al. (6) reported that treating liver graft IRI with prostaglandin E1 significantly increased the recurrence-free survival rates of recipients with HCC. A mouse model mimicking the recurrence of HCC after liver transplantation suggested that remote ischemic preconditioning offers protection against ischemia-mediated accelerated HCC recurrence (8). Matteo et al. (32) reported that the performance of hypothermic oxygenated liver perfusion before liver implantation appears advantageous to protect against HCC recurrence after liver transplantation, despite extended tumor criteria. In the current study, IRI was largely prevented. Here, we compared the

difference in the postoperative recurrence rate between the IFLT and CLT groups. To correct selection biases and confounding factors, propensity score matching was performed. The tumor parameters, including tumor size, number, AFP level, tumor grade, microvascular infiltration and preoperative downstage treatment, were consistent between the two groups in our study. Both groups of patients received DBD liver donation without warm ischemia time, and IRI can be largely reduced even completely prevented by performing IFLT. An univariate and multivariate Cox regression analysis was performed in our study, and showed surgical procedure (CLT *vs* IFLT) was an independent prognostic factor for RFS in HCC patients following liver transplantation. In the Kaplan–Meier analysis, the recurrence free survival rates at 1 and 3 years after LT in recipients with HCC in the IFLT group were significantly higher than those in the CLT group both in the entire cohort and propensity-matched cohort (P=0.006 and P=0.048, respectively). These results together indicated that IFLT provides greater benefit than CLT in terms of the reduction in post-LT HCC recurrence, which supports that IRI had an impact on tumor recurrence after liver transplantation and that preventing or reducing IRI can reduce the HCC recurrence rate after liver transplantation.

The significance of IFLT in liver transplantation for HCC may not only improve the prognosis but also may expand the donor pool. Organ shortages are a problem to be solved worldwide, and patients with HCC who exceed the Milan or UCSF standard rarely have the opportunity to obtain a suitable liver. Marginal organs have greater vulnerability to IRI, such as older donors and fatty livers (33). Because China still in its early stages in developing an organ donation system based on deceased citizens, most donations originate from primary care hospitals, because of the lack of both basic medical equipment and doctors experienced with managing donors, these donors often suffer from multiple risk factors such as unstable blood circulation, hypoproteinemia, infection, and electrolyte disturbance. To be honest, we are relatively cautious about donor selection. Therefore, our initial experience is often based with a very young donors, which is a limitation of the study. However, IFLT can protect these marginal donor livers from IRI damage. Our previous studies reported the successful use of marginal donor livers (such as with hyperbilirubinemia or 85–95% macrovesicular steatosis) in LT recipients using IFLT (14, 34). Therefore, we recommend increasing the utilization of extended donor criteria or marginal donor liver grafts in recipients with HCC by performing IFLT in the future due to the benefit of IFLT-mediated reduction in IRI and post-LT HCC recurrence.

Our research has several limitations. First, IFLT is only carried out in a single center, and the overall sample size is insufficient. In the future, we will promote IFLT technology in multiple centers to increase the number of HCC patients to verify the significance of IFLT in reducing postoperative tumor recurrence. Second, there were not enough cases to perform stratified studies for different tumor stages. We will increase the number of HCC patients at different stages to explore the significance of IFLT in HCC patients within the standard or beyond the standard. Third, IFLT technology is currently limited to DBD donors, and we will explore the implementation of IFLT on DCD donors in the future. At that time, whether IFLT can reduce the recurrence rate of tumors after DCD donor liver transplantation still needs further research.

In conclusion, clinically, IRI increases the recurrence rate of HCC after liver transplantation. IFLT can significantly reduce IRI damage and has the potential to be a useful strategy to reduce HCC recurrence after liver transplantation.

DATA AVAILABILITY STATEMENT

The original contributions presented in the study are included in the article/supplementary materials, further inquiries can be directed to the corresponding author/s.

ETHICS STATEMENT

All the procedures were performed in accordance with the ethical standards of the responsible committee on human experimentation (institutional and national) and with the Helsinki Declaration of 1964 and later versions. The study was approved by the Institutional Ethics Committee for Clinical Research and Animal Trials of the First Affiliated Hospital of Sun Yat-sen University and informed consent waiver was granted by the IEC given the retrospective, minimal risk nature of the study. No organs from executed prisoners were transplanted into any of the patients reported in this study.

AUTHOR CONTRIBUTIONS

YT and TW were responsible for writing the manuscript. FL, QiZ, ZC, and JG were responsible for data collection and statistics. WJ, QiaZ, DW, and MC were responsible for the revision of the manuscript. ZG and XH were responsible for the design of the project. All authors contributed to the article and approved the submitted version.

FUNDING

Supported by grants as follows: the National Natural Science Foundation of China (81970564, 81471583, 81570587 and 81770410), Guangdong Basic and Applied Basic Research Foundation (2020A1515011557), the Key Clinical Specialty Construction Project of National Health and Family Planning Commission of the People's Republic of China, the Guangdong Provincial Key Laboratory Construction Projection on Organ Donation and Transplant Immunology (2013A061401007, 2017B030314018), Guangdong Provincial international Cooperation Base of Science and Technology (Organ Transplantation) (2015B050501002), Guangdong Provincial

Natural Science Funds for Major Basic Science Culture Project (2015A030308010), Guangdong Provincial Natural Science Funds for Distinguished Young Scholars (2015A030306025), Special support program for training high level talents in Guangdong Province (2015TQ01R168), Pearl River Nova Program of Guangzhou (201506010014), Science and Technology Program of Guangzhou (201704020150), Sun Yat-sen University Young Teacher Key Cultivate Project (17ykzd29) and "Elite program" specially supported by China organ transplantation development foundation.

ACKNOWLEDGMENTS

Highly appreciate professor Shunjun Fu team for providing guidance in statistical analysis in this article.

REFERENCES

1. Bray F, Ferlay J, Soerjomataram I, Siegel R, Torre L, Jemal A. Global Cancer Statistics 2018: GLOBOCAN Estimates of Incidence and Mortality Worldwide for 36 Cancers in 185 Countries. *CA: Cancer J Clin* (2018) 68 (6):394–424. doi: 10.3322/caac.21492
2. Song TJ, Ip EW, Fong Y. Hepatocellular Carcinoma: Current Surgical Management. *Gastroenterology* (2004) 127(5 Suppl 1):S248–60. doi: 10.1053/j.gastro.2004.09.039
3. Citores MJ, Lucena JL, de la Fuente S, Cuervas-Mons V. Serum Biomarkers and Risk of Hepatocellular Carcinoma Recurrence After Liver Transplantation. *World J Hepatol* (2019) 11(1):50–64. doi: 10.4254/wjh.v11.i1.50
4. Agopian VG, Harlander-Locke M, Zarrinpar A, Kaldas FM, Farmer DG, Yersiz H, et al. A Novel Prognostic Nomogram Accurately Predicts Hepatocellular Carcinoma Recurrence After Liver Transplantation: Analysis of 865 Consecutive Liver Transplant Recipients. *J Am Coll Surg* (2015) 220 (4):416–27. doi: 10.1016/j.jamcollsurg.2014.12.025
5. Kornberg A, Küpper B, Tannapfel A, Katenkamp K, Thrum K, Habrecht O, et al. Long-Term Survival After Recurrent Hepatocellular Carcinoma in Liver Transplant Patients: Clinical Patterns and Outcome Variables. *Eur J Surg Oncol* (2010) 36(3):275–80. doi: 10.1016/j.ejso.2009.10.001
6. Orci LA, Lacotte S, Delaune V, Slits F, Oldani G, Lazarevic V, et al. Effects of the Gut-Liver Axis on Ischaemia-Mediated Hepatocellular Carcinoma Recurrence in the Mouse Liver. *J Hepatol* (2018) 68(5):978–85. doi: 10.1016/j.jhep.2017.12.025
7. Nagai S, Yoshida A, Facciuto M, Moonka D, Abouljoud MS, Schwartz ME, et al. Ischemia Time Impacts Recurrence of Hepatocellular Carcinoma After Liver Transplantation. *Hepatology* (2015) 61(3):895–904. doi: 10.1002/hep.27358
8. Kornberg A, Witt U, Kornberg J, Friess H, Thrum K. Extended Ischemia Times Promote Risk of HCC Recurrence in Liver Transplant Patients. *Dig Dis Sci* (2015) 60(9):2832–9. doi: 10.1007/s10620-015-3541-z
9. Huang H, Tohme S, Al-Khafaji AB, Tai S, Loughran P, Chen L, et al. Damage-Associated Molecular Pattern-Activated Neutrophil Extracellular Trap Exacerbates Sterile Inflammatory Liver Injury. *Hepatology* (2015) 62 (2):600–14. doi: 10.1002/hep.27841
10. Man K, Ng KT, Lo CM, Ho JW, Sun BS, Sun CK, et al. Ischemia-Reperfusion of Small Liver Remnant Promotes Liver Tumor Growth and Metastases–Activation of Cell Invasion and Migration Pathways. *Liver Transpl* (2007) 13 (12):1669–77. doi: 10.1002/lt.21193
11. Oldani G, Crowe LA, Orci LA, Slits F, Rubbia-Brandt L, de Vito C, et al. Pre-Retrieval Reperfusion Decreases Cancer Recurrence After Rat Ischemic Liver Graft Transplantation. *J Hepatol* (2014) 61(2):278–85. doi: 10.1016/j.jhep.2014.03.036
12. Li CX, Ling CC, Shao Y, Xu A, Li XC, Ng KT, et al. CXCL10/CXCR3 Signaling Mobilized-Regulatory T Cells Promote Liver Tumor Recurrence After Transplantation. *J Hepatol* (2016) 65(5):944–52. doi: 10.1016/j.jhep.2016.05.032
13. Yang F, Zhang Y, Ren H, Wang J, Shang L, Liu Y, et al. Ischemia Reperfusion Injury Promotes Recurrence of Hepatocellular Carcinoma in Fatty Liver *via* ALOX12-12hete-GPR31 Signaling Axis. *J Exp Clin Cancer Res CR* (2019) 38 (1):489. doi: 10.1186/s13046-019-1480-9
14. He XS, Guo ZY, Zhao Q, Ju WQ, Wang DP, Wu LW, et al. The First Case of Ischemia-Free Organ Transplantation in Humans: A Proof of Concept. *Am J Transplant* (2018) 18(3):737–44. doi: 10.1111/ajt.14583
15. Zhang Z, Tang Y, Zhao Q, Wang L, Zhu C, Ju W, et al. Association of Perfusion Characteristics and Posttransplant Liver Function in Ischemia-Free Liver Transplantation. *Liver Transpl* (2020) 26(11):1441–54. doi: 10.1002/lt.25825
16. Olthoff KM, Kulik L, Samstein B, Kaminski M, Abecassis M, Emond J, et al. Validation of a Current Definition of Early Allograft Dysfunction in Liver Transplant Recipients and Analysis of Risk Factors. *Liver Transpl* (2010) 16 (8):943–9. doi: 10.1002/lt.22091
17. Zhai Y, Petrowsky H, Hong J, Busuttil R, Kupiec-Weglinski J. Ischaemia-Reperfusion Injury in Liver Transplantation–From Bench to Bedside. *Nat Rev Gastroenterol Hepatol* (2013) 10(2):79–89. doi: 10.1038/nrgastro.2012.225
18. Souidi N, Stolk M, Seifert M. Ischemia-Reperfusion Injury: Beneficial Effects of Mesenchymal Stromal Cells. *Curr Opin Organ Transplant* (2013) 18(1):34–43. doi: 10.1097/MOT.0b013e32835c2a05
19. Nasralla D, Coussios CC, Mergental H, Akhtar MZ, Butler AJ, Ceresa CDL, et al. A Randomized Trial of Normothermic Preservation in Liver Transplantation. *Nature* (2018) 557(7703):50–6. doi: 10.1038/s41586-018-0047-9
20. Reddy S, Greenwood J, Maniakin N, Bhattacharjya S, Zilvetti M, Brockmann J, et al. Non-Heart-Beating Donor Porcine Livers: The Adverse Effect of Cooling. *Liver Transpl* (2005) 11(1):35–8. doi: 10.1002/lt.20287
21. Eisenbach C, Encke J, Merle U, Gotthardt D, Weiss KH, Schneider L, et al. An Early Increase in Gamma Glutamyltranspeptidase and Low Aspartate Aminotransferase Peak Values are Associated With Superior Outcomes After Orthotopic Liver Transplantation. *Transplant Proc* (2009) 41(5):1727–30. doi: 10.1016/j.transproceed.2009.01.084
22. Wadei HM, Lee DD, Croome KP, Mai ML, Golan E, Brotman R, et al. Early Allograft Dysfunction After Liver Transplantation Is Associated With Short- and Long-Term Kidney Function Impairment. *Am J Transplant* (2016) 16 (3):850–9. doi: 10.1111/ajt.13527
23. Deschenes M. Early Allograft Dysfunction: Causes, Recognition, and Management. *Liver Transpl* (2013) 19 Suppl 2:S6–8. doi: 10.1002/lt.23746
24. Mazzaferro V, Llovet JM, Miceli R, Bhoori S, Schiavo M, Mariani L, et al. Predicting Survival After Liver Transplantation in Patients With Hepatocellular Carcinoma Beyond the Milan Criteria: A Retrospective, Exploratory Analysis. *Lancet Oncol* (2009) 10(1):35–43. doi: 10.1016/s1470-2045(08)70284-5
25. Gouw AS, Balabaud C, Kusano H, Todo S, Ichida T, Kojiro M. Markers for Microvascular Invasion in Hepatocellular Carcinoma: Where do We Stand? *Liver Transpl* (2011) 17 Suppl 2:S72–80. doi: 10.1002/lt.22368
26. Berry K, Ioannou GN. Serum Alpha-Fetoprotein Level Independently Predicts Posttransplant Survival in Patients With Hepatocellular Carcinoma. *Liver Transpl* (2013) 19(6):634–45. doi: 10.1002/lt.23652
27. Hameed B, Mehta N, Sapisochin G, Roberts JP, Yao FY. Alpha-Fetoprotein Level > 1000 Ng/mL as an Exclusion Criterion for Liver Transplantation in Patients With Hepatocellular Carcinoma Meeting the Milan Criteria. *Liver Transpl* (2014) 20(8):945–51. doi: 10.1002/lt.23904
28. Jassem W, Xystrakis E, Ghnewa YG, Yuksel M, Pop O, Martinez-Llordella M, et al. Normothermic Machine Perfusion (NMP) Inhibits Proinflammatory Responses in the Liver and Promotes Regeneration. *Hepatology* (2019) 70 (2):682–95. doi: 10.1002/hep.30475
29. Ling Q, Liu J, Zhuo J, Zhuang R, Huang H, He X, et al. Development of Models to Predict Early Post-Transplant Recurrence of Hepatocellular Carcinoma That Also Integrate the Quality and Characteristics of the Liver Graft: A National Registry Study in China. *Surgery* (2018) 16(8):1–10. doi: 10.1016/j.surg.2018.01.022

30. Kulik LM, Fisher RA, Rodrigo DR, Brown RSJr., Freise CE, Shaked A, et al. Outcomes of Living and Deceased Donor Liver Transplant Recipients With Hepatocellular Carcinoma: Results of the A2ALL Cohort. *Am J Transplant* (2012) 12(11):2997–3007. doi: 10.1111/j.1600-6143.2012.04272.x
31. Man K, Fan ST, Lo CM, Liu CL, Fung PC, Liang TB, et al. Graft Injury in Relation to Graft Size in Right Lobe Live Donor Liver Transplantation: A Study of Hepatic Sinusoidal Injury in Correlation With Portal Hemodynamics and Intragraft Gene Expression. *Ann Surg* (2003) 237(2):256–64. doi: 10.1097/01.Sla.0000048976.11824.67
32. Mueller M, Kalisvaart M, O'Rourke J, Shetty S, Parente A, Muller X, et al. Hypothermic Oxygenated Liver Perfusion (HOPE) Prevents Tumor Recurrence in Liver Transplantation From Donation After Circulatory Death. *Ann Surg* (2020) 272(5):759–65. doi: 10.1097/sla.0000000000004258
33. Xu J, Sayed BA, Casas-Ferreira AM, Srinivasan P, Heaton N, Rela M, et al. The Impact of Ischemia/Reperfusion Injury on Liver Allografts From Deceased After Cardiac Death Versus Deceased After Brain Death Donors. *PloS One* (2016) 11(2):e0148815. doi: 10.1371/journal.pone.0148815
34. Huang C, Chen Z, Wang T, He X, Chen M, Ju W. A Marginal Liver Graft With Hyperbilirubinemia Transplanted Successfully by Ischemia-Free Liver Transplantation. *Ann Transl Med* (2021) 9(5):425. doi: 10.21037/atm-20-6296

Conflict of Interest: The authors declare that the research was conducted in the absence of any commercial or financial relationships that could be construed as a potential conflict of interest.

Publisher's Note: All claims expressed in this article are solely those of the authors and do not necessarily represent those of their affiliated organizations, or those of the publisher, the editors and the reviewers. Any product that may be evaluated in this article, or claim that may be made by its manufacturer, is not guaranteed or endorsed by the publisher.

frontiers in Surgery

ORIGINAL RESEARCH
published: 14 December 2021
doi: 10.3389/fsurg.2021.764450

Comparative *ex vivo* Investigations on the Cutting Quality of the CO_2 Laser and the Diode Pumped Er:YAG Laser

Holger Wurm[1]*, *Patrick Johannes Schuler*[2], *Florian Hausladen*[1], *René Graesslin*[2], *Thomas Karl Hoffmann*[2], *Karl Stock*[1] *and Elisabeth Friederike Reins*[2]

[1] *Institut für Lasertechnologien in der Medizin und Meßtechnik, Ulm University, Ulm, Germany,* [2] *Department of Otorhinolaryngology, Head and Neck Surgery, Ulm University Medical Center, Ulm, Germany*

Objectives: A sufficient histological evaluation is a key pillar in oncological treatment, especially in situations of cancer of unknown primary. CO2 laser technology is used in clinical routine of soft tissue surgery because of its cutting quality and availability. Diode pumped solid state Er(bium):YAG laser systems promise a higher cutting efficiency and minor thermal damages. The aim of this study was to compare both laser systems with respect to their suitability for cutting soft tissue.

Methods: A setup was realized which enables comparable experiments with the clinical CO_2 laser (AcuPulse 40ST DUO, Lumenis) and the Er:YAG laser system (DPM 40, Pantec Biosolutions AG). Fresh mucosal samples of porcine tongues were used to determine the influence of laser power and sample velocity on cutting depth and thermal damage width for both lasers. In addition, for the Er:YAG laser, the influence of the pulse repetition rate was examined additionally. For analysis, images of histological sections were taken.

Results: In all experiments, the Er:YAG laser shows a significantly higher cutting depth ($P < 0.0001$) and less thermal damage width ($P < 0.0001$) than the CO_2 laser. For example, at an average power of 7.7 W and a sample velocity of 5 mm/s the Er:YAG laser shows a mean cutting depth of 1.1 mm compared to the CO_2 laser with 500 µm. While the Er:YAG laser shows a mean thermal damage width of 70 µm compared to 120 µm. Furthermore, the Er:YAG enables the adjustment of the cutting depth and thermal damage width by varying the irradiation parameters. A decrease of the repetition rate leads to a reduction of thermal damage. For example, a repetition rate of 100 Hz results in a thermal damage width of 46 µm compared to 87 µm at 800 Hz at an average power of 7.7 W and a cutting velocity = 5 mm/s while a homogenous cutting quality can be achieved.

Conclusions: In conclusion, the results of these *ex vivo* experiments demonstrate significant advantages of the diode pumped Er:YAG laser system for soft tissue ablation compared to the CO_2 laser, in particular regarding cutting efficiency and thermal damage width.

Keywords: CO_2 laser, Er:YAG laser, diode pumped, high repetition rate, 2.94 µm, head and neck surgery, oncology

OPEN ACCESS

Edited by:
Marco Riva,
University of Milan, Italy

Reviewed by:
Helena Jelinkova,
Czech Technical University in Prague, Czechia
Fabio Ferreli,
Humanitas University, Italy

***Correspondence:**
Holger Wurm
holger.wurm@ilm-ulm.de

Specialty section:
This article was submitted to Surgical Oncology, a section of the journal Frontiers in Surgery

Received: *18 October 2021*
Accepted: *25 November 2021*
Published: *14 December 2021*

Citation:
Wurm H, Schuler PJ, Hausladen F, Graesslin R, Hoffmann TK, Stock K and Reins EF (2021) Comparative ex vivo Investigations on the Cutting Quality of the CO_2 Laser and the Diode Pumped Er:YAG Laser. Front. Surg. 8:764450. doi: 10.3389/fsurg.2021.764450

INTRODUCTION

Laser surgery is used in various procedures in head and neck surgery. It has become an alternative to open surgery in the excision of tumors in hard-to-reach regions like the larynx and hypopharynx, reducing the risk of injuring surrounding organs and often preserving their functions (1, 2). Due to the high absorption coefficient of its wavelength ($\lambda = 10.6\,\mu m$; $\mu_a = 800\ cm^{-1}$) in water the CO_2 laser shows a more efficient and precise soft tissue cutting compared to other lasers, working with vaporization (3) and has therefore become the standard in head and neck laser surgery over the past decades (4–7).

While simultaneous coagulation during the ablation process leads to local hemostasis and the reduction of reconstruction needs (1, 8–10), laser irradiation may also cause thermal damage width of the surrounding tissue. The reason for this is the gaussian spatial beam profile and the continuous wave (cw) operating mode which is true for the most of available CO_2 lasers. Especially when evaluating the infiltrating potential of small lesions or in situations of cancer of unknown primary, it is very important to minimize peripheral damage in order to allow sufficient histological evaluation (11). Furthermore, a prolonged wound healing in comparison to cold surgery has been described (8).

Especially from these points of view the Er:YAG laser shows some decisive advantages. In contrast to the CO_2 laser, fibers (e.g., sapphire, germanium oxide or ZBLAN fibers) are available for the Er:YAG, which is particularly useful for endoscopic applications. The ablation efficiency of the Erbium laser is even higher compared to the CO_2 laser (12, 13). The reason is the higher absorption coefficient in water (Er:YAG laser: $\lambda = 2.94\,\mu m$, $\mu_a = 1*10^4\ cm^{-1}$, Er:YSGG laser: $\lambda = 2.79\,\mu m$, $\mu_a = 4*10^3\ cm^{-1}$) and the pulsed operation mode which leads to higher powers within one laser pulse compared to a cw-system of comparable average power. This leads to so called thermomechanical ablation, in which the massive increase in volume of the water during rapid evaporation results in very efficient tissue ablation (14–16). Furthermore, the more Top-Hat like beam profile, caused by a higher number of laser modes, leads to much steeper temperature gradients at the edges of the sections and thus to significantly fewer thermal side effects such as coagulation and carbonization. But the comparable low repetition rate of the flashlamp pumped Erbium lasers does not allow homogeneous cutting which has left it irrelevant for tumor surgery up to now. The new diode pumped Er:YAG laser system enabling pulse repetition rates up to 2 kHz might eliminate this disadvantage. Furthermore, it offers adjustable pump current as well as a variable pulse duration from 1 to 1,000 µs and offers a better beam quality which allows to couple into fibers with 200 µm core size (11, 17). In prior *in vitro* studies we have already shown that smooth and homogeneous cuts can be achieved in both soft and hard tissue with thermally damaged zones adjustable over a wide range from about 50 µm to > 1,000 µm (18–21).

In this *in vitro* study we compare the cutting characteristics of the new diode pumped Er:YAG laser to a standard clinical CO_2 laser system using the same clinically approved irradiation parameters on mucosa of the tongue.

TABLE 1 | Parameters of the used laser systems.

	CO_2 laser	Diode pumped Er:YAG laser
Type	AcuPulse 40ST DUO	DPM40
Manufacturer	Lumenis	Pantec
Wavelength	10.6 µm	2.94 µm
Max. optical power Φ_{max}	40 W	40 W
Operation mode	SuperPulse	Pulsed (50 Hz–2 kHz)
Beam quality factor M^2	≈ 1 (TEM00)	≈25
Focal length f'	300 mm	66.2 mm
Beam waist / Spot diameter	500 µm	500 µm

MATERIALS AND METHODS

Sample Preparation

The laser cuts were performed on the mucosa of fresh porcine tongues from the slaughter. For this, equivalent tissue samples (thickness = 1 cm) were cut from the lateral part of the tongue. Each parameter setting was performed on 3 different samples. Cutting depth and thermal damage were measured in six different histological sections, respectively ($n = 18$).

Laser Systems and Experimental Setup

Table 1 shows the most important parameters of the used laser systems. The experimental setup is shown in **Figure 1**. For the CO_2 laser the standard focusing unit (f = 300 mm; spot diameter = 500 µm) was used. The beam of the Er:YAG laser was coupled into a sapphire fiber (core diameter 425 µm, NA = 0.12) and the fiber output end was imaged onto the sample surface by a specially raytracing designed optic (f' = 66.2 mm) (OpticStudio 20, Zemax) which leads to an almost homogeneous irradiated circular area (diameter = 500 µm) in the image plane of the optics. The measured depth of focus was about 5 mm. A mirror joint arm connects the CO_2 laser with the irradiation optics (f' = 300 mm), which forms a Gaussian beam waist in the focal plane. The irradiation spot of the Er:YAG laser and the beam waist of the CO_2 laser were positioned next to each other in a distance of 100 mm in order to allow a reliable switching between the lasers using the same translation stage. The exact size and the position of the image / focus plane were analyzed by moving irradiated photographic paper (burn paper) through the image / focus plane region with a computer-controlled translation stage (Corvus Eco & 3xLS110, Pi miCos GmbH) at a speed of 30 mm/s and low pulse repetition rate. Therefore, the burn paper was moved 10 mm in x- and z-direction simultaneously with equal velocities. The ablation marks of the laser pulses on the paper were analyzed with microscope and the correct positions saved in the control software of the translation stage. The sample was positioned on a holder adapted to the translation stage which allows a defined positioning and movement of the sample during irradiation. After determination of the position all cuts were performed with the translation stage in the image plane / focal plane.

By using a computer-controlled shutter unit in the beam path of the Er:YAG laser it was possible to reproduce the same

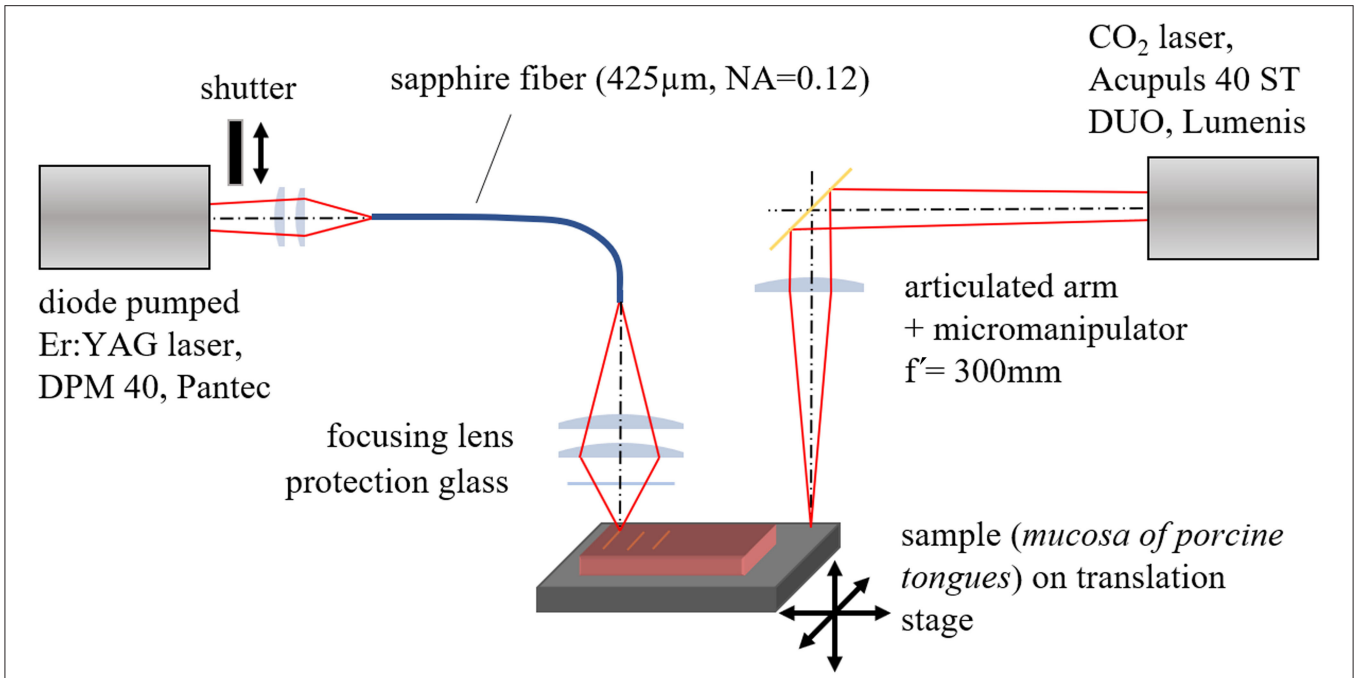

FIGURE 1 | Experimental setup for irradiation of the samples with defined parameters.

procedure for each sample: (a) switching the laser on, (b) waiting for about 10 s to stabilize the laser operation, (c) starting the movement of the sample, (d) opening the shutter automatically when constant sample velocity is reached. After one cycle with a sample movement of typically 10 mm the shutter was closed and the sample stopped. The procedure for the CO_2 laser was performed in a similar way, using the foot switch instead of the computer-controlled shutter, which leads to an inaccuracy at the beginning and end of the cut. For this reason, the histological sections were taken from the middle part of the cut. The setup is shown in **Figure 1**.

Prior to the experiments the laser power of the CO_2 laser was set to 10 W which is a typically used value for soft tissue cutting in a clinical setting. The resulting laser power in the beam waist (7.7 W) was measured by a power meter (30(150)A, OPHIR and Nova II, OPHIR) and this value was also used for the Er:YAG laser. To adjust the laser power the pulse peak current of the Er:YAG laser was kept constant (300 A) and the pulse duration was varied.

Analysis of the Samples

During the irradiation, the cutting process was recorded by a CMOS-sensor camera (MQ042CG-CM, software XIMEA Cam Tool, XIMEA GmbH) adapted on a surgical microscope (OPMI 6-CFC on Universal S3 stand, Carl Zeiss).

To analyze the cutting geometry and to maintain the tissue structure the samples were stored in 4 % formalin solution (neutral buffered formalin) for 72 h for fixation. After embedding in paraffin, the histological sections were prepared and stained with Azan. For image acquisition and evaluation a light microscope (Axiophot, Carl Zeiss) equipped with a digital camera (ProgRes C12plus, Jenoptic) with capture and processing software (Jenoptic, ProgRes Capture Pro, Version 2.5) was used. This software also allowed to measure the thermal damage and the depth of the cuts as shown in **Figure 2**. The measured thermal damage width includes coagulation and carbonization.

Statistical Analysis

Statistical analysis was performed using GraphPad Prism six software (GraphPad Software). Data was tested for normal distribution using D'Agostino–Pearson omnibus normality test. Parametric data from **Figure 3** was analyzed using the two-way analysis of variance (ANOVA) to determine differences between two grouping variables. Parametric data from **Figure 5** was evaluated using the one-way ANOVA to determine differences between the three velocity groups for the same mean power. Significance was set at $p < 0.05$.

Experiments

The following investigations were performed:

- Comparative experiments with a laser power of 7.7 W and various cutting velocities (2, 5, 10 mm/s). Er:YAG laser parameter: repetition rate = 200 Hz, pulse duration = 154 µs.
- Investigation of the influence of repetition rate (100, 200, 400 and 800 Hz) on to the cutting depth and thermal damage width for the Er:YAG laser (laser power = 7.7 W).
- Investigation of the influence of laser power on to the cutting depth and thermal damage width for the Er:YAG laser at various cutting velocities (2, 5, and 10 mm/s) at a repetition rate of 200 Hz.

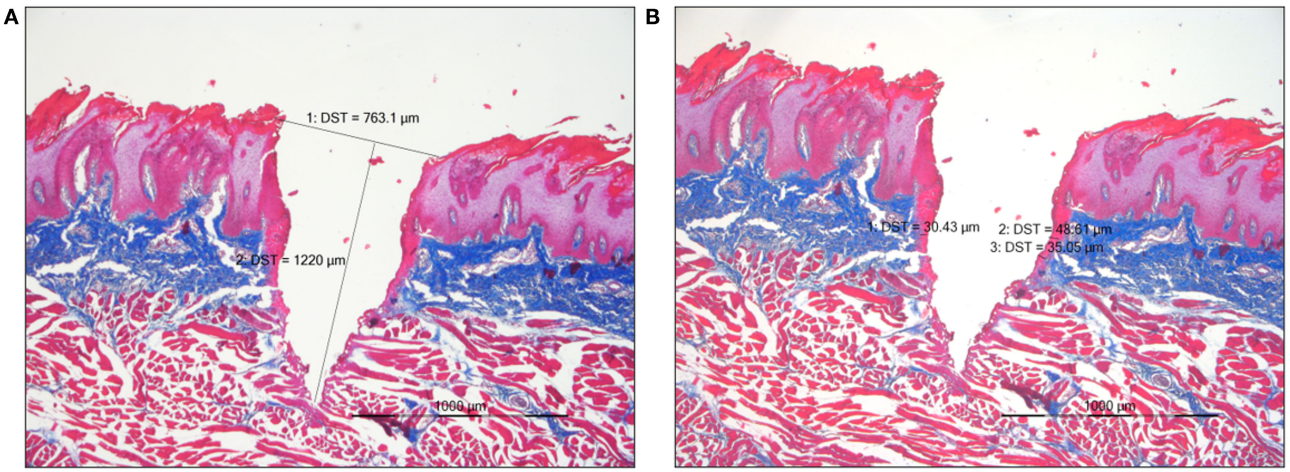

FIGURE 2 | (A) Measurement of the cutting depth in a histological section of pork tongue mucosa. Er:YAG, Azan staining, light microscopy at a magnification of 20x. **(B)** Measurement of the thermal damage width in a histological section of pork tongue mucosa. Er:YAG, Azan staining, light microscopy at a magnification of 20x.

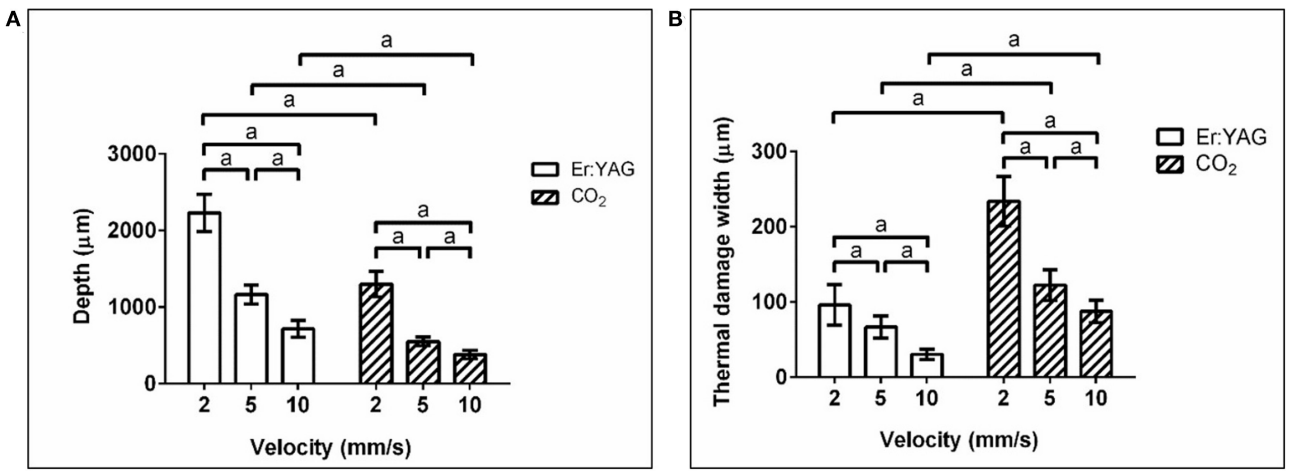

FIGURE 3 | (A) Mean value and standard deviation of the measured cutting depths ($^{a}P < 0.0001$) and **(B)** thermal damage width ($^{a}P < 0.0001$) for the Er:YAG laser with 200 Hz repetition rate and the CO_2 laser at various cutting velocity (laser power = 7.7 W), measured in the histological sections.

RESULTS

Comparison of CO_2 Laser and Er:YAG Laser

While performing the experiments it was observed that the homogeneity of the cuts of both laser systems is comparable. While the cut made by the CO_2 laser shows thermal damage up to carbonization, the cut of the Er:YAG laser doesn't. Immediately after cutting, the cutting walls collapsed to a certain extent. The corresponding histological section showed that the cut of the CO_2 laser is broader and minor deep compared to the Er:YAG laser. The thermal damage in the histological section of the CO_2 laser is more pronounced compared to the Er:YAG laser and vacuoles as well as carbonization are visible at the edges of the CO_2 laser cuts.

Figure 3 shows the mean values and standard deviations of the cutting depth (left) and the thermal damage width (right) for both lasers and the various cutting velocities. For both lasers the cutting depth increases with decreasing cutting velocity. The cuts generated by the Er:YAG laser are about two times deeper compared to the CO_2 laser cuts.

Furthermore, it can be seen that the thermal damage width for the CO_2 laser cuts is at least twice as wide as for the Er:YAG laser cuts at all speeds.

Influence of the Repetition Rate on the Cutting Depth and Thermal Damage Width for the Er:YAG Laser

Figure 4 shows the resulting mean values and standard deviations of the cutting depth (A) and thermal

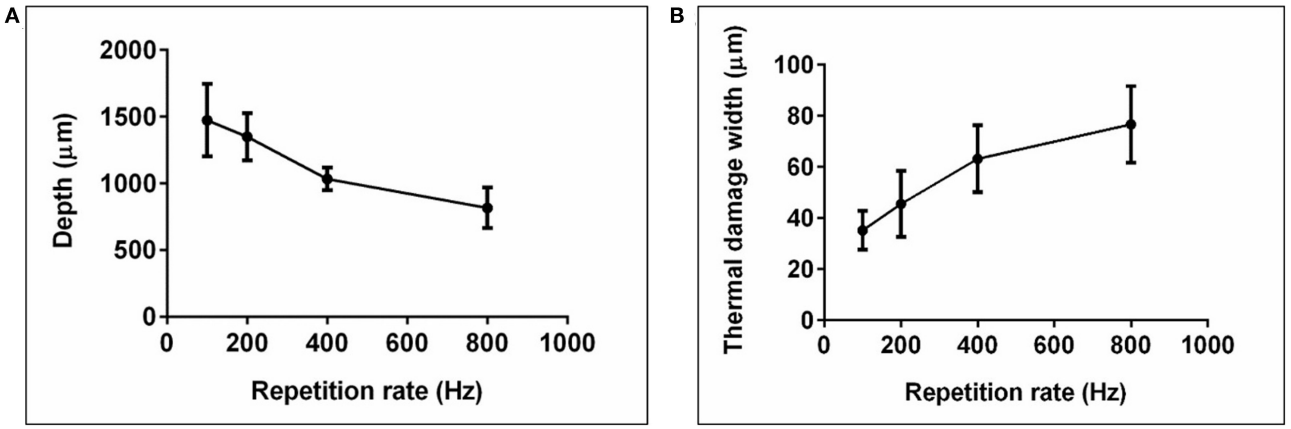

FIGURE 4 | (A) Mean value and standard deviation of the measured cutting depth and **(B)** thermal damage width, applied over the repetition rate (Er:YAG laser, laser power = 7.7 W, cutting velocity = 5 mm/s).

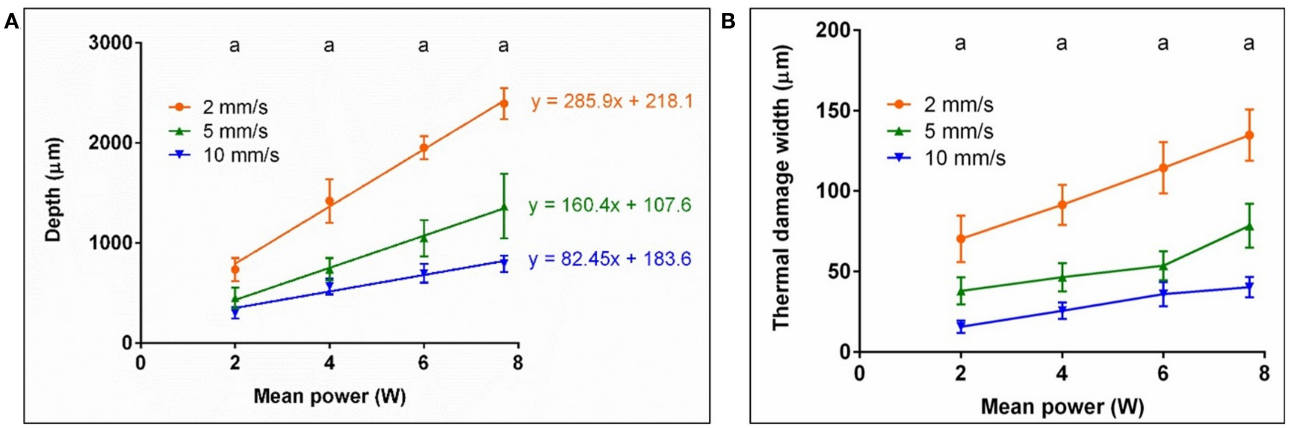

FIGURE 5 | (A) Mean value and standard deviation of the measured cutting depths ($^{a}P < 0.0001$, significant differences between velocities, for the same mean power) and **(B)** thermal damage widths ($^{a}P < 0.0001$, significant differences between velocities, for the same mean power) applied over the laser power and for various cutting velocities (Er:YAG laser, repetition rate = 200 Hz); in **(A)** linear regressions are shown for the different velocities, including the corresponding equation.

damage width (B), depicted over the repetition rate. With increasing repetition rate, the cutting depth decreases while the thermal damage width increases.

Influence of the Laser Power on the Cut Depth and Thermal Damage at Various Cutting Velocities for the Er:YAG Laser

In **Figure 5**, the resulted mean values and standard deviations of the cutting depth (A) and thermal damage width (B) are depicted over the laser power. Both the cutting depth and the thermal damage width increase with laser power. An increase of the cutting velocity leads to a decrease of both measured values. Especially the cutting depth shows an almost linear behavior with increasing laser power.

DISCUSSION

In this *in vitro* study on mucosa of fresh porcine tongues we were able to achieve a higher cutting depth (factor ≈ 2) as well as a less pronounced thermal damage of surrounding tissue at comparable homogeneity using the diode pumped Er:YAG laser compared to a standard clinical CO_2 laser system at clinically approved irradiation parameters.

Both results were at least qualitatively expected due to the higher absorption of the Er:YAG laser radiation in soft tissue and the highly efficient thermomechanical ablation mechanism compared to vaporization. This and the more Top-Hat shaped beam profile in the image plane explain the lack of carbonization when using the diode pumped Er:YAG laser which is expected to be beneficial in terms of better wound healing (8).

The parameters velocity, repetition rate and mean power (pulse energy) have a significant influence on the thermal damage and cutting depth and will be discussed in the following.

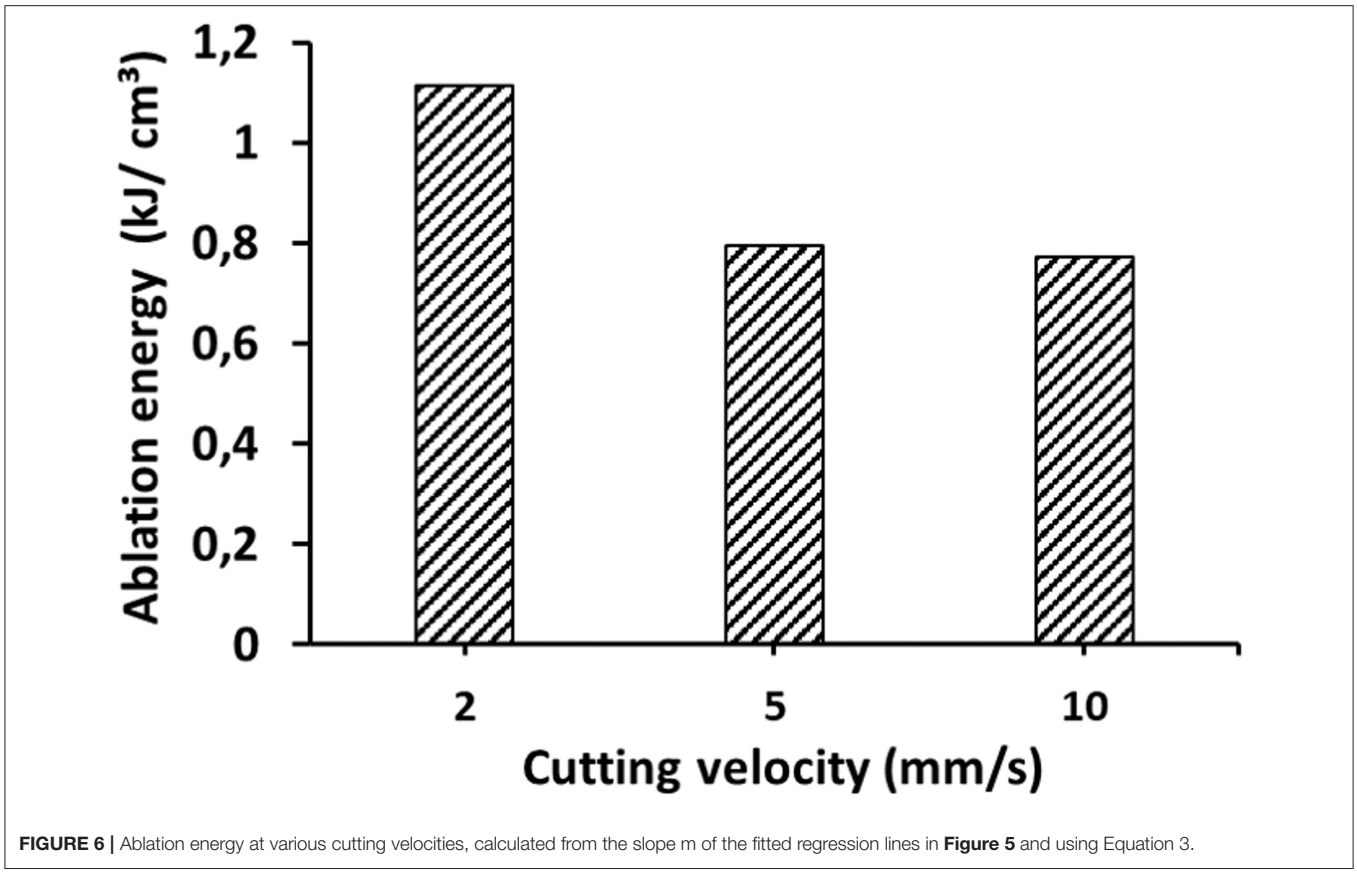

FIGURE 6 | Ablation energy at various cutting velocities, calculated from the slope m of the fitted regression lines in **Figure 5** and using Equation 3.

The observed decline of cutting depth with increasing cutting velocity (**Figure 3**) can be explained by the reduced irradiation time per position and therefore a decrease of applied laser energy. This decrease of applied energy per position subsequently leads to the observed reduction of the thermal damage width with increasing cutting velocity.

It is already well known, that at constant mean laser power with rising pulse repetition rates the cutting depth decreases and the thermal damage increases. This can be explained by the increase in the number of pulses per position with increasing repetition rate. The energy to reach the ablation threshold must be introduced into the tissue for each pulse, which leads to increased outflow of energy into the surrounding tissue with a higher number of pulses and thus to the observed increase in thermal damage width and a decrease in cutting depth (**Figure 4**).

In **Figure 5**, for all cutting velocities an almost linear correlation between the mean power (and therefore the pulse energy) and the depth of the cuts can be observed. The irradiation time per position follows the equation:

$$t = \frac{\varnothing_F}{v} \tag{1}$$

with the spot diameter $\varnothing_F$ and the cutting velocity v. Assuming that the cutting width is equal to the laser spot diameter, the ablation volume ΔV can be calculated from the irradiated Area A and Δz as follows:

$$\Delta V = A \bullet \Delta z = \frac{1}{4} \bullet \varnothing_F{}^2 \bullet \Delta z \tag{2}$$

From m and t, the necessary ablation energy per volume $\Delta E/\Delta V$ can be calculated by:

$$\frac{\Delta E}{\Delta V} = \frac{\Delta P \bullet t}{A \bullet \Delta z} = \frac{t}{A \bullet m} = \frac{\varnothing_F}{v \bullet A \bullet m} = \frac{\varnothing_F}{v \bullet \frac{1}{4} \bullet \varnothing_F{}^2 \bullet m}$$
$$= \frac{1}{\frac{1}{4} \bullet \varnothing_F \bullet m \bullet v} \tag{3}$$

Figure 6 shows the calculated values $\Delta E/\Delta V$ for the various cutting velocities. The observed decrease of the ablation energy with increasing cutting velocity can be explained (in a similar manner as above) by the decrease in the number of pulses per position with increasing cutting velocity. All calculated values for the ablation energy are significantly lower than the values found in literature (1.5–5 kJ/cm²) (22–25). One possible reason for this could be the top-hat-like beam profile in our experiment.

We were able to achieve homogenous cuts with increased cutting depth compared to the CO_2 laser. From the perspective of a surgeon the assessment of the right cutting depth requires experience, like with every new tool, to avoid injuring underlying structures. A more effective laser cutting tool, however, might

shorten the operation time and thus offer an economic advantage that needs to be evaluated.

Histological studies on the thermal damage width of the CO_2 laser cut showed the obliteration of small vessels that allows simultaneous hemostasis. The authors also emphasized the lack of reconstruction needs by creating a sealed wound bed (8). Often open surgery with the risk of injuring surrounding organs is the only surgical alternative when trying to reach structures like the laryngopharynx. The thermal damage, however, prevented migration of inflammatory cells as well as spouting of new capillaries and therefore delayed wound healing by several days (26).

A smaller thermal damage width could lead to a higher rate of postoperative bleeding events. On the other hand, a thinner necrotic area could contain scaring, lead to a faster restitution of organ function and therefore prevent the delay of adjuvant therapy.

A thinner thermal damage width could also be a benefit when evaluating the margins of histological samples. If squamous cell carcinoma of unknown primary in the head and neck first presents as cervical lymph node metastases laser surgery is frequently used to take systematic samples from the mucosa of the oropharynx. The management of unknown primary must always include at least a bilateral tonsillectomy and a mucosectomy of the tongue base (27). Primary cancer cell nests can be very small and are not always detectable via positron emission tomography beforehand, but prognosis is significantly better if the primary can be located (28). In this case it is very important to minimize peripheral damage in order to allow sufficient histological evaluation (11).

In conclusion, these experiments demonstrate a higher ablation efficiency with significantly reduced thermal damage and without carbonization. Furthermore, the expand of the thermal damage width can be varied via the repetition rate. Due to the high repetition rates of over 100 Hz and by that the high overlap of the individual pulses, clear cutting edges can be achieved even at high velocities. In combination with the already shown excellent suitability for hard tissue ablation, for example used in stapedotomy, we see a high potential for developing a unique clinical system based on the diode pumped Er:YAG laser. A configuration with similar properties to the CO_2 laser systems available on the market could be achieved by using a fiber with the smallest possible core diameter and small NA (Numerical Aperture), the end of which would then be imaged onto the tissue on the surgical microscope via suitable imaging optics and an adapted micromanipulator. Furthermore, this configuration would also be very well suited to integrate a therapeutic feedback system, for example OCT or temperature measurement systems, as already described in the literature (29–31). *In vivo* experiments need to be prepared to assess hemostasis, scarring and histological evaluation as well as patient comfort regarding pain and inflammation.

DATA AVAILABILITY STATEMENT

The raw data supporting the conclusions of this article will be made available on request by the authors, without undue reservation.

AUTHOR CONTRIBUTIONS

HW, FH, and KS concepted and developed the optical design for the Er:YAG laser. TH and RG were planning and organizing the experiments with the clinical laser. HW, FH, and ER realized the setup for both laser systems. HW and ER were performing the experiments. HW, ER, and PS were analyzing the histological sections. HW and FH were performing the statistical analysis. HW, KS, ER, and PS wrote sections of the manuscript. All authors contributed to manuscript revision, read, and approved the submitted version.

ACKNOWLEDGMENTS

The authors wish to thank Andrea Böhmler for sample preparation and preparation of the histological sections and stains as well as Pantec Biosolutions AG for financial support.

REFERENCES

1. Vilaseca I, Blanch JL, Bernal-Sprekelsen M. Transoral laser surgery for hypopharyngeal carcinomas. *Curr Opin Otolaryngol Head Neck Surg.* (2012) 20:97–102. doi: 10.1097/MOO.0b013e32834fa8fe
2. Guimarães AV, Dedivitis RA, Matos LL, Aires FT, Cernea CR. Comparison between transoral laser surgery and radiotherapy in the treatment of early glottic cancer: a systematic review and meta-analysis. *Sci Rep*. (2018) 8:1–7. doi: 10.1038/s41598-018-30218-x
3. Hale GM, Querry MR. Optical constants of water in the 200-nm to 200-μm wavelength region. *Appl Opt.* (1973) 12:555–63. doi: 10.1364/AO.12.000555
4. Bertino G, Degiorgi G, Tinelli C, Cacciola S, Occhini A, Benazzo M. CO2 laser cordectomy for T1–T2 glottic cancer: oncological and functional long-term results. *Arch OtorhinoLaryngol.* (2015) 272:2389–95. doi: 10.1007/s00405-015-3629-2
5. Zhang Y, Liang G, Sun N, Guan L, Meng Y, Zhao X, et al. Comparison of CO2 laser and conventional laryngomicrosurgery treatments of polyp and leukoplakia of the vocal fold. *Int J Clin Exp Med.* (2015) 8:18265–74.
6. Motta G, Esposito E, Motta S, Tartaro G, Testa D. CO2 laser surgery in the treatment of glottic cancer. *Head Neck.* (2005) 27:566–74. doi: 10.1002/hed.20135
7. Jovanovic S, Schönfeld U, Scherer H. CO2 laser stapedotomy with the "one-shot" technique–clinical results. *Otolaryngol Head Neck Surg.* (2004) 131:750–7. doi: 10.1016/j.otohns.2004.05.008
8. Lippert BM, Teymoortash A, Folz BJ, Werner JA. Wound healing after laser treatment of oral and oropharyngeal cancer. *Lasers Med Sci.* (2003) 18:36–42. doi: 10.1007/s10103-002-0244-4
9. Grinnell F. Fibronectin and wound healing. *J Cell Biochem.* (1984) 26:107–16. doi: 10.1002/jcb.240260206
10. Clark RA. Fibronectin matrix deposition and fibronectin receptor expression in healing and normal skin. *J Invest Dermatol.* (1990) 94:128S–34S. doi: 10.1111/1523-1747.ep12876104
11. Romeo U, Libotte F, Palaia G, Del Vecchio A, Tenore T, Visca P, et al. Histological in vitro evaluation of the effects of Er:YAG laser on oral soft tissues. *Lasers Med Sci.* (2011) 27:749–53. doi: 10.1007/s10103-011-0969-z

12. Nagel D. The Er:YAG laser in ear surgery: first clinical results. *Lasers Surg Med.* (1997) 21:79–87. doi: 10.1002/(sici)1096-9101(1997)21:1<79::aid-lsm12>3.0.co;2-4
13. Arnoldner C, Schwab B, Lenarz T. Clinical results after stapedotomy: a comparison between the Erbium: Yttrium-Aluminum-Garnet laser and the conventional technique. *Otol Neurotol.* (2006) 27:458–65. doi: 10.1097/00129492-200606000-00005
14. Zweig AD. A thermo-mechanical model for laser ablation. *J Appl Phys.* (1991) 70:1684–91. doi: 10.1063/1.349537
15. Majaron B, Plestenjak P, Lukač M. Thermo-mechanical laser ablation of soft biological tissue: modeling the micro-explosions. *Appl Phys B.* (1999) 69:71–80. doi: 10.1007/s003400050772
16. Nahen K, Vogel A. Plume dynamics and shielding by the ablation plume during Er:YAG laser ablation. *J Biomed Opt.* (2002) 7:165–78. doi: 10.1117/1.1463047
17. Heinrich A, Hagen C, Vizhanyo A, Krammer P, Summer S, Gross S, et al. High power, diode-pumped Er:YAG lasers for soft and hard tissue applications. In: *Medical Laser Applications and Laser-Tissue Interactions V (2011), paper 80921C* (Optical Society of America) (2011) 8092:243–8. doi: 10.1117/12.888255
18. Stock K, Hausladen F, Hibst R. Investigations on the potential of a novel diode pumped Er:YAG laser system for dental applications. In: *Lasers in Dentistry XVIII* (International Society for Optics and Photonics) (2012) 8208:55–61. doi: 10.1117/12.908382
19. Stock K, Diebolder R, Hausladen F, Wurm H, Lorenz S, Hibst R. Primary investigations on the potential of a novel diode pumped Er:YAG laser system for bone surgery. In: *Photonic Therapeutics and Diagnostics IX*. (International Society for Optics and Photonics) (2013) 85656D. doi: 10.1117/12.2004123
20. Stock K, Meitinger D, Hausladen F, Stegmayer T, Wurm H. Primary investigations on defined thermal effects on soft tissue using a diode pumped Er:YAG laser system. In: *Optical Interactions with Tissue and Cells XXX* (International Society for Optics and Photonics) (2019) 10876:156–63. doi: 10.1117/12.2509674
21. Stock K, Reins E, Schuler PJ, Wurm H. Comparative in-vitro investigations on the cutting quality of the CO2 laser and the diode pumped Er:YAG laser. In: *Imaging, Therapeutics, and Advanced Technology in Head and Neck Surgery and Otolaryngology 2020* (International Society for Optics and Photonics) (2020) 11213:29–35. doi: 10.1117/12.2545849
22. Kaufmann R, Hibst R. Pulsed Er:YAG- and 308 nm UV-excimer laser: an in vitro and in vivo study of skin-ablative effects. *Lasers Surg Med.* (1989) 9:132–40. doi: 10.1002/lsm.1900090208
23. Walsh JT, Deutsch TF. Er:YAG laser ablation of tissue: measurement of ablation rates. *Lasers Surg Med.* (1989) 9:327–37. doi: 10.1002/lsm.1900090404
24. Hibst R, Kaufmann R. Effects of laser parameters on pulsed Er-YAG laser skin ablation. *Laser Med Sci.* (1991) 6:391–7. doi: 10.1007/BF02042461
25. Dickinson MR, Charlton A, King TA, Freemont AJ, Bramley R. Studies of Er-YAG laser interactions with soft tissue. *Laser Med Sci.* (1991) 6:125–31. doi: 10.1007/BF02032539
26. Werner JA, Lippert BM, Rudert H, Godbersen GS. Vergleichende Untersuchungen zur Revaskularisation der Schleimhaut des oberen Aerodigestivtraktes nach Skalpell-, CO2- und Nd:YAG-Laserinzision. In: H. Feldmann, E. Stennert, eds. *Teil II: Sitzungsbericht* Verhandlungsbericht. Berlin, Heidelberg: Springer (1993). p. 32–33. doi: 10.1007/978-3-642-84996-1_29
27. Di Maio P, Iocca O, De Virgilio A, Ferreli F, Cristalli G, Pellini R, et al. Role of palatine tonsillectomy in the diagnostic workup of head and neck squamous cell carcinoma of unknown primary origin: a systematic review and meta-analysis. *Head Neck.* (2019) 41:1112–21. doi: 10.1002/hed.25522
28. Kuta V, Williams B, Rigby M, Hart R, Trites J, MacKay C, et al. Management of head and neck primary unknown squamous cell carcinoma using combined positron emission tomography-computed tomography and transoral laser microsurgery. *Laryngoscope.* (2018) 128:2307–11. doi: 10.1002/lary.27034
29. Katta N, McElroy AB, Estrada AD, Milner TE. Optical coherence tomography image-guided smart laser knife for surgery. *Lasers Surg Med.* (2018) 50:202–12. doi: 10.1002/lsm.22705
30. Chang W, Fan Y, Zhang X, Liao H. An intelligent theranostics method using optical coherence tomography guided automatic laser ablation for neurosurgery. *2018 40th Annual International Conference of the IEEE Engineering in Medicine and Biology Society (EMBC)*. Honolulu (2018). doi: 10.1109/EMBC.2018.8513016
31. Yaroslavsky I, Boutoussov D, Vybornov A, Perchuk I, Meleshkevich V, Altshuler G. Ex vivo evaluation of super pulse diode laser system with smart temperature feedback for contact soft-tissue surgery. In: *Lasers in Dentistry XXIV* (International Society for Optics and Photonics) (2018) 10473:82–87. doi: 10.1117/12.2291115

Conflict of Interest: The experiments were partially financially supported by Pantec Biosolutions AG.

The authors declare that the research was conducted in the absence of any commercial or financial relationships that could be construed as a potential conflict of interest.

frontiers in Oncology

ORIGINAL RESEARCH
published: 17 December 2021
doi: 10.3389/fonc.2021.716470

Endoscopic Versus Surgical Therapy for Early Esophagogastric Junction Adenocarcinoma Based on Lymph Node Metastasis Risk: A Population-Based Analysis

Hua Ye[1,2,3], *Ping Chen*[2,3], *Yi-Fan Wang*[1] *and Xiu-Jun Cai*[1]*

[1] Department of General Surgery, Sir Run Run Shaw Hospital, Zhejiang University School of Medicine, Hangzhou, China, [2] Department of Gastrointestinal and Hernia Ward, HwaMei Hospital, University Of Chinese Academy Of Sciences, Ningbo, China, [3] Key Laboratory of Diagnosis and Treatment of Digestive System Tumors of Zhejiang Province, Ningbo, China

OPEN ACCESS

Edited by:
Patrick J. Schuler,
Ulm University Medical Center,
Germany

Reviewed by:
Giovanni Capovilla,
Johannes Gutenberg University Mainz,
Germany
Aleksandar M. Cvetković,
University of Kragujevac, Serbia

***Correspondence:**
Xiu-Jun Cai
srrsh_cxj@zju.edu.cn

Specialty section:
This article was submitted to Surgical Oncology, a section of the journal Frontiers in Oncology

Received: 28 May 2021
Accepted: 22 November 2021
Published: 17 December 2021

Citation:
Ye H, Chen P, Wang Y-F and Cai X-J (2021) Endoscopic Versus Surgical Therapy for Early Esophagogastric Junction Adenocarcinoma Based on Lymph Node Metastasis Risk: A Population-Based Analysis. Front. Oncol. 11:716470. doi: 10.3389/fonc.2021.716470

Background: In this study, we aimed to compare the prognosis and lymph node metastasis (LNM) risk in patients with early-stage esophagogastric junction (EGJ) adenocarcinoma after endoscopic treatment (ET) or radical surgery.

Methods: We collected data from eligible patients based on the Surveillance, Epidemiology, and End Results (SEER) database between 2004 and 2016. Logistic regression analysis was used to determine independent predictors of LNM (examination of at least 16 lymph nodes). Cox regression analysis and propensity score-matched (PSM) analysis were subsequently utilized to compare the overall survival (OS) and cancer-specific survival (CSS) of patients treated with ET or radical surgery.

Results: In total, 3708 patients were identified. Among them, 856 patients had greater than or equal to 16 examined lymph nodes (LNs) (LNE≥16). The LNM rates were 18.8% in all patients 8.3% in T1a patients and 24.6% in T1b patients. Independent predictors of LNM were submucosal invasion, tumor size ≥3cm and decreasing differentiation (P<0.05). The LNM rate decreased to approximately 5.3% in T1b tumors with well differentiation and tumor size <3cm. However, the LNM incidence increased to 17.9% or 33.3% in T1a tumors with poor differentiation or with both tumor size≥3cm and poor differentiation. Cox regression analysis demonstrated CSS was not significantly different in early-stage EGJ adenocarcinoma patients undergoing ET and those treated with radical surgery (HR= 1.004, P=0.974), which were robustly validated after PSM analysis. Moreover, subgroup analysis stratified by T1a and T1b showed similar results.

Conclusions: The findings of this study indicated ET as an alternative to radical surgery in early EGJ adenocarcinoma.

Keywords: endoscopic treatment, surgery, esophagogastric junction adenocarcinoma, lymph node metastasis, survival

INTRODUCTION

In recent years great changes have been made in the clinical intervention for early malignant and precancerous lesions of the upper gastrointestinal (GI) tract, from radical surgery to endoscopic treatment. The incidence of esophagogastric junction (EGJ) adenocarcinoma has been rapidly rising in Western countries in the last few decades (1). A similar trend has been observed in Asia, probably due to the available eradication therapy for Helicobacter pylori (H.pylori), a high prevalence of gastroesophageal reflux disease and obesity, and dietary factors (2), and partly shared with those of gastric adenocarcinoma, i.e. H.pylori infection and dietary factors (3). As a minimally invasive approach, endoscopic submucosal dissection (ESD) or endoscopic mucosal resection (EMR) is also curative for superficial GI malignancies, including esophageal, gastric, and colonic lesions (4). Moreover, due to the varied incidence of lymph node metastasis (LNM) in esophageal and gastric cancer, there are also differences in the curative resection criteria of ESD/EMR between esophageal and gastric cancer (5, 6). However, it is unknown which curative resection criteria are better for EGJ adenocarcinoma since the incidence of metastatic EGJ adenocarcinoma remains unknown. It is noteworthy that inaccessible assessment of pathologic lymph node (LN) is considered the main drawback of endoscopic treatment (ET), as it can significantly affect patients' survival in the case of metastatic LNs. Therefore, clinical decision-making in early-stage EGJ adenocarcinoma can be optimized by better pretreatment LNM risk stratification according to both patient and tumor features.

In this study, eligible patients from the Surveillance, Epidemiology, and End Results (SEER) database were utilized to determine preoperative predictors of LNM, followed by a comparison of the effects of radical surgery and ET on long-term survival in early-stage EGJ adenocarcinoma. Finally, an early-stage EGJ adenocarcinoma therapeutic algorithm was proposed for patients at acceptable risk for ET.

MATERIALS AND METHODS

Origins of Materials

The National Cancer Institute (NCI) supports the SEER database, which records data on tumor incidence and survival by covering almost 28% of the population in the USA from diverse geographic regions (18 cancer registries) from 2004 to 2016. The collection and recoding of SEER data were performed using data items and codes based on the North American Association of Central Cancer Registries (NAACCR) (7). Access to the SEER database was obtained, and our study gained institutional approval.

Inclusion and Exclusion Criteria

In total, 3708 patients were enrolled. The inclusion criteria were as follows: (1) year of diagnosis (from 2004 to 2016); (2) patients were 18 years or older; (3) histological type included adenocarcinoma (8140), mucinous adenocarcinoma (MAC) (8480), and signet ring cell cancer (SRCC) (8490); (4) available active follow-up data; and (5) patients with T1 EGJ adenocarcinoma (site codes, C15.5, C16.0, C16.1, and C16.2) treated with either ET, radical surgery According to the records in the SEER database, ET referred to endoscopic treatment for local tumor excision with pathology specimen. In addition, the definition of radical surgery was all forms of partial esophagus removal along with partial or total gastrectomy (6). At least 16 regional lymph nodes (LNs) were examined after surgical resection. The exclusion criteria were as follows: (1) distant metastasis; (2) patients who received neoadjuvant therapy; (3) patients who had more than one primary malignancy, except those with EGJ as the first diagnosis; (4) patients who died within 1 month, which was mostly caused by surgical complications; and (5) patients undergoing local tumor destruction without a pathological specimen.

There are controversies over the staging classification system for esophagogastric junction adenocarcinoma. The cancers involving it with epicenters no more than 2cm into the gastric cardia are staged as adenocarcinomas of the esophagus and those with more than 2cm involvement of the gastric cardia are staged as gastric cancers (8). Studies have shown that patients with ≥ 16 pathologically examined LNs (eLNs) have better prognoses as compared to those with < 16 eLNs (9). The American Joint Committee on Cancer (AJCC) advocates for the retrieval of at least 16 LNs for optimizing the radicality of D2 lymphadenectomies and enabling proper staging of gastric cancer (10). Therefore, we selected patients with radical surgical resection and dissection of at least 16 lymph nodes for further analysis of LNM risks in patients with early-stage EGJ adenocarcinoma.

Statistical Analysis

Age at diagnosis, race, year of diagnosis, marital status, gender, tumor size, differentiation grade, survival (months), number of examined LNs, LNM, histology, and death cause were collected from the SEER database. The main endpoints included overall survival (OS) and cancer-specific survival (CSS).

For comparisons among groups, categorical variables were analyzed by Fisher's exact test or Pearson's test. Risk factors for LNM were determined by both univariate and multivariate logistic regression models, shown as odds ratios (ORs) along with 95% confidence intervals (CIs). Moreover, adjusted hazard ratios (HRs) along with 95% CIs were calculated by both univariate and multivariate Cox regression models. Additionally, PSM analysis was performed by using the 1:1 "nearest neighbor" match paradigm, aiming at further adjustment of variations in general data and bias minimization. The following covariates histology, grade, race, gender, age, T stage, tumor size, year of diagnosis, and marital status were used in PSM analysis. After matching, we compared two groups with control for covariate balance and similarity in baseline covariates between groups, and two matched groups were compared according to the study objectives. Statistical analysis was performed by R software version R-3.6.2 (The R Foundation

for Statistical Computing, Vienna, Austria) as well as SPSS version 23.0 (SPSS Inc., Chicago, IL, USA). GraphPad Prism 6.0 (GraphPad Software, San Diego, CA) was employed to plot survival curves. A two-sided P value < 0.05 suggested statistical significance.

RESULTS

Patient Characteristics

In total, 3708 eligible patients were included (surgical therapy: n = 2418, 65.2%; ET: n = 1290, 34.8%). Among them, 3708 patients were male and the remaining 610 were female. The median age at diagnosis was 67 years, ranging from 22 to 97 years (mean ± SD:66.35 ± 10.61 years). The median follow-up was 44 months, ranging between 1 and 155 months. In total, 1610 patients had radical surgery of partial esophagus removal along with partial gastrectomy and 808 had the radical surgery of partial esophagus removal along with total gastrectomy. Detailed data on patient demographics as well as tumor characteristics are shown in **Table 1**.

LNM Risks in Early-Stage EGJ Adenocarcinoma

In total, we collected information from 856 patients with EGJ adenocarcinoma diagnosed between 2004 and 2016 with at least 16 LNs examined who received surgical resection. The overall LNM rate was 18.8% (161/856). When stratified by pT stage, LNM rates were 8.3% (25/300) and 24.6% (122/496) in T1a and T1b patients, respectively. LNM rate decreased to 5.3% (2/38) in well-differentiated T1b tumors with a tumor size<3cm; while LNM incidence increased to 17.9% (12/67) in poorly-differentiated T1a tumors, and rose to as high as 33.3% (5/15) in poorly-differentiated tumors exceeding 3cm in size. Given that the tumor size is a key determinant of LNM, 722 patients with known tumor sizes were selected for further univariate and multivariate logistic regression analyses to identify risk factors for LNM. Consequently, we robustly found that tumor size, tumor grade, and pT stage were significant predictive indicators for LNM. LNM rate was significantly higher in T1b than T1a tumors (OR: 2.168, 95% CI: 1.273-3.692, P=0.004). Compared with small tumors that were less than 1cm in size, the risk of LNM was increased in tumor sizes exceeding 3 cm (OR=5.484, 95% CI: 2.688-11.187, P <0.001) in multivariate analysis. The incidence of LNM was also significantly higher in tumors with poor/moderate differentiation or undifferentiation than those with well differentiation (OR 2.824, 95% CI: 1.071-7.443, P=0.036; OR 4.783, 95% CI 1.812-12.624, P= 0.002, respectively) in multivariate analysis. The detailed patient characteristics are summarized in **Table 2**. According to the present NCCN guidelines, ET is recommended for T1a tumors but is less definitive for T1b tumors.

LNM Rates in T1a Tumors

The rate of LNM in T1a tumor sizes exceeding 3 cm was 23.8% (10/42) compared with 6.1% (12/197) in tumors <3 cm in size. Compared with small tumors less than 1cm in size, the risk of LNM was increased in tumor sizes exceeding 3 cm (OR=4.662, 95% CI: 1.407-15.442, P =0.012) in multivariate analysis. The presence of LNM was 4.8% (3/62), 7.0% (8/115), and 17.9% (12/67) in well-differentiated, moderately differentiated, and poorly/undifferentiated T1a tumors, respectively. The incidence of LNM was higher in poorly differentiated T1a cancer compared with well-differentiated examples (OR3.611,95% CI: 0.865-15.085, P =0.078) in multivariate analysis. The details of other tumor features is shown in **Table 3**.

LNM Rates in T1b Tumors

We further compared the LNM rate in T1b tumors between tumor size exceeding 3 cm and tumors <3 cm, which was 42.7% (56/131) versus 19.3% (61/316). The incidence of LNM was higher in Signet ring cell carcinoma (OR 2.073, 95% CI: 1.006-4.273, P = 0.048) than in well-differentiated tumors. Compared with small tumors of less than 1cm in size, the risk of LNM was increased in tumor sizes exceeding 3 cm (OR=5.935, 95% CI: 2.183-16.134, P<0.001). The presence of LNM was 6.4% (3/47), 21.4% (47/220), and 32.9% (70/213) in well-differentiated, moderately differentiated, and poorly/undifferentiated T1b tumors, respectively. LNM incidence was higher in poorly-differentiated than well-differentiated T1b tumors (OR 7.287, 95%CI: 1.674-31.725, P=0.008) in multivariate analysis. The details of other tumor features are shown in **Table 3**.

Patient Survival

The mean OS in the surgical therapy and ET groups was 105 months (95% CI 103–108), 97 months (95% CI 93–102) respectively. The log-rank test showed that overall survival was similar in patients treated by surgical therapy and ET (p=0.065). Survival curves of the two groups were displayed in **Figure 1A**. The mean CSS was 121 months (95% CI 118–123) and 126 months (95% CI 122–131) in the surgical therapy, ET groups, respectively. The log-rank test revealed that the CSS survival of patients treated by surgical therapy was significantly worse than those treated by ET (P<0.001). The survival curves of the two groups are displayed in **Figure 1B**, after propensity score matching. Furthermore, The mean OS in the radical surgery of partial esophagus removal along with partial gastrectomy, total gastrectomy, and ET groups was 107 months (95% CI 103–110), 103months (95% CI 99–108), and 97 months (95% CI 93–102) respectively. A log-rank test showed that OS was similar in patients treated by the radical surgery of partial esophagus removal along with partial gastrectomy, total gastrectomy, and ET groups (p=0.081). The mean CSS in the radical surgery of partial esophagus removal along with partial gastrectomy, total gastrectomy, and ET groups was 121 months (95% CI 118–124), 120months (95% CI 116–124), and 127 months (95% CI 122–131) respectively. The log-rank test revealed that the CSS survival of patients treated by ET was significantly better than those treated by surgery of partial gastrectomy group (P=0.002) and those treated by surgery of total gastrectomy group (P=0.001).The multivariate Cox regression models showed that OS (ET: HR 1.220, 95% CI: 1.059-1.406, P =0.006) and CSS (ET:

TABLE 1 | Baseline characteristics of patients treated with ES and ET for early-stage esophageal cancer before and after the propensity score-matched (1:1 matching).

Characteristic	Before matched		Statistic	p	After matched		Statistic	p
	Surgery N=2418,%	ET N=1290,%			Surgery N=920,%	ET N=920,%		
Gender			χ^2 = 4.104	0.043			χ^2 = 0.434	0.510
Female	376 (15.6)	234 (18.1)			166 (18.0)	177 (19.2)		
Male	2042 (84.4)	1056 (81.9)			754 (82.0)	743 (80.8)		
Age (years)			χ^2 = 190.802	<0.001			χ^2 = 5.161	0.160
Up to 49	170 (7.0)	39 (3.0)			36 (3.9)	37 (4.0)		
50-64	985 (40.7)	360 (27.9)			304 (33.0)	297 (32.3)		
65-79	1114 (46.1)	650 (50.4)			478 (52.0)	452 (49.1)		
80+	149 (6.2)	241 (18.7)			102 (11.1)	134 (14.6)		
Race			χ^2 = 2.270	0.321			χ^2 = 3.222	0.200
White	2270 (93.9)	1221 (94.7)			874 (95.0)	864 (93.9)		
Black	56 (2.3)	32 (2.5)			24 (2.6)	21 (2.3)		
Others*	92 (3.8)	37 (2.9)			22 (2.4)	35 (3.8)		
Tumor size (cm)			χ^2 = 374.707	<0.001			χ^2 = 4.393	0.355
<1	511 (21.1)	351 (27.2)			258 (28.0)	236 (25.7)		
1-2	571 (23.6)	211 (16.4)			196 (21.3)	178 (19.3)		
2-3	420 (17.4)	86 (6.7)			72 (7.8)	84 (9.1)		
3+	431 (17.8)	70 (5.4)			70 (7.6)	66 (7.2)		
Not stated	485 (20.1)	572 (44.3)			324 (35.2)	356 (38.7)		
Year of diagnosis			χ^2 = 337.009	<0.001			χ^2 = 2.772	0.428
2004-2006	577 (23.9)	116 (9.0)			113 (12.3)	104 (11.3)		
2007-2009	675 (27.9)	189 (14.7)			188 (20.4)	183 (19.9)		
2010-2012	555 (23.0)	315 (24.4)			232 (25.2)	212 (23.0)		
2013-2016	611 (25.3)	670 (51.9)			387 (42.1)	421 (45.8)		
Marital status			χ^2 = 15.807	<0.001			χ^2 = 5.671	0.059
Married	1687 (69.8)	819 (63.5)			609 (66.2)	560 (60.9)		
Single/widowed	402 (16.6)	270 (20.9)			173 (18.8)	203 (22.1)		
Other/unknown	329 (13.6)	201 (15.6)			138 (15.0)	157 (17.1)		
T stage			χ^2 = 400.549	<0.001			χ^2 = 1.844	0.398
T1a	979 (40.5)	927 (71.9)			592 (64.3)	595 (64.7)		
T1b	1226 (50.7)	226 (17.5)			235 (25.5)	217 (23.6)		
T1x	213 (8.8)	137 (10.6)			93 (10.1)	108 (11.7)		
Grade			χ^2 = 279.570	<0.001			χ^2 = 4.461	0.216
Well-differentiated	346 (14.3)	210 (16.3)			160 (17.4)	134 (14.6)		
Moderately differentiated	1019 (42.1)	438 (34.0)			352 (38.3)	338 (36.7)		
Poorly/Undifferentiated	726 (30.0)	191 (14.8)			167 (18.2)	182 (19.8)		
Unknown	327 (13.5)	451 (35.0)			241 (26.2)	266 (28.9)		
Histology			χ^2 = 21.284	<0.001			χ^2 = 0	1.0
Adenocarcinoma	2270 (93.9)	1255 (97.3)			887 (96.4)	887 (96.4)		
Mucinous carcinoma	25 (1.0)	8 (0.6)			8 (0.9)	8 (0.9)		
Signet ring cell carcinoma	123 (5.1)	27 (2.1)			25 (2.7)	25 (2.7)		

*ET, Endoscopic therapy; T1a,tumor invades the lamina propria or muscularis mucosa; T1b, tumor invades the submucosa; T1x, unknown T1a or T1b.*American Indian/Alaska Native, Asian/Pacific Islander.*

HR1.004, 95% CI: 0.807-1.249, P=0.974.) compare with the surgical therapy group. Moreover, univariate and multivariate Cox regression models consistently revealed that tumor size (≥2cm), year of diagnosis, pT stage, LNM, Grade(Poorly/Undifferentiated), histology (Signet ring cell carcinoma), marital status, and old age (≥65years) were significant prognostic indicators for both OS and CSS (**Table 4**).

PSM

In total, 920 patient pairs were included in the PSM analysis. Patient features and tumor characteristics of both surgical therapy and ET groups after propensity matching were displayed in **Table 1**. As a result, all matched variables were balanced between two groups (all P > 0.05). Survival analysis and log-rank test revealed worse OS in the ET group than surgical therapy group (**Figure 1C**). There was no significant difference in CSS (**Figure 1D**). Moreover, Cox proportional hazard regression revealed significant differences in OS (HR = 1.488, 95% CI 1.240-1.786; P < 0.001) and no significant differences in CSS (HR = 1.112, 95% CI:0.866-1.429; P = 0.405) between surgical therapy and ET groups. The details of other tumor features are shown in **Table 5**.

Subgroup Analysis

The 920 patient pairs were further categorized into T1a and T1b groups. After adjustment of both patient demographics and tumor variables, surgical therapy and ET related CSS (HR = 1.085, 95% CI 0.760-1.550; P = 0.653), (HR = 1.335, 95% CI: 0.856-2.083; P = 0.203) were not significantly different in T1a and T1b patients (shown in **Table 6**).

TABLE 2 | Logistic regression analysis of the risk factors for lymph node metastasis in early-stage esophagogastric junction cancer (LNE≥16).

Characteristic	Univariate analysis		Multivariate analysis	
	OR (95% CI)	*P*	OR (95% CI)	*P*
Gender				
Female	Reference			
Male	1.216 (0.762-1.942)	0.412		
Age (years)				
Up to 49	Reference			
50-64	0.904 (0.455-1.794)	0.773		
65-79	0.946 (0.480-1.865)	0.872		
80+	1.910 (0.737-4.948)	0.183		
Race				
White	Reference			
Black	0.236 (0.031-1.785)	0.162		
Others*	1.135 (0.510-2.525)	0.756		
Tumor size (cm)				
<1	Reference		Reference	
1-2	2.556 (1.256-5.201)	0.010	1.699 (0.813-3.554)	0.159
2-3	3.403 (1.638-7.070)	0.001	1.930 (0.896-4.156)	0.093
3+	8.868 (4.496-17.490)	<0.001	5.524 (2.716-11.234)	<0.001
Not stated	1.350 (0.576-3.166)	0.490	1.130 (0.466-2.738)	0.787
pT stage				
T1a	Reference		Reference	
T1b	3.588 (2.271-5.670)	<0.001	2.162 (1.311-3.565)	0.003
T1x	3.348 (1.622-6.912)	0.001	2.729 (1.234-6.035)	0.013
Year of diagnosis				
2004-2006	Reference			
2007-2009	1.410 (0.830-2.397)	0.204		
2010-2012	1.174 (0.690-1.998)	0.553		
2013-2016	0.986 (0.586-1.661)	0.959		
Marital status				
Married	Reference			
Single/widowed	1.258 (0.789-2.006)	0.335		
Other/unknown	0.881 (0.517-1.501)	0.640		
Grade				
Well-differentiated	Reference		Reference	
Moderately differentiated	3.614 (1.518-8.602)	0.004	2.539 (1.042-6.186)	0.040
Poorly/Undifferentiated	7.558 (3.202-17.840)	<0.001	4.325 (1.774-10.544)	0.001
Unknown	1.158 (0.341-3.932)	0.814	1.275 (0.358-4.533)	0.708
Histology				
Adenocarcinoma	Reference		Reference	
Mucinous carcinoma	1.332 (0.274-6.480)	0.723	0.611 (0.115-3.253)	0.563
Signet ring cell carcinoma	2.331 (1.322-4.110)	0.003	1.798 (0.965-3.350)	0.065

LNE, Number of examined lymph nodes; OR, odd ratio; 95% CI,95% confidence intervals; pT, pathologic tumor; T1a,tumor invades the lamina propria or muscularis mucosa; T1b, tumor invades the submucosa.

**American Indian/Alaska Native, Asian/Pacific Islander.*

DISCUSSION

Accumulated studies have demonstrated that EGJ adenocarcinoma is a separate entity from gastric or esophageal malignancies due to unique clinicopathological characteristics and patient survival (11, 12). The majority of EGJ carcinomas are handled by surgical intervention, including esophagectomy along with total or proximal gastrectomy, which, however, greatly attenuates postoperative living quality and is accompanied by a high risk of complications. The rate of postoperative complications is reported to be 33-39% according to a systematic review (13). ESD is particularly suitable for patients with early-stage proximal gastric cancer, who, otherwise, are generally treated with total gastrectomy. If patients are managed with ESD, the whole stomach can be preserved, along with better life quality (14). Due to the unknown incidence of LNM in EGJ adenocarcinoma, there is no consensus on the indication of endoscopic resection for superficial EGJ adenocarcinoma.

To our knowledge, our study is the largest to date concerning LNM rates in early-stage EGJ adenocarcinoma after eliminating patients with less than 16 examined LNs. We found that the LNM rate in early-stage EGJ adenocarcinoma was as high as 18.8% (161/856). LNM rates stratified by pT stage were 8.3% (25/300) in T1a and 24.6% (122/496) in T1b. Moreover, the rate of LNM decreased to 5.3% (2/38) in well-differentiated T1b tumors with tumor size<3cm; and LNM rate increased to 17.9% (12/67) in poorly differentiated T1a tumors, and to 33.3% (5/15) in poorly differentiated T1a tumors with tumor size>3cm. Overall, there is limited information concerning the LNM rate in superficial EGJ adenocarcinoma. According to the study by

TABLE 3 | Logistic regression analysis of the risk factors for lymph node metastasis in T1a and T1b esophagogastric junction cancer (LNE≥16).

Characteristic	T1a				T1b			
	Univariate analysis		Multivariate analysis		Univariate analysis		Multivariate analysis	
	OR (95% CI)	*P*	OR (95% CI)	*P*	OR (95% CI)	*P*	OR (95% CI)	*P*
Gender								
Female	Reference				Reference			
Male	1.710 (0.493-5.930)	0.398			1.216 (0.706-2.095)	0.481		
Age (years)								
Up to 49	Reference				Reference			
50-64	0.687 (0.207-2.276)	0.539			1.029 (0.390-2.716)	0.954		
65-79	0.433 (0.121-1.548)	0.198			1.076 (0.413-2.801)	0.881		
80+	Omitted				1.875 (0.551-6.379)	0.314		
Race								
White	Reference				Reference			
Black	Omitted				1.053 (0.410-2.699)	0.915		
Others*	1.067 (0.131-8.691)	0.952			0.352 (0.037-3.374)	0.365		
Tumor size (cm)								
<1	Reference		Reference		Reference		Reference	
1-2	1.516 (0.422-5.446)	0.524	1.342 (0.364-4.943)	0.658	2.410 (0.882-6.587)	0.086	2.036 (0.732-5.666)	0.173
2-3	1.617 (0.295-8.846)	0.580	1.126 (0.191-6.633)	0.896	2.686 (0.969-7.447)	0.058	2.292 (0.809-6.490)	0.118
3+	6.062 (1.928-19.060)	0.002	4.673 (1.421-15.371)	0.011	7.019 (2.622-18.791)	<0.001	6.091 (2.239-16.570)	<0.001
Not stated	1.003 (0.231-4.355)	0.996	0.984 (0.219-4.423)	0.983	1.068 (0.289-3.943)	0.921	1.042 (0.277-3.921)	0.951
Year of diagnosis								
2004-2006	Reference				Reference			
2007-2009	0.486 (0.128-1.851)	0.290			1.611 (0.850-3.053)	0.144		
2010-2012	0.736 (0.254-2.132)	0.573			1.239 (0.655-2.344)	0.511		
2013-2016	0.623 (0.216-1.796)	0.381			0.974 (0.526-1.806)	0.934		
Marital status								
Married	Reference				Reference		Reference	
Single/widowed	0.597 (0.170-2.092)	0.420			1.759 (1.012-3.055)	0.045	1.780 (0.981-3.232)	0.058
Other/unknown	0.531 (0.119-2.370)	0.406			0.888 (0.469-1.681)	0.715	0.879 (0.448-1.724)	0.707
Grade								
Well-differentiated	Reference		Reference		Reference		Reference	
Moderately differentiated	1.470 (0.376-5.754)	0.580	1.543 (0.380-6.259)	0.544	3.985 (1.184-13.404)	0.026	3.005 (0.872-10.359)	0.081
Poorly/Undifferentiated	4.291 (1.149-16.021)	0.030	3.909 (0.973-15.708)	0.055	7.179 (2.154-23.931)	0.001	4.944 (1.440-16.970)	0.011
Unknown	0.728 (0.117-4.527)	0.734	0.820 (0.127-5.298)	0.835	2.095 (0.317-13.835)	0.442	1.496 (0.207-10.794)	0.690
Histology								
Adenocarcinoma	Reference		Reference		Reference		Reference	
Mucinous carcinoma	11.727 (0.709-193.969)	0.085	5.434 (0.185-160.030)	0.327	0.667 (0.077-5.776)	0.713	0.497 (0.053-4.627)	0.539
Signet ring cell carcinoma	1.466 (0.316-6.791)	0.625	0.76 (0.146-4.036)	0.755	2.578 (1.320-5.037)	0.006	2.025 (0.980-4.184)	0.057

LNE, Number of examined lymph nodes; OR, odd ratio; 95% CI,95% confidence intervals; T1a,tumor invades the lamina propria or muscularis mucosa.
**American Indian/Alaska Native, Asian/Pacific Islander.*

Gertler, LNM was only detectable in pT1b tumors (18%) but not in pT1a among superficial EGJ adenocarcinoma (15), which was also similarly reported by Stein (16). Moreover, Koufuji, et al. reported no LNM in T1 EGJ carcinoma (17). Of the above studies, the relatively inadequate sample size might be the most significant drawback. Zhu, et al. reported that the overall LNM rate of superficial EGJ carcinoma was 21.75%, which is 11.41% and 26.50% in mucosal cancer and submucosal cancer, respectively. The results of the above study are consistent with our findings and another study concerning surgically resected pT1 EGJ carcinoma (18, 19).

Previous studies have shown that tumor size, pathological differentiation, lymphovascular invasion, and infiltration depth are risk factors for LNM in gastric and esophageal cancer (15, 19). In our study, similar predictors of LNM involvement were revealed, including tumor size, differentiation type, and depth of invasion. To be specific, poor tumor differentiation (including moderately/poorly differentiated and undifferentiated) and

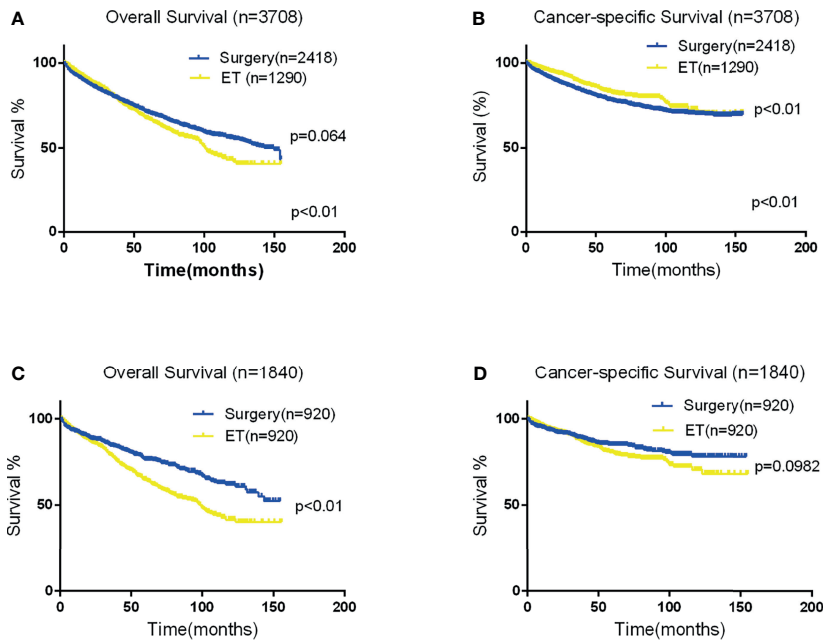

FIGURE 1 | Kaplan-Meier curves for OS and CSS. Panels **(A, B)** depict the overall and CSS of the Two groups in the original data set, and panels **(C, D)** depict the OS and CSS of the two group after propensity score matching.

tumor sizes exceeding 3 cm increased LNM risk. Tumor differentiation is the most potent predictor. Therefore, endoscopic intervention might be proper for low-risk patients, while, high-risk patients should be managed by surgical resection in consideration of the high risk of LNM.

Our study revealed that the CSS survival of patients treated by surgical therapy was significantly worse than those treated by ET (P<0.001). Subset analysis of survival of ET vs surgery including radical surgery of partial esophagus removal along with partial gastrectomy group and total gastrectomy group. A log-rank test revealed that the CSS survival of patients treated by ET was significantly better than those treated by surgery of partial gastrectomy group (P=0.002) and those treated by surgery of total gastrectomy group (P=0.001). Better survival of the ET group in the overall population is related to the selection bias of patients with less advanced tumors than surgery groups. Previous research has revealed that age, T stage and tumor differentiation are independently correlated with poor prognosis (20–22) Due to the bias caused these parameters which can interfere with the comparison of ET and surgical therapy, multivariate Cox regression analysis and PSM were performed. ET and surgical therapy were associated with similar CSS in patients with early-stage EGJ adenocarcinoma. Additionally, subgroup analysis stratified by T stage also showed similar outcomes. PSM analysis also revealed consistent outcomes, which could decrease selection bias associated with diverse clinical features of ET and surgical therapy. We identify an OS benefit of surgery compared to ET (HR = 1.488, 95% CI:1.240-1.786; P < 0.001), but no CSS difference between surgical therapy and ET groups after PSM (HR = 1.112, 95% CI:0.866-1.429; P=0.405). Patients in the ET group may have more non-oncological basic diseases and are more likely to have non-oncological death cases. Therefore, the OS of the ET group is worse than that of the surgery group. The authors found that patients with sm1 cancers, classified by a submucosal invasion of < 500μm, and tumors smaller than 3 cm had no LNMs. Nevertheless, with a deep submucosal invasion of ≥500μm stratified by sm2 and sm3, the incidence of LNM increased to 28.6%, irrespective of tumor size. The above outcomes suggest that ESD can be safely used to treat patients with sm1 and tumor size < 3 cm, which is beyond the proposed guidelines (6, 23). Most patients with T1b tumors should be treated by surgical intervention due to the high LNM rate (24.6%). Nevertheless, LNM incidence in T1b cancer with all low-risk tumor characteristics was only 5.3%. Hence, definitive ET must be cautiously determined on submucosal cancers without other high-risk characteristics. The multivariate Cox regression models showed that no significant differences in CSS (HR = 1.004, 95% CI: 0.807-1.249, P=0.974) between surgical therapy and ET groups. Moreover, Cox proportional hazards regression revealed no significant differences in CSS (HR = 1.112, 95% CI:0.866-1.429; P = 0.405) between surgical therapy and ET groups after PSM. Therefore, ET might be a valid alternative to surgical therapy to treat early EGJ adenocarcinoma, especially in elderly patients. Marital status is not a risk factor for LNM in gastric and esophageal cancer in our study. Cox proportional hazards regression revealed that for marital status there were significant differences in OS and CSS. Divorce, widowhood, and other reasons for living alone might increase the risk of adopting bad lifestyle habits. Previous research has shown that an

TABLE 4 | Cox regression analysis of OS and CSS in patients with early-stage esophagogastric junction cancer.

Characteristic	OS				CSS			
	Univariate analysis		Multivariate analysis		Univariate analysis		Multivariate analysis	
	HR (95% CI)	*P*	HR (95% CI)	*P*	HR (95% CI)	*P*	HR (95% CI)	*P*
Gender								
Female	Reference				Reference			
Male	0.998 (0.896-1.112)	0.975			0.968 (0.855-1.097)	0.612		
Race								
White	Reference		Reference		Reference		Reference	
Black	1.353 (1.084-1.689)	0.007	1.187 (0.949-1.484)	0.133	1.351 (1.044-1.748)	0.022	1.104 (0.851-1.431)	0.457
Others*	0.830 (0.656-1.049)	0.119	0.818 (0.646-1.036)	0.095	0.918 (0.705-1.195)	0.523	0.908 (0.696-1.185)	0.477
Tumor size (cm)								
<1	Reference		Reference		Reference		Reference	
1-2	1.507 (1.257-1.807)	<0.001	1.144 (0.952-1.375)	0.152	1.879 (1.474-2.394)	<0.001	1.284 (1.004-1.641)	0.046
2-3	2.115 (1.762-2.538)	<0.001	1.309 (1.084-1.579)	0.005	2.778 (2.183-3.537)	<0.001	1.469 (1.146-1.882)	0.002
3+	4.139 (3.531-4.851)	<0.001	1.564 (1.317-1.856)	<0.001	6.456 (5.224-7.979)	<0.001	1.906 (1.521-2.390)	<0.001
Not stated	2.943 (2.525-3.430)	<0.001	1.389 (1.180-1.635)	<0.001	4.176 (3.392-5.141)	<0.001	1.682 (1.349-2.096)	<0.001
Year of diagnosis								
2004-2006	Reference		Reference		Reference		Reference	
2007-2009	0.868 (0.784-0.962)	0.007	0.900 (0.812-0.997)	0.044	0.887 (0.786-1.001)	0.051	0.942 (0.834-1.063)	0.333
2010-2012	0.690 (0.616-0.773)	<0.001	0.741 (0.660-0.831)	<0.001	0.697 (0.611-0.795)	<0.001	0.793 (0.694-0.907)	0.001
2013-2016	0.659 (0.582-0.747)	<0.001	0.770 (0.677-0.875)	<0.001	0.630 (0.545-0.727)	<0.001	0.807 (0.697-0.935)	0.004
Marital status								
Married	Reference		Reference		Reference		Reference	
Single/widowed	1.436 (1.306-1.578)	<0.001	1.191 (1.080-1.312)	<0.001	1.530 (1.371-1.707)	<0.001	1.249 (1.116-1.398)	<0.001
Other/unknown	1.142 (1.016-1.284)	0.027	1.182 (1.050-1.332)	0.006	1.232 (1.077-1.409)	0.002	1.252 (1.092-1.435)	0.001
T stage								
T1a	Reference						Reference	
T1b	1.205 (1.083-1.340)	0.001	1.192 (1.061-1.340)	0.003	1.403 (1.229-1.601)	<0.001	1.313 (1.137-1.517)	<0.001
T1x	3.905 (3.553-4.292)	<0.001	1.443 (1.292-1.612)	<0.001	5.153 (4.594-5.779)	<0.001	1.596 (1.400-1.818)	<0.001
Treatment								
Surgery	Reference						Reference	
ET	1.092 (0.960-1.241)	0.180	1.220 (1.059-1.406)	0.006	0.693 (0.578-0.831)	<0.001	0.830 (0.682-1.010)	0.062
RT	6.111 (5.573-6.702)	<0.001	3.700 (3.271-4.185)	<0.001	7.031 (6.311-7.834)	<0.001	4.024 (3.483-4.649)	<0.001
LNM								
No	Reference		Reference		Reference		Reference	
Yes	2.275 (2.066-2.504)	<0.001	1.507 (1.361-1.668)	<0.001	2.728 (2.453-3.035)	<0.001	1.614 (1.443-1.805)	<0.001
Grade								
Well-differentiated	Reference		Reference		Reference		Reference	
Moderately differentiated	1.573 (1.349-1.834)	<0.001	1.084 (0.928-1.267)	0.310	1.780 (1.466-2.162)	<0.001	1.097 (0.900-1.336)	0.358
Poorly/Undifferentiated	2.368 (2.031-2.761)	<0.001	1.245 (1.060-1.461)	0.007	3.122 (2.577-3.783)	<0.001	1.393 (1.141-1.700)	0.001
Unknown	1.216 (1.026-1.440)	0.024	0.873 (0.734-1.037)	0.121	1.325 (1.069-1.642)	0.010	0.898 (0.722-1.116)	0.332
Histology								
Adenocarcinoma	Reference		Reference		Reference		Reference	
Mucinous carcinoma	2.136 (1.574-2.899)	<0.001	1.792 (1.319-2.435)	<0.001	2.262 (1.602-3.194)	<0.001	1.796 (1.270-2.540)	0.001
Signet ring cell carcinoma	1.779 (1.531-2.068)	<0.001	1.191 (1.018-1.393)	0.029	1.960 (1.657-2.319)	<0.001	1.184 (0.994-1.410)	0.059
Age (years)								
Up to 49	Reference		Reference				Reference	
50-64	1.192 (0.943-1.505)	0.141	1.161 (0.918-1.467)	0.213	1.038 (0.803-1.343)	0.774	1.006 (0.776-1.303)	0.966
65-79	1.908 (1.521-2.394)	<0.001	1.659 (1.320-2.085)	<0.001	1.514 (1.180-1.943)	0.001	1.298 (1.009-1.670)	0.043
80+	4.358 (3.452-5.502)	<0.001	2.447 (1.929-3.106)	<0.001	3.669 (2.841-4.737)	<0.001	1.937 (1.491-2.518)	<0.001

ET, Endoscopic therapy; RT, Radiotherapy; LNM, lymph node metastasis; HR, Hazard ratio; 95% CI,95% confidence intervals; T1a,tumor invades the lamina propria or muscularis mucosa; T1b, tumor invades the submucosa; T1x, unknown T1a or T1b.

**American Indian/Alaska Native, Asian/Pacific Islander.*

increased risk of esophagogastric cancers is associated with the status of being unmarried and having a low level of education and a low income (24). But after PSM Cox proportional hazards regression revealed that marital status had no significant differences in OS and CSS. The associations require attention in terms of identifying high-risk individuals.

Diagnostic ER is considered as potentially curative and also has a more accurate evaluation of invasion depth than endoscopic ultrasonography (EUS) (25), which is a feasible and reasonable final step in all early-stage EGJ adenocarcinoma. Pathologic assessment on ER samples could assist further therapeutic strategies, which should simultaneously consider patient-related parameters. Moreover, a multidisciplinary team involving surgeons, medical oncologists, and endoscopists is necessary for clinical decision-making. For patients with older age or multiple comorbidities, a higher probability of leaving

TABLE 5 | Cox regression analysis of OS and CSS in patients with early-stage esophagogastric junction cancer after propensity score matching.

Characteristic	OS				CSS			
	Univariate analysis		Multivariate analysis		Univariate analysis		Multivariate analysis	
	HR (95% CI)	*P*	HR (95% CI)	*P*	HR (95% CI)	*P*	HR (95% CI)	*P*
Gender								
Female	Reference				Reference			
Male	1.029 (0.819-1.293)	0.807			1.031 (0.751-1.414)	0.851		
Race								
White	Reference				Reference			
Black	1.182 (0.667-2.098)	0.567			0.720 (0.268-1.934)	0.515		
Others*	0.901 (0.508-1.598)	0.722			0.693 (0.286-1.680)	0.417		
Tumor size (cm)								
<1	Reference		Reference		Reference		Reference	
1-2	1.369 (1.028-1.822)	0.031	1.115 (0.833-1.491)	0.465	1.360 (0.908-2.038)	0.136	1.046 (0.692-1.581)	0.831
2-3	1.685 (1.190-2.386)	0.003	1.159 (0.811-1.657)	0.418	2.029 (1.277-3.223)	0.003	1.324 (0.822-2.134)	0.248
3+	2.157 (1.507-3.087)	<0.001	1.489 (1.029-2.153)	0.035	2.658 (1.664-4.245)	<0.001	1.652 (1.016-2.687)	0.043
Not stated	1.318 (1.033-1.681)	0.026	1.085 (0.841-1.400)	0.529	1.385 (0.982-1.955)	0.063	1.126 (0.785-1.614)	0.520
Year of diagnosis								
2004-2006	Reference		Reference		Reference		Reference	
2007-2009	0.780 (0.614-0.990)	0.041	0.733 (0.575-0.933)	0.012	0.785 (0.561-1.099)	0.158	0.705 (0.502-0.992)	0.045
2010-2012	0.578 (0.443-0.755)	<0.001	0.564 (0.428-0.742)	<0.001	0.560 (0.389-0.806)	0.002	0.517 (0.355-0.752)	0.001
2013-2016	0.615 (0.459-0.823)	0.001	0.558 (0.412-0.756)	<0.001	0.560 (0.379-0.827)	0.004	0.476 (0.317-0.714)	<0.001
Marital status								
Married	Reference				Reference			
Single/widowed	1.219 (0.986-1.508)	0.068			1.226 (0.914-1.645)	0.174		
Other/unknown	0.849 (0.644-1.119)	0.245			0.852 (0.583-1.244)	0.406		
T stage								
T1a	Reference		Reference		Reference		Reference	
T1b	1.920 (1.567-2.351)	<0.001	1.494 (1.203-1.857)	<0.001	2.310 (1.755-3.041)	<0.001	1.705 (1.270-2.289)	<0.001
T1x	2.082 (1.618-2.680)	<0.001	1.784 (1.374-2.316)	<0.001	2.499 (1.778-3.512)	<0.001	2.087 (1.464-2.976)	<0.001
Treatment								
ES	Reference		Reference		Reference		Reference	
ET	1.599 (1.337-1.913)	<0.001	1.488 (1.240-1.786)	<0.001	1.229 (0.962-1.570)	0.099	1.112 (0.866-1.429)	0.405
Grade								
Well-differentiated	Reference		Reference		Reference		Reference	
Moderately differentiated	1.246 (0.941-1.649)	0.124	1.148 (0.875-1.506)	0.822	1.251 (0.851-1.839)	0.254	1.025 (0.693-1.514)	0.903
Poorly/Undifferentiated	1.668 (1.233-2.258)	0.001	1.196 (0.874-1.636)	0.264	1.937 (1.292-2.903)	0.001	1.323 (0.868-2.017)	0.193
Unknown	0.788 (0.584-1.063)	0.118	0.752 (0.554-1.021)	0.067	0.664 (0.432-1.021)	0.062	0.621 (0.401-0.962)	0.033
Histology								
Adenocarcinoma	Reference		Reference		Reference		Reference	
Mucinous carcinoma	1.855 (0.829-4.152)	0.133	1.116 (0.488-2.550)	0.795	3.031 (1.249-7.353)	0.014	1.810 (0.725-4.517)	0.204
Signet ring cell carcinoma	2.042 (1.304-3.199)	0.002	1.297 (0.808-2.082)	0.281	2.413 (1.379-4.220)	0.002	1.373 (0.759-2.486)	0.295
Age (years)								
Up to 49	Reference		Reference		Reference		Reference	
50-64	0.982 (0.526-1.834)	0.956	1.024 (0.547-1.916)	0.941	0.559 (0.283-1.105)	0.094	0.574 (0.289-1.141)	0.113
65-79	1.796 (0.982-3.286)	0.057	1.685 (0.918-3.095)	0.092	0.980 (0.514-1.868)	0.952	0.881 (0.459-1.692)	0.704
80+	4.969 (2.687-9.188)	<0.001	3.821 (2.051-7.118)	<0.001	3.078 (1.593-5.948)	0.001	2.158 (1.102-4.226)	0.025

ET, Endoscopic therapy; HR, Hazard ratio; 95% CI,95% confidence intervals; T1a,tumor invades the lamina propria or muscularis mucosa; T1b, tumor invades the submucosa; T1x, unknown T1a or T1b.

**American Indian/Alaska Native, Asian/Pacific Islander.*

positive LNs may be acceptable for a lower morbidity procedure. Conversely, aggressive surgical therapy should be considered among young patients even with low risks of LNM.

In this large population-based study, our findings are mainly based on real-world outcomes. To our knowledge, this is the first population-based study to describe the long-term survival of ET in comparison with surgery for early-stage EGJ adenocarcinoma. Nevertheless, certain limitations must be acknowledged, Firstly, relevant data on lymphovascular invasion, the deep distance of submucosal invasion, and macroscopic type are inaccessible in the SEER database, which are potential risk factors for LNM. The absence of these variables might affect the accurate assessment of LNM. Secondly, the applied models are simplified and only use available and accepted measures, which do not adequately account for all variables associated with subject outcomes. The lack of records of surgical complications in the SEER database affects results on the influence of complications and cancer survival. We excluded patients who died within one month after surgery to reduce the impact of surgical complications. Additionally, the lack of a comorbidity index may have an impact on assessing patients' choice of treatment modality, as older patients and those with a higher Comorbidity Index had lower odds of being treated with

TABLE 6 | Cox regression analysis of CSS in patients with T1a and T1b esophagogastric junction cancer after propensity score matching.

Characteristic	T1a				T1b			
	Univariate analysis		Multivariate analysis		Univariate analysis		Multivariate analysis	
	HR (95% CI)	*P*	HR (95% CI)	*P*	HR (95% CI)	*P*	HR (95% CI)	*P*
Gender								
Female	Reference				Reference			
Male	1.005 (0.640-1.579)	0.982			1.252 (0.706-2.219)	0.442		
Race								
White	Reference				Reference			
Black	Omitted				0.697 (0.097-5.011)	0.720		
Others*	1.310 (0.536-3.205)	0.554			Omitted			
Tumor size (cm)								
<1	Reference		Reference		Reference		Reference	
1-2	1.126 (0.642-1.975)	0.680	1.038 (0.589-1.829)	0.897	1.380 (0.693-2.748)	0.359	1.495 (0.721-3.100)	0.280
2-3	1.815 (0.912-3.612)	0.089	1.546 (0.767-3.115)	0.223	1.553 (0.733-3.292)	0.250	1.638 (0.754-3.559)	0.212
3+	2.167 (1.062-4.425)	0.034	2.184 (1.056-4.517)	0.035	2.133 (0.958-4.749)	0.064	1.503 (0.637-3.545)	0.352
Not stated	1.234 (0.792-1.921)	0.353	1.248 (0.788-1.976)	0.346	1.039 (0.510-2.119)	0.915	1.055 (0.498-2.233)	0.889
Year of diagnosis								
2004-2006	Reference		Reference		Reference			
2007-2009	0.781 (0.494-1.234)	0.290	0.835 (0.525-1.330)	0.448	1.208 (0.577-2.527)	0.617		
2010-2012	0.611 (0.369-1.011)	0.055	0.615 (0.363-1.042)	0.070	0.789 (0.373-1.670)	0.536		
2013-2016	0.458 (0.249-0.842)	0.012	0.449 (0.238-0.848)	0.014	0.948 (0.448-2.006)	0.888		
Marital status								
Married	Reference				Reference			
Single/widowed	1.171 (0.767-1.790)	0.465			1.446 (0.897-2.331)	0.130		
Other/unknown	0.916 (0.542-1.546)	0.741			0.798 (0.379-1.678)	0.551		
Treatment								
surgery	Reference		Reference		Reference		Reference	
ET	1.083 (0.764-1.536)	0.654	1.085 (0.760-1.550)	0.653	1.341 (0.877-2.049)	0.175	1.335 (0.856-2.083)	0.203
Grade								
Well-differentiated	Reference		Reference		Reference		Reference	
Moderately differentiated	1.059 (0.636-1.764)	0.824	0.972 (0.580-1.629)	0.915	1.479 (0.657-3.331)	0.344	1.246 (0.543-2.863)	0.604
Poorly/Undifferentiated	1.505 (0.848-2.669)	0.162	1.117 (0.614-2.031)	0.717	2.364 (1.043-5.357)	0.039	2.053 (0.882-4.776)	0.095
Unknown	0.627 (0.367-1.072)	0.088	0.536 (0.309-0.929)	0.026	1.909 (0.751-4.851)	0.175	1.936 (0.749-5.005)	0.173
Histology								
Adenocarcinoma	Reference		Reference		Reference		Reference	
Mucinous carcinoma	3.494 (0.863-14.140)	0.079	4.054 (0.989-16.618)	0.052	2.108 (0.517-8.601)	0.299	2.476 (0.587-10.455)	0.217
Signet ring cell carcinoma	2.826 (1.240-6.441)	0.013	1.876 (0.770-4.571)	0.166	1.115 (0.352-3.530)	0.853	0.619 (0.185-2.072)	0.437
Age (years)								
Up to 49	Reference		Reference		Reference		Reference	
50-64	0.858 (0.303-2.431)	0.773	0.801 (0.282-2.280)	0.678	0.199 (0.061-0.650)	0.007	0.209 (0.059-0.738)	0.015
65-79	1.270 (0.461-3.497)	0.644	1.050 (0.378-2.913)	0.926	0.422 (0.151-1.180)	0.100	0.460 (0.152-1.392)	0.169
80+	4.341 (1.537-12.257)	0.006	3.060 (1.061-8.827)	0.039	0.976 (0.343-2.780)	0.964	0.966 (0.316-2.955)	0.952

ET, Endoscopic therapy; RT, Radiotherapy; LNM, lymph node metastasis; HR, Hazard ratio; 95% CI,95% confidence intervals; T1a,tumor invades the lamina propria or muscularis mucosa; T1b, tumor invades the submucosa.

**American Indian/Alaska Native, Asian/Pacific Islander.*

surgery. Selection biases are unavoidable in the retrospective analysis. Therefore, to reduce bias as much as possible, we applied the PSM method to ensure that the clinical data between the ET group and the surgery group were consistent, such as age, gender, tumor size, etc. Finally, although PSM was further performed in this study, the results must be cautiously interpreted due to the fraction of unmatched patients.

CONCLUSION

This population-based study reveals that LNM risk is significantly increased in submucosal compared with intramucosal tumors. In subgroup analysis, patients with poorly-differentiated T1a cancers with a size of >3 cm had an increased LNM rate than those with T1b cancers without other high-risk factors. These data suggest disease heterogeneity among patients with early-stage EGJ adenocarcinoma, which must be identified to select the optimal resection strategy. Therefore, we believe that national guidelines for the management of early-stage EGJ adenocarcinoma should include all high risk features for LNM and stage-specific surgery therapy mortality. ET is thus a valid alternative to surgery for T1a tumors and well-differentiated T1b tumors with a tumor size of <3cm in early EGJ adenocarcinoma, especially for older patients. ET is a minimally invasive surgery

with less trauma and higher quality of life compared to traditional surgery.

DATA AVAILABILITY STATEMENT

The datasets presented in this study can be found in online repositories. The names of the repository/repositories and accession number(s) can be found below: The datasets analyzed in this study are collected from SEER repository (https://seer.cancer.gov/).

AUTHOR CONTRIBUTIONS

HY, Y-FW, and X-JC participated in the design of this project, interpretation of data, and drafting and critical revision of the article and provided final approval of the version to be submitted. HY and PC completed the data collection and analysis. All authors contributed to the article and approved the submitted version.

FUNDING

This study was supported by the Medical Scientific Research Foundation of Zhejiang Province, China (Grant No. 2021KY1010). Key Laboratory of Diagnosis and Treatment of Digestive System Tumors of Zhejiang Province (2019E10020), the Ningbo Clinical Research Center for Digestive System Tumors (Grant No. 2019A21003), and the HwaMei Research Foundation of Ningbo No.2 Hosptial, China (Grant No. 2020HMKY55). Health Young Technical Backbone Talents Foundation of Ningbo.

ACKNOWLEDGMENTS

The authors acknowledge the efforts of the Surveillance, Epidemiology, and End Results (SEER) Program tumor registries in the creation of the SEER database. The interpretation and reporting of these data are the sole responsibility of the authors.

REFERENCES

1. Buas MF, Vaughan TL. Epidemiology and Risk Factors for Gastroesophageal Junction Tumors: Understanding the Rising Incidence of This Disease. *Semin Radiat Oncol* (2013) 23:3–9. doi: 10.1016/j.semradonc.2012.09.008
2. Kauppila JH, Lagergren J. The Surgical Management of Esophago-Gastric Junctional Cancer. *Surg Oncol* (2016) 25:394–400. doi: 10.1016/j.suronc.2016.09.004
3. Derakhshan MH, Malekzadeh R, Watabe H, Yazdanbod A, Fyfe V, Kazemi A, et al. Combination of Gastric Atrophy, Reflux Symptoms and Histological Subtype Indicates Two Distinct Aetiologies of Gastric Cardia Cancer. *Gut* (2008) 57:298–305. doi: 10.1136/gut.2007.137364
4. Toyonaga T, Man-i M, East JE, Nishino E, Ono W, Hirooka T, et al. 1,635 Endoscopic Submucosal Dissection Cases in the Esophagus, Stomach, and Colorectum: Complication Rates and Long-Term Outcomes. *Surg Endosc* (2013) 27:1000–8. doi: 10.1007/s00464-012-2555-2
5. Kuwano H, Nishimura Y, Oyama T, Kato H, Kitagawa Y, Kusano M, et al. Guidelines for Diagnosis and Treatment of Carcinoma of the Esophagus April 2012 Edited by the Japan Esophageal Society. *Esophagus Off J Jpn Esophageal Soc* (2015) 12:1–30. doi: 10.1007/s10388-014-0465-1
6. Japanese Gastric Cancer Association. Japanese Gastric Cancer Treatment Guidelines 2018 (5th Edition). *Gastric Cancer Off J Int Gastric Cancer Assoc Jpn Gastric Cancer Assoc* (2020) 24:1–21. doi: 10.1007/s10120-020-01042-y
7. Wingo PA, Jamison PM, Hiatt RA, Weir HK, Gargiullo PM, Hutton M, et al. Building the Infrastructure for Nationwide Cancer Surveillance and Control–a Comparison Between the National Program of Cancer Registries (NPCR) and the Surveillance, Epidemiology, and End Results (SEER) Program (United States). *Cancer Causes Control CCC* (2003) 14:175–93. doi: 10.1023/A:1023002322935
8. Rice TW, Ishwaran H, Ferguson MK, Blackstone EH, Goldstraw P. Cancer of the Esophagus and Esophagogastric Junction: An Eighth Edition Staging Primer. *J Thorac Oncol Off Publ Int Assoc Study Lung Cancer* (2017) 12:36–42. doi: 10.1016/j.jtho.2016.10.016
9. Biondi A, D'Ugo D, Cananzi FC, Papa V, Borasi A, Sicoli F, et al. Does a Minimum Number of 16 Retrieved Nodes Affect Survival in Curatively Resected Gastric Cancer? *Eur J Surg Oncol J Eur Soc Surg Oncol Br Assoc Surg Oncol* (2015) 41:779–86. doi: 10.1016/j.ejso.2015.03.227
10. In H, Solsky I, Palis B, Langdon-Embry M, Ajani J, Sano T. Validation of the 8th Edition of the AJCC TNM Staging System for Gastric Cancer Using the National Cancer Database. *Ann Surg Oncol* (2017) 24:3683–91. doi: 10.1245/s10434-017-6078-x
11. Hasegawa S, Yoshikawa T, Aoyama T, Hayashi T, Yamada T, Tsuchida K, et al. Esophagus or Stomach? The Seventh TNM Classification for Siewert Type II/III Junctional Adenocarcinoma. *Ann Surg Oncol* (2013) 20:773–9. doi: 10.1245/s10434-012-2780-x
12. Ichihara S, Uedo N, Gotoda T. Considering the Esophagogastric Junction as a 'Zone'. *Dig Endosc Off J Jpn Gastroenterological Endosc Soc* (2017) 29(Suppl 2):3–10. doi: 10.1111/den.12792
13. Haverkamp L, Ruurda JP, van Leeuwen MS, Siersema PD, van Hillegersberg R. Systematic Review of the Surgical Strategies of Adenocarcinomas of the Gastroesophageal Junction. *Surg Oncol* (2014) 23:222–8. doi: 10.1016/j.suronc.2014.10.004
14. Yoshinaga S, Gotoda T, Kusano C, Oda I, Nakamura K, Takayanagi R. Clinical Impact of Endoscopic Submucosal Dissection for Superficial Adenocarcinoma Located at the Esophagogastric Junction. *Gastrointestinal Endosc* (2008) 67:202–9. doi: 10.1016/j.gie.2007.09.054
15. Gertler R, Stein HJ, Schuster T, Rondak IC, Höfler H, Feith M. Prevalence and Topography of Lymph Node Metastases in Early Esophageal and Gastric Cancer. *Ann Surg* (2014) 259:96–101. doi: 10.1097/SLA.0000000000000239
16. Stein HJ, Feith M, Mueller J, Werner M, Siewert JR. Limited Resection for Early Adenocarcinoma in Barrett's Esophagus. *Ann Surg* (2000) 232:733–42. doi: 10.1097/00000658-200012000-00002
17. Koufuji K, Shirouzu K, Aoyagi K, Yano S, Miyagi M, Imaizumi T, et al. Surgery and Clinicopathological Features of Gastric Adenocarcinoma Involving the Esophago-Gastric Junction. *Kurume Med J* (2005) 52:73–9. doi: 10.2739/kurumemedj.52.73
18. Zhu M, Cao B, Li X, Li P, Wen Z, Ji J, et al. Risk Factors and a Predictive Nomogram for Lymph Node Metastasis of Superficial Esophagogastric Junction Cancer. *J Gastroenterol Hepatol* (2020) 35(9):1524–31. doi: 10.1111/jgh.15004
19. Dubecz A, Kern M, Solymosi N, Schweigert M, Stein HJ. Predictors of Lymph Node Metastasis in Surgically Resected T1 Esophageal Cancer. *Ann Thorac Surg* (2015) 99:1879–85; discussion 1886. doi: 10.1016/j.athoracsur.2015.02.112
20. Wani S, Drahos J, Cook MB, Rastogi A, Bansal A, Yen R, et al. Comparison of Endoscopic Therapies and Surgical Resection in Patients With Early Esophageal Cancer: A Population-Based Study. *Gastrointestinal Endosc* (2014) 79:224–32.e221. doi: 10.1016/j.gie.2013.08.002
21. Njei B, McCarty TR, Birk JW. Trends in Esophageal Cancer Survival in United States Adults From 1973 to 2009: A SEER Database Analysis. *J Gastroenterol Hepatol* (2016) 31:1141–6. doi: 10.1111/jgh.13289
22. Ngamruengphong S, Wolfsen HC, Wallace MB. Survival of Patients With Superficial Esophageal Adenocarcinoma After Endoscopic Treatment vs Surgery. *Clin Gastroenterol Hepatol Off Clin Pract J Am Gastroenterological Assoc* (2013) 11:1424–9.e1422; quiz e1481. doi: 10.1016/j.cgh.2013.05.025
23. Pyo JH, Lee H, Min YW, Min BH, Lee JH, Kim KM, et al. Indication for Endoscopic Treatment Based on the Risk of Lymph Node Metastasis in Patients With Siewert Type II/III Early Gastric Cancer. *Gastric Cancer Off J Int Gastric Cancer Assoc Jpn Gastric Cancer Assoc* (2018) 21:672–9. doi: 10.1007/s10120-017-0789-3

24. Lagergren J, Andersson G, Talbäck M, Drefahl S, Bihagen E, Härkönen J, et al. Marital Status, Education, and Income in Relation to the Risk of Esophageal and Gastric Cancer by Histological Type and Site. *Cancer* (2016) 122:207–12. doi: 10.1002/cncr.29731
25. Pouw RE, Heldoorn N, Alvarez Herrero L, ten Kate FJ, Visser M, Busch OR, et al. Do We Still Need EUS in the Workup of Patients With Early Esophageal Neoplasia? A Retrospective Analysis of 131 Cases. *Gastrointestinal Endosc* (2011) 73:662–8. doi: 10.1016/j.gie.2010.10.046

Conflict of Interest: The authors declare that the research was conducted in the absence of any commercial or financial relationships that could be construed as a potential conflict of interest.

frontiers in Oncology

ORIGINAL RESEARCH
published: 20 December 2021
doi: 10.3389/fonc.2021.771863

Comparative Analysis of Two Surgical Treatment Options for Giant Cell Tumor of the Proximal Femur: Extended Curettage and Segmental Resection

*Yuhao Yuan[1], Qing Liu[1], Yupeng Liu[1], Ziyi Wu[1], Wei Zhong[1], Hongbo He[1] and Wei Luo[1,2]**

[1]Department of Orthopaedics, Xiangya Hospital, Central South University, Changsha, China, [2]National Clinical Research Center for Geriatric Disorders, Xiangya Hospital, Changsha, China

OPEN ACCESS

Edited by:
Patrick J. Schuler,
Ulm University Medical Center,
Germany

Reviewed by:
Amin Karimi,
Shahid Beheshti University of Medical Sciences, Iran
Ismail Tawfeek Badr,
University of Menoufia, Egypt
José Manuel Pinto Silva Casanova,
University of Coimbra, Portugal
Khodamorad Jamshidi,
Iran University of Medical Sciences, Iran

***Correspondence:**
Wei Luo
luowei0928@126.com

Specialty section:
This article was submitted to Surgical Oncology, a section of the journal Frontiers in Oncology

Received: 07 September 2021
Accepted: 22 November 2021
Published: 20 December 2021

Citation:
Yuan Y, Liu Q, Liu Y, Wu Z, Zhong W, He H and Luo W (2021) Comparative Analysis of Two Surgical Treatment Options for Giant Cell Tumor of the Proximal Femur: Extended Curettage and Segmental Resection. Front. Oncol. 11:771863. doi: 10.3389/fonc.2021.771863

Aim: As a locally destructive intermediate bone tumor with low incidence, high recurrence rate, and difficulty in reconstruction, giant cell tumor of bone (GCTB) in the proximal femur has no unified surgical treatment standard. This study aimed to compare the differences in local recurrence, reconstruction durability, and postoperative function after treatment with either extended curettage (EC) or segmental resection (SR) for GCTB in the proximal femur so as to provide constructive suggestions for the rational selection of EC or SR operation scheme.

Patients and Methods: 29 patients (15 men and 14 women) were included in this retrospective study, with a mean age of 32.1 years. According to the division method of proximal femur of International Society Of Limb Salvage (ISOLS), there was 1 case in the H1 area, 17 cases in the H2 area, 10 cases in the H1+H2 area, and 1 case in the H1+H2+H3 area. Among them were 11 cases of Campanacci grade II GCTB, 18 cases of Campanacci grade III GCTB, and 7 cases with pathological fractures. All patients underwent either EC or SR surgery. The Musculoskeletal Tumor Society (MSTS) score was used for patient evaluation. The operation effectiveness was analyzed according to the Mankin evaluation standard. Regular follow-up was performed to evaluate the recurrence rate, limb function, and long-term complications of the two surgical methods.

Results: All patients were followed up for a mean of 60.4 months. Local recurrence occurred in one of 19 patients treated with EC (5.3%) and one of 10 patients treated with SR (10%). The MSTS score of lower limb function in patients in the EC group was better compared to patients in the SR group (P = 0.002). Complications occurred in 2 cases (10.5%) and 5 cases (50%) in the EC group (osteoarthritis, osteonecrosis) and SR group (joint stiffness, infection, prosthesis loosening), respectively, with significant differences between the two groups (P = 0.03). The operation effectiveness was analyzed according to the Mankin evaluation standard. The EC group showed an optimal rate of 94.7% (18/19) as opposed to 80% (8/10) in the SR group.

Conclusions: For GCTB in the proximal femur, when the tumor does not extensively involves the surrounding soft tissues, the articular surface was not damaged, and there is no pathological fracture with apparent displacement, EC surgery should be fully considered.

Keywords: proximal femur, giant cell tumor of bone, extended curettage, segment resection, surgical options

INTRODUCTION

Giant cell tumor of bone (GCTB) is a common primary bone tumor and possesses characteristics of unpredictable biological behavior, severe bone erosion, and a high recurrence rate (1). Studies have shown that GCTB accounts for about 20% of all benign bone tumors, with malignant transformation occurring in about 10% of GCTB and lung metastasis occurring in 1% to 4% of patients. The age of onset is mainly between 20 and 40 years old, women are more common (2). In addition, it is defined as a locally destructive intermediate bone tumor due to its strong bone and soft tissue invasiveness. The epiphyseal regions of the distal femur and proximal tibia are the most common sites, accounting for about 60% - 70% of GCTB in all body parts (3). However, the prognosis varies according to the anatomical site of GCTB. Hence the study of GCTB in different anatomical parts is a must (2, 3).

The incidence rate of GCTB in the proximal femur is relatively low, accounting for only about 5.5% of GCTB. Still, it has the features of a high recurrence rate and poor prognosis (4). The lesions are mainly located in the femoral neck and intertrochanteric. As this region is an essential mechanical conduction pathway of the human body, the probability of pathological fracture is higher than that of GCTB around the knee joint. Although fewer cases can extend to the joint cavity, they can penetrate the subchondral bone and seriously affect the function of the hip joint (5). Besides, considering the blood supply, osteonecrosis is more likely to occur in the progression and treatment of proximal femoral GCTB. Furthermore, previous studies have identified that the postoperative local recurrence is more frequent with a high complication rate of proximal femoral GCTB (6–8). These factors lead to the tortuous dilemma in the treatment of proximal femoral GCTB. The aim of our treatment of proximal femoral GCTB at this stage is primarily to completely remove the lesions, reduce the recurrence rate, restore the flatness of the joint surface and prevent complications. These will help restore the normal biological function of the hip joint to the greatest extent and achieve a satisfactory survival prognosis. Therefore, the treatment of proximal femoral GCTB is more challenging. At present, there are few literature reports on proximal femoral GCTB, and there is no unified treatment principle (9). The choice of surgical methods is also controversial, which mainly include extended curettage (EC) and bone cement filling, segmental resection (SR), and tumor hip prosthesis reconstruction (10, 11). Although both treatments can achieve satisfactory results, the prognosis is inconsistent in the reviews, and each has its advantages and drawbacks. The former can preserve the articular surface, but secondary osteoarthritis, osteonecrosis, and local recurrence (12) are the main downsides. Although the latter shows low local recurrence rates, it comes with limitations such as limited prosthesis life, revision, infection, and poor joint function (13), especially for young patients.

Here in, we retrospectively analyzed cases of proximal femoral GCTB with complete clinical data through a single center. This study aims to study the clinical efficacy of EC and SR on proximal femoral GCTB and analyze the differences between the two surgical methods in terms of recurrence rate, functional reconstruction, postoperative complications, etc. The aim is to provide a theoretical basis for standardizing the treatment scheme and prospective research.

Abbreviations: EC, extended curettage; SR, segmental resection; GCTB, giant cell tumor of the bone; ISOLS, International Society Of Limb Salvage; MSTS, musculoskeletal tumor society; CT, computed tomography; MRI, magnetic resonance imaging; DHS, dynamic hip screw.

PATIENTS AND METHODS

Patients

From February 2010 to June 2018, 37 consecutive patients with a diagnosis of GCTB of the proximal femoral were treated at the Xiangya Hospital Bone Tumor Center. In this retrospective study, the inclusion criteria were: (1) the lesion was located in the proximal femur and confirmed as GCTB by histopathological diagnosis; (2) GCTB patients who were initially treated in the bone tumor treatment center of our hospital and undergone a primary operation; (3) and postoperative follow-up of more than 24 months with integrated data. The exclusion criteria were: (1) Presence of primary or secondary malignant giant cell tumor of bone (once the preoperative imaging data show that the tumor may deteriorate, we would take preoperative puncture biopsy to determine the diagnosis); (2) patients hospitalized for local recurrence or complications after treatment in other hospitals. According to the above criteria, among the 37 patients, 2 patients developed malignant changes, 4 were lost to follow-up, and 2 were admitted to our department due to postoperative complications after treatment in other hospitals. Finally, a total of 29 patients were included in this study. The localization of the lesion was performed using the International Society of Limb Salvage (ISOLS) zoning method: the tumor located in the femoral head was identified as the H1 zone, those between the femoral head and neck junction and the distal plane of the lesser trochanter as the H2 zone (**Figure 1**), and those in the distal plane of the lesser trochanter as the H3 zone (14). In addition, preoperative X-ray, computed tomography(CT), and magnetic resonance imaging(MRI) were used to evaluate the scope of tumor invasion, record whether pathological fracture and

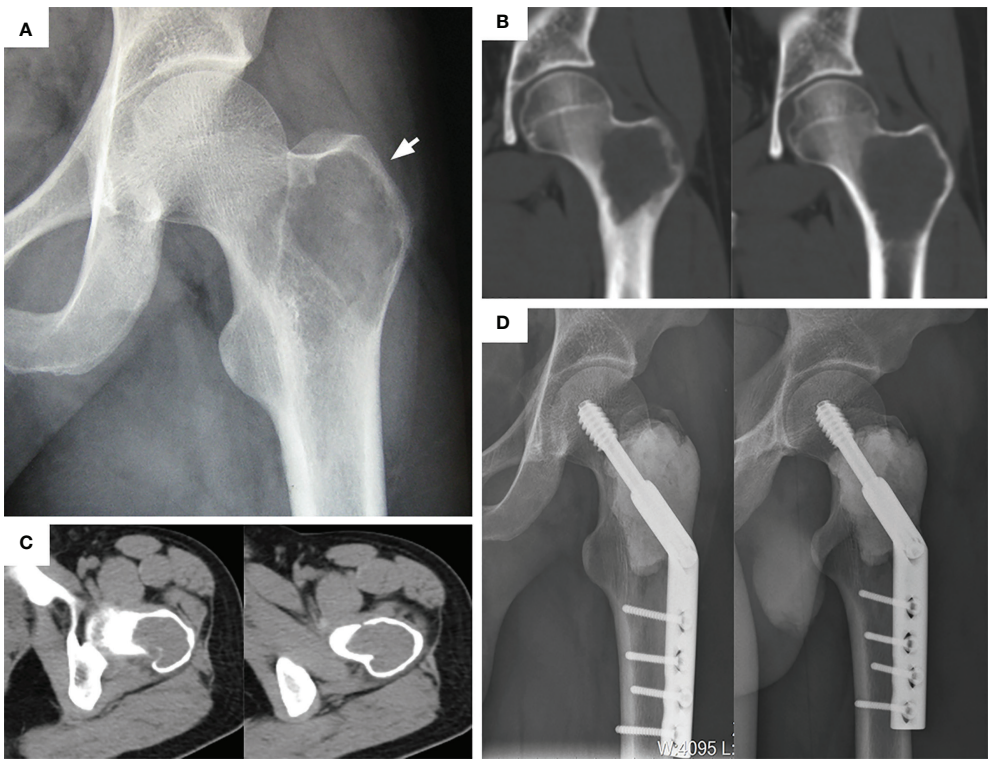

FIGURE 1 | Typical preoperative and postoperative manifestations of EC for H2 type GCTB of proximal femur. **(A)** Apparent osteolytic lesions can be seen in the greater trochanter (arrow). **(B)** A coronal plane CT scan showed that the tumor invaded the femoral neck and intertrochanteric space. **(C)** CT transverse section showed that the bone cortex around the lesion was thin but not completely penetrated. **(D)** After extended curettage, allogeneic bone and bone cement filling, and DHS plate fixation. The anteroposterior and lateral radiographs was rechecked at 29 months.

displacement were present, and Campanacci imaging grade was used to evaluate its performance (15). All the above patients and their guardians have signed informed consent. This study has been approved by the Ethics Committee of Xiangya Hospital of Central South University.

Surgical Technique

The following procedure was used: for EC operation, a longitudinal incision was taken at the lateral side of the proximal thigh, with the tensor fascia lata and lateral femoral muscle membrane cut. This fully exposes the lesion (**Figure 2A**), and a bone drill was used to drill holes along the periphery of the fenestration at the proximal femur. To prevent splitting fractures, the fenestration should be sufficiently large to remove the tumor tissue completely. Curettes of different sizes (**Figure 2B**) were used, and the surrounding bone ridge was cleaned with a high-speed grinding drill (**Figure 2C**). The cavity wall was cauterized with a high-frequency electric knife. The tumor cavity was flushed with a high-pressure sterilization water gun (**Figure 2D**). A 10% Iodine tincture was applied meticulously using a surgical cotton ball and left for at least 1 minute (**Figures 2E, F**) to eliminate residual tumor cells. The surface of subchondral bone was filled with allogeneic bone (**Figure 2G**), then the main nail was implanted, and the remaining bone defect was filled with bone cement. It is worth noting that the allogeneic bone was filled below the subchondral bone with a thickness of at least 1 cm. Finally, with the assistance of a C-arm machine, the dynamic hip screw (DHS) steel plate was accurately inserted (**Figure 2H**), washed with normal saline, and the wound was closed. The procedure of SR operation was as follows: The posterolateral approach of the hip was used, the tumor boundary was fully exposed, and the soft tissue within 1 cm outside the tumor capsule and bony tissue within 2~3cm were removed entirely to achieve marginal resection. Healthy soft tissues were retained during the resection process, especially the lateral femoral muscle, to cover the prosthesis. A distal osteotomy was performed 2~3 cm away from the tumor. The anterior soft tissue was separated with dislocation of the femoral head while protecting the sciatic nerve, and the tumor segment was wholly removed. Measure the bone length of the excised segment, reconcile the bone cement, and a customized femoral prosthesis was inserted. The intercondylar connecting plane and the thick line of the femur were used as a reference to control the rotation of the prosthesis so that the femoral neck was tilted forward by 15°.

Patients in the EC group avoided weight-bearing for 2 weeks after the surgery and gradually transitioned from non-weight, semi-weight bearing to full-weight bearing with the support of crutches. Patients in the SR group began non-weight-bearing hip flexion and extension in bed 3 days after the surgery, semi-weight

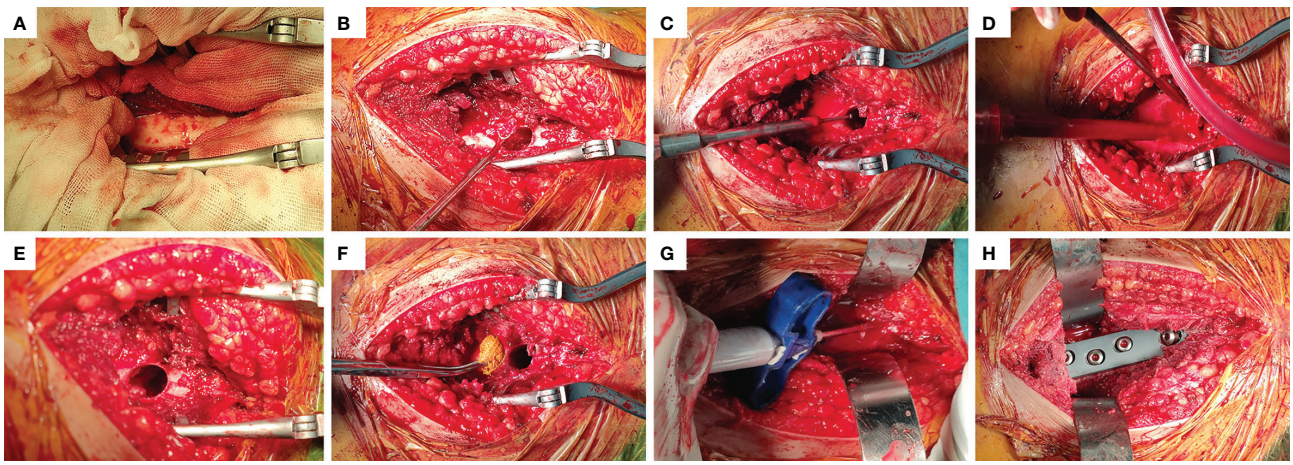

FIGURE 2 | Main steps of EC surgery. **(A)** Fenestration was performed in the lateral position near the lesion. **(B)** Complete removal of the tumor tissue visible with curettes of different sizes. **(C)** The bone ridge in the tumor cavity was removed with a high-speed grinding drill. **(D)** the tumor cavity was flushed with a high-pressure sterilization water gun. **(E, F)** The cavity wall was wiped with a cotton ball soaked with 10% Iodine tincture. **(G)** Allogeneic bone was implanted into the subchondral bone with a thickness of at least 1cm, and the rest was filled with bone cement. **(H)** Driving DHS steel plate to stabilize mechanical stress.

bearing and hip function exercises began 1-week post-surgery, semi squatting was practiced with the aid of crutches 3 weeks after surgery, and achieved normal life function score within 3 months.

Follow-Up and Evaluation

The first reexamination was started in the first month after surgery, and follow-ups were conducted every 3 months in the first year after surgery, every 6 months in the second year, and then yearly, largely as outpatient follow-ups. The follow-up examinations included local X-rays, CT or MRI, and other routine auxiliary examinations. For those with lung metastasis before operation, we usually recheck chest CT every three months after operation. For those without lung metastasis before operation, we usually recheck every six months after operation. In addition, the functional status of the hip joint on the affected side was thoroughly checked with the aim to assess the postoperative tumor prognosis, functional prognosis, and complications. The evaluation methods were as follows: Kellgren-Lawrence (K-L) grade (16) was used to evaluate the severity of osteoarthritis, Musculoskeletal Tumor Society (MSTS) score (17) was used to evaluate the functional changes, Ficat classification (18) was used to monitor the status of femoral head necrosis, and Mankin evaluation standard (19) was used to evaluate the surgical efficacy. In addition, infection, prosthesis loosening, immune rejection, fracture, and recurrence were recorded, and the latest follow-up was to be taken as the final recorded.

Statistical Analysis

SPSS version 20 (SPSS Inc., Chicago, IL, USA) was used to analyze the collected data, determine the relationship between different variables, and compare the therapeutic effects and prognostic outcomes of the two operations. The quantitative data were expressed as mean ± standard deviation, and conform to normally distributed. The difference of mean between the two groups was analyzed by independent sample t-test. Chi-square test or Fisher's exact test were used to analyze the qualitative data expressed in frequency. $P < 0.05$ was deemed as statistically significant.

RESULTS

According to the original data of patients (**Table 1**), there were 19 patients (11 men and 8 women) in the EC group, with an average age of 32.3 years (range, 19-52). This group included 10 cases of Campanacci grade II and 9 cases of Campanacci grade III. 12 cases were located in the H2 area (**Figure 1**), 6 cases in the H1 + H2 area (**Figure 3**), 1 case in H1 + H2 + H3 area (**Figure 4**), and 2 cases had pathological fractures before the procedure. On the other hand, there were 10 patients (4 men and 6 women) in the SR group, with an average age of 31.8 years (range, 22-49). This group included 1 case of Campanacci grade II, 9 cases of Campanacci grade III. 1 case was located in the H1 area, 5 cases in the H2 area, 4 cases in the H1 + H2 area, and 8 cases had pathological fractures before the procedure. Besides, in all patients, no tumor cells were found in the adjacent tissues selected during the operation.

Oncology Prognosis

In this study, the average follow-up time of the EC group was 57.5 months (range, 26-137). Among the 19 patients, 1 patient (5.3%) developed local soft-tissue recurrence 17 months after surgery: this patient had a pathological fracture without apparent displacement before surgery and was treated with expanded curettage in consideration of the patient's young age. In the second surgery, local resection was carried out, and the healing and recovery were fair. The follow-up results were satisfactory

TABLE 1 | Demographic and clinical follow-up data of patientBC, bone cement; AB, allogeneic bone; EC, extended curettage; SR, segmental resection; MSTS, musculoskeletal tumor society.

Patients Number/ Gender	Age/Location	Filler Materials	Disease Course (Month)	Therapeutic Modalities	Follow-up (Month)	Campanacci Grade	Pathological Fracture	Post-op MSTS Score	Post-Op recurrence	Complications
1/F	40/H1+2	BC +AB	9	EC	119	II	N	25	N	osteoarthritis
2/M	24/H2	BC	6	SR	86	II	Y	28	N	N
3/M	31/H1+2+3	BC+AB	12	EC	74	II	N	30	N	N
4/M	49/H1+2	BC	8	SR	52	III	Y	22	N	joint stiffness
5/F	29/H2	BC+AB	15	EC	91	III	Y	27	Y	N
6/M	25/H1+2	BC	18	SR	46	III	N	28	N	N
7/F	48/H2	BC	11	SR	61	III	Y	23	N	infection
8/F	41/H2	AB	17	EC	37	II	N	29	N	N
9/M	39/H1+2	BC+AB	18	EC	137	III	N	27	N	N
10/M	52/H2	BC+AB	5	EC	44	III	N	28	N	N
11/F	22/H1	BC	10	SR	121	III	N	21	N	Prosthesis loosening
12/M	27/H2	AB	6	EC	26	II	N	29	N	N
13/M	19/H2	AB	15	EC	57	II	Y	27	N	N
14/F	30/H1+2	BC	21	SR	65	III	Y	26	N	N
15/F	34/H2	BC	11	SR	40	III	Y	25	N	N
16/F	36/H2	AB	14	EC	41	II	N	27	N	N
17/F	24/H2	BC	17	SR	125	III	Y	21	Y	joint stiffness
18/M	33/H2	BC+AB	20	EC	28	III	N	30	N	N
19/F	21/H2	AB	7	EC	36	II	N	29	N	N
20/M	32/H1+2	BC	13	SR	27	III	Y	27	N	N
21/M	27/H2	BC+AB	16	EC	44	III	N	28	N	N
22/F	30/H2	BC	9	SR	36	III	Y	26	N	joint stiffness
23/M	38/H1+2	BC+AB	7	EC	50	III	N	28	N	N
24/M	31/H1+2	BC+AB	10	EC	31	III	N	29	N	N
25/F	28/H2	AB	19	EC	38	II	N	28	N	N
26/F	40/H2	AB	18	EC	47	II	N	26	N	N
27/M	37/H1+2	BC+AB	6	EC	79	III	N	24	N	osteonecrosis
28/F	24/H1+2	BC+AB	15	EC	50	III	N	29	N	N
29/M	20/H2	AB	17	EC	63	II	N	27	N	N

BC, bone cement; AB, allogeneic bone; EC, extended curettage; SR, segmental resection; MSTS, musculoskeletal tumor society.

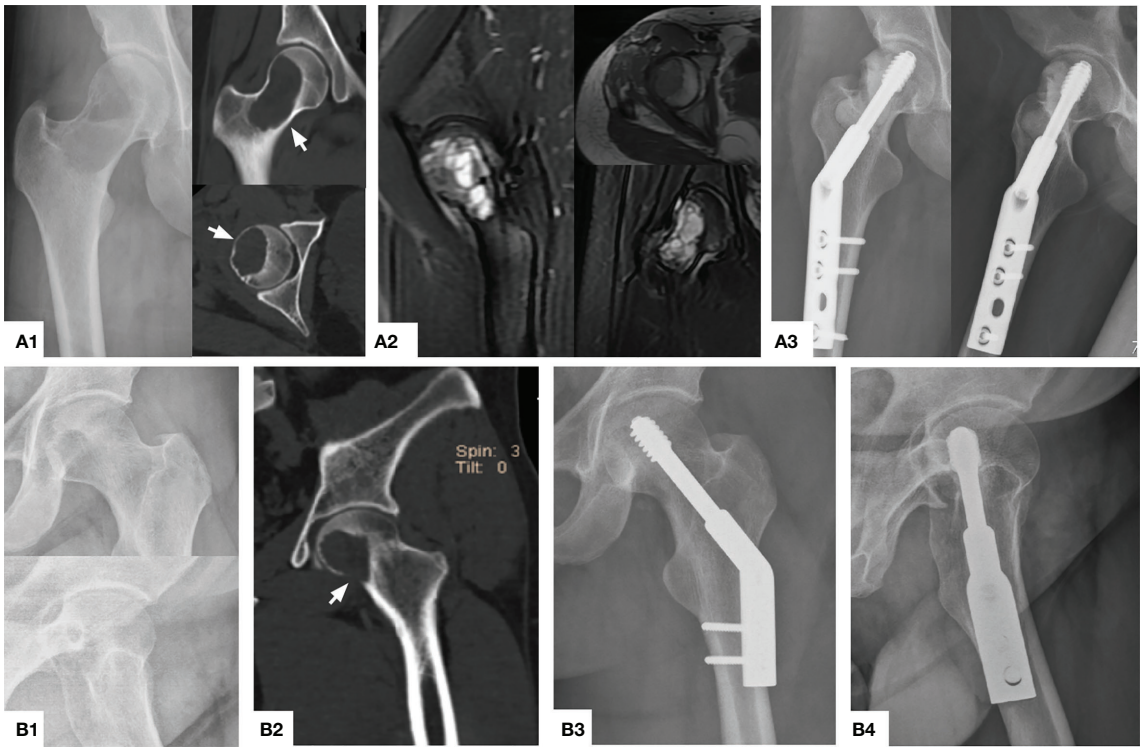

FIGURE 3 | Typical preoperative and postoperative manifestations of EC for H1+H2 type GCTB of proximal femur. **(A1)** A 40 year female patient with osteolytic changes occurred in the whole femoral neck extending upwards to the femoral head (arrow). **(A2)** MRI showed that most of the lesions were medium to high-intensity signals without the involvement of the surrounding soft tissue. **(A3)** The X-ray showed that the bone graft was satisfactory and the internal fixation was firm 26 months after operation. **(B1, B2)** A 31 year male patient with obvious quasi-circular transparent area can be seen under the femoral head, accumulating down the femoral neck, and partial perforation of the bone cortex can be seen (arrow). **(B3, B4)** The bone healed satisfactorily and effective internal fixation 32 months after operation.

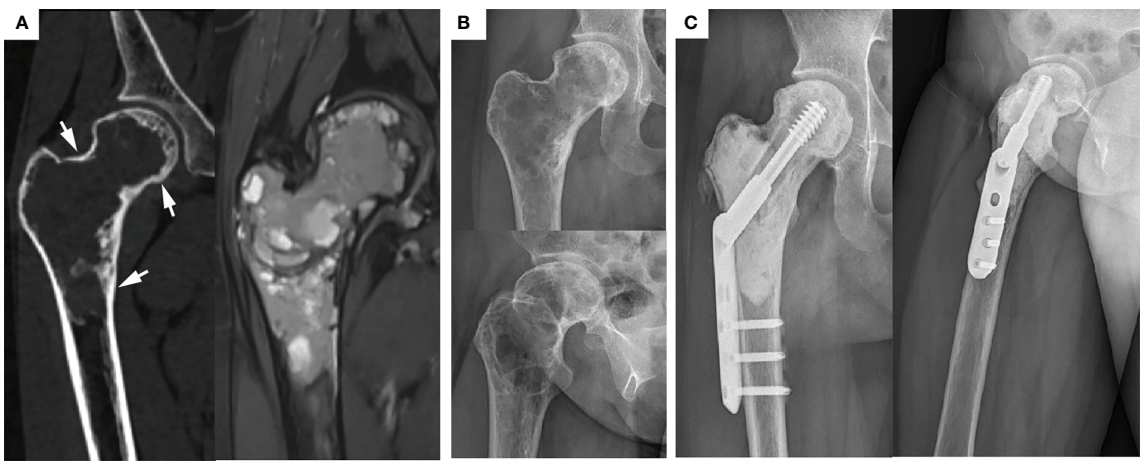

FIGURE 4 | Typical preoperative and postoperative manifestations of EC for H1+H2+H3 type GCTB of proximal femur. **(A)** Preoperative CT and MRI showed that the femoral head, femoral neck, and subtrochanteric were invaded, but the lesions were still wrapped in the bone cortex (arrow). **(B)** Preoperative X-ray showed typical "soap bubble-like" changes. **(C)** Due to the extensive involvement of the lesion and the significant reduction of bone strength, the allogeneic fibula was placed in parallel above DHS and achieved a desirable prognosis 3 years after operation.

after 74 months. Another case had lung metastasis before surgery, but there were no secondaries after resection of pulmonary nodules under endoscopy, and tumor-free survival was achieved.

The average follow-up time of the SR group was 65.9 months (range, 27-125). Of the 10 patients, 1 patient (10%) developed local recurrence of the distal part of the prosthesis and was located in the proximal femur, 2 years after surgery. This was confirmed by pathological biopsy as GCTB. Therefore, tumor segment resection and artificial prosthesis construction were performed again. There was no recurrence and metastasis after 8 years of follow-up. Unfortunately, this patient suffered from local hip joint functional impairment due to two major invasive operations. In addition, there were no lung metastases in this group of patients before or after surgery.

In general, only 1 patient (5.3%, 10%) in both groups had a relapse, and the recurrence rate was not statistically different (P=1.000). Besides, results of the univariate analysis showed no significant correlation between gender, pathological fractures, surgical methods, lesion locations, Campanacci grades, and the recurrence of proximal femur GCTB (**Table 2**).

Function and Treatment Evaluation

The MSTS scoring system of bone and soft tissue tumors was used as a reference for postoperative functional evaluation. The EC group had an average score of 27.6 (range, 24-30), while the SR group had an average score of 24.7 (range, 21-28). Results of the statistical analysis identified that the EC group obtained better postoperative functional recovery than the SR group (P = 0.002). In addition, according to the Mankin evaluation standard, the surgical effect was comprehensively evaluated, and the excellent and good rates were calculated. In the EC group, 17 cases were rated as excellent, 1 was rated as good, and 1 was poor. In contrast, in the SR group, 8 cases were rated as excellent, and 2 were rated as poor; The overall excellent and good rates of the two groups were compared (EC group, 94.7%; SR group, 80%), EC group was slightly higher (P = 0.560) (**Table 2**).

Complications

Among the 19 patients in the EC group, 1 patient developed hip arthritis (K-L grade 2) at the 102 month of postoperative follow-up but with no apparent pain and joint deformities, currently under conservative treatment. Another patient developed necrosis of the femoral head (Ficat stage I). Although the articular surface was not involved before the operation, the tumor invaded the subchondral bone of the femoral head in a wide range. Therefore, the local blood supply under the femoral head might have been affected during the extended curettage. Non-steroidal anti-inflammatory drugs and drugs to improve local microcirculation (prostaglandin E1) were temporarily given, the course of prostaglandin E1 was 3 months, 5ug/day, 14 days/month. In contrast, 3 patients developed varying degrees of joint stiffness in the SR group, and satisfactory results were obtained after standardized functional rehabilitation training. In addition, 1 patient suffered from a peri-prosthetic delayed infection at 5 months postoperatively, which was well-controlled after debridement, lavage, and drainage. Another patient suffered from a slight loosening of the prosthesis, but

TABLE 2 | Data statistics and analysis of patients.

Variable	EC group (n = 19)	SR group (n = 10)	P-value
Mean age, (sd)	32.3 ± 8.5	31.8 ± 9.6	
Gender, n (%)			
M	11	4	
F	8	6	
Campanacci Grade, n (%)			
II	10	1	
III	9	9	
location			
H1	0	1	
H2	12	5	
H1+2	6	4	
H1+2+3	1	0	
Pathological fracture, n (%)	2	8	<0.0001
Disease course(month)	12.9 ± 5.0	12.4 ± 4.8	
Duration of follow-up (month)	57.5 ± 30.4	65.9 ± 34.4	0.779
Local recurrence, n (%)	1 (5.3%)	`1 (10%)	1.000
Post-op MSTS score	27.6± 1.6	24.7± 2.8	0.002
Complication, n (%)			
osteoarthritis	1	0	
joint stiffness	0	3	
infection	0	1	
osteonecrosis	1	0	
Prosthesis loosening	0	1	
total	2 (10.5%)	5 (50%)	0.03
Reoperation, n (%)	1 (5.3%)	2 (20%)	
Excellent and good rate	18 (94.7%)	8 (80%)	0.560

EC, extended curettage; SR, segmental resection; MSTS, musculoskeletal tumor society.

this did not affect the routine work and life of the patient. Due to financial reasons, the patient refused active treatment and continued with regular follow-up. Overall, the incidence of complications in the SR group (50%) was higher than that in the EC group (10.5%), the comparison being statistically significant (P = 0.03) (**Table 2**).

DISCUSSION

Proximal femoral GCTB, as an intermediate tumor with low incidence, local invasiveness, and strong bone destructiveness, can easily cause puncture of the cortical bone and pathological fractures (20). With the development of surgical technology and the improvement of adjuvant therapy, open surgery is the most effective treatment for most patients with GCTB. Extended curettage and segmental tumor resection are often used in clinical practice (10, 11). Still, even in the most commonly seen cases of GCTB of the knee joint, when combined with pathological fractures or Campanacci grade III, the choice of the two surgical methods remains controversial (20, 21). There are even fewer systematic studies for GCTB of the proximal femur to clarify the reference criteria for surgical selection.

In the past, due to the insufficient resection edge of the tumor, the recurrence rate of curettage and bone grafting was as high as 40%-60% (2, 22). Now, with the continuous improvement of the understanding of the invasiveness of GCTB, some scholars put forward the concept of extended curettage, using high-speed grinding and drilling to remove the invaded bone in the lesions. Pulse washing and application of chemical agents (phenol, alcohol, Iodine tincture, or zinc chloride) were used to further treat the tumor cavity to reduce postoperative recurrence rate (23, 24). Iodine tincture with a concentration of 10%, which can denature the cell membrane of tumor cells and induce coagulative necrosis. It has slight irritation to the solid substance of bone, so it plays an ideal role as a local tumor killer. In this study, after high-speed drilling, electric knife cauterization, pulse sterilized water, and iodophor smearing, the recurrence rate (5.3%) was effectively controlled. It was slightly lower than the extensive data research of our department (7.2%) (3) and significantly better than other single-center retrospective studies (25, 26). Moreover, the commonly used reconstruction materials after GCTB extended curettage include autologous bone, allogeneic bone, or bone cement (27, 28). Bone cement with good mechanical stress was used to fill the tumor cavity's primary body reconstruction. Furthermore, bone cement can dissipate a lot of heat during solidification and physically inactivate the residual tumor cells around the tumor cavity. However, some studies have reported that using bone cement only to fill the expanded bone defect after the scraping promotes thermal injury of articular cartilage and non-fusion of the cement-subchondral bone interface (29). Radev BR et al. (30) recommend allogeneic bone transplantation (at least 3mm thick) at the subchondral bone to avoid this complication. This surgical technique also coincides with our study: when reconstructing bone defects, the subchondral bone was first filled with allogeneic bone, usually 10mm in thickness, and soaked with hydrogen peroxide before use, to remove its immunogenicity. Finally, bone cement is supplemented. Only 1 case in the EC group developed hip arthritis without surgery and obtained a satisfactory prognosis through the above multi-dimensional treatment methods.

Enlarged curettage of proximal femoral GCTB increases the risk of pathological fracture of the femoral neck. Errani C (31) and Lun D et al. (32) believe that the maximum diameter of the lesion shown by imaging exceeds 50% of the femoral neck, and the mechanical strength may be damaged, the bone cortex is involved in an extensive range, and may be further damaged during tumor curettage, resulting in pathological fractures. In the above cases, preventive internal fixation is required. In this group, 17 patients were treated with prophylactic DHS internal fixation, 2 patients with pathological fractures were reconstructed directly with DHS, and postoperative fractures were not observed. The trabecular bone pores at the proximal tuberosity of the femur are larger, and the tumor invasion may be more extensive, which indicates a more thorough removal. However, the bone of the femoral calcar is dense, which significantly impacts the mechanical strength of the proximal femur after destruction, this requires more attention during reconstruction. For proximal femoral GCTB, the tumor is first removed while preserving the joint, mechanical strength is then restored. If these conditions can be met at the same time, EC surgery should be chosen.

SR is a surgical method of segmental resection of the tumor, mega prosthesis implantation, and reconstruction. The indications for SR in this study include pathological fractures with evident displacement or Campanacci grade III proximal femoral GCTB while disrupting the integrity of the articular surface of the femoral head (**Figure 5**). SR is recommended for its excellent tumor prognosis. Van der Heijden L et al. (33) reported that for GCTB with pathological fractures, the local recurrence rate in SR was significantly lower than that of EC. Hindiskere S. et al. (34) and Klenke FM et al. (35) summarized multi-institutional retrospective studies, according to their experience, consider that SR has unique advantages in controlling the local recurrence rate of GCTB, SR is suitable for cases with a massive invasion of surrounding soft tissue. Interestingly, Balke M et al. (36) found that SR remains a wise choice for recurrent or worsening GCTB since it can effectively control the local recurrence rate. Therefore, SR is still a valuable treatment for high-grade and highly aggressive GCTB of the proximal femur. However, with advanced surgical techniques and treatment possibilities, preservation of joint function is preferred. The complications of SR, such as decreased limb functions, postoperative infection, long-term prosthesis loosening, and sinking, cannot be overlooked. Besides, it destroys the original joint structure while creating a large surgical wound and is associated with more intraoperative and postoperative bleeding, which hamper the target of optimal functional prognosis.

It was reported that aseptic loosening and prosthesis infection are the main reasons for the failure of prosthesis reconstruction after proximal femoral tumor (37). Xu G et al. (38) performed SR plus custom-made prosthesis reconstruction on 19 patients with

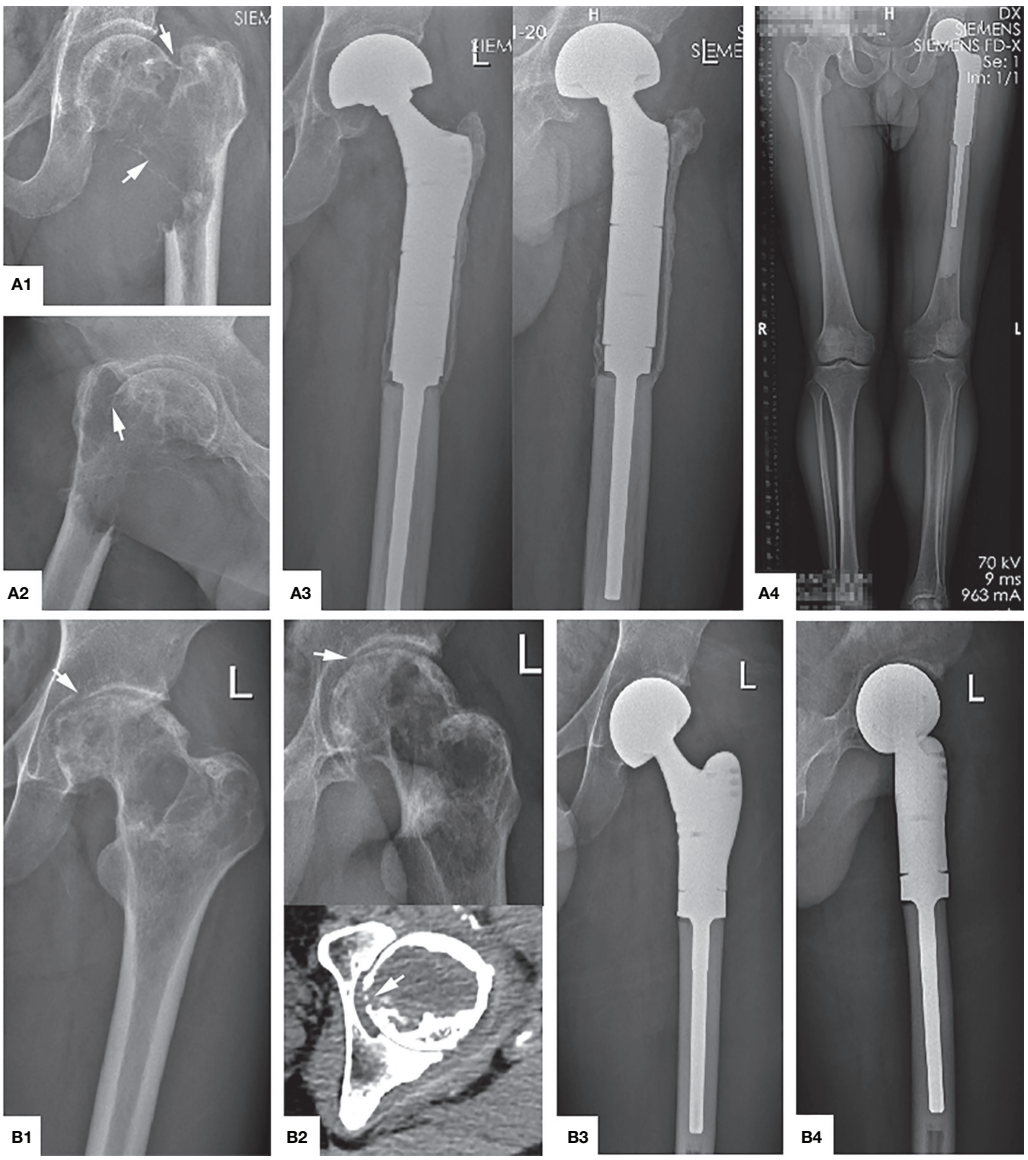

FIGURE 5 | Main indications and typical preoperative and postoperative manifestations of SR. **(A1, A2)** The tumor has completely eroded the proximal femur, and a significantly displaced pathological fracture has occurred (arrow), which is Campanacci grade III. **(A3, A4)** Anteroposterior, lateral, and full-length of both lower limbs radiographs showed that the position of the prosthesis was adequate, there was no transparent band around, and the force line was normal 4 years after operation. **(B1)** The femoral head is compressed to flat due to osteolysis destruction (arrow). **(B2)** The articular surface was also damaged and ruptured (arrow). **(B3, B4)** The X-ray shows the contraposition and alignment of the artificial joint prosthesis were satisfactory 41 months after operation.

proximal femoral tumors. 26% of the patients suffered from complications: 2 cases needed prosthesis removal, 2 cases developed deep infections around the acetabulum, and 2 cases developed acetabular wear. Abou Senna WG et al. (39) reported the complication rate after prosthesis replacement for proximal femoral tumors as 45%. The most common complication was periprosthetic infections in 10 cases (16.7%), followed by aseptic loosening in 7 cases (11.7%). These studies suggest that with the extension of survival and follow-up time, patients with SR plus prosthesis replacement will likely face many complications, leading to secondary revision surgery. In addition, the joint functions will be gradually lost, increasing the economic burden of patients, and it remains tough to obtain a satisfactory functional prognosis at the same time. These factors must be considered during the initial SR operation.

The indications of SR and EC are different, but their long-term outcome can be compared in order to find the balance point in the treatment of proximal femoral GCTB. This study's analysis and comparison established that the recurrence rate between the EC group (5.3%) and SR group (10%) was similar. Interestingly, there

was no statistical difference, suggesting that EC can also obtain a satisfactory local control rate. However, in terms of functional recovery, the MSTS score of the EC group (27.6 ± 1.6) was significantly higher than that of the SR group (24.7 ± 2.8). Meanwhile, the incidence of complications in the EC group (10.5%) was significantly lower than that in the SR group (50%), with both groups achieving satisfactory excellent and good rates (EC versus SR, 94.7% versus 80%). Summing up the above results, there are substantial differences in the long-term functional prognosis and complication rates between EC and SR, which must be regarded as an essential factor in surgical decision-making. In addition, with the emergence of microwave ablation and denosumab adjuvant therapy, both may downgrade the surgery so that more patients can receive EC surgery (6, 24). In short, the author believes that EC can effectively control the local recurrence rate and obtain ideal postoperative function for patients with Campanacci grades II and III without extensive soft tissue invasion or pathological fracture without evident displacement. On the other hand, SR is more suitable for patients with GCTB of the proximal femur with damaged articular surfaces that cannot be preserved or from pathological fractures with obvious displacement.

This study is a single-center retrospective analysis but contains some shortcomings: (1) due to the low incidence rate of GCTB in the proximal femur, the total number of cases in this study is relatively small, therefore, larger samples and more extensive data analysis are required in the future; (2) Although all follow-up time were > 2 years, the duration needs to be extended for the analysis of the long-term survival rate of artificial joint prostheses.

CONCLUSION

In conclusion, functional reconstruction and recurrence control play a vital role for GCTB in the proximal femur. When the tumor does not extensively involves the surrounding soft tissues, the articular surface is not damaged, and there is no pathological fracture with apparent displacement, EC should be fully considered to achieve optimal joint function and survival prognosis, In other cases, SR surgery is also a wise choice.

DATA AVAILABILITY STATEMENT

The original contributions presented in the study are included in the article/supplementary material. Further inquiries can be directed to the corresponding author.

ETHICS STATEMENT

All patients and their families provided informed consent, and the study design was approved by the Research Ethics Committee of Xiangya Hospital.

AUTHOR CONTRIBUTIONS

YY and WL were in charge of the study design. HH, WL, QL, YL, WZ, and YY screened patients and collected relevant follow-up data. YY, QL, ZW, and YL analyzed the data. The manuscript was written by YY and WL. WL checked the manuscript. All authors contributed to the article and approved the submitted version.

FUNDING

This work was supported by the Hunan Youth Science and Technology Innovation Talent Project (2020RC3058), and the Research project of Hunan health and Family Planning Commission (C20180785).

REFERENCES

1. Klenke FM, Wenger DE, Inwards CY, Rose PS, Sim FH. Recurrent Giant Cell Tumor of Long Bones: Analysis of Surgical Management. *Clin Orthop Relat Res* (2011) 469(4):1181–7. doi: 10.1007/s11999-010-1560-9
2. Niu X, Zhang Q, Hao L, Ding Y, Li Y, Xu H, et al. Giant Cell Tumor of the Extremity: Retrospective Analysis of 621 Chinese Patients From One Institution. *J Bone Joint Surg Am* (2012) 94(5):461–7. doi: 10.2106/JBJS.J.01922
3. He H, Zeng H, Luo W, Liu Y, Zhang C, Liu Q. Surgical Treatment Options for Giant Cell Tumors of Bone Around the Knee Joint: Extended Curettage or Segmental Resection? *Front Oncol* (2019) 9:946. doi: 10.3389/fonc.2019.00946
4. Shi J, Zhao Z, Yan T, Guo W, Yang R, Tang X, et al. Surgical Treatment of Benign Osteolytic Lesions in the Femoral Head and Neck: A Systematic Review. *BMC Musculoskelet Disord* (2021) 22(1):549. doi: 10.1186/s12891-021-04442-y
5. Wijsbek AE, Vazquez-Garcia BL, Grimer RJ, Carter SR, Abudu AA, Tillman RM, et al. Giant Cell Tumour of the Proximal Femur: Is Joint-Sparing Management Ever Successful? *Bone Joint J* (2014) 96-B(1):127–31. doi: 10.1302/0301-620X.96B1.31763
6. Ke J, Cheng S, Yao MY, Chu X, Wang M, Zeng XL, et al. Novel Strategy of Curettage and Adjuvant Microwave Therapy for the Treatment of Giant Cell Tumor of Bone in Extremities: A Preliminary Study. *Orthop Surg* (2021) 13 (1):185–95. doi: 10.1111/os.12865
7. Cho HS, Park IH, Han I, Kang SC, Kim HS. Giant Cell Tumor of the Femoral Head and Neck: Result of Intralesional Curettage. *Arch Orthop Trauma Surg* (2010) 130(11):1329–33. doi: 10.1007/s00402-009-1026-2
8. Errani C, Tsukamoto S, Ciani G, Donati DM. Present Day Controversies and Consensus in Curettage for Giant Cell Tumor of Bone. *J Clin Orthop Trauma* (2019) 10(6):1015–20. doi: 10.1016/j.jcot.2019.09.017
9. Montgomery C, Couch C, Emory CL, Nicholas R. Giant Cell Tumor of Bone: Review of Current Literature, Evaluation, and Treatment Options. *J Knee Surg* (2019) 32(4):331–6. doi: 10.1055/s-0038-1675815
10. Dabak N, Gocer H, Cirakli A. Advantages of Pressurized-Spray Cryosurgery in Giant Cell Tumors of the Bone. *Balkan Med J* (2016) 33(5):496–503. doi: 10.5152/balkanmedj.2016.150473
11. Gulia A, Puri A, Prajapati A, Kurisunkal V. Outcomes of Short Segment Distal Radius Resections and Wrist Afusion With Iliac Crest Bone Grafting for Giant Cell Tumor. *J Clin Orthop Trauma* (2019) 10(6):1033–7. doi: 10.1016/j.jcot.2019.09.024
12. Sirin E, Akgulle AH, Topkar OM, Sofulu Ö, Baykan SE, Erol B. Mid-Term Results of Intralesional Extended Curettage, Cauterization, and Polymethylmethacrylate Cementation in the Treatment of Giant Cell

Tumor of Bone: A Retrospective Case Series. *Acta Orthop Traumatol Turc* (2020) 54(5):524–9. doi: 10.5152/j.aott.2020.19082
13. Bai WZ, Guo SB, Zhao W, Yu XC, Xu M, Zheng K, et al. Comparison of Outcomes of 2 Surgical Treatments for Proximal Humerus Giant Cell Tumors: A Multicenter Retrospective Study. *J Shoulder Elbow Surg* (2019) 28(11):2103–12. doi: 10.1016/j.jse.2019.04.010
14. Sakayama K, Sugawara Y, Kidani T, Miyawaki J, Fujibuchi T, Kamei S. Diagnostic and Therapeutic Problems of Giant Cell Tumor in the Proximal Femur. *Arch Orthop Trauma Surg* (2007) 127(10):867–72. doi: 10.1007/s00402-007-0419-3
15. Campanacci M, Giunti A, Olmi R. Metaphyseal and Diaphyseal Localization of Giant Cell Tumors. *Chir Organi Mov* (1975) 62(1):29–34. doi: 10.1038/ajg.2012.107
16. Kellgren JH, Lawrence JS. Radiological Assessment of Osteo-Arthrosis. *Ann Rheum Dis* (1957) 16(4):494–502. doi: 10.1136/ard.16.4.494
17. Enneking WF, Dunham W, Gebhardt MC, Malawar M, Pritchard DJ. A System for the Functional Evaluation of Reconstructive Procedures After Surgicl Treatment of Tumors of the Musculoskeletal System. *Clin Orthop Relat Res* (1993) 286):241–6. doi: 10.1007/978-1-4471-5451-8_128
18. Jawad MU, Haleem AA, Scully SP. In Brief: Ficat Classification: Avascular Necrosis of the Femoral Head. *Clin Orthop Relat Res* (2012) 470(9):2636–9. doi: 10.1007/s11999-012-2416-2
19. Mankin HJ, Gebhardt MC, Jennings LC, Springfield DS, Tomford WW. Long-Term Results of Allograft Replacement in the Management of Bone Tumors. *Clin Orthop* (1996) 324:86–97. doi: 10.1097/00003086-199603000-00011
20. Lin F, Hu Y, Zhao L, Zhang H, Yu X, Wang Z, et al. The Epidemiological and Clinical Features of Primary Giant Cell Tumor Around the Knee: A Report From the Multicenter Retrospective Study in China. *J Bone Oncol* (2016) 5 (1):38–42. doi: 10.1016/j.jbo.2016.02.001
21. Basu MA, Chawla SP. Giant Cell Tumor of Bone: An Update. *Curr Oncol Rep* (2021) 23(5):51. doi: 10.1007/s11912-021-01047-5
22. Sung HW, Kuo DP, Shu WP, Chai YB, Li SM. Giant-Cell Tumor of Bone: Analysis of Two Hundred and Eight Cases in Chinese Patients. *J Bone Joint Surg Am* (1982) 64(5):755–61. doi: 10.2106/00004623-198264050-00015
23. Errani C, Tsukamoto S, Leone G, Righi A, Akahane M, Tanaka Y, et al. Denosumab May Increase the Risk of Local Recurrence in Patients With Giant-Cell Tumor of Bone Treated With Curettage. *J Bone Joint Surg Am* (2018) 100(6):496–504. doi: 10.2106/JBJS.17.00057
24. Perrin DL, Visgauss JD, Wilson DA, Griffin AM, Abdul Razak AR, Ferguson PC, et al. The Role of Denosumab in Joint Preservation for Patients With Giant Cell Tumour of Bone. *Bone Joint J* (2021) 103-B(1):184–91. doi: 10.1302/0301-620X.103B1.BJJ-2020-0274.R1
25. Jamshidi K, Zandrahimi F, Haji ABM, Arefpour AM, Bagherifard A, Al-Baseesee HH, et al. Extended Curettage Versus En Bloc Resection for the Treatment of Grade 3 Giant Cell Tumour of the Knee With Pathologic Fracture: A Retrospective Study. *Int Orthop* (2021) 45(1):289–97. doi: 10.1007/s00264-020-04836-y
26. Takeuchi A, Suwanpramote P, Yamamoto N, Shirai T, Hayashi K, Kimura H, et al. Mid- to Long-Term Clinical Outcome of Giant Cell Tumor of Bone Treated With Calcium Phosphate Cement Following Thorough Curettage and Phenolization. *J Surg Oncol* (2018) 117(6):1232–8. doi: 10.1002/jso.24971
27. Fan H, Zeng X, Wang X, Zhu R, Pei G. Efficacy of Prevascularization for Segmental Bone Defect Repair Using Beta-Tricalcium Phosphate Scaffold in Rhesus Monkey. *Biomaterials* (2014) 35(26):7407–15. doi: 10.1016/j.biomaterials.2014.05.035
28. Dimitriou R, Jones E, McGonagle D, Giannoudis PV. Bone Regeneration: Current Concepts and Future Directions. *BMC Med* (2011) 9:66. doi: 10.1186/1741-7015-9-66
29. Wu M, Yao S, Xie Y, Yan F, Deng Z, Lei J, et al. A Novel Subchondral Bone-Grafting Procedure for the Treatment of Giant-Cell Tumor Around the Knee: A Retrospective Study of 27 Cases. *Medicine (Baltimore)* (2018) 97:e13154. doi: 10.1097/MD.0000000000013154
30. Radev BR, Kase JA, Askew MJ, Weiner SD. Potential for Thermal Damage to Articular Cartilage by PMMA Reconstruction of a Bone Cavity Following Tumor Excision: A Finite Element Study. *J Biomech* (2009) 42:1120–6. doi: 10.1016/j.jbiomech.2009.02.005
31. Errani C, Ruggieri P, Asenzio MA, Toscano A, Colangeli S, Rimondi E, et al. Giant Cell Tumor of the Extremity: A Review of 349 Cases From a Single Institution. *Cancer Treat Rev* (2010) 36(1):1–7. doi: 10.1016/j.ctrv.2009.09.002
32. Lun D, Hu Y, Huang H, Xia Q, Miao J, Yu J. Femoral Neck of Anterolateral and Lateral Combined Approach Tumor Curettage, Bone Grafting and Internal Fixation. *Chin J Orthop* (2011) 31(2):119–25. doi: 10.3760/cma.j.issn.0253-2352.2011.02.003
33. Van der Heijden L, Dijkstra PD, Campanacci DA, Gibbons CL, van de Sande MA. Giant Cell Tumor With Pathologic Fracture: Should We Curette or Resect? *Clin Orthop Relat Res* (2013) 471:820–9. doi: 10.1007/s11999-012-2546-6
34. Hindiskere S, Errani C, Doddarangappa S, Ramaswamy V, Rai M, Chinder PS. Is a Short-Course of Preoperative Denosumab as Effective as Prolonged Therapy for Giant Cell Tumor of Bone? *J Clin Orthop Relat Res* (2020) 478:2522–33. doi: 10.1097/CORR.0000000000001285
35. Klenke FM, Wenger DE, Inwards CY, Rose PS, Sim FH. Giant Cell Tumor of Bone: Risk Factors for Recurrence. *Clin Orthop Relat Res* (2011) 469:591–9. doi: 10.1007/s11999-010-1501-7
36. Balke M, Ahrens H, Streitbuerger A, Koehler G, Winkelmann W, Gosheger G, et al. Treatment Options for Recurrent Giant Cell Tumors of Bone. *J Cancer Res Clin Oncol* (2009) 135:149–58. doi: 10.1007/s00432-008-0427-x
37. Henderson ER, Groundland JS, Pala E, Dennis JA, Wooten R, Cheong D, et al. Failure Mode Classification for Tumor Endoprostheses: Retrospective Review of Five Institutions and a Literature Review. *J Bone Joint Surg Am* (2011) 93:418–29. doi: 10.2106/JBJS.J.00834
38. Xu G, Miwa S, Yamamoto N, Hayashi K, Tsuchiya H. Pedicle Frozen Autograft-Prosthesis Composite Reconstructions for Malignant Bone Tumors of the Proximal Femur. *BMC Musculoskelet Disord* (2020) 21:81. doi: 10.1186/s12891-020-3112-0
39. Abou Senna WG, Ebeid WA, Abdel Moneim M, Saladin M, Hasan BZ, Badr IT, et al. Long-Term Outcome of Patients With Primary or Secondary Tumors of the Proximal Femur Treated by Bipolar Modular Tumor Prosthesis. *Arch Orthop Trauma Surg* (2020) 8:581–6. doi: 10.1007/s00402-020-03581-6

Conflict of Interest: The authors declare that the research was conducted in the absence of any commercial or financial relationships that could be construed as a potential conflict of interest.

frontiers in Oncology

ORIGINAL RESEARCH
published: 12 January 2022
doi: 10.3389/fonc.2021.733510

Self-Expandable Metallic Stent Implantation Combined With Bronchial Artery Infusion Chemoembolization in the Treatment of Lung Cancer With Complete Atelectasis

*Xiaobing Li[1], Meipan Yin[1], Pengfei Xie[1], Ying Liu[2], Xiangnan Li[3], Yu Qi[3], Yaozhen Ma[1], Chunxia Li[1] and Gang Wu[1]**

[1] Department of Interventional Radiology, The First Affiliated Hospital of Zhengzhou University, Zhengzhou, China, [2] Department of Respiratory, The First Affiliated Hospital of Zhengzhou University, Zhengzhou, China, [3] Department of Thoracic Surgery, The First Affiliated Hospital of Zhengzhou University, Zhengzhou, China

OPEN ACCESS

Edited by:
Patrick J. Schuler,
Ulm University Medical Center,
Germany

Reviewed by:
Beatrice Aramini,
University Hospital of Modena, Italy
Wei-Lin Wang,
Zhejiang University, China
Katerina Malagari,
National and Kapodistrian
University of Athens, Greece

***Correspondence:**
Gang Wu
wuganghenan2004@zzu.edu.cn

Specialty section:
This article was submitted to
Surgical Oncology,
a section of the journal
Frontiers in Oncology

Received: 30 June 2021
Accepted: 15 December 2021
Published: 12 January 2022

Citation:
Li X, Yin M, Xie P, Liu Y, Li X, Qi Y,
Ma Y, Li C and Wu G (2022)
Self-Expandable Metallic Stent
Implantation Combined With
Bronchial Artery Infusion
Chemoembolization in the
Treatment of Lung Cancer With
Complete Atelectasis.
Front. Oncol. 11:733510.
doi: 10.3389/fonc.2021.733510

Background: Atelectasis is a common complication of lung cancer, and there are few reports about the treatment methods. This study retrospectively analyzed the safety and effectiveness of endotracheal metal stent implantation combined with arterial infusion chemoembolization in the treatment of non-small cell lung cancer with complete atelectasis.

Methods: The clinical data of patients with non-small cell lung cancer and complete atelectasis treated by self-expandable metallic stent implantation combined with arterial infusion chemotherapy were retrospectively analyzed. The clinical efficacy was evaluated and postoperative adverse reactions were observed. Progression-free survival and overall survival were analyzed by Kaplan-Meier method.

Results: In all, 42 endotracheal metallic stents were implanted in 42 patients under fluoroscopy. 5–7 days after stent implantation, CT showed that 24 patients (57.1%) had complete lung recruitment, and that 13 (31.0%) had partial lung recruitment. The technical success rate was 100%, and the clinical success rate was 88.1% (37/42). 5–7 days after stent implantation, bronchial artery infusion chemoembolization was performed in all patients. The median progression-free survival and overall survival were 6 months (95% CI: 2.04-9.66) and 10 months (95% CI: 7.22-12.79), respectively.

Conclusion: Self-expandable metallic stent implantation combined with arterial infusion chemoembolization may be an effective and safe strategy in the treatment of lung cancer with atelectasis clinically.

Keywords: lung cancer, atelectasis, self-expandable metallic stent, bronchial artery infusion chemoembolization, interventional radiology

INTRODUCTION

Atelectasis in lung cancer often results from severe tracheal or bronchial obstruction due to cancer invasion. Subsequently, diminished alveolar air severely leads to substantial lung tissue damage, such as atrophy and collapse. According to associated reports, the incidence rate of lung cancer is 10–40% (1–3). The survival time of untreated lung cancer patients with atelectasis isn't beyond 2 months, and patients often die of asphyxia, infection, or ventilator support-related complications (4). Lung cancer with complete atelectasis refers to the atelectasis of the whole lung, which often results in a dyspneic symptom. As the common therapeutic methods, radiotherapy or intravenous chemotherapy can hardly relieve airway obstruction in a short time, in contrast with the potential local tissue swelling and aggravate dyspnea subsequently.

Self-expandable metallic stent (SEMS) is widely used in the treatment of airway stenosis due to its significant advantage in the relieving airway stenosis and dyspnea (5–9). However, there are few reports on SEMS being applied in the treatment of lung cancer with atelectasis (10), because the SEMS cannot suppress the invasion of tumor tissue to the surrounding areas. The spread of cancer through the mesh of the stent causes airway restenosis, which affects the long-term efficacy of SEMS in the treatment of atelectasis.

Bronchial arterial transcatheter arterial chemoembolization (BA-TACE) infuses chemotherapeutic drugs directly into the tumor-feeding artery to increase the local drug concentration and destroy cancer cells effectively. It has been demonstrated that infusion chemotherapeutic drugs in small doses ensures the therapeutic effect and avoid severe side effects. Bronchial artery embolization can further improve the curative effect by blocking the tumor-feeding artery and tumor vascular bed (11–13). This study evaluated the safety and efficacy of SEMS implantation combined with BA-TACE in the treatment of lung cancer with complete atelectasis, which provides a preliminary clinically evidence for promotion the combined therapy.

MATERIALS AND METHODS

Patients

In this retrospective study, we analyzed the clinical data of patients with lung cancer with complete atelectasis who received the combined therapy in the Department of Interventional Radiology of our hospital, from June 2012 to May 2020. Patients' medical records, imaging data, operation records, and follow-up results were analyzed. The following inclusion criteria were applied: ① non-small cell lung cancer diagnosed by histological examination; ② complete atelectasis confirmed by CT imaging; and ③ sequential treatment combined with SEMS implantation and BA-TACE. The exclusion criteria were as follows: ① patients without BA-TACE after stent implantation; ② patients without stent implantation before BA-TACE; and ③ patients who received any other type of treatments in the course of the combined therapy.

This study protocol was approved by the ethics investigation committee of the First Affiliated Hospital of Zhengzhou University. Ethical approval code: SS-2018-25. Written informed consent was obtained from each patient during questionnaire administration for the collection and analysis of applicable clinical data.

Preoperative Preparation

Blood routine, electrolytes, coagulation function, tumor markers, liver and kidney function, and electrocardiogram results were examined before the operation. The location, degree, and length of stenosis, atelectasis, and pleural effusion were confirmed by plain and enhanced chest CT. In this study, all stents used were bare. The diameter of the stent was about 10% larger than that of the trachea and main bronchus in the mediastinal window of chest CT. The airway obstruction is at least 1 cm away from the carina or larynx, a straight tubular tracheal stent should be used; the obstruction in the carina area, a Y-shaped endotracheal stent is preferred, and the obstruction in distal of the main bronchus, a small Y-shaped tracheal stent should be used. The SEMS used in the study was manufactured by Nanjing Micro-Tech Medical Company (Nanjing City, Jiangsu Province, China).

SEMS Implantation Therapy

The patients were administered intramuscular diazepam (10 mg) and anisodamine (10 mg) and intravenous dexamethasone (10 mg), 30 min before the procedure. The procedures were performed under fluoroscopic guidance, without the use of bronchoscopy. Interventional radiologists placed the stent under local anesthesia. Patients lay on the examination bed, with ECG monitoring. A gag was used to open the mouth. Oxygen was administered *via* a nasal catheter, and a sputum aspirator was prepared. Under fluoroscopy, a 0.035-inch hydrophilic guide wire (Cook Corporation, Bloomington, IN, USA) and a 5 F vertebral artery catheter (Cordis Company, New Jersey, USA) were introduced transorally into the trachea or bronchus. Then, 5 mL of 2% lidocaine and 5 mL of 0.01% epinephrine were quickly sprayed *via* the catheter. Tracheography was performed to determine the location of airway stenosis. After the guide wire and catheter pass through the stenosis, the guide wire was withdrawn. Retract the catheter while injecting contrast agent for airway imaging. We could use this technique to define the distal end of the stenotic component of the main bronchus. Exchange with stiff guide wire into one side bronchus, 9 F sheath tubes was placed along guide wire. Another 0.035-inch hydrophilic hard wire was introduced for Y-shaped or small Y-shaped stenting. In general, the bronchial component of the stent was slowly released 0.5 to 1 cm beyond the distal end of the stenotic component of the main bronchus. After the stent was successfully inserted, the sputum aspiration tube was introduced for sputum drainage to avoid suffocation (5, 14).

The patients were given aerosol inhalation and anti-inflammatory treatment after SEMS implantation, and their vital signs were closely monitored. A repeat CT was performed 5–7 days after the implantation to observe the position of the stent, degree of expansion, and lung recruitment.

Bronchial Artery Infusion Chemoembolization

The BA-TACE procedure was performed 5–7 days after SEMS implantation and when the dyspnea was relieved. BA-TACE chemotherapy regimen: comprised epirubicin 30–50 mg, nedaplatin 40–60 mg, and raltitrexed 4 mg.

The Seldinger technique was used to puncture the femoral artery. The location of the tumor- feeding artery was determined by bronchial arteriography. If necessary, a 2.7-F micro guide superselective catheter was used. The dose of chemotherapy drugs is decided during the procedure on the basis of the number of blood supply arteries and the degree of tumor staining (15). Each drug was dissolved in 150–200 mL solution and injected into the tumor-feeding artery at a constant rate of 10 mL/min. Subsequently, 350–560 μm gelatin sponge particles (in absence of hemoptysis) or PVA particles (in presence of hemoptysis) were used to embolize the tumor-feeding artery (13).

The patients were treated with proton pump inhibitors, antiemetics, antibiotics, and expectorants. BA-TACE was performed 1–3 times at 4-week intervals according to the degree of tumor shrinkage. Chest CT was reexamined before each BA-TACE to evaluate atelectasis and its curative effect on the tumor.

Evaluation

The chest CT and DSA images were analyzed by two experienced interventional radiologists. The curative effect of lung recruitment was divided into complete lung recruitment, partial lung recruitment, no lung recruitment, and progressive atelectasis (16). Dyspnea patients were divided into five grades based on dyspnea score (17). In this study, progression-free survival (PFS) and overall survival (OS) were used as the outcome measures. After treatment with airway stenting and BA-TACE, absence of any serious operation-related event was considered as technical success. An improvement of clinical symptoms or of the atelectasis on CT after SEMS implantation was considered as clinical success.

The adverse events during and after treatment were recorded in detail. Adverse events were graded according to the American standard for common adverse reaction terminology (version 5.0).

Statistical Analysis

SPSS software (version 23.0, IBM, Armonk, NY, USA) was used for all statistical analysis. Data are presented as medians, mean ± standard deviation, or percentages. Overall survival (OS) was calculated by the Kaplan-Meier method. OS was calculated from the day of histologic diagnosis to the date of death or last follow-up. P values <0.05 indicated statistical significance.

RESULTS

A total of 42 patients [33 males and 9 females, age: 37–86 (mean: 60.6 ± 11.32) years] were enrolled in this study. There were 30 cases of dyspnea (dyspnea score > 1), 15 cases of cough (35.7%), four cases of hemoptysis (9.5%), two cases of eating obstruction (4.8%), one case of chest pain (2.4%), and one case of fever (2.4%). Among those with comorbid diseases, seven patients had hypertension (16.7%), eight had type 2 diabetes (19.0%), one had coronary heart disease (2.4%), and three had chronic lung disease (7.1%).

The clinical characteristics of the patients are shown in **Table 1**.

SEMS Implantation and Clinical Results

In all, 42 SEMS were implanted in 42 patients under fluoroscopic guidance, including four straight tubular stents, five L-shaped stents, 31 large Y-shaped stents, and two small Y-shaped stents. The success rate of stent implantation was 100%. The operation time of stent implantation ranged from 4–42 (mean: 14.2 ± 7.11) minutes. There were no serious events such as massive hemorrhage, asphyxia, or death related to the operation. The status of stent placement, stent type, location, and degree of airway stenosis are shown in **Table 2**. The types and sizes of stents are shown in **Table 3**.

TABLE 1 | Baseline Characteristics of Study Patients (N=42).

Variables	Data
Histological type	
Squamous cell carcinoma	33 (78.6)
Adenocarcinoma	8 (19.0)
Adenosquamous carcinoma	1 (2.4)
TNM stage	
III	24 (57.1)
IV	28 (66.7)
Dyspnea classification(N=30)	
2	4 (9.3)
3	17 (39.5)
4	6 (14.0)
5	3 (7.0)
Location of atelectasis	
Right lung	28 (65.1)
Left lung	14 (33.3)
Previous treatment	
Chemotherapy	22 (52.4)
Radiotherapy	5 (11.6)
Surgery	5 (11.6)
^{125}I seed implantation	4 (9.3)

TABLE 2 | Statistics of stent placement.

Data	
Emergency	10 (23.8)
Non-emergency	32 (76.2)
Severity of airway obstruction	
III	10 (23.8)
IIV	12 (28.6)
Narrow part	
Trachea + Carina	9 (21.4)
Carina + Right main bronchus	5 (11.9)
Carina + Light main bronchus	9 (21.4)
Carina + Left and right bronchus	10 (23.8)
Light main bronchus	3 (7.1)
Right main bronchus	6 (14.3)

TABLE 3 | The stent types and dimensions.

Stent Types	n	Median Diameter (mm)	Median Length (mm)
Straight tubular stents	4	20 (20-20)	50 (40-60)
L-shaped stents	5	Main tube 20 (20-20)	Main tube 40 (30-60)
		Branches 13 (10-14)	Branches 25 (20-40)
Large Y-shaped stents	31	Main tube 22 (12-22)	Main tube 40 (30-55)
		Left branches 12 (8–14)	Left branches B30 (10–35)
		Right branches 12 (10–14)	Right branches 15 (10–50)
Small Y-shaped stents	2	Main tube 12 (12-12)	Main tube 22.5 (20–25)
		Branches 10 (10-10)	Branches 13 (10–15)

After 5 to 7 days of stent implantation, CT showed that 24 patients (57.1%) had complete lung recruitment, and 13 patients (31.0%) had partial lung recruitment. The technical success rate was 100%, and the clinical success rate was 88.1% (37/42). Five patients (11.9%) had no lung recruitment; hence, they were treated with sputum aspiration and ablation under fiberoptic bronchoscopy. Eventually, their clinical symptoms and atelectasis improved. The oxygen saturation was >94%, and the dyspnea score showed significant improvement, with 13, 11, and 6 patients showing a score of 0, 1, and 2.

BA-TACE

Twenty-seven, 11, and 4 patients underwent one, two, and three BA-TACE procedure, respectively. A total of 70 arteries in 42 patients were confirmed as tumor-feeding arteries by angiography, with an average of 1.67 ± 0.55 arteries per patient

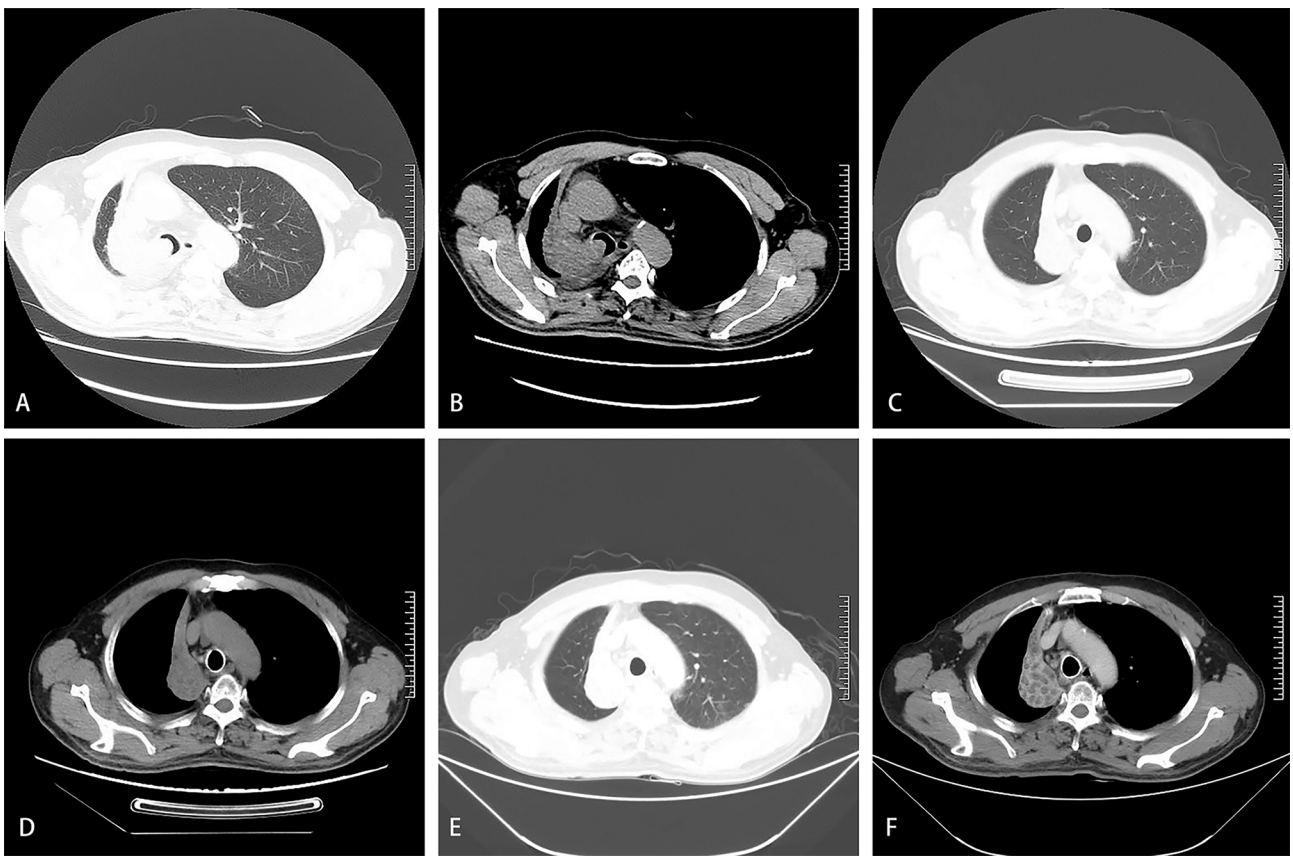

FIGURE 1 | A 61-year-old man was diagnosed with squamous cell carcinoma of the right lung 8 months ago. He had progressive dyspnea for 3 days. The dyspnea score was 5. Chest computed tomography on admission showed complete atelectasis in the lung window **(A)** and the mediastinal window **(B)**. Repeated computed tomography in the lung window **(C)** and the mediastinal window **(D)** showed a reduction in the size of the tumor in the right lung one month after the first BA-TACE. Repeated computed tomography in the lung window **(E)** and the mediastinal window **(F)** showed obvious necrosis in the tumor area one month after the second BA-TACE.

(range: 1-3), including 46 bronchial arteries, 7 internal thoracic arteries, 1 esophageal artery, 1 thyroid neck trunk, and 15 intercostal arteries.

All 42 patients were successfully treated with chemotherapy *via* the tumor-feeding artery: 38 patients were treated with gelatin sponge and four were treated with PVA particles. Typical cases are shown in **Figures 1**–**3**.

Four weeks after the last BA-TACE treatment, the patient received subsequent treatment. Eight patients received targeted therapy, 10 received intravenous chemotherapy, eight received radiotherapy, five received radioactive seed implantation, six received chemotherapy and PD-1 treatment, and six did not receive any anti-tumor treatment until the end of follow-up.

Survival

The median PFS was 6.0 months (95% CI: 2.04–9.66), and the median OS was 10.0 months (95% CI: 7.22–12.79). The 6- and 12-month survival rates were 71.4% and 42.3%, respectively (**Figures 4**, **5**).

Until the end of the follow-up period, four patients survived and were followed up for 9–26 months. Dyspnea did not recur in these 4 patients. In all, 38 patients died of the following causes: massive hemoptysis (n=1), cerebrovascular accident (n=3), pulmonary infection (n=14), cardiac arrest (n=4, one had coronary heart disease), heart failure (n=3), and cachexia caused by tumor (n=13). Among the 39 patients who died, 18 experienced recurrent dyspnea.

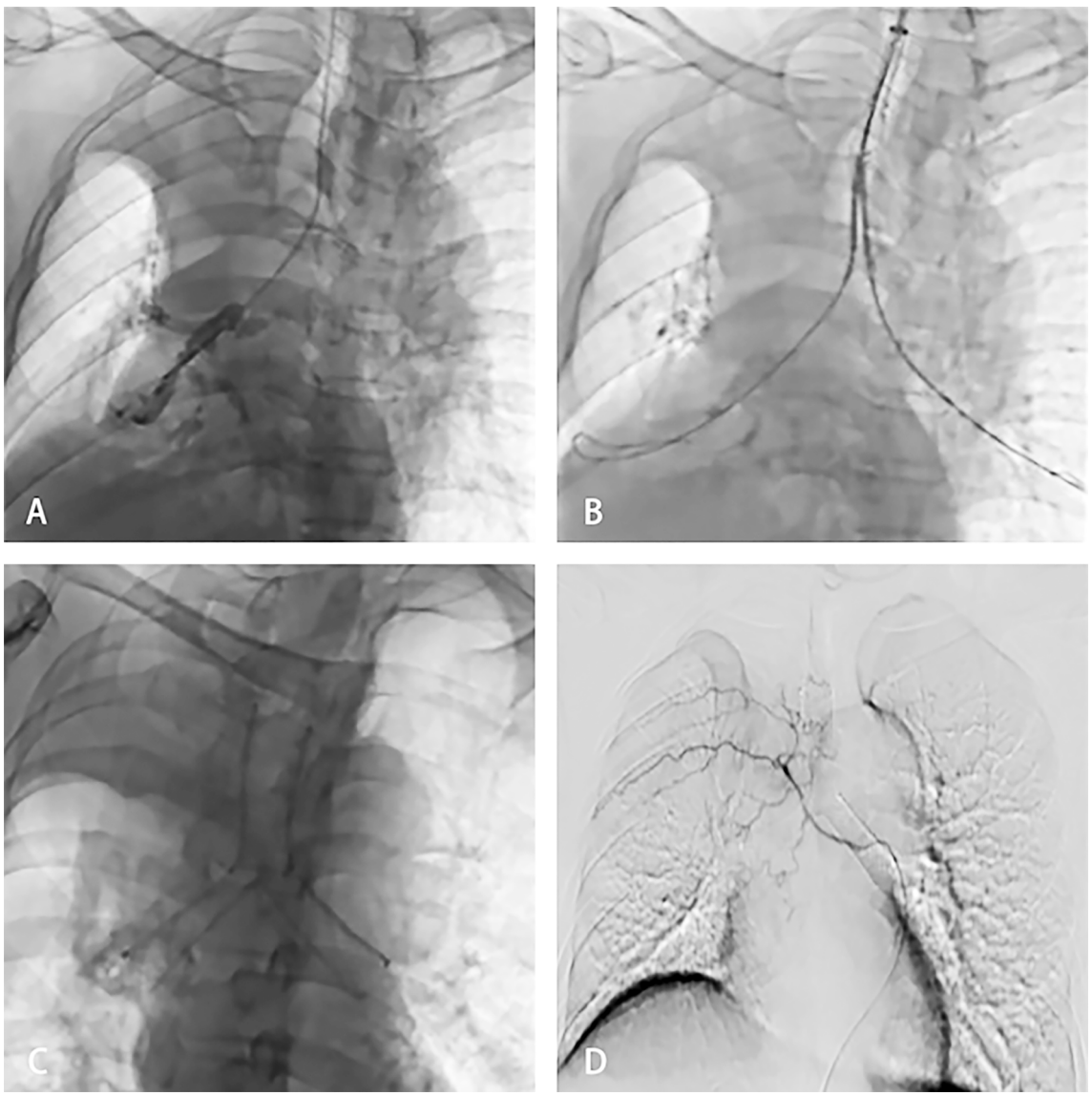

FIGURE 2 | The patient was then treated with SEMS implantation and BA-TACE. Bronchography showed complete blockage of the distal right main bronchus and carina **(A)**. The stent delivery system was inserted under fluoroscopic guidance to reach the right blocked bronchus **(B)**. Fluoroscopy showed release of the Y-shaped stent **(C)**. Arteriography showed that the arteries were thickened and areas of abnormal staining were visible **(D)**.

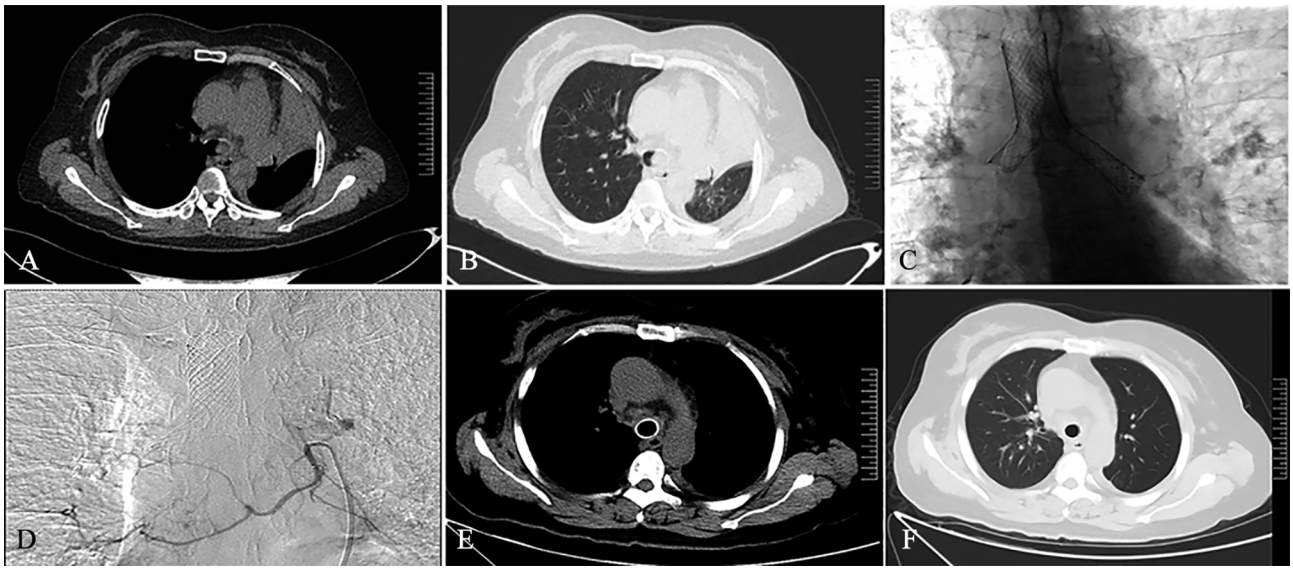

FIGURE 3 | A 45-year-old female patient was diagnosed with left lung squamous cell carcinoma 2 weeks ago. She had dyspnea for 1 week. Chest computed tomography on admission showed atelectasis on the left side in the mediastinal window **(A)** and lung window **(B)**. The patient subsequently received SEMS implantation **(C)** and BA-TACE **(D)** treatment. One month after treatment, the patient's reexamination of CT showed complete left lung recruitment in the mediastinal window **(E)** and the lung window **(F)**, and the tumor treatment effect was complete remission.

Adverse Events

Eight patients (19.0%) had poor expectoration after SEMS implantation, which improved after sputum suction under bronchoscopy. The postoperative adverse events included hemoptysis, nausea, vomiting, fever, elevated serum alanine, and aspartate aminotransferase levels, and decreased platelet count. All the adverse events were classified as grade 1 (**Table 4**).

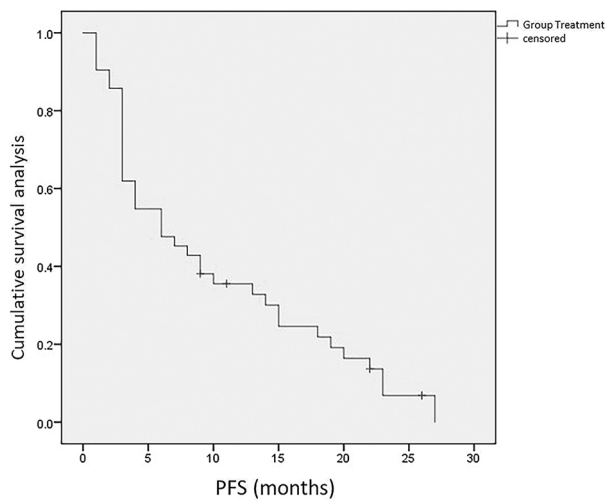

FIGURE 4 | Kaplan-Meier curve for PFS.

DISCUSSION

In lung cancer progression, atelectasis with dyspnea and insufficient ventilation is a common complication, affecting the quality of life (18). Owing to complication, old age, physical status, and other factors, traditional radiotherapy and chemotherapy are not effective for lung cancer with atelectasis (19). Previous report has exhibited the low efficiency of molecular targeted therapy (e.g., tyrosine kinase inhibitors) (20). The efficacy of other treatment methods such as radioactive seed implantation between tumor tissues and traditional Chinese herb in the treatment of advanced lung cancer remains to be verified (21–23).

Fast and accurate placement of the intraairway stent guarantees the successful operation. Thus, the successful placement of stent under fluoroscopy requires highly skilled operators. As a palliative interventional therapy, stent placement can rapidly relieve atelectasis caused by airway obstruction and improve ventilation, but there are related complications (24), such as irritative cough, stimulating granulation tissue hyperplasia, tracheal perforation, hemoptysis, asphyxia, and death, which ultimately influence the long-term curative effect. The stent implantation can only improve dyspnea and provide opportunities for later treatment.

Pulmonary tumors are considered to be fed through two different vascular systems, comprising low-pressure pulmonary arterial circulation and high-pressure systemic arterial circulation, including the bronchial artery (1, 25). BA-TACE is considered as a good choice for the treatment of advanced lung cancer. BA-TACE has a high rate of successful tumor reduction

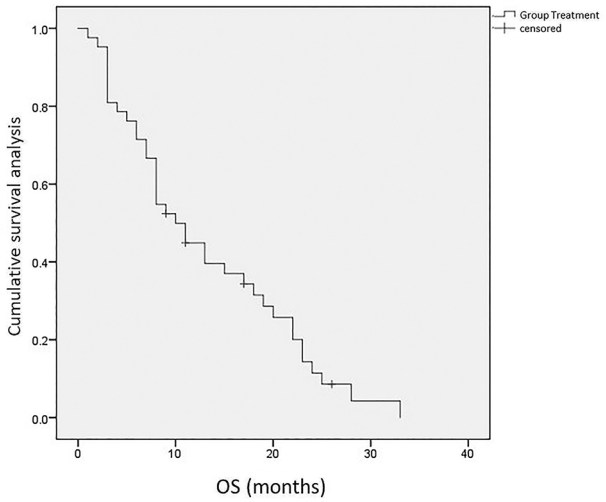

FIGURE 5 | Kaplan-Meier curve for OS.

in a short time, less adverse reactions, and high repeatability (13, 26, 27). BA-TACE combined with SEMS can not only suppress tumor but also relieve symptoms, improve lung recruitment rate, and maintain the airway stent patency rate. Arteriography to find all the tumor-feeding arteries plays a key role in BA-TACE treatment. We judge whether all the arteries have been found based on the consistency of the position and shape of the tumor presented in the arteriography and CT.

However, BA-TACE may lead to serious complications such as cerebral infarction, spinal cord injury, esophageal perforation, and tracheal perforation (28, 29). Identifying the spinal artery and the abnormal communication between the bronchial artery and the pulmonary vein is a prerequisite to avoid serious adverse events such as paraplegia and cerebral infarction. According to our experience, careful operation, use of microcatheter when necessary (Typical cases are shown in **Figures 6**), and selection of types and models of embolic materials (the selection of permanent embolic materials for patients with hemoptysis, and the use of gelatin sponge for patients without hemoptysis) are details that result in a high technical success rate and low incidence of adverse events (30).

There are few reports on the clinical efficacy of sequential treatment of lung cancer with atelectasis by SEMS implantation and BA-TACE. There is only one report about retrospective analysis of bronchoscopic implantation of ^{125}I radioactive seeds for the treatment of lung cancer with complete atelectasis (16), the limitation of this technique is that it can only be applied to patients with mild dyspnea and without hemoptysis.

The main limitation of this study is that it is a single center, retrospective, and observational analysis, with a limited number

TABLE 4 | Adverse events and subsequent treatment (N=42).

Adverse events	Data	Treatment	Effect
Intraoperative			
cough	11(26.2)	10 mg dexamethasone intravenous bolus	relief
Postoperative			
Grade 1 nausea/vomiting	9 (21.4)	Antiemetic treatment	relief
Grade 1 fever	6 (14.3)	Antipyretic treatment	relief
ALT/AST increase			
Grade 1	5 (11.9)	Hepatoprotective treatment	relief
Thrombocytopenia Grade 1	3 (7.1)	Platelet Ascending treatment	relief
Chest pain grade 1	13 (31.0)	Symptomatic treatment	relief
Abdominal pain grade 1	1 (2.4)	Symptomatic treatment	relief
Hemoptysis	6 (14.3)	Hemostatic treatment	relief

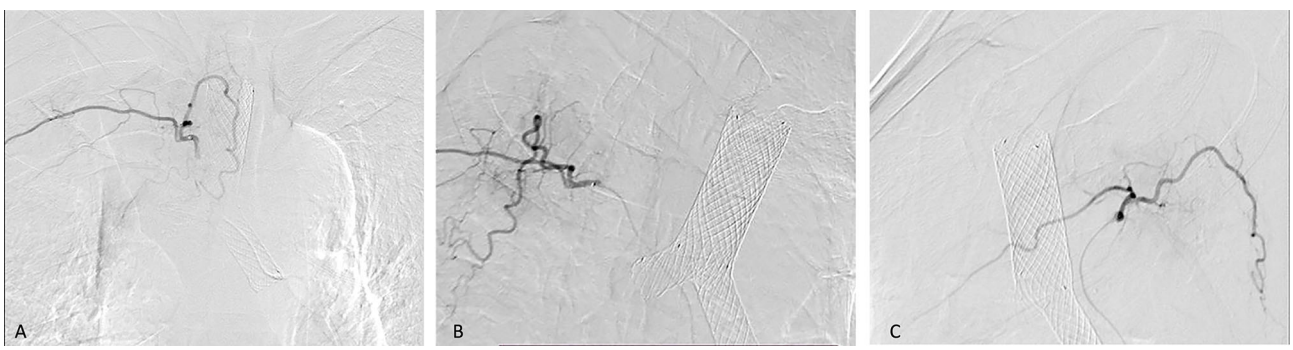

FIGURE 6 | Bilateral bronchial arteriography shows the vascular distribution of the embolized tumor. A 57-year-old man was diagnosed with right lung squamous cell carcinoma and right atelectasis. He underwent BA-TACE after airway stent placement. In Figures **(A–C)**, we use bilateral bronchial angiography to find the vascular distribution of the tumor, and use a microcatheter for infusion chemoembolization.

of cases and no control group for comparison. More prospective and large-scale clinical controlled trials are needed in the future.

This study shows that SEMS combined with BA-TACE is an effective and safe method in the treatment of non-small cell lung cancer with atelectasis, which can be attempted clinically. Large-scale randomized clinical trials need to be carried out to further confirm the results of this study.

DATA AVAILABILITY STATEMENT

The original contributions presented in the study are included in the article/supplementary material. Further inquiries can be directed to the corresponding author.

ETHICS STATEMENT

This study protocol was approved by the ethics investigation committee of the First Affiliated Hospital of Zhengzhou University. Ethical approval code:SS-2018-25. The patients/participants provided their written informed consent to participate in this study.

AUTHOR CONTRIBUTIONS

XiaoL and GW contributed in the study design, data collection, data analysis, data interpretation, literature search, and writing of the article. MY contributed in the literature search and writing of the article. PX and YL contributed in the data collection, analysis, and interpretation. XiangL, YQ, YM, and CL contributed in the data analysis and data interpretation. All authors contributed to the article and approved the submitted version.

ACKNOWLEDGMENTS

The authors thank their colleagues in the interventional operating room.

REFERENCES

1. Kwint M, Conijn S, Schaake E, Knegjens J, Rossi M, Remeijer P, et al. Intra Thoracic Anatomical Changes in Lung Cancer Patients During the Course of Radiotherapy. *Radiother Oncol* (2014) 113:392–7. doi: 10.1016/j.radonc.2014.10.009
2. Karlsson K, Nyman J, Baumann P, Wersäll P, Drugge N, Gagliardi G, et al. Retrospective Cohort Study of Bronchial Doses and Radiation-Induced Atelectasis After Stereotactic Body Radiation Therapy of Lung Tumors Located Close to the Bronchial Tree. *Int J Radiat Oncol Biol Phys* (2013) 87:590–5. doi: 10.1016/j.ijrobp.2013.06.2055
3. Elsayad K, Kriz J, Reinartz G, Scobioala S, Ernst I, Haverkamp U, et al. Cone-Beam CT-Guided Radiotherapy in the Management of Lung Cancer: Diagnostic and Therapeutic Value. *Strahlenther Onkol* (2016) 192:83–91. doi: 10.1007/s00066-015-0927-y
4. Bolliger CT, Sutedja TG, Strausz J, Freitag L. Therapeutic Bronchoscopy With Immediate Effect: Laser, Electrocautery, Argon Plasma Coagulation and Stents. *Eur Respir J* (2006) 27:1258–71. doi: 10.1183/09031936.06.00013906
5. Han X, Al-Tariq Q, Zhao Y, Li L, Cheng Z, Wang H, et al. Customized Hinged Covered Metallic Stents for the Treatment of Benign Main Bronchial Stenosis. *Ann Thorac Surg* (2017) 104:420–5. doi: 10.1016/j.athoracsur.2017.01.116
6. Ma J, Han X, Wu G, Jiao D, Ren K, Bi Y. Outcomes of Temporary Partially Covered Stent Placement for Benign Tracheobronchial Stenosis. *Cardiovasc Intervent Radiol* (2016) 39:1144–51. doi: 10.1007/s00270-016-1353-y
7. Huang S, Xu J, An Z, Yuan P, Xu H, Lv W, et al. Clinical Assessment of Airway Stent Placement in Patients With Malignant Airway Lesions. *J Thorac Dis* (2018) 10:3277–88. doi: 10.21037/jtd.2018.06.01
8. Verma A, Phua CK, Wu QM, Sim WY, Rui AW, Goh SK, et al. Our Clinical Experience of Self-Expanding Metal Stent for Malignant Central Airway Obstruction. *J Clin Med Res* (2017) 9:58–63. doi: 10.14740/jocmr2811w
9. Andreetti C, D'Andrilli A, Ibrahim M, Rendina EA. Treatment of a Complex Tracheobronchial Malignant Stenosis With a Modified Conical Semicovered Self-Expanding Stent. *J Thorac Cardiovasc Surg* (2013) 146:488–9. doi: 10.1016/j.jtcvs.2013.03.007
10. Wu G, Li Z, Jiao D, Han X. Sequential Interventional Treatment of Right-Sided Lung Cancer With Complete Lung Atelectasis: A Case Report. *J Thorac Cardiovasc Surg* (2016) 152:e65–7. doi: 10.1016/j.jtcvs.2016.05.012
11. Huang J, Zhang T, Ma K, Fan P, Liu Y, Weng C, et al. Clinical Evaluation of Targeted Arterial Perfusion of Verapamil and Chemotherapeutic Drugs in Interventional Therapy of Advanced Lung Cancer. *Cancer Chemother Pharmacol* (2013) 72:889–96. doi: 10.1007/s00280-013-2271-1
12. Shang B, Li J, Wang X, Li D, Liang B, Wang Y, et al. Clinical Effect of Bronchial Arterial Infusion Chemotherapy and CalliSpheres Drug-Eluting Beads in Patients With Stage II-IV Lung Cancer: A Prospective Cohort Study. *Thorac Cancer* (2020) 11:2155–62. doi: 10.1111/1759-7714.13522
13. Zeng Y, Yin M, Zhao Y, Liu Y, Li X, Qi Y, et al. Combination of Bronchial Arterial Infusion Chemotherapy Plus Drug-Eluting Embolic Transarterial Chemoembolization for Treatment of Advanced Lung Cancer-A Retrospective Analysis of 23 Patients. *J Vasc Interv Radiol* (2020) 31:1645–53. doi: 10.1016/j.jvir.2020.06.007
14. Li ZM, Wu G, Han XW, Ren KW, Zhu M. Radiology-Guided Forceps Biopsy and Airway Stenting in Severe Airway Stenosis. *Diagn Interv Radiol* (2014) 20:349–52. doi: 10.5152/dir.2014.12118
15. Nakanishi M, Demura Y, Umeda Y, Mizuno S, Ameshima S, Chiba Y, et al. Multi-Arterial Infusion Chemotherapy for Non-Small Cell Lung Carcinoma–Significance of Detecting Feeding Arteries and Tumor Staining. *Lung Cancer* (2008) 61:227–34. doi: 10.1016/j.lungcan.2007.12.017
16. Lu M, Pu D, Zhang W, Liao J, Zhang T, Yang G, et al. Trans-Bronchoscopy With Implantation of (125)I Radioactive Seeds in Patients With Pulmonary Atelectasis Induced by Lung Cancer. *Oncol Lett* (2015) 10:216–22. doi: 10.3892/ol.2015.3204
17. Ferrazza AM, Martolini D, Valli G, Palange P. Cardiopulmonary Exercise Testing in the Functional and Prognostic Evaluation of Patients With Pulmonary Diseases. *Respiration* (2009) 77:3–17. doi: 10.1159/000186694
18. Pang Z, Ding N, Dong W, Ni Y, Zhang T, Qu X, et al. Prognostic Effects of Preoperative Obstructive Pneumonitis or Atelectasis and Comparison With Tumor Size in Non-Small Cell Lung Cancer. *J Thorac Dis* (2017) 9:768–78. doi: 10.21037/jtd.2017.02.88
19. Ambroggi M, Biasini C, Toscani I, Orlandi E, Berte R, Mazzari M, et al. Can Early Palliative Care With Anticancer Treatment Improve Overall Survival and Patient-Related Outcomes in Advanced Lung Cancer Patients? A Review of the Literature. *Support Care Cancer* (2018) 26:2945–53. doi: 10.1007/s00520-018-4184-3
20. Inal C, Yilmaz E, Piperdi B, Perez-Soler R, Cheng H. Emerging Treatment for Advanced Lung Cancer With EGFR Mutation. *Expert Opin Emerg Drugs* (2015) 20:597–612. doi: 10.1517/14728214.2015.1058778
21. Chen S, Yu L, Jiang C, Zhao Y, Sun D, Li S, et al. Pivotal Study of Iodine-131-Labeled Chimeric Tumor Necrosis Treatment Radioimmunotherapy in Patients With Advanced Lung Cancer. *J Clin Oncol* (2005) 23:1538–47. doi: 10.1200/JCO.2005.06.108
22. He XR, Han SY, Li PP. Recent Highlights of Chinese Medicine for Advanced Lung Cancer. *Chin J Integr Med* (2017) 23:323–30. doi: 10.1007/s11655-016-2736-2

23. Li QW, Qiu B, Wang B, Zhang J, Chen L, Zhou Y, et al. Comparison of Hyper- and Hypofractionated Radiation Schemes With IMRT Technique in Small Cell Lung Cancer: Clinical Outcomes and the Introduction of Extended LQ and TCP Models. *Radiother Oncol* (2019) 136:98–105. doi: 10.1016/j.radonc.2019.03.035
24. Lee HJ, Labaki W, Yu DH, Salwen B, Gilbert C, Schneider A, et al. Airway Stent Complications: The Role of Follow-Up Bronchoscopy as a Surveillance Method. *J Thorac Dis* (2017) 9:4651–9. doi: 10.21037/jtd.2017.09.139
25. Nakanishi M, Yoshida Y, Natazuka T. Prospective Study of Transarterial Infusion of Docetaxel and Cisplatin to Treat Non-Small-Cell Lung Cancer in Patients Contraindicated for Standard Chemotherapy. *Lung Cancer* (2012) 77:353–8. doi: 10.1016/j.lungcan.2012.04.006
26. Yuan Z, Li WT, Ye XD, Dong S, Peng WJ. Intra-Arterial Infusion Chemotherapy for Advanced Non-Small-Cell Lung Cancer: Preliminary Experience on the Safety, Efficacy, and Clinical Outcomes. *J Vasc Interv Radiol* (2013) 24:1521–8.e4. doi: 10.1016/j.jvir.2013.05.065
27. Zhu J, Zhang HP, Jiang S, Ni J. Neoadjuvant Chemotherapy by Bronchial Arterial Infusion in Patients With Unresectable Stage III Squamous Cell Lung Cancer. *Ther Adv Respir Dis* (2017) 11:301–9. doi: 10.1177/1753465817717169
28. Tanaka O, Hashimoto S, Narimatsu Y, Fujiwara H, Kurata T, Okuda S, et al. Can Selective CT Angiography Reduce the Incidence of Severe Complications During Transcatheter Arterial Embolization or Infusion Chemotherapy for Thoracic Diseases. *Diagn Interv Radiol* (2006) 12:201–5.
29. Fellows KE. Control of Massive Hemoptysis by Embolization of Intercostal Arteries. *Radiology* (1981) 140:249–50. doi: 10.1148/radiology.140.1.249-c
30. Mal H, Rullon I, Mellot F, Brugière O, Sleiman C, Menu Y, et al. Immediate and Long -Term Results of Bronchial Artery Embolization for Life-Threatening Hemoptysis. *Chest* (1999) 115:996–1001. doi: 10.1378/chest.115.4.996

Conflict of Interest: The authors declare that the research was conducted in the absence of any commercial or financial relationships that could be construed as a potential conflict of interest.

frontiers in Oncology

ORIGINAL RESEARCH
published: 03 February 2022
doi: 10.3389/fonc.2022.828432

aBVA Procedure by Uniportal Video-Assisted Thoracoscopic Surgery for Right Upper Peripheral Lung Cancer: A Randomized Trial

*Kaiying Wang, Jian Zhang, Jianglun Li, Langbo Liu, Zhongben Tang and Xiaojun Du**

Department of Thoracic Surgery, The Affiliated Hospital of Guizhou Medical University, Guiyang, China

Objective: This study aims to determine the optimal dividing order of anatomic pulmonary resection under uniportal video-assisted thoracoscopic surgery (uni-VATS) for patients with right upper peripheral lung cancer.

Methods: Patients who met the eligibility criteria were randomly allocated into the aBVA and VAB groups. In the aBVA group, the surgical procedure proceeded from the posterior to the anterior region (from the deeper to the superficial site). In the VAB group, the dissection orders were vein first followed by arterial branches, followed by the bronchus. Clinical data were collected and analyzed.

Results: Sixty patients were randomly allocated to the aBVA group (n = 30) and the VAB group (n = 30). The operation time in the aBVA group (230.500 ± 68.360 min) was significantly shorter than that in the VAB group (305.600 ± 107.821 min) (p = 0.01). The blood loss in the aBVA group (104.000 ± 70.935 ml) was significantly lower than that in the VAB group (391.000 ± 625.175 ml) (p = 0.01). Two patients in the VAB group underwent conversion to 2-portal VATS. The number of lymph nodes (13.367 ± 5.436 vs. 10.333 ± 7.279, p = 0.072) and lymph node stations (5.067 ± 1.574 vs. 4.467 ± 2.345, p = 0.567) were comparable between the two groups. The differences in the postoperative drainage tube time (5.033 ± 3.113 vs. 6.467 ± 4.447 days, p = 0.278) and hospital stay (8.233 ± 3.390 vs. 9.433 ± 4.523 days, p = 0.361) were not significantly different between the two groups.

Conclusion: Compared with the VBA procedure, aBVA is easier for patients with right upper peripheral lung cancer who undergo uni-VATS lobectomy.

Keywords: lung cancer, uniportal, VATS, procedure, lobectomy

OPEN ACCESS

Edited by:
Patrick J. Schuler, Ulm University Medical Center, Germany

Reviewed by:
Beatrice Aramini, University Hospital of Modena, Italy
Angelo Carretta, Vita-Salute San Raffaele University, Italy

***Correspondence:**
Xiaojun Du
xj.du@foxmail.com

Specialty section:
This article was submitted to Surgical Oncology, a section of the journal Frontiers in Oncology

Received: *03 December 2021*
Accepted: *12 January 2022*
Published: *03 February 2022*

Citation:
Wang K, Zhang J, Li J, Liu L, Tang Z and Du X (2022) aBVA Procedure by Uniportal Video-Assisted Thoracoscopic Surgery for Right Upper Peripheral Lung Cancer: A Randomized Trial. Front. Oncol. 12:828432. doi: 10.3389/fonc.2022.828432

INTRODUCTION

Lung cancer has the second highest incidence and highest mortality rate of cancer in both men and women worldwide (1). It is well known that surgical resection plays an important role in the comprehensive treatment of nonsmall cell lung cancer (NSCLC). In patients with NSCLC who underwent surgery, the right upper lobe had the highest incidence rate (23.8% to 47.0%) among the

five lung lobes (2–7). The current National Comprehensive Cancer Network (NCCN) guidelines for NSCLC suggest that for medically operable disease, resection is the preferred local treatment modality (other modalities include stereotactic ablative radiotherapy, thermal ablation such as radiofrequency ablation, and cryotherapy), and that anatomic pulmonary resection is preferred for the majority of patients with NSCLC (8). However, the optimal order of anatomical hilar resections remains controversial. In addition, the NCCN guidelines for NSCLC also suggest that video-assisted thoracoscopic surgery (VATS) or minimally invasive surgery (including robotic-assisted approaches) should be strongly considered for patients with no anatomical or surgical contraindictions (8). With the advantages of direct view, easy learning, reduced operation time and postoperative drainage duration, decreased postoperative pain and hospitalization, diminished inflammatory response, and faster access to chemotherapy (3, 9, 10), uniportal VATS (uni-VATS) has been widely accepted and used. Therefore, in this study, we attempted to distinguish the optimal order of anatomical pulmonary resection under uni-VATS for patients with right upper peripheral lung cancer.

MATERIALS AND METHODS

Study Design

This project was designed as a pilot, prospective, randomized controlled study and was approved by the Human Ethics Committee and the Research Ethics Committee of the Affiliated Hospital of Guizhou Medical University (Guizhou, China; approval no. 2021-475). Written informed consent was obtained from the parents or legal guardians for the use of their data in scientific research at the beginning of enrollment.

Patient Recruitment

Eligibility criteria included peripheral NSCLC diagnosed by preoperative computed tomography (CT) scan and pathological findings, operable disease confirmed by preoperative evaluation, and male or female patients. The exclusion criteria were as follows: peripheral massive lesion involving the hilar, calcification of hilar lymph nodes, and complications that were planned to be simultaneously managed by surgery or other surgical contraindications that might impact the perioperative outcomes of surgery, such as seriously poor cardiopulmonary function.

Randomization

Patients who met the eligibility and exclusion criteria were randomly allocated into the aBVA and VAB groups by minimization (11, 12) based on clinicopathological characteristics, including age, sex, pathology, and TNM stage as the eighth edition of the TNM Classification for Lung Cancer (13).

Surgical Procedure

All surgical procedures were performed by the same team. The details of the procedure we used were similar to those described previously (14). However, there were some components that should be reiterated. The incision, approximately 3.0 to 4.0 cm long, was performed at the fifth intercostal space, between the anterior axillary line and posterior axillary line. A small disposable plastic wound protector was used to stretch the incision. A 30°, 10-mm high-definition camera thoracoscope was used to provide a panoramic view and placed at the posterior part of the incision. Wedge resection of the lesions was then performed first in both groups. The main differences between the two groups were the order of the hilar structures to be dissected. In the aBVA group (**Figure 1** and **Video S1**), the procedure proceeded from the posterior to the anterior region (from the deeper to the superficial site). The fissure was stapled first if it was incomplete using the tunnel technique (15), and the posterior ascending artery ("a" in aBVA) was then cut followed by the upper bronchus. The upper arterial branches (including variant arterial branches) were then stapled as well as the upper vein simultaneously with a stapler as the last step.

To shorten the operation duration and reduce the risk of vessel injury, the hilar lymph nodes and surrounding tissue were dissociated from the mediastinum and pushed to the distal end (not removed from the chest right now), which was extracted along with the upper lung in a protective bag when the lobectomy was completed and removed *in vitro* for histopathological examination.

In the VAB group (**Figure 2** and **Video S2**), the dissecting orders were as follows: the upper vein was stapled first, followed by the upper arterial branches and variant arterial branches, stapling the fissure if it was incomplete. The posterior ascending

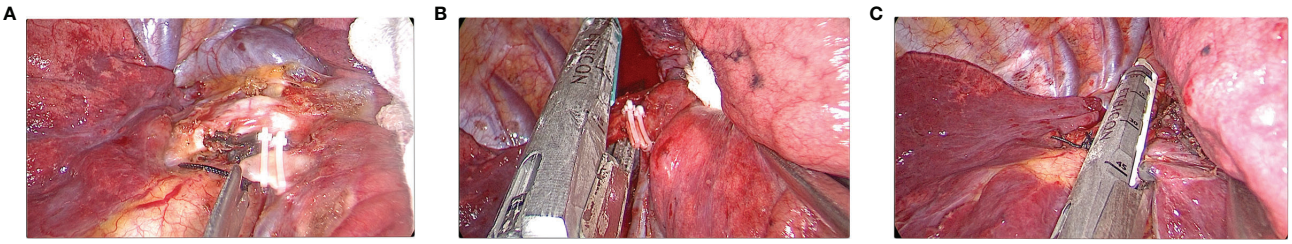

FIGURE 1 | The main steps of the aBVA procedure. **(A)** Cutting the posterior ascending artery ("a" in aBVA), **(B)** stapling the upper bronchus, and **(C)** stapling the upper arterial branches (including variant arterial branches) as well as upper vein simultaneously.

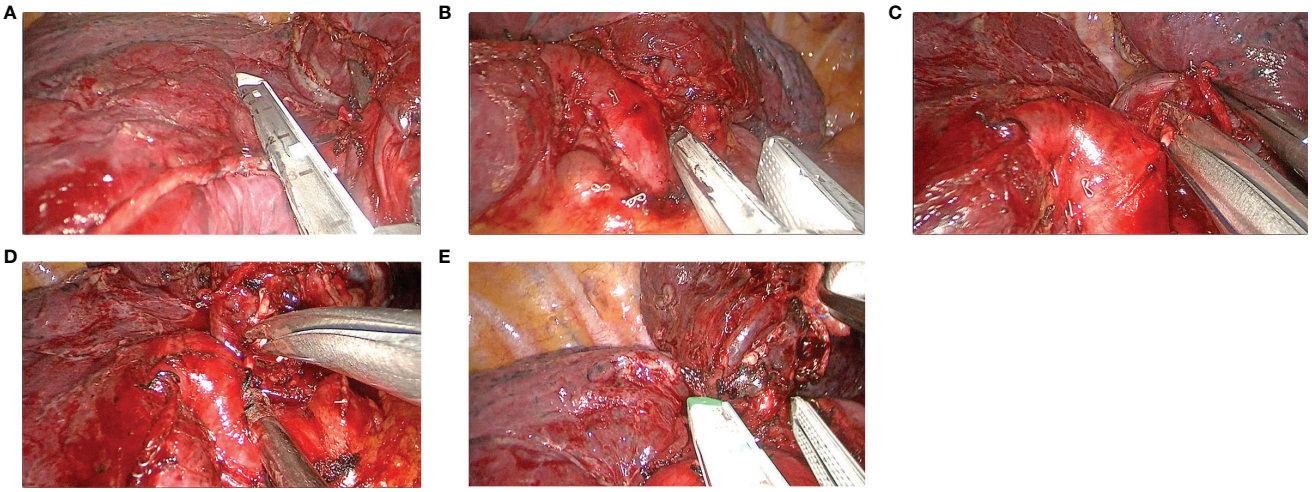

FIGURE 2 | The main steps of the VAB procedure. **(A)** Stapling the upper vein, **(B)** stapling the upper arterial branches, **(C)** cutting the variant arterial branches, **(D)** cutting the posterior ascending artery, and **(E)** stapling the upper bronchus.

artery was then cut, and the upper bronchus was stapled as the last step.

When the fissure was complete, lobectomy was easier and faster in both groups because the artery in the fissure was exposed, and no lung parenchyma was incised. As a rule, in both groups, double ligation was used for all vessels less than 10 mm in diameter; otherwise, a stapler was used. Systemic node dissection was performed to remove the right upper and lower paratracheal, subcarinal, paraesophageal, and pulmonary ligament lymph nodes. At the end of the surgery, one intercostal drain was placed through the incision, as described previously (16), and was removed postoperatively when the daily drainage was <200 ml with no air leakage and sufficient lung expansion on chest X-rays. Patients were usually discharged the day after the chest tube removal and were routinely followed up after 1 week, every 3 months until 2 years postoperatively, and every 6 months thereafter.

Conversion to Multiportal VATS or Thoracotomy

The surgeons made the decision to convert to multiportal VATS if the operation was difficult to proceed or thoracotomy when uncontrolled bleeding occurred. If conversion to multiportal VATS was required, a 1.2-cm assistant incision at the midaxillary line or another 1.2 cm assistant incision at the posterior axillary line was performed at the seventh intercostal space. When conversion to thoracotomy was needed, anterior and posterior extension of the uniportal incision to about 10 cm in length at the fifth intercostal space was made.

Data Collection and Statistical Analysis

All clinical data were collected from the institutional database, anesthesia and surgical notes, and medical and nursing records. Descriptive statistics were used to describe the demographic characteristics. Continuous variables were presented as mean ± standard deviation (mean ± SD), and categorical variables are presented as numbers and percentages. When variances were equal, a two-sample unpaired *t*-test with equal variance was used for continuous variables. For unequal variances, the two-sample Wilcoxon rank-sum (Mann-Whitney) test was used. χ^2 or Fisher's exact test was used for binary categorical data, and results are presented as odds ratios (ORs) and 95% confidence intervals (CIs). Statistical analysis was performed using Stata 15.0 (StataCorp LP). All statistical tests were two sided, and $p < 0.05$ was considered to indicate a statistically significant difference.

RESULTS

Sixty consecutive patients with right upper peripheral NSCLC were randomly allocated to the aBVA group ($n = 30$) and the VAB group ($n = 30$). The differences in the clinicopathological characteristics between the aBVA and VAB groups were not significant (**Table 1**). The operating time in the aBVA group (230.500 ± 68.360 min) was significantly lower than that in the VAB group (305.600 ± 107.821 min) ($p = 0.01$). Consequently, the blood loss in the aBVA group (104.000 ± 70.935 ml) was significantly lower than that in the VAB group (391.000 ± 625.175 ml) ($p = 0.01$). Two patients in the VAB group underwent conversion to 2-portal VATS because of difficulty in placing the stapler around the superior pulmonary vein due to a lack of angle. The number of lymph nodes (13.367 ± 5.436 vs. 10.333 ± 7.279, $p = 0.072$) and lymph node stations (5.067 ± 1.574 vs. 4.467 ± 2.345, $p = 0.567$) were comparable between the two groups. The differences in the postoperative drainage tube time (5.033 ± 3.113 vs. 6.467 ± 4.447 days, $p = 0.278$) and hospital stay (8.233 ± 3.390 vs. 9.433 ± 4.523 days, $p = 0.361$) were not significant between the two groups (**Table 2**). No uncontrolled bleeding or perioperative death occurred, and no conversion to thoracotomy was needed in either group.

TABLE 1 | Differences in clinicopathological characteristics between the VAB and aBVA groups.

Characteristics	VAB group	aBVA group	*p*
Sex			
Female	18	14	0.301
Male	12	16	
Age	59.933 ± 8.103	58.033 ± 7.360	0.345
Pathology			
SCC	4	8	0.197
AC	26	22	
T			
1a	4	5	0.343*
1b	12	7	
1c	5	3	
2a	7	14	
2b	1	0	
3	1	1	
N			
0	23	24	0.809*
1	2	3	
2	5	3	
Stage			
I	16	15	0.356*
IIA	4	9	
IIB	5	2	
IIIA	5	4	

SCC, squamous cell carcinoma; AC, adenocarcinoma.
**Fisher's exact test.*

DISCUSSION

The current NCCN guidelines for NSCLC suggest that anatomical pulmonary resection is preferred for the majority of patients with NSCLC (8). However, the optimal order for anatomical resection remains controversial. Traditionally, it has been suggested that the pulmonary vein be cut first to avoid dissemination of tumor cells, which could consequently lead to blood micrometastasis and treatment failure (17–21). However, other studies concluded that the sequence of ligation of pulmonary vessels did not seem to influence oncological outcomes or survival (22–24). Despite the controversy, we still performed wedge resections first for the sake of clarity in the present study.

In addition, the NCCN guidelines for NSCLC suggest that VATS or minimally invasive surgery (including robotic-assisted approaches) should be strongly considered for patients with no anatomical or surgical contraindictions (8). With the advantages of direct view, easy learning, less operation time and postoperative drainage duration, decreased postoperative pain and hospitalization, diminished inflammatory response, and faster access to chemotherapy (3, 9, 10), uni-VATS has been widely accepted and used. Therefore, anatomical right upper pulmonary resection was performed using uni-VATS in this study.

The results of this study demonstrated that the operation time (230.500 ± 68.360 vs. 305.600 ± 107.821 min, $p = 0.01$) and blood loss (104.000 ± 70.935 vs. 391.000 ± 625.175 ml, $p = 0.01$) in the aBVA group were significantly shorter than those in the VAB group. These results were in accordance with those of a previous retrospective study by Zhai et al. (22). These advantages may be attributed to the change in the hilar cutting order. It is well known that in the VAB procedure, the upper pulmonary vein is the most difficult structure to divide first with a stapler through a single incision because it is difficult to achieve better angles for stapler insertion. Many solutions have been attempted, for example, using

TABLE 2 | Differences in surgical outcomes between the VAB and aBVA groups.

Characteristics	VAB group	aBVA group	*p*
Surgical time (min)	305.600 ± 107.821	230.500 ± 68.360	0.001*
Blood loss (ml)	391.000 ± 625.175	104.000 ± 70.935	<0.001*
No. LN removed (*n*)	10.333 ± 7.279	13.367 ± 5.436	0.072
No. LNS removed (*n*)	4.467 ± 2.345	5.067 ± 1.574	0.567*
Conversion (*n*)			
No	28	30	0.492**
Yes	2	0	
Tube stay (days)	6.467 ± 4.447	5.033 ± 3.113	0.278*
Hospital stay (days)	9.433 ± 4.523	8.233 ± 3.390	0.361*

LN, lymph nodes; LNS, lymph node station.
**Wilcoxon rank-sum (Mann-Whitney) test; **Fisher's exact test.*

curved-tip staplers or polymer vascular clips, ligation of the vein using sutures, and cutting the upper arterial branches first (9, 10, 14). When the aBVA procedure is used, it is easy to cut the posterior ascending artery first and the upper bronchus with a stapler through a single incision because they are farther away from the incision. It is easier then to cut the upper pulmonary vein as well as the upper arterial branches (including variant arterial branches), as they have increased degrees of freedom.

The results of this study also showed that the number of lymph nodes (13.367 ± 5.436 vs. 10.333 ± 7.279, $p = 0.072$) and lymph node stations (5.067 ± 1.574 vs. 4.467 ± 2.345, $p = 0.567$) were comparable between the two groups. The differences in the postoperative drainage tube time (5.033 ± 3.113 vs. 6.467 ± 4.447 days, $p = 0.278$) and hospital stay (8.233 ± 3.390 vs. 9.433 ± 4.523 days, $p = 0.361$) were not significantly different between the two groups. This implies that the aBVA procedure can achieve short-term surgical outcomes similar to those of the VAB procedure.

The present study had some limitations. It failed to compare the two procedures in patients with central lung cancer and lacked the results of long-term surgical outcomes. Further investigation is required to address these issues.

CONCLUSION

In conclusion, for patients with right upper peripheral lung cancer, compared with the VAB procedure under uni-VATS, the aBVA procedure is easier and can achieve the same short-term surgical outcomes; therefore, it is worth promoting the application of the aBVA procedure in clinics.

DATA AVAILABILITY STATEMENT

The raw data supporting the conclusions of this article will be made available by the authors, without undue reservation.

ETHICS STATEMENT

The studies involving human participants were reviewed and approved by the ethics board of the Affiliated Hospital of Guizhou Medical University. The patients/participants provided their written informed consent to participate in this study.

AUTHOR CONTRIBUTIONS

KW, JZ, LL, JL, ZT, and XD analyzed and interpreted the data. KW, LL, and JL were major contributors in writing the manuscript. KW, ZT, and XD confirm the authenticity of all the raw data. All authors read and approved the final manuscript.

FUNDING

This study was partly funded by the Beijing Xisike Clinical Oncology Research Foundation (grant no. Y-Q201801-006) and the Science and Technology Fund Project of the Health Commission of Guizhou Province (grant no. Gzwjkj2020-1-111).

SUPPLEMENTARY MATERIAL

The Supplementary Material for this article can be found online at: https://www.frontiersin.org/articles/10.3389/fonc.2022.828432/full#supplementary-material

Supplementary Video 1 | The main steps of the aBVA procedure.

Supplementary Video 2 | The main steps of the VAB procedure.

REFERENCES

1. Siegel RL, Miller KD, Jemal A. Cancer Statistics, 2020. *CA A Cancer J Clin* (2020) 70:7–30. doi: 10.3322/caac/21590
2. Flores RM, Park BJ, Dycoco J, Aronova A, Hirth Y, Rizk NP, et al. Lobectomy by Video-Assisted Thoracic Surgery (VATS) Versus Thoracotomy for Lung Cancer. *J Thorac Cardiovasc Surg* (2009) 138:11–8. doi: 10.1016/j.jtcvs.2009.03.030
3. Matsuura N, Igai H, Ohsawa F, Yazawa T, Kamiyoshihara M. Uniport vs. Multiport Video-Assisted Thoracoscopic Surgery for Anatomical Lung Resection-Which Is Less Invasive? *J Thorac Dis* (2001) 13:244–51. doi: 10.21037/jtd-20-2759
4. Menna C, Poggi C, Andreetti C, Maurizi G, Ciccone AM, D'Andrilli A, et al. Does the Length of Uniportal Video-Assisted Thoracoscopic Lobectomy Affect Postoperative Pain? Results of a Randomized Controlled Trial. *Thorac Cancer* (2020) 11:1765–72. doi: 10.1111/1759-7714.13291
5. Lim CG, Shin KM, Lim JS, Lim JK, Kim HJ, Kim WH, et al. Predictors of Conversion to Thoracotomy During Video-Assisted Thoracoscopic Surgery Lobectomy in Lung Cancer: Additional Predictive Value of FDG-PET/CT in a Tuberculosis Endemic Region. *J Thorac Dis* (2017) 9:2427–36. doi: 10.21037/jtd.2017.07.40
6. Byun CS, Lee S, Kim DJ, Lee JG, Lee CY, Jung I, et al. Analysis of Unexpected Conversion to Thoracotomy During Thoracoscopic Lobectomy in Lung Cancer. *Ann Thorac Surg* (2015) 100:968–73. doi: 10.1016/j.athoracsur.2015.04.032
7. Samson P, Guitron J, Reed MF, Hanseman DJ, Starnes SL. Predictors of Conversion to Thoracotomy for Video-Assisted Thoracoscopic Lobectomy: A Retrospective Analysis and the Influence of Computed Tomography–Based Calcification Assessment. *J Thorac Cardiovasc Surg* (2013) 145:1512–8. doi: 10.1016/j.jtcvs.2012.05.028
8. Ettinger DS, Wood DE, Aisner D, Akerley W, Bauman JR, Bharat A, et al. *NCCN Clinical Practice Guidelines in Oncology: Non-Small Cell Lung Cancer. Version 5. 2021* (2021). Available at: https://www.nccn.org/guidelines/guidelines-detail?category=1&id=1450 (Accessed June 16, 2021).
9. Gonzalez-Rivas D. Uniportal Thoracoscopic Surgery: From Medical Thoracoscopy to non-Intubated Uniportal Video-Assisted Major Pulmonary Resections. *Ann Cardiothorac Surg* (2016) 5:85–91. doi: 10.21037/acs.2016.03.07
10. Gonzalez-Rivas D, Paradela M, Fernandez R, Delgado M, Fieira E, Mendez L, et al. Uniportal Video-Assisted Thoracoscopic Lobectomy: Two Years of Experience. *Ann Thorac Surg* (2013) 95:426–32. doi: 10.1016/j.arthoracsur.2012.10.070
11. Taves DR. Minimization: A New Method of Assigning Patients to Treatment and Control Groups. *Clin Pharmacol Ther* (1974) 15:443–53. doi: 10.1002/cpt1974155443
12. Treasure T, MacRae KD. Minimisation: The Platinum Standard for Trials? Randomisation Doesn't Guarantee Similarity of Groups; Minimistaion Does. *BMJ* (1998) 317:362–3. doi: 10.1136/bmj.317.7155.362
13. Goldstraw P, Chansky K, Crowley J, Rami-Porta R, Asamura H, Eberhardt WEE, et al. The IASLC Lung Cancer Staging Project: Proposals for Revision of the TNM Stage Groupings in the Forthcoming (Eighth) Edition of the TNM

Classification for Lung Cancer. *J Thorac Oncol* (2016) 11:39–51. doi: 10.1016/j.jtho.2015.09.009
14. Gonzalez-Rivas D, Fieira E, Delgado M, Mendez L, Fernandez R, de la Torre M. Uniportal Video-Assisted Thoracoscopic Lobectomy. *J Thorac Dis* (2013) 5:12. doi: 10.3978/j.issn.2071-1439.2013.07.30
15. Decaluwe H, Sokolow Y, Deryck F, Stanzi A, Depypere L, Moons J, et al. Thoracoscopic Tunnel Technique for Anatomical Lung Resections: A 'Fissure First, Hilum Last' Approach With Staplers in the Fissureless Patient. *Interact Cardiovasc Thorac Surg* (2015) 21:2–7. doi: 10.1093/icvts/ivv048
16. Du X, Chen G, Tian D, Xie L, Zhou H. Modified Tube Fixation Technique for Uniportal Video-Assisted Thoracic Surgery. *VATS* (2018) 3:45–5. doi: 10.21037/vats.2018.10.03
17. Sawabata N, Funaki S, Hyakutake T, Shintani Y, Fujiwara A, Okumura M. Perioperative Circulating Tumor Cells in Surgical Patients With non-Small Cell Lung Cancer: Does Surgical Manipulation Dislodge Cancer Cells Thus Allowing Them to Pass Into the Peripheral Blood? *Surg Today* (2016) 46:1402–9. doi: 10.1007/s00595-016-1318-4
18. Duan X, Zhu Y, Cui Y, Yang Z, Zhou S, Han Y, et al. Circulating Tumor Cells in the Pulmonary Vein Increase Significantly After Lobectomy: A Prospective Observational Study. *Thorac Cancer* (2019) 10:163–9. doi: 10.1111/1759-7714.12925
19. Sawabata N, Nakamura T, Kawaguchi T, Watanabe T, Ouji NS, Ito T, et al. Circulating Tumor Cells Detected Only After Surgery for Non-Small Cell Lung Cancer: Is it a Predictor of Recurrence? *J Thorac Dis* (2020) 12:4623–32. doi: 10.21037/jtd-20-1636
20. Hashimoto M, Tanaka F, Yoneda K, Takuwa T, Matsumoto S, Okumura Y, et al. Positive Correlation Between Postoperative Tumor Recurrence and Changes in Circulating Tumor Cell Counts in Pulmonary Venous Blood (pvCTC) During Surgical Manipulation in non-Small Cell Lung Cancer. *J Thorac Dis* (2018) 10:298–306. doi: 10.21037/jtd.2017.12.56
21. Long X, Wu B, Zhang W, Lv G, Yu D, Peng J, et al. Effects of Vessel Interruption Sequence During Lobectomy for Non-Small Cell Lung Cancer: A Systematic Review and Meta-Analysis. *Front Surg* (2021) 8:694005. doi: 10.3389/fsurg.2021.694005
22. Zhai H-R, Yang X-N, Nie Q, Liao RQ, Dong S, Li W, et al. Different Dissecting Orders of the Pulmonary Bronchus and Vessels During Right Upper Lobectomy Are Associated With Surgical Feasibility and Postoperative Recovery for Lung Cancer Patients. *Chin J Cancer* (2017) 36:53. doi: 10.1186/s40880-017-0220-9
23. Kozak A, Alchimowicz J, Safranow K, Wojcik J, Kochanowski L, Kubisa B, et al. The Impact of the Sequence of Pulmonary Vessel Ligation During Anatomic Resection for Lung Cancer on Long-Term Survival – A Prospective Randomized Trial. *Adv Med Sci* (2013) 58:156–63. doi: 10.2478/v10039-012-0061-3
24. Refaely Y, Sadetzki S, Chetrit A, Simansky DA, Paley M, Modan B, et al. The Sequence of Vessel Interruption During Lobectomy for non–Small Cell Lung Cancer: Is it Indeed Important? *J Thorac Cardiovasc Surg* (2003) 125:1313–20. doi: 10.1016/s0022-5223(03)00022-9

Conflict of Interest: The authors declare that the research was conducted in the absence of any commercial or financial relationships that could be construed as a potential conflict of interest.

frontiers in Oncology

ORIGINAL RESEARCH
published: 11 February 2022
doi: 10.3389/fonc.2022.810367

Improving the Quality of Human Upper Urinary Tract Specimens by Cryobiopsy

Jan T. Klein[1†], *Axel John*[1], *Lars Bohnert*[1], *Markus D. Enderle*[2], *Walter Linzenbold*[2] *and Christian Bolenz*[1*]

[1] Department of Urology, University of Ulm, Ulm, Germany, [2] Department of Research and Basic Technologies, Erbe Elektromedizin GmbH, Tuebingen, Germany

OPEN ACCESS

Edited by:
Aali Jan Sheen,
Manchester Royal Infirmary,
United Kingdom

Reviewed by:
Julia Heinzelbecker,
Saarland University Hospital, Germany
Giuseppe Simone,
Regina Elena National Cancer Institute,
Hospital Physiotherapy Institutes
(IRCCS), Italy

***Correspondence:**
Christian Bolenz
christian.bolenz@uniklinik-ulm.de

†ORCID:
Jan T. Klein
orcid.org/0000-0002-9884-8733

Specialty section:
This article was submitted to
Surgical Oncology,
a section of the journal
Frontiers in Oncology

Received: 06 November 2021
Accepted: 05 January 2022
Published: 11 February 2022

Citation:
Klein JT, John A, Bohnert L,
Enderle MD, Linzenbold W and
Bolenz C (2022) Improving the
Quality of Human Upper Urinary
Tract Specimens by Cryobiopsy.
Front. Oncol. 12:810367.
doi: 10.3389/fonc.2022.810367

Objective: The quality of histopathological specimens obtained from the upper urinary tract with conventional flexible ureterorenoscopic biopsy needs to be improved. We investigated the feasibility and biopsy quality of specimens obtained by cryobiopsy, compared with standard ureterorenoscopic biopsy techniques in a human ex vivo model.

Materials and Methods: Human ureters obtained from nephrectomy specimens (N=12) were dissected and canulated with an ureteral access sheath. Ureterorenoscopic biopsies were randomly obtained from different sites of the renal pelvic caliceal system using different types of instruments. The performance of two newly developed flexible cryoprobes with outer diameters of 1.1 mm (CB11) and 0.9 mm (CB09) was compared with that of the biopsy forceps(FB) and Bigopsy®(BiG) and two different Dormia baskets N-Gage (NG) and Zero-Tip (ZT). We assessed the feasibility of the various biopsy techniques based on the number of biopsy attempts needed to obtain macroscopically discernible biopsies. The specimens were examined histopathologically for size, biopsy quality, presence of various artifact types, and representativeness.

Results: Biopsies taken with the cryoprobes showed a higher biopsy quality than biopsies taken with the comparative instruments. The CB11 provided significantly larger biopsies than forceps biopsies and also than biopsies with ZT. The CB09 was able to collect larger samples when compared with the FB and BiG biopsy forceps. There were no significant differences in artifact area, except for the CB11 cryoprobe compared with the NG. To clarify the results a subdivision of larger or smaller than 20% artifact area was performed. A significant difference was found between CB11 and the forceps biopsies, as well as between CB11 and NG and ZT in favor of the cryoprobe. The representation of the histopathological sample was also determined. Biopsies taken with CB11 were more representative compared with forceps biopsies BiG and FB and basket biopsies NG and ZT.

Conclusions: In a standardized comparative ex vivo setting, larger biopsies were obtained by using the cryobiopsy technique with the CB11 probe. Qualitatively, cryobiopsy specimens were overlaid by fewer artifacts and a higher biopsy quality was achieved in histopathologic examination compared with standard instrumentation. Further stepwise development will transfer the promising cryobiopsy technique into the clinical setting.

Keywords: upper tract urinary cancer, cryobiopsy, biopsy devices, UTUC, new biopsy devices

INTRODUCTION

Upper urinary tract carcinoma (UTUC) is a relatively rare entity, representing 5-10% of all urothelial carcinomas (1). UTUC has similar morphology as bladder carcinomas and almost all UTUCs are urothelial in origin. Surprisingly, UTUCs are much more frequently invasive compared to urothelial carcinoma of the urinary bladder at the time of diagnosis (1). Organ-preserving treatment strategies have been developed for many other tumor entities and are also available for UTUC under certain conditions (1). The decision for or against a kidney-preserving therapy procedure is based on a correct histological classification of the tumor into low- or high-risk tumor. Histopathological grading and staging are essential for determining treatment options and prognoses. Without biopsies, the diagnosis rate is only 50-60%. With additional ureterorenoscopic biopsies, the rate is 80-90%. The biopsy procedure used must allow for a differentiation between these two groups. The type of biopsy technique influences the diagnosis. The combination of forceps biopsy and Dormia basket shows the best biopsy quality to date (1). However, despite current biopsy instruments and procedures, a considerable number of biopsies are proven to be too small and of insufficient diagnostic value due to artifact overlay. This means that sampling is prone to errors and does not allow a reliable diagnosis in every case. In a quarter of all cases, adequate grading cannot be performed because the tissue sample is too small (1-2mm) or crush artifacts and associated disturbances of the tissue architecture occur (2). Restaging or regrading after radical nephroureterectomy is required in approximately one third of all cases (3). It was reported that biopsies <1mm may not allow for reliable diagnosis (4). The quality of the preparation depends on the type of biopsy forceps used. Novel frontloading biopsy forceps are superior to the classic backloading ones, especially for flat or sessile lesions (5). To overcome these limitations, the arsenal of biopsy instruments is expanded to include the "Dormia baskets". For papillary lesions, basket biopsy is particularly suitable (5).

There is a trend toward understaging; for example, 45% of tumors initially classified as Ta have to be graded to pT1 or higher postoperatively. Some tumor entities, such as carcinoma *in situ*, almost completely escape diagnoses. Thus, histopathologic diagnosis needs much improvement (6).

Improving the diagnostic accuracy is currently subject to several research projects. For this purpose, non-invasive diagnostic techniques such as narrowband imaging, optical coherence tomography, confocal laser microscopy or photodynamic diagnostics have been investigated. These technologies improve the optical detection of tumor tissue and allow an in-situ assessment of tumor tissue. However, this does not affect the biopsy quality itself.

The cryoprobe itself is already used in other medical fields, such as in the ablation of tumors or in the treatment of atrial fibrillation (7, 8). Cryotechnology has been successfully and diagnostically used on humans in pulmonology for transbronchial lung biopsies in suspected interstitial lung diseases (9). Larger, higher quality samples with fewer complications can be obtained from human tissue (10–12). The sample size depends on the type of tissue, the probe diameter, the application time and the contact pressure (13). In addition, despite the freezing process, molecular markers can be retained in the tissue, which indicates that the tissue integrity remains intact (14). Ureterorenoscopic cryobiopsy could decisively improve the quality of the histopathological biopsate obtained, thus making a significant contribution to organ preservation in UTUC.

We have previously shown that cryobiopsy is feasible in the upper urinary tract of porcine kidneys. In this animal study, larger samples with a low artifact load have been successfully obtained (15). In addition, compared to the other biopsy devices, the cryoprobe did not produce crush artifacts and consistently yielded pathologically assessable samples. There are no data in the literature on the use of cryobiopsy in the human upper urinary tract. In order to evaluate the feasibility and value of cryobiopsy in this field, the use of the cryoprobe was performed in an ex vivo experiment on the human urinary tract.

MATERIALS AND METHODS

Study Design and Patient Selection

The study had a controlled, prospective, single-blinded, monocentric design. Patients for whom removal of the kidney was indicated for various reasons were enrolled in the study. Patients with renal tumors and patients with high-risk UTUC requiring nephrectomy were included. To determine the feasibility of cryobiopsy, the sample volume, and the artifact area, we also included patients with chronic kidney disease and clinically non-functioning kidneys (e.g., chronic pyelonephritis or shrunken kidney) that needed to be removed for appropriate indications, such as hypertension, chronic urinary tract infection, or recurrent pain. In total, N=12 patients were enrolled in the study.

Patients with florid local renal inflammation, systemic inflammation in the context of sepsis or acute renal trauma who required emergency nephrectomies and transplant kidneys were excluded because the pathomorphological changes expected in these patients could have confounded the results. In addition, patients under 18 years of age, pregnant patients and patients unable to give their own consent were excluded. This study was approved by the local ethic review board.

Cryoprobe

Two disposable types of cryoprobes (Erbe Elektromedizin GmbH, Germany) were used in this study: one with an outer diameter of 1.1 mm (CB11), which is already available on the market, and one prototype of a new cryoprobe with an outer diameter of 0.9 mm (CB09). The cryoprobes are connected to a standard carbon dioxide gas pressure cylinder *via* the control unit, the ERBEKRYO2 device (Erbe Elektromedizin GmbH, Germany), which are inserted in retrograde into the ureterorenoscope. Activation and activity duration, and thus ice ball formation at the cryoprobe tip, can be determined *via* a foot pedal connected to the control unit.

The principle of the cryoprobe is based on the Joule-Thomson effect, which describes a temperature reduction through the sudden decompression of a gas (here CO_2). The probe itself consists of an outer tube, an inner lumen and an outer lumen. In the inner lumen, the compressed gas flows at a pressure of approximately 55 bar to the tip of the probe, where an abrupt decompression of the gas occurs resulting in the cooling of the metal probe tip. The gas flows through the outer lumen back to the control unit and is released to the room.

The metal tip is brought into contact with the tissue to be biopsied. The activated metal tip of the cryoprobe cools the tissue. Very fine ice crystals form initially, and on further activation, an ice ball encloses the tissue undergoing biopsy. The ice crystals cause the tissue to adhere to the metal surface of the probe, so that the sample adheres to the metal tip by adhesion and can be released from the tissue dressing with a jerk of the probe.

Two factors determine the sample size: first, the probe contact pressure, which can be determined manually by the surgeon. Second, which is the most influencing factor that can be set on the control unit, is the freezing duration.

To obtain optimal biopsy sizes, it is important that the ice ball surrounding the tissue is not too large, so that the ice ball's adhesion to the tissue is weaker than to the probe; otherwise, this would cause the ice ball to detach from the probe tip. In addition, the sample must be large enough to allow for histopathological evaluation. We have determined these parameters to be optimal at a sampling time of 7 seconds for both cryoprobes. In this case, cell morphology is preserved despite the freezing process and the sampling can reliably succeed.

The timer of the ERBEKRYO device starts as soon as the pedal is pressed and can be read on a connected display or can be detected acoustically. With the cryoprobe, biopsies can be taken both tangentially or frontally. After the specified activation time, the probe and endoscope are pulled out as a unit with a jerk movement through the ureteral access sheath, as the sample adhering to the probe is too large to fit through the working channel of the endoscope. After the extraction process is complete, the cryoprobe is deactivated and the ice ball forms back. The biopsy detaches from the metal tip and can be preserved in a formalin-containing container for pathology.

Ex Vivo Model Human Nephrectomy Specimen

The nephrectomy specimen was harvested. One specimen was a nonfunctional hydronephrotic kidney, seven kidneys had been removed for locally advanced renal cell carcinoma, and four kidneys had been removed for upper tract urothelial carcinoma. The ureter was dissected, dilated and a ureteral access sheath (Navigator®, 13/15 Ch, 28cm, (Boston Scientific, Marlborough, Massachusetts, US) was inserted and fixed. In order to create an optimal basis for comparison, we always used a brand-new disposable flexible ureterorenoscope LithoVue® (Boston Scientific, Marlborough, Massachusetts, US). The biopsies were performed under 0,9% saline irrigation with the different devices in a randomized order. The experimental setup is shown in **Figure 1**. The following biopsy instruments were used: two different disposable cryoprobes with outer diameters of 1.1 mm (CB11) and 0.9 mm (CB09) (Erbe Elektromedizin, Tuebingen, Germany), reusable biopsy forceps (FB) for flexible ureteroscopy (No. 829.601, Richard Wolf GmbH, Knittlingen, Germany), and a frontloading disposable biopsy forceps for the upper urinary tract (BIGopsy® No. BLB-024115, Cook Medical, Bloomington, IN, US). Additionally, two different tipless Dormia baskets were used: a front grasping N-Gage® basket (No. NGE-022115, 2.2F Cook Medial, Bloomington, IN, US) (NG) and a side grasping Dormia basket: Zero-Tip® (No. 390105; UPN M0063901050, Boston Scientific, Marlborough, Massachusetts, US) (ZT) (**Figure 2**). This corresponds with the standard instruments for biopsies in the upper urinary tract. For data processing, a study ID was determined for each patient and recorded in an Excel spreadsheet in CRF format, which ensured the pseudonymization of the patients. Only when the data were complete and representative were they entered into the study database. A histopathological examination was performed using a standard microscope (Axio Vision LE REL 4.4; Carl Zeiss Microimaging, Göttingen, Germany). Up to three biopsies were obtained with each probe. The number of biopsy attempts and potential biopsies obtained per instrument, per kidney in all twelve kidney specimens examined are shown in **Table 1**.

We assessed whether it was generally possible to obtain a biopsy with the different devices, regardless of the quality or quantity of the biopsy. "Yes" meant that a macroscopically identifiable sample could be obtained within 3 attempts and hence feasible, "no" meant that a sample could not be obtained. This was assessed immediately after each biopsy.

The biopsy reliability was determined by the number of times a biopsy had to be performed before a sample was successfully obtained. The number was recorded. The tissue sample was considered "not obtained" if macroscopic tissue could not be obtained, even on the third attempt. Subsequently, whether a sample could already be successfully obtained was analyzed during the first biopsy attempt.

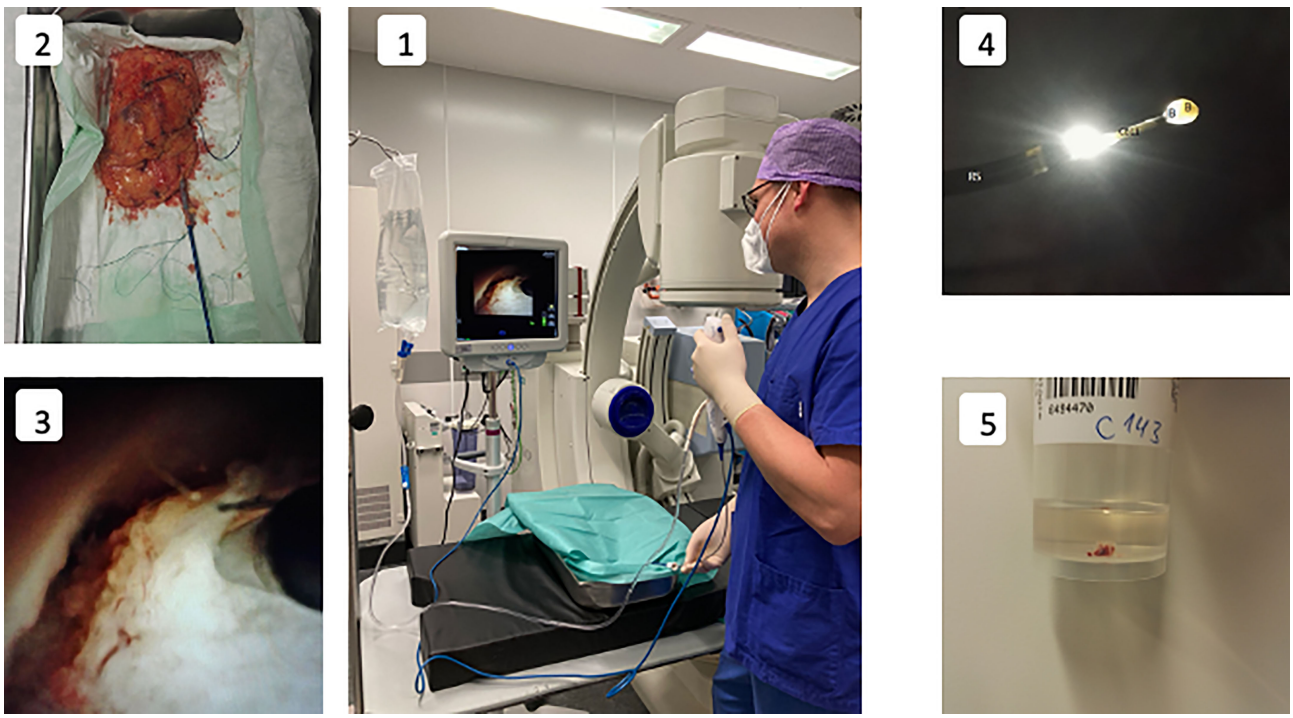

FIGURE 1 | Experimental setup and procedure. 1: Experiment setup-surgeon performing a endoscopic biopsy under irrigation with sodium chloride solution utilising a digital ureterorenoscope. 2: Kidney specimen with attached ureter cannulated with an access sheath. 3: Endoscopic visualization of cryoprobe (CB11) in the renal pelvicocaliceal system almost in contact with the tissue, shortly before activation. 4: Ureteroscope (RS) after biopsy with the cryoprobe (CB11) with ice ball (IB) adhering to the tip of the cryoprobe and a biopsy specimen (B) enclosed within. 5: Container for the biopsy specimen. The formalin solution cotains a macroscopically visible cryobiopsy specimen.

Histopathologic Evaluation

All obtained biopsy specimens were fixed in 4.5% neutral buffered formalin, processed into paraffin blocks, and stained with hematoxylin and eosin. Subsequently, the samples were analyzed by the reference pathologist (TB) using a predefined histology score for the following parameters: Total area of the specimen in mm^2, biopsy quality score, percentage of artifact area and presence of squeeze artifacts. The biopsy area was determined based on the length and width of the sample. There is already a scheme for assessing quality from pneumology (13, 16), which has been adapted in more detail for urology (15). The histopathologic quality score is evaluated using an ordinal scale and was also assessed by an experienced pathologist (TB). The artifact area was defined by the area fraction of the artifacts in relation to the cross-sectional area of the sample. A specimen was considered representative if, first, it was large enough to perform a histopathologic examination, second, it had an artifact score of 0-1, and third, if the quality was rated at least at 2.

Statistical Analyses

Statistical analysis of the samples was performed using IBM SPSS Statistics version 27 for Windows (released 2020, Armonk, NY, IBM Corp.). The chi-square test was used to test whether two categorically distributed variables were statistically different. We used this test to determine whether the biopsy was successful in the first attempt and to examine whether it was possible to obtain samples at all. We also used it to calculate whether the specimens differed significantly in their artifact area, by dividing them into specimens with an artifact area greater than 20% and also less than 20%. The chi-square test was used to test representativeness for statistical significance. A one-way analysis of variance (ANOVA) with Welch correction was used for unpaired data from the Gaussian distribution with unequal standard deviation, with a Dunnett multiple comparison correction for multiple comparisons as *post hoc* analysis. This was used to compare the cross-sectional area of the samples. The Kruskal-Wallis H test was used to test rank-based nonparametric values between two or more groups of independent variables. In this case, our post-hoc nonparametric test was the Dunn multiple comparison test. We used these tests to examine the percent artifact area and biopsy score. Descriptive statistics were reported using standard deviation and mean, or median and range for nonparametric distribution. Rank correlation was calculated using the Spearman rank correlation coefficient. Plots were presented using the mean ± the standard error of the mean.

RESULTS

No difference was found between CB11 and CB09 when directly compared in any of the factors examined. The analysis focused

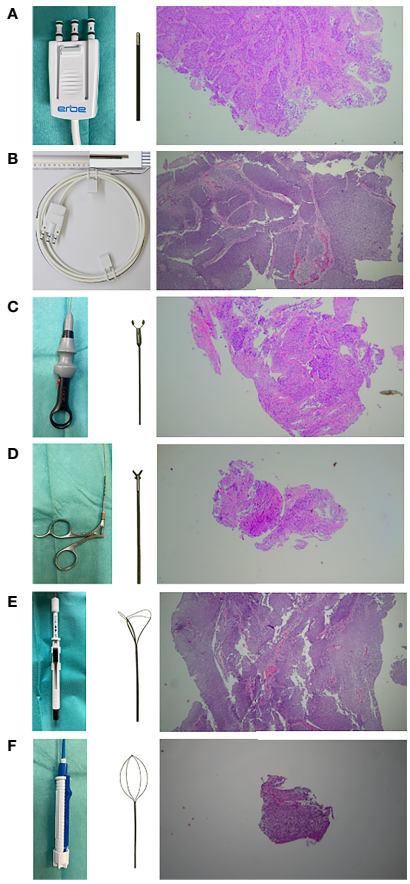

FIGURE 2 | Overview of the instruments used and exemplary representation of the histological specimen (HE strain, 20x magnification) obtained. **(A, B)** cryoprobe with outer diameters of 1.1 mm and 0.9 mm (Erbe Elektromedizin, Tuebingen, Germany). (CB11) & (CB09) **(C)** frontloading disposable biopsy forceps for the upper urinary tract (BIGopsy No. BLB-024115, Cook Medical, Bloomington, IN, US). (BiG) **(D)** reusable biopsy forceps for flexible ureteroscopy (No. 829.601, Richard Wolf GmbH, Knittlingen, Germany). (FB) **(E)** tipless front grasping Dormia basket N-Gage (No. NGE-022115, 2.2F Cook Medial, Bloomington, IN, US). (NG) **(F)** tipless side grasping Dormia basket: Zero-Tip (No. 390105; UPN M0063901050, Boston Scientific, Marlborough, Massachusetts, US). (ZT).

on the performance of the cryoprobes in comparison to the other devices. **Table 2** shows the summary of the results for the different factors.

Biopsies were obtained with each instrument. The cutoff was set at 3 biopsy attempts. A total of 175 histologically evaluable biopsies were obtained from 266 biopsy attempts (**Table 2**). Forceps biopsies were superior to the other techniques, with the BiG being superior to all other instruments tested in terms of biopsy collection feasibility. 36/36 biopsies (Bx) were taken with the BiG (100%) and 31/36Bx with the FB (88%). Both cryoprobes were slightly less effective. 29/36 Bx (80.6%) were retrieved with the CB09 and 30/36 Bx (83%) with the CB11. The least efficient technique was the Dormia basket biopsy. 23/36 (63%) of biopsies were obtained with the NG Dormia basket and 26/36 (72%) with the ZT (**Figure 3**).

At 66.7%, the BiG was the most efficient device for obtaining a biopsy in the first bite, followed immediately by the two cryoprobes. Both CB09 and CB11 proved to be almost as efficient as the BiG, with 63.9% biopsies in the first attempt. The FB took the first bite in half of the cases (50%), while the Dormia baskets NG (33.3%) and ZT (36.1%) proved to be less efficient than forceps biopsies. (**Figure 4**)

The average area of the biopsies obtained with the cryoprobes CB11 and CB09 yielded the largest samples with 14.5 mm^2 and 12.7 mm^2, respectively. The basket biopsies were also of sufficient size, at NG 9.5 mm^2 and 6.7 mm^2. Relatively little tissue could be obtained with forceps biopsies: BiG 4.3 mm^2 and FB 1.4 mm^2. The CB11 yielded significantly larger biopsies than the FB ($p<0.005$), the BiG ($p<0.005$) and the Dormia basket ZT ($p=0.037$). The CB09 collected significantly larger samples compared to the FB ($p<0.005$) and the BiG ($p<0.005$) (**Figure 5**).

Consequently, the quality of CB11 and CB09 were superior to all other devices in terms of biopsy quality (**Figure 6**).

The average area of the biopsy specimen overlaid with artifacts was determined. Interestingly, the pronounced artifact overlays were seen in the biopsies obtained with the Dormia baskets ZT (33%) and NG basket (48%). This was followed by the forceps biopsies FB (28%) and BiG (24%) and the least artifact overlays were obtained from the cryo-tissue sample CB11 (11%) and CB09 (19%). Due to a wide distribution of measured values, there were no significant differences between the cryoprobes and

TABLE 1 | Possible numbers of biopsy attempts and possible biopsies to be obtained per instrument, per kidney, for all twelve kidney specimens examined including the trial results.

Parameter	Minimum	Maximum
Possible number of attempts		
per device per kidney	3	9
using all six devices per kidney	3*6 = 18	9*6 = 54
in N=12 kidneys	3*6*12 = 216	9*6*12 = 658
Possible number of biopsies		
per device per kidney	0	3
using all six devices per kidney	0	3*6 = 18
in N=12 kidneys	0	3*6*12 = 216
Trial results (N=12 kidneys, 6 devices)		
Number of attempts performed	266	
Number of biopsies obtained	175	

TABLE 2 | Comparison of the parameters: feasibility, reliability, mean biopsy area, mean artifact area, artifact scores, pathology score and representativeness score of the different devices.

	Feasibility in 3 attempts in %	Reliability biopsy on first attempt in %	Mean biopsy areaIn mm^2(SD)	Mean artifact area in %	Artifact score 0-1 in %	Artifact score 2-3 in %	Patho score mean AU	Rep score In %
CB11	83	63.9	14.5 (±9.7)	11	89.7	10.3	4.9	89.7
CB09	80.6	63.9	12.7 (±6.0)	19	77.8	22.2	4.7	77.8
BiG	100	66.7	4.3 (±5.8)	24	69.3	30.7	3.2	80.6
FB	88	50	1.4 (±2.1)	28	65.2	34.8	3.6	60.9
NG	63	33.3	9.5 (±11.6)	48	53.3	46.7	3.3	53.3
ZT	72	36.1	6.7 (±7.9)	33	59.1	40.9	2.9	54.5

All devices were listed on the y-axis: cryoprobe 1.1mm, cryoprobe 0.9mm, disposable biopsy forceps BIGopsy®, standard biopsy forceps, Dormia basket Cook-N-Gage and Dormia basket Zero-Tip. SD, standard deviation.

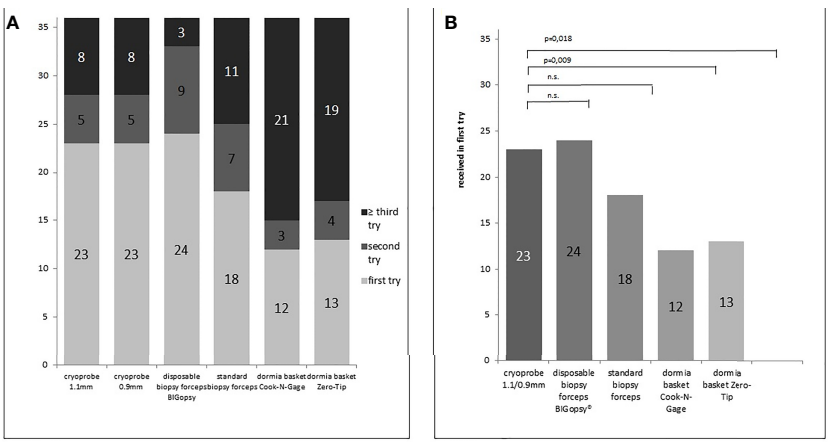

FIGURE 3 | Number of biopsy attempts per biopsy device **(A)** and number of sample already received in the first biopsy attempt **(B)**. P values in B determined via chi-square test (n.s. = not significant). Samples were collected using the different biopsy devices (disposable biopsy forceps BIGopsy®, standard biopsy forceps, Dormia basket Cook-N-Gage and Dormia basket Zero-Tip-x-axis).

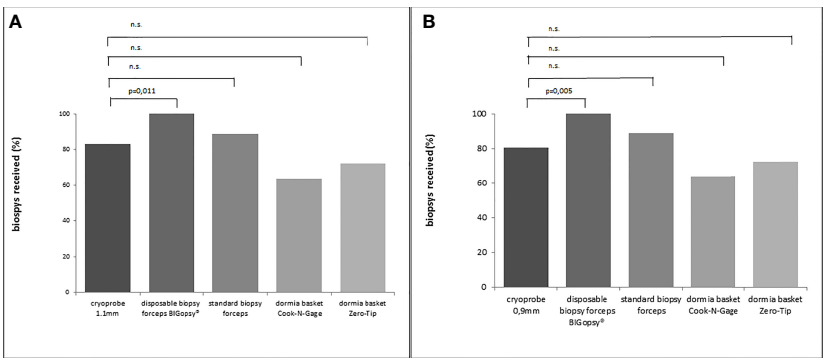

FIGURE 4 | Percentage x/n from actual biopsies obtained (x) vs. number of attempts (n). In **(A)** cryoprobe 1.1mm vs other devices (disposable biopsy forceps BIGopsy®, standard biopsy forceps, Dormia basket Cook-N-Gage and Dormia basket Zero-Tip-x-axis). In **(B)** cryoprobe 0.9mm vs other devices. P values were determined by chi-square test (n.s., not significant).

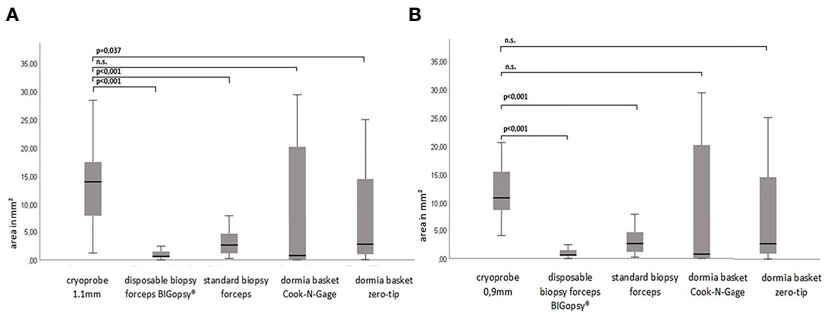

FIGURE 5 | The biopsy size of the paraffine in mm^2. P-values via Welch ANOVA for variance inhomogeneity with Dunn's multiple comparison of means. ANOVA, analysis of variance, Graph: median ± 95% confidence interval (n.s. = not significant). In **(A)** cryoprobe 1.1 mm vs. other deviced (disposable biopsy forceps BIGopsy®, standard biopsy forceps, Dormia basket Cook-N-Gage and Dormia basket Zero-Tip- x-axis. In **(B)** cryoprobe 0.9mm vs other devices.

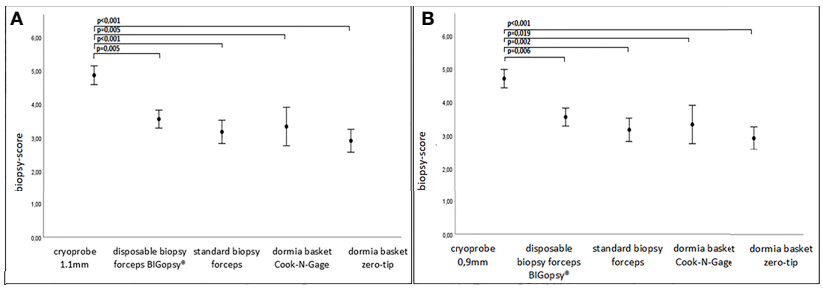

FIGURE 6 | Biopsy score in A.U (arbitrary unit). P values were collected via rank based nonparametric Kruskall-Wallis test, post hoc test via Dunn's multiple comparison of means. Graph: mean ± standard error of the mean (1x). In **(A)** cryoprobe 1.1mm vs other devices (disposable biopsy forceps BIGopsy®, standard biopsy forceps, Dormia basket Cook-N-Gage and Dormia basket Zero-Tip-x-axis). In **(B)** cryoprobe 0.9mm vs other devices.

the other devices, with the exception of the CB11 compared to the Dormia basket NG (**Figure 7**).

A subgroup analysis was performed to identify the differences more clearly. In the subgroup analysis, the artifact area was categorized as less than (artifact score 0 & 1) and larger than 20% (artifact score 2 & 3). Tissue was the least altered by the cryoprobe removal, resulting in a low artifact score (0–1). CB11 (89.7%) and CB09 (77.8%) preserved tissue best with a low artifact score. Forceps biopsies with FB (65.2%) and BiG (69.3) showed inferior tissue preservation. Biopsy with the Dormia basket was the most overshadowed by higher grade artifacts, but was still able to achieve an artifact score of 0-1 in > 50% of cases: NG (53.3%) and ZT (59.1%). The statistical analyses showed that a significant difference was observed between the CB11 and the BiG (p=0.049), the FB (p=0.032), and the NG (p=0.006) and ZT Dormia baskets (p=0.011) in favor

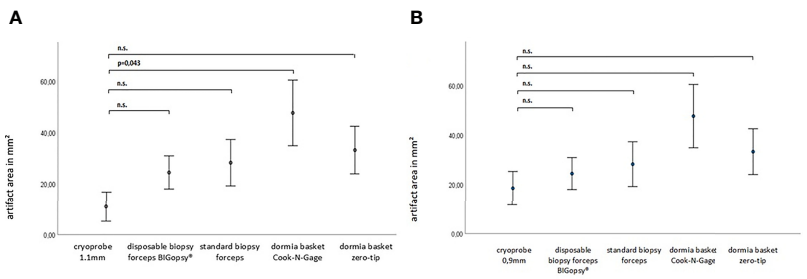

FIGURE 7 | The artifact area within the paraffine section in mm^2. P-values via Welch ANOVA for variance inhomogeneity with Dunn's multiple comparison of means.ANOVA, analysis of variance, Graph: means ± standard error of the mean (1x) (n.s. = not significant). In **(A)** cryoprobe 1.1 mm vs. other deviced (disposable biopsy forceps BIGopsy®, standard biopsy forceps, Dormia basket Cook-N-Gage and Dormia basket Zero-Tip- x-axis. In **(B)** cryoprobe 0.9mm vs other devices.

of the CB11. This trend was also observed for CB09, but the values were not statistically better (**Figures 8** and **9**).

Taken together, the CB11 achieved the best results compared to the other instruments with representative tissue samples in 90% of cases. The superior quality of samples obtained with the CB11 proved statistically significant compared to the BiG (p=0.049), FB (p=0.014), NG (p=0.006) and ZT (p=0.004). The CB09 with 78% representative samples did not prove to be more representative than all the other devices used (**Figure 10**).

DISCUSSION

Preliminary studies in the ex vivo porcine model using CB11 showed that the ureterorenoscopic cryobiopsy of the upper urinary tract is feasible (15). In our ex vivo study of human tissue, cryobiopsy also proved feasibility and reliability comparable to forceps biopsy (BiG, FB), and was more reliable as a Dormia basket biopsy (NG, ZT). The flat lesions and scarless tumor-free tissues were also biopsied in the study, which explains the comparatively poor performance of the baskets, which are normally very effective for exophytic lesions.

A distinct advantage of cryoprobe biopsy is that flat lesions can be biopsied due to the possibility to contact the tissue tangentially and the size of the biopsy can be controlled by the activation time of the probe. In addition, the lack of forceps blades and the cold exposure of the tissue results in fewer squeezing artifacts and better preservation of the different tissue layers (15). For a successful biopsy an optimal tissue sample under ideal freedom of movement and perfect visibility is desirable.

The handling of cryoprobe-guided biopsy is relatively simple for the experienced endourologist. The probe is inserted in retrograde through the instrument channel. The tip of the probe is blunt enough not to damage the inside of the endoscope. The tip of the probe is clearly visible in the image and, in contrast to BiG, only obscures a fraction of the endoscopic monitor image compared to the FB, even more with the 0.9 mm cryoprobe prototype. Although there was nearly no difference between the two cryoprobes, the 0.9 mm probe was slightly more bendable and showed a better irrigation flow rate compared to the 1.1 mm (data not shown), which can be explained by the small outer diameter (15).

One disadvantage is, that the probe must be passed through an access sheath; there is debate as to whether this is a potential risk to the patient from a tumor biology perspective. However, the cryoprobe must always be taken together with the endoscope. Particularly in the case of biopsy in the lower calyx group with a steep calyx neck angle, a tissue enclosed ice ball may be sheared off the tip of the cryoprobe by the edge of the access sheath when the instrument is withdrawn. Theoretically, in these cases a secondary removal of the specimen using a dormia basket should be technically feasible.

The therapeutic spectrum of UTUC is diverse and associated with different risks and long-term consequences for the patient, depending on the method chosen. A purely visual ureteroscopic decision would misclassify 30% of tumors (17). Biopsy can increase the diagnostic rate to as high as 90% (18), but in biopsies taken with conventional biopsy techniques, only one in four specimens collected is diagnostic (19). If diagnosis is not possible due to incorrect biopsies, reinterventions are likely to occur with the renewed risk for patients of bleeding, ureteral perforation, tumor spillage or urinary tract infections. If the

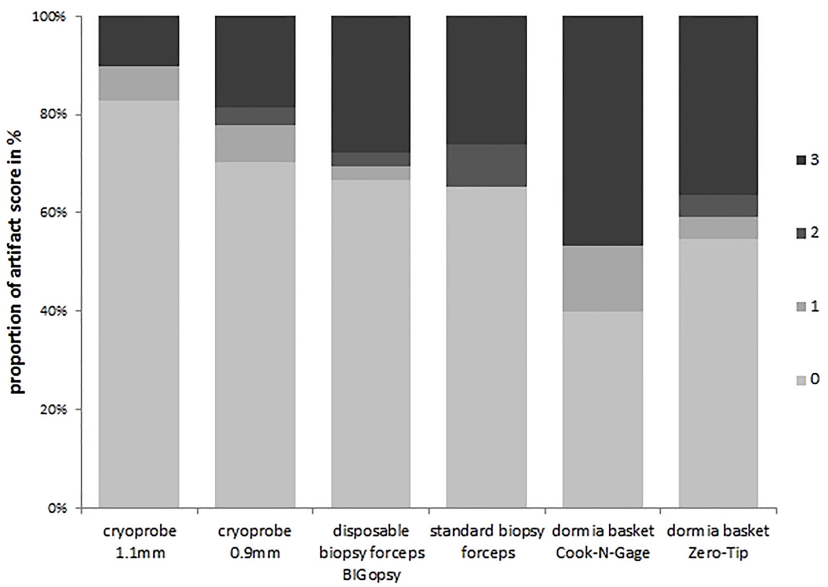

FIGURE 8 | Percent artifact scores per category were determined by dividing the number of biopsies per artifact score category by the number of total biopsies. All biopsies were previously assigned to an artifact score category.The devices were listed on the x-axis:cryoprobe 1.1mm, cryoprobe 0.9mm,disposable biopsy forceps BIGopsy®, standard biopsy forceps, Oormia basket Cook N-Gage and Oonnia basket Zero-Tip.

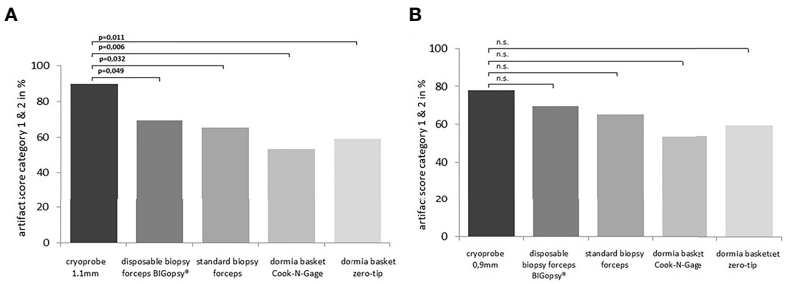

FIGURE 9 | The relevant number of biopsies on the total biopsies falling into artifact score category 0 or 1 [score in A.U.(arbitrary unit)] were compared among each other. In **(A)** cryoprobe 1.1 mm vs.other devices (disposable biopsy forceps BIGopsy®, standard biopsy forceps, Dormia basket Cook N-Gage and Dormla basket Zero-Tip-x-axis). In **(B)** cryoprobe 0.9mm vs.other devices. P values were determined by chi-square test (n.s. = not significant).

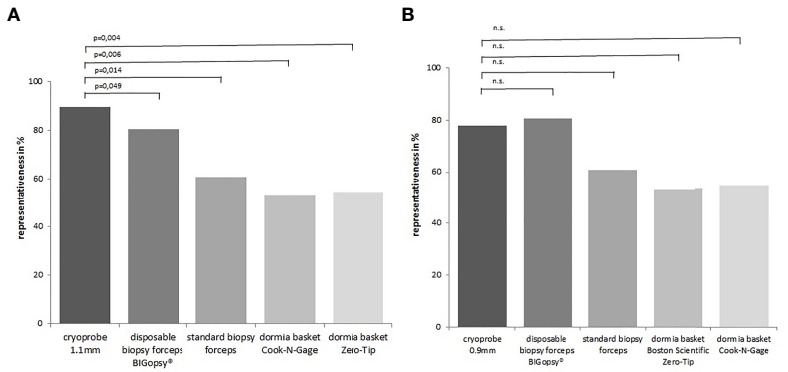

FIGURE 10 | The proportion of representative samples in the total biopsy number. Representative = sufficient size + artifact score category 0/1+ biopsy score 2 6. In **(A)** cryoprobe1.1 mm vs. other devices (disposable biopsy forceps BIGopsy®, standard biopsy forceps, Dormia basket Cook-N-Gage and Dormia basket Zero-Tip-x-axis). In **(B)** cryoprobe 0.9 mm vs other devices. P value-s were determined by chi-square test (n.s. = not significant).

primary diagnosis is incorrect, necessary radical surgical therapy is delayed with a potentially worse outcome for the patient.

For low-risk carcinomas, kidney-preserving endoscopic interventions are the method of choice (20). However, correct staging is crucial (21). Rojas et al. demonstrated that 57% of biopsies were classified as understaged, which may lead to erroneous renal preservation procedures despite invasive tumors (22). A high proportion of biopsies still cannot be utilized. Al-Qahtani et al. listed 10 of 40 biopsies as too small and not evaluable. Tavor et al. also showed 25% non-evaluable biopsies, and in a study by Breda et al., 66 of 302 (21.8%) biopsies were not evaluable (6, 18, 19). Cryobiopsy with a high level of representativeness could be an alternative to reduce the error rate.

A key advantage of the cryoprobe is the ability for the surgeon to adjust the sample size by the activation time, and the contact pressure of the probe on the tissue (13, 23). This gives the surgeon, in contrast to all previous biopsy techniques, the possibility to control the biopsy size.

The question arises whether a larger sample volume actually affects histopathological assessment, and in this regard, the literature contains inconsistent results.

The concordance between the biopsy grading and the final histopathologic diagnosis on the explanted organ ranges from 67% to 93% (22, 24–27). Compared with 5.9/2.4F biopsy forceps, a Dormia basket, and standard 3.6/3F biopsy forceps, Lama et al. concluded that the size and quality of the specimen had no effect on grading (28). This was determined in a retrospective setting comparing specimens from 145 patients with subsequent nephrectomies. Rojas et al. also demonstrated that biopsy volume did not affect grading in 54 patients. Nevertheless, they showed that biopsy-based staging in particular has great potential for improvement (22). Consistently, Tavora et al. reported that in cases where a definitive diagnosis could not be made by experts, this was mainly due to biopsy size, cell architecture, and squeeze artifacts in 21.05% of the specimens (19). Williams et al. showed that larger tissue specimens are better able to demonstrate the architecture of the lesion, which seems particularly important in the diagnosis of low-grade tumors, which tend to have fewer memorable cytologic features than high-grade UTUCs (27).

Correct staging is often not possible, which, in turn, can complicate treatment decisions. Rojas et al., in a study of 51

patients, showed that correct staging was present in only 43% of patients (22). Brown et al. attempted to draw conclusions about staging from bioptic grading. They calculated positive predictive values for staging in the different grading groups. Patients with G3 UTUC had pT3 or higher tumors in 43% of the cases. Patients with high-grade biopsies had pT2 UTUCs in 66% of the cases. In contrast, 72% of patients with low-grade biopsies had a final histologic staging of less than pT2 (29). This was confirmed by another study with a PPV of 60% for high-grade biopsies (24). Brien et al. showed that of 74 patients with high-grade biopsies, 62% had a T2 tumor on the final histopathologic evaluation, and 68% with low-grade biopsies were actually classified as maximum T1 (30).

Overall, the trend is toward undergrading and understaging. In a direct comparison between biopsy and subsequent nephroureterectomy, tumors had to be upstaged in a study by Margolin et al. (31). For Guarnizo et al., in 10 of the 22 cases (45%) from pTa, pT1+ was elevated (range pT1 to pT3) (25). Smith et al. also had to upgrade 24 (43%) of their patients from low-grade, non-invasive to high-grade invasive (32).

Since staging is composed of tumor infiltration depth, among other factors, it is reasonable to assume that incorrect staging occurs because the surgeon tends to perform biopsies too shallowly, rather than too deeply, to avoid perforation and bleeding, particularly in the ureter. Stewart et al. suggest that the tunica muscularis in the upper urinary tract is more likely to be completely infiltrated because it has a very thin layer (33). However, a pTa tumor entails different therapy than a pT1+ tumor (34). Given these findings, it is clearly advantageous to use the instrument for the biopsy that provides the best quality and size of the tissue sample. Whether the cryoprobe also produces an improvement in staging needs to be investigated in further studies. For example, by using the cryoprobe in addition to the standard 3F biopsy forceps in the study by Guarnizo et al. and then comparing the results (25).

A recent meta-analysis by Nowak et al. evaluated the risk of developing a bladder tumor after ureterorenoscopic biopsy has been performed. An association was shown between biopsied and non-biopsy patients. The group of biopsied patients showed a higher incidence rate of tumors in the urinary bladder. Seeding of floating tumor cells may occur but the exact mechanisms for this have not been determined. The study collectives were too different for this. The application of various techniques, such as the use of a ureteral sheath as protection against recurrence in the urinary bladder, also showed no improvement (35). The extent to which cryobiopsy can circumvent this phenomenon is not yet clear. In contrast to other biopsy techniques, in cryobiopsy the biopsy specimen is tightly enclosed by the ice ball and cell spreading may thus be reduced. However, this still needs to be investigated in further studies.

Our study has some limitations. The number of samples and trials required was calculated in a power analysis before the start of the study and was determined with N=12 samples. However, a higher number of trials would increase the statistical power. The primary endpoint of the study was the feasibility of cryobiopsy of human urothelial tissue in the upper urinary tract and that endpoint was met. Not all nephrectomy specimens contained tumor tissue, so statistical power is limited. However, urothelial tumor tissue is more fragile compared to normal urothelium, so this effect can be considered marginal. Flat lesions and fibrous tissues were included in the study. This explains the reduced specimen size using the Dormia baskets. A questionnaire about the handling of the different probes would have been beneficial for evaluating the handling of the different instruments.

CONCLUSIONS

Cryobiopsy on human urothelial tissue of the upper urinary tract is feasible. This includes urothelium, fibrous und tumor tissue. Significantly larger and higher quality samples compared to the standard armamentarium of upper tract biopsies could be obtained using both cryoprobes CB11. The cross-sectional area of the biopsy after the microscopy of the paraffin sections in mm^2 was significantly increased, compared with conventional biopsy methods. Furthermore, fewer squeezing artifacts were observed. Overall, our results indicated that cryoprobes, especially the CB11, can help improve diagnostics and therapy decision-making in UTUC. *In vivo* studies need to confirm the advantages of cryobiopsy in a clinical setting.

DATA AVAILABILITY STATEMENT

The original contributions presented in the study are included in the article/supplementary material. Further inquiries can be directed to the corresponding author.

ETHICS STATEMENT

The studies involving human participants were reviewed and approved by Ethikkommission der Universität Ulm Helmholtzstraße 20 (Oberer Eselsberg) Protocol Nr: 66/20. The patients/participants provided their written informed consent to participate in this study.

AUTHOR CONTRIBUTIONS

The authors confirm contribution to the paper as follows: study conception and design: JK, CB, WL, ME. Data collection: JK, AJ, LB. Analysis and interpretation of results: JK, WL, LB. Draft manuscript preparation: JK, LB, WL, AJ. All authors reviewed the results and approved the final version of the manuscript.

FUNDING

The Cryoprobes used in the study and the cryodevice (Erbekryo) were provided by Erbe Elektromedizin, Tübingen, Germany free of charge. The processing costs of the ethics application before the local ethics board were covered by the company Erbe Elektromedizin, Tübingen, Germany. The funder was not involved in the study design, collection, analysis, interpretation of data, the writing of this article or the decision to submit it for publication.

REFERENCES

1. Rouprêt M, Babjuk M, Burger M, Capoun O, Cohen D, Compérat EM, et al. European Association of Urology Guidelines on Upper Urinary Tract Urothelial Carcinoma: 2020 Update. *Eur Urol* (2021) 79(1):62–79. doi: 10.1016/j.eururo.2020.05.042
2. Tavora F, Fajardo DA, Lee TK, Lotan T, Miller JS, Miyamoto H, et al. Small Endoscopic Biopsies of the Ureter and Renal Pelvis: Pathologic Pitfalls. *Am J Surg Pathol* (2009) 33:1540–6. doi: 10.1097/PAS.0b013e3181aec42a
3. Smith AK, Stephenson AJ, Lane BR, Larson BT, Thomas AA, Gong MC, et al. Inadequacy of Biopsy for Diagnosis of Upper Tract Urothelial Carcinoma: Implications for Conservative Management. *Urology* (2011) 78:82–6. doi: 10.1016/j.urology.2011.02.038
4. Margolin EJ, Matulay JT, Li G, Meng X, Chao B, Vijay V, et al. Discordance Between Ureteroscopic Biopsy and Final Pathology for Upper Tract Urothelial Carcinoma. *J Urol* (2018) 199:1440–5. doi: 10.1016/j.juro.2018.02.002
5. Breda A, Territo A, Sanguedolce F, Basile G, Subiela JD, Reyes HV, et al. Comparison of Biopsy Devices in Upper Tract Urothelial Carcinoma. *World J Urol* (2018) 37:1899–905. doi: 10.1007/s00345-018-2586-y
6. Clements T, Messer JC, Terrell JD, Herman MP, Ng CK, Scherr DS, et al. High-Grade Ureteroscopic Biopsy is Associated With Advanced Pathology of Upper-Tract Urothelial Carcinoma Tumors at Definitive Surgical Resection. *J Endourol* (2012) 26:398–402. doi: 10.1089/end.2011.0426
7. Akkaya E, Berkowitsch A, Zaltsberg S, Greiss H, Hamm CW, Sperzel J, et al. Second-Generation Cryoballoon Ablation for Treatment of Persistent Atrial Fibrillation: Three-Year Outcome and Predictors of Recurrence After a Single Procedure. *J Cardiovasc Electrophysiol* (2018) 29:38–45. doi: 10.1111/jce.13372
8. He XZ, Wang QF, Han S, Wang HQ, Ye YY, Zhu ZY, et al. Cryo-Ablation Improves Anti-Tumor Immunity Through Recovering Tumor Educated Dendritic Cells in Tumor-Draining Lymph Nodes. *Drug Des Devel Ther* (2015) 9:1449–58. doi: 10.2147/DDDT.S76592
9. Montufar F, Moral LD, Labarca G, Folch E, Majid A, Fernandez-Bussy S. Transbronchial Cryobiopsies and Cryotherapy in Lung Diseases. *Rev Med Chil* (2018) 146:1033–40. doi: 10.4067/s0034-98872018000901033
10. Babiak A, Hetzel J, Krishna G, Fritz P, Moeller P, Balli T, et al. Transbronchial Cryobiopsy: A New Tool for Lung Biopsies. *Respiration* (2009) 78:203–8. doi: 10.1159/000203987
11. Fruchter O, Fridel L, Rosengarten D, Raviv Y, Rosanov V, Kramer M R. Transbronchial Cryo-Biopsy in Lung Transplantation Patients: First Report. *Respirology* (2013) 18:669–73. doi: 10.1111/resp.12037
12. Hetzel J, Eberhardt R, Herth FJF, Petermann C, Reichle G, Freitag L, et al. Cryobiopsy Increases the Diagnostic Yield of Endobronchial Biopsy: A Multicentre Trial. *Eur Respir J* (2012) 39:685–90. doi: 10.1183/09031936.00033011
13. Franke KJ, Linzenbold W, Nuessle D, Enderle M, Boesmueller H, Nilius G, et al. A New Tool for Transbronchial Cryobiopsies in the Lung: An Experimental Feasibility *Ex Vivo* Study. *Respiration* (2016) 91:228–34. doi: 10.1159/000443990
14. Hetzel J, Hetzel M, Hasel C, Moeller P, Babiak A. Old Meets Modern: The Use of Traditional Cryoprobes in the Age of Molecular Biology. *Respiration* (2008) 76:193–7. doi: 10.1159/000135934
15. Klein JT, Berger F, Linzenbold W, Jager L, Enderle MD, Bosmuller H, et al. Cryobiopsy in the Upper Urinary Tract: Preclinical Evaluation of a Novel Device. *Urology* (2019) 123:273–9. doi: 10.1016/j.urology.2018.10.003
16. Yarmus LB, Semaan RW, Arias SA, Feller-Kopman D, Ortiz R, Bosmuller H, et al. A Randomized Controlled Trial of a Novel Sheath Cryoprobe for Bronchoscopic Lung Biopsy in a Porcine Model. *Chest* (2016) 150:329–36. doi: 10.1016/j.chest.2016.01.018
17. El-Hakim A, Weiss GH, Lee BR, Smith A D. Correlation of Ureteroscopic Appearance With Histologic Grade of Upper Tract Transitional Cell Carcinoma. *Urology* (2004) 63:647–50. doi: 10.1016/j.urology.2003.10.076
18. Al-Qahtani SM, Legraverend D, Gil-Diez de Medina S, Sibony M, Traxer O. Can We Improve the Biopsy Quality of Upper Urinary Tract Urothelial Tumors? Single-Center Preliminary Results of a New Biopsy Forceps. *Urol Int* (2014) 93:34–7. doi: 10.1159/000354875
19. Tavora F, Fajardo DA, Lee TK, Lotan T, Miller JS, Miyamoto H, et al. Small Endoscopic Biopsies of the Ureter and Renal Pelvis: Pathologic Pitfalls. *Am.J.Surg.Pathol* (2009) 33:1540–6. doi: 10.1097/PAS.0b013e3181aec42a
20. Raman JD. Kidney Sparing Surgery for Upper-Tract Urothelial Carcinoma. Minerva. *Urol Nefrol* (2016) 68:359–71.
21. Roupret M, Xylinas E, Colin P, Houede N, Comperat E, Audenet F, et al. French ccAFU Guidelines - Update 2018-2020: Upper Tract Urothelial Carcinoma. *Prog Urol* (2018) 28(Suppl 1):R34–47. doi: 10.1016/j.purol.2018.07.284
22. Rojas CP, Castle SM, Llanos CA, Santos Cortes JA, Bird V, Rodriguez S, et al. Low Biopsy Volume in Ureteroscopy Does Not Affect Tumor Biopsy Grading in Upper Tract Urothelial Carcinoma. *Urol Oncol* (2013) 31:1696–700. doi: 10.1016/j.urolonc.2012.05.010
23. Jabari H, Sami R, Fakhri M, Kiani A. Different Protocols for Cryobiopsy Versus Forceps Biopsy in Diagnosis of Patients With Endobronchial Tumors. *Pneumologia* (2012) 61:230–3.
24. Clements T, Messer JC, Terrell JD, Herman MP, Ng CK, Scherr DS, et al. High-Grade Ureteroscopic Biopsy is Associated With Advanced Pathology of Upper-Tract Urothelial Carcinoma Tumors at Definitive Surgical Resection. *J Endourol* (2012) 26:398–402. doi: 10.1089/end.2011.0426
25. Guarnizo E, Pavlovich CP, Seiba M, Carlson DL, Vaughan ED, Sosa R E. Ureteroscopic Biopsy of Upper Tract Urothelial Carcinoma: Improved Diagnostic Accuracy and Histopathological Considerations Using a Multi-Biopsy Approach. *J Urol* (2000) 163:52–5. doi: 10.1016/S0022-5347(05)67970-0
26. Keeley FX, Kulp DA, Bibbo M, McCue PA, Bagley D H. Diagnostic Accuracy of Ureteroscopic Biopsy in Upper Tract Transitional Cell Carcinoma. *J Urol* (1997) 157:33–7. doi: 10.1016/S0022-5347(01)65273-X
27. Williams SK, Denton KJ, Minervini A, Oxley J, Khastigir J, Timoney AG, et al. Correlation of Upper-Tract Cytology, Retrograde Pyelography, Ureteroscopic Appearance, and Ureteroscopic Biopsy With Histologic Examination of Upper-Tract Transitional Cell Carcinoma. *J Endourol* (2008) 22:71–6. doi: 10.1089/end.2007.9853
28. Lama DJ, Safiullah S, Patel RM, Lee TK, Balani JP, Zhang L, et al. Multi-Institutional Evaluation of Upper Urinary Tract Biopsy Using Backloaded Cup Biopsy Forceps, a Nitinol Basket, and Standard Cup Biopsy Forceps. *Urology* (2018) 117:89–94. doi: 10.1016/j.urology.2018.03.040
29. Brown GA, Matin SF, Busby JE, Dinney CP, Grossman HB, Pettaway CA, et al. Ability of Clinical Grade to Predict Final Pathologic Stage in Upper Urinary Tract Transitional Cell Carcinoma: Implications for Therapy. *Urology* (2007) 70:252–6. doi: 10.1016/j.urology.2007.03.051
30. Brien JC, Shariat SF, Herman MP, Ng CK, Scherr DS, Scoll B, et al. Preoperative Hydronephrosis, Ureteroscopic Biopsy Grade and Urinary Cytology Can Improve Prediction of Advanced Upper Tract Urothelial Carcinoma. *J Urol* (2010) 184:69–73. doi: 10.1016/j.juro.2010.03.030
31. Margolin EJ, Matulay JT, Li G, Meng X, Chao B, Vijay V, et al. Discordance Between Ureteroscopic Biopsy and Final Pathology for Upper Tract Urothelial Carcinoma. *J Urol* (2018) 199:1440–5. doi: 10.1016/j.juro.2018.02.002
32. Smith AK, Stephenson AJ, Lane BR, Larson BT, Thomas AA, Gong MC, et al. Inadequacy of Biopsy for Diagnosis of Upper Tract Urothelial Carcinoma: Implications for Conservative Management. *Urology* (2011) 78:82–6. doi: 10.1016/j.urology.2011.02.038
33. Stewart GD, Bariol SV, Grigor KM, Tolley DA, McNeill S A. A Comparison of the Pathology of Transitional Cell Carcinoma of the Bladder and Upper Urinary Tract. *BJU Int* (2005) 95:791–3. doi: 10.1111/j.1464-410X.2005.05402.x
34. Freifeld Y, Krabbe LM, Clinton TN, Woldu SL, Margulis V. Therapeutic Strategies for Upper Tract Urothelial Carcinoma. *Expert Rev Anticancer Ther* (2018) 18:765–74. doi: 10.1080/14737140.2018.1481395
35. Nowak L, Krajewski W, Chorbińska J, Kiełb P, Sut M, Moschini M, et al. The Impact of Diagnostic Ureteroscopy Prior to Radical Nephroureterectomy on Oncological Outcomes in Patients With Upper Tract Urothelial Carcinoma: A Comprehensive Systematic Review and Meta-Analysis. *J Clin Med* (2021) 10 (18):4197. doi: 10.3390/jcm10184197

Conflict of Interest: ME and WL are employed by Erbe Elektromedizin GmbH, Tuebingen Germany.

The remaining authors declare that the research was conducted in the absence of any commercial or financial relationships that could be construed as a potential conflict of interest.

this article, or claim that may be made by its manufacturer, is not guaranteed or endorsed by the publisher.

frontiers in Oncology

ORIGINAL RESEARCH
published: 15 March 2022
doi: 10.3389/fonc.2022.768635

Surgical Resection of Intraocular Tumors (Partial Transscleral Sclerouvectomy Combined With Mircoinvasive Vitrectomy and Reconstruction of the Eyeball) in Asian Patients: Twenty-Five Years Results

*Nan Zhou, Ping Wang, Xiaolin Xu, Yueming Liu and Wenbin Wei**

Beijing Tongren Eye Center, Beijing Key Laboratory of Intraocular Tumor Diagnosis and Treatment, Medical Artificial Intelligence Research and Verification Laboratory of the Ministry of Industry and Information Technology, Beijing Tongren Hospital, Capital Medical University, Beijing, China

OPEN ACCESS

Edited by:
Patrick J. Schuler, Ulm University Medical Center, Germany

Reviewed by:
Yingjie Wang, Peking Union Medical College Hospital (CAMS), China
Ibadulla Mirzayev, Ankara University, Turkey

***Correspondence:**
Wenbin Wei
weiwenbintr@163.com

Specialty section:
This article was submitted to Surgical Oncology, a section of the journal Frontiers in Oncology

Received: *31 August 2021*
Accepted: *28 January 2022*
Published: *15 March 2022*

Citation:
Zhou N, Wang P, Xu X, Liu Y and Wei W (2022) Surgical Resection of Intraocular Tumors (Partial Transscleral Sclerouvectomy Combined With Mircoinvasive Vitrectomy and Reconstruction of the Eyeball) in Asian Patients: Twenty-Five Years Results. Front. Oncol. 12:768635. doi: 10.3389/fonc.2022.768635

Objective: To describe the outcome of intraocular tumor resection by partial transscleral sclerouvectomy (PTSU) combined with micro-invasive vitrectomy and reconstruction of the eyeball (MVRE) in Asian patients.

Design, Methods and Participants: This retrospective, interventional cohort study included 366 patients who underwent PTSU combined with MVRE for intraocular tumors both in adult and pediatric age groups. The medical records of these patients were reviewed for clinical, operative, and histopathological features.

Main Outcome Measures: Globe salvage, best corrected visual acuity (BCVA), surgical side effects, tumor control, and tumor-related metastasis and death.

Results: The mean follow-up duration was 87 months (median, 66; range, 1-303 months). Among the 366 patients, the mean age was 8.5 years (median, 7; range, 1-19 years) in the 37 pediatric patients, and was 43 years (median, 42; range, 20-51) in 329 adult patients. The tumor mainly involved the ciliary body (n=136; 37.2%) and choroid (n=86; 23.5%). The common pathologic diagnosis of the 366 patients was as follows. In the pediatric age group, histopathologic examination revealed positive tumor margins in 37 patients mainly including ciliary body medulloepithelioma (8/37), ciliary body melanocytoma (13/37) and uveal melanoma (5/37). In the adult group, the pathological diagnosis mainly included melanoma (195/329), RPE adenoma (21/329), amelanotic melanoma (13/329), ciliary body adenoma of nonpigmented epithelium (19/329),

schwannoma/neurilemmoma (11/329), melanocytoma (24/329), and leiomyoma (9/329). The globe salvage rate was 81.1% in the pediatric age groups (<20 years), and 93.6% in the adult group (≥20 years), respectively. Of the 338 salvaged eyes, final BCVA was 20/20 to 20/40 in 16 (4.7%), 20/40 to 20/80 in 58 (17.2%), 20/80 to 20/200 in 160 (47.3%), and ≤ 20/200 in 104 (30.8%). Early side effects included corneal edema in 28 (7.7%) patients, hyphema in 46 (12.6%), and vitreous hemorrhage in 76 (21%) patients. Postoperative side effects included proliferative vitreoretinopathy (PVR) in 67 (18.3%), late cataract in 42 (11.5%), and glaucoma in 18 (5%) patients. Local tumor recurrence was detected in 20 patients (5.5%) at a mean interval of 23.6 months, including melanoma (n=19) and medulloepithelioma (n=1). Enucleation was necessary in 28 (7.7%) cases owing to recurrence in 15 (53.6%), eye prophylaxis with high-grade malignancy in 5 (17.8%), and blind painful eye in 8 (28.6%) cases. Kaplan-Meier estimated for 5, 10-year metastasis rate and metastasis-related death rate (95%CI) in 213 UM patients were 3.2% (1.4%-7.0%), 6.9% (3.8%-12.3%); and 3.5% (1.6%-7.6%), 7.6% (4.2%-13.5%), respectively.

Conclusions: As a surgically challenging procedure, PTSU combined with MVRE offers several theoretical advantages over enucleation and radiotherapy. It can achieve control of most intraocular tumors, preserve useful vision, and maintain a cosmetically normal eye.

Keywords: surgical resection procedure, intraocular tumors, globe salvage, useful vision, control of tumors

HIGHLIGHTS

Intraocular tumors are a rare condition, which not only spare vision but also endanger life. Choosing an appropriate management technique for controlling intraocular tumors, saving the eyeball, and preserving useful vision is important for improving the quality of life of patients.

INTRODUCTION

Intraocular tumors are a rare condition in the population, which not only can cause loss of vision, but also endanger life. The incidence and prevalence of intraocular tumors occurring in pediatric patients and adults are different, and the same type of neoplasm maybe has different clinicopathological features in pediatric patients and adults. There are several benign tumors, malignant tumors, and simulating lesions that can occur in the eyes of the pediatrics or adults, including retinoblastoma, uveal melanoma (UM), hemangioma, medulloepithelioma, nevus, iris and ciliary body melanocytoma, and others. Treatment strategies for the management of these lesions included observation for benign, nonprogressive lesions and intervention for malignant or progressively enlarging tumors. Depending on the size, location and type of the tumor, interventional methods included cryotherapy, thermotherapy, surgical excision, plaque brachytherapy, laser photocoagulation, radiotherapy, chemotherapy, and enucleation (1). The treatment purpose for intraocular tumors is to control the tumor, prolong life, and preserve the eyeball and even useful vision. Surgical resection can be performed as a primary treatment or as a salvage procedure after another form of therapy.

Resection (surgical excision) is a technically challenging method in which a "trap-window" is created in the eye to allow entry and removal of a mass, followed by subsequent globe repair. It is designed to preserve useful vision and maintain a cosmetically normal eye. This technique is mainly used for ciliary body, choroidal and pigment epithelial tumors, and rare retinal tumors. Resection is classified based on the tissue involved as iridectomy, iridocyclectomy, iridogoniocycletomy, iridocyclochoroidectomy, iridogoniocyclochoroidectomy, partial lamellar sclerouvectomy (PLSU) (1–5), or local resection *via* 23- to 25-gauge micro-invasive vitrectomy for the excision of intraocular tumors, which we have termed as partial transscleral sclerouvectomy (PTSU) combined with micro-invasive vitrectomy and reconstruction of the eyeball (MVRE). Previous studies have termed surgical excision "en bloc" or "eye wall" resection (6–8). There are few previous studies that have evaluated the success of surgical resection for UMs in Caucasian adults (2–11), while the published literature is lacking the outcomes of local resection of intraocular tumors in the Asian population. Herein, to further explore the potential benefits of this surgical procedure, we reported an analysis of the outcomes of PTSU combined with MVRE for intraocular tumors in the pediatric and adult groups in the Asian population.

METHODS

The clinical records of all patients who underwent PTSU combined with MVRE from Jun 6, 1995 to Oct 26, 2020 at the Beijing Tongren Hospital were analyzed. The study and data collection were compliant with the principles of the Declaration of Helsinki. The study was approved by the Institutional Review

Board of Beijing Tongren Hospital, and written informed consent was obtained from all participants. Asian patients who underwent surgery were included in this study; those under the age of 20 years were included in the pediatric group and those over the age of 20 years were in the adult group. The operative procedure was performed by senior ophthalmologists (WB. W).

The collected clinical data included patient demographics, associated ocular and systemic disease, treatment history, ocular symptoms, best corrected visual acuity (BCVA), and intraocular pressure (IOP). The evaluated tumor characteristics included tumor location, tumor configuration (mushroom, dome, plateau, or lentiform), tumor size (largest basal diameter and thickness in millimeters [mm]), surface features, color, pigmented (including dark black, brown or mixed) or nonpigmented, exudative retinal detachment, vitreous hemorrhage, secondary effects on adjacent structures, and extraocular extension. Largest tumor basal diameter and tumor thickness were measured by standard ocular Color Doppler ultrasonography (CDU). Surgical findings including intraoperative and postoperative period were noted. A record of the histopathological features was listed. Long-term outcomes such as tumor control, BCVA, surgical side effects, and tumor-related metastasis and death were assessed.

Patient Selection

The decision to perform PTSU combined with MVRE was dependent on several factors, including tumor location, tumor size, tumor type, secondary effects of tumor, BCVA, and patient preference (3, 4). Other options for treatment based on the tumor type included observation, thermotherapy, plaque brachytherapy, and enucleation. Although the selection was case-based, PTSU combined with MVRE was generally applied for tumors measuring<18 mm in diameter and tumors with no evidence of vitreous invasion (3) or extraocular extension. Tumor thickness was a less important factor for considering PTSU combined with MVRE. For benign lesions, surgical resection was attempted only if the BCVA was compromised, causing secondary glaucoma, or if there was a high risk of amblyopia owing to astigmatism. For malignant lesions, the advantages and disadvantages of alternative treatments (such as plaque brachytherapy, radiotherapy and enucleation) were discussed with the patient before proceeding with PTSU combined with MVRE.

Operative Procedure

PTSU Combined With MVRE

Local resection was performed in all patients *via* partial transscleral sclerouvectomy (PTSU) combined with 23 to 25-gauge micro-invasive vitrectomy and reconstruction of the eyeball (MVRE). The key operative procedure has been described in previous studies (1–3). For ciliary body or choroidal tumors, a limbal peritomy was created centered on the tumor meridian and the adjacent rectus muscles were isolated and tagged with 4-0 silk sutures. If the tumor margin underlaid a rectus muscle, then muscle disinsertion was performed, tagging with double armed 5-0 vicryl sutures. The episcleral blood vessels or sentinel vessels were cauterized gently and bare sclera was exposed over the tumor. The tumor margins were identified by transillumination and marked on the sclera with a marking pen. A ladder-shaped scleral flap was then created with a 2-mm margin from the tumor edge. In most cases, a posteriorly hinged flap was created to facilitate good wound edge apposition during the closure; however, when the tumor was anterior and within the iris and/or ciliary body, an anterior hinged flap was created. Ocular decompression by pars plana micro-invasive vitrectomy facilitated local excision by reducing retinal bulging through the scleral window. If the ciliary body tumor was small, a three-port vitrectomy was deemed unnecessary. A single infusion cannula was placed to stabilize intraocular pressure and reform the globe. Vitrectomy can be performed before, during, and/or after scleral flap dissection. Bipolar cauterization was performed on the uvea around the tumor for hemostasis. The uvea was carefully incised for the entire circumference of the tumor and cautious separation of the uveal mass from the underlying tissue (retina and vitreous) was subsequently achieved. For choroidal tumors, when the whole tumor body was separated from the sclera, floating in the pool of perfluorocarbon liquid, then the tumor was extracted through the scleral flap. The mass was safely removed and placed on a cardboard in formalin. Vitreous loss is often encountered when the ciliary body is the main area of tumor involvement because the thin nonpigmented ciliary epithelium is often adherent to the resected specimen (4, 5). In these scenarios, a 23 to 25-gauge micro-invasive vitrectomy was considered and performed. The scleral flap was closed with interrupted 8-0 nylon sutures depending on the location and size of the defect. The sutures were placed approximately 1.5-2 mm apart. The globe was reformed with balanced salt solution (BSS), injected through the pars plana. The structure of the eyeball was restored. The previously detached rectus muscle was resutured to its insertion and conjunctiva was reapproximated and closed with 8-0 vicryl sutures.

For iris tumors, either a scleral flap was made as described above or a limbal incision was created. A 15° microsurgical knife was used to create a paracentesis port 90° away from the main incision and a viscoelastic material was injected into the anterior chamber. The main incision was created using a 15° knife and is enlarged using a 3.2 microsurgical knife or 11th blade. The iris tumor was removed en bloc using Vannas capsulotomy scissors avoiding the pupillary rim. If the pupillary margin was removed, pupilloplasty was performed using 10-0 Prolene sutures in some patients. The anterior chamber was refilled with BSS and the flap or incision was sutured using interrupted 8-0 or 10-0 nylon sutures.

Statistical Analysis

Data collected on continuous scale, including age (years), largest tumor basal diameter, and tumor thickness (millimeters), were expressed as mean, median, minimum and maximum. Kaplan-Meier analysis was performed to estimate the cumulative probability of metastasis and death. Factors relevant to metastasis and metastasis related death of UM patients after performing PTSU with MVRE were evaluated by univariate and multivariable Cox regression analyses. Hazard ratios and 95%

CIs were calculated for each risk factor. P-value < 0.05 was considered to be statistically significant different. All analyses were performed using Stata version 15.0 (StataCorp LLC, College Station, TX, USA).

RESULTS

Clinical Characteristics of Patients

In all, 366 patients (Asian/Chinese) who underwent PTSU combine with MVRE from Jun 6, 1995 to Oct 26, 2020. The mean age was 8.5 years (median, 7; range, 1–19) in the 37 pediatric patients, and was 43 years (median, 42; range, 20–51) in the 329 adult patients, respectively (**Tables 1**, **2**). Clinical features of the tumor are listed in **Table 1**.

In the pediatric age group, BCVA at presentation was 20/20 to 20/40 in 2 (5%) eyes, 20/40 to 20/80 in 5 (13%), 20/80 to 20/200 in 6 (16%), and ≤ 20/200 in 24 (65%) eyes. The mean largest tumor basal diameter was 11.2 mm (median, 10.5; range, 3.9-20.1), and the mean thickness was 6.5 mm (median, 6.7; range, 1.5-12.1). The tumor was clinically pigmented in 22 (59.5%) and nonpigmented in 15 (40.5%) patients. The other associated findings at presentation included sentinel vessel in 30 (81%), corneal blood staining in 1 (3%), band-shaped corneal degeneration in 12 (32.4%), pseudohypopyon in 1 (3%) (**Figure 1A**), hyphema in 1 (3%), elevated IOP >21 mmHg in 2 (6%), rubeosis in 7 (19%), iris stromal seeding in 4 (11%), iris cyst in 2 (6%), dislocation of lens in 8 (21.6%), angle seeding in 1 (3%), cataract in 9 (24.3%), and feeder or drainer vessel in 1 (3%) patient.

In the adult group, BCVA at presentation was 20/20 to 20/40 in 33 (10%) of eyes, 20/40 to 20/80 in 76 (23%), 20/80 to 20/200 in 146 (44%), and ≤ 20/200 in 74 (23%) eyes. The mean tumor largest basal diameter was 9.1 mm (median, 8.8; range, 1.5–22.2), and the mean thickness was 6.4 mm (median, 6.6; range, 0.3–16.4). The tumor was clinically pigmented in 238 (72.3%) and nonpigmented in 91 (27.7%) patients. The other associated findings at presentation included sentinel vessel in 185 (56.2%), pseudohypopyon in 2 (0.6%), rubeosis in 2 (0.6%), iris cyst in 2 (0.6%), dislocation of lens in 66 (20.1%), angle seeding in 3 (0.9%), elevated IOP >21 mmHg in 10 (3%), cataract in 6 (1.8%), yellowish retinal exudation in 29 (8.8%), secondary exudative retinal detachment in 245 (74.8%), vitreous hemorrhage in 16 (4.9%), vitreous pigment dissemination in 8 (2.4%), exudative macular detachment in 56 (17%), surface wrinkling retinopathy in 22 (6.7%), and feeder or drainer vessel in 25 (7.6%) patients. The most relevant sign of ciliary body tumors is a prominent episcleral (sentinel) vessel.

TABLE 1A | Surgical Resection (Partial Transscleral Sclerouvectomy Combine with Mircoinvasive Vitrectomy and Reconstruction of the Eyeball) of Intraocular Tumors in 37 Children: Demographic and Clinical Features.

Features	Patients n n (%), n=37
Age (yrs), mean (median; range)	8.5, (7, 1-19)
Gender	
Male	21 (56.8%)
Female	16 (43.2%)
Race	
Asian	37 (100%)
Tumor location	
Iris	2 (5.4%)
Ciliary body	24 (64.9%)
Iris+ciliary body	2 (5.4%)
Ciliary body+choroid	2 (5.4%)
Choroid	4 (10.8%)
Retina	1 (2.7%)
Iris+ciliary body+choroid	2 (5.4%)
Tumor size (mm), mean (median, range)	
Largest tumor basal diameter	11.2 (10.5; 3.9-20.1)
Tumor thickness	6.5 (6.7; 1.5-12.1)
Histopathologic diagnosis	
Medulloepithelioma	8 (21.6%)
Melanocytoma	16 (43.3%)
Iris	1 (6.3%)
Ciliary body	11 (68.7%)
Iris+ciliary body	2 (12.5%)
Iris+ciliary body+ choroid	2 (12.5%)
Melanoma	5 (13.5%)
Pigmented	4 (80%)
Ciliary body-mixed cell	1 (25%)
Choroid-epithelioid	1 (25%)
Choroid-spindle cell	1 (25%)
Choroid-mixed cell	1 (25%)
Non-pigmented	1 (20%)
Choroid-mixed cell	1 (100%)
Schwannoma	1 (2.7%)
Leiomyoma	2 (5.4%)
Nevus	2 (5.4%)
Ciliary body	1 (50%)
Choroid	1 (50%)
Inflammatory granuloma	2 (5.4%)
Hemangioma	1 (2.7%)

Intraoperative Course

Performed surgeries included iridectomy in 29 (8%), iridogoniocyclectomy in 18 (5%), iridogoniocyclochoroidectomy in 201 (55%), and cyclochoroidectomy in 84 (23%) patients. Limbal-based incision (with no flap) was used in 33 (9%) patients; a fornix-based flap was created in 293 (80%) patients. Muscle disinsertion was required in 6 (1.6%) patients to gain access to the surgical site. Standard three-port micro-invasive vitrectomy was performed in 337 (92%) patients for ensuring stabilized intraocular pressure and reattachment of the retina at resection (23 to 25-gauge). On completion of tumor removal, pupillary reconstruction was performed in 29 (8%) patients using Prolene sutures; repair with donated sclera was performed for sealing the wound in 6 (1.6%) patients. Intraoperative hyphema was noted in 40 (11%), vitreous hemorrhage in 70 (19%), and subretinal hemorrhage in 2 (0.5%) patients. No patient developed suprachoroidal expulsive hemorrhage.

Pathology

The pathological diagnosis of the 366 patients is listed in **Tables 1**, **2**. In the pediatric age group, histopathological examination revealed positive tumor margins in 33 patients including those with medulloepithelioma (ciliary body in 8 patients; **Figures 1A–F**), melanocytoma (ciliary body in 13 patients, choroid in 2 patients, iris in 1 patient) (**Figures 2**, **3**), melanoma (ciliary body in 1 patient, choroid in 4 patients),

TABLE 1B | Surgical Resection (Partial Transscleral Sclerouvectomy Combine with Mircoinvasive Vitrectomy and Reconstruction of the Eyeball) of Intraocular Tumors in 329 Adult: Demographic and Clinical Features.

Feature	Patients n (%), n=329
Age (yrs), mean (median; range)	43 (42; 20-51)
Gender	
Male	159 (48.3%)
Female	170 (51.7%)
Race	
Asian	329 (100%)
Tumor location	
Conjunctiva	4 (1.2%)
Iris	27 (8.2%)
Ciliary body	111 (33.7%)
Iris+ciliary body	16 (4.9%)
Ciliary body+choroid	55 (16.6%)
Choroid	82 (24.9%)
Retina	33 (10.1%)
Tumor size (mm), mean (median, range)	
Largest tumor basal diameter	9.1 (8.8; 1.5-22.2)
Tumor thickness	6.4 (6.6; 0.3-16.4)
Histopathologic diagnosis	
Melanoma	**208 (63.2%)**
Pigmented	195 (93.7%)
Conjunctiva	2 (1.1%)
Iris-spindle	13 (6.7%)
Iris-mixed cell	6 (3.2%)
Iris+ciliary body-spindle	5 (2.6%)
Iris+ciliary body-mixed cell	3 (1.6%)
Ciliary body-mixed cell	40 (20.6%)
Ciliary body-epithelioid	6 (3.2%)
Ciliary body-spindle	7 (3.6%)
Choroid-epithelioid	9 (4.6%)
Choroid-spindle cell	20 (11.0%)
Choroid-balloon	2 (1.1%)
Choroid-mixed cell	35 (17.9%)
Ciliary body + choroid-mixed cell	17 (8.8%)
Ciliary body + choroid-epithelioid	2 (1.1%)
Ciliary body + choroid–spindle	28 (14.4%)
Non-pigmented	**13 (6.3%)**
Ciliary body-epithelioid (1), spindle (1),mixed cell (4)	6 (46.2%)
Choroid-mixed cell (1), epithelioid (1)	2 (15.4%)
Ciliary body + choroid- spindle (4), epithelioid (1)	5 (38.4%)
Melanocytoma	24 (7.3%)
Iris	2 (8.3%)
Ciliary body	12 (50%)
Iris+ciliary body	8 (33.3%)
Choroid	2 (8.3%)
Schwannoma (neurilemmoma)	**11 (3.3%)**
Ciliary body	5 (45.5%)
Choroid	5 (45.5%)
Ciliary body+Choroid	1 (9.1%)
Leiomyoma	**9 (2.7%)**
Ciliary body	6 (66.7%)
Choroid	3 (33.3%)
Inflammatory granuloma	3 (0.9%)
Retinoblastoma	5 (1.5%)
Malignant medulloepithelioma	1 (0.3%)
Ciliary body adenoma of nonpigmented epithelium	19 (5.8%)
CPE adenoma	5 (1.5%)
RPE adenoma	21 (6.3%)
Pigmented	16 (76.2%)
Non-pigmented	5 (23.8%)
RPE adenocarcinoma (choroid)	1 (0.3%)
RPE hamartoma	1 (0.3%)
Nevus	1 (0.3%)
Retinal capillary hemangioma	2 (0.6%)
MALT lymphoma	4 (1.2%)
Solitary fibrous tumor	1 (0.3%)
Glioneuroma	2 (0.6%)
Ameloblastoma	1 (0.3%)
Glomangioma	1 (0.3%)
Inflammatory pseudotumor	1 (0.3%)
Allelocytoma	1 (0.3%)
Neurofibroma (choroid)	1 (0.3%)
Amyloidosis	2 (0.6%)
Plasmacytoma	1 (0.3%)
Others	
Iris metastatic tumor	3 (0.9%)
Iris foreign body	1 (0.3%)

CPE, ciliary body pigmented epithelial adenoma.

leiomyoma (ciliary body in 2 patients), schwannoma (ciliary body in 1 patient), hemangioma (retina in 1 patient), and inflammatory granuloma (iris in 2 patients), nevus (ciliary body in 1 patient, choroid 1 patient).

In the adult group, histopathological examination revealed positive tumor margins in 321 patients including those with melanoma (conjunctiva in 2 patients, iris in 19 patients, ciliary body in 61 patients, choroid in 113 patients), amelanotic melanoma (ciliary body in 6 patients, choroid in 7 patients), malignant medulloepithelioma (ciliary body in 1 patient), RPE adenoma (21 patients), RPE adenocarcinoma (1 patient), ciliary body adenoma of nonpigmented epithelium (19 patients), leiomyoma (ciliary body in 6 patients, choroid in 3 patients; **Figure 4**), schwannoma/neurilemmoma (ciliary body in 6 patients, choroid in 5 patients; **Figure 5**), retinal hemangioma (2 patients), well-differentiated retinoblastoma (3 patients), melanocytoma (iris in 2 patients, ciliary body in 20 patients, choroid in 2 patients), amyloidosis (vitreous and retina in

TABLE 2 | Surgical Resection (Partial Transscleral Sclerouvectomy Combine with Mircoinvasive Vitrectomy and Reconstruction of the Eyeball) of Intraocular Tumors in 366 Patients: Early and Late Surgical Side Effects.

Side effects	n (%)
Early postoperative side effects (< 2 weeks)	
Corneal edema	28 (7.7%)
Hyphema	46 (12.6%)
Descemet's folds	19 (51%)
Vitreous hemorrhage	76 (21%)
Elevated IOP	46 (12.6%)
Late posterative effects (> 2 weeks)	
Hypotony	2 (0.5%)
Proliferative vitreoretinopathy	67(18.3%)
Cataract	42 (11.5%)
Glaucoma	18 (5%)
Vitreous hemorrhage (nonresolving)	2 (0.5%)
Recurrent retinal detachment	7 (2%)
Sympathetic ophthalmia	1 (0.3%)

IOP, intraocular pressure.

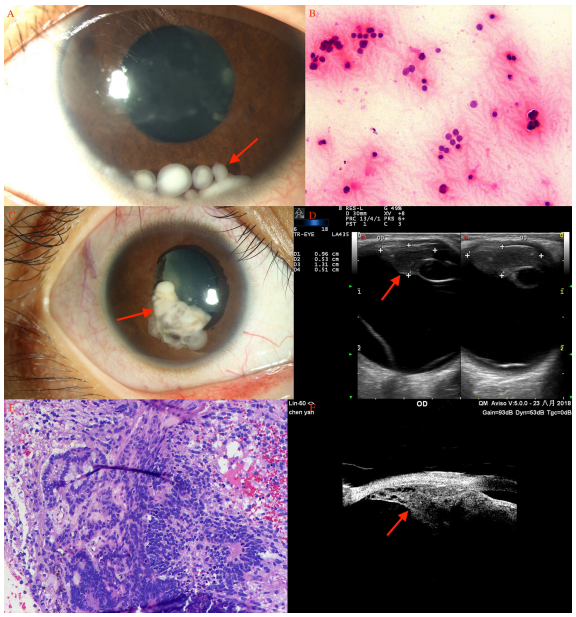

FIGURE 1 | Ciliary body medulloepithelioma of a 5-year-old boy. **(A)** The pompom-like pseudohypopyon (arrow) in the anterior chamber (original magnifications × 16). (left eye) **(B)** The anterior-chamber fine-needle aspiration biopsy showed small, round blue tumor cells, with small bland nuclei and relatively abundant eosinophilic cytoplasm, arranged in nest bulk (hematoxylin-eosin [HE], original magnifications×200). **(C)** Medulloepithelioma of a 17-year-old girl. A markedly white tumor (arrow) in the pupil area with iris involvement (leukocoria), a prominent episcleral (sentinel) vessel, and rubeosis were noted (arrow). **(D)** CDI showed lesions (arrow) with low-to-moderate internal reflectivity and sharply demarcated borders; cystic components were seen. **(E)** Histopathology revealed ciliary body medulloepithelioma. **(F)** UBM of ciliary body tumor with iris invasion (iridociliary tumor, arrow) showed low-to-medium internal reflectivity and loss of the acute angle shape.

2 patients), RPE hamartoma (1 patient), MALT-lymphoma (choroid in 1 patient), solitary fibrous tumor (choroid in 1 patient), ameloblastoma (choroid in 1 patient), glomangioma (ciliary body in 1 patient), glioneuroma (choroid in 1 patient, ciliary body and choroid in 1 patient), neurofibroma (choroid in 1 patient), inflammatory granuloma (iris in 2 patients, choroid in 1 patient), metastatic tumor (iris in 3 patients), allelocytoma (choroid in 1 patient), plasmacytoma (choroid in 1 patient), and inflammatory pseudotumor (choroid in 1 patient).

Among the 366 patients, 3 pediatric patients (0.8%) and 13 adult patients (3.6%) were incorrectly diagnosed preoperatively *via* clinical assessment. The preoperative incorrect diagnosis included 2 cases of medulloepithelioma (preoperatively diagnosed as retinoblastoma and hemangioma), 1 case of granuloma (preoperatively diagnosed as amelanotic melanoma), 13 cases of amelanotic melanoma (preoperatively diagnosed as neurilemmoma and atypical hemangioma), melanoma (preoperatively diagnosed as RPE adenoma), gliosis (preoperatively diagnosed as adenoma), melanocytoma (preoperatively diagnosed as melanoma), leiomyoma (preoperatively diagnosed as amelanotic adenoma), and a patient with nevus (preoperatively diagnosed as transscleral melanoma).

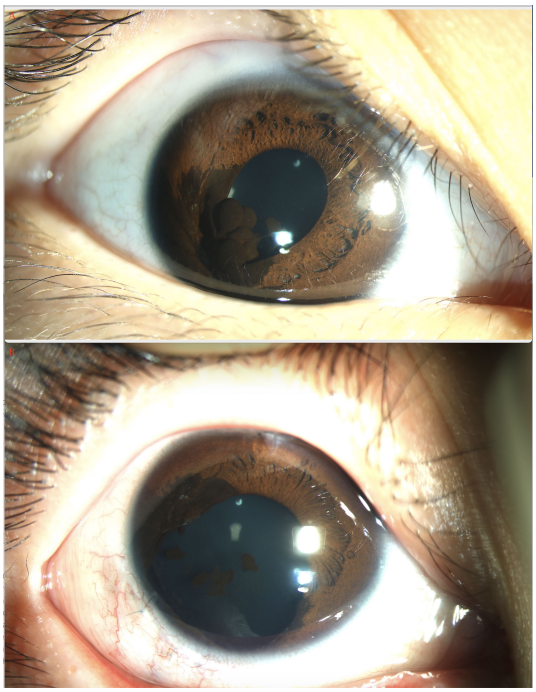

FIGURE 2 | Iris melanocytoma (arrow) of a 7-year-old girl before **(A)** and after **(B)** iridectomy.

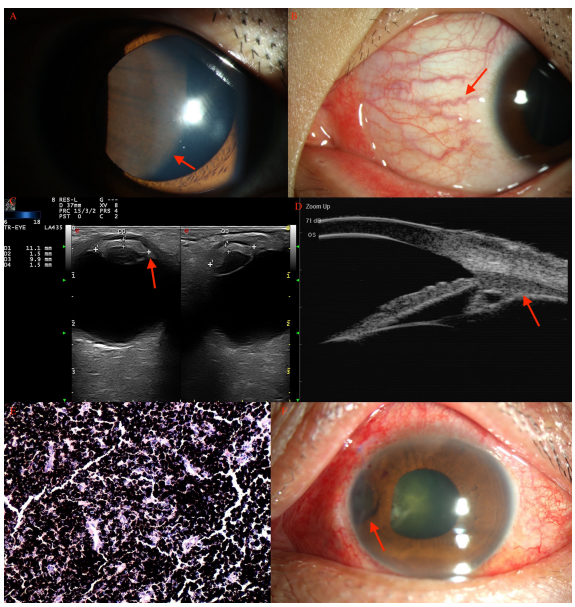

FIGURE 3 | Ciliary body melanocytoma (**A**, arrow) of a 15-year-old boy, with prominent sentinel vessels (**B**, arrow). **(C)** CDI revealed lesions (arrow) with moderate internal reflectivity with irregular borders. **(D)** UBM showed a mass (arrow) pushing the normal iris posteriorly. **(E)** Histopathology revealed an amount of melanin in the tumor cells, with a small, round, normochromic, and regular nucleus. **(F)** After PTSU combined with MVRE.

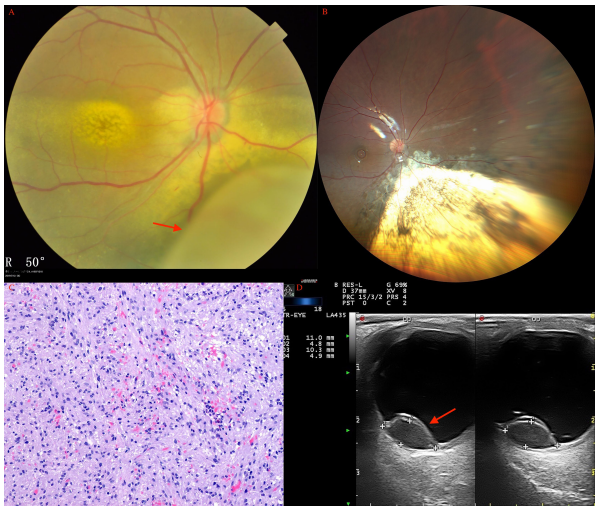

FIGURE 4 | Choroidal leiomyoma (arrow) of a 27-year-old woman before **(A)** and after **(B)** PTSU combined with MVRE. **(C)** Photomicrograph of leiomyoma showing bundles of spindle cells with blunt-ended oval nuclei (HE, ×100). **(D)** CDI revealed a pedunculated mass (arrow) with inconsistent reflectivity of moderate intensity, and arterial blood signals in the tumor.

Surgical Side Effects

Postoperative side effects are listed in **Table 2**. Early side effects included corneal edema in 28 (7.7%), hyphema in 46 (12.6%), and vitreous hemorrhage in 76 (21%) patients. Late side effects included proliferative vitreoretinopathy (PVR) in 67 (18.3%), late cataract in 42 (11.5%), glaucoma in 18 (5%), recurrent retinal detachment in 7 (2%), hypotony in 2 (0.5%), non-resolving vitreous hemorrhage in 2 (0.5%), and sympathetic ophthalmia in 1 (0.3%) patients. PVR occurred at mean 12 months after surgery. Postoperative cataract surgery was performed in 7 (19%) patients and scleral buckling was performed in 3 (11%) patients (2 cases of rhegmatogenous retinal detachment). The management of glaucoma included topical therapy for 10, trabeculectomy for 3, cyclophotocoagulation for 2, and glaucoma tube shunt for 3 patients.

Outcomes

The mean follow-up duration was 87 months (median, 66; range, 1-303 months). Among the 366 patients, local tumor recurrence was detected in 20 (5.5%) patients at a mean interval of 23.6 months, including melanoma (n = 19) and medulloepithelioma (n = 1) (**Figure 6**). This was treated with I-125 plaque brachytherapy in 4 patients with melanoma and 1 patient with medulloepithelioma, and enucleation in 15 patients with melanoma. Overall, 28 (7.7%) patients underwent enucleation after a mean interval of 8.2 months (median 4.5; range, 1-26 months). The reason for enucleation was tumor recurrence in 15 (53.6%), prophylaxis for high-grade malignancy or tumors invading the optic nerve in 5 (17.9%), and blind painful eye caused by neovascular glaucoma (NVG) in 8 (28.5%) patients. Among the 338 salvaged eyes, the final BCVA was 20/20 to 20/40 in 16 (4.7%), 20/40 to 20/80 in 58 (17.2%), 20/80 to 20/200 in 160 (47.3%), and ≤ 20/200 in 104 (30.8%) patients (**Table 3**). There were no cases of orbital recurrence, metastasis or death at a mean of 97.0 months of follow-up.

In this study, 4 patients (11%) underwent surgery at <3 years of age. The diagnoses in these patients were ciliary body medulloepithelioma (n = 3), and ciliary body melanocytoma (n = 1). After a mean follow-up of 40.0 months, no patient had a

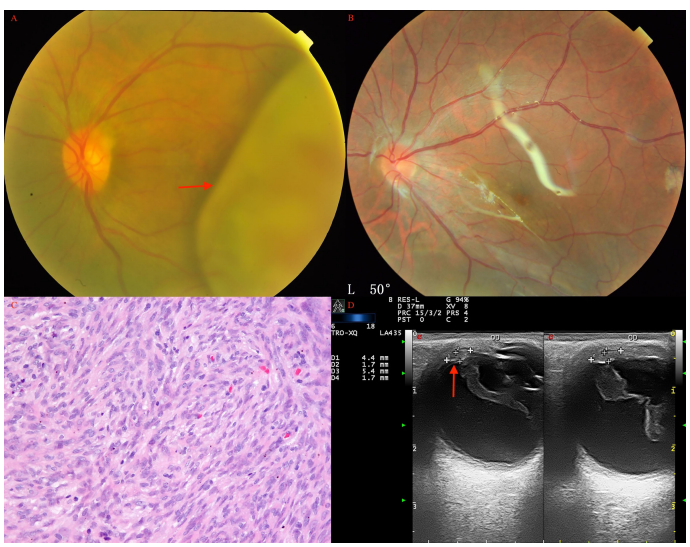

FIGURE 5 | Choroidal schwannoma/neurilemmoma (arrow) in a 43-year-old man before **(A)** and after **(B)** PTSU combined with MVRE. **(C)** Histopathology revealed that the tumor consisted of spindle cells in a fascicular arrangement with long eosinophilic cytoplasmic processes and cells loosely arranged in a mucoid matrix (HE, × 200); **(D)** CDI showed two pedunculated masses (arrow) with inconsistent reflectivity of moderate intensity and no choroidal excavation, with arterial blood signals in the tumor.

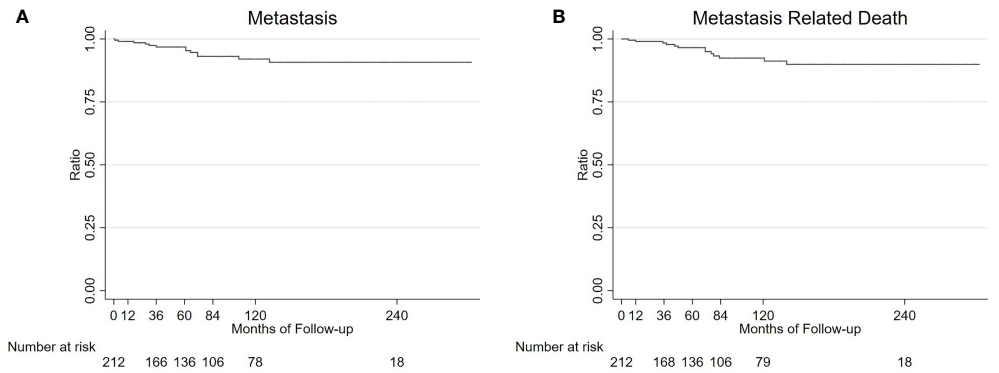

FIGURE 6 | Survival analysis of 213 UM patients. Kaplan-Meier estimated that the 1, 3, 5, 7, and 10-year metastasis rates and metastasis related death rate (95% CI) in 213 UM patients were 0.5% (0.1%-3.3%), 3.2% (1.4%-7.0%), 3.2% (1.4%-7.0%), 6.9% (3.8%-12.3%), and 6.9% (3.8%-12.3%) **(A)**; and 1.0% (0.2%-3.4%), 1.6% (0.5%-4.8%), 3.5% (1.6%-7.6%), 7.6% (4.2%-13.5%), and 7.6% (4.2%-13.5%) **(B)**, respectively.

recurrence and the globe was salvaged in all patients. Infant eye surgeries are more challenging because of the increased pliability of the sclera causing an increased tendency to collapse during surgery. Hence, surgery was considered only if the lesion was obstructing the visual axis and inducing amblyopia in infants.

Medulloepithelioma

In this study, medulloepithelioma was diagnosed in 8 (22%) patients in the pediatric age group (**Figures 1A–F**) and only 1 patient in the adult group. The lesions were primarily located in the ciliary body, and rubeosis (n=8, 89%) was a common manifestation combined with medulloepithelioma.

In the pediatric age group, the age group for medulloepithelioma ranged from 1 to 17 years, and it observed in 6 (75%) males and 2 (25%) females. Iridogoniocyclectomy was performed in all using a limbal-based flap in 2 (25%) and a fornix-based flap in 6 (75%) patients. Tumor recurrence was noted in 1 (11.1%) patient at 3 months. The recurrence was treated with I-125 plaque brachytherapy in 1 patient, but enucleation was ultimately required because of high-grade malignancy in pathological analysis. Medulloepithelioma was relatively common in children but usually was misdiagnosed during preoperative assessment. Medulloepithelioma in two patients was clinically diagnosed as retinoblastoma and hemangioma, and 2 patients with retinoblastoma were diagnosed to have medulloepithelioma preoperatively. After a mean follow-up duration of 22.5 months, no patient was noted to have documented metastasis.

Malignant medulloepithelioma that occurred in adults was extremely rare; only 1 patient with malignant medulloepithelioma was clinically diagnosed to have amelanotic melanoma or adenoma preoperatively.

Melanocytoma

There were 16 (43%) pediatric patients and 24 (7.3%) adult patients with a histopathological diagnosis of melanocytoma in this study (**Figure 3**). Among pediatric patients, the age group for melanocytoma ranged from 3 to 9 years, and gender was male in 9 (56.3%) and female in 7 (43.8%). The lesions were primarily located in the ciliary body (n = 13; 81.2%) with anterior chamber angle involvement, choroid (n = 2; 12.5%), and iris (n = 1; 6.3%). Sentinel vessel (n = 16, 100%), corneal blood staining/corneal edema (n=13, 81.2%), and rubeosis (n=4, 25%) were common manifestations accompanying melanocytoma. Iridogoniocyclectomy was performed in all patients using a limbal-based flap in 6 (37.5%) and a fornix-based flap in 10 (62.5%). Melanocytoma was common in children and mainly located in the ciliary body with angle involvement; necrosis was noted in the tumor.

Among the adult patients, the age group for melanocytoma ranged from 20 to 56 years, and gender was male in 6 (25%) and female in 18 (75%). The lesions were primarily located in the ciliary body (n = 20; 83.4%), iris (n = 2; 8.3%), and choroid (n = 2; 8.3%). The elevated IOP>21 mmHg (n = 10; 41.7%), pigmented in iris (n = 22, 91.7%), optic atrophy (n = 9, 37.5%), and sentinel vessel (n = 18, 75%) were common

TABLE 3A | BCVA of 366 patients before and after surgery of PTSU and MVRE.

BCVA	Pediatric age group		Adult group	
-	Before surgery (n=37)	After surgery (n=30)	Before surgery (n=329)	After surgery (n=308)
20/20~20/40	2 (5.4%)	1 (3.3%)	33 (10.0%)	15 (4.9%)
20/40~20/80	5 (13.5%)	0 (0%)	76 (23.1%)	58 (18.8%)
20/80~20/200	6 (16.2%)	8 (26.7%)	146 (44.4%)	152 (49.4%)
≤20/200	24 (64.9%)	21 (70%)	74 (22.5%)	83 (26.9%)
Enucleation	**n=7**		**n=21**	

TABLE 3B | BCVA of 213 UM patients before and after surgery of PTSU and MVRE.

BCVA	Pediatric age group		Adult group	
-	Before surgery (n=5)	After surgery (n=2)	Before surgery (n=208)	After surgery (n=188)
20/20~20/40	0 (0%)	0 (0%)	39 (18.8%)	14 (7.4%)
20/40~20/80	0 (0%)	0 (0%)	39 (18.8%)	15 (8.0%)
20/80~20/200	0 (0%)	0 (0%)	84 (40.3%)	97 (51.6%)
≤20/200	2 (100%)	2 (100%)	46 (22.1%)	62 (33.0%)
Enucleation	**n=3**		**n=20**	

manifestations accompanying tumors. Melanocytoma occurrence in adults was relatively common and was diagnosed clinically as melanoma preoperatively. Small ciliary body melanocytoma was commonly misdiagnosed as glaucoma and even a trabeculectomy surgery was performed (n = 6, 25%). Iridogoniocyclectomy was performed in all patients using a limbal-based flap in 8 (33%) and a fornix-based flap in 16 (66%). The intraocular pressure was normal after the surgery (n = 10).

Melanoma

There were 213 patients with the histopathological diagnosis of melanoma in this study, 5 were pediatrics and 208 were adults. Among pediatric patients, the mean age was 6 years (median 5; range, 2–11 years). Among the 5 pediatric patients, 2 (40%) were male and 3 (60%) were female; 4 lesions were pigmented and 1 was non-pigmented. The tumors were primarily located in the ciliary body (n = 1; 20%), and choroid (n = 4; 80%). The pathological cell type was identified to be epithelioid in 1 (20%), spindle cell in 1 (20%), and mixed cell type in 3 (60%) patients. After a mean follow-up period of 148 months, 3 (60%) patients were found to have a recurrence and no patient had documented metastasis. Two cases of the recurrences were treated with enucleation and the third was treated with I-125 plaque brachytherapy.

Among adults, the mean age was 43.8 years (median, 44; range, 21–70 years). Among the 208 patients, 111 (53.4%) were male and 97 (46.6%) were female. The tumors were 13 in nonpigmented and pigmented in 195 patients. The tumors were primarily located in the ciliary body (n = 67; 32.2%), and choroid (n = 122; 58.7%). The pathological cell type was epithelioid in 20 (9.5%), spindle cell in 78 (37.5%), and mixed cell type in 106 (51.0%) patients. After a mean follow-up duration of 24.1 months, 16 (7.7%) patients were noted to have a recurrence with 13 patients had developing hepatic metastasis, and 3 patients along with orbit extension; 13 patients with recurrences were treated with enucleation and 3 patients were treated with I-125 plaque brachytherapy.

Kaplan-Meier analysis estimated that the 1, 3, 5, 7, and 10-year metastasis rates and metastasis related death rates (95% CI) in 213 UM patients were 0.5% (0.1%-3.3%), 3.2% (1.4%-7.0%), 3.2% (1.4%-7.0%), 6.9% (3.8%-12.3%), 6.9% (3.8%-12.3%); and 1.0% (0.2%-3.4%), 1.6% (0.5%-4.8%), 3.5% (1.6%-7.6%), 7.6% (4.2%-13.5%),7.6% (4.2%-13.5%) (**Figure 6**), respectively. Multivariable analysis showed no significant factors having different relative risks for metastasis and metastasis related death, including older age, sex, tumor base, tumor thickness, color and pathological type (**Supplementary Tables 1, 2**).

DISCUSSION

Intraocular tumors are uncommon and the types of intraocular tumors that occurred in the pediatric age group and the adult age group are different, which can often clinically lead to a misdiagnosis. In our selected cases, PTSU combined with MVRE was used as a primary globe-preserving treatment to prevent irradiation or enucleation and to conserve useful visual acuity. Some authors have reported the experience and outcome with local resection of intraocular tumors in the Caucasian population (3–12). However, most of the reported series (2–12) have not subcategorized patients with intraocular tumors based on the pediatric and adult age groups; particularly, the effectiveness of local resection in Asian population is still unknown.

PTSU combined with MVRE is successful for globe salvage, and is designed to remove tumor lesions, preserve vision and maintain a cosmetically normal eye. However, it is a surgically difficult procedure that can sometimes lead to adverse effects in the immediate and late postoperative period. Shields et al. (4) reported the postoperative course of 95 patients treated with PLSU for ciliary body and choroidal tumors. In their series, the most common intraoperative side effect was vitreous hemorrhage (83%) and subretinal or intraretinal hemorrhage (35%). Late postoperative side effects included cataract development in 34% and retinal detachment requiring surgery in 17%. A study by Naumann et al. (13) included 68 patients with iris and ciliary body tumors treated with en bloc excision. The main intraoperative issue in their study was vitreous hemorrhage in 35%, and the main postoperative side effect was cataract development in 32% patients. In our study, the most common immediate postoperative adverse side effect was vitreous hemorrhage (21%) and the most common postoperative adverse effect was PVR (18.3%). These side effects were often mild and had minor effects on the patients.

In literature concerning adult Caucasian patients regarding UM resection, globe-salvage has been achieved in 71% to 81% patients and final visual acuity of ≥20/40 is achieved in 50% to 53% patients (3, 9, 14). Ramasubramanian (5) reported 19 pediatric UM resections, with globe salvage in 76% patients and a final visual acuity of ≥20/40 in 64% patients. In our study on pediatric UM resection, globe salvage was reported in

80% patients, and final BCVA of ≥20/40 was achieved in 3.2% patients. In our study on adult UM resection, globe salvage was reported in 91.8% patients, and a final BCVA of ≥20/40 was achieved in 7.3% patients. The relatively low results for BCVA were associated with vitrectomy and a long follow-up duration.

In the present study, melanoma was the most common diagnosis (63.0%) in adult patients, followed by melanocytoma (7.3%), RPE adenoma (6.4%), and ciliary body adenoma of nonpigmented epithelium (5.7%). Melanoma was primarily located in the choroid (58.7%) and ciliary body (32.2%). Collaborative Ocular Melanoma Study (COMS) disclosed that melanoma-related mortality at 10 years was 17% to 18% for medium melanoma, and the patients underwent I-125 plaque brachytherapy, and 40% to 45% for large melanoma, wherein the patients underwent pre-enucleation radiation (15–18). In our previous study, we found the 5, 10-year UM metastasis rate and metastasis-related death (95% CI) in 1151 Asian UM patients were 15.5% (12.3%-19.5%), 24.5% (17.6% -33.6%); and 7.5% (5.3%-10.7%), 11.9% (8.1%-17.2%), respectively. Of these, 929 patients underwent the management of I-125 plaque brachytherapy (19). In this study, there were 213 medium-sized UM patients who underwent local resection, Kaplan-Merier analysis revealed that 5, 10-year metastasis rates and metastasis-related death rates (95% CI) in 213 UM patients were 3.2% (1.4%-7.0%), 6.9% (3.8%-12.3%); and 3.5% (1.6%-7.6%), 7.6% (4.2%-13.5%), respectively. The probable low rate of metastasis in this study maybe because of patient selection bias. Multivariate analysis revealed that the pathological type had no significant factors having different relative risks of metastasis and metastasis-related death in patients with UMs, the results were inconsistent with previous studies in which found that the presence of epithelioid tumor cells was one of the predictors (20). Considering the Racial differences and patient selection bias further studies were needed to evaluate its influence on UM onset among the Asian population. Iris tumors are less likely to metastasize and smaller tumors mainly located in the ciliary body are more preferable to be treated with PTSU combined with MVRE. In addition, during the mean follow-up duration of 24.1 months, a low recurrence rate of 7.7% (16/208) was noted, requiring subsequently rescue therapy. There was no metastasis-related death at the end of the follow-up. Based on the above mentioned findings, local resection has excellent effective outcomes.

In not completely conformity with the previous studies (5, 21–23), several special clinical features were noted in a large proportion of our pediatric patients: melanoma rarely occurred in the pediatric age group (n = 5), and no cases of metastatic disease and death were observed. However, UM was reported to occur with a frequency of 1.1% among all UMs in Caucasian patients<20 years of age. Of these, 12% to 21% arise in the iris and 88% to 79% from the ciliary body and choroid (21, 22). In a study by Shields et al. (22) including 106 patients with UM aged <20 years old, the rate of metastasis was 4.7% and the rate of death from metastasis was 2.8%. They noted that melanoma in the pediatric age group of patients was more likely to be pigmented, with melanoma located in the iris, more remote from the foveola and optic disc, and with a smaller tumor basal diameter and thickness (22). The rate of metastasis was significantly lower in patients aged <20 years (22).

Melanocytoma was the most commonly diagnosed in our pediatric age group; this result was inconsistent with a previous study (5). In Ramasubramanian's (5) pediatric series, the most common diagnosis was medulloepithelioma. Frank et al. (23) reported the clinical features and management of 10 melanocytoma of the ciliary body. In their series, 1 patient was a child and the other 9 patients were adults. No recurrences were reported among the 10 patients who underwent management by iridocyclectomy. Melanocytomas of the ciliary body, although having the benign nature, have a propensity for invasion of the chamber angle structures and a tendency to recur. In this series, there were 16 pediatrics and 24 adult patients with melanocytoma; the mean largest tumor basal diameter was 11 mm vs 7 mm, and the mean tumor thickness was 4 mm vs 3 mm, respectively. Furthermore, we noted the different clinical features of melanocytoma between pediatrics and adults. Melanocytoma in pediatric patients was often with a larger tumor basal diameter and thickness, and more likely to be accompanied with hyphema. Further, 12 of the 16 pediatric patients (75%) showed local extension to the anterior chamber angle structures and intrascleral limbal plexuses. Of the 24 adult patients, 10 (41.7%) and 9 (37.5%) showed elevated preoperative IOP and optic disc atrophy, respectively. Moreover, 22 (91.7%) patients had remarkable pigmentation with dispersed fine dark spots distributed on the iris at presentation. Local extension or invasion of the chamber angle of the tumor was only observed in 2 (13%) patients. Pathological findings reported that mitosis was usually absent. Invasion of the chamber angle structures was observed histologically in 9 patients from the pediatric age group. Extensive necrosis was seen in 9 of 10 tumors, and malignant changes were noted in another. In contrast, these pathological features were not noted in the adult group.

In addition, although a melanocytoma of the ciliary body can usually be distinguished by histopathological criteria, clinically it may be difficult to distinguish from malignant melanoma before surgery. Like melanocytomas, ciliary body melanomas are usually slow-growing tumors (21, 22). Accordingly, we also do not rely on tumor growth as a differentiating factor. For the above reasons, if technically feasible, we favor iridocyclectomy or PTSU combined with MVRE over observation of darkly pigmented tumors of the ciliary body. Limbal incision was performed in all patients, and during the follow-up period, there was no recurrence was observed.

Medulloepithelioma was a relatively common diagnosis (21.6%) in pediatric patients. Medulloepithelioma is a congenital tumor that usually arises from the ciliary body, and most are accompanied with intratumoral cysts. In Ramasubramanian's (5) series of 4 medulloepithelioma, they found medulloepithelioma was the most commonly misdiagnosed tumor preoperatively. In Zimmerman's series (24) of 56 intraocular medulloepitheliomas, 45 (80%) were treated initially with iridocyclectomy but subsequently required enucleation: 20% developed extraocular extension and 7% died of tumor-related causes. In Canning's

(25) series of 16 patients with medulloepithelioma, 4 patients were initially treated with resection but all eventually needed enucleation. In our study, there were 9 patients with histopathological diagnosis of medulloepithelioma and 1 out of 9 patients ultimately required enucleation (globe salvage rate, 88.9%). None of the patients in our study developed extraocular disease or metastasis. We found that rubeosis is a common manifestation presented with medulloepithelioma (89%); thus, it maybe another clinical characteristic of this rare tumor.

The selected criteria and treatment guidelines we follow are based on experience from our patient series and from previous reports. Considering the controversy of fine-needle aspiration biopsy, given that there is potential for dissemination of tumor cells (26), we do not routinely choose to perform this procedure for speculated malignant lesions, including the simulated neoplastic lesions. In our series, there were 3 cases of adult-onset well-differentiated retinoblastoma without metastasis or death postoperatively, and the gene testing has confirmed the diagnosis lately. Regardless, an optimal treatment should be interpreted with caution because of the rarity of adult retinoblastoma.

In summary, PTSU combined with MVRE is an acceptable treatment option for benign and malignant intraocular tumors and simulating lesions in the pediatric age group and adult group, allowing globe-salvaging with the possibility of maintaining useful vision and favorable survival of the patients. The adverse effect rates are similar between the pediatric and the adult populations and enucleation is eventually needed in approximately 7.7% of patients. Patients with iris and ciliary body UM show benefits *via* local resection, and enucleation is needed only in few cases. Surgical resection of an intraocular tumor in its entirety with careful assessment of pathological features and gene analysis may have more potential benefits to favorable long-term outcomes.

SYPNOSIS

In this work, we described the outcomes of intraocular tumor resection by partial transscleral sclerouvectomy (PTSU) combined with micro-invasive vitrectomy and reconstruction of the eyeball (MVRE) in 366 Asian patients in 25 years. The adverse effect rates were similar between the pediatric and the adult populations and enucleation waseventually needed in approximately 7.7% of patients. These findings suggested that local resection has excellent effective outcomes in patients with intraocular tumors.

DATA AVAILABILITY STATEMENT

The original contributions presented in the study are included in the article/**Supplementary Material**. Further inquiries can be directed to the corresponding author.

ETHICS STATEMENT

The studies involving human participants were reviewed and approved by Institutional Review Board of Beijing Tongren Hospital. Written informed consent to participate in this study was provided by the participants' legal guardian/next of kin. Written informed consent was obtained from the individual(s), and minor(s)' legal guardian/next of kin, for the publication of any potentially identifiable images or data included in this article.

AUTHOR CONTRIBUTIONS

WW: Examination of patient, interpretation of results, writing the manuscript. NZ: Interpretation of results and writing/ reviewing of manuscript. XX: Interpretation of results and reviewing of manuscript. PW: Reviewing of manuscript. YL: Examination and treatment of patient. All authors read and approved the final manuscript.

FUNDING

The National Natural Science Foundation of China (Nr. 81272981), the Beijing Natural Science Foundation (Nr. 7151003) provided financial support.

SUPPLEMENTARY MATERIAL

The Supplementary Material for this article can be found online at: https://www.frontiersin.org/articles/10.3389/fonc.2022.768635/full#supplementary-material

REFERENCES

1. Shields JA, Shields CL. *Intraocular Tumors: An Atlas and Textbook. 2nd*. Philadelphia: Lippincott Williams and Wilkins (2008) p. 6–58.
2. Lee CS, Rim TH, Kwon HJ, Yi JH, Lee SC. Partial Lamellar Sclerouvectomy of Ciliary Body Tumours in a Korean Population. *Am J Ophthalmol* (2013) 156:36–42.e1. doi: 10.1016/j.ajo.2013.01.026
3. Shields JA, Shields CL. Surgical Approach to Lamellar Sclerouvectomy for Posterior Uveal Melanomas: The 1986 Schoenberg Lecture. *Ophthalmic Surg* (1988) 19:774–80. doi: 10.3928/0090-4481-19881101-04
4. Shields JA, Shields CL, Shah P, Sivalingam V. Partial Lamellar Sclerouvectomy for Ciliary Body and Choroidal Tumors. *Ophthalmology* (1991) 98:971–83. doi: 10.1016/S0161-6420(91)32194-8
5. Ramasubramanian A, Shields CL, Kytasty C, Mahmood Z, Shah SU, Shields JA. Resection of Intraocular Tumors (Partial Lamellar Sclerouvectomy) in the Pediatric Age Group. *Ophthalmology* (2012) 119(12):2507–13. doi: 10.1016/j.ophtha.2012.06.044
6. Mirzayev I, Gündüz AK, Okçu Heper A. Partial Lamellar Sclerouvectomy Surgery for Anteriorly Located Uveal Tumour Resection: A 20-Year Experience. *Eye (Lond)* (2021). doi: 10.1038/s41433-021-01545-7

7. Char DH, Miller T, Crawford JB. Eye-Wall Resection. *Trans Am Ophthalmol Soc* (2000) 98:153–9.
8. Weinstein GW, Quayle WH. An En Bloc Technique for the Resection of Anterior Uveal Tumors. *Am J Ophthalmol* (1979) 88:519 –23. doi: 10.1016/0002-9394(79)90657-3
9. Char DH, Miller T, Crawford JB. Uveal Tumour Resection. *Br J Ophthalmol* (2001) 85:1213–9. doi: 10.1136/bjo.85.10.1213
10. Damato BE, Paul J, Foulds WS. Predictive Factors of Visual Outcome After Local Resection of Choroidal Melanoma. *Br J Ophthalmol* (1993) 77:616 –23. doi: 10.1136/bjo.77.10.616
11. Peyman GA, Gremillion CM. Eye Wall Resection in the Management of Uveal Neoplasms. *Jpn J Ophthalmol* (1989) 33:458–71.
12. Memmen JE, McLean IW. The Long-Term Outcome of Patients Undergoing Iridocyclectomy. *Ophthalmology* (1990) 97:429–32. doi: 10.1016/S0161-6420(90)32562-9
13. Naumann GO, Rummelt V. Block Excision of Tumors of the Anterior Uvea: Report on 68 Consecutive Patients. *Ophthalmology* (1996) 103:2017–27. doi: 10.1016/S0161-6420(96)30392-8
14. Damato B. The Role of Eyewall Resection in Uveal Melanoma Management. *Int Ophthalmol Clin* (2006) 46:81–93. doi: 10.1097/01.iio.0000195862.71558.c8
15. Diener-West M, Earle JD, Fine SL, et al. Collaborative Ocular Melanoma Study Group. The COMS Randomized Trial of Iodine 125 Brachytherapy for Choroidal Melanoma, III: Initial Mortality Findings: COMS Report No. 18. *Arch Ophthalmol* (2001) 119(7):969–82. doi: 10.1001/archopht.119.7.969
16. Collaborative Ocular Melanoma Study Group. The COMS Randomized Trial of Iodine 125 Brachytherapy for Choroidal Melanoma, V: 12-Year Mortality Rates and Prognostic Factors: COMS Report No. 28. *Arch Ophthalmol* (2006) 124(12):1684– 93. doi: 10.1001/archopht.124.12.1684
17. Collaborative Ocular Melanoma Study Group. The Collaborative Ocular Melanoma Study (COMS) Randomized Trial of Pre-Enucleation Radiation of Large Choroidal Melanoma, II: Initial Mortality Findings: COMS Report No. 10. *Am J Ophthalmol* (1998) 125(6):779–96. doi: 10.1016/s0002-9394(98)00039-7
18. Hawkins BSCollaborative Ocular Melanoma Study Group. The Collaborative Ocular Melanoma Study (COMS) Randomized Trial of Pre-Enucleation Radiation of Large Choroidal Melanoma, IV: 10-Year Mortality Findings and Prognostic Factors: COMS Report No. 24. *Am J Ophthalmol* (2004) 138(6):936–51. doi: 10.1016/j.ajo.2004.07.006
19. Zhou N, Zhang R, Xu X, Liu Y, Wei W. Clinical Characteristics of Uveal Melanoma and Association of Metastasis of Uveal Melanoma With Congenital Oculocutaneous Melanosis in Asian Patients: Analysis of 1151 Consecutive Eyes. *Ophthalmol Retina* (2021) 5(11):1164–72. doi: 10.1016/j.oret.2021.01.001
20. Damato BE, Paul J, Foulds WS. Risk Factors for Metastatic Uveal Melanoma After Trans-Scleral Local Resection. *Br J Ophthalmol* (1996) 80:109–16. doi: 10.1136/bjo.80.2.109
21. Shields CL, Shields JA, Milite J, De Potter P, Sabbagh R, Menduke H. Uveal Melanoma in Teenagers and Children: A Report of 40 Cases. *Ophthalmology* (1991) 98:1662– 6. doi: 10.1016/S0161-6420(91)32071-2
22. Shields CL, Kaliki S, Furuta M, Mashayekhi A, Shields JA. Clinical Spectrum and Prognosis of Uveal Melanoma Based on Age at Presentation in 8,033 Cases. *Retina* (2012) 32:1363–72. doi: 10.1097/IAE.0b013e31824d09a8
23. LoRusso FJ, Boniuk M, Font RL. Melanocytoma (Magnocellular Nevus) of the Ciliary Body: Report of 10 Cases and Review of the Literature. *Ophthalmology* (2000) 107(4):795–800. doi: 10.1016/s0161-6420(99)00151-7
24. Broughton WL, Zimmerman LE. A Clinicopathologic Study of 56 Cases of Intraocular Medulloepitheliomas. *Am J Ophthalmol* (1978) 85:407–18. doi: 10.1016/S0002-9394(14)77739-6
25. Canning CR, McCartney AC, Hungerford J. Medulloepithelioma (Diktyoma). *Br J Ophthalmol* (1988) 72:764 –7. doi: 10.1136/bjo.72.10.764
26. Karcioglu ZA, Gordon RA, Karcioglu GL. Tumor Seeding in Ocular Fine Needle Aspiration Biopsy. *Ophthalmology* (1985) 92:1763–7. doi: 10.1016/S0161-6420(85)34105-2

Conflict of Interest: The authors declare that the research was conducted in the absence of any commercial or financial relationships that could be construed as a potential conflict of interest.

frontiers in Oncology

ORIGINAL RESEARCH
published: 25 March 2022
doi: 10.3389/fonc.2022.800449

Development and Validation of a Preoperative Nomogram for Predicting Benign and Malignant Gallbladder Polypoid Lesions

Shuai Han[1], *Yu Liu*[2], *Xiaohang Li*[1], *Xiao Jiang*[3], *Baifeng Li*[1], *Chengshuo Zhang*[1] *and Jialin Zhang*[1]*

[1] Department of Hepatobiliary Surgery, The First Hospital of China Medical University, Shenyang, China, [2] Department of Radiology, The First Hospital of China Medical University, Shenyang, China, [3] Department of Endocrinology and Metabolism, The Second Hospital of Dalian Medical University, Dalian, China

OPEN ACCESS

Edited by:
Patrick J. Schuler, Ulm University Medical Center, Germany

Reviewed by:
Jose M. Ramia, Hospital General Universitario de Alicante, Spain
Stefano Francesco Crinò, University of Verona, Italy

***Correspondence:**
Jialin Zhang
jlz2000@yeah.net

Specialty section:
This article was submitted to Surgical Oncology, a section of the journal Frontiers in Oncology

Received: *23 October 2021*
Accepted: *23 February 2022*
Published: *25 March 2022*

Citation:
Han S, Liu Y, Li X, Jiang X, Li B, Zhang C and Zhang J (2022) Development and Validation of a Preoperative Nomogram for Predicting Benign and Malignant Gallbladder Polypoid Lesions. Front. Oncol. 12:800449. doi: 10.3389/fonc.2022.800449

Purpose: The purpose of this study was to develop and validate a preoperative nomogram of differentiating benign and malignant gallbladder polypoid lesions (GPs) combining clinical and radiomics features.

Methods: The clinical and imaging data of 195 GPs patients which were confirmed by pathology from April 2014 to May 2021 were reviewed. All patients were randomly divided into the training and testing cohorts. Radiomics features based on 3 sequences of contrast-enhanced computed tomography were extracted by the Pyradiomics package in python, and the nomogram further combined with clinical parameters was established by multiple logistic regression. The performance of the nomogram was evaluated by discrimination and calibration.

Results: Among 195 GPs patients, 132 patients were pathologically benign, and 63 patients were malignant. To differentiate benign and malignant GPs, the combined model achieved an area under the curve (AUC) of 0.950 as compared to the radiomics model and clinical model with AUC of 0.929 and 0.925 in the training cohort, respectively. Further validation showed that the combined model contributes to better sensitivity and specificity in the training and testing cohorts by the same cutoff value, although the clinical model had an AUC of 0.943, which was higher than 0.942 of the combined model in the testing cohort.

Conclusion: This study develops a nomogram based on the clinical and radiomics features for the highly effective differentiation and prediction of benign and malignant GPs before surgery.

Keywords: gallbladder polypoid lesions, radiomics, nomogram, computed tomography, risk factors

INTRODUCTION

Gallbladder polypoid lesions (GPs), as a common gallbladder disease, represent a wide spectrum of lesions that protrude inward from the wall of the gallbladder. In past decades, the prevalence of GPs has been increasing on account of the abuse of abdominal imaging methods, affecting approximately 4%–10% of adults worldwide (1, 2). Clinically, most gallbladder polyps are benign, and only a minority are malignant polyps. Unfortunately, the prognosis and clinical management of them are quite different (3–5). Thus, it is crucial to differentiate benign and malignant GPs preoperatively.

Recently, predictions of malignant GPs have been reported based on the features of patients and GPs. However, it has been proven difficult to differentiate between benign and malignant GPs relying on these features (6–8). Radiomics is an emerging method whose final goal is to dig up the existing medical images that we can get the high-dimensional information, hence aiding in clinical decision-making. In clinical practice, contrast-enhanced computed tomography (CECT) is in common use for GPs, benefited to evaluate the relationship of the tumor and surrounding tissues and consequently accurately diagnose GPs (9). Therefore, a tool for the early identification of malignant GPs is developed through this research.

MATERIALS AND METHODS

Patient Selection

The study ultimately included 195 patients with gallbladder polypoid lesions which were ≥10 mm and proven by pathology during April 2014 to May 2021. The inclusion criteria included the following (1) patients who underwent surgical treatment and were diagnosed, confirmed pathologically; (2) the maximum diameter of GPs ≥10 mm; and (3) CECT performed in all patients within 1 month prior to the operation. The exclusion criteria included the following: (1) patients had undergone some operation or treatment before surgery including radio-chemotherapy and percutaneous transhepatic gallbladder drainage; (2) the lesion had invaded the surrounding tissues obviously; and (3) the GPs could not be displayed clearly for the gallbladder wall edema accompanied by a large amount of inflammatory exudate due to acute cholecystitis and respiratory artifacts. All the patients were randomly divided into a training cohort and a testing cohort in the ratio of 7:3.

Clinical Feature

Clinical characters of patients and CT imaging features, measured by experienced radiologists, were collected and recorded from electronic medical records, retrospectively. The cutoff points of age were confirmed, and patients were divided into two groups based on the principle of maximum Youden's index: patients who were younger than 56 years and not. If any of the gallbladder diseases symptoms existed, such as upper abdominal pain, nausea and vomiting, cutaneous, or sclera icterus, they were recorded as positive. The diameter of the lesion was recorded at the horizontal slice of the largest size of the lesion. In addition, the GPs were divided by the gallbladder anatomical location strictly, which was defined as gallbladder neck, fundus, or body. The base that means the basal morphology of GPs was divided into sessile and pedunculated for the angle between the basement mucosa and protuberance of the GPs with reference to Yamada's classification where the sessile lesions refer to the angle >90° while the pedunculated lesions are defined as angle <90° (10). It would be defined as multiple if there were more than one lesion, and the lesion which had the largest diameter was considered as the target lesion. Each parameter was compared between the benign and malignant gallbladder polypoid lesion groups with univariate correlation analysis in the training cohort. Thereafter, the parameters that associated with the benignity and malignancy of the GPs were identified by a multivariate logistic regression analysis.

Imaging

Three CT scanners were included in this study, namely, Somatom Definition Flash CT (Siemens Healthineers, Erlangen, Germany), Aquilion ONE CT (Toshiba Corporation, Tokyo, Japan), and BrillianceICT (Royal Philips Electronics, Amsterdam, Netherlands). The most recent record will be selected if the patient has multiple CECT examination records. All patients were first given a plain scan in a conventional supine position, then an enhanced scan. Arterial phase, portal venous phase, and delayed phase were performed at 25 to 30 s, 60 to 70 s, and 160 to 180 s after the injection of a non-ionic contrast agent. In addition, the whole original medical image is resampled to the same voxel spacing by the linear interpolation algorithm, and the differences of scanning parameters in different scanner modes are eliminated. The new data points in the original image are reconstructed within the range of known data points.

Segmentation

The resampled sequences including arterial-phase, portal-phase, and delayed-phase CT images were imported to segment a structure software application called ITK-SNAP (http://www.itksnap.org, version 3.8.0), and the volume-of-interest (VOI) segmentation was manually delineated by a doctor with the years of radiology experience without seeing the patient's clinical information or pathological diagnosis. Then, the delineated segmentations were reviewed carefully by a senior doctor who has 30 years of radiology experience.

Radiomics Feature Extraction and Selection

"PyRadiomics," an open-source package for standardizing the extraction of radiomics data (https://github.com/Radiomics/pyradiomics), was used to extract 107 radiomics features from each phase of preprocessed sequence CT image and the segmented VOI. The extracted features can be classified into seven categories including 14 Shape-based features, 18 First-Order Statistics features, 24 Gray-Level Co-occurrence Matrix features, 16 Gray-Level Run Length Matrix features, 16 Gray-Level Size Zone Matrix features, 14 Gray-Level Dependence Matrix features, and 5 Neighboring Gray Tone Difference Matrix features. All the features were standardized by the

following formula: features = (f − μ)/std. First, Pearson correlation analysis was performed to identify the redundant features. Features with the mean absolute correlation higher than 0.8 were considered redundant and would be randomly eliminated by a high correlation filter, leaving only one. Then, the least absolute shrinkage and selection operator (LASSO) method with tenfold cross-validation was used to iteratively screen the most significant features in the training cohort until the feature coefficients were not zero. Rad-score was calculated based on these features by the formula shown as follows:

$$Rad-score = \beta_0 + \beta_1 x\,(f_1 - \mu_1)/std_1 + \beta_2 x\,(f_2 - \mu_2)/std_2 + \cdots \beta_n x\,(f_n - \mu_n)/std_n$$

f = {f_i, i = 1, 2, ···, n} indicates the selected radiomics features; μ = {μ_i, i = 1, 2, ···, n}

and std = {std_i, i = 1, 2, ···, n} indicates the mean value and the standard deviation of each feature and β = {β_i, i = 0, 1, ···, n} indicates the LASSO regression coefficient.

Nomogram Building and Validation

After the clinical and radiomics significant parameters were identified in the training cohort, three models could be constructed in the training cohort with clinical features, radiomics features, or both of them, respectively. The receiver operating characteristic (ROC) curve and calibration curve were used to compare and evaluate the predictive ability of the models for GP benignity and malignancy in both the training and testing cohorts. Then, the area under the curve (AUC) was calculated and the cutoff value in the training cohort based on the maximum Youden's index criterion was confirmed. On the same cutoff value, the sensitivity and specificity were achieved in both the training and testing cohorts. After assessment, the most robust model would be used to construct a nomogram. The whole process is shown in **Figure 1**.

Statistical Analysis

Continuous data were expressed using the mean ± standard deviation (SD) or median [interquartile range (IQR) as appropriate. Continuous variables were analyzed using Student's t-test or Mann–Whitney U test appropriately. Categorical variables were analyzed using the x^2 test or Fisher exact test. All statistical analyses were completed by R language software (version 4.0.5). The packages named "ResourceSelection," "PredictABEL," "pROC," "rms," "glmnet," "RROC," "Hmisc," and "rmda" were used.

RESULTS

Patient Characteristics

A total of 195 patients were included in the study, including 136 in the training cohort and 59 in the testing cohort. In the training cohort, 92 patients with benign and 44 patients with malignant cystic polypoid lesions were enrolled, respectively. In the testing cohort, 40 patients have benign and 19 patients have malignant gallbladder polypoid lesions. The characteristics of patients in the training cohort are detailed in **Table 1**. The statistical

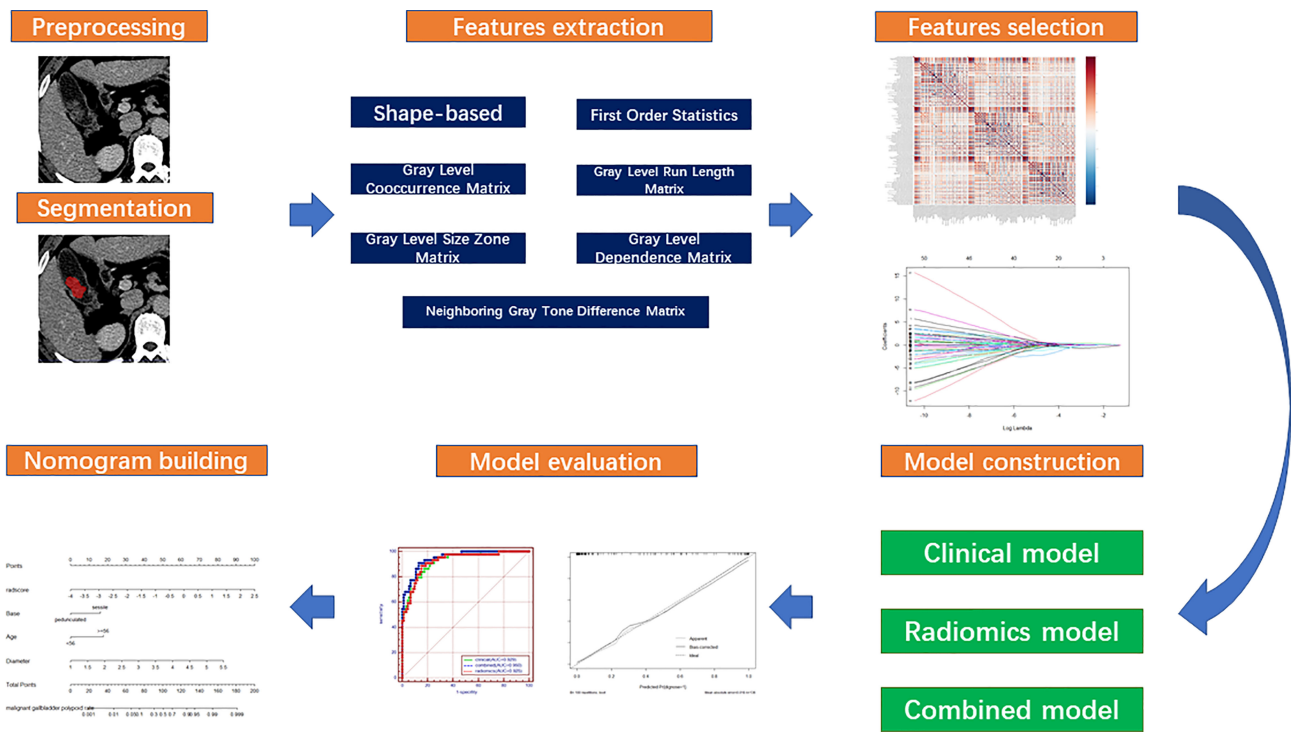

FIGURE 1 | Study workflow.

TABLE 1 | Demographics and clinical characteristics.

Parameters	Level	Overall 136	Benign 92	Malignant 44	p
Age (%)	<56	62 (45.6)	54 (58.7)	8 (18.2)	<0.001
	>=56	74 (54.4)	38 (41.3)	36 (81.8)	
Sex (%)	female	89 (65.4)	61 (66.3)	28 (63.6)	0.91
	male	47 (34.6)	31 (33.7)	16 (36.4)	
Diabetes (%)	absent	115 (84.6)	79 (85.9)	36 (81.8)	0.72
	present	21 (15.4)	13 (14.1)	8 (18.2)	
Hypertension (%)	absent	103 (75.7)	77 (83.7)	26 (59.1)	0.004
	present	33 (24.3)	15 (16.3)	18 (40.9)	
BMI (kg/m^2)		25.95 [22.17, 30.10]	25.05 [21.87, 30.57]	27.55 [22.90, 29.70]	0.421
Symptoms (%)	absent	91 (66.9)	64 (69.6)	27 (61.4)	0.45
	present	45 (33.1)	28 (30.4)	17 (38.6)	
CA199 (%)	absent	108 (79.4)	75 (81.5)	33 (75.0)	0.514
	present	28 (20.6)	17 (18.5)	11 (25.0)	
CA125 (%)	absent	135 (99.3)	91 (98.9)	44 (100.0)	1
	present	1 (0.7)	1 (1.1)	0 (0.0)	
AFP (%)	absent	128 (94.1)	85 (92.4)	43 (97.7)	0.437
	present	8 (5.9)	7 (7.6)	1 (2.3)	
CEA (%)	absent	110 (80.9)	73 (79.3)	37 (84.1)	0.671
	present	26 (19.1)	19 (20.7)	7 (15.9)	
RBC (10^{12}/L)		4.57 (0.50)	4.62 (0.49)	4.48 (0.51)	0.126
HGB (g/L)		137.83 (15.98)	138.35 (16.32)	136.75 (15.38)	0.587
PLT (10^9/L)		227.50 [197.50, 254.25]	229.00 [202.75, 257.50]	210.50 [190.25, 239.75]	0.078
INR		1.00 [1.00, 1.02]	1.00 [1.00, 1.02]	1.00 [1.00, 1.02]	0.493
WBC (10^9/L)		5.67 [4.67, 7.02]	5.74 [4.64, 6.61]	5.46 [4.75, 7.37]	0.559
NE (10^9/L)		3.16 [2.54, 3.97]	3.14 [2.55, 3.97]	3.23 [2.48, 4.69]	0.614
LY (10^9/L)		1.92 [1.55, 2.35]	1.93 [1.61, 2.33]	1.75 [1.50, 2.38]	0.462
ALB (g/L)		40.69 (4.00)	41.37 (3.98)	39.27 (3.68)	0.004
ALT (U/L)		17.50 [12.00, 24.25]	17.50 [12.00, 24.00]	18.00 [12.00, 27.75]	0.622
DBIL (μmol/L)		3.10 [2.50, 4.70]	3.10 [2.48, 4.82]	3.10 [2.58, 4.43]	0.961
TBIL (μmol/L)		11.30 [8.70, 15.45]	11.70 [9.15, 15.93]	10.50 [8.30, 13.35]	0.35
Location (%)	Bottom/body	124 (91.2)	88 (95.7)	36 (81.8)	0.019
	Neck	12 (8.8)	4 (4.3)	8 (18.2)	
Number (%)	Single	92 (67.6)	58 (63.0)	34 (77.3)	0.143
	Multiple	44 (32.4)	34 (37.0)	10 (22.7)	
Base (%)	Pedunculated	47 (34.6)	41 (44.6)	6 (13.6)	0.001
	sessile	89 (65.4)	51 (55.4)	38 (86.4)	
Diameter (cm)		1.60 [1.19, 2.30]	1.29 [1.07, 1.73]	2.43 [1.95, 3.35]	<0.001
Stones (%)	Absent	115 (84.6)	78 (84.8)	37 (84.1)	1
	Present	21 (15.4)	14 (15.2)	7 (15.9)	

meaningful characteristics were identified as significant with $p < 0.1$ by univariate analysis, among whom three characteristics were selected for $p < 0.01$ in multivariate logistic regression analysis by entering methods including age (odds ratio (OR) = 8.28, p = 0.003), base (OR = 6.96, p = 0.006), and diameter (OR = 14.68, $p < 0.001$) (**Table 2**). Taking three factors above as independent variables, a logistic regression model was constructed and evaluated. The sensitivity and specificity were 0.773, 0.935 in the training cohort and 0.737, 0.950 in the testing cohort, respectively, and the AUC was 0.929, 0.943, respectively.

Radiomics Features

After importing the original images and VOI segmentation files into the Pyradiomics package, 321 radiomics features of each patient were extracted and then normalized. Subsequently, Pearson's correlation coefficients of all 321 radiological features

TABLE 2 | Multivariate analysis of risk factors related with malignant GPs.

Parameters		Odds ratio	95% CI	p
Age	<56 vs. ≥56	8.28	2.05-33.46	0.003
Base	Pedunculated vs. sessile	6.96	1.77-27.46	0.006
diameter		14.68	4.38-49.16	<0.001

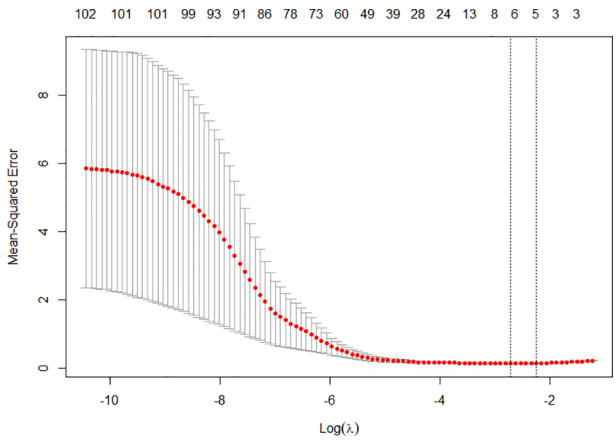

FIGURE 2 | The tenfold cross-validation was repeated 100 times to generate the optimal value in the LASSO model. Six non-zero coefficients were chosen at the standard of lambda that gave the minimum binomial deviance.

for each patient and highly correlated features were randomly excluded, after which a total of 104 radiomics features remained. Six features with non-zero coefficients were finally filtrated by the LASSO logistic regression (**Figure 2**). Taking 6 radiomics factors into the radiomics model, Rad-score was calculated in the training cohort and testing cohort. The sensitivity and specificity were 0.886, 0.848 in the training cohort and 0.737, 0.925 in the testing cohort, respectively, and the AUC was 0.925, 0.920, respectively.

Development, Performance, and Validation of the Combined Model

As aforementioned, we incorporated clinical features in conjunction with radiomics signatures into the multivariate logistic regression in the training cohort and obtained the combined logistic regression model. The sensitivity and specificity were 0.909, 0.870 in the training cohort and 0.842, 0.925 in the testing cohort, which performed more equally and appropriately as a screening model corresponding to other two models, and the AUC was 0.950, 0.942 (**Figures 3A, B**), respectively. Aside this, the calibration curves of the combined model in both training cohort and testing cohort showed that the discrete experimental lines were almost overlapping with or close to the diagonal line (**Figures 4A, B**), which indicated that the calibration of the combined model in identifying the benignity and malignancy of GPs was high. Moreover, the Hosmer–Lemeshow test yielded non-significant p values, 0.824 in the training cohort and 1.000 in the testing cohort, which also showed good calibration power.

DISCUSSION

Gallbladder lesions are broadly divided into wall thickening (GWT) and polypoid lesions (GPs) according to the morphology performance in imaging modalities that GWTs should be determined as wall thickening of 4 mm or more, while GPs are defined as focal elevation or protrusions that are distinguishable from the surrounding mucosa including early gallbladder cancer and neoplastic and non-neoplastic polyps (11, 12). For instance, the most common type of non-neoplastic polyp is cholesterol polyp, which accounts for about 60% of gallbladder polyps and tends to remain benign. Adenomas are truly neoplastic polyps with a definite potential to develop into a malignant state. Unfortunately, benign and malignant gallbladder polyps are difficult to distinguish because of their similar morphology, and there are currently no reliable predictive biomarkers for the diagnosis of GPs larger than 10 mm (13–15). At present, it is well accepted and recommended that, when polyps are larger than 10 mm, cholecystectomy should be performed because gallbladder polyps that are large-sized (≥10 mm) or rapidly growing must be regarded as potentially malignant (16–19). About the choice of initial surgical methods for GPs, laparoscopic cholecystectomy is recommended for GPs larger than 10 mm unless the malignant one is highly preoperative suspected without taking account of any other factors that might interfere with surgery, while the final approach of surgery is determined by intraoperative frozen sections and postoperative histopathology. Although the most definite surgical approach for malignant GPs is unsettled, it is widely recognized that open cholecystectomy with partial liver and lymph node resection when necessary or laparoscopic cholecystectomy is appropriate to achieve better prognosis according to invasive GPs or not. Therefore, it is important to preoperatively identify malignant GPs based on which can we take the proper surgical techniques such as avoidance of gallbladder perforation and bile spillage, use of a protective bag for specimen extraction, and intraoperative frozen sections or open cholecystectomy (13, 20, 21). Actually, there was only 0.690 of sensitivity in clinical preoperative diagnosis at our database (**Table 3**). Considering the moderate diagnostic accuracy, we developed and validated a nomogram incorporating clinical and radiomics features for individualized preoperative prediction and differentiation of benign and malignant GPs. The results showed that the study provided a prediction tool by which patients with

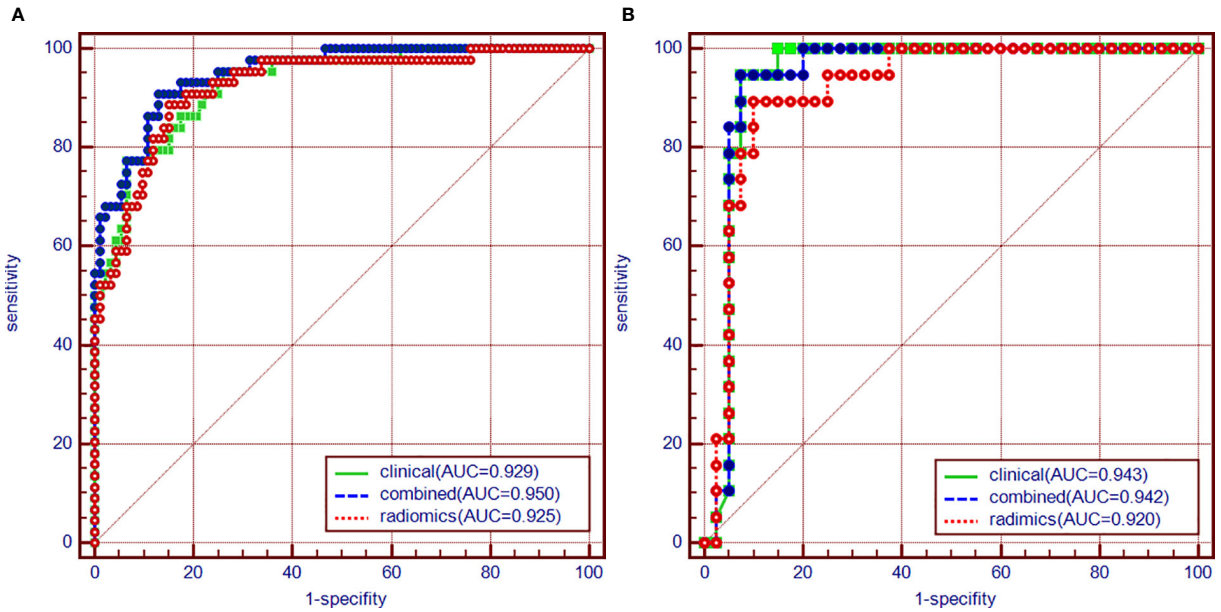

FIGURE 3 | **(A)** Diagnostic efficiency of 3 models using ROC analysis in the training cohort. **(B)** Diagnostic efficiency of 3 models using ROC analysis in the testing cohort.

gallbladder polyps ≥10 mm in size can be identified before surgery and had a favorable discrimination and calibration.

For the selection of clinical characteristics and imaging features, previous studies have confirmed that several clinical risk factors were closely related to the benignity and malignancy of the GPs (7, 13). Similarly, we found that age, base, and diameter were significantly associated with the benignity and malignancy of the GPs in this study. In total, 26 candidate features were reduced to 3 features that influenced the benignity and malignancy of the GPs as independent factors after the univariate correlation analysis and multivariate logical regression in the training cohort. Actually, the presence of gallstones appears to be a risk factor for malignancy of GPs in previous studies but not ours. One possible contributing factor was that the increased risk caused by gallstones is most likely attributable to greater local epithelial irritation and chronic inflammation leading to dysplasia, which were presented with GWTs and excluded from our study.

In addition, traditional radiographic diagnosis by visual observation is usually limited by human visual perception, while radiomics was a useful tool, which enables quantification of diseases by extracting information that cannot be directly recognized by the human brain from images and ultimately assists the surgeon especially in diagnosis and efficacy prediction (6, 8, 11). For the achievement of the radiomics signature from image, ultrasonography (US) is one of the most effective screening methods used for assessment of GPs. The diagnostic performance of US can be further improved by the use of high-resolution US, contrast-enhanced US, and endoscopic US. Yuan et al. showed that contrast-enhanced US is preferred over CT for the diagnosis of neoplastic and non-neoplastic GPs; Andrea et al. reported the use of contrast-enhanced endoscopic US for the characterization of mural nodules within pancreatic cystic neoplasms; and Antonio et al. described a method of contrast-enhanced harmonic endoscopic ultrasound-guided fine-needle aspiration versus standard fine-needle aspiration in pancreatic masses (11, 22–24). However, we noted the limitation of ultrasonography (US) that the slices they selected in two-dimensional imaging may not cover the cancerous lesions area and the sensitivity and accuracy of US are highly dependent on the diagnostic skill of sonographers. Magnetic resonance imaging based on high b-value diffusion-weighted imaging has been applied as a non-invasive modality in distinguishing between benign and malignant GPs, but the sensitivity and specificity of magnetic resonance imaging are unsatisfying owing to the "T2 shine-through" effect (6, 13). Yet, CECT is a widespread used modality and is adopted most frequently to distinguish between benign and malignant gallbladder polypoid lesions, and it was adopted on a single phase by previous investigations (10). The potential of radiomics to predict the characteristics of tumors, among whom CT-based radiomics has been widely applied in liver, lung, and pancreatic tumors, has been demonstrated (25–27). However, there have been a few reports on CECT-based radiomics in predicting benign and malignant GPs. To the best of our knowledge, this study is the first attempt to provide a comprehensive analysis of the benignity and malignancy of the GPs involving three phases of CECT. In addition, High Correlation filter was used to eliminate one radiomics feature randomly which was considered highly correlated with another from the same or different phases of the same patient. The least absolute shrinkage and selection operator (LASSO) method with tenfold cross-validation was used for subsequent feature selection to avoid overfitting. Therefore, 321 candidate

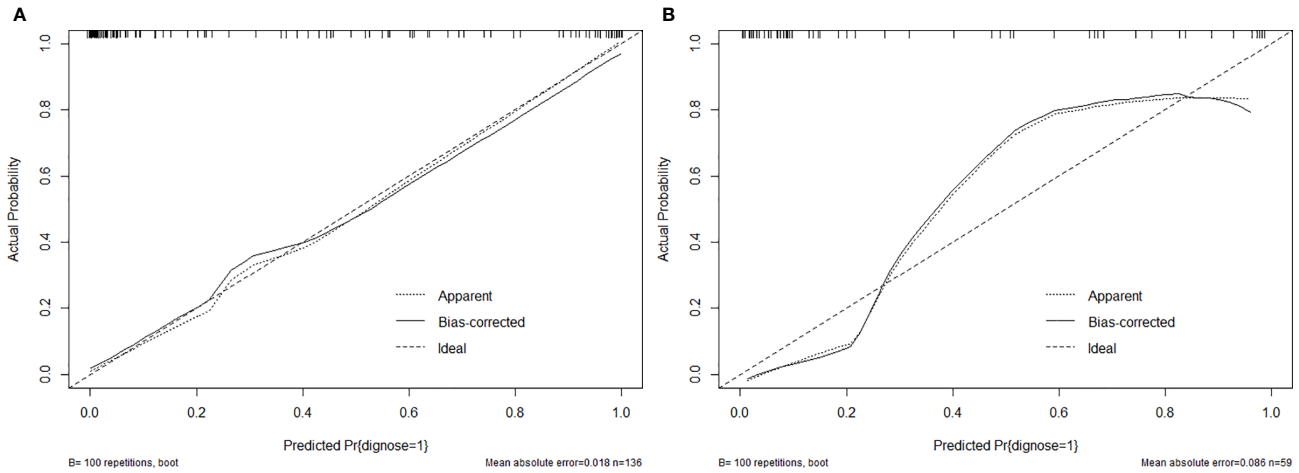

FIGURE 4 | **(A)** Calibration curves of combined model in the training cohort. **(B)** Calibration curves of combined model in the testing cohort.

TABLE 3 | The sensitivity and specificity of clinical diagnosis for malignant gallbladder polypoid-lesions were 0.6190 and 0.8939, respectively.

Clinical diagnosis / Pathology diagnosis	Benign	Malignant
Benign	118	14
Malignant	24	39

radiomics features were narrowed down to 6 potential predictors by High Correlation filter and LASSO method.

A clinical model that included 3 independent factors was constructed, while a radiomics model that incorporated 6 radiomics features and a combined model with Rad-score calculated by the radiomics model as well as 3 clinical features in the clinical model were established. The performance of the combined model in ROC was significantly more excellent than other models in the training cohort, which was identified as the best model for its superior sensitivity and specificity in the testing cohort at the situation of the same cutoff value with the training cohort, although the AUC of the combined model was less than the clinical model in the testing cohort probably due to the small sample size, on which the model can have the potential to identify more malignant GPs in external data. A nomogram was depicted based on the combined model (**Figure 5**).

Clinically, for GP patients with difficulty in diagnosis, after adjusting the balance of extra economic costs of CECT and clinical benefit, our data suggest that patients at high risk of

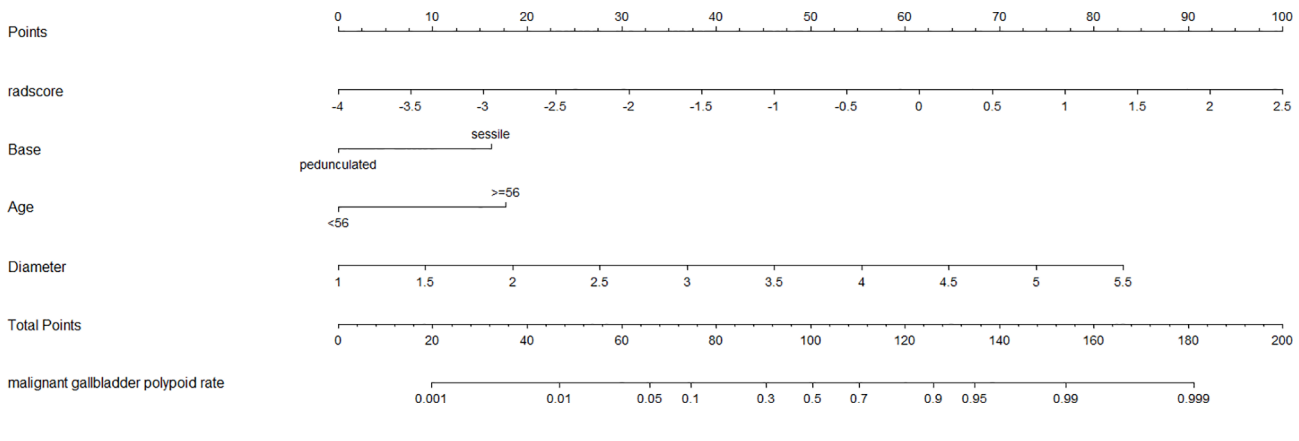

FIGURE 5 | The developed nomogram based on combined model.

malignant GPs according to our combined model should be treated with proper surgical approaches.

CONCLUSION

The proposed combined model can provide a novel approach to effectively evaluate benign and malignant GPs, which assist compensatorily in the preoperative decision-making of malignant risk of lesions ≥10 mm in size.

DATA AVAILABILITY STATEMENT

The raw data supporting the conclusions of this article will be made available by the authors, without undue reservation.

ETHICS STATEMENT

This study was approved by the Institutional Review Board of The First Hospital of China Medical University and the requirement for informed consent was waived based on the nature of a retrospective study.

AUTHOR CONTRIBUTIONS

SH and YL collected and analyzed the data. SH and XL drafted the manuscript. XJ and BL were involved in manuscript reviewing. CZ and JZ designed the study. All authors contributed to the article and approved the submitted version.

REFERENCES

1. Choi Y, Do J, Seo S, Lee S, Oh H, Min Y, et al. Prevalence and Risk Factors of Gallbladder Polypoid Lesions in a Healthy Population. *Yonsei Med J* (2016) 57:1370–5. doi: 10.3349/ymj.2016.57.6.1370
2. Lin W, Lin D, Tai D, Hsieh S, Lin C, Sheen I, et al. Prevalence of and Risk Factors for Gallbladder Polyps Detected by Ultrasonography Among Healthy Chinese: Analysis of 34 669 Cases. *J Gastroenterol Hepatol* (2008) 23:965–9. doi: 10.1111/j.1440-1746.2007.05071.x
3. Xu A, Zhang Y, Hu H, Zhao G, Cai J, Huang A. Gallbladder Polypoid-Lesions: What Are They and How Should They be Treated? A Single-Center Experience Based on 1446 Cholecystectomy Patients. *J Gastrointestinal Surg* (2017) 21:1804–12. doi: 10.1007/s11605-017-3476-0
4. Babu B, Dennison A, Garcea G. Management and Diagnosis of Gallbladder Polyps: A Systematic Review. *Langenbecks Arch Surg* (2015) 400:455–62. doi: 10.1007/s00423-015-1302-2
5. Singh S, Agarwal AK. Gallbladder Cancer: The Role of Laparoscopy and Radical Resection. *Ann Surg* (2009) 250:494–5; author reply 495. doi: 10.1097/SLA.0b013e3181b490d9
6. Ogawa T, Horaguchi J, Fujita N, Noda Y, Kobayashi G, Ito K, et al. High B-Value Diffusion-Weighted Magnetic Resonance Imaging for Gallbladder Lesions: Differentiation Between Benignity and Malignancy. *J Gastroenterol* (2012) 47:1352–60. doi: 10.1007/s00535-012-0604-1
7. Cha B, Hwang J, Lee S, Kim J, Cho J, Kim H, et al. Pre-Operative Factors That Can Predict Neoplastic Polypoid Lesions of the Gallbladder. *World J Gastroenterol* (2011) 17:2216–22. doi: 10.3748/wjg.v17.i17.2216
8. Zhou W, Li G, Ren L. Triphasic Dynamic Contrast-Enhanced Computed Tomography in the Differentiation of Benign and Malignant Gallbladder Polypoid Lesions. *J Am Coll Surgeons* (2017) 225:243–8. doi: 10.1016/j.jamcollsurg.2017.04.014
9. Aerts H. The Potential of Radiomic-Based Phenotyping in Precision Medicine: A Review. *JAMA Oncol* (2016) 2:1636–42. doi: 10.1001/jamaoncol.2016.2631
10. Yang X, Liu Y, Guo Y, Chai R, Niu M, Xu K. Utility of Radiomics Based on Contrast-Enhanced CT and Clinical Data in the Differentiation of Benign and Malignant Gallbladder Polypoid Lesions. *Abdominal Radiol (New York)* (2020) 45:2449–58. doi: 10.1007/s00261-020-02461-2
11. Okaniwa S. How Can We Manage Gallbladder Lesions by Transabdominal Ultrasound? *Diagnostics (Basel)* (2021) 11:784. doi: 10.3390/diagnostics11050784
12. Yu M, Kim Y, Park H, Jung S. Benign Gallbladder Diseases: Imaging Techniques and Tips for Differentiating With Malignant Gallbladder Diseases. *World J Gastroenterol* (2020) 26:2967–86. doi: 10.3748/wjg.v26.i22.2967
13. Xu A, Hu H. The Gallbladder Polypoid-Lesions Conundrum: Moving Forward With Controversy by Looking Back. *Expert Rev Gastroenterol Hepatol* (2017) 11:1071–80. doi: 10.1080/17474124.2017.1372188
14. Zielinski M, Atwell T, Davis P, Kendrick M, Que FG. Comparison of Surgically Resected Polypoid Lesions of the Gallbladder to Their Pre-Operative Ultrasound Characteristics. *J Gastrointest Surg* (2009) 13:19–25. doi: 10.1007/s11605-008-0725-2
15. Kim S, Kim H, Yang D, Ryu J, Won KY. Gallbladder Carcinoma: Causes of Misdiagnosis at CT. *Clin Radiol* (2016) 71:e96–109. doi: 10.1016/j.crad.2015.10.016
16. Yang H, Sun Y, Wang Z. Polypoid Lesions of the Gallbladder: Diagnosis and Indications for Surgery. *Br J Surg* (1992) 79:227–9. doi: 10.1002/bjs.1800790312
17. Gallahan W, Conway J. Diagnosis and Management of Gallbladder Polyps. *Gastroenterol Clinics North America* (2010) 39:359–67, x. doi: 10.1016/j.gtc.2010.02.001
18. Boulton R, Adams D. Gallbladder Polyps: When to Wait and When to Act. *Lancet (London England)* (1997) 349:817. doi: 10.1016/S0140-6736(05)61744-8
19. Mainprize K, Gould S, Gilbert J. Surgical Management of Polypoid Lesions of the Gallbladder. *Br J Surg* (2000) 87:414–7. doi: 10.1046/j.1365-2168.2000.01363.x
20. Lundgren L, Muszynska C, Ros A, Persson G, Gimm O, Andersson B, et al. Management of Incidental Gallbladder Cancer in a National Cohort. *Br J Surg* (2019) 106:1216–27. doi: 10.1002/bjs.11205
21. Papageorge M, de Geus S, Woods A, Ng S, Drake F, Cassidy M, et al. Undertreatment of Gallbladder Cancer: A Nationwide Analysis. *Ann Surg Oncol* (2021) 28:2949–57. doi: 10.1245/s10434-021-09607-6
22. Yuan Z, Liu X, Li Q, Zhang Y, Zhao L, Li F, et al. Is Contrast-Enhanced Ultrasound Superior to Computed Tomography for Differential Diagnosis of Gallbladder Polyps? A Cross-Sectional Study. *Front Oncol* (2021) 11:657223. doi: 10.3389/fonc.2021.657223
23. Lisotti A, Napoleon B, Facciorusso A, Cominardi A, Crinò S, Brighi N, et al. Contrast-Enhanced EUS for the Characterization of Mural Nodules Within Pancreatic Cystic Neoplasms: Systematic Review and Meta-Analysis. *Gastrointestinal Endoscopy* (2021) 94(5):881–9.e5. doi: 10.1016/j.gie.2021.06.028
24. Facciorusso A, Mohan B, Crinò S, Ofosu A, Ramai D, Lisotti A, et al. Contrast-Enhanced Harmonic Endoscopic Ultrasound-Guided Fine-Needle Aspiration Versus Standard Fine-Needle Aspiration in Pancreatic Masses: A Meta-Analysis. *Expert Rev Gastroenterol Hepatol* (2021) 15:821–8. doi: 10.1080/17474124.2021.1880893
25. Zhang W, Yang R, Liang F, Liu G, Chen A, Wu H, et al. Prediction of Microvascular Invasion in Hepatocellular Carcinoma With a Multi-Disciplinary Team-Like Radiomics Fusion Model on Dynamic Contrast-Enhanced Computed Tomography. *Front Oncol* (2021) 11:660629. doi: 10.3389/fonc.2021.660629
26. Li Q, He X, Fan X, Zhu C, Lv J, Luo T. Development and Validation of a Combined Model for Preoperative Prediction of Lymph Node Metastasis in Peripheral Lung Adenocarcinoma. *Front Oncol* (2021) 11:675877. doi: 10.3389/fonc.2021.675877

27. Palumbo D, Mori M, Prato F, Crippa S, Belfiori G, Reni M, et al. Prediction of Early Distant Recurrence in Upfront Resectable Pancreatic Adenocarcinoma: A Multidisciplinary, Machine Learning-Based Approach. *Cancers* (2021) 13:4938. doi: 10.3390/cancers13194938

Conflict of Interest: The authors declare that the research was conducted in the absence of any commercial or financial relationships that could be construed as a potential conflict of interest.

Publisher's Note: All claims expressed in this article are solely those of the authors and do not necessarily represent those of their affiliated organizations, or those of the publisher, the editors and the reviewers. Any product that may be evaluated in this article, or claim that may be made by its manufacturer, is not guaranteed or endorsed by the publisher.

frontiers in Oncology

ORIGINAL RESEARCH
published: 28 March 2022
doi: 10.3389/fonc.2022.797349

Transcatheter Arterial Chemoembolization in Combination With High-Intensity Focused Ultrasound for Intermediate and Advanced Hepatocellular Carcinoma: A Meta-Analysis

Yun-Bing Wang[1,2], Rong Ma[2], Zhi-Biao Wang[1], Qiu-Ling Shi[1,3], Lian Zhang[1], Wen-Zhi Chen[1], Jian-Ping Gong[2] and Jin Bai[1]**

[1] State Key Laboratory of Ultrasound in Medicine and Engineering, College of Biomedical Engineering, Chongqing Medical University, Chongqing, China, [2] Department of Hepatobiliary Surgery, The Second Affiliated Hospital of Chongqing Medical University, Chongqing, China, [3] School of Public Health and Management, Chongqing Medical University, Chongqing, China

Background: The study was conducted to explore whether high-intensity focused ultrasound (HIFU) can improve the effect of transcatheter arterial chemoembolization (TACE) in intermediate and advanced hepatocellular carcinoma (HCC).

Methods: PubMed, Embase, Cochrane Library, Web of Science, Wanfang Data, CQVIP, China National Knowledge Infrastructure (CNKI), and Chinese Biomedical (CBM) databases were searched for randomized controlled trials (RCTs) comparing the effect of TACE in combination with HIFU group (group A) to TACE alone group (group B) in treating intermediate and advanced HCC. The primary outcomes were overall survival (OS) rate and tumor response rate. The odds ratio (OR) and 95% confidence interval (CI) for each study were calculated and then pooled with fixed effects model or random effects model. Sensitivity analyses and subgroup analyses were conducted. A publication bias was also evaluated.

Results: After literature selection, eleven RCTs involving 803 patients were included in this meta-analysis. This meta-analysis revealed that group A was associated with an increased 6-month OS rate (OR = 0.20), 12-month OS rate (OR = 0.23), 24-month OS rate (OR = 0.32), and overall response rate (WHO criterion, OR = 0.22; RECIST criterion, OR = 0.30). Furthermore, subgroup analyses showed no bias in the result. Given the limited number of studies that reported major complications, no additional meta-analysis of complication was conducted. Despite no special treatment, any complication following HIFU treatment was found to subside within 3-7 days.

OPEN ACCESS

Edited by:
Lueder Alexander Kahrs, University of Toronto Mississauga, Canada

Reviewed by:
Kunal Bharat Gala, Tata Memorial Hospital, India
Tommaso Stecca, ULSS2 Marca Trevigiana, Italy

***Correspondence:**
Jin Bai
sajinbai@cqmu.edu.cn
Jian-Ping Gong
300381@cqmu.edu.cn

Specialty section:
This article was submitted to Surgical Oncology, a section of the journal Frontiers in Oncology

Received: *18 October 2021*
Accepted: *22 February 2022*
Published: *28 March 2022*

Citation:
Wang YB, Ma R, Wang ZB, Shi QL, Zhang L, Chen WZ, Gong JP and Bai J (2022) Transcatheter Arterial Chemoembolization in Combination With High-Intensity Focused Ultrasound for Intermediate and Advanced Hepatocellular Carcinoma: A Meta-Analysis. Front. Oncol. 12:797349. doi: 10.3389/fonc.2022.797349

Conclusion: TACE in combination with HIFU is associated with increased OS and tumor response in intermediate and advanced HCC. Current evidence supports the use of HIFU after TACE treatment in intermediate and advanced HCC.

Keywords: transcatheter arterial chemoembolization, high-intensity focused ultrasound, combination, hepatocellular carcinoma, meta-analysis

INTRODUCTION

Primary liver cancer is the sixth most commonly diagnosed cancer and the third leading cause of cancer death worldwide in 2020 (1). Hepatocellular carcinoma (HCC) accounts for 75-85% of all liver cancer cases. As the majority of HCC patients are diagnosed at an intermediate or advanced stage and are not surgical candidates, transcatheter arterial chemoembolization (TACE) is the primary treatment option. Previous studies found that after two consecutive TACE sessions, 22.5% of patients had no objective response, attributed to TACE failing to produce complete necrosis of HCC (2, 3). Combining TACE with local ablation techniques such as microwave ablation, radiofrequency ablation, cryoablation, and high-intensity focused ultrasound (HIFU) has been shown to improve overall survival rates when compared to TACE alone (4–7).

For HCC, HIFU has proven a non-invasive therapy option (8). HIFU was described as a new ablative strategy for small liver cancer in the clinical practice guidelines of the European Association for the Study of the Liver (EASL) (9). HIFU is also regarded as a key therapeutic approach for ablation in the Medical Administration of the National Health and Health Commission of the People's Republic of China guidelines for primary liver cancer (2019 edition) (10). TACE in combination with HIFU, on the other hand, has not been recommended by any guidelines for intermediate or advanced HCC. This is most likely due to the fact that HIFU is still in its infancy and its efficacy has yet to be validated (11).

Several studies have investigated the impact of combining TACE and HIFU in patients with intermediate and advanced HCC when compared to TACE alone (7, 11–20). However, these studies did not show consistent conclusion that TACE in combination with HIFU has a better overall survival or tumor response than TACE alone. Therefore, a meta-analysis is necessary to comprehensively demonstrate the efficacy of TACE in conjunction with HIFU in HCC.

In this study, we intended to conduct a meta-analysis by searching multiple online databases thoroughly. In addition, we performed subgroup analyses based on variables such as sample size, age, and tumor size to explore whether the conclusion is valid. This meta-analysis utilizes the primary outcomes of overall survival and tumor response to evaluate if TACE in conjunction with HIFU is more effective than TACE alone in the management of intermediate and advanced HCC. This study was conducted in accordance with the guidelines for the "Preferred Reporting Items for Systematic Reviews and Meta-Analyses (PRISMA)" (21).

Abbreviations: HCC, Hepatocellular carcinoma; TACE, Transcatheter arterial chemoembolization; HIFU, High-intensity focused ultrasound; EASL, European association for the study of the liver; PRISMA, Preferred reporting items for systematic reviews and meta-analyses; CNKI, China national knowledge infrastructure; CBM, Chinese biomedical; RCTs, Randomized controlled trials; MeSH, Medical subject headings; IRB, Institutional review board; OS, Overall survival; CR, Complete response; PR, Partial response; SD, Stable disease; PD, Progressive disease; OR, Odds ratio; CI, Confidence interval; HR, Hazard ratio.

MATERIALS AND METHODS

Search Strategy

The protocol of this meta-analysis was registered on the international prospective register of systematic reviews database (PROSPERO: CRD42020203484). PubMed, Embase, Cochrane Library, Web of Science, Wanfang Data, CQVIP, China National Knowledge Infrastructure (CNKI), and Chinese Biomedical (CBM) databases were searched for randomized controlled trials (RCTs) that compared the effects of TACE in combination with HIFU and TACE alone in treating HCC that were published before October 6, 2021. Medical subject headings (MeSH) and free words were combined for literature retrieval. We mainly used the following search terms: "HIFU", "high-intensity focused ultrasound", "focused ultrasound", "FUAS", "focused ultrasound ablation surgery", "TACE", "Transarterial chemoembolization", "HCC", and "hepatocellular carcinoma". No language was limited during the literature search. Institutional Review Board (IRB) approval and written consent were not required for conducting this meta-analysis.

Inclusion and Exclusion Criteria

Inclusion criteria: 1) studies where the patients were diagnosed with primary intermediate or advanced HCC. The original study should demonstrate that patients with intermediate or advanced liver cancer were included. The diagnostic criterion, which could be TNM or BCLC grade, was not restricted. 2) Studies where patients in the TACE combined with HIFU group (group A) received HIFU after TACE treatment, whereas patients in the TACE alone group (group B) received only TACE. 3) Studies where any of the primary or secondary outcomes was reported. The primary outcomes were the 6-month overall survival (OS) rate, 12-month OS rate, 24-month OS rate, and tumor response. OS was defined as the period from the date of certain treatment to the date of death from any cause. Tumor response was evaluated according to WHO criterion, RECIST criterion, RECIST 1.1 criterion, modified RECIST criterion, or other criteria. Tumor response was usually assessed one month after treatment. Each criterion included the classification of complete

response (CR), partial response (PR), stable disease (SD), and progressive disease (PD). Tumor response was reflected by overall response rate, which was calculated using the formula "CR+PR". Post-treatment complication was the secondary outcome. 4) Only RCTs were considered for this study. Exclusion criteria: 1) The full text was not available; 2) the study belonged to animal experiment; 3) the study was not related to our subject; or 4) the study used other therapies that were combined with group A or group B.

Study Selection, Data Extraction, and Assessment of Methodological Quality

Two reviewers (YBW and RM) examined the full texts independently and extracted the data. Any disagreements among reviewers were resolved by consulting with another senior coauthor. We collected the following data: first author, publication year, region, study design, intervention technique, sample size, age, gender, Child-pugh grade, clinical stage, tumor size, percentage of single tumor, and outcomes. The Cochrane handbook was utilized to assess the methodological quality of the included RCTs (22).

Statistical Analysis

When the survival rate for specific months in a study was not available but the survival curve was provided, the survival rate was calculated using Engauge Digitizer software (version 10.8). The pooled value was calculated using the Mantel-Haenszel method as well as the study-specific odds ratio (OR) and 95% confidence interval (CI) for the categorical variables. When significant statistical heterogeneity was identified, the outcomes were combined using random effects model. Otherwise, the fixed effects model would be employed. Stata software (version 16.0) was used for data synthesis. Heterogeneity between different studies was evaluated by the I^2 statistic and the chi-squared test. When $P < 0.05$, significant heterogeneity was identified. Furthermore, I^2 value $\leq 50\%$, $50\% < I^2$ value $\leq 75\%$, and I^2 value $> 75\%$ were considered to be low, moderate, and high heterogeneity, respectively. When high heterogeneity was detected, the potential origins would be explored. Sensitivity analysis was performed using the "leave one out" method. Publication bias was evaluated using Begg's test and Egger's test and was shown by funnel plot. $P < 0.05$ was considered statistically significant.

RESULTS

Characteristics of the Included Studies

We obtained 4580 citations after performing a literature search. We started by removing duplicate studies, retaining 3896 citations. Next, we further excluded 3835 citations after we screened the titles and abstracts for relevance, yielding 61 citations that were reviewed for further consideration. Finally, for quantitative synthesis, 11 RCTs (7, 11–20) that fit the inclusion criteria of this meta-analysis were identified. Literature selection is summarized in **Figure 1**.

The included studies were published between 2005 and 2019. When combined, our study included 399 patients in group A and 404 patients in group B. In group A, HIFU ablation was conducted after TACE treatment. Six of the 11 RCTs (11, 13–15, 18, 19) identified the time interval between HIFU and TACE, approximately 2-4 weeks. One study set the time interval as one week (7). Four studies (12, 16, 17, 20) did not report the time interval. All study provided the information about the age and sex. Eight of the elven studies reported that they included patients with mean age >52. Among the 11 RCTs, nine RCTs included intermediate and advanced HCC, and the remaining two studies included advanced HCC. Seven RCTs said they used TNM stage, and four studies did not report the criteria they used. Furthermore, eight RCTs reported the Child-Pugh score, while three studies did not. Seven of the eight studies showed that they included patients with Child-pugh A or B. Only one study included patients with Child-pugh C in both groups. The detailed characteristics of the included studies are shown in **Table 1**.

Methodological quality of the RCTs is shown in **Supplementary Figure 1**. As indicated, five RCTs (12, 13, 16, 19, 20) reported random sequence generation methods. All trials used randomization, but no strategies for allocation concealment were reported. As a result, the possibility of selection bias in most studies is regarded to be uncertain. One study by Wu F et al. (19) reported that the operator who performed TACE was blinded, but other operators as well as participants were not. Furthermore, as other studies did not report that they blinded participants and personnel, the risk of performance bias for all studies is high. Only the study by Wu F et al. (19) blinded the outcome assessment, so the risk of detection bias for all studies is high. As four of the studies did not specify whether or not follow-up was completed, the risk of attrition bias is undetermined. No study was found to have selective reporting, so the risk of reporting bias is low. Additionally, no other bias was found.

Meta-Analysis of Overall Survival

The 6-month OS rate in group A (87.12%) was significantly higher than that in group B (62.83%) [OR = 0.20; 95% CI = 0.13 to 0.33; $P < 0.001$; **Figure 2A**], with low heterogeneity ($P = 0.27$; $I^2 = 21.4\%$), according to the meta-analysis of seven studies (7, 13–16, 18, 19). This difference was supported by subgroup analyses based on sample size, age, and tumor size (**Supplementary Table 1**). Furthermore, a meta-analysis of seven studies (7, 13–16, 18, 19) revealed that the 12-month OS rate in group A (73.11%) was significantly higher than that in group B (44.24%) [OR = 0.23; 95% CI = 0.12 to 0.47; $P < 0.001$; **Figure 2B**], with moderate heterogeneity ($P = 0.046$; $I^2 = 53.3\%$). This difference was again supported by subgroup analyses based on sample size, age, and tumor size (**Supplementary Table 1**). Additionally, meta-analysis of four studies (7, 13, 16, 18) showed that the 24-month OS rate in the group A (50.83%) was significantly higher than that in the group B (30.0%) [OR = 0.32; 95% CI = 0.19 to 0.54; $P < 0.001$; **Figure 2C**], with low heterogeneity ($P = 0.39$; $I^2 = 1.4\%$). The result of subgroup analyses based on different sample size and age supported this difference (**Supplementary Table 1**).

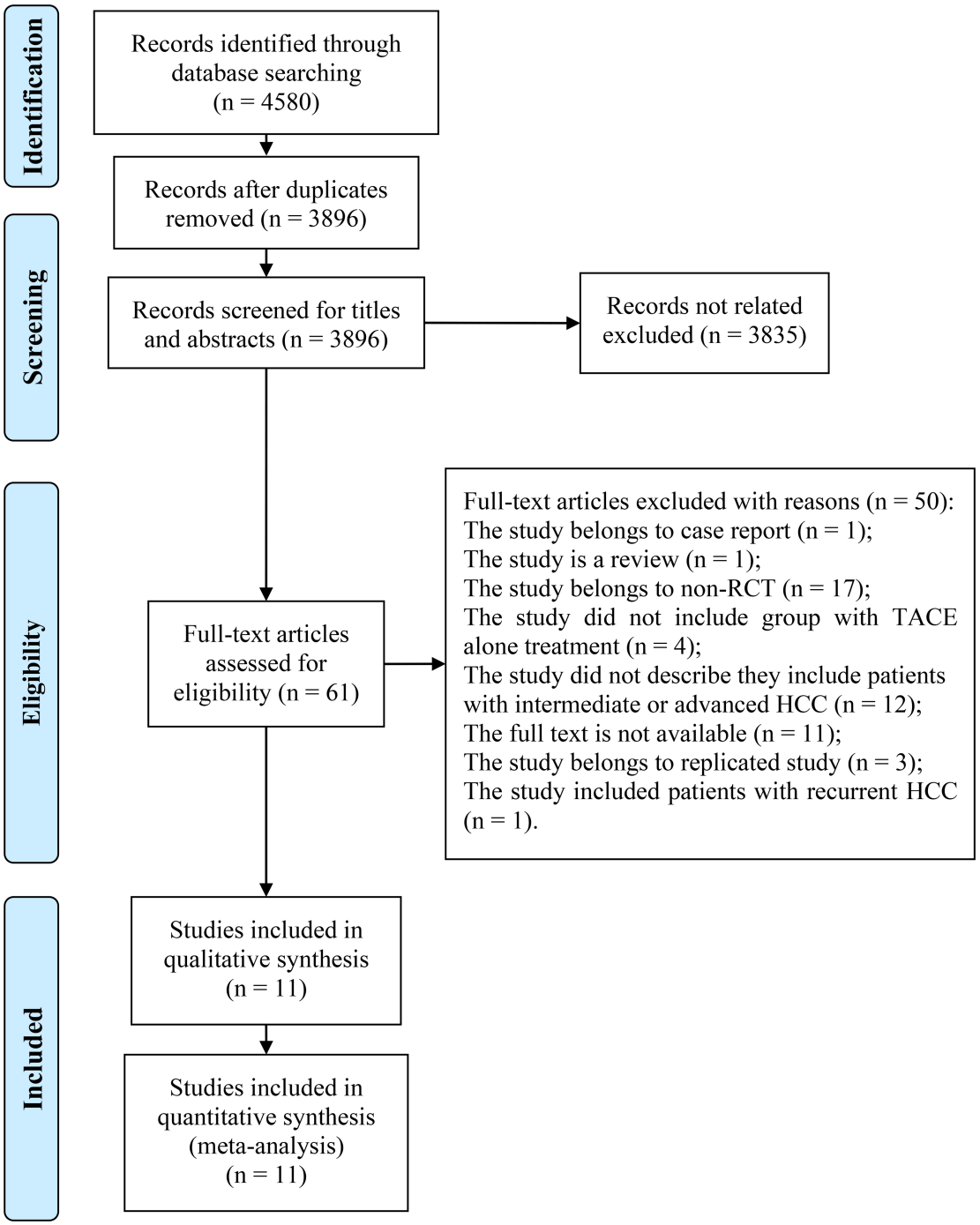

FIGURE 1 | Flow diagram of literature selection. A flow diagram of the literature selection process is shown. We found 4580 citations after searching eight online databases. The titles and abstracts were then reviewed for relevance. We identified 61 citations and reviewed them using their full-texts. Finally, for qualitative and quantitative synthesis, we included eleven RCTs. RCT, randomized controlled trial; TACE, transcatheter arterial chemoembolization; HCC, hepatocellular carcinoma.

Meta-Analysis of Tumor Response

Among the eleven studies included, one study (18) did not report the outcome of tumor response, four studies (12, 16, 17, 20) reported tumor response based on WHO criterion, three studies (11, 14, 15) reported tumor response using the RECIST criterion, one study (7) reported tumor response using the modified RECIST criterion, and two studies (13, 19) reported tumor response using other criteria. Considering that different criteria

TABLE 1 | Characteristics of the included studies.

First author (Year)	Group	No. of patients	Age, y, mean (SD[a])	Sex (Male/ Female)	Child-pugh grade (A/B/C)	Clinical stage for all patients in each study	Tumor size, cm, mean (SD[a])	Single tumor, %	6-,12-,24-months OS rate	CR/PR/ SD[b]/PD
Wu F (2005)(19)	A	24	47 ± 12.6	15/9	24/0/0	Advanced HCC (TNM stage IVa)	10.03(No SD[a])	25.00	80.15[c] (80.4-85.4)[d]/42.9/NA	All patients: NA
	B	26	44.5 ± 8.4	21/5	24/2/0		11.26 (No SD[a])	34.62	13.2/0/NA	
Chen WZ (2005) (18)	A	61	52.5 ± 13.1	49/12	59/2/0	Intermediate and advanced HCC (TNM stage III and IV)	9.8 ± 2.9	All patients: NA	82.41/65.14/ 31.37	All patients: NA
	B	66	53.4 ± 13.6	55/11	65/1/0		9.4 ± 2.8		44.42/12.48/ 6.2	
Cao W (2009) (17)	A	30	All patients: 40.9 (No SD[a])	All patients: 43/17	All patients: 18/42/0	Intermediate and advanced HCC (TNM stage II, III, and IV)	All patients: 3.9 (No SD[a])	All patients: NA	All patients: NA	3/18/8/1
	B	30								1/12/12/ 5
Li P (2013) (15)	A	25	59.40 ± 11.79	22/3	17/8/0	Intermediate and advanced HCC (TNM stage III and IV)	All patients: NA	All patients: NA	72/59.1/NA	1/20/2/2
	B	22	58.27 ± 12.15	18/4	11/11/0				48/31.8/NA	0/14/2/6
Du JK (2013) (16)	A	34	56(No SD[a])	21/13	All patients: A or B	Intermediate and advanced HCC (no criteria reported)	All patients: NA	All patients: NA	100/94.12/ 52.94	3/21/10/ 1
	B	34	53(No SD[a])	19/15					91.12/76.47/ 35.29	0/11/18/ 5
Dong WH (2015) (14)	A	34	60.5 ± 7.6	30/4	21/13/0	Intermediate and advanced HCC (TNM stage III and IV)	All patients: NA	All patients: NA	79.4/76.5/NA	2/27/2/3
	B	31	61.3 ± 9.2	28/3	16/15/0				54.8/51.6/NA	1/18/5/7
Fu SY (2015) (13)	A	36	All patients: 57.32 (median)	All patients: 40/36	All patients: 56/20/0	Intermediate and advanced HCC (TNM stage III and IV)	All patients: 2.5-11.0(range)	All patients: NA	94.4/66.7/36.1	All patients: NA
	B	40							82.5/47.5/15	
Wang RJ (2018) (12)	A	30	53.5 ± 13.6	19/11	All patients: NA	Intermediate and advanced HCC (no criteria reported)	All patients: NA	All patients: NA	All patients: NA	4/18/7/1
	B	30	53.4 ± 12.5	20/10						0/10/17/ 3
Luo Y (2019) (11)	A	45	All patients: 58.34 ± 2.95	All patients: 52/38	All patients: NA	Intermediate and advanced HCC (no criteria reported)	All patients: 11.16 ± 3.28	All patients: NA	All patients: NA	15/23/5/ 2
	B	45								6/22/11/ 6
Zhang Q (2019) (7)	A	50	56 ± 11	25/25	9/20/21	Intermediate and advanced HCC (TNM stage II, III, IV)	All patients: NA	All patients: NA	96.70[c]/92.57[c]/ 84.17[c]	20/25/5/ 0
	B	50	55 ± 10	26/24	10/19/21				89.70[c]/85.98[c]/ 70.91[c]	15/15/ 10/0
Liang W (2018) (20)	A	30	53.5 ± 13.6	19/11	All patients: NA	Advanced HCC (no criteria reported)	All patients: NA	All patients: NA	All patients: NA	4/18/7/1
	B	30	53.4 ± 12.5	20/10						0/10/17/ 3

[a]The SD means standard deviation; [b]The SD means one of the tumor response, which is stable disease; [c]The OS rate was calculated by our study; [d]The range was reported by the original study; Group A, TACE in combination with HIFU; Group B, TACE alone; TACE, transcatheter arterial chemoembolization; HIFU, high-intensity focused ultrasound; CR, complete response; PR, partial response; PD, progressive disease; NA, not available; OS, overall survival; HCC, hepatocellular carcinoma.

defined the tumor response differently, we performed a meta-analysis based on each reported criterion.

Meta-analysis of four studies (12, 16, 17, 20) using WHO criterion showed that the overall response rate in the group A (71.77%) was significantly higher than that in the group B (35.48%) (OR = 0.22; 95% CI = 0.13 to 0.37; P < 0.001; **Figure 3A**), with no heterogeneity (P = 0.85; I^2 = 0). The result of subgroup analyses based on sample size < 70 and age < 57 supported this difference (**Supplementary Table 2**). Meta-analysis of three trials (11, 14, 15) using RECIST criterion showed that the overall response rate in the group A (84.62%) was significantly higher than that in the group B (62.24%) (OR = 0.30; 95% CI = 0.15 to 0.59; P < 0.001; **Figure 3B**), with no heterogeneity (P = 0.98; I^2 = 0). The result of subgroup analyses based on sample size < 70 and age ≥ 57 supported this difference (**Supplementary Table 2**).

Posttreatment Complications

The posttreatment complications from each study were extracted and summarized in **Supplementary Table 3**. As shown, one study (11) reported two serious complications: digestive tract hemorrhage and renal failure. The group A was associated with a lower percentage of digestive tract hemorrhage compared to the group B (P = 0.049). However, renal failure showed no difference between the two groups. No other studies reported serious

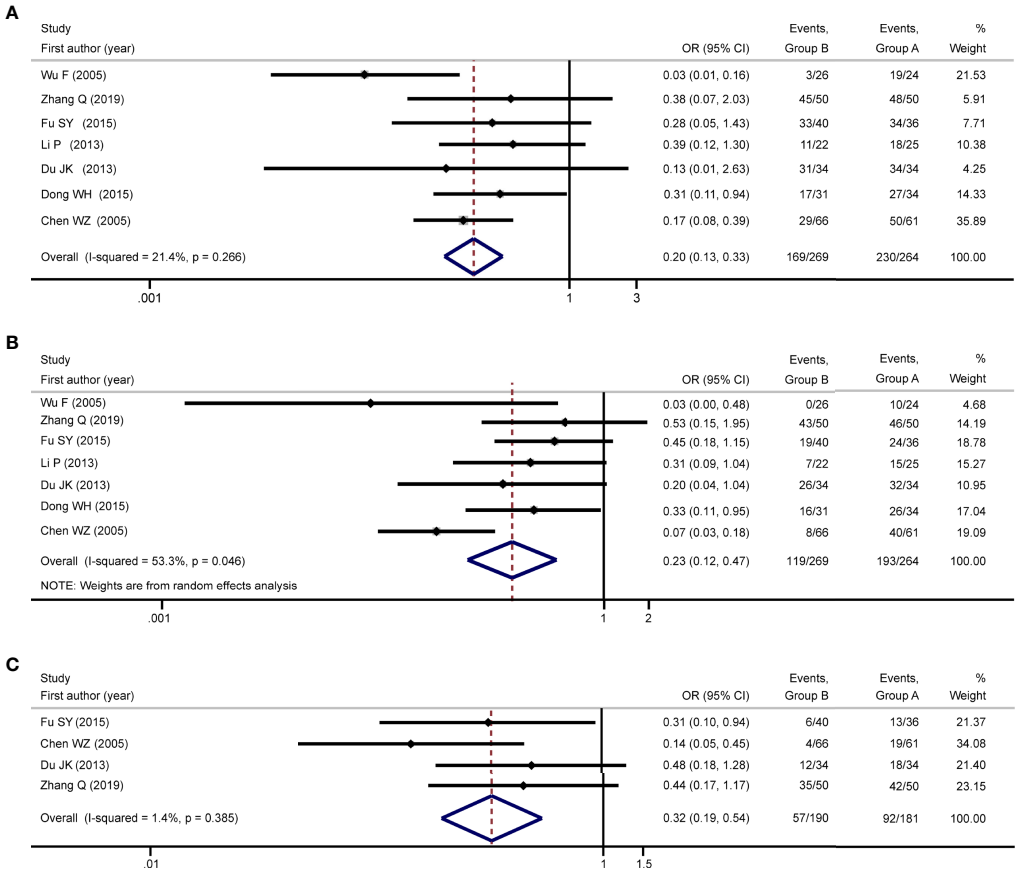

FIGURE 2 | Meta-analysis of overall survival. Meta-analysis of overall survival was conducted with the outcomes of 6-month OS rate, 12-month OS rate, and 24-month OS rate, respectively. Results of the meta-analyses showed that group A was associated with increased 6-month OS rate [OR: 0.20; 95% CI: 0.13-0.33; **(A)**], 12-month OS rate [OR: 0.23; 95% CI: 0.12-0.47; **(B)**], and 24-month OS rate [OR: 0.32; 95% CI: 0.19-0.54; **(C)**] compared to group B, and no high statistical heterogeneities were detected. Group A: TACE in combination with HIFU; Group B: TACE alone; TACE, transcatheter arterial chemoembolization; HIFU, high-intensity focused ultrasound; OS, overall survival; OR, odds ratio; CI, confidence interval.

complications. In the group A, some mild complications, such as fever, skin burn, mild local pain, and subcutaneous edema, were reported in these studies. These mild complications usually rapidly resolved within 3-7 days after HIFU treatment without special treatment. No additional meta-analysis was performed due to the limited number of serious complications reported.

Sensitivity Analyses

Sensitivity analyses were conducted on 6-month OS rate, 12-month OS rate, 24-month OS rate, and overall response rate (with WHO criterion and RECIST criterion). Utilizing the "leave one out" method, we found that the difference in any meta-analysis between group A and group B was still statistically significant and had not been changed.

Publication Bias

To evaluate publication bias, the outcome of the 6-month OS rate was used. Begg's test (P=1.00), Egger's test (P=0.82), and the Begg's funnel plot (**Figure 4**) all indicate that there was no publication bias. Each dot in the funnel plot represents a study. As shown in the figure, the points are symmetrical on both sides of the reference line.

DISCUSSION

HIFU was first proposed for treatment in 1932, when Freundlich H, Collner K, and Rogowski F found the medium's propensity to heat tissue (23). The JC HIFU tumor treatment system was first developed and utilized in clinic by the Ultrasound Institute of Chongqing Medical University in 1997. HIFU is a non-invasive technique of local thermal ablation. Its basic premise is to focus low-energy ultrasound *in vitro* on the target tissue *in vivo*, resulting in coagulative necrosis *via* ultrasound's biological effects such as thermal effect, cavitation effect, and mechanical impact (24). At present, HIFU technology is mainly used in benign and malignant solid tumors and benign diseases of uterus, prostate and other organs. As HIFU can ablate the local tumor while being monitored through ultrasound or MRI, it is considered both safe and accurate. When compared to

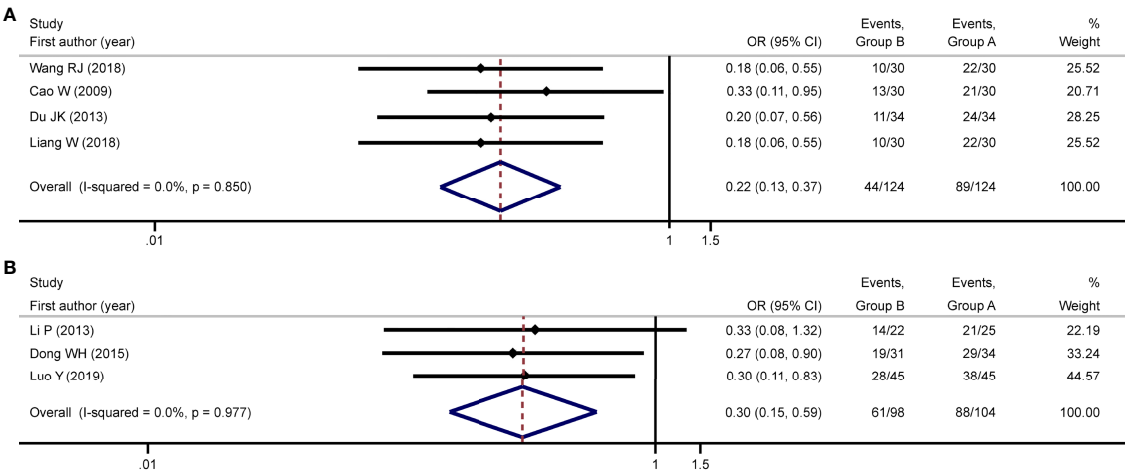

FIGURE 3 | Meta-analysis of tumor response. Meta-analysis of tumor response was conducted using studies with WHO criterion and RECIST criterion, respectively. Using studies reporting tumor response with WHO criterion, the meta-analysis found group A was associated with improved overall response rate compared to group B [OR: 0.22; 95% CI: 0.13-0.37; **(A)**]. Using studies reporting tumor response with RECIST criterion, the meta-analysis found group A was associated with improved overall response rate compared to group B [OR: 0.30; 95% CI: 0.15-0.59; **(B)**]. No heterogeneity was detected in either meta-analysis. Group A: TACE in combination with HIFU; Group B: TACE alone; TACE, transcatheter arterial chemoembolization; HIFU, high-intensity focused ultrasound; OR, odds ratio; CI, confidence interval.

traditional surgical resection, HIFU technology is minimally invasive, therefore it can be utilized as an alternate treatment when traditional surgery is not feasible.

Our meta-analysis found that the 6-month, 12-month, and 24-month OS in group A were significantly better compared to group B. The meta-analysis also indicated that group A was associated with increased overall response rate compared to group B. Therefore, our meta-analysis found that HIFU combined with TACE had better short-term and long-term efficacy than TACE alone. Furthermore, the heterogeneity of the meta-analysis for each outcome was not high. The result of subgroup analyses based on different sample size, age, and tumor size was consistent with the result of the meta-analyses including all studies. In addition, sensitivity analyses found the result of the meta-analyses was not influenced by any single study. Additionally, our study identified no evidence of publication bias, implying that the literature search was comprehensive. These additional analyses, taken collectively, imply that the conclusion of our meta-analysis is reliable.

In our meta-analysis, we summarized the incidence of complications in both groups. Common complications induced by HIFU included fever, skin burn, mild local pain, and subcutaneous edema, which rapidly resolved 3-7 days after HIFU treatment without special treatment (25). It is worth noting that HIFU may also cause severe complications, such as bleeding and renal failure. However, the incidence rate of these severe complications is very low (26). Of note, among the included studies, two serious complications (renal failure and digestive tract hemorrhage) were reported in one study (11). For the incidence rate of renal failure, group A (n=1) and group B (n=0) showed no difference. However, for digestive tract hemorrhage, group B (n=6) exhibited a higher incidence rate compared to group A (n=1). The reason behind this is unexplained in the original study, and it may need to be investigated further in the future. In any case, our data suggested that TACE in conjunction with HIFU is safe for patients with intermediate and advanced HCC.

TACE is a major treatment for intermediate and advanced liver cancer. TACE has the ability to obstruct the arterial blood supply of liver cancer cells. Liver cancer, however, has a dual blood supply from the hepatic artery and the portal vein. In addition, the tumor may develop neovascularization and collateral circulation. These factors lead to incomplete tumor necrosis and affect the efficacy of TACE. In order to kill tumor cells as much as possible,

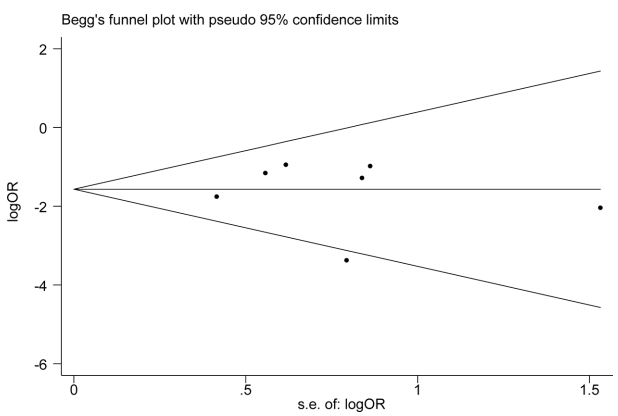

FIGURE 4 | Evaluation of publication bias. Begg's funnel plot was used to detect publication bias in 6-month OS rate. Each dot in the funnel plot represents a study. Those points are symmetrical on both sides of the reference line, indicating no publishing bias. OS, overall survival; OR, odds ratio.

TACE treatment often needs to be carried out many times. Repeated TACE could lead to chemotherapeutic cytotoxicity and aggravate the fibrosis progression, thus leads to the deterioration of liver function (27). When combined with other treatment methods, a synergistic anticancer effect can be achieved, and the survival time of patients can be prolonged as much as possible. A single treatment is frequently insufficient to achieve a satisfactory curative effect. More and more patients are opting for a multidisciplinary combination treatment (28). TACE treatment is an integral part of this multidisciplinary approach. At present, TACE therapy has been reported to be combined with HIFU, radiofrequency ablation, radiotherapy, targeted therapy and immunotherapy to improve the curative effect.

In this meta-analysis, we found that the combination of TACE and HIFU was better than TACE alone in the treatment of intermediate and advanced liver cancer. TACE's therapeutic impact can be enhanced by HIFU, which may be due to the following processes. First, HIFU can induce tumor coagulative necrosis, which can enhance the death of localized tumor cells following TACE treatment and consolidate the therapeutic efficacy of TACE (29). Second, after TACE treatment, liver cancer cells near the portal vein may remain, and HIFU helps to eliminate these residual tumor cells. Furthermore, HIFU aids in the exposure of tumor antigens and the induction of an anti-tumor immune response, which may improve the efficacy of liver cancer treatment (30). Considering the role of HIFU after TACE treatment, the findings of our study showed that in clinical practice, if possible, combination with HIFU should be promoted for patients with intermediate and advanced HCC, rather than consecutive TACE.

Our research has some limitations. First, despite the fact that our study solely included RCTs, there were certain bias risks. For instance, because blinding of participants and personnel, as well as blinding of outcome assessment, are difficult to implement, performance bias and detection bias are difficult to avoid. Second, despite our best efforts to incorporate studies from various countries, all of the included studies identified were from China. This could be due to a variety of factors, including: 1) China had a high HCC disease burden, with many patients diagnosed with intermediate or advanced HCC (31); and 2) China developed and applied the JC HIFU system in clinic early, which has been subsequently recommended for the treatment of HCC. Whether TACE in combination with HIFU benefits patients from other countries as well still needs to be validated by further studies. Third, some details about TACE or HIFU therapy were not explored in this meta-analysis. The primary reason was due to limited information being reported in the original studies. More information, such as the frequencies of TACE or HIFU, the time spent on treatment, and the time interval between TACE and HIFU, are hoped to be reported and studied in future research. Furthermore, whether a single or multiple lesions were treated is critical for tumor treatment. In the study conducted by Wu F, et al, the entire tumors in combination group were treated with HIFU. According to another study conducted by Cao W, et al, a number of the patients did not achieve complete tumor ablation. The reasons mentioned were the tumor overlaps with the ribs, is adjacent to or invades the hepatic duct or gallbladder, and so cannot be completely ablated. For other studies, whether single lesions were treated or multiple was not reported in detail. Nevertheless, given that additional tumor ablation can lessen a patient's tumor load and prolong the patient's life, it could be argued that tumors in certain patients should be treated as much as possible. In any case, it is expected that future study should focus on how many lesions were treated.

Fourth, our study did not use hazard ratio (HR) as the effect size, but used OR instead. The main reason is that HR in most studies was not provided. So, to better evaluate the survival benefit from HIFU, further original studies would better consider HR as the effect size. Furthermore, the number of studies included in the meta-analysis is limited. We intended to incorporate as many studies as possible by searching all literature libraries recognized by academia. After completing our manuscript, we revisited our literature search by rescanning these databases. However, only the initial eleven studies were subsequently identified. Although the number of studies is limited, the results are reliable. The findings are useful for guiding clinical treatment. This meta-analysis could be updated when new studies are released in the future.

CONCLUSION

TACE in combination with HIFU is associated with increased OS and tumor response compared to TACE alone in patients with intermediate and advanced HCC. The use of HIFU after TACE treatment in intermediate and advanced HCC is supported by current evidence.

DATA AVAILABILITY STATEMENT

The original contributions presented in the study are included in the article/**Supplementary Material**. Further inquiries can be directed to the corresponding authors.

ETHICS STATEMENT

Ethical review and approval was not required for the study on human participants in accordance with the local legislation and institutional requirements. Written informed consent for participation was not required for this study in accordance with the national legislation and the institutional requirements.

AUTHOR CONTRIBUTIONS

Conception and design: Y-BW, R M, Z-BW, Q-LS, J-PG, and JB. Collection and assembly of data: Y-BW and RM. Data analysis and interpretation: All authors. Manuscript writing: All authors. J-PG and JB contributed equally to this work. All authors contributed to the article and approved the submitted version.

FUNDING

The study was funded by Chongqing medical scientific research project (Joint project of Chongqing Health Commission and Science and Technology Bureau: No. 2021MSXM139).

SUPPLEMENTARY MATERIAL

The Supplementary Material for this article can be found online at: https://www.frontiersin.org/articles/10.3389/fonc.2022.797349/full#supplementary-material

REFERENCES

1. Sung H, Ferlay J, Siegel RL, Laversanne M, Soerjomataram I, Jemal A, et al. Global Cancer Statistics 2020: GLOBOCAN Estimates of Incidence and Mortality Worldwide for 36 Cancers in 185 Countries. *CA Cancer J Clin* (2021) 71(3):209–49. doi: 10.3322/caac.21660
2. Choi J, Lee D, Shim JH, Kim KM, Lim YS, Lee YS, et al. Evaluation of Transarterial Chemoembolization Refractoriness in Patients With Hepatocellular Carcinoma. *PloS One* (2020) 15(3):e0229696. doi: 10.1371/journal.pone.0229696
3. Liu HC, Shan EB, Zhou L, Jin H, Cui PY, Tan Y, et al. Combination of Percutaneous Radiofrequency Ablation With Transarterial Chemoembolization for Hepatocellular Carcinoma: Observation of Clinical Effects. *Chin J Cancer Res* (2014) 26(4):471–7. doi: 10.3978/j.issn.1000-9604.2014.08.18
4. Kim W, Cho SK, Shin SW, Hyun D, Lee MW, Rhim H. Combination Therapy of Transarterial Chemoembolization (TACE) and Radiofrequency Ablation (RFA) for Small Hepatocellular Carcinoma: Comparison With TACE or RFA Monotherapy. *Abdom Radiol (NY)* (2019) 44(6):2283–92. doi: 10.1007/s00261-019-01952-1
5. Li W, Ni CF. Current Status of the Combination Therapy of Transarterial Chemoembolization and Local Ablation for Hepatocellular Carcinoma. *Abdom Radiol (NY)* (2019) 44(6):2268–75. doi: 10.1007/s00261-019-01943-2
6. Liu C, Li T, He JT, Shao H. TACE Combined With Microwave Ablation Therapy vs. TACE Alone for Treatment of Early- and Intermediate-Stage Hepatocellular Carcinomas Larger Than 5 Cm: A Meta-Analysis. *Diagn Interv Radiol* (2020) 26(6):575–83. doi: 10.5152/dir.2020.19615
7. Zhang Q, Bian SQ, Lv W, Kou D, Hu HL, Guo SS, et al. Observation of Efficacy of TACE Combined With HIFU on Patients With Middle-Advanced Liver Cancer. *Eur Rev Med Pharmacol Sci* (2019) 23(3):239–46. doi: 10.26355/eurrev_201908_18653
8. Sehmbi AS, Froghi S, Oliveira de Andrade M, Saffari N, Fuller B, Quaglia A, et al. Systematic Review of the Role of High Intensity Focused Ultrasound (HIFU) in Treating Malignant Lesions of the Hepatobiliary System. *HPB (Oxford)* (2021) 23(2):187–96. doi: 10.1016/j.hpb.2020.06.013
9. European Association for the Study of the Liver. EASL Clinical Practice Guidelines: Management of Hepatocellular Carcinoma. *J Hepatol* (2018) 69(1):182–236. doi: 10.1016/j.jhep.2018.03.019
10. Medical administration of National Health and Health Commission of the people's Republic of China. Guidelines for Diagnosis and Treatment of Primary Liver Cancer in China (2019 Edition). *Chin J Hepatol* (2020) 28(2):112–28. doi: 10.3760/cma.j.issn.1007-3418.2020.02.004
11. Luo Y, Jiang Y. Comparison of Efficiency of TACE Plus HIFU and TACE Alone on Patients With Primary Liver Cancer. *J Coll Physicians Surg Pak* (2019) 29(5):414–7. doi: 10.29271/jcpsp.2019.05.414
12. Wang RJ. Clinical Effect of TACE Combined With Focused Ultrasound in the Treatment of Intermediate and Advanced Liver Cancer. *Henan Med Res* (2018) 27(18):3312–3. doi: 10.3969/j.issn.1004-437X.2018.18.018
13. Fu SY, Ren RX, Wang MJ, Chen YL, Jiang BH, Zhang Q. Clinical Observation of TACE Combined With HIFU in the Treatment of Middle and Advanced Primary Hepatocellular Carcinoma. *J China Pharm* (2015) 26(35):4978–80. doi: 10.6039/j.issn.1001-0408.2015.35.28
14. Dong WH, Gu JP, Zha MB. Clinical Effect of Transcatheter Arterial Chemoembolization in Combination With High Intensity Focused Ultrasound Therapy for Advanced Stage of Hepatic Carcinoma. *J Trop Med* (2015) 15(4):496–9.
15. Li P. Clinical Study of TACE in Combination With High Intensity Focused Ultrasound Therapy for III and IV Stage of Hepatic Carcinoma. *Shanxi Med Univ* (2013), 1–50. doi: 10.7666/d.Y2339403
16. Du JK, Li GH, He WH, Ma XJ, Huang CJ, He HJ. Clinical Research on TACE Combined With Focused Ultrasound Sword in Treatment of Mid-Late Stage Liver Cancer. *Chin J Modern Med* (2013) 23(21):97–101. doi: 10.3969/j.issn.1005-8982.2013.21.022
17. Cao W, Wu FW, Wan Y, Zhang HX. The Changes of Serum TSGF and AFP Levels in Patients With Primary Liver Cancers After TACE Combined With HIFU Treatment. *Modern Oncol Med* (2009) 17(10):1930–2. doi: 10.3969/j.issn.1672-4992.2009.10.041
18. Chen WZ, Zhang L, Zhu H, Wang ZB, Wu F, Li KQ, et al. High Intensity Focused Ultrasound Combined With Transcatheter Arterial Chemoembolization in the Treatment of Intermediate and Advanced Primary Liver Cancer. *Proc 4th Natl Symposium Interventional Ther Gastrointestinal Malignant Lesions* (2005) 91–2.
19. Wu F, Wang ZB, Chen WZ, Zou JZ, Bai J, Zhu H, et al. Advanced Hepatocellular Carcinoma: Treatment With High-Intensity Focused Ultrasound Ablation Combined With Transcatheter Arterial Embolization. *Radiology* (2005) 235(2):659–67. doi: 10.1148/radiol.2352030916
20. Liang W. Clinical Treatment Effect of TACE Combined With Focused Ultrasound Knife in Advanced Liver Cancer. *Adv Mod Oncol Res* (2018) 4(3):28–30. doi: 10.30564/amor.v4i3.281
21. Moher D, Liberati A, Tetzlaff J, Altman DG. PRISMA Group. Preferred Reporting Items for Systematic Reviews and Meta-Analyses: The PRISMA Statement. *PloS Med* (2009) 6(7):e1000097. doi: 10.1371/journal.pmed.1000097
22. Higgins JPT, Green S. Cochrane Handbook for Systematic Reviews of Interventions Version 5.1.0 [Updated March 2011]. *The Cochrane Collaboration* (2011). Available at: www.cochrane-handbook.org.
23. Lynn JG, Zwemer RL, Chick AJ, Miller AE. A New Method for the Generation and Use of Focused Ultrasound in Experimental Biology. *J Gen Physiol* (1942) 26(2):179–93. doi: 10.1085/jgp.26.2.179
24. Bachu VS, Kedda J, Suk I, Green JJ, Tyler B. High-Intensity Focused Ultrasound: A Review of Mechanisms and Clinical Applications. *Ann BioMed Eng* (2021) 49(9):1975–91. doi: 10.1007/s10439-021-02833-9
25. Li JJ, Gu MF, Luo GY, Liu LZ, Zhang R, Xu GL. Complications of High Intensity Focused Ultrasound for Patients With Hepatocellular Carcinoma. *Technol Cancer Res Treat* (2009) 8(3):217–24. doi: 10.1177/153303460900800306
26. Cheung TT, Chu FS, Jenkins CR, Tsang DS, Chok KS, Chan AC, et al. Tolerance of High-Intensity Focused Ultrasound Ablation in Patients With Hepatocellular Carcinoma. *World J Surg* (2012) 36(10):2420–7. doi: 10.1007/s00268-012-1660-7
27. Qu K, Yan Z, Wu Y, Chen Y, Qu P, Xu X, et al. Transarterial Chemoembolization Aggravated Peritumoral Fibrosis *via* Hypoxia-Inducible Factor-1α Dependent Pathway in Hepatocellular Carcinoma. *J Gastroenterol Hepatol* (2015) 30(5):925–32. doi: 10.1111/jgh.12873
28. Lu J, Zhao M, Arai Y, Zhong BY, Zhu HD, Qi XL, et al. Clinical Practice of Transarterial Chemoembolization for Hepatocellular Carcinoma: Consensus Statement From an International Expert Panel of International Society of Multidisciplinary Interventional Oncology (ISMIO). *Hepatobiliary Surg Nutr* (2021) 10(5):661–71. doi: 10.21037/hbsn-21-260
29. Sengupta S, Balla VK. A Review on the Use of Magnetic Fields and Ultrasound for Non-Invasive Cancer Treatment. *J Adv Res* (2018) 14:97–111. doi: 10.1016/j.jare.2018.06.003
30. Daher S, Massarwa M, Benson AA, Khoury T. Current and Future Treatment of Hepatocellular Carcinoma: An Updated Comprehensive Review. *J Clin Transl Hepatol* (2018) 6(1):69–78. doi: 10.14218/JCTH.2017.00031
31. Liu X, Qin S. Immune Checkpoint Inhibitors in Hepatocellular Carcinoma: Opportunities and Challenges. *Oncologist* (2019) 24(Suppl 1):S3–S10. doi: 10.1634/theoncologist.2019-IO-S1-s01

Conflict of Interest: The authors declare that the research was conducted in the absence of any commercial or financial relationships that could be construed as a potential conflict of interest.

Publisher's Note: All claims expressed in this article are solely those of the authors and do not necessarily represent those of their affiliated organizations, or those of the publisher, the editors and the reviewers. Any product that may be evaluated in

this article, or claim that may be made by its manufacturer, is not guaranteed or endorsed by the publisher.

frontiers | Frontiers in Oncology

ORIGINAL RESEARCH
published: 28 April 2022
doi: 10.3389/fonc.2022.822983

What Are the Results of Limb Salvage Surgery for Primary Malignant Bone Tumor in the Forearm?

Weifeng Liu[1,2*], *Yongkun Yang*[1,2], *Tao Jin*[1,2], *Yang Sun*[1,2], *Yuan Li*[1,2], *Lin Hao*[1,2], *Qing Zhang*[1,2] *and Xiaohui Niu*[1,2*]

[1] Department of Orthopaedic Oncology Surgery, Beijing Jishuitan Hospital, Peking University, Beijing, China, [2] Fourth Medical College of Peking University, Beijing, China

OPEN ACCESS

Edited by:
Patrick J. Schuler,
Ulm University Medical Center,
Germany

Reviewed by:
Johanna Patricia Adevoso Canal,
University of the Philippines Manila,
Philippines
Michael Wagels,
Queensland Health, Australia
Seiichi Matsumoto,
Cancer Institute Hospital of Japanese
Foundation for Cancer Research,
Japan

***Correspondence:**
Weifeng Liu
liuweifengjst@126.com
Xiaohui Niu
niuxiaohui@263.net

Specialty section:
This article was submitted to
Surgical Oncology,
a section of the journal
Frontiers in Oncology

Received: 26 November 2021
Accepted: 21 March 2022
Published: 28 April 2022

Citation:
Liu W, Yang Y, Jin T, Sun Y, Li Y,
Hao L, Zhang Q and Niu X (2022) What
Are the Results of Limb Salvage
Surgery for Primary Malignant
Bone Tumor in the Forearm?
Front. Oncol. 12:822983.
doi: 10.3389/fonc.2022.822983

Background and Objectives: After diagnosing a primary bone tumor involving the forearm, various excision strategies and reconstruction methods must be considered. This study explored the oncological and functional outcomes of limb salvage surgery for primary malignant bone tumors in the forearm.

Methods: Patients with primary forearm bone tumors (n = 369) were retrospectively analyzed between 2000 and 2017. There were 266 patients with radial tumors, and 46 (17.3%) were malignant, whereas 103 patients had ulnar lesions and 22 (21.4%) were malignant tumors. The oncological results, prognostic factors, and functional results after limb salvage surgery of forearm malignancies were analyzed.

Results: The follow-up averaged 72.1 (7–192, median 62.5) months. Fifty-six patients who received limb salvage surgery were included in the final evaluation. Radius resection was performed in 38 patients, and distal radius (25 patients) was most frequent. Ulnar resection was performed in 18 patients, and the proximal ulna (13 patients) was most frequent. The surgical margins obtained were intralesional in 3 patients, marginal in 8 patients and wide in 45 patients. Local recurrence occurred in 11 patients (19.6%), and distant metastasis occurred in 14 patients (25%). The 5-year recurrence-free survival rate was 79.8%. Unplanned excision, ulnar involvement, proximal forearm location and inadequate surgical margins were associated with recurrence. The overall 5-year and 10-year survival rates were 83.5 and 71.7%, respectively. Distant metastasis was a poor prognostic factor for the survival rate. Forty-two patients were evaluated by MSTS score with an average of 27.9 ± 1.5.

Conclusions: The incidence of radial malignant tumors is higher than that of ulnar lesions. The distal radius and the proximal ulna are the most frequently involved sites. Unplanned excisions, ulnar tumors, proximal forearm tumors, and inadequate surgical margin are the risk factors for local recurrence. Distant metastasis is an independent poor prognostic factor of death. The oncology control and functional results of limb salvage surgery were satisfactory.

Keywords: forearm, sarcoma, limb salvage, recurrence, metastasis, prognosis

INTRODUCTION

Primary bone tumors arising from the ulna and radius are rare compared with soft tissue tumors (1). Benign bone tumors accounted for most of the forearm tumors. Therefore, according to the general definition a disease is considered rare when it affects fewer than 1 in 2,000 people (2), the location of forearm accounted for 1–2% in all primary malignant bone tumors and surgical treatment is more challenging (3). Many tendons in the forearm are responsible for fine movement of the hand, and tumors often involve essential structures in this narrow space. As a result, the hand function will be significantly reduced after wide resection of the tumors.

Muramatsu (4) suggested the key for local control with forearm tumors was the safe surgical margin. A surgical margin of 5 cm in other sites is easily achieved, but it is challenging in the forearm. The reconstruction following tumor resection is also controversial, with three main problems: (1) some sarcomas are difficult to remove safely; (2) the defects and methods of reconstruction are varied, requiring individual design, and (3) the oncological evaluation and functional assessment need long-term follow up. How could we draw the appropriate surgical treatment strategies, it is urgently necessary to accumulate evidence-based evidence for these rare tumors.

This study included forearm primary malignant bone tumors to clarify (1) the epidemiological characteristics of primary malignant bone tumors in the forearm; (2) the oncological results and related risk factors; and (3) reconstruction methods and functional results after tumor resection.

MATERIALS AND METHODS

Inclusion and Exclusion Criteria

With institutional review board (I.R.B.) approval, all patients in this study underwent limb salvage surgery for primary sarcoma of the forearm. Inclusion criteria were (1) primary malignant tumor of radius/ulna; (2) limb salvage surgery with resection of the tumor; (3) complete imaging (X-ray, CT, and MRI) and clinical data; (4) oncology results and complications can be evaluated; (5) follow-up time was more than 12 months, or oncological events (local recurrence, distant metastasis, or death) occurred within 12 months. The exclusion criteria were (1) bone defect and reconstruction were not involved; (2) amputation; (3) no surgical treatment or rejection of treatment; (4) incomplete imaging and follow-up data.

General Characteristics

Patients with primary bone tumors (n = 369) of the forearm at the Beijing Jishuitan Hospital were analyzed retrospectively. There were 266 radial tumors, and 46 patients (17.3%) had malignant lesions. Forty of these 46 patients underwent limb salvage surgery and were thus eligible for inclusion in this study. There were 103 ulnar tumors, and 22 patients (21.4%) had malignant lesions. Twenty of these 22 patients underwent limb salvage surgery and were thus eligible for inclusion. Fifty-six of these 60 eligible patients followed up for more than 12 months and enrolled in the final study (**Figure 1**).

The local evaluation included X-ray, CT, and MRI of the forearm in all patients. Staging evaluation included chest CT and bone scans. A preoperative biopsy was performed for tumors suspected of malignancy. The surgical strategy for tumor resection was based on preoperative imaging. Preoperative chemotherapy was recommended for patients younger than 55 y with high-grade sarcoma involvement.

The collected data included

1. *Surgical procedure*: All these surgical strategies were decided by the Jishuitan sarcoma multidisciplinary team with the same theory and techniques, and all the surgeons were all in our musculoskeletal tumor team. Margin was defined as follows: Intralesional: Piecemeal debulking or curettage, which may leave macroscopic disease; Marginal: Shell out en bloc through pseudocapsule or reactive zone, which may leave either "satellite" or "skip" lesions; Wide: Intracompartmental en bloc with a cuff of normal tissue, which may leave "skip" lesions, Radical: Extracompartmental en bloc entire compartment with no tumor residual (5). We elaborate on the location of the lesion in the long bone, the proportion of resection in the whole bone and the reconstructive method recorded.

High-grade malignant bone tumors contained osteosarcoma, Ewing's sarcoma, and undifferentiated pleomorphic sarcoma received preoperative chemotherapy, which facilitates to protect the vascular nerve tract, reduced reaction zone, and is conducive to limb salvage procedure. Otherwise, limb salvage will not be performed if the response to chemotherapy is poor or if blood vessels are involved.

2. *Oncological concerns*: local relapse and recurrence-free interval, distant metastasis, and death were noted and documented in this study.
3. *Functional parameters*: the complications and MSTS (musculoskeletal tumor society) scores (6) were included in the final evaluation.

Statistical Methods

Follow-up time was calculated from the date of operation to the last follow-up or death date. Comparison between subgroups was made using chi-square and t-tests. Wilcoxon method was used for correlation comparison of abnormal distribution grade data, with Mann–Whitney for independent samples. Local recurrence-free survival (LRFS), distant metastasis-free survival (DMFS), and overall survival (OS) were calculated using the Kaplan–Meier method. Univariate analysis for prognostic factors was

Abbreviations: CT, Computed Tomography; MRI, Magnetic Resonance Imaging; MSTS, Musculoskeletal Tumor Society; UE, Unplanned Excision; LRFS, Local Recurrence Free Survival; DMFS, Distant Metastasis Free Survival; OS, overall survival; ICBG, Iliac Crest Bone Graft.

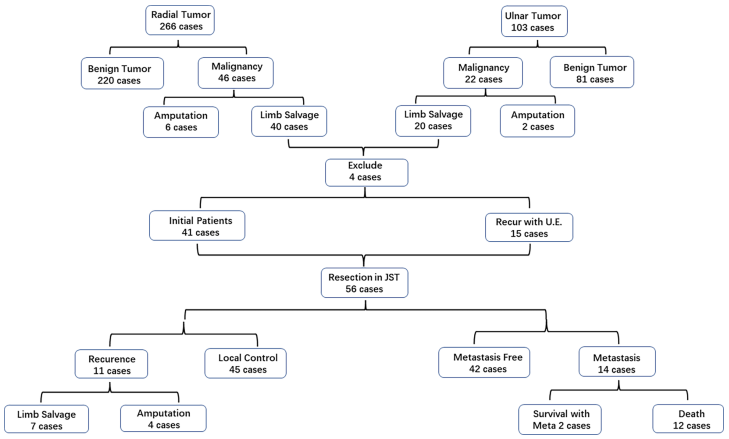

FIGURE 1 | Overview of case enrollment and treatment process in this study.

performed using the log-rank test. Multivariate analyses of factors predicting outcome were performed using Cox regression. A *P*-value of 0.05 or less for two-sided comparisons was considered statistically significant. All analyses were carried out using the SPSS 21.0 software package (IBM, USA).

RESULTS

Patients and Tumor Characteristics

There were forty-six patients with radial malignant tumors, accounting for 17.3% of 266 total radial tumors, and twenty-two patients with ulnar malignant tumors accounting for 21.4% of 103 total ulnar tumors.

Of the 46 patients with primary malignant bone tumor of the radius, limb salvage surgery was performed in 40 patients and amputation in 6 patients. In 22 patients with malignancy of ulna, limb salvage surgery was performed in 20 patients and amputation in 2 patients. Fifty-six patients followed up for more than 12 months, or progression within 12 months were included in the final evaluation (**Table 1**). There were 34 men (60.7%) and 22 women (39.3%) with a mean age of 27.8 (5–73, median 20.0) years. The follow-up averaged 72.1 (7–192, median 62.5) months.

Based on the pathological diagnosis, osteosarcoma was reported in 17 patients (30.4%), Ewing's sarcoma in 10 patients (17.9%), undifferentiated pleomorphic sarcoma in 7 patients (12.5%), low-grade central osteosarcoma in 6 patients (10.7%), chondrosarcoma in 6 patients (10.7%), bone angiosarcoma in 2 patients (3.6%), epithelioid sarcoma in 2 patients (3.6%), parosteal osteosarcoma, low-grade mixed tumor, low-grade myofibroblastic sarcoma, malignant giant cell tumor of bone, spindle cell sarcoma and clear cell sarcoma in 1 patient (1.8%), respectively. There were 17 cases (30.4%) of low-grade sarcoma and 39 cases (69.6%) of high-grade sarcoma based on histology (7, 8).

Tumor Local Control

Of 56 limb salvage procedures in this study, 15 patients (15/56, 26.8%) were recurrent cases following unplanned excision (UE) in another hospital and were referred to our center with reoperation (Group 1), meanwhile, 41 patients (41/56, 73.2%) underwent initial surgery in our hospital (Group 2). In all patients of this study, local recurrence eventually occurred in 11 patients (11/56, 19.6%; see **Table 2**) at the end of follow-up after our surgery. Six patients in Group 1 (6/15, 40%) had recurrences after re-operation done at other hospitals. This is higher than the recurrence rate if the initial surgery was performed in our center (Group 2) (5/41, 12.2%) (P = 0.02) (**Figure 2**). The median recurrence-free time for these 11 recurrent cases was 12 (2–38) months, and 90% of the recurrences occurred within three years (10/11). There were 4 cases who eventually had to undergo amputations in these 11 recurrent cases (4/11, 36.4%). The local resection was performed in 7 cases (63.6%), and one case had a second recurrence. The 3-year and 5-year recurrence-free survival rates were 81.9 and 79.8%, respectively. The recurrence rate with inadequate (marginal or intralesional) margins was significantly higher than adequate (wide) resections. Univariate analysis (**Table 3**) shows the history of UE (P = 0.015), ulnar tumor (P = 0.016), tumor located in the proximal forearm (P = 0.021), and inadequate surgical margin (P <0.001) were associated with recurrence (**Figure 3**).

Postoperative Complications and Functional Evaluation

The bone defects after radial tumor resection were divided into proximal 1/3, distal 1/3, and more than 1/3 defect. The proximal 1/3 defect did not receive reconstruction. The distal 1/3 defect received an autogenous iliac bone graft and wrist joint fusion with internal fixation (**Figure 4**). The more than 1/3 defect from distal to proximal radius received the following procedures: (1) ulna osteotomy and fixation with the end of radius,

TABLE 1 | Patients, Tumor Characteristics and Outcomes in 56 Patients.

Characteristics	N (%)	Local recurrence	Metastasis	Death
Gender				
Male	34 (61)	8	11	9
Female	22 (39)	3	3	3
Age				
<50	48 (86)	10	12	10
≥50	8 (14)	1	2	2
Major histologic type				
Osteosarcoma	17 (30)	3	6	5
Ewing sarcoma	10 (18)	2	3	3
Pleomorphic undifferentiated sarcoma	7 (13)	1	2	2
chondrosarcoma	6 (11)	1	0	0
Other than above	16 (28)	4	3	2
Status at presentation				
Initial	41 (73)	5	9	8
Unplanned excision	15 (27)	6	5	4
Grade				
Low	17 (30)	4	2	2
High	39 (70)	7	12	10
Involved bone				
Radius	38 (68)	4	10	9
Ulna	18 (32)	7	4	3
Anatomic location				
Proximal 1/3	19 (34)	7	7	6
Middle 1/3	10 (18)	2	1	1
Distal 1/3	27 (48)	2	6	5
Bone Resection				
defect <1/3	18 (32)	3	5	4
1/3≤defect<2/3	24 (43)	6	6	5
2/3≤defect	14 (25)	2	3	3
Margin				
Intracapsular	3 (5)	2	1	1
Marginal	8 (14)	5	5	4
Wide	45 (81)	4	8	7
Chemotherapy				
Neoadjuvant	28 (50)	5	9	8
Adjuvant	33 (59)	7	10	8
No chemo	23 (41)	4	4	4

(2) ulna centralization and wrist arthrodesis with internal fixation (**Figure 5**), (3) long segment fibula autograft and fixation (less than 1/2 defect), and (4) ipsilateral ulnar osteotomy to replace the radial defect (**Figure 6**).

After resecting the ulnar tumor, the proximal 1/3 defect was treated with (1) elbow prosthesis replacement and (2) inactivated replantation. More than 2/3 defect of the middle segment was treated with (1) elbow prosthesis combined with free vascularized fibula grafting and (2) brachioradialis elbow arthroplasty (**Figure 7**). The distal 1/3 defect did not receive reconstruction. Although we have performed different methods in reconstruction, the majority is biological reconstruction, which determined relatively few subsequent complications.

Ten patients (10/56, 17.8%) developed postoperative complications: internal fixation failure in 5 patients, limb

TABLE 2 | Local Recurrences by Tumor Type, Grade, Location, Margins.

No.	Histology	Post-op interval	Grade	Bone	Location	Status	Margin	Outcome	Follow-up months
1	Osteosarcoma	2	High	Radius	Distal 1/3	Unplanned excision	Inadequate	Death	7
2	Osteosarcoma	38	High	Radius	Distal 1/3	Initial	Inadequate	NED	123
3	Spindle cell sarcoma	11	Low	Radius	Distal 1/3	Unplanned excision	Inadequate	Death	19
4	Ewing sarcoma	12	High	Ulna	Proximal 1/3	Initial	Adequate	Death	24
5	Ewing sarcoma	28	High	Ulna	Proximal 1/3	Unplanned excision	Adequate	Death	40
6	Osteosarcoma	5	High	Ulna	Middle 1/3	Initial	Inadequate	Death	92
7	Chondrosarcoma	24	Low	Ulna	Proximal 1/3	Initial	Inadequate	NED	48
8	Low grade central osteosarcoma	27	Low	Ulna	Proximal 1/3	Initial	Adequate	NED	42
9	Clear cell sarcoma	5	Low	Radius	Proximal 1/3	Unplanned excision	Inadequate	Death	11
10	Pleomorphic undifferentiated sarcoma	16	High	Ulna	Proximal 1/3	Unplanned excision	Adequate	NED	43
11	Epithelioid sarcoma	11	High	Ulna	Proximal 1/3	Unplanned excision	Inadequate	SWT	30

Inadequate, Intracapsular and Marginal; Adequate, Wide; NED, No evidence of disease; SWT, Survival with tumor.

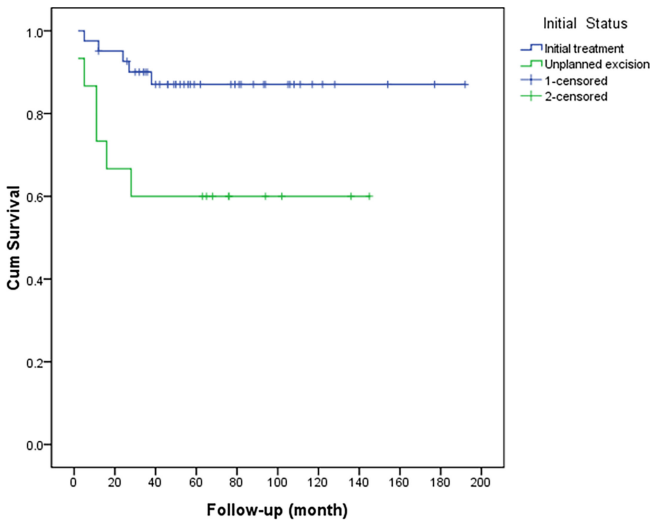

FIGURE 2 | Comparison of recurrence-free survival between patients with recurrence after unplanned excision and those with initial treatment (P = 0.015).

shortening deformity, wrist silver fork deformity, prosthetic aseptic loosening, inactivated bone graft joint subluxation, and bone graft nonunion in 1 patient, respectively. Seven patients (7/10, 70%) underwent revision: 5 patients with fixation failure received re-fixation, one patient with nonunion received iliac graft again, and one patient with limb shortening deformity received limb extension by external fixator. The other three patients underwent routine observations without revision.

Twenty-two patients with ulna centralization lost rotational function, but flexion/extension and other fine movements were not significantly limited. At the final follow-up, functional scores were analyzed for both survivor and final limb salvage patients, because 12 patients died and 4 patients underwent amputation due to recurrence (2 patients were repeated), so 42 patients were included in the final functional evaluation. The MSTS score with an average of 27.9 ± 1.5. The function of patients with limb salvage was satisfactory, and the final limb salvage rate was 92.9% (52/56).

Distant Metastasis and Overall Survival

The follow-up averaged 72.1 (7–192, median 62.5) months. None of the patients had metastatic disease at presentation and distant metastasis was observed in 14 patients (14/56, 25%) during the follow-up, there were seven osteosarcomas, three Ewing sarcomas, two undifferentiated pleomorphic sarcomas, and two low-grade central osteosarcomas developed metastatic disease, 12 (12/14, 85.7%) of them had high-grade sarcomas. The median time from surgery to the development of distant metastasis was 15 (2–64) months, with 6 (42.9%) metastases occurring within 1 year and 12 cases (85.7%) within two years. The median time from the development of distant metastases to death was 11 (1–84) months. Eleven cases (78.6%) involved only lung metastases, 3 cases (21.4%) involved multiple sites of lung and bone metastases (one scapula, one thoracic vertebra, and one femoral shaft).

The 2-year and 5-year metastasis-free survival rates were 78.6 and 76.0%, respectively. The metastasis-free survival rates with adequate (wide) margins and inadequate (marginal or intralesional) margins were 80.4 and 43.6%, respectively (P = 0.008). The 5-year survival rates of high-grade and low-grade tumors were 81.7 and 88.2%, respectively (P = 0.427).

At the end of follow-up in Oct 2021, forty-two patients survived without tumor, two patients survived with metastatic disease, and twelve cases died of metastasis. The median survival time of dead patients was 29 (7–92) months. The overall 5-year and 10-year survival rates were 83.5 and 71.7%, respectively (**Figure 8**). Univariate analysis showed inadequate surgical margins (P = 0.048), local recurrences (P <0.001) and distant metastases (P <0.001) were associated with death. Multivariate analysis of the risk ratio model showed only distant metastases were significant independent poor prognostic factors of overall survival (P <0.001) (**Table 4**).

DISCUSSION

The incidence of primary malignant bone tumors of the forearm is low. Limited previous studies describe a large case series of bone tumors in the forearm, most of which are soft tissue tumors (9–11). The complex anatomy in the narrow forearm space leads to difficulties of limb salvage surgery and poor function after limb salvage surgery for treating bone sarcoma. In the forearm tumors treated in our center at the past 18 years, more benign tumors were found than malignant tumors, and more soft tissue sarcoma was found than primary bone malignant tumors (1). Many reports on soft tissue sarcoma in the forearm have been published (12), while only some case reports on bone sarcoma have been found (13, 14). The primary malignant tumors in the forearm only occupied 18.4% (68/369) of all primary bone tumors in this study. Although the number of malignant cases

TABLE 3 | Outcomes in Univariate Analysis of Prognostic Factors (n = 56).

Variable		Local recurrence-free survival (%)	Distant metastasis-free survival (%)	Disease specific overall survival (%)
Gender				
	Male	76.1	64.6	65.6
	Female	85.6	86.4	86.4
	P-value	0.377	0.152	0.392
Age				
	<50	78.8	74.1	74.2
	≥50	85.7	65.6	43.8
	P-value	0.620	0.986	0.609
Grade				
	Low	76.5	88.2	88.2
	High	81.4	67.0	67.7
	P-value	0.651	0.178	0.427
Bone Site				
	Radius	88.9	71.0	71.8
	Ulna	66.1	77.8	66.1
	P-value	0.016	0.762	0.662
Anatomic location				
	Proximal 1/3	62.3	51.3	48.1
	Middle & Distal 2/3	88.3	80.1	79.5
	P-value	0.021	0.119	0.065
Status				
	Initial	87.0	74.3	72.2
	Unplanned excision	60.0	66.7	72.7
	P-value	0.015	0.419	0.409
Margin				
	Adequate	90.8	80.4	80.9
	Inadequate	36.4	43.6	48.5
	P-value	0.000	0.008	0.048
Chemotherapy				
	Neoadjuvant & Adjuvant	78.2	79.1	70.8
	No chemo	82.2	68.7	72.5
	P-value	0.741	0.321	0.833
Local recurrence				
	Yes	NA	36.4	26.5
	No	NA	82.2	81.8
	P-value	NA	0.000	0.000
Metastasis				
	Yes	NA	NA	0
	No	NA	NA	100
	P-value	NA	NA	0.000

in the radius is much greater than that in the ulna, the proportion of malignant ulnar tumors is higher. Therefore, tumors in the ulna are much more likely to be malignant, although the number of malignant tumors in the radius is dominant. This distribution characteristic has not been described previously (15, 16).

In this study, eleven cases (11/56, 19.6%) had local recurrence in the final follow-up. Six of the 15 patients (6/15, 40%) underwent UE before recurrence developed. These factors may be relevant with the high recurrence rate: improper surgical approach, surgical field contamination, and compartment barrier destruction resulted in the spread of the tumors; the biological behavior of recurrent tumors was more aggressive (17, 18). A significant advantage in recurrence-free survival for primary tumors was observed, and their imaging findings were "milder" than those of UE tumors. Because of the high risk of recurrence, radical resection and even amputation should be considered.

Following univariate analysis, tumors located in the ulna and proximal forearm showed a significantly higher risk of local recurrence, the above characteristics were not found in previous studies (12, 19, 20). Compared with bone sarcomas, soft tissue sarcomas of the forearm have predominantly been previously reported, and which was focused on tumor size associated with recurrence (21). Bosma et al. (22) analyzed the different recurrence risks of sarcoma at different sites, and Pradhan et al. (23) compared forearm sarcoma with other sites. However, the different recurrence rates between different sites in the forearm had not previously been analyzed due to the small sample sizes of the studies.

With less soft tissue attached, the coverage is more difficult for limb salvage in the ulna. The proximal anatomical structure is more complex than the distal forearm. The radial nerve, brachial artery, attachment of muscles at the proximal forearm, and juxtaposition of the elbow joint may lead to inadequate resection margins due to the necessary preservation of essential structures. All these factors may contribute to the increase in the ulnar recurrence rate. For ulna malignancies, especially proximal involvement, the implementation of limb salvage needs to be repeatedly evaluated.

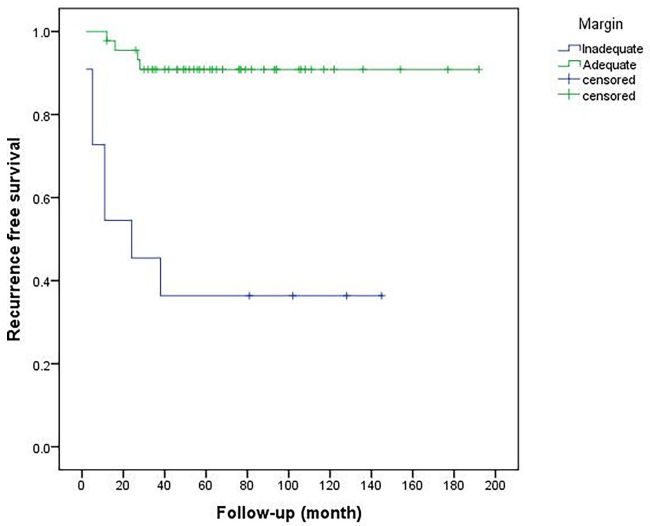

FIGURE 3 | Comparison of recurrence-free survival between inadequate and adequate surgical margins (P < 0.001).

The influence of surgical margins on local recurrence has been investigated in many studies (12). Most researchers define adequate margins as wide or extra-compartmental resections. Muramatsu et al. (4) used a 2-cm margin for high-grade sarcomas and a 1-cm margin for low-grade sarcomas, achieving a satisfactory local recurrence rate of 11%. In this study, the inadequate surgical margin increased the recurrence rate significantly. Intralesional and marginal resection was 63% (7/11), while the recurrence rate of adequate margins was 8.9% (4/45). We planned the surgical strategy according to preoperative imaging, and we used the postoperative specimen and pathological slides to evaluate the surgical margin. This was consistent in most cases. Sometimes the postoperative evaluation does not reach the ideal-planned margin. Such outcomes suggest that limb salvage surgery needs to be re-evaluated if it is difficult to achieve a safe margin.

Daecke et al. (19) reported that the metastasis rate of high-grade bone sarcoma in the forearm was 24%, and the 5-year survival rate was 86.2%, which was better than that in other sites. The current study showed that 14 patients (14/56, 25%) had metastases, and the 5-year survival rate of high-grade sarcoma was 81.7%, slightly lower than that of low-grade sarcoma but without statistical significance. The data suggest that (1) lower tumor load in the forearm leads to a lower risk of metastasis than other anatomical locations are unknown, many other variables that contribute to the risk of metastasis (2), perioperative chemotherapy was performed in most high-grade sarcomas, which reduced metastatic risk.

Whether recurrence affects metastases and survival is controversial (24, 25), some studies suggested that safe margins only affect recurrence, which does not increase metastases and reduce survival (26–28). However, more studies have demonstrated the contrary result (9, 29, 30). The current study showed that margins and recurrence were significantly associated with metastasis and survival following univariate analysis. But only metastasis was an independent risk factor for

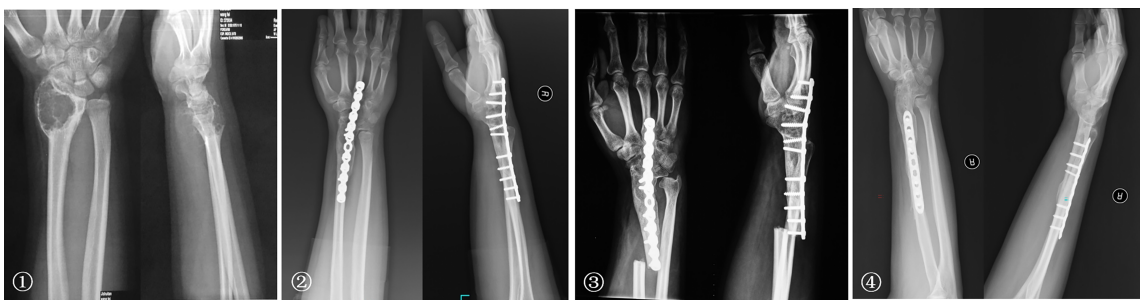

FIGURE 4 | ① The preoperative radiographs of a 29-year-old man with chondrosarcoma. ② Treatment included a distal radius resection and autogenous iliac bone graft with wrist joint fusion. ③ Fracture was caused by trauma eight years after surgery, and internal fixation was performed again. ④ Rotation function of the forearm is shown 192 months postoperatively.

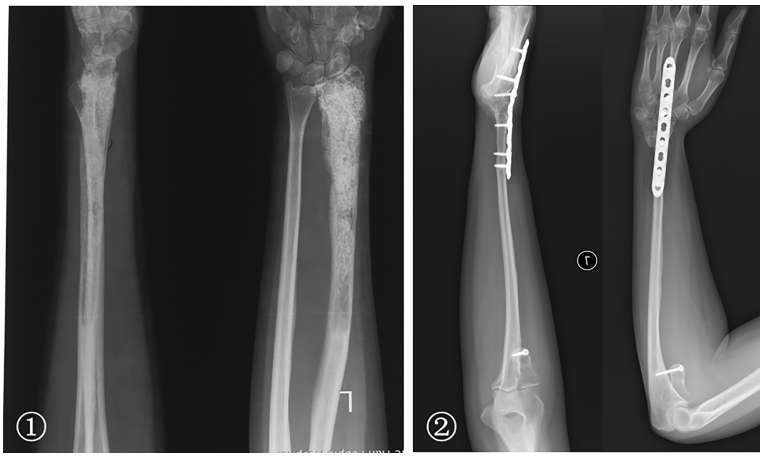

FIGURE 5 | ① A 29-year-old woman with low-grade central osteosarcoma of the middle and distal radius underwent unplanned excision and tumor recurrence. ② Radius resection and ulna centralization with wrist joint fusion was performed; satisfactory bone healing but a loss of forearm rotation is shown 65 months postoperatively.

death from the multivariate analysis. Perhaps recurrence causes repeated operations and prolongs tumor-bearing time, which potentially changes of tumor biological behavior and increases the risk of metastases. The overall 5-year survival rates were 83.5%, the 5-year survival rates of high-grade and low-grade tumors were 81.7 and 88.2% respectively in our study. It was better than the 5-year survival rate of 67% and similar to survival at 5-year following limb salvage surgery of 86% in other reports (19, 23). The results validated the concept of safe margins—local control—reduction of metastases—improvement of survival need more evidence to back up.

The premise of function is oncological safety. The anatomical features of two bones in the forearm have extensive influence on rotation and hand function. Since there is no weight-bearing, it is important to ensure flexibility for the forearm and hand. Defects of the distal ulna and proximal radius have little effect on function, and reconstruction is unnecessary. More challenges result from 2/3 or more defects in the middle and distal radius and 2/3 or more defects in the middle and proximal ulna. For the treatment strategy of the distal radius, wrist arthrodesis with structural iliac crest bone graft was chosen (ICBG) for the defect within 7 cm, and good results were achieved (31). For defects over 7 cm, the ulna is directly displaced to centralization. This method is practical and straightforward, but the loss of rotation is not negligible. A segment autogenous fibula transplantation or translocating the ipsilateral ulna as a vascularized autograft to reconstruct the distal radius defects were adopted (32, 33) to maintain rotation. This relatively complex method showed better function and preferred wrist arthrodesis to obtain a stable joint (31). Compared to a few joint replacement options for the distal

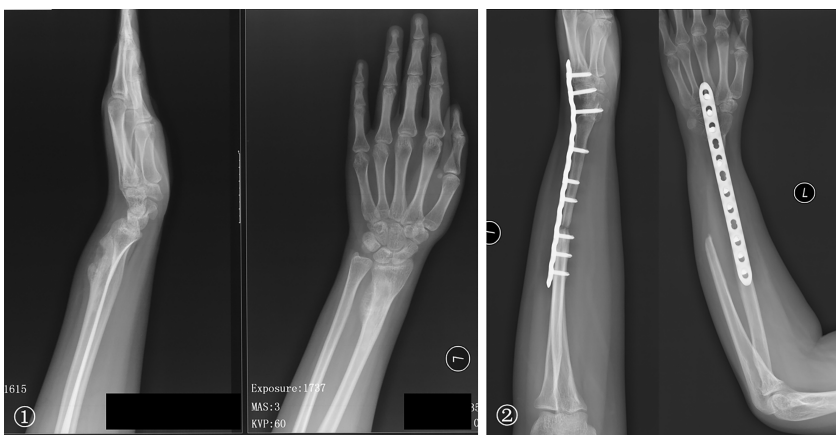

FIGURE 6 | ① The preoperative radiographs of a 19-year-old woman with low-grade central osteosarcoma of the distal radius. ② Treatments included a distal radius resection; ipsilateral ulnar osteotomy to replace the radial defect. Wrist joint fusion was performed; the satisfactory bone healing of the forearm and rotation function is shown 50 months postoperatively.

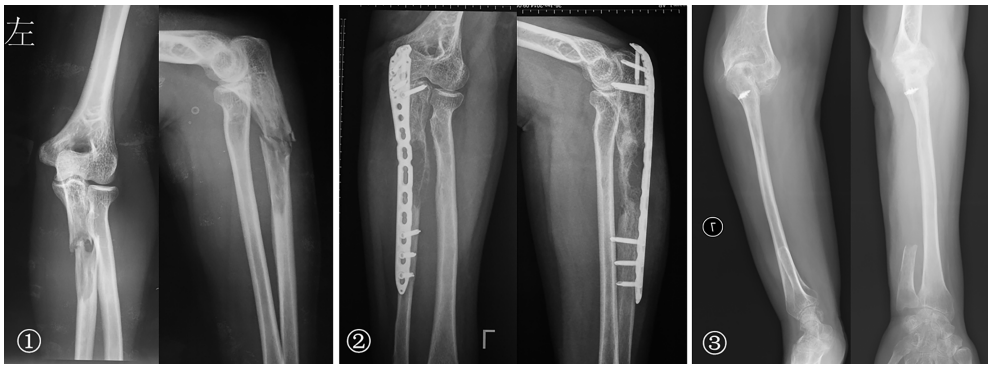

FIGURE 7 | ① The preoperative radiographs of a 51-year-old woman with osteosarcoma of the proximal ulna. ② An unplanned excision and tumor recurrence occurred. ③ The radial head was displaced and inserted into the intercondylar of the humerus after proximal ulna resection; the rotation function of the forearm is shown 76 months postoperatively.

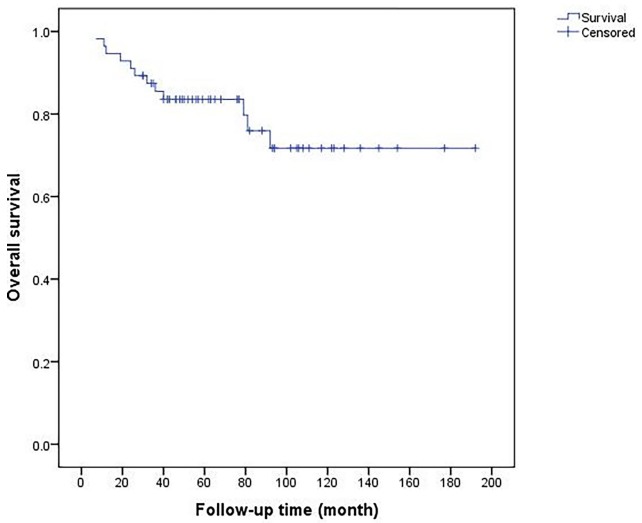

FIGURE 8 | Overall 5-year and 10-year survival rates of 56 patients were 83.5 and 71.7%, respectively.

radius (34), prosthesis replacement is a routine and applicable method for proximal ulna defects. Brachioradialis elbow arthroplasty between the proximal radius and humeral condyle was designed, yielding satisfactory function. It is challenging to cover skin defects due to extensive resections in recurrent cases. Instead, it is preferred to execute microsurgery and flap technology (16, 35). In this study, three patients received flap coverage, and two patients underwent free vascularized fibula grafting with satisfactory postoperative results.

This study has some limitations. Firstly, this is a retrospective analysis spanning 18 years, and there were homogeneity differences in the choice of chemotherapy and surgical techniques. Secondly, this is a single institution report, which lacks multiple center coordination to correct the bias in the enrollment of patients and treatment methods. Finally, this study only included limb salvage cases, which did not compare with the outcomes of amputation. Thus, the selection bias of tumor load and site led to overestimating the survival rate of patients with forearm malignancy.

TABLE 4 | Outcomes in Multivariate Analysis of Prognostic Factors.

Variable		Wald	Odds Ratio	*P*-Value	95% CI	
					Lower	Upper
Margin	Adequate	0.202	1	0.653	0.574	2.424
	Inadequate		1.180			
LR	No	0.752	1	0.386	0.484	6.529
	Yes		1.778			
Metastasis	No	13.864	1	0.000	7.006	530.539
	Yes		60.966			

LR, Local recurrence.

CONCLUSIONS

This study is the most extensive, single-institution case analysis of limb salvage treatment for primary malignant bone tumors in the forearm. A history of unplanned surgery, tumors located in the ulna, proximal forearm, and inadequate surgical margin are important factors leading to local recurrence. To improve local control, limb salvage should be used with caution in patients who underwent unplanned excision. Amputation may be a better choice for high-risk patients with proximally located soft tissue masses adjacent to vascular and nerve tracts. Metastasis is an independent poor prognostic factor of survival. Multidisciplinary collaboration for the systematic treatment of metastatic patients is a potentially effective way to reduce the mortality of these malignant tumors. Limb salvage surgery for malignant bone tumors of the forearm showed a high overall survival rate and relatively satisfactory functional recovery.

DATA AVAILABILITY STATEMENT

The original contributions presented in the study are included in the article/supplementary material. Further inquiries can be directed to the corresponding authors.

ETHICS STATEMENT

The studies involving human participants were reviewed and approved by the Beijing Jishuitan Hospital. Written informed consent to participate in this study was provided by the participants' legal guardian/next of kin.

AUTHOR CONTRIBUTIONS

WL and XN conceived and designed the study. WL,YY, TJ, YS, YL, LH and QZ undertook the study. WL and YY analyzed and interpreted the clinical data. WL drafted the manuscript. WL, YY and XN reviewed and edited the manuscript. All authors listed have made a substantial,direct, and intellectual contribution to the work and approved it for publication.

FUNDING

This research was supported by the National Key R&D Program of China (Grant No. 2021YFC2400500), Beijing Municipal Administration of Hospitals Incubating Program (PX2021015), Beijing Natural Science Foundation (L212042), Beijing Jishuitan Hospital Elite Young Scholar Programme (XKGG202105), Chinese Society of Clinical Oncology (CSCO) Research Foundation (Y-2019GCTB-002, Y-young2019-070), National Natural Science Foundation of China (51973021).

ACKNOWLEDGMENTS

The authors thank Chung Ming Chan and G. Douglas Letson who reviewed the manuscript, and Tao Wang, Fajun Yang, Feng Yu, and Hairong Xu, for their contribution to the data collection of this study.

REFERENCES

1. Niu X, Xu H, Inwards CY, Li Y, Ding Y, Letson GD, et al. Primary Bone Tumors: Epidemiologic Comparison of 9200 Patients Treated at Beijing Ji Shui Tan Hospital, Beijing, China, With 10 165 Patients at Mayo Clinic, Rochester, Minnesota. *Arch Pathol Lab Med* (2015) 139(9):1149–55. doi: 10.5858/arpa.2014-0432-OA
2. Haendel M, Vasilevsky N, Unni D, Bologa C, Harris N, Rehm H, et al. McMurry J Et Al: How Many Rare Diseases are There? *Nat Rev Drug Discov* (2020) 19(2):77–8. doi: 10.1038/d41573-019-00180-y
3. Picci P, Manfrini M, Fabbri N, Gambarotti M, Vanel D. *Atlas of Musculoskeletal Tumors and Tumorlike Lesions, The Rizzoli Case Archive*. Switzerland: Springer (2014).
4. Muramatsu K, Ihara K, Yoshida K, Tominaga Y, Hashimoto T, Taguchi T. Musculoskeletal Sarcomas in the Forearm and Hand: Standard Treatment and Microsurgical Reconstruction for Limb Salvage. *Anticancer Res* (2013) 33 (10):4175–82.
5. Enneking WF, Spanier SS, Goodman MA. A System for the Surgical Staging of Musculoskeletal Sarcoma. *Clin Orthop Relat Res* (1980) 153):106–20. doi: 10.1097/00003086-198011000-00013
6. Enneking WF, Dunham W, Gebhardt MC, Malawar M, Pritchard DJ. A System for the Functional Evaluation of Reconstructive Procedures After Surgical Treatment of Tumors of the Musculoskeletal System. *Clin Orthop Relat Res* (1993) 286):241–6. doi: 10.1097/00003086-199301000-00035
7. Coindre JM. Grading of Soft Tissue Sarcomas: Review and Update. *Arch Pathol Lab Med* (2006) 130(10):1448–53. doi: 10.5858/2006-130-1448-GOSTSR
8. Christopher DM, Fletcher JAB, Pancras CW, Hogendoorn FM. *WHO Classification of Tumours of Soft Tissue and Bone*. Lyon: International Agency for Research on Cancer (2013).
9. Stojadinovic A, Leung DH, Hoos A, Jaques DP, Lewis JJ, Brennan MF. Analysis of the Prognostic Significance of Microscopic Margins in 2,084 Localized Primary Adult Soft Tissue Sarcomas. *Ann Surg* (2002) 235(3):424–34. doi: 10.1097/00000658-200203000-00015
10. Popov P, Tukiainen E, Asko-Seljavaara S, Huuhtanen R, Virolainen M, Virkkunen P, et al. Soft-Tissue Sarcomas of the Upper Extremity: Surgical Treatment and Outcome. *Plast Reconstr Surg* (2004) 113(1):222–30; discussion 231-22. doi: 10.1097/01.PRS.0000095946.90511.1D
11. Bansal K, Prasad A, Shahi P, Sehgal A, Kamal S. Extraosseus Ewing's Sarcoma of the Forearm. *Cureus* (2020) 12(7):e9051. doi: 10.7759/cureus.9051
12. Baroudi MR, Ferguson PC, Wunder JS, Isler MH, Mottard S, Werier JA, et al. Forearm Soft Tissue Sarcoma: Tumors Characteristics and Oncologic Outcomes Following Limb Salvage Surgery. *J Surg Oncol* (2014) 110(6):676–81. doi: 10.1002/jso.23686
13. Puri A, Gulia A, Byregowda S, Ramanujan V. Reconstruction of the Elbow and Forearm for Ewing Sarcoma of the Ulna: A New Biological Technique. *Int J Shoulder Surg* (2016) 10(2):85–8. doi: 10.4103/0973-6042.180721
14. Cahayadi SD, Antoro A, Swandika B. A Giant Cell-Rich Osteosarcoma of the Proximal Ulnar Bone Treated by Elbow Arthroplasty: A Case Report. *Int J Surg Case Rep* (2019) 58:157–61. doi: 10.1016/j.ijscr.2019.04.017
15. KK U. *Dahlin's Bone Tumors-General Aspects and Data on 11,087 Cases. 5th Edition*. Philadelphia: Lippincott-Raven Publishers (1996).
16. Rosenberg AE. WHO Classification of Soft Tissue and Bone, Fourth Edition: Summary and Commentary. *Curr Opin Oncol* (2013) 25(5):571–3. doi: 10.1097/01.cco.0000432522.16734.2d
17. Yang Z, Niu N, Tang J, Wu L, He J, Shi J. Reconstruction of Forearm Support With Ulnar Translocation After Resection of Chondrosarcoma in the Proximal Radius. *Orthopade* (2020) 49(11):1006–12. doi: 10.1007/s00132-020-03903-x
18. Bilgeri A, Klein A, Lindner LH, Nachbichler S, Knösel T, Birkenmaier C, et al. The Effect of Resection Margin on Local Recurrence and Survival in High Grade Soft Tissue Sarcoma of the Extremities: How Far Is Far Enough? *Cancers (Basel)* (2020) 12(9):2560. doi: 10.3390/cancers12092560
19. Daecke W, Bielack S, Martini AK, Ewerbeck V, Jurgens H, Kotz R, et al. Osteosarcoma of the Hand and Forearm: Experience of the Cooperative Osteosarcoma Study Group. *Ann Surg Oncol* (2005) 12(4):322–31. doi: 10.1245/ASO.2005.06.002
20. Landau MJ, Badash I, Yin C, Alluri RK, Patel KM. Free Vascularized Fibula Grafting in the Operative Treatment of Malignant Bone Tumors of the Upper Extremity: A Systematic Review of Outcomes and Complications. *J Surg Oncol* (2018) 117(7):1432–9. doi: 10.1002/jso.25032
21. England P, Hong Z, Rhea L, Hirbe A, McDonald D, Cipriano C, et al. Does Advanced Imaging Have a Role in Detecting Local Recurrence of Soft-Tissue Sarcoma? *Clin Orthop Relat Res* (2020) 478(12):2812–20. doi: 10.1097/CORR.0000000000001351
22. Bosma SE, Rueten-Budde AJ, Lancia C, Ranft A, Dirksen U, Krol AD, et al. Individual Risk Evaluation for Local Recurrence and Distant Metastasis in Ewing Sarcoma: A Multistate Model: A Multistate Model for Ewing Sarcoma. *Pediatr Blood Cancer* (2019) 66(11):e27943. doi: 10.1002/pbc.27943
23. Pradhan A, Reddy KI, Grimer RJ, Abudu A, Tillman RM, Carter SR, et al. Osteosarcomas in the Upper Distal Extremities: Are Their Oncological Outcomes Similar to Other Sites? *Eur J Surg Oncol* (2015) 41(3):407–12. doi: 10.1016/j.ejso.2014.11.038
24. Pisters PW, Leung DH, Woodruff J, Shi W, Brennan MF. Analysis of Prognostic Factors in 1,041 Patients With Localized Soft Tissue Sarcomas of the Extremities. *J Clin Oncol* (1996) 14(5):1679–89. doi: 10.1200/JCO.1996.14.5.1679

25. Yang JC, Chang AE, Baker AR, Sindelar WF, Danforth DN, Topalian SL, et al. Randomized Prospective Study of the Benefit of Adjuvant Radiation Therapy in the Treatment of Soft Tissue Sarcomas of the Extremity. *J Clin Oncol* (1998) 16(1):197–203. doi: 10.1200/JCO.1998.16.1.197
26. Tanabe KK, Pollock RE, Ellis LM, Murphy A, Sherman N, Romsdahl MM. Influence of Surgical Margins on Outcome in Patients With Preoperatively Irradiated Extremity Soft Tissue Sarcomas. *Cancer* (1994) 73(6):1652–9. doi: 10.1002/1097-0142(19940315)73:6<1652::AID-CNCR2820730617>3.0.CO;2-X
27. Heinemann M, Ranft A, Langer T, Jurgens H, Kreyer J, Vieth V, et al. Recurrence of Ewing Sarcoma: Is Detection by Imaging Follow-Up Protocol Associated With Survival Advantage? *Pediatr Blood Cancer* (2018) 65(7): e27011. doi: 10.1002/pbc.27011
28. Spraker-Perlman HL, Barkauskas DA, Krailo MD, Meyers PA, Schwartz CL, Doski J, et al. Factors Influencing Survival After Recurrence in Osteosarcoma: A Report From the Children's Oncology Group. *Pediatr Blood Cancer* (2019) 66(1):e27444. doi: 10.1002/pbc.27444
29. Zhao R, Yu X, Feng Y, Yang Z, Chen X, Wand J, et al. Local Recurrence Is Correlated With Decreased Overall Survival in Patients With Intermediate High-Grade Localized Primary Soft Tissue Sarcoma of Extremity and Abdominothoracic Wall. *Asia Pac J Clin Oncol* (2018) 14(2):e109-15. doi: 10.1111/ajco.12807
30. Dickinson IC, Whitwell DJ, Battistuta D, Thompson B, Strobel N, Duggal A, et al. Surgical Margin and its Influence on Survival in Soft Tissue Sarcoma. *ANZ J Surg* (2006) 76(3):104–9. doi: 10.1111/j.1445-2197.2006.03615.x
31. Wang T, Chan CM, Yu F, Li Y, Niu X. Does Wrist Arthrodesis With Structural Iliac Crest Bone Graft After Wide Resection of Distal Radius Giant Cell Tumor Result in Satisfactory Function and Local Control? *Clin Orthop Relat Res* (2017) 475(3):767–75. doi: 10.1007/s11999-015-4678-y
32. Gundavda MK, Agarwal MG, Reddy R, Katariya A, Bhadiyadra R. Does a Modified Technique to Achieve Arthrodesis of the Wrist After Resection of the Distal Radius and Translocating the Ipsilateral Ulna as a Vascularized Graft to Reconstruct the Defect Improve Grip Strength and Outcomes Scores? *Clin Orthop Relat Res* (2021) 479(6):1285–93. doi: 10.1097/CORR.0000000000001604
33. McLean JM, Clayer M, Stevenson AW, Samson AJ. A Modified Ulnar Translocation Reconstruction Technique for Campanacci Grade 3 Giant Cell Tumors of the Distal Radius Using a Clover Leaf Plate. *Tech Handb Up Extrem Surg* (2014) 18(3):135–42. doi: 10.1097/BTH.0000000000000053
34. Guzik G. The Use of a Custom-Made Prosthesis in the Treatment of Chondrosarcoma of Distal Radius. *Ortop Traumatol Rehabil* (2016) 18 (1):65–72. doi: 10.5604/15093492.1198866
35. Muramatsu K, Ihara K, Doi K, Hashimoto T, Taguchi T. Sarcoma in the Forearm and Hand: Clinical Outcomes and Microsurgical Reconstruction for Limb Salvage. *Ann Plast Surg* (2009) 62(1):28–33. doi: 10.1097/SAP.0b013e3181743a11

Conflict of Interest: The authors declare that the research was conducted in the absence of any commercial or financial relationships that could be construed as a potential conflict of interest.

Publisher's Note: All claims expressed in this article are solely those of the authors and do not necessarily represent those of their affiliated organizations, or those of the publisher, the editors and the reviewers. Any product that may be evaluated in this article, or claim that may be made by its manufacturer, is not guaranteed or endorsed by the publisher.

frontiers | Frontiers in Oncology

ORIGINAL RESEARCH
published: 16 May 2022
doi: 10.3389/fonc.2022.829369

Preliminary Study of a Modular MR-Compatible Robot for Image-Guided Insertion of Multiple Needles

*Amanda M. Aleong[1], Thomas Looi[1,2], Kevin Luo[2], Zhiling Zou[2], Adam Waspe[1,2], Satwinder Singh[2], James M. Drake[1,2] and Robert A. Weersink[1,3,4]**

[1] The Institute of Biomedical Engineering, University of Toronto, Toronto, ON, Canada, [2] The Centre of Image Guided Innovation and Therapeutic Intervention in the Hospital for Sick Children, Toronto, ON, Canada, [3] The Department of Medical Biophysics, University of Toronto, Toronto, ON, Canada, [4] The Department of Radiation Oncology, University of Toronto, Toronto, ON, Canada

Percutaneous needle-based interventions such as transperineal prostate brachytherapy require the accurate placement of multiple needles to treat cancerous lesions within the target organ. To guide needle placement, magnetic resonance imaging (MRI) offers excellent visualization of the target lesion without the need for ionizing radiation. To date, multi-needle insertion relies on a grid template, which limits the ability to steer individual needles. This work describes an MR-compatible robot designed for the sequential insertion of multiple non-parallel needles under MR guidance. The 6-DOF system is designed with an articulated arm to extend the reach of the robot. This strategy presents a novel approach enabling the robot to maneuver around existing needles while minimizing the footprint of the robot. Forward kinematics as well as optimization-based inverse kinematics are presented. The impact of the robot on image quality was tested for four sequences (T1w-TSE, T2w-TSE, THRIVE and EPI) on a 3T Philips Achieva system. Quantification of the signal-to-noise ratio showed a 46% signal loss in a gelatin phantom when the system was powered on but no further adverse effects when the robot was moving. Joint level testing showed a maximum error of 2.10 ± 0.72°s for revolute joints and 0.31 ± 0.60 mm for prismatic joints. The theoretical workspace spans the proposed clinical target surface of 10 x 10 cm. Lastly, the feasibility of multi-needle insertion was demonstrated with four needles inserted under real-time MR-guidance with no visible loss in image quality.

Keywords: robotics, needle insertion, MRI, brachytherapy, biopsy

OPEN ACCESS

Edited by:
Patrick J. Schuler, Ulm University Medical Center, Germany

Reviewed by:
Mengying Shi, University of Massachusetts Lowell, United States
Leon R. Schild, Ulm University Medical Center, Germany

***Correspondence:**
Robert A. Weersink
robert.weersink@rmp.uhn.ca

Specialty section:
This article was submitted to Surgical Oncology, a section of the journal Frontiers in Oncology

Received: *05 December 2021*
Accepted: *21 March 2022*
Published: *16 May 2022*

Citation:
Aleong AM, Looi T, Luo K, Zou Z, Waspe A, Singh S, Drake JM and Weersink RA (2022) Preliminary Study of a Modular MR-Compatible Robot for Image-Guided Insertion SWof Multiple Needles. Front. Oncol. 12:829369. doi: 10.3389/fonc.2022.829369

1 INTRODUCTION

The insertion of multiple needles for minimally invasive procedures such as prostate brachytherapy is a time-consuming task with needle deflection and tissue deformation presenting the primary challenges to accurate placement. In particular, the treatment of localized prostate cancer using focal therapies such as high-dose rate brachytherapy and thermal laser ablation presents an opportunity to optimize needle placement thereby minimizing the number of needles to be inserted and

reducing the risk to the patient. To date, state-of-the-art magnetic resonance (MR)-guided needle insertion typically uses a template grid registered to the MR image space to place the needles at planned locations based on pre-insertion images (1). The patient must be moved out of the MR bore to place each needle and returned to the bore to acquire verification images, leading to a procedure time of 3-5 hours on average for a multi-needle case. Robotic systems are being explored to improve patient access in closed-bore MR systems and enable needle steering under image guidance. Eliminating the need to move the patient is expected to reduce the overall procedure time and improve the needle targeting accuracy. However, due to challenges associated with clinical translation, there has been a shift in focus from automated needle insertion under continuous MR-guidance to passive needle guidance with intermittent MR imaging for the verification of needle placement.

Existing robotic systems focus primarily on the guidance of single-needle procedures wherein each needle is removed before subsequent needles are inserted. The mechanics of inserting a single needle through soft tissue to reach deep-seated targets has been investigated extensively. Efforts to reduce needle deflection due to needle-tissue interaction has led to steering mechanisms that utilize axial rotation and lateral force at the base of the needle to adjust the needle trajectory (2–4).

A brief review of clinically-tested, MR-compatible robots provides insight into the limitations of available systems. For single needle insertion, the MrBot is a 6-DOF, pneumatically driven benchtop system developed at John Hopkins for use in the MR environment to facilitate transrectal prostate biopsy (5). The robot evolved out of a previously automated steerable system but was adapted for manual insertion to aid clinical translation. The FDA-approved system reported an MRI-based needle targeting accuracy of 2.55 mm (6). Few robotic systems have been developed for guiding multiple needle insertions. Recently, Cepek et al. presented MR PING, a 5-DOF bench-top guidance system currently undergoing clinical trials for focal laser ablation in the prostate (7). The system positions a small grid template *via* manual joint manipulation and is then locked in place once satisfactory alignment to the target has been achieved, with no subsequent steering possible once the grid is locked. Using the grid, needle insertions were confined to the same orientation resulting in a median needle guidance error of 3.5 mm over 37 insertions. Upon further inspection, needle deflection was identified as the main limiting factor in system accuracy. Another strategy for guiding multi-needle insertion was presented by Podder et al (8). The system was developed for ultrasound-guided brachytherapy seed placement. Simultaneous multi-needle insertion was achieved using actuated channels in a template grid to steer multiple needles. The results showed seed placement within 0.2 mm of the plan, confirming the benefits of needle steering. The systems presented limit the ability to steer non-parallel needles and constrains all needles to a single orientation thereby limiting access to optimal insertion paths for individual needles. The targeting errors observed for the first two systems presented are consistent with errors seen in the clinic for traditional template-based procedures.

In practice, the needle steering models that predict deflection based on tissue models and forces at the base of the needle are often complex and computationally expensive, limiting their feasibility in real-time applications (3, 9). Real-time MR offers additional feedback that may be used to reduce the model complexity and facilitate closed-loop control systems. As such, a robotic system that is compatible with real-time imaging is needed. Critically, there should be minimal impact on image quality when the robot's joints are in motion. The signal-to-noise ratio (SNR) provides a suitable metric for gauging the impact of the robot on the MR. Furthermore, there is need for a system that overcomes the specific challenges associated with the insertion of multiple needles. Namely, entry-point and trajectory constraints imposed by placing needles next to each other and the need to change the needle that the robot is guiding without excessive movement of the patient. In addition, the presence of needles in the tissue affects the tissue deformation and target shift for subsequent needles.

This work presents a novel strategy to sequentially drive the insertion of multiple non-parallel needles under real-time MR-guidance. A modular robotic system is described with an articulated arm to extend the robot's reach into a closed-bore MR system and a hinge-based needle guide to support needle release for subsequent needle insertions. This strategy enables the robot to maneuver around existing needles while minimizing the footprint of the robot. The system aligns the needle guide along a specified path and is designed to support future work on the adjustment of the needle trajectory to minimize needle deflection during insertion for each target point. This paper reports on the conceptual design and preliminary validation of a robot for sequential non-parallel needle insertion under continuous image guidance using custom pre-clinical gel phantoms designed to mimic the entry force properties of tissue. The gel phantoms allow for measurements in a controlled setting to confirm (and correct if necessary) the robot functionality before we move to further studies using *ex vivo* tissue samples and pre-clinical animal studies.

2 SYSTEM OVERVIEW

2.1 Design and Specifications

The robot described herein is developed for transdermal needle insertion, in the inferior to superior direction, under real-time MR guidance, aligning with requirements described by recent guidance documents on image-guided robotic interventions (10, 11). Critically, the operation of the robot is designed to have no adverse impact on image quality by either its presence in the MR bore or during the robotic adjustment of a needle. All components of the robot are made with MR safe or MR conditionally safe materials according to American Society for Testing and Materials guidelines. The main components of the robot body were machined from Delrin, aluminum, brass, and acrylic. The end effector was 3D printed using stereolithography (PolyJet, Stratasys) using VeroWhite (Stratasys) plastic. Further, all parts were visibly inspected prior to assembly. The joints are

actuated by non-magnetic ultrasonic rotary motors (USR30/60-E3M, Shinsei Co., Japan). The current system is built to accommodate passive, hand-driven insertion. The end effector i.e. the needle guide mechanism that attaches to the last link of the robot, is designed to be interchangeable to support future modifications for automation. For clinical use, the robot can be replaced with sterile covers and the 3D printed needle guide can be removed and sterilized using standard ethylene oxide gas protocols.

The planned robot workspace covers the full extent of the target organ (initially the prostate) with a constrained surface for needle insertion. It is designed to access all positions and orientations for needle entry-points for an expected range of patient sizes. Based on clinical experience for our initial scenario of prostate insertions, the target surface consists of a 10 x 10 cm transverse region allowing access to a 10 x 10 x 5 cm target cube up to 10 cm below the skin. The angle of approach covers a range between ±5° about the coronal and ±15° about the sagittal. The robot is also designed to accommodate access to the patient during needle insertion and allows easy release of the needle to facilitate multiple needle insertions. Both hardware and software safety interrupts are included to ensure patient safety. Furthermore, the motion of the robot joints are constrained to prevent collision with the patient, clinician, and magnet during normal operation.

Additional criteria considered when designing the robot are listed herein. The end effector should align to an entry point at the specified position and an orientation with a translational error under 1 mm and a rotational error under 1° in phantom tests to meet clinical requirements and remain competitive with existing systems (10–13). The system should be rigid enough to generate an insertion force of up to 2 N to allow the clinician to make adjustments at the needle entry point without causing unnecessary damage to the tissue or deformation of the robot links (14, 15). Furthermore, the motors and attached mechanisms should allow small adjustments to the needle trajectory for needle steering without interfering with other needles already in place. Specifically, adjustments on the order of 1 mm and 1° to the end effector position and orientation should be feasible without interfering with the clinician workspace.

To establish base functionality, the initial iteration of the system is built to accommodate hand-driven needle insertion *via* a custom needle guide while future modifications will support an automated approach.

2.2 Hardware

The system consists of the robot, the control box, and a computer console for interfacing with the robot and communicating with the MR. The robot consists of a planar Cartesian base and an articulated arm, able to move in 6 dimensions. It consists of 3 prismatic joints (P) and 3 rotary joints (R), as shown in **Figure 1**, with a PPRRRP configuration and an interchangeable end effector.

The 6-DOF robot is further divided into 3 sections. The base consists of two prismatic lead screw joints (axial and lateral) providing planar motion. The arm consists of 3 rotational joints: the pivot, the elbow and the shoulder. Lastly, the end effector attaches to a 1D lead screw for extension along the insertion direction. The elbow and end lead screw are driven by independent belt mechanisms.

The end effector for manual needle insertion, shown in **Figure 2**, was designed to enable needles to be easily swapped out on the robot, without undue effort on the clinician's part or excessive movement of the patient bed. It enables the tip of the needle guide to be positioned as close to the skin as possible to minimize the deflection due to torque on the needle as it enters the tissue. To reduce the space between needles, the footprint of the needle guide was minimized to allow the sequential placement of multiple needles while still being rigid enough to guide the needle and maintain its trajectory. Lastly, the modular design of the robot end effector allows it to be easily swapped out or adapted for other modes of operation. The custom-designed 3D-printed needle guide is connected to the robot *via* a mounting plate and incorporates a hinge mechanism to release

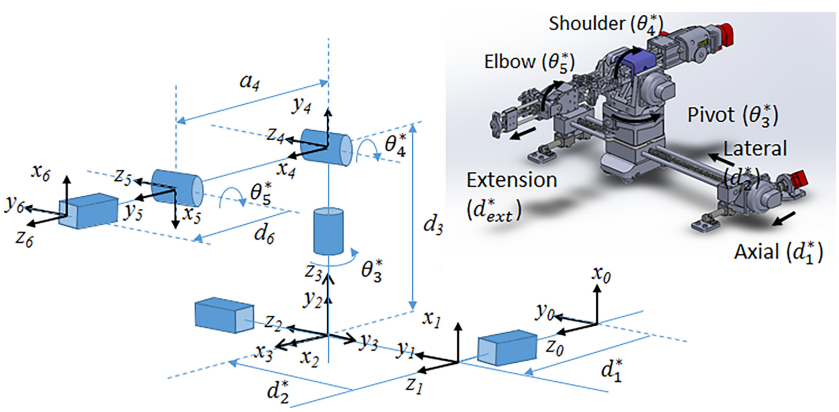

FIGURE 1 | (Left) Joint-level schematic of robot showing coordinate systems and movement of each joint; (right) CAD rendering of the 6-DOF robot showing joint motion.

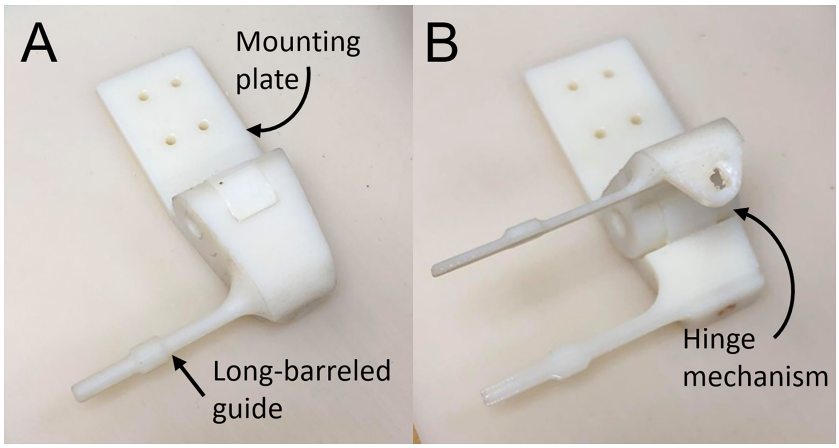

FIGURE 2 | End effector needle guide in **(A)** closed and **(B)** open configuration.

the needle after insertion. It features a long barrel to enable the needle guide to access the target surface while maneuvering around needles that have already been inserted.

The control box consists of 2 USB4 controllers (US Digital) and 7 motor drivers housed in a metal case with fans and vents placed for optimal cooling. The motor drivers were calibrated by Shinsei Co. for operation with 10 m MR-compatible shielded connecting cables. The control box connects to the robot *via* D-sub filtered connectors (API Technologies 56-705-003) which were used to minimize the electromagnetic impact of the robot on the MR field. Specifically, the connectors filter noise induced through communication between the control box outside the room and the robot inside the MR room.

2.3 Robot Control Workflow

The robot control workflow describes the overall process from registering the robot with the MR-guidance system, to selecting the target, driving the robot and inserting a sequence of needles as shown in **Figure 3**. The robot is manually mounted on the MR bed and registered to the MR image space as described in 2.3.1. After registration, the Z-frame is removed by the operator and the target volume is imaged to select the desired needle poses. A plan is generated using the inverse kinematic workflow described in 2.3.3 to drive the robot to each target. With the target phantom still in the bore, the robot is driven automatically to the next target. The needle is then inserted into the guide and the operator has the choice to manually drive the needle insertion or automatically drive the needle in using the extension joint. At this point, the real-time MR slice is manually aligned to the expected insertion path and the sequence is initiated to monitor the needle during insertion. Once the needle is fully inserted further adjustments may be made by manual or automatic retraction of the needle. Automatic MR slice alignment and needle tracking is currently under development and is being reported elsewhere. Finally, the needle is manually released from the guide and the workflow proceeds to the next target.

Figure 3A shows the procedure workflow and **Figure 3B** shows the inverse kinematic workflow for a single needle insertion as described in detail below.

2.3.1 MR to Robot Registration

A z-frame fiducial phantom was used to register the MRI coordinate space to the robot coordinate space (13, 16). The robot is placed on the MR bed and a homing system is used to drive the robot to a known joint configuration. The homing system consists of a set of limit switches used to detect when a joint has been driven to the edge of its working range. After driving each joint to their respective limit, the joints were then driven a known distance or angle to the desired home configuration and the Z-frame was connected rigidly to the last joint, as shown in **Figure 4**. By acquiring an image of the Z-frame, the pose of the Z-frame with respect to the magnet isocenter can be determined as described in (13, 16). Equation 1 describes the transformation of a point in MR coordinate space, $\mathbf{p}_{MR}$, to the same point described in the robot coordinate space, $\mathbf{p}_{Robot}$.

$$\mathbf{p}_{Robot} = T_{Z-Frame}^{Robot} * T_{MR}^{Z-frame} * p_{MR} \quad (1)$$

$T_{Z-Frame}^{Robot}$ is the transformation from the robot to the z_frame obtained by homing and $T_{MR}^{Z-frame}$ is the transformation from the Z-frame to the MR isocenter obtained by imaging the Z-frame. Using this mapping, a target selected in an MR image can be defined in robot coordinate space and passed to the inverse kinematic workflow to determine a suitable set of joint angles for needle alignment.

2.3.2 Forward Kinematics

The pose of the end effector encompasses its position and orientation. In this section, we describe the forward kinematics formulation that maps the pose of each joint to that of the end effector. To begin, we define 6 joint variables (d_1, d_2, θ_3, θ_4, θ_5, d_6)

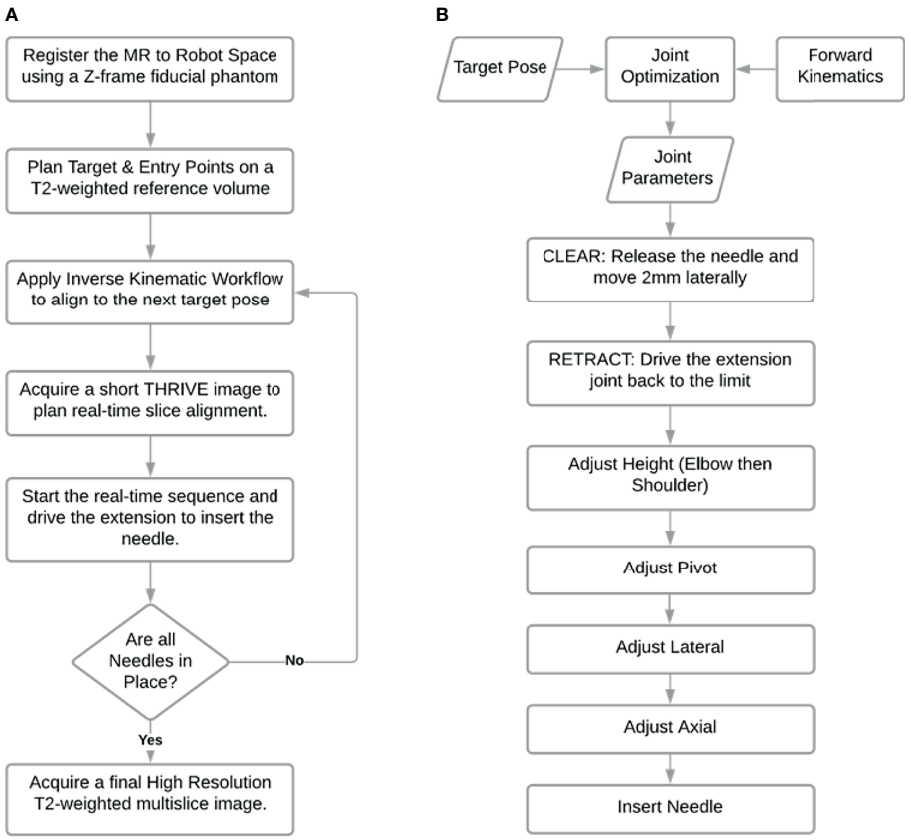

FIGURE 3 | Workflow of needle insertions. **(A)** Procedure workflow; **(B)** Single needle insertion inverse kinematic workflow represented by third step in workflow **(A)**.

each corresponding to a joint shown in **Figure 1**. The mathematical expression relating the inertial frame of reference, frame 0, to the end effector was then defined according to the modified Denavit-Hartenberg (D-H) convention (17). Using this convention, each joint is assigned a Cartesian coordinate frame and the following set of four D-H parameters may be used to determine the relationship between frame *i* and frame *i-1*. The link length, a_{i-1}, describes the distance between $\mathbf{z}_{i-1}$ to $\mathbf{z}_i$ along the $\mathbf{x}_{i-1}$ direction. The twist angle, α_{i-1}, describes the angle from $\mathbf{z}_{i-1}$ to $\mathbf{z}_i$ about the $\mathbf{x}_{i-1}$ axis. The joint

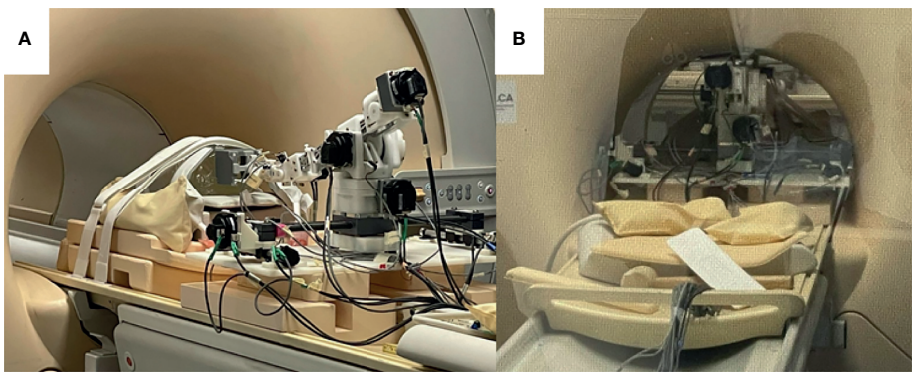

FIGURE 4 | Robot setup in MRI bore. **(A)** Robot in place on MR bed with a z-frame fiducial phantom attached to the front of the extension joint; **(B)** Robot advanced into the bore of the MRI with phantom at isocenter.

offset, d_i, describes the displacement between $\mathbf{x}_{i-1}$ to $\mathbf{x}_i$ along the $\mathbf{z}_i$ direction. Lastly, the joint angle, θ_i, describes the angle from $\mathbf{x}_{i-1}$ to $\mathbf{x}_i$ about the $\mathbf{z}_i$ axis.

For the 5-DOF robot, 6 coordinate frames are required to establish the relationship between all the successive link-joint pairs, as shown in **Figure 1**. The transformation matrix, T_i^{i-1} given by the expression in Equation 2 defines the translation and rotation of frame *i* with respect to frame *i-1* using the D-H parameters described for $i = 0, \ldots, 5$.

$$T_i^{i-1} = \begin{bmatrix} cos\theta_i & -sin\theta_i & 0 & a_{i-1} \\ sin\theta_i cos\alpha_{i-1} & cos\theta_i \sin\alpha_{i-1} & -sin\alpha_{i-1} & -d_i sin\alpha_{i-1} \\ sin\theta_i sin\alpha_{i-1} & cos\theta_i sin\alpha_{i-1} & cos\alpha_{i-1} & d_i cos\alpha_{i-1} \\ 0 & 0 & 0 & 1 \end{bmatrix} \quad (2)$$

Table 1 summarizes the D-H parameters for the robot according to the modified D-H convention. With frames assigned to all the links, a series of matrix multiplications establishes the translation and orientation of frame 5 with respect to frame 0.

$$T_6^0 = T_1^0 * T_2^1 * T_3^2 * T_4^3 * T_5^4 \quad (3)$$

Frame 6 is decoupled from the final pose of the end effector and is used primarily to advance the needle guide to the surface of the skin for hand driven procedures or ultimately to drive automated needle insertion along the intended direction. The final end effector offset assumes that joint 6 is fully extended.

The kinematic solution of the robot was determined by Equation 3. Using the D-H parameters from **Table 1** and the variable joint angles (d_1, d_2, θ_3, θ_4, θ_5) the position and orientation of the end-effector can be computed. The final joint variable, d_6, determines the proximity to the skin for the hand-driven case or the depth of insertion in the direction of joint 5 for the robot-driven case.

2.3.3 Inverse Kinematic Workflow

The inverse kinematics workflow described herein encompasses both the inverse kinematic formulation used to determine the specific joint configuration needed to place the end effector at a desired pose as well as the motion plan i.e. the sequence of joint motions needed to move to the target pose. To position the needle guide along the desired needle path, a pose is required based on an entry point through the skin and a target point inside the tissue (usually a tumor). Rather than being simply perpendicular to the axial plane, the orientation of the needle guide is usually defined by the need to have a treatment device align with the long axis of a target or to avoid intersecting other organs as shown in **Figure 5**. With the robot initially registered to a default home position, the joint configuration needed for alignment of the end effector to the target pathway is calculated by the joint optimization process described at the end of this section. As a critical step in sequential multi-needle insertion, the procedure to release the needle and clear its path is incorporated for all needles after the first insertion. In addition, the order of the joint motion is important due to patient proximity and is described in detail by the workflow shown in **Figure 3B**.

The inverse kinematics is formulated as a constrained optimization problem. It should be noted that the pivot directly determines the yaw angle while the shoulder and the elbow together determine both the height and the pitch angle of insertion, thus, accommodating for a range of entry points and patient sizes. The last joint (d_6) acts as the insertion joint and therefore is not considered while computing the necessary joint configuration for a given target. The first five joint values are computed *via* inverse kinematics to position the last joint for insertion. In other words, the optimal joint configuration, as determined by inverse kinematics, positions the end of the last rotary joint at the desired needle insertion pose.

The inverse kinematics were computed in Matlab using the *fmincon* function, a non-linear solver for constrained optimization problems. Given a target pose, the solver uses a gradient descent algorithm to search the bounded joint space for a suitable set of parameters that minimize the Euclidean error between target position and the position of the end effector. The position of the end effector is computed by applying forward kinematics to each proposed set of joint values. The bounds of the search space are determined by the operating range for each joint. Further constraints are applied to define the desired orientation of the target. These are equality constraints,

$$\theta_3 = C_1 . \quad (4)$$

$$\theta_4 + \theta_5 = C_2 . \quad (5)$$

where C_1 and C_2 are constants defined by the target yaw (the angle about the z-axis of frame 0) and pitch (the angle about the y-axis of frame 0) angles respectively. In summary, the solver tests a range of joint values within the bounded space and returns the joint values that minimize the error function.

TABLE 1 | Joint definitions and D-H parameters.

Number (*i*)	Joint Type	Joint Name	Link Length $a_{(i-1)}$	Twist Angle $\alpha_{(i-1)}$	Offset d_i	Joint Angle θ_i
1	Prismatic	Axial	0	0	d_1	0
2	Prismatic	Lateral	0	-π/2	d_2	-π/2
3	Rotary	Pivot	0	-π/2	d_3	θ_3
4	Rotary	Shoulder	0	π/2	0	θ_4
5	Rotary	Elbow	a_4	0	0	θ_5 - π/2
6	Prismatic	Extension	0	-π/2	d_6	π

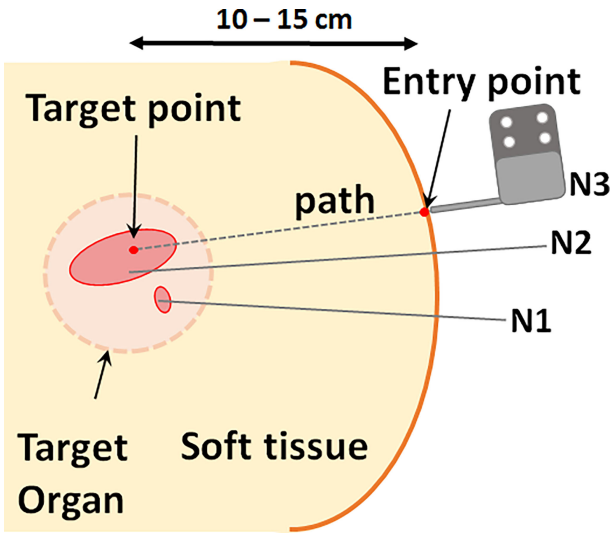

FIGURE 5 | Schematic of needle typical clinical needle insertion scenario. Multiple needles are inserted at varying orientations for optimal coverage of the target volume. Each needle path, or pose, is defined by a point in the target and an entry point.

3 METHODS

3.1 MR Compatibility Test

The robot was tested on a 3T Philips Achieva system with a 60 cm diameter bore and, with minor modifications, will be compatible with similar clinical MRI systems. Four clinically-relevant image sequences were investigated for qualitative uniformity in the images as well as quantitative changes in SNR. T1-weighted turbo spin echo (TSE), T2-weighted TSE and ultrafast gradient echo (THRIVE) sequences may be used for anatomical landmarking and pre-operative treatment planning. High resolution T2-weighted TSE is additionally used to confirm the final placement of the needles in a typical brachytherapy procedure. The gradient echo-echo planar imaging sequence (FFE-EPI) provides a means to monitor needle insertion in near real-time using the magnitude portion of the image. The imaging parameters used for each of the sequences are summarized in **Table 2**. Two phantoms were used to assess the impact of the robot on the image quality for each type of sequence. A saline phantom was used to provide a standardized reference for quality assurance as is done at our institution. A gelatin phantom was used because it can be quickly and easily prepared and its similar water content to tissue results in MRI SNR and contrast that is generally representative of tissue. Further, their mechanical properties can be modified to mimic insertion into tissue. A saline phantom (Philips QA fluid grid phantom) was placed at the isocenter of the magnet and imaged with: (1) the robot in position ready for needle insertion but switched off (Power Off) and (2) the robot in place and powered on (Power On) and (3) the robot being remotely driven during acquisition (Moving). The process was repeated for a gelatin phantom. Additional scans were acquired in the gelatin phantom with a catheter and guiding titanium alloy trocar (6F) inserted (Trocar) while the robot was powered on. Finally, an image set was acquired with the guiding trocar removed and the catheter left in place (Catheter). Image signal-to-noise and qualitative uniformity were assessed for each image using the Philips DICOMViewer. The SNR was calculated as the difference between the mean signal in a region of interest (ROI) inside the phantom and the mean signal in a region outside the phantom divided by the standard deviation of the region outside of the phantom. Multiple ROIs (4-5 depending on the space) were used to obtain the average SNR across the phantom.

3.2 Theoretical Workspace Simulation

The forward kinematics were used to simulate the workspace of the robot end effector in Matlab for the feasible range of joint angles. The workspace shows the volume of points that can be accessed by the end effector without considering the constraints imposed by the MR and patient which are subject to change. A

TABLE 2 | Scan parameters for each MR sequence.

Sequence	Resolution (mm)	Slice Thickness (mm)	FA (°)	TE (ms)	TR (ms)
T2w TSE	1.56 x 1.56	3	160	79	4000
T1w TSE	1.56 x 1.56	3	160	10	750
THRIVE	1.56 x 1.56	1	15	2	20
FFE-EPI	1.56 x 1.56	5	19.5	20	25

sample segmentation of a prostate volume was obtained from a clinical case study and plotted as a reference landmark relative to the robot workspace. A potential needle trajectory is shown passing through the feasible workspace outside the skin and accessing the prostate which may be up to 10 cm superior of the skin.

3.3 Joint-Level Testing

The joint-level uncertainty was measured by repeatedly driving each joint over a set distance for a range of available joint values. Optical tracking (Polaris Vega, NDI, Waterloo, Canada) was used to assess the accuracy of each joint movement by fixing an optical marker to the end effector and recording its position and orientation in real-time. Each joint was driven back and forth, 10 times in each direction in steps of 5mm for prismatic joints and steps of 5° for revolute joints. Means and standard deviations were calculated for each isolated joint motion.

3.4 Workflow Assessment for Sequential Needle Insertion

To assess the feasibility of sequential needle insertion using the designed end effector, a benchtop test was performed in a gelatin phantom. A gel phantom was marked with seven insertion points on the proximal face of the phantom as illustrated in **Figure 9A**. Insertion points and insertion angles are reported as [*X, Y,* R_x, R_y], where R_x and R_y indicate rotation about the *X* and *Y* axis. Given the designed target surface of 10 x 10 cm, poses were selected at the upper and lower angled bounds of the target space (5: [50, 0, -15, 0], 3: [-50, 0, 15, 0]). Distances are in mm and angles are in degrees. Two poses were selected at the extreme left and right of the target space (1: [0, -50, 0, -10], 7: [0, 50, 0, 10]). Three parallel poses were selected in the central zone of the target surface to demonstrate the feasible resolution for horizontal and vertical insertion (4: [0, 0, 0, 0], 2: [0, 5, 0, 0], 6: [5, 0, 0, 0]). For this study a flat insertion surface was assumed with constant insertion depth (z-axis). The order of the targets was selected to follow a left to right insertion pattern, but future work will consider the optimal sequence for insertion to minimize target motion while avoiding collision with other needles. The robot was driven to each target position in the order shown in the diagram by entering the appropriate joint values with the needle guide closed. At each position, a needle was inserted *via* the needle guide at the desired pose. The needle was then released by opening the needle guide and the process was repeated for the other six entry points. Needle positions and orientations were chosen to demonstrate the range of motion of the robot.

3.5 Needle Insertion Under Real-Time MRI

The feasibility of sequential multi-needle insertion under real-time MRI was assessed in a gelatin phantom using the workflow described in 2.3. The robot was set up in the MR bore and registered to the imaging space as described in 2.3.1. A THRIVE image of the phantom was acquired using the imaging parameters from **Table 2**. Four target points were delineated at various positions and angles on the transverse surface of the phantom. For each target the inverse kinematics were determined using the bore-constrained robot range of motion. For each target, the needle guide was driven to the planned position and orientation and real-time MR images (FFE-EPI from Table II) were acquired while the needle was being inserted. To assess the image quality of the real-time sequence while a needle was being inserted, automated needle insertion was simulated by positioning the needle tip at the surface of the gel and taping the shaft of the needle to the fully retracted needle guide. The needle guide was driven forward, and the progression of the needle was visualized under continuous FFE-EPI. After all the needles were inserted, a final T2w-TSE was acquired with trocars removed to assess the placement of the needles.

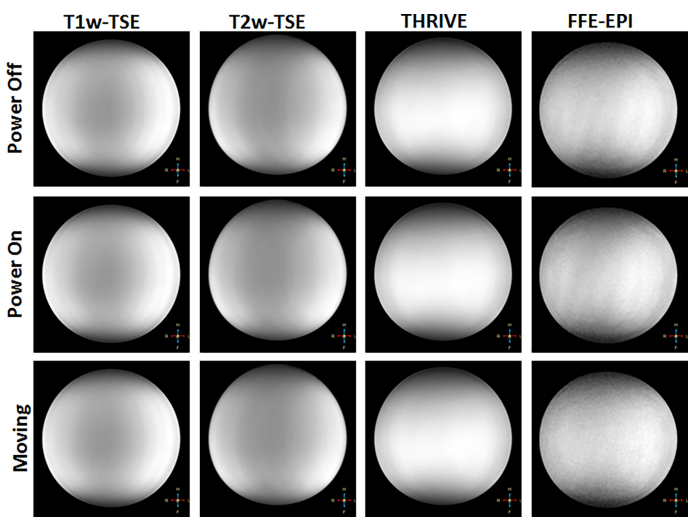

FIGURE 6 | Representative images showing qualitative changes in MR images of a saline phantom for different sequences (in columns) and with the robot powered off (top row), powered on (middle row) and robot moving (bottom row).

4 RESULTS

4.1 MR Compatibility

Figure 6 shows representative images of the Saline phantom for each sequence and robot condition. No visible change is observed when the robot is powered on or moving thus confirming the qualitative uniformity of the images for the working robot. The measured SNR values for both the saline and gelatin phantom are summarized by the graphs in **Figure 7**. The graph shows the mean over the SNR samples and the standard deviation represented as error bars. The four to five SNR samples measured for each case was used to run a one-way analysis of variance test to determine whether there was a significant difference in the group means for each type of sequence. The most dramatic change in SNR was observed by powering on the robot. In the saline phantom, a significant difference ($p < 0.05$) was observed for the T1-weighted TSE ($p = 0.0083$). Using a multiple comparison test, it was determined that power off was significantly different from power on ($p = 0.0467$) and moving ($p = 0.0076$). In the gelatin, the SNR showed greater variability for each case compared to the saline phantom and no significant difference was observed for the group means for each sequence.

4.2 Theoretical Workspace

The robot spans 65 cm in height and 30 cm laterally with 6 cm in depth at its widest point. The workspace covers the proposed clinical target surface of 10 x 10 cm. This is confirmed by the plot of the feasible workspace of the robot relative to a sample anatomical target (**Figure 8**).

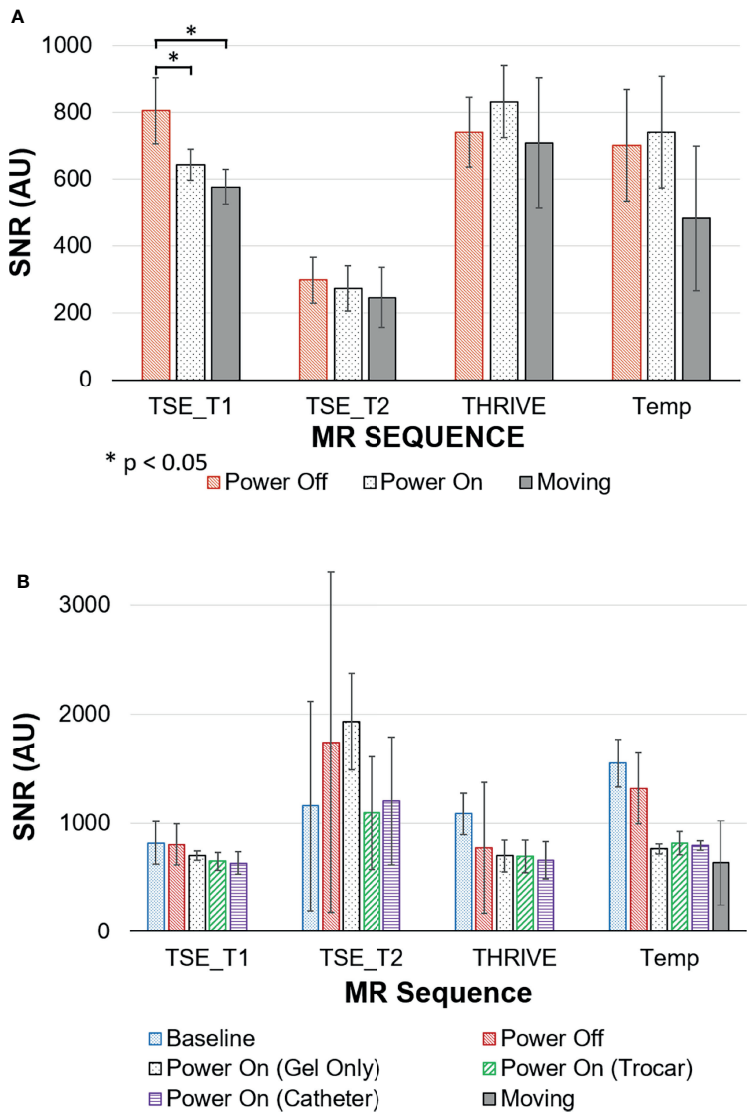

FIGURE 7 | Signal to Noise ratios (SNR) for MRI sequences with the robot in different states of use measured in **(A)** saline phantom; **(B)** gelatin phantom.

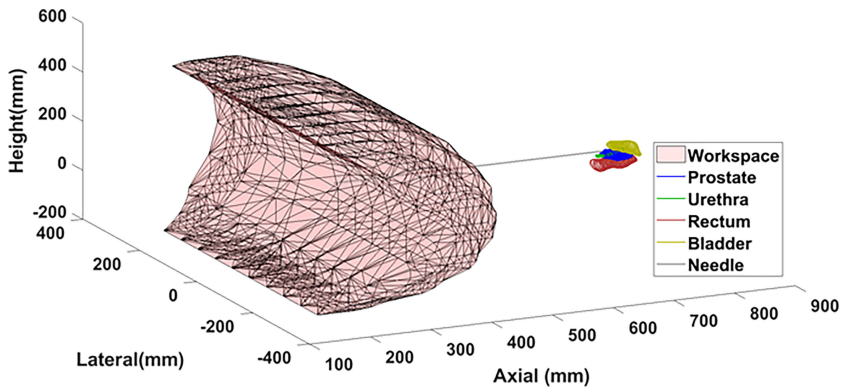

FIGURE 8 | Theoretical workspace computed using forward kinematics relative to sample anatomical landmarks.

4.3 Joint Level Accuracy

The mean error and standard deviation for each joint are reported in **Table 3**. Joint level testing showed errors between (0.08 ± 0.05) to (0.31 ± 0.60) mm for the lateral and axial prismatic joints. The revolute joints powered by belt-drive resulted in the largest errors of (2.10 ± 0.72) to (1.80 ± 0.48) ° for the shoulder and elbow respectively. The majority of the joint inaccuracy for the revolute joints appears to be systematic and the precision of the joint motion falls within the design specifications of 1 mm for prismatic joints and 1° for revolute joints.

4.4 Workflow Assessment for Sequential Needle Insertion

Figure 9 shows photographs of the needle guide and phantom during needle insertion. In order from top-middle to bottom middle: photographs after insertions of needles 1, 3, 4 and 7. Each needle was successfully placed at its respective target point without interference with other needles, demonstrating the maneuverability of the robot for multi-needle insertion. Needles were placed at four boundary points of the desired target surface to confirm the range of motion of the robot. In addition, three needles were placed in the central zone of the phantom with 5mm spacing in the horizontal and vertical directions to demonstrate that the feasible resolution of needle placement is consistent with that of a standard clinical grid template. **Figure 9** (bottom right) shows the final arrangement of the needles in an isometric view with the needle guide in place just after release of the last needle. The offset between needles 2 and 4 was 5 mm, well within clinical requirements.

TABLE 3 | Measured joint level errors.

	Error Mean	Error Standard Deviation
Axial (mm)	0.31	0.60
Lateral (mm)	0.08	0.05
Pivot (°)	0.20	0.19
Shoulder (°)	2.10	0.72
Elbow (°)	1.80	0.48

4.5 Needle Insertion Under Real-Time MRI

The four needles were successfully inserted using the robot under real-time imaging. **Figure 10** shows the time-lapse images of a second needle being inserted to the right of the first needle. A video of the needle insertion is available in the supplementary material. The final TSE image of the phantom shows the four needles in place at various orientations with a 49 mm spread in the anterior-posterior direction and lateral spread of 22 mm.

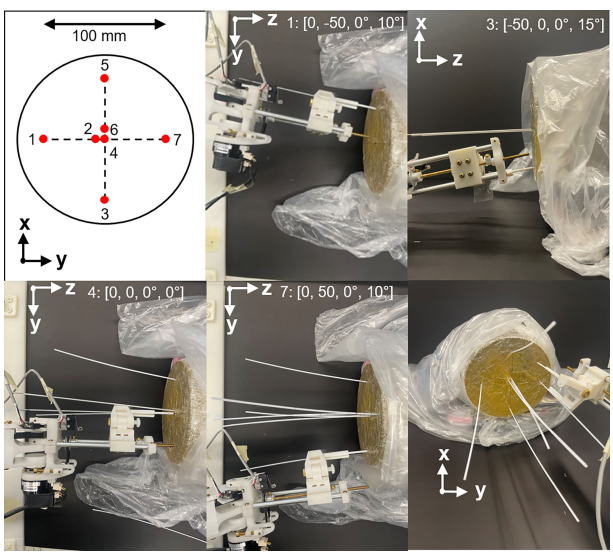

FIGURE 9 | Example of multiple needle insertion by the robot using a gel phantom. Top left: needle insertion plan with numbers indicating order of insertion. In order from top-middle to bottom middle: photographs showing needle insertions at needles 1, 3, 4 and 7. Axis indicators show the perspective of each photograph. Insertion points and insertion angles are shown in each photograph as [X, Y, R_x, R_y]. Bottom right: isometric view after insertion of all needles.

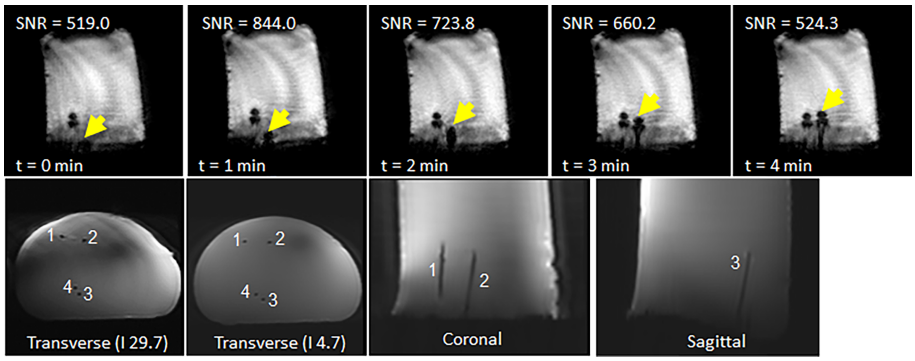

FIGURE 10 | (top row) Representative time-lapse images of showing progression of a second needle inserted to the right of a needle already in place. (bottom row) Final scan of phantom after insertion of four needles: (left) axial scan close to phantom surface; (middle) axial scan close to needle tips; and (right) coronal scan.

5 DISCUSSION

The results demonstrate the feasibility of robotically-guided multi-needle insertion under real-time MR guidance tissue-simulating gel phantoms. The robot showed minimal effect on the quality of the MR images and, crucially, sufficient signal was retained to visualize the needle during robot-driven insertion under real-time MR. Our plans are to progress to *ex vivo* and *in vivo* pre-clinical samples to verify these results in scenarios more representative of the clinical setting.

MRI is routinely used for guiding therapies because its soft-tissue contrast enables identification of targets, such as in the prostate, gynecology and neurological tumors. For prostate focal therapy, treatments such as high dose rate brachytherapy and phototherapies require insertion of multiple needles into the target. Compared to other MR-guided robotic systems, which insert parallel needles, our system is capable of inserting multiple needles at different orientations. We demonstrated that multiple needles could be inserted independently in both horizontal and vertical planes without interference from neighboring needles, with a minimum separation of ~5mm. We don't anticipate any limit in the number of needles that can be inserted except in the space between and the orientations of the inserted needles. For prostate focal therapies, the typical number of catheters ranges between 3-10 needles, similar to our demonstration of seven needles. We therefore expect that our robot can be applied to these treatments. By inserting multiple needles at different orientations, we anticipate that better targeting can be achieved with fewer needles. Each needle can be appropriately angled to fully cover the target while avoiding other structures that could interfere with insertion, such as the pubic arch for lateral tumors, the urethra for medial and anterior targets, or the rectum for posterior targets. With fewer catheter insertions, a reduction in total procedure time may also be observed.

The SNR analysis revealed that the robot did not have a significant impact on the signal in the case of the tissue-like gelatin. Large fluctuations were seen in the gelatin. In all cases low values were observed for the background signal with values ranging from 0.48 to 10.13. As such, small changes in the noise had a severe scaling effect on the estimation of the SNR. This suggests that fluctuations in the noise of the image was a major contributing factor to the wide spread seen for the SNRs. Another contributing factor may be local inhomogeneities in the gelatin phantom. In contrast, the standardized saline phantom images showed relatively stable SNR values and provided a baseline reference supporting the hypothesis that the robot had no major impact on the signal quality with the exception of the T1-weighted TSE. Despite the change in SNR, it was determined that sufficient signal was retained to ensure the viability of the robot as an insertion tool in the MR environment.

Joint level testing confirmed that the robot will conform to the desired specifications with a few modifications required. Currently, the elbow joint is powered by a drive belt through a worm gear to the ultrasonic motor. During joint testing, the elbow exhibited a form of hysteresis whereby driving the joint upwards (against gravity) was slightly different versus driving downwards (towards gravity). Further inspection points to a possible improvement as the height of the belt teeth is too short resulting in the belt not engaging with the gear connected to the joint. The largest errors were observed due to backlash when changing direction. This may be due to both the spacing of the belt teeth and slack in the belt tension when engaging the driving gear in the opposite direction. In the joint test data, similar behaviour was observed for the shoulder joint where the inner gear of the gearbox may be slipping. Another possible source of error could be the plastic worm gears used in the pivot and elbow joints which can exhibit some deformation at the gear teeth. For future work, these plastic worm gears will be replaced with aluminum-based worm gears.

The preliminary workflow test for multi-needle insertion revealed several important factors for future consideration. The end effector requires construction from a stronger material with greater precision to minimize any slack in the needle guide during insertion. The order of insertion must be defined during the planning phase to ensure minimal interference between needles during insertion. Future work will explore the automatic optimization of the needle insertion plan and establish communication between the planning software and

the robot control system. The current setup requires manual release of the needle which is not ideal for an in-bore patient set-up. A major benefit of the current design is the ease with which new end effectors each may be adapted to a specific needle type or procedure. Examples include angling the body of the needle guide for ease of access, changes for left or right-handed insertion and changing the gauge of the guide hole. To account for the characterized joint inaccuracies, an offset was applied during the MR guidance test.

Further evaluation of the functional workspace, the targeting accuracy, and the force output of the system is in progress. Additional tests will be conducted to assess the cumulative error associated with driving the robot in free space with and without the presence of a magnetic field. Lastly, the end effector will be modified to achieve automated needle insertion.

The large needle artefact observed in the MR images is a characteristic of imaging at 3 Tesla. It is expected that for a typical 1.5T clinical scanner the needle localization will improve. With real-time MR images of the needle being fed back from the scanner, an automatic AI-based needle segmentation may be used to localize the needle in the image and predict deviations from the target path. We hypothesize that using such an approach will aid in earlier detection of needle deflection and will allow smaller adjustments at the entry point to correct for needle deflection, compared to intermittent verification images. To support small adjustments, a secondary mode of operation may be employed by the robot. In the case of needle correction, the kinematic workflow must be modified as the needle is already partially inserted in the patient, generally along the planned path but with some deviation of the tip from the planned trajectory. As such, the motion along several coordinates is constrained by tissue. The user will have the ability to switch between multiple control pathways to minimize needle deflection and overcome the tissue restrictions. For example, the user may employ the following strategy: (i) retract along extension until the needle is behind the point of deflection and (ii) adjust the joint configuration so that position of the end effector tip is maintained but is in a slightly different orientation. The optimal strategy for correction of needle deflection requires further investigation but will benefit greatly from the information on the true needle position provided by real-time MRI.

6 CONCLUSION

The robot described in this paper supports multi-needle insertion under real-time MR-guidance. The robot is specifically designed to allow individual needle manipulation and thus enables future implementation of corrective motions to minimize needle deflection during insertion. The robotic system, equipped with real-time MRI feedback, has the potential to improve the safety and efficiency of MR-guided percutaneous procedures such as prostate brachytherapy.

DATA AVAILABILITY STATEMENT

The raw data supporting the conclusions of this article will be made available by the authors, without undue reservation.

AUTHOR CONTRIBUTIONS

AA conceptualized and assisted in the robot design, assisted in the kinematics design, developed registration with MR imaging and tested its performance and wrote the manuscript. TL conceptualized, designed and assembled equipment and assisted in testing and assisted in writing. SS designed kinematics. KL designed and assembled equipment. AW assisted with MRI design and imaging. ZZ developed user interface and robotic homing system. JD provided resource towards the robot design and testing facilities. RW conceptualized and assisted in the robot design and co-wrote the manuscript. All authors contributed to the article and approved the submitted version.

FUNDING

This research was supported by Siemens Healthcare Canada Ltd., Canadian Institutes of Health Research Mitacs Accelerate Program (Grant No MITACS IT12238) and the Natural Sciences and Engineering Research Council (Grant No 506721). Siemens Healthcare Canada provided direct funding to the project through the sponsored research agreement between Siemens Healthcare Canada and RW (through University Health Network, Toronto, CA, UHN-2015-MR-1-Jaffray) and by matching the contribution of Mitacs Accelerate Program in support of the graduate student. They had no influence on the experiments or the content of the manuscript and have no exclusive rights to the results or output of the research.

ACKNOWLEDGMENTS

We would like to thank Pascal Voyer-Nguyen, Eric Godden and Heidi Aleong for their contributions to hardware development and image analysis. Also, many thanks to Daniel Lin for project support, Warren Foltz for lending his MR expertise and Alejandro Berlin for his clinical expertise.

SUPPLEMENTARY MATERIAL

The Supplementary Material for this article can be found online at:: https://www.frontiersin.org/articles/10.3389/fonc.2022.829369/full#supplementary-material

REFERENCES

1. Ménard C, Susil RC, Choyke P, Gustafson GS, Kammerer W, Ning H, et al. MRI-Guided HDR Prostate Brachytherapy in Standard 1.5t Scanner NIH Public Access. *Int J Radiat Oncol Biol Phys* (2004) 59:1414–23. doi: 10.1016/j.ijrobp.2004.01.016
2. Lehmann T, Rossa C, Usmani N, Sloboda R, Tavakoli M. Deflection Modeling for a Needle Actuated by Lateral Force and Axial Rotation During Insertion in Soft Phantom Tissue. *Mechatronics* (2017) 48(October):42–53. doi: 10.1016/j.mechatronics.2017.10.008
3. Dimaio SP, Salcudean SE. Needle Steering and Motion Planning in Soft Tissues. *IEEE Trans Biomed Eng* (2005) 52(6):965–74. doi: 10.1109/TBME.2005.846734
4. Reed KB, Majewicz A, Kallem V, Alterovitz R, Goldberg K, Cowan NJ, et al. *Robot-Assisted Needle Steering*. IEEE Robotics and Automation Magazine New York: IEEE (2011). 35–46 p.
5. Stoianovici D, Kim C, Petrisor D, Jun C, Lim S, Ball MW, et al. MR Safe Robot, FDA Clearance, Safety and Feasibility of Prostate Biopsy Clinical Trial. *IEEE/ASME Trans Mechatronics*. (2017) 22(1):115–26. doi: 10.1109/TMECH.2016.2618362
6. Stoianovici D, Song D, Petrisor D, Ursu D, Mazilu D, Mutener M, et al. "MRI Stealth" Robot for Prostate Interventions. *Min. Invasive. Ther Allied Technol* (2007) 16(4):241–8. doi: 10.1080/13645700701520735
7. Cepek J, Chronik BA, Lindner U, Trachtenberg J, Davidson SRH, Bax J, et al. A System for MRI-Guided Transperineal Delivery of Needles to the Prostate for Focal Therapy. *Med Phys* (2013) 40(1):1–15. doi: 10.1118/1.4773043
8. Podder TK, Buzurovic I, Huang K, Yu Y. MIRAB: An Image-Guided Multichannel Robot for Prostate Brachytherapy. *Int J Radiat OncolBioPhys*. (2010) 78(3):S810. doi: 10.1016/j.ijrobp.2010.07.1876
9. Li P, Yang Z, Jiang S. Needle-Tissue Interactive Mechanism and Steering Control in Image-Guided Robot-Assisted Minimally Invasive Surgery: A Review. *Med Biol Eng Comput* (2018) 56(6):931–49. doi: 10.1007/s11517-018-1825-0
10. Podder TK, Beaulieu L, Caldwell B, Cormack RA, Crass JB, Dicker AP, et al. AAPM and GEC-ESTRO Guidelines for Image-Guided Robotic Brachytherapy: Report of Task Group 192. *Med Phys* (2014) 41(10):101501–2. doi: 10.1118/1.4895013
11. Monfaredi R, Cleary K, Sharma K. MRI Robots for Needle-Based Interventions: Systems and Technology. *Ann Biomed Eng* (2018) 46(10):1479–97. doi: 10.1007/s10439-018-2075-x
12. Tilak G, Tuncali K, Song SE, Tokuda J, Olubiyi O, Fennessy F, et al. 3t MR-Guided in-Bore Transperineal Prostate Biopsy: A Comparison of Robotic and Manual Needle-Guidance Templates. *J Magn Reson Imaging* (2015) 42(1):63–71. doi: 10.1002/jmri.24770
13. Song S-E, Tokuda J, Hata N, Fennessy FM, Oguro S, Fedorov A, et al. In-Bore Setup and Software for 3T MRI-Guided Transperineal Prostate Biopsy. *Phys Med Biol* (2012) 57(18):5823–40. doi: 10.1088/0031-9155/57/18/5823
14. Podder T, Clark D, Sherman J, Fuller D, Messing E, Rubens D, et al. *In Vivo* Motion and Force Measurement of Surgical Needle Intervention During Prostate Brachytherapy. *Med Phys* (2006) 33(8):2915–22. doi: 10.1118/1.2218061
15. Jiang S, Li P, Yu Y, Liu J, Yang Z. Experimental Study of Needle-Tissue Interaction Forces: Effect of Needle Geometries, Insertion Methods and Tissue Characteristics. *J Biomech* (2014) 47(13):3344–53. doi: 10.1016/j.jbiomech.2014.08.007
16. Tokuda J, Song SE, Tuncali K, Tempany C, Hata N. Configurable Automatic Detection and Registration of Fiducial Frames for Device-To-Image Registration in MRI-Guided Prostate Interventions. *Lect. Notes Comput Sci (including. subseries. Lect. Notes Artif Intell Lect. Notes Bioinformatics).* (2013) 8151 LNCS(PART 3):355–62. doi: 10.1007/978-3-642-40760-4_45
17. Craig JJ. *Introduction to Modern Robotics: Mechanics, Planning, and Control*. Prentice Hall. New York: Pearson (2004).

Conflict of Interest: AA received support from Mitacs Accelerate Program.

The remaining authors declare that the research was conducted in the absence of any commercial or financial relationships that could be construed as a potential conflict of interest.

This research was supported by Siemens Healthcare Canada Ltd., and the Natural Sciences and Engineering Research Council.

Advantages of publishing in Frontiers

OPEN ACCESS
Articles are free to read for greatest visibility and readership

FAST PUBLICATION
Around 90 days from submission to decision

HIGH QUALITY PEER-REVIEW
Rigorous, collaborative, and constructive peer-review

TRANSPARENT PEER-REVIEW
Editors and reviewers acknowledged by name on published articles

Frontiers
Avenue du Tribunal-Fédéral 34
1005 Lausanne | Switzerland

Visit us: www.frontiersin.org
Contact us: frontiersin.org/about/contact

REPRODUCIBILITY OF RESEARCH
Support open data and methods to enhance research reproducibility

DIGITAL PUBLISHING
Articles designed for optimal readership across devices

FOLLOW US
@frontiersin

IMPACT METRICS
Advanced article metrics track visibility across digital media

EXTENSIVE PROMOTION
Marketing and promotion of impactful research

LOOP RESEARCH NETWORK
Our network increases your article's readership